class of resistance temperature sensor (Sec. 5.4.5) based on semiconductor type materials that exhibit a wide range of temperature coefficients. The resistivity depends upon the material used to form the thermistor. Both negative (NTC) and positive temperature coefficient (PTC) devices can be produced. Commercially available thermistor forms are beads, probes, disks, and rods. The characteristics of thermistor output are shown in Fig. 5.9. The exact relationship between temperature and resistance depends on the material used for the sensor, but the general form of the output can be expressed by the equation

$$R = R_O \cdot e^{\beta(1/T - 1/T_O)} \tag{5.5}$$

where R = resistance at temperature T in ohms
R_O = resistance at temperature T_O in ohms
e = base of natural log
T, T_O = absolute temperature in K
β = indicator of shape of NTC curve

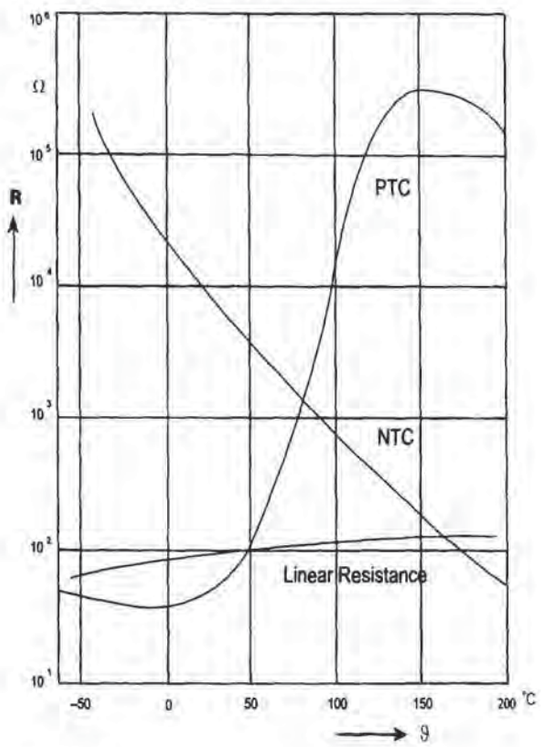


FIGURE 5.9 Thermistor output versus temperature.

This accounts for the high degree of nonlinearity in the output. However, the thermistor's nonlinearity can either be tolerated in many automotive applications, or corrected by an MCU or by circuit techniques. In the case of the water temperature indicator, for example, the thermistor's resistance is matched to a normal operating point on the gage; thus, the nonlinearity during conditions that generate higher temperature is not a problem.

Thermistors have a usable temperature range from –250 to +650 °C. Recent developments in automotive thermistors have focused on techniques to reduce cost and improve the manufacturability and reliability.

PETITIONER'S EXHIBIT 1002
US PATENT NO. 6,581,565

5.4.2 Thermocouples

Thermocouples are used frequently during the development phase of the vehicle because of their low cost, the broad range of temperature measurements that are possible from a single thermocouple such as iron-constantan, ease of extending the range through other materials, ease in obtaining a variety of form factors (especially small shapes), ease in forming the thermocouple, and ease in interfacing to temperature-recording equipment. The thermocouple type, wire size, and construction are factors that allow different units to be used from –250 to +1700 °C.

A thermocouple is formed by a pair of dissimilar conductors connected at one end. A voltage output E, proportional to the difference in temperature T_1 and T_2, is the basis of thermoelectric temperature measurements, also known as the Seebeck effect.

Thermocouple junctions can be formed by welding, soldering, or pressing materials together. Measurements can be made very easily; however, the highest accuracy is obtained by taking into account a number of factors, including reference junction considerations and a number (five) of laws that govern thermocouple behavior. Common types and their operating characteristics are shown in Table 5.5.

TABLE 5.5 Common Thermocouples and Application Factors

	Conductor		Temperature	Standard error	Seebeck
ISA code	Positive	Negative	Range, °C	Limit, °C	Coefficient, μV/°C
E*	Chromel	Constantan	0 to +316	±2	62
J*	Iron	Constantan	0 to +277	±2	51
T*	Copper	Constantan	–59 to +93	±1	40
K*	Chromel	Alumel	0 to +277	±2	40
N*	Nicrosil	Nisil	0 to +277	±2	38
S*	Platinum†	Platinum	0 to +538	±3	7
R*	Platinum‡	Platinum	0 to +538	±3	7

* Other temperature ranges and error limits are available.
† 10% Rhodium.
‡ 13% Rhodium.

5.4.3 Bimetallic Switch

A bimetallic temperature switch uses two metal strips with different coefficients of linear expansion that are welded together. Increasing temperature causes the strips to warp predictably. A switch point can be established by an initial calibration that indicates that a critical temperature has been reached and provides an input to an electronic control unit or a lamp indication. Switch types can be disk or cantilever construction. The use of switches does not require analog-to-digital conversion in control systems with microcontrollers, but provides limited information (only above or below a desired operating point) about the system. Early engine control systems used a disk switch in the air cleaner to indicate operation below 13 °C and a cantilever design in the engine coolant to indicate temperature above 71 °C.

5.4.4 Potentiometer Temperature Sensor

A bimetallic actuator can be combined with a high-resolution potentiometer to provide a temperature sensor for automotive applications. The linear movement of the bimetallic stack is transmitted by a stainless steel tube and measured as a distance by a conductive plastic film potentiometer providing a linear indication of temperatures up to 650 °C. The time constant for the sensor is approximately 70 s.

PETITIONER'S EXHIBIT 1002
US PATENT NO. 6,581,565

5.4.5 RTDs

A resistive temperature detector, or RTD, made of platinum is the highest inherent accuracy temperature sensor. The RTD has an output that varies with temperature based on the following equation:

$$\text{RTD} = R_O \cdot (1 + A \cdot T + B \cdot T^2) \tag{5.6}$$

where RTD = value of RTD at 0 °C in ohms and is 100 Ω for Pt100 and 200 Ω for Pt200
A = detector constant = $3.908 \cdot 10^{-3}$ ($°C^{-1}$) for Pt100
B = detector constant = $-5.802 \cdot 10^{-7}$ ($°C^{-2}$) for Pt100
T = temperature in °C

A constant current is applied to the RTD to obtain a voltage output over the range from −200 to +850 °C. Linearity can be within 3.6 percent for a range of 0 to 850 °C.

Other metals like nickel, nickel-iron alloy, copper, and aluminum can also be used for the RTDs. In addition to wire-wound RTDs, thin-film techniques also allow an RTD to be applied to a substrate, such as ceramic or silicon.

5.4.6 Semiconductor Techniques

Several semiconductor parameters vary linearly over the operating temperature range. As shown in Fig. 5.10, the gate threshold voltage of a power MOSFET changes from 1.17 to 0.69 times its 25 °C value when the temperature increases from −40 to 150 °C. Also, the breakdown voltage of the power MOSFET varies from 0.9 to 1.18 times its value at 25 °C over the same −40 to 150 °C temperature range (Fig. 5.10). These relationships are frequently used to determine the critical temperature (junction temperature) of semiconductor components in actual circuit operation. External package-level temperature measurements can be several degrees different than the junction temperature, especially during rapid, high-energy switching events. The actual junction temperature and the resulting effect on semiconductor parameters must be taken into account for the proper application of semiconductor devices. Semiconductors can be used for sensing temperature within their operating temperature range.

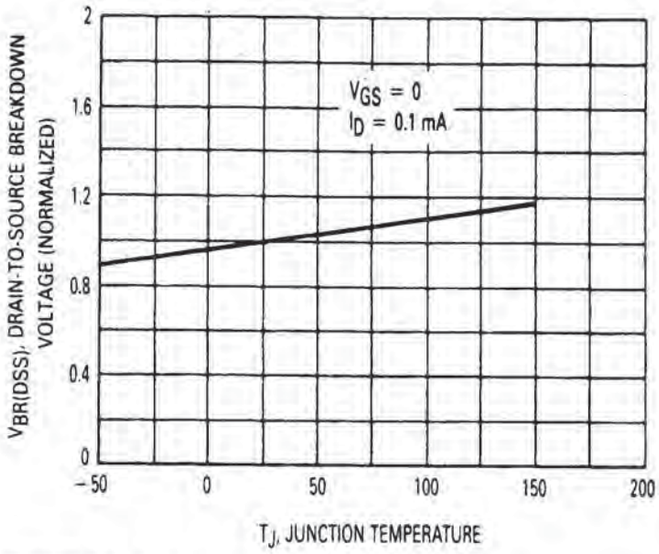


FIGURE 5.10 Breakdown voltage versus temperature.

PETITIONER'S EXHIBIT 1002
US PATENT NO. 6,581,565

The most commonly referenced transistor temperature measurement is the V_{BE} relationship to temperature. A silicon temperature sensor that utilizes this effect has a nominal output of 730 mV at –40 °C and an output of 300 mV at 150 °C. The linearity of this device is shown in Fig. 5.11. The total accuracy is within ±3.0 mV including nonlinearity which is typically within ±1 °C in the range of –40 to 150 °C. The readings are made with a constant (collector) current of 0.1 mA passing through the device to minimize the effect of self-heating of the junction.

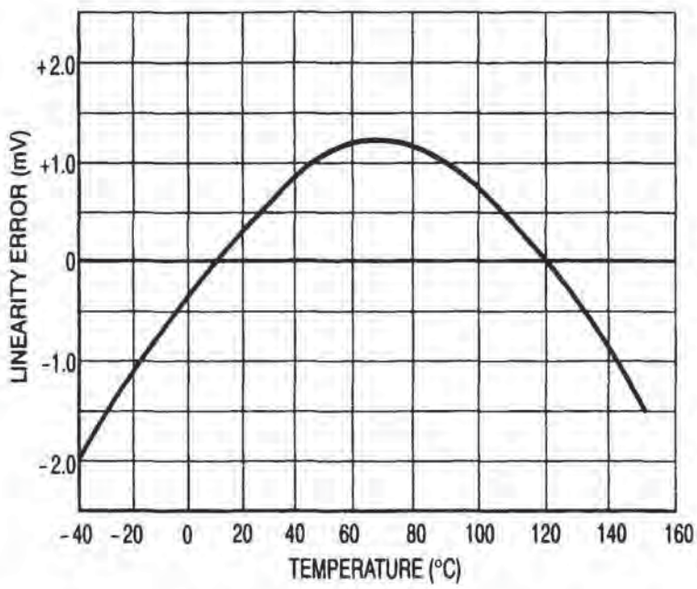


FIGURE 5.11 Linearity of silicon temperature sensor.

The linear relationship of the V_{BE} of a transistor to temperature provides a considerable improvement in accuracy over a thermistor. However, the limited operating range of semiconductor temperature sensors (–40 to 150 °C) has limited their application in vehicles. To be cost-effective in automotive applications, semiconductor sensing is usually incorporated with other sensing or interface devices.

An RTD (Sec. 5.4.5) with an aluminum metal film has been integrated with a semiconductor process to provide a temperature sensor that can directly drive the analog-to-digital input in a microcontroller unit (MCU). The sensor has better than ±2 percent accuracy over a –50 to 150 °C temperature range. On-chip linearization techniques avoid look-up table linearization by the MCU.

Another integrated semiconductor temperature sensor uses the fact that two identical transistors operating at a constant ratio of collector current densities r results in the difference in base-emitter voltages being $(kT) \cdot (\ln r)$. Both Boltzman's constant k and the charge of an electron q are constant, so the resulting voltage is directly proportional to absolute temperature. The voltage is then converted to a current by low-temperature coefficient thin-film resistors.

Polysilicon diodes and resistors can be produced as part of a power MOSFET semiconductor manufacturing process and used as temperature-sensing elements to determine the junction temperature of the device. The thermal sensing that is performed by the polysilicon elements is a significant improvement over power device temperature sensing that is performed by an external temperature-sensing element. An extreme thermal gradient exists between the maximum junction temperature at the top (active area) of the power device and the remote point which is able to be measured by a thermistor or thermocouple. Placing the thermal-sensing element inside the package improves the measurement process considerably.

PETITIONER'S EXHIBIT 1002
US PATENT NO. 6,581,565

By sensing with poly resistors or diodes, the sensor can be located close to the center of the power device near the source bond pads where the current density is the highest and, consequently, the highest die temperature occurs. The thermal conductivity of the oxide that separates the polysilicon diodes from the power device is two orders of magnitude less than that of silicon. However, because the layer is thin, the polysilicon element offers an accurate indication of the actual peak junction temperature.

A very low on-resistance power FET that incorporates a temperature sensing diode is shown in Fig. 5.12. The power device achieves an on-resistance of 5 milliohms (including packaging resistance) at 25 °C utilizing a production power FET process. The power FET process was chosen instead of a power IC process because a large die size was required to meet the power dissipation requirements of a very cost sensitive application. A minor modification (the addition of a single masking layer) to a production power FET process allows both sensing and protection features to be integrated. Devices that are produced using the SMARTDISCRETE technology, as this approach is called by Motorola, are one way to provide more cost-effective, smart power semiconductors, especially for high-current or low on-resistance power applications.

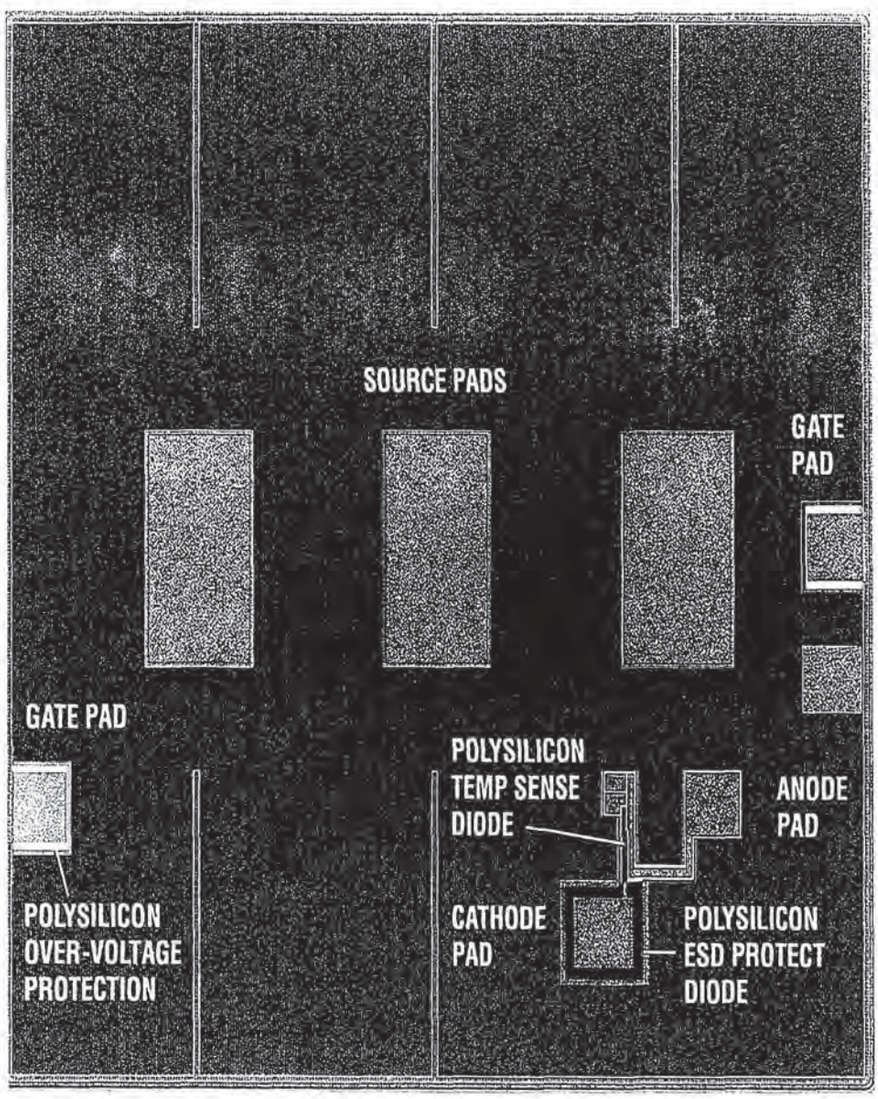


FIGURE 5.12 Temperature sensor integrated in power MOSFET. *(Die photomicrograph Courtesy Motorola Inc.)*

PETITIONER'S EXHIBIT 1002
US PATENT NO. 6,581,565

An accurate indication of the maximum die temperature is obtained by monitoring the output voltage when a constant current is passed through the integrated polysilicon diode(s). A number of diodes are actually provided in the design. A single diode has a temperature coefficient of 1.90 mV/°C. Two or more diodes can be placed in series if a larger output is desired. For greater accuracy, the diodes can be trimmed during wafer-level testing by blowing fusible links made from polysilicon. The response time of the diodes is less than 100 μs which has allowed the device to withstand a direct short across an automobile battery with external circuitry providing shutdown prior to device failure. The sensing capability also allows the output device to provide an indication (with additional external circuitry) if the heatsinking is not proper when the unit is installed in a module or if a change occurs in the application which would ultimately cause a failure.

A smart power IC, like Motorola's SMARTMOS™ process, can have multiple power drivers integrated on a single monolithic piece of silicon. Each of these drivers can have a temperature sensor integrated to determine the proper operating status and shut off only a specific driver if a fault occurs. The temperature sensor is basically a band gap reference. In this case, two diodes' junctions are biased with different current densities. Circuitry in the smart power IC process establishes a voltage reference and a trip point.

5.4.7 Thermostat (Mechanical Temperature Sensing)

The earliest method of temperature regulation used in vehicles is still in use today—the thermostat. The expansion element usually activates a valve which redirects the flow of coolant into a radiator bypass line when a specific temperature is reached.

5.4.8 Fiber Optic Temperature Sensors

High-temperature sensors capable of operating up to 1800 °C have been developed using optical fibers. The response time of the sensor is on the order of 500 ms and the accuracy is within ±0.5 percent. The noncontact sensor uses a single optical fiber that has an outside diameter of 0.5 to 1.0 mm. The probe structure is critical to the sensor's sensitivity and the distance coefficient that relates the detection surface area to the distance at which the probe will be placed for measurement.

A sapphire fiber optic sensor has been developed to measure high temperatures such as those found near the tip of a spark plug during combustion. The sensor can withstand temperatures up to 4000 °C and has an accuracy of 0.2 percent at 1000 °C. The sensor has been used to identify knock and to characterize flame front propagation.

5.4.9 Temperature Indicators

Temperature-indicating materials have been developed with melting points that can be calibrated to ±1 °C. When the temperature of the device is exceeded, a phase change occurs and the material changes color. The material is available in paint, patch, pellet, and applicator stick form. Temperature ranges from 38 to 1371 °C are available. This kind of indication is useful during the development phase of automotive components to verify that a critical design temperature has not been exceeded.

5.4.10 Infrared Temperature Sensing

Blackbody emittance is the basis for infrared (IR) thermometry. Objects at temperatures above –273 °C emit radiant energy in an amount proportional to the fourth power of their

PETITIONER'S EXHIBIT 1002
US PATENT NO. 6,581,565

temperature. An IR sensor consists of collecting optics, lenses, and/or fiber optics, spectral filtering, and a detector as the front end. The primary characteristic of the optics is the field of view (FOV) which allows a specific target to be measured at a prescribed distance.

Infrared sensors have been used extensively for noncontact temperature measurements in process control. In automobiles, infrared sensors use temperature variations to produce a monochrome image in night vision systems. Board-level temperature testing also utilizes IR-sensing techniques to identify hot spots and potential failure points.

5.4.11 Thermal Actuators/Thermal Cooling

Chemical sensors like the oxygen sensor described in Sec. 5.2.6 require a minimum operating temperature to be effective. Semiconductor technology allows platinum and silicon heaters and temperature sensors to be produced on a thin diaphragm, or window, etched into a silicon substrate. Temperatures can be produced in the window which exceed 1200 °C, while the supporting rim of silicon remains essentially at room temperature. This ability may allow fast-response sensors to be developed for vehicle applications.

Other silicon development activity using micromachining techniques may allow heat pipes and silicon-level heatsinks to remove heat more effectively from rapidly switching semiconductor devices.

5.5 HUMIDITY SENSORS

Humidity sensors are used extensively during vehicle and component development, especially in determining the ability to withstand humidity and temperature cycling tests. Engine performance can be affected by humidity. A sensor that can pass rigorous automotive qualification tests and meet the desired specifications and cost criteria would provide additional input for the engine control system. In a less rugged application, HVAC systems may benefit from the input from humidity sensors. Humidity sensors are not used on production vehicles at the present time. However, some potential techniques that are used in development and nonautomotive applications are described in this section.

Techniques to measure humidity are listed in Table 5.6. Most of these are actually laboratory instruments. The most well known approach to humidity measurements is the use of wet bulb and dry bulb thermomometer readings interpreted through the use of a psychrometric chart which relates all basic humidity readings. The effect of humidity on polymers and the use of semiconductor-processing techniques has created actual sensors that do not require the constant calibration, have less drift, improved reliability, and potentially can achieve automotive cost objectives. Three sensing techniques that have potential for future vehicle use are capacitive, resistive, and oxidized porous silicon.

5.5.1 Capacitive Humidity Sensors

A thin-film polymer capacitive-type relative humidity sensor can be produced by using semiconductor technology. The dielectric constant of the polymer thin film changes linearly with changes in atmospheric relative humidity. A desirable feature, in addition to long-term stability and operation to 180 °C, is fast wet-up/dry-down performance.

A temperature sensor can easily be added to the RH sensor, which increases the operating range and the functionality.

PETITIONER'S EXHIBIT 1002
US PATENT NO. 6,581,565

TABLE 5.6 Techniques for Measuring Humidity/Moisture

Principle	Type measurement
Gravimetric hygrometer	Instrument
Pressure-humidity generator	Instrument
Wet bulb/dry bulb (psychrometer)	Instrument
Hair element	Instrument
Electric conductivity	Instrument
Dew cell	Instrument
Chilled mirror	Instrument
Karl Fisher titration	Instrument
Electrolytic	Instrument
Lithium chloride	Instrument
Capacitance hygropolymer	Production sensor
Bulk polymer (resistance)	Production sensor
Thin-film polymer (capacitance)	Production sensor
Gold/aluminum oxide	Production sensor
Oxidized porous silicon (OPS)	Experimental sensor

5.5.2 Resistive Humidity Sensors

Both surface and bulk polymer resistance sensors have been developed for measuring relative humidity. In bulk polymer film units, mobile ions are released from the molecular structure with increased humidity levels resulting in orders-of-magitude change in resistance over the operating range. Diode temperature compensation is used to improve accuracy over the temperature range. With an ac excitation at 1 kHz, a change from 10 to 100 percent RH produces a corresponding resistance variation from $2 \cdot 10^7$ to $2 \cdot 10^3$ ohms.

5.5.3 Oxidized Porous Silicon

A capacitive-type sensor has been developed that uses oxidized porous silicon (OPS) as a moisture-absorbing dielectric between the electrodes of the capacitor. An electrolysis process is used to create a thin porous layer on the top of a silicon wafer. The silicon is converted to OPS by a high-temperature treatment in either oxygen or steam. Metal electrodes are deposited on the top and back of the OPS to complete the capacitive structure.

When water vapor contacts the sensor, it permeates through the porous structure between the electrodes. The response of a typical sensor increases 800 percent when exposed to an RH change from 1 to 40 percent. Since semiconductor techniques are used in the manufacturing process, the potential to integrate signal conditioning and other sensors may provide an attractive solution for future vehicle sensing requirements.

5.6 CONCLUSIONS

Several factors are influencing the temperature-sensing requirements for future vehicles. The ultra-efficient vehicle will operate at higher temperatures and utilize brake energy-recovery. Both of these aspects will increase the temperature environment for other vehicle components.

The requirements for sensors in future vehicle systems include improved performance (sensitivity) and reliability in spite of operating at higher temperatures, lower cost, space and weight reduction, greater functionality including diagnostics and self-test, and ease of inter-

PETITIONER'S EXHIBIT 1002
US PATENT NO. 6,581,565

facing with an MCU for adaptive control and interchangeability. The capability of semiconductor technology to provide sensing information for failure detection provides a means for increased reliability in several vehicle subsystems.

All trademarks are the property of their respective owners.

GLOSSARY

Accuracy A comparison of the actual output signal of a device to the true value of the input. The various errors (such as linearity, hysteresis, repeatability, and temperature shift) attributing to the accuracy of a device are usually expressed as a percent of full-scale output (FSO).

Maximum operating temperature The maximum body temperature at which the thermistor will operate for an extended period of time with acceptable stability of its characteristics. This temperature is the result of the internal or external heating, or both, and should not exceed the maximum value specified.

Negative temperature coefficient (NTC) An NTC thermistor is one in which the zero-power resistance decreases with an increase in temperature.

Operating temperature range The range of temperature between minimum and maximum temperature at which the output will meet the specified operating characteristics.

Self-generating Providing an output signal without applied excitation, such as a thermoelectric transducer.

Self-heating Internal heating resulting from electric energy dissipated within the unit.

Storage temperature range The range of temperature between minimum and maximum which can be applied without causing the sensor (unit) to fail to meet the specified operating characteristics.

Temperature coefficient of full-scale span The percent change in the full-scale span per unit change in temperature relative to the full-scale span at a specified temperature.

Temperature hysteresis The difference in output at any temperature in the operating temperature range when the temperature is approached from the minimum operating temperature and when approached from the maximum operating temperature with zero input applied.

Thermal time constant The thermal time constant is the time required for a thermistor to change to 63.2 percent of the total difference between its initial and final body temperature when subjected to a step function change in temperature under zero-power conditions.

Transfer function A mathematical, graphical, or tabular statement of the influence which a system or element has on the output compared at the input and output terminals.

BIBLIOGRAPHY

Automotive Electronics Reliability Handbook, SAE, Warrendale, Pa., 1987.
Automotive Handbook, Robert Bosch GmbH, 1986.

PETITIONER'S EXHIBIT 1002
US PATENT NO. 6,581,565

BR923/D Discrete and Special Technologies Group Reliability Audit Report 1Q90, Motorola Semiconductor Products Sector, Phoenix, Ariz.

Collings, N., W. Cai, T. Ma, and D. Ball, "A linear catalyst temperature sensor for exhaust gas ignition (EGI) and on board diagnostics of misfire and catalyst efficiency," SAE SP-957, *U.S. and European Automotive Technology Emissions Technology,* International Congress and Exposition, Detroit, March 1–5, 1993.

De Vera, D., T. Glennon, A. A. Kenny, M. A. H. Khan, and M. Mayer, "An automotive case study," *Quality Progress,* June 1988, pp. 35–38.

Dosher, J., "Smart and active sensors," *Proceedings of Sensors Expo West,* 1991, pp. 103C-1–6.

Hao, T., E. F. Malinowski, and C-C. Liu, "High temperature fiber optic sensor for industrial applications," *Proceedings of Sensors Expo West,* San Jose, Calif., March 2–4, 1993, pp. 227–228.

Norton, Harry N., "Section 10—Transducers and Sensors," in D. G. Fink and D. Christiansen (eds.), *Electronics Engineers' Handbook* (3d ed.), McGraw-Hill, New York, 1989.

Pressure Sensor Device Data, Motorola Semiconductor Products Sector, Phoenix, Ariz., 1993.

Recommended Environmental Practices for Electronic Equipment Design, SAE J1211, Warrendale, Pa., Nov. 1978.

Temming, J., "Measuring seat comfort," *Automotive Engineering,* July 1993, pp. 25–30.

PETITIONER'S EXHIBIT 1002
US PATENT NO. 6,581,565

CHAPTER 6
EXHAUST GAS SENSORS

**H.-M. Wiedenmann, G. Hötzel,
H. Neumann, J. Riegel, and H. Weyl**
Robert Bosch GmbH
Lambda Oxygen Sensor Development

6.1 BASIC CONCEPTS

6.1.1 Combustion

The sole products of complete fuel combustion are the nontoxic substances carbon dioxide and water:

$$C_mH_n + \left(m + \frac{n}{4}\right) 0_2 \rightarrow m\,CO_2 + \frac{n}{2}\,H_2O \tag{6.1}$$

The theoretical air requirement for this process is 14.7 kg air for each kilogram of fuel; this corresponds to approximately 10 m^3 air per liter of fuel. The air/fuel ratio is defined as stoichiometric when the engine is supplied with the exact quantity of air required for complete combustion.

6.1.2 Definition of Normalized air/fuel Ratio Lambda

The mixture ratio is defined by the normalized air/fuel ratio lambda (λ):

$$\lambda = \frac{\text{current air-fuel ratio}}{\text{stoichiometric air-fuel ratio}} \tag{6.2}$$

Because the conditions within the engine do not correspond to the absolute ideal required for perfect combustion, a number of products of incomplete combustion occur, even if a stoichiometric air/fuel ratio ($\lambda = 1$) is maintained. Thus, the CO_2 and H_2O are joined by CO, H_2, and HC (hydrocarbons C_xH_y) along with corresponding amounts of not reacted (free) oxygen. The water-gas equilibrium defines the ratio of CO to H_2. At high combustion temperatures, the N_2 and O_2 in the air supply form nitrous oxides such as NO, NO_2, N_2O (generic designation: NO_x).

6.1.3 Composition of Untreated Exhaust Gas

The composition of the exhaust gases entering the catalytic converter (untreated or raw emissions) varies according to the quality of combustion and, even more importantly, as a function

PETITIONER'S EXHIBIT 1002
US PATENT NO. 6,581,565

of the normalized air/fuel ratio lambda (λ) (Fig. 6.1). Rich mixtures (lambda < 1, excess fuel) produce high concentrations of CO, H_2, and HC, while lean mixtures (lambda > 1, excess oxygen) generate higher levels of NO_x and free oxygen. The lower combustion-chamber temperatures associated with mixture ratios of lambda > 1.2 result in reductions in NO_x concentrations accompanied by increased HC concentrations. Maximum emissions of CO_2 (greenhouse gas) occur at a slightly lean mixture (lambda ≈ 1.1).

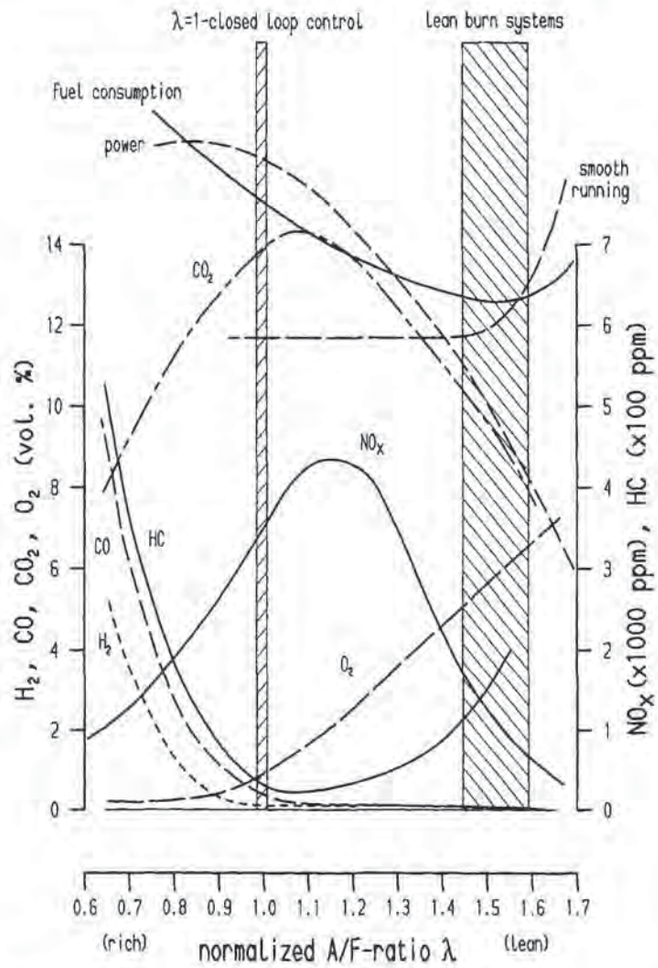


FIGURE 6.1 Typical curves for fuel consumption, power, smoothness, and composition of raw exhaust gases relative to lambda in a spark-ignition engine.

6.1.4 Lambda Closed-Loop Control: Design Concepts

Lambda Control Ranges. The main elements considered in defining the range of the lambda closed-loop control system (Table 6.1) are engine design, emission limits, fuel consumption, and the requirements for performance and smooth running.

Treatment of Exhaust Gases. Catalytic treatment of exhaust gases is essential for achieving compliance with the stringent current United States emission standards (Table 6.2). In the catalytic process, CO, H_2, and HC are oxidized to form CO_2 and H_2O, while the constituents of

PETITIONER'S EXHIBIT 1002
US PATENT NO. 6,581,565

TABLE 6.1 Lambda Control Ranges

	Lambda = 1—spark ignition engine	Lean-burn concept	Lean-mix concept	Diesel engine
Lambda-control range	Lambda = 1 ± < 0.005	1.4–1.7	1.4–1.7 and lambda = 1	1.1–7
Target	Opt. catalytic aftertreatment	Fuel economy low CO, HC, (NO_x)*	Improved fuel economy within allowable emission	Reduced emissions particles and NO_x
Lambda sensors	Lambda = 1 sensor	Lean A-F sensor	Wide-range A-F sensor	Lean A-F sensor
Exhaust gas aftertreatment	Three-way-catalyst (TWC)	Oxi-cat NO_x-cat*	TWC NO_x-cat*	Particle filter* NO_x-cat*
Control concepts	Conventional or continuous	Continuous	Lean: continuous lambda = 1: conventional	Full-load and EGR-control
Series production	Discont. control	—	Yes	—

* Not available yet.
TWC: three-way-catalyst; Oxi-cat: oxidation-catalyst; NO_x-cat: NO_x-reduction-catalyst.

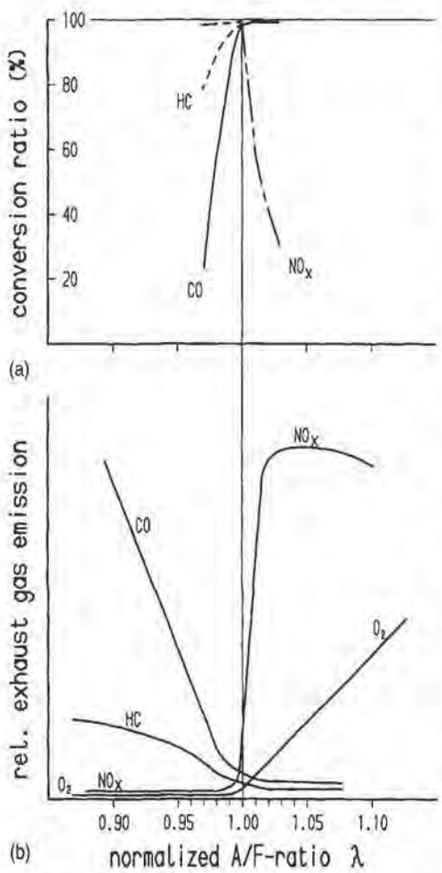


FIGURE 6.2 (*a*) Conversion rates for CO, NO_x, and HC in a new three-way catalytic converter; (*b*) typical curve for exhaust-gas composition downstream from a new three-way catalytic converter.

NO_x are reduced to N_2 and O_2. A three-way catalytic converter TWC (selective catalytic converter) and closed-loop control system featuring a lambda sensor are essential elements in achieving adequate reductions in all three pollutants (Fig. 6.2). The engine must be operated within a narrow range of $|\Delta\lambda| < 0.005$ at lambda = 1.

Oxidation catalysts are sometimes employed to reduce CO and HC emissions from lean-burn and diesel engines. Meanwhile, NO_x reduction catalysts and particle filters are being developed for future applications (Table 6.1).

Lambda Closed-Loop Control. Lambda closed-loop control is incorporated in the engine's electronic control system. The control system regulates lambda upstream from the catalytic converter with the aid of an oxygen sensor. System lag results in relatively long control-response delays, especially at low rpm. For this reason, the system must incorporate a pilot-control function capable of adjusting the mixture to the desired lambda with the highest possible degree of precision. This arrangement makes it possible to avoid excessive control deviations and harmful emission peaks of the kind that lead to high emission levels and reduced vehicle performance.

Conventional Closed-Loop Lambda Control. The closed-loop control concept pre-

PETITIONER'S EXHIBIT 1002
US PATENT NO. 6,581,565

TABLE 6.2 Summary of Emission Levels for Spark-Ignition Engines
(Status: July 1992)

		Exhaust emission limits						
	Start of sale	HC	CO	NO_x	HC + NO_x	Unit	Remarks	
California	MY 1993	0.25	3.4	0.4	—	g/mile		
	MY 1994	0.125	3.4	0.2	—	g/mile	TLEV 10 %	% of fleet,
	MY 1997	0.075	3.4	0.2	—	g/mile	LEV 25 %	stepwise
	MY 1997	0.04	1.7	0.2	—	g/mile	ULEV 2 %	increase
	MY 1998	0.0	0.0	0.0	—	g/mile	ZEV 2 %	
USA (Fed.)	MY 1983	0.41	3.4	1.0	—	g/mile		
	MY 1994	0.25	3.4	0.4	—	g/mile		
	MY 2003	0.125	1.7	0.2	—	g/mile	on need	
Japan	4/1981	0.25	2.1	0.25	—	g/km	10-mode	
EG	1992	—	2.72	—	0.97	g/km	MVEG I	
	10/1996	0.15	2.1	0.3	—	g/km	MVEG II	proposal parliament
		—	2.2	—	0.5	g/km		proposal commission
	1996	—	1.5	—	0.2	g/km	MVEG III	proposal Germany

TLEV: Transitional Low-Emission Vehicles
ULEV: Ultra Low-Emission Vehicles
LEV: Low-Emission Vehicles
ZEV: Zero-Emission Vehicles
MVEG: Motor Vehicle Emission Group

sently in use in spark-ignition engines is based on 2-point lambda = 1 control (Fig. 6.3) with the mixture composition oscillating around the optimum lambda. When the exhaust mixture shifts from rich to lean, the voltage from a lambda = 1 probe drops from approximately 800 mV (lambda < 1) to approximately 100 mV (lambda > 1), with a steep signal change (lambda jump) occurring at lambda = 1 (Sec. 6.2.1). Once the signal from the sensor crosses beyond the specified threshold value (e.g., 450 mV), the system responds by progressively leaning out the mixture until the probe signal drops below this border again. Once this process is completed, the system reverts to graduated mixture enrichment. Depending upon the system lag, the subsequent control-oscillation rate will lie in the 0.5 . . . 5 Hz range, with an amplitude of $\Delta\lambda = \pm 0.01 \ldots 0.05$ relative to the median lambda. During the lean-operation period, the catalytic converter stores oxygen for release during the rich-mixture phases. This arrangement ensures high conversion rates despite the control oscillations. Preferably an algorithm with proportional plus integral characteristics (PI controller) is used. Variations in system lag and integrator pitch affect the amplitude and the frequency of the oscillations. The proportional factors have to be adapted. Because load and rpm have a major effect on system lag, control parameters are defined and stored in a load/rpm control map.

Continuous Lambda = 1 Control. A continuous lambda = 1 control can be employed to achieve substantially smaller control deviations, providing attendant reductions in emissions, especially when used with aged catalytic converters. An oxygen sensor with a roughly linear or linearized lambda characteristic curve is required for this arrangement (Secs. 6.2.5 and 6.2.6).

6.1.5 On-Board Diagnosis (OBD II)

From the 1994 model year onward, on-board devices capable of monitoring the operation of all emission-relevant vehicle components will be required in the United States. Pollutant emission sensors (see Sec. 6.6) to measure levels of CO, NO_x, and HC emissions downstream from the catalytic converter represent an ideal means of monitoring the performance of both converter and oxygen sensor. Unfortunately, there are still no sensors of this type suitable for

PETITIONER'S EXHIBIT 1002
US PATENT NO. 6,581,565

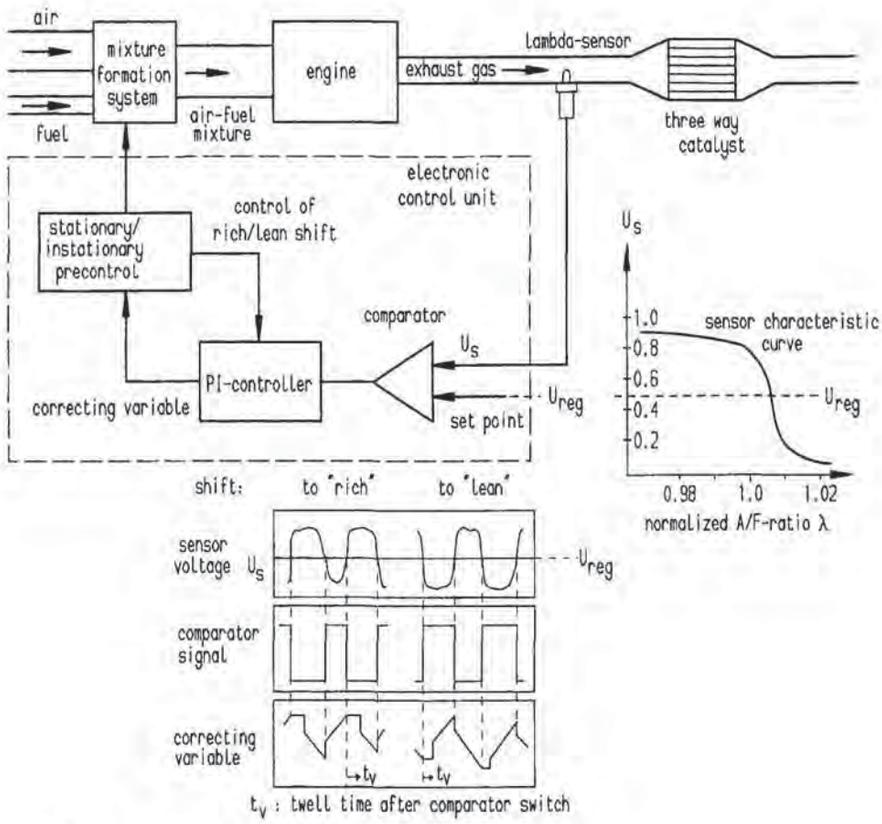


FIGURE 6.3 Operating diagram for lambda control.

use in the engine's exhaust stream. As an alternative, there exist concepts that employ a second oxygen sensor behind the catalytic converter to detect aging in the converter and/or the lambda sensor.

6.2 PRINCIPLES OF EXHAUST GAS SENSORS FOR LAMBDA CONTROL

6.2.1 Lambda = 1 Sensor: Nernst Type (ZrO_2)

Sensing Mechanism. In principle, the lambda sensor operates as a solid-electrolyte galvanic oxygen-concentration cell (Fig. 6.4). A ceramic element consisting of zirconium dioxide and yttrium oxide is employed as a gas-impermeable solid electrolyte. This mixed oxide is an almost perfect conductor of oxygen ions over a wide temperature range (Sec. 6.3). The solid electrolyte is designed to separate the exhaust gas from the reference atmosphere. Both sides feature catalytically active platinum electrodes. At the inner electrode (air; $pO_2'' - 0.21$ bar), the electron reaction

$$O_2 + 4e^- \rightarrow 2\,O^{2-} \tag{6.3}$$

incorporates oxygen ions in the electrolyte. These migrate to the outer electrode (exhaust gas; pO_2' variable $< pO_2''$), where the counterreaction occurs at the three-phase boundary (elec-

PETITIONER'S EXHIBIT 1002
US PATENT NO. 6,581,565

trolyte-platinum-gas). A counteractive electrical field is created, and an electrical voltage U_s corresponding to the partial-pressure ratio is generated in accordance with the Nernst equation:

$$U_s = \frac{RT}{4F} \ln \frac{pO_2''}{pO_2'} \tag{6.4}$$

where R = general gas constant
F = Faraday's constant
T = absolute temperature
pO_2 = partial pressure of oxygen

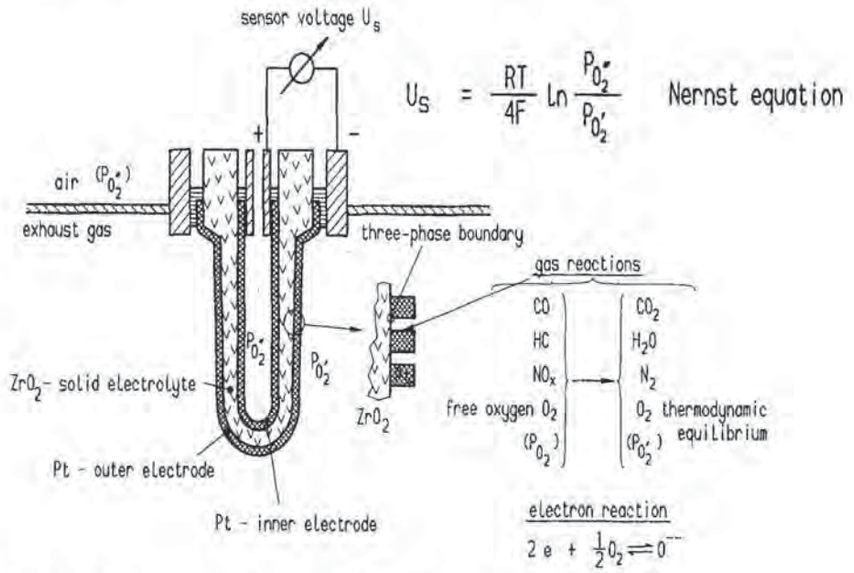


FIGURE 6.4 Diagram illustrating design and operation of a lambda = 1 sensor.

Catalytic Process. Measurements of oxygen content can only serve as the basis for unambiguous conclusions regarding the lambda of the exhaust gas when a state of thermodynamic gas equilibrium is established at the catalytically active electrodes on the oxygen sensor (residual oxygen). The absolute concentrations of the individual components in the engine's exhaust gases fluctuate across a wide range in accordance with the instantaneous operating conditions (warm-up, acceleration, steady-state operation, deceleration). The oxygen sensor must thus be capable of converting the gas mixture that it receives into a state of complete thermodynamic equilibrium. The resulting requirements are a high level of catalytic activity at the electrode and a protective layer capable of limiting the gas quantity. Should it prove impossible to achieve thermodynamic equilibrium at the electrode, the sensor's lambda signal will be erroneous.

Characteristic Curve. The concentration of residual oxygen fluctuates exponentially (by several orders of 10) in the vicinity of a stoichiometric air/fuel mixture (lambda = 1). In accordance with Eq. (6.4), this leads to massive variations in sensor voltage (lambda = 1 jump) with the characteristic lambda curve (Fig. 6.5).

Reference Atmosphere. Ambient air is the most commonly used O_2 reference. Alternatives include a metal-metal oxide mixture or a pumped reference medium. With this method, an O_2 reference pumping current is superimposed on the voltage measurement to generate an approximately constant O_2 partial pressure at the encapsulated reference electrode.

PETITIONER'S EXHIBIT 1002
US PATENT NO. 6,581,565

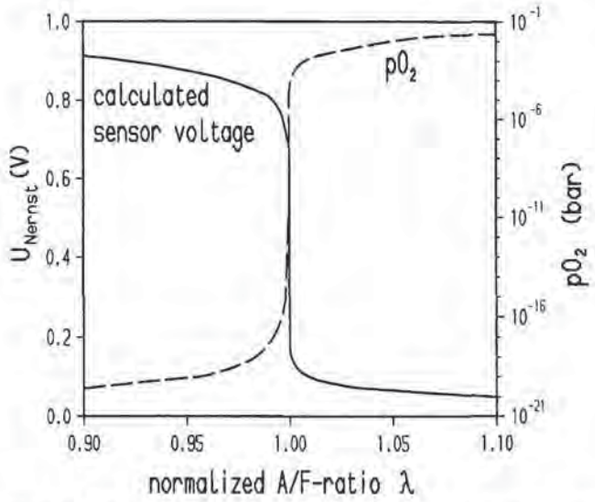


FIGURE 6.5 Equilibrium partial pressure of oxygen pO_2 and resulting curve for Nernst voltage at ≈ 700 °C relative to the normalized air-fuel ratio lambda.

6.2.2 Lambda = 1 Sensor: Semiconductor Type

Sensing Mechanism. Oxidic semiconductors such as TiO_2 and $SrTiO_3$ rapidly achieve equilibrium with the oxygen partial pressure in the surrounding gas phase at relatively low temperatures. Changes in the partial pressure of the adjacent oxygen produce variations in the oxygen vacancy concentration of the material (TiO_{2-x} respectively $SrTiO_{3-x}$), thereby modifying its volume conductivity.

$$R_T = A\ pO_2^n \exp\left(\frac{E}{kT}\right) \tag{6.5}$$

where R_T = semiconductor resistance
A = constant
E = activation energy
k = Boltzmann constant
T = absolute temperature
$n \approx 1/4$.

This effect, which is exploited to determine lambda, is also superposed by the conductivity's temperature dependence. Electrical resistance and sensor response times are both inversely proportional to temperature, as equilibrium is achieved more rapidly through diffusion in the oxygen vacancies.

Design. The ability to dispense with an O_2 reference allows an extremely simple design featuring an integrated heater. The porous semiconductor thick-film layer is generally positioned and sintered onto a planar Al_2O_3 substrate between two electrodes. Thin-film layers are also being developed as an alternative.

Characteristic Curve. At lambda = 1, the sensor layer displays an extreme change in conductivity due to the large pO_2 variation (see Sec. 6.2.1 and Fig. 6.5). When new, TiO_2 sensors provide essentially the same response as ZrO_2-based lambda = 1 probes. Variations in the rates of increase for lean and rich resistance and for response time occur over its lifetime, with the emission-control system undergoing a significant shift toward lean.

PETITIONER'S EXHIBIT 1002
US PATENT NO. 6,581,565

Principles of Operation. A voltage is applied to the TiO_2 resistor R_T and a serial reference resistor. The voltage drop at the serial resistor depends on R_T, respectively on lambda. In a three-pole version, the applied voltage is taken from the heater voltage; for the four-pole version (insulated ground) a separate supply is employed. Temperature compensation may be required, depending upon the specific application.

6.2.3 Lean A/F Sensor: Nernst Type

Sensing Mechanism. It is always possible to employ a potentiometric lambda = 1 sensor (Sec. 6.2.1) as a lean A/F sensor by using the flat part of the Nernst voltage curve (Sec. 6.4 and Fig. 6.5) to derive the values at lambda > 1. The diminutive characteristic sensor voltages in this lambda range (U_S < 65 mV at lambda > 1.05) mean that stringent requirements for consistency must be met. Minute voltage deviations of just a few mV are sufficient to produce substantial errors in lambda.

Design. For this reason, special sensors must be employed in applications in which quantitative determination of lambda > 1.05 is required. To this end, special electrode manufacturing techniques are used to enhance catalytic activity, while a power heater (18 W) is used in conjunction with a protection tube featuring a lower gas-flow rate to provide a more constant ceramic temperature.

Principles of Operation. A high-output input amplifier is required for measurement of the low voltage levels associated with lean exhaust gases. In vehicle testing, lambda control has proven effective when used together with a classical mixture regulator. Even alternating operation (lambda = 1 and lean) with a sensor in the same vehicle is possible. Depending upon accuracy requirements, lean operation is possible in a range extending to lambda ≈ 1.5.

Nonautomotive Applications. Lambda-controlled operation can be employed to maintain narrow tolerances and to limit drift in oil- and gas-fired units; the benefits include low fuel consumption, enhanced safety, and lower emissions. The use of sensors in stationary power plants—for instance, in central heating plants—is particularly interesting as a potential means of dealing with fluctuations in the calorific content of the fuel.

6.2.4 Lean A/F Sensor: Limiting-Current Type

Sensing Mechanism. An external electrical voltage is applied to two electrodes on a heated ZrO_2 electrolyte to pump O_2 ions from the cathode to the anode (electrochemical O_2 pumping cell) (Fig. 6.6*a*). When a diffusion barrier impedes the flow of O_2 molecules from the exhaust gas to the cathode, the result is current saturation beyond a certain pumping voltage threshold (limiting current condition). Because the resulting limiting current I_l is roughly proportional to the exhaust gas' oxygen concentration c_{O2}

$$I_l = 4FD \frac{Q}{L} c_{O2} \tag{6.6}$$

where F = Faraday's constant
D = diffusion coefficient
Q = effective diffusion cross section
L = effective diffusion length

Design. Figure 6.6*b* provides a schematic illustration of this sensor type featuring planar technology and an integrated electric heater element.

PETITIONER'S EXHIBIT 1002
US PATENT NO. 6,581,565

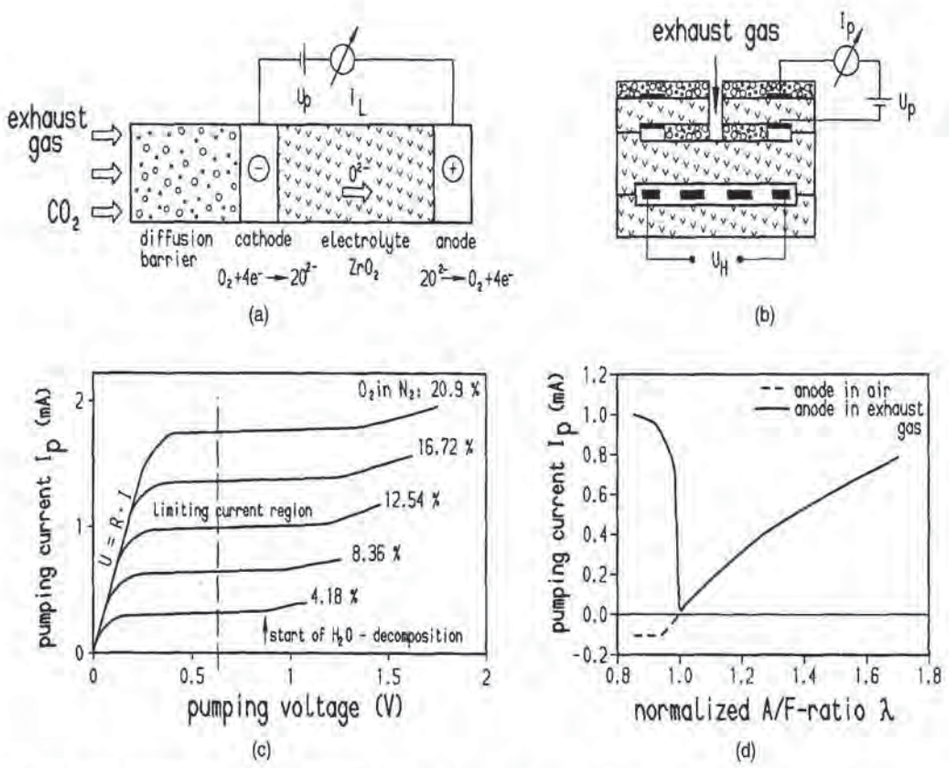


FIGURE 6.6 Limiting current sensor: (*a*) principle of operation; (*b*) schematic diagram; (*c*) current/voltage characteristics; (*d*) response curve as function of lambda.

Characteristic Curve. Figure 6.6c shows the current-voltage pattern for a limiting current sensor at various O_2 concentrations. If, at a constant pumping voltage, the pumping current is entered above lambda instead of c_{O2}, the resulting curve will correspond to Fig. 6.6*d*. In lean exhaust gas, the signal drops in response to reductions in lambda as indicated in Eq. (6.7), but below lambda = 1 there is a radical surge. This response pattern is at variance with the basic theory, and can be explained as the result of decomposition effects at the cathode. As a result, this sensor is only suitable for use in lean gases. Depending upon the design of the diffusion barrier (pore radius to free path length for the gas molecules, according to the proportion of gas phases to Knudsen diffusion), various relationships are observed between pumping current (measurement signal) and exhaust pressure and sensor temperature.

Principles of Operation. Depending on the accuracy requirements, a stable operating temperature in the range 600 to 800 °C is needed. Pumping voltages must always be selected to satisfy the conditions for limiting current. In addition, this limiting current has to be calibrated due to the manufacture scattering of the diffusion gap.

6.2.5 Wide-Range A/F Sensor: Single-Cell

Design and Operation. When the anode of a limiting current sensor of the type described in Sec. 6.2.4 is exposed to reference air instead of to the exhaust gas, the total voltage U_S at the probe will be the sum of the effective pumping voltage U_P and a superimposed Nernst voltage U_N.

$$U_S = U_P + U_N \tag{6.7}$$

PETITIONER'S EXHIBIT 1002
US PATENT NO. 6,581,565

In operation, holding U_S to, as an example, 500 mV will produce a positive pumping voltage in lean exhaust gases ($U_N < 500$ mV); the diffusion limits the rate at which O_2 is pumped from the cathode to the anode. At lambda = 1 ($U_N \approx 500$ mV), the pumping voltage and, with it, the pumping current drop toward zero. In rich exhaust gas ($U_N > 500$ mV), the effective pumping voltage U_P becomes negative, causing oxygen to be pumped from the reference air electrode to the exhaust gas electrode ($I_P < 0$), where it reacts with the rich gas components CO, H_2, and HC.

Characteristic Curve. The pumping current displays a uniform upward trend between mildly rich and extremely lean lambda values (Fig. 6.6*d*).

Applications. This type of sensor is in series production as a thimble-type design for lean-mix concepts. In this application, operation as a limiting current sensor is restricted to lean conditions; during operation at lambda = 1, the pumping voltage is switched off and the Nernst voltage serves as the control signal.

6.2.6 Wide-Range A/F Sensor: Dual-Cell

Design. Skillful combination of a limiting-current sensor with a Nernst concentration cell on a single substrate will produce a dual-cell wide-range A/F sensor. The pumping and concentration cells are made of ZrO_2. Each cell is coated with two porous platinum electrodes, and they

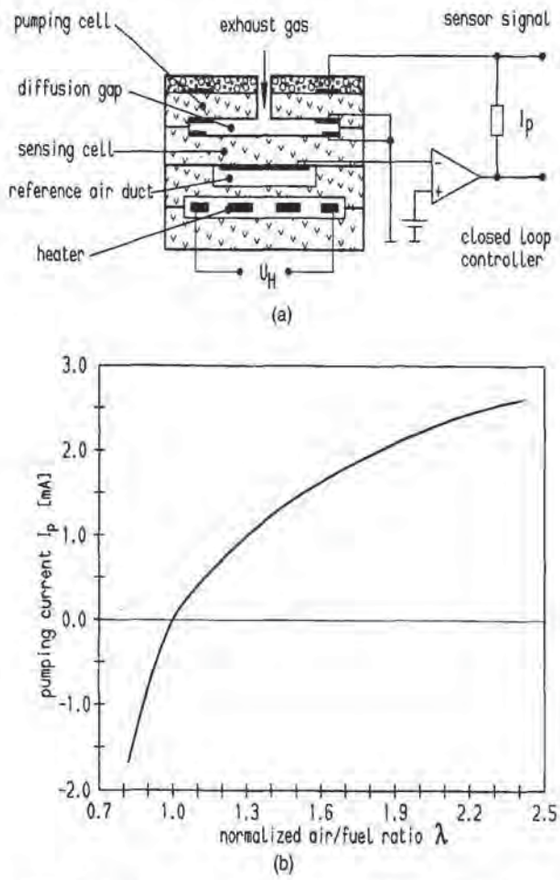


FIGURE 6.7 Dual-cell wide-range A-F sensor: (*a*) schematic diagram; (*b*) response curve as function of lambda ($T_{gas} \approx 400$ °C, $P_H \approx 12$ W).

PETITIONER'S EXHIBIT 1002
US PATENT NO. 6,581,565

are arranged with a measurement gap of approximately 10 to 50 μm in height between them. A gas-intake opening in the solid electrolyte connects this measurement gap to the exhaust gas while the gap is serving as a diffusion barrier to control limiting current (Fig. 6.7).

Operation Mode. An electronic circuit regulates the current applied to the pumping cell to maintain a constant gas composition (for instance, lambda = 1) in the measurement gap. This corresponds to a Nernst-cell voltage of $U_N \approx 450$ mV. If the exhaust gas is lean, the pumping cell drives the oxygen outward from the measurement gap. If the exhaust gas is rich, the flow direction is reversed and oxygen from the surrounding exhaust gas (e.g., from decomposition of CO_2 and H_2O) is pumped into the measurement gap.

Characteristic Curve. The pumping current is proportional to the oxygen concentration (or oxygen requirement). With the attendant electronic control circuitry, an unambiguous, linear signal increase over a wide lambda range of 0.7 < lambda < infinite (air) can be obtained if the current is calibrated due to the manufacture scattering (Fig. 6.7). The integrated heating element provides an operating temperature in excess of 600 °C.

6.3 TECHNOLOGY OF CERAMIC EXHAUST GAS SENSORS

6.3.1 ZrO_2-based Sensors

The zirconium dioxide used to manufacture oxygen sensors is not pure; instead, the solid electrolyte consists of a mixed oxide, ZrO_2/Y_2O_3. The Y_2O_3 concentration used for actual applications lies in the 4 to 5 mol% range. This level is commensurate with optimum sensor operation in the important properties of ion conductivity, thermal stability, and mechanical strength.

Ion Conductivity. The substitution of trivalent yttrium ions for quadrivalent zirconium ions leads to the formation of oxygen vacancies through which the oxygen ions can move. Initially, the increases in ion conductivity are roughly proportional to the rise in Y_2O_3 content, as they are accompanied by a simultaneous rise in the number of oxygen vacancies. This pattern is observed with yttrium as well as with other bi- and trivalent alkaline earth metals, at least until a certain level of defect concentration is reached. Beyond this limit, the mutual influence of the vacancies reaches such levels that any further increases in defect concentration are accompanied by reductions in ion conductivity. The maximum is obtained at approximately 9 to 10 mol% Y_2O_3.

Phase Composition and Mechanical Stability. At room temperature, zirconium dioxide is monocline. It becomes tetragonal (metastable) above 1200 °C, and assumes a cubic form beyond 2370 °C. Yttrium doping can be employed to partially or completely stabilize the tetragonal and cubic modification, even at room temperature (PSZ—partially stabilized zirconium; FSZ—fully stabilized zirconium, above approximately 10 mol%, with certain manufacturing processes 7 to 8 mol% Y_2O_3). ZrO_2, with an essentially monocline structure, does not display sufficient resistance to temperature fluctuations for application in automotive exhaust systems—the changes in the geometry of the individual crystallites which accompany the phase transition lead to fatigue symptoms in the ceramic material. At the same time, the cubic phase does not possess the physical strength required to resist the physical shocks and thermal stresses. However, good mechanical characteristics can be obtained by using partially stabilized ceramic materials, with maximum strength being achieved within the range of 2 to 4 mol% Y_2O_3.

Manufacture of Partially Stabilized ZrO_2 Ceramics. The most common procedure consists of mixing and grinding the ZrO_2 and Y_2O_3 together (mixed oxide). The differences in the

PETITIONER'S EXHIBIT 1002
US PATENT NO. 6,581,565

length of the diffusion paths—the two oxides are located adjacently as separate powder particles—do not generally produce a completely homogeneous distribution of yttrium in the ZrO_2. Thus, both fully stabilized cubic crystallites and tetragonal crystallites can be formed during the sintering process. During the phase transition to monocline ZrO_2 that takes place during cooling, the latter provoke internal tension, causing the ceramic material to harden. Certain combinations of yttrium concentration and manufacturing techniques can be employed to obtain exclusively tetragonal crystallites, which remain stable even after cooling (TSZ—tetragonal stabilized zirconia). Due to the absence of a phase transition within the temperature range associated with the intended application, stabilized tetragonal zirconium dioxide displays a virtually constant coefficient of thermal expansion. Both of the partially stabilized ZrO_2 ceramics described here are used in the manufacture of oxygen sensors.

6.3.2 Thimble-Type Sensors

Shaping. The ceramic base (Fig. 6.4) is shaped in the usual manner with dry pressing of granulated ZrO_2 and subsequent grinding of the compact material.

Electrodes. The application of the gas-permeable platinum electrodes is one of the most critical processes in the manufacture of oxygen sensors. A basic distinction is made between two different procedures:

Thin-Film Process. In this process, a thin microporous platinum layer (electrode thickness < 1 μm) is applied to the previously sintered base using one of three methods: thermal evaporation, sputtering, or chemical deposition with subsequent thermal treatment.

Thick-Film Process. In this process, a (for example) platinum-cermet layer (mixture of noble metal and ceramic phase) is printed onto the unsintered base (electrode thickness 5 to 10 μm).

As far as actual operation is concerned, the salient difference between the two processes resides in the fact that the three-phase boundary required for the conversion of oxygen (common border of platinum, zirconia, and gas phase) remains restricted to the surface of the base when thin-film electrodes are used. In contrast, the use of thick-film cermet electrodes with a ceramic phase of ZrO_2 results in a substantially larger border area along with enhanced high-temperature adhesion.

Protective Layer. As the outer electrode is exposed to the exhaust gases, a suitable protective layer, combining the requisite porosity with optimal adhesive properties, is essential to ensure the long-term stability of the oxygen sensor. In the conventional plasma or flame-spraying process, a porous layer 50 to 300 μm in thickness (e.g., magnesium spinel) is applied to the sintered and electrodes-equipped base. A cofiring technique with ZrO_2-based protective layers or a combination of both processes is being employed in the production of a new generation of oxygen sensors with enhanced long-term stability.

Well-defined porosity levels must be maintained to ensure satisfactory operation. With cofired protective layers, the required porosity level can be obtained by using organic pore-forming substances, which are burned out during sintering, or by adding a second, sinter-inactive ceramic phase, such as Al_2O_3. Porous protective layers also provide a diffusion barrier for the exhaust-gas molecules before they reach the electrodes. These layers thus exercise a determining influence on the sensor's control characteristics because the components of the exhaust gas which exhibit various diffusion coefficients are not in a state of thermodynamic equilibrium (see Sec. 6.4). This effect can be partially neutralized through defined pigmentation in the protective layers, which not only display catalytic characteristics, but can also inhibit contamination.

6.3.3 Planar Oxygen Sensors

The planar oxygen sensor derives its designation from the fact that, as opposed to the thimble-type sensor, its design arranges all operating layers in plain, consecutive surfaces. The

PETITIONER'S EXHIBIT 1002
US PATENT NO. 6,581,565

technology applied in their manufacture is quite similar to the multilayer technology employed to produce ceramic multilayer capacitors and high-density electronic circuit boards (e.g., MCM—multichip modules).

Manufacture of Ceramic Green Sheet. First, an organic binder phase is added to the ZrO_2 powder in a tape-casting process to produce ceramic substrate layers.

Printing on the Ceramic Green Sheet. A screen-printing process (thick-film process) is employed to attach the individual function groups, e.g., galvanic cell, pumping cell, reference-air duct and heater (see also Sec. 6.2) to the green tape in the desired layer sequence. Several printed layers are generally required for each side of the tape; these layers can also consist of various inorganic materials.

Lamination. A number of screen-printed substrates can be stacked and laminated (bonded in a process combining temperature and pressure) to form composite structures representing virtually any desired level of complexity. A simplified version of a lambda = 1 sensor in planar technology is illustrated in Fig. 6.8.

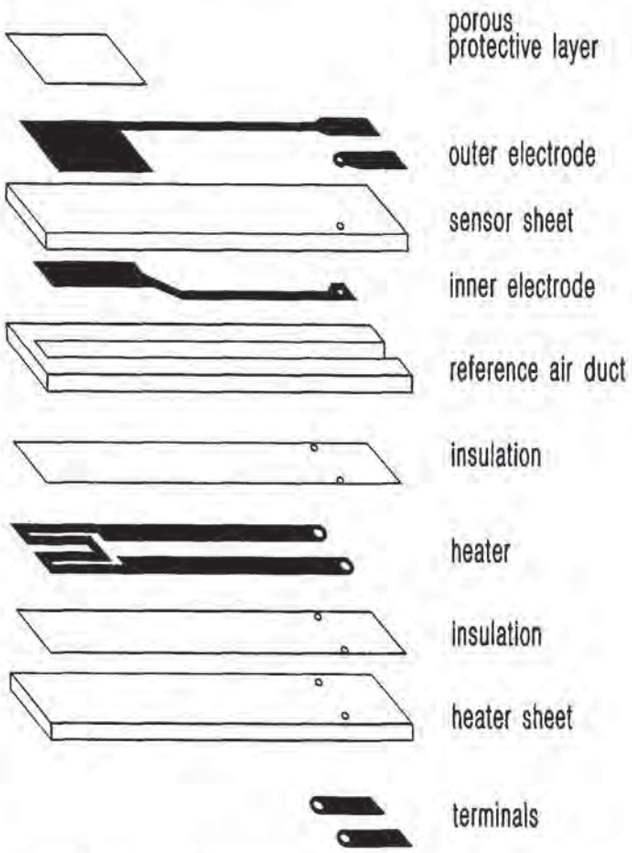


FIGURE 6.8 Layer structure of planar lambda = 1 sensor.

Advantages of Planar Technology. The application of surface-design technology also provides an additional advantage by making it possible to combine a number of individual elements on a single substrate for subsequent separation (multiple application) and sintering to form monolithic sensors with integrated heating elements. The coefficients of thermal expan-

PETITIONER'S EXHIBIT 1002
US PATENT NO. 6,581,565

sion of the ZrO_2, cermet, and insulation layers must be precisely matched to ensure that the resulting ceramic elements display adequate thermal and mechanical stability.

Sensor elements manufactured with this new technology offer a number of advantages: the integration of heater and sensor provides a single unit with a lower total thermal mass, allowing substantial reductions in the continuous heating requirement (30 to 40 percent of that required with a thimble-type sensor), shorter delay between activation and readiness for active control, and smaller sensor dimensions. These characteristics make the unit ideal for meeting the demands of the modern motor vehicle (reductions in energy requirements, weight and space savings, and more stringent emission requirements). In addition, planar technology is an essential factor in obtaining complicated operating abilities such as those found in the dual-cell wide-range A/F sensor (see Sec. 6.2.6).

6.3.4 Al_2O_3-based Sensors

Sensors for oxygen and other exhaust gases which employ variations in the conductivity of the sensor material (TiO_2, SnO_2, etc.) to detect changes in the gas concentration are usually designed as planar sensors. The preferred substrate material is Al_2O_3. As the combinations of functions (e.g., heater, electrodes, etc.) are essentially those required with planar ZrO_2 sensors, the manufacturing techniques are also quite similar. Al_2O_3 provides advantages in the form of lower material costs and a simplified internal structure, made possible by the fact that Al_2O_3 maintains its good insulation properties at high temperatures. A disadvantage, particularly in terms of long-term stability, is the difficulty with sintering and sensor-material adhesion, as cofiring technology cannot be employed for this procedure.

6.3.5 Construction

Figure 6.9 shows completely assembled a heated thimble sensor and a planar lambda sensor. Although similar in external appearance—the planar sensor is somewhat shorter and narrower—the two units differ substantially in their respective internal structures. The differences are largely a result of the fact that heater and sensor in the heated thimble-type sensor are two separate components requiring assembly and electrical contact. Various ceramic support components are incorporated to enhance structural integrity and to ensure an impermeable seal between the reference air and the exhaust gases while also providing a degree of impact protection for the sensor unit. On the exhaust-gas side, the sensor elements receive both physical and thermal protection from a protection tube. Due to its basic design configuration, the planar sensor element does not share the rotational symmetry of its thimble-type counterpart. Thus, it must be installed in a specific position; the protection tube features a partial double wall to facilitate orientation. The offset inlet openings provide a uniform flow of exhaust gases past the measurement electrode, regardless of its position relative to the exhaust-gas stream. Thermal insulation from the exhaust gases is also improved.

Although unheated thimble-type sensors are still on the market, they are becoming less important due to the increasing demands for precision of emission control systems.

6.4 FACTORS AFFECTING THE CONTROL CHARACTERISTICS OF LAMBDA = 1 SENSORS

6.4.1 Factors Affecting the Static Curve

Due to the porous protective layer around the electrode, the steep voltage change in the sensor's characteristic curve does not occur at precisely lambda = 1; instead, it is displaced a small

PETITIONER'S EXHIBIT 1002
US PATENT NO. 6,581,565

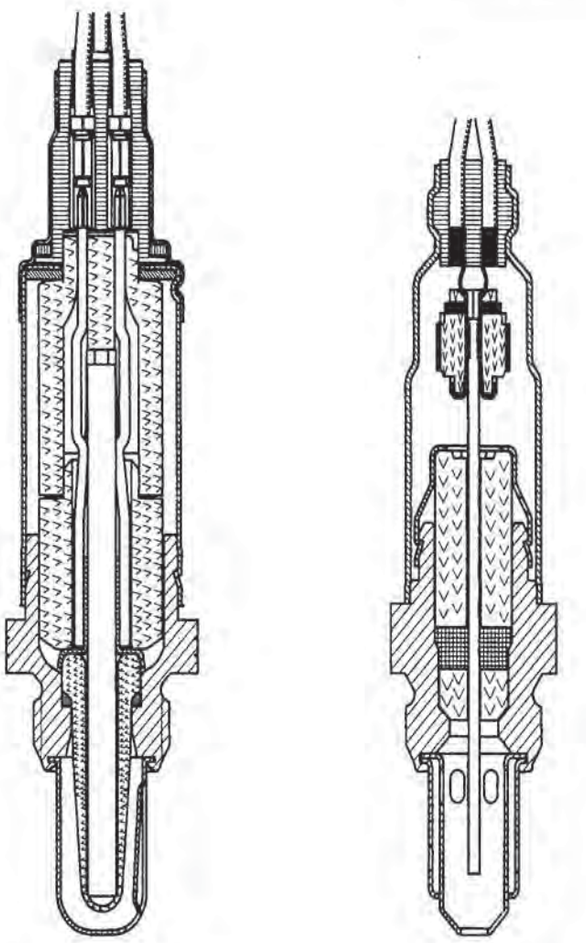


FIGURE 6.9 Construction of thimble-type and planar-type oxygen sensors.

amount into the lean range. The lower the porosity of the protective layer, the greater the diffusion of H_2 relative to O_2 toward the electrode. This phenomenon induces changes in the lambda value at the electrode relative to the lambda of the exhaust gas, the electrode detects richer exhaust gas and the lambda characteristic curve is displaced into the lean range.

Lean Shift. The lean shift is caused by exhaust-gas residue, such as oil ash and SiO_2, which partially plug the pores of the protective layer, and by reductions in sensor temperature.

Rich Shift. Fractures and flake-off of the protective layer lead to reductions in response times and shift the static characteristic curve toward rich. Electrode deactivation, especially due to lead contamination, will produce a flatter static response curve, as free, unconverted oxygen will also be detected. This effect also displaces the switchpoint threshold toward a lower lambda. A similar effect occurs when the reference atmosphere is contaminated (Chemical Shift Down, or CSD), for instance, with exhaust gases or water. Figure 6.10 shows typical characteristic curves for these conditions.

PETITIONER'S EXHIBIT 1002
US PATENT NO. 6,581,565

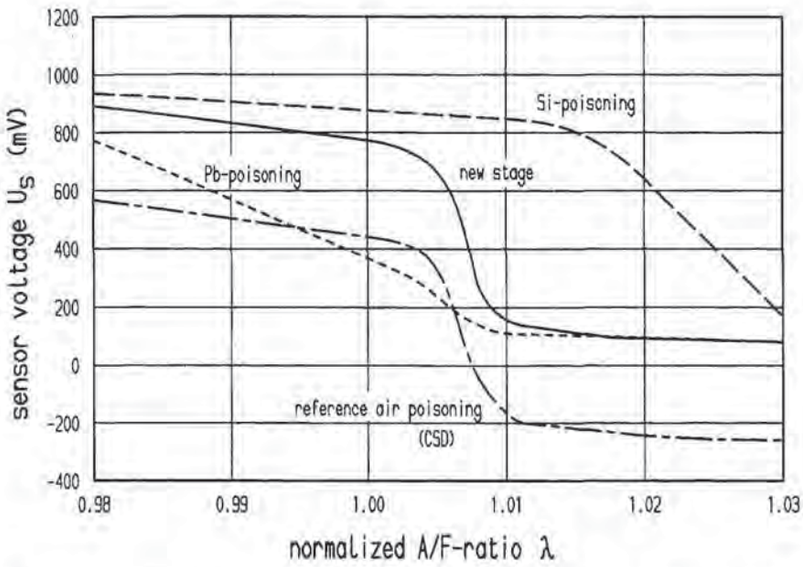


FIGURE 6.10 Effects of contamination on the static response curve of a lambda = 1 sensor as measured at laboratory test stand at $T_{gas} \approx 350$ °C.

6.4.2 Factors Affecting Sensor Dynamics and Control State

Factors. The control state (adjusted lambda) depends upon a number of factors. These include static sensor characteristics, sensor dynamics and asymmetry in sensor response times (switching times), t_{rs} (rich to switchpoint) during the surge from rich to lean, and t_{ls} (lean to switchpoint) during the jump from lean to rich. The sensor switching times t_{rs} and t_{ls} are strongly influenced by the configuration of the protection tube, the protective layer, and the sensor's temperature. Without the protection tube, switching times of less than 10 ms have been measured for ZrO_2 sensors with $T_{ceramic} \approx 900$ °C. However, such rapid response times are neither necessary nor desirable with many of the systems presently in use.

Response Times. An increase in response time that is not accompanied by a variation in the differential between t_{rs} and t_{ls} results in worse emissions with a constant control state due to the fact that the control amplitude increases while the conversion rate of the catalytic converter is reduced (see sec. 6.1.4 and Fig. 6.2).

Asymmetry. An asymmetrical increase in the response times t_{rs} and t_{ls} will also affect the control state due to the lambda shift.

Lean Shift. A pronounced increase in t_{rs} leads to a displacement toward lean. This can occur for any of several reasons. The dwell time in the rich exhaust gas is determined by control frequency and amplitude, and affects t_{rs} through the adsorption of CO and HC. Should the protective layer be obstructed (for instance, by oil ash), or should the sensor temperature drop, t_{rs} will generally rise more than t_{ls}.

Rich Shift. In contrast, a more pronounced rise in t_{ls} will lead to a displacement toward the rich range. The conversion rate of the electrode and the protective layer exercise a major influence on t_{ls}. Lead deposits diminish catalytic activity, causing t_{ls} to rise without exercising any substantive effect on t_{rs}.

Temperature. As a general rule, the susceptibility to sensor contamination is inversely proportional to electrode temperature. The factors determining the temperature of the ceramic material are the heater, the gas temperature, the gas flow rate (rpm, load), and the protection

PETITIONER'S EXHIBIT 1002
US PATENT NO. 6,581,565

tube. Depending upon the installation location, the ceramic temperature generally lies between 350 and 1000 °C for exhaust temperatures ranging between 150 and 900 °C. The flow velocity of the gas varies between 2 m/s at idle, 40 m/s at moderate rpm and load, and up to 80 m/s under full load. The influence exercised by gas temperature and the protection tube can be seen in Fig. 6.11. The ceramic temperature has a major effect on the controlled lambda. A protection tube providing a lower gas flow (see Fig. 6.11: 1 hole/4 flaps) and a higher heater

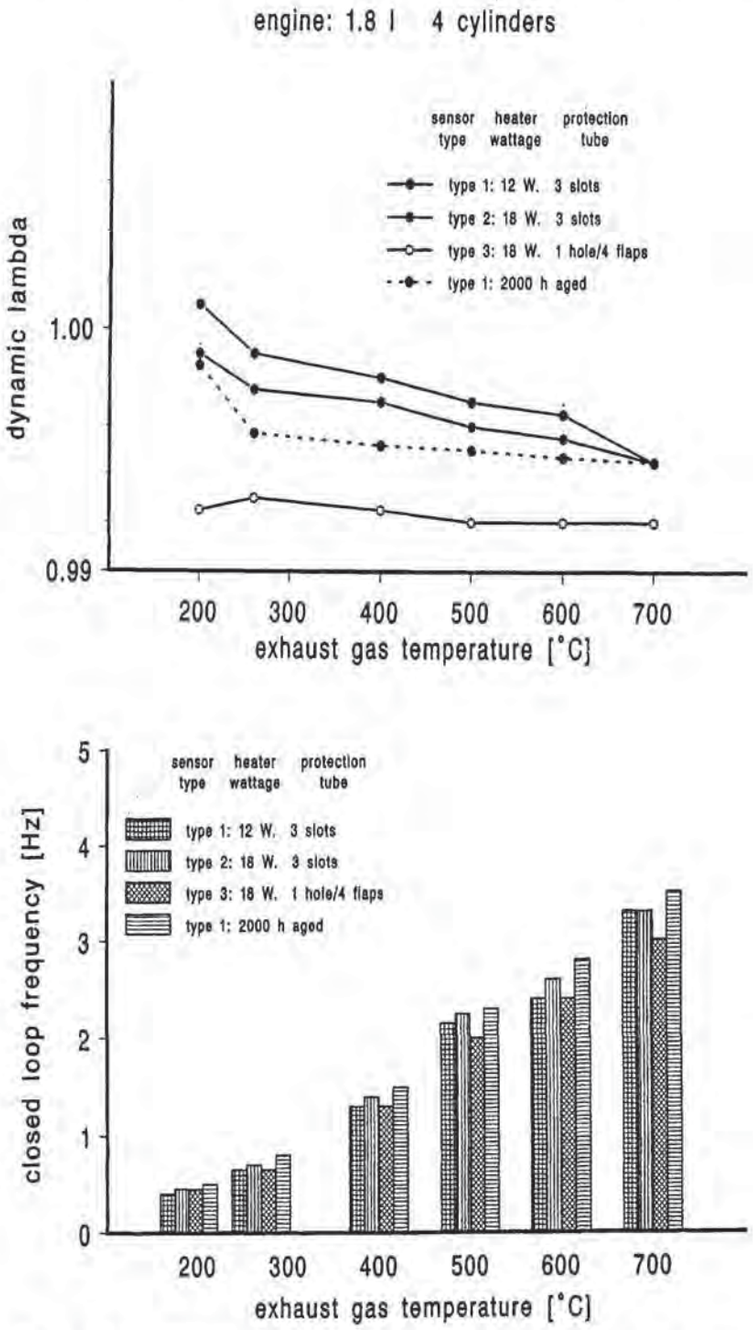


FIGURE 6.11 Effects of exhaust-gas temperature (rpm) on dynamic lambda and control frequency.

PETITIONER'S EXHIBIT 1002
US PATENT NO. 6,581,565

power (18 W) will lead to higher ceramic temperatures with enhanced temperature consistency relative to exhaust temperature. This measure is employed to obtain a more stable controlled lambda. The lambda value displays a moderate rich shift compared to that obtained with a more open tube (see Fig. 6.11: 3 slots) and 12 W heater power.

System Lag. System lag is dependent on the sensor's installation position (0.2 to 2 m downstream from the exhaust manifold, with approx. 1 meter downstream from the exhaust valve being typical) and the gas velocity as determined by load, rpm, and the exhaust pipe diameter. It can be up to 500 ms at idle, and drops down to delays as low as 20 ms at full load. The sensor (protection tube, heater power) is of secondary significance (Fig. 6.11). The influence of sensor response times (t_{ts}, t_{ls}) on the control state increases as a function of their share of the total system lag.

tv Shift. The cumulative effect of all extraneous influences is a slight lean control state of the lambda = 1 sensor. Electronic compensation for the lean shift is available in the form of an asymmetrical control-oscillation pattern (see Sec. 6.1.4). This is provided either by means of a switching delay after the sensor surge (tv shift, Fig. 6.3), through variations in the controller's surge amplitude, and/or via asymmetrical ramp slope. Those parameters for the electronic lambda displacement which vary according to load and rpm can be stored as a program map in the electronic control unit (ECU). This method can be employed for lambda corrections up to $|\Delta\lambda| \leq 0.015$.

6.5 APPLICATIONS

6.5.1 Operating Conditions

Environmental Factors. Table 6.3 provides a summary of the types and magnitudes of the major stress factors affecting the sensor. Beyond the actual function of the sensor itself, optimal selection and precise mixture of all applied materials (ceramics, metals, synthetics) are essential factors in obtaining the thermal, mechanical, and chemical characteristics needed to achieve the obligatory extended service life of over 100,000 miles.

Sensor Installation Location. Because it is of determining significance for both external influences and control function, correct sensor location is a critical factor in calibrating the performance of the total lambda-control system. The sensor must be far enough from the exhaust valves to ensure that it monitors representative exhaust gases for all cylinders, but near enough to hold system lag to acceptable levels. Both factors affect emissions.

Thermal Stress. Thermal stresses at the sensor stem from the high-potential exhaust-gas temperatures as well as from the temperature gradients that occur. Exhaust temperature is essentially a function of engine speed, and can reach a maximum of 1000 °C at the sensor on high-performance engines. The most extreme temperature gradients at the sensor occur during hard driving directly in the wake of a warm start at which the exhaust system and the sensor have already cooled off. These conditions can produce exhaust-gas temperature gradients of up to 500 K/s.

Thermal Shock. In the warm-up phase following a cold start, condensation on the pipe walls can cause the ceramic material to crack once the electric heater warms it beyond the critical temperature of approximately 300 °C. Accumulations of condensation can be largely avoided by locating the sensor as close as possible to the engine to provide rapid heating of the upstream exhaust pipe. Depending upon the specific vehicle, a time delay for switching on the sensor heater may be required.

PETITIONER'S EXHIBIT 1002
US PATENT NO. 6,581,565

TABLE 6.3 Overview of Stress Factors for Exhaust Gas Sensors

Mechanical stress	Stress caused by environmental conditions	Thermal stress	Stress caused by exposition to exhaust gas
Vibrational stress (<1300 m/s²) by engine vibration (<5 kHz) by pulsation of the exhaust gas (< ±300 mbar) by ambient wind (cable, <10 Hz)	Splash water, gush of water (in case containing NaCl, $CaCl_2$, $MgCl_2$)	Exhaust gas temperature (150 °C ... 1000 °C)	Exhaust gas composition ch between lambda = 0.85 (fuel load enrichment) and lambda infinite (overrun fuel)
Stone impact (<1.5 Nm)	Dust (organic, inorganic origin)	Exhaust gas temperature gradients at cold start (<500 K/s) at overrun fuel cutoff (<200 K/s)	Catalyst poisoning from fuel additives: permissible lead content: <0.013 g/l sulfur content: <0.1 % Br-, Cl-compounds
Installation/removal (torque about 50 Nm when assembled)	Oil, dirt undercarriage protection	Temperature increase after engine stalling (<300 °C at cable outlet)	Oil ash (Ca-, P-, S-, Zn-compounds up to 1 kg within ~60000)
Wire pull test (>70 N)	Fluctuation of the electrical supply system (9 ... 15 V)	Radiant heat (may require corresponding protective measures)	Miscellaneous corrosion products (e.g., Fe-oxides)
Handling (shock load up to 1000 g)	EMC (<200 V/m)		Condensation water
	Variation of climatic conditions (–40 °C ... +50 °C, 10 ... 100% rel. humidity)		

Mechanical Stresses. The main sources of mechanical stress on the sensor are vibration, exhaust-gas pulsation, stone impact, and cable tension (Table 6.3).

Sealing. The cable outlet of the sensor must be sealed to prevent water splash from penetrating to its interior and distorting the reference air (see Sec. 6.4.1 and Fig. 6.10). At the same time, the sealing element must be flexible enough to absorb the accelerative forces associated with vibration as well as any tensile forces transmitted through the cable.

6.5.2 Emission Certification

It would be impossible for a vehicle equipped only with an unregulated catalytic converter and lacking an oxygen sensor to achieve compliance with the American emission standards. When a regulated catalytic converter is used together with an oxygen sensor, emissions remain well below the limits. Even after vehicle mileage corresponding to more than 100,000 miles, the sensor limits emission increases to a minimum (Fig. 6.12). The introduction of a new system must be accompanied by precise calibration of the engine-control system to match the production tolerances and aging characteristics which affect the sensor's control response. The considerable effects that temperature and aging exercise on the catalytic converter must also be considered.

Durability Tests

Life Cycle. To determine aging behavior, the sensors undergo a standard durability test in the exhaust-gas stream of a test engine. The test cycle is designed to simulate combined urban and rural operation, and has been adopted by many automobile manufacturers as a standard program. The mean average speed is approximately 100 km/h for a midrange car. All newly developed products must withstand 2000 h (more than 100,000 miles) operation in this program without failure.

Hot Durability Testing. In a substantially more demanding test, essentially consisting of simulated full-load operation, the sensors must survive at least 1000 h (roughly 100,000 miles). The main stress factors for the sensors in these tests are thermal exposure (exhaust-gas temperatures reaching 950 °C, housing temperatures up to 650 °C), exhaust gas loads, and vibration.

PETITIONER'S EXHIBIT 1002
US PATENT NO. 6,581,565

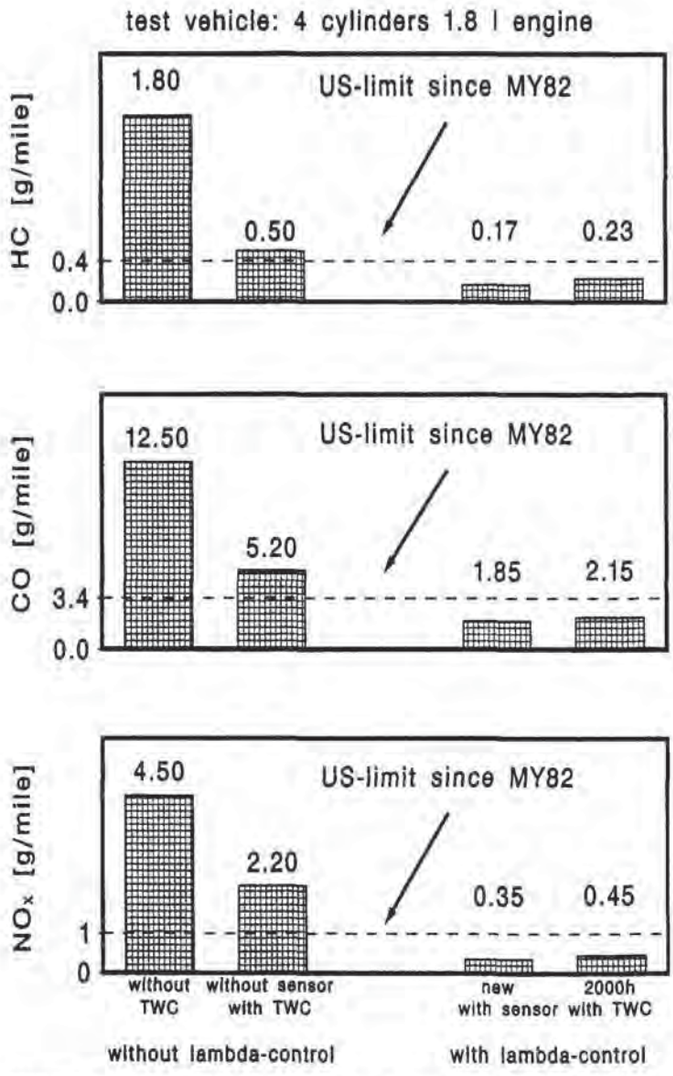


FIGURE 6.12 Comparison of emissions levels without catalytic converter, with unregulated converter, with controlled converter (new and old sensors, converter approx. 10,000 km).

Durability Testing of Contamination Resistance. Short durability tests featuring higher levels of Pb, Si, and oil are employed to determine the sensor's resistance to contamination damage.

6.6 SENSOR PRINCIPLES FOR OTHER EXHAUST GAS COMPONENTS

Sensors capable of monitoring the levels of the regulated toxic exhaust substances—CO, NO_x, and HC—would be desirable as elements of the On-Board Diagnosis systems (OBD I and OBD II) specified by the California Air Resources Board. Due to the extreme operating con-

PETITIONER'S EXHIBIT 1002
US PATENT NO. 6,581,565

ditions, only a few of the many tested configurations have a chance to be used in engine-exhaust gas.

6.6.1 Mixed-Potential Sensors

Sensing Mechanism. If reduced catalytic activity prevents gas equilibrium from being achieved at the electrode of a galvanic ZrO_2 cell, competing reactions can occur. These, in turn, prevent a state of reduction/oxidation equilibrium in the oxygen, and lead to the formation of a mixed potential. This potential is determined by electrode activity, temperature, and gas composition. It is difficult to design manufacturing techniques that can consistently produce electrodes capable of maintaining specific, defined rates of catalytic activity over extended periods of time. Every change in electrode activity (for instance, due to aging) leads to a variation in mixed potential. Pt electrodes give rise to a mixed potential at very low temperatures, with extended response delays relative to lambda sensors. Other electrode materials with lower rates of catalytic activity continue to provide a mixed potential at higher temperatures, making it possible to achieve response times < 1 s.

Selectivity. Careful selection of electrode materials, operating temperature, and selective precatalyzation layers offers opportunities for improving selectivity.

Operation Mode. Because the effect is temperature-sensitive, a constant sensor temperature must be regulated in the range of 300 to 600 °C, depending upon the individual application.

6.6.2 Semiconductor Gas Sensors

Sensing Mechanism

Ceramic and Thick-Film Layers. On the surface of nonstoichiometric metal oxides such as SnO_2, TiO_2, In_2O_3, and Fe_2O_3 (*n*-type semiconductors), oxygen is absorbed and dissociated in air at high temperatures and is bonded to the crystal lattice. This leads to the formation of a thin depletion layer at the crystallite surface with a resultant arch in the potential curve. This phenomenon produces reductions in surface conductivity and higher intercrystalline resistance at the boundaries between two crystallites; this is the major factor determining the total resistance of the polycrystalline metal oxide. Oxidation gases such as CO, H_2, and C_xH_y, which react with surface oxygen, increase the density of charge carriers in the boundary layer and reduce the potential barrier. Reduction gases, such as NO_x and SO_x raise the potential barrier and, with it, the surface/intercrystalline resistance.

Thin-Film Layers. Compared to porous polycrystalline materials, thin-film layers display only limited numbers of crystalline boundaries at the layer surface for reaction with the exhaust gases. The depletion-layer barrier makes up a substantial proportion of the layer thickness on thin-film devices, meaning that changes in charge-carrier density within the barrier layer due to adsorbed gases will also result in substantial variations in the total resistance.

Selectivity. Selected doping materials and temperatures can be employed to achieve selectivity for CO, HC, or NO_x. The resistance of metal-oxide semiconductors is always a function of the partial pressure of the O_2.

Specific Influences of Exhaust Gas. Engine exhaust gas with minimal, highly variable O_2 partial pressures is characterized by a high level of O_2 cross-axis sensitivity. Within the lambda = 1 to lambda < 1 operating range, an irreversible long-term change in sensor resistance leading to disintegration of the metal oxide is also possible. High operating temperatures are conducive to the diffusion of oxygen vacancies and doping materials. When amplified by sintering effects, these lead to resistance drift and attenuated sensor response.

PETITIONER'S EXHIBIT 1002
US PATENT NO. 6,581,565

Standard operating temperatures for metal-oxide gas sensors range from 100 to 500 °C, with up to 600 °C being seen in some restricted applications. With SnO_2, a high level of selectivity for, for example, CO can be achieved at temperatures as low as the 100 to 200 °C range. However, the response times can be measured in minutes. At higher temperatures, in the 300 to 550 °C range, response times of less than 1 s can be obtained, but with reduced selectivity.

6.6.3 Catalytic Gas Sensors

Sensing Mechanism. The catalytic gas sensor is essentially a temperature sensor featuring a catalytically active surface. An exothermic reaction (basically an oxidation reaction in air) at the catalytically active surface causes the temperature of the sensor to rise. The increase in temperature is proportional to the concentration of an oxidation gas in an excess-oxygen atmosphere. A temperature sensor of the same basic design—but without the catalytic response—is employed to enhance sensitivity and to provide temperature compensation by means of differential-signal evaluation. Materials employed for the temperature sensor include coiled Pt wire, Pt thin-film and thick-film layers, transistors, and NTC and PTC thermistors.

Operating Conditions. Catalytic gas sensors are relatively insensitive and can be employed in a range >1000 ppm. Excess oxygen is required to monitor concentrations. Due to the sensitivity to flow rate, these units are generally operated in flowheads with diffusion limiters. Measurement and reference sensors must be exposed to the same flow conditions, with no mutual thermal influences. Symmetrical configurations in pellet form are thus preferred over planar shapes. Operating temperatures for commercial sensors are in the 500 to 600 °C range, but extension to higher temperatures is possible. The requirement for long-term stability in the catalytic converter is the limiting factor governing the operating temperature. Catalytic gas sensors are not selective, instead providing a summing signal for all combustion gases. Thus catalytic sensors for application in exhaust gases are restricted to monitoring the state of the catalytic converter.

BIBLIOGRAPHY

Arndt, J., "Ceramics and Oxides," in W. Göpel, J. Hesse, and J. N. Zemel (eds.), *Sensors—Fundamentals and General Aspects,* vol. 1, S.252 ff, VCH Verlagsgesellschaft, Weinheim, 1989.

Barnes, G. J., R. L. Klimisch, and B. B. Krieger, "Equilibrium Considerations in Catalytic Emission Control," SAE Paper 730200, *SAE National Automobile Engineering Meeting,* Detroit, Jan. 1973.

Bosch, *Automotive Electric/Electronic Systems,* VDI, Düsseldorf, May 1987.

Bosch, *Automotive Handbook,* VDI-Verlag, Düsseldorf, 1986.

Duecker, H., K.-H. Friese, and W.-D. Haecker, "Ceramic Aspects of the Bosch Lambda-Sensor," SAE Paper 750223, *SAE National Automobile Engineering Meeting,* Detroit, 1975.

Gruber, H. U., and H. M. Wiedenmann, "Three Years Field Experience with the Lambda-Sensor in Automotive Control Systems," SAE Paper 800017, *SAE National Automobile Engineering Meeting,* Detroit, Feb. 1980.

Moseley, P. T., and B. C. Tofield (eds.), *Solid State Gas Sensors,* Adam Hilger, Bristol and Philadelphia, 1987.

Saji, K., "Characteristics of Limiting Current-Type Oxygen Sensor," *J. Electrochem. Soc.: Electrochem. Science and Technology,* vol. 134, no. 10, 1987, pp. 534–542.

Saji, K., H. Kondo, T. Takeuchi, and I. Igarashi, "EMF Characteristics of Zirconia Oxygen Sensor in Nonequilibrium Gas Mixtures Containing Combustible Gas and Oxygen," *Proc. 1st Sensor Symposium,* Tsukuba, Japan, June 1981, pp. 103–107.

Soejima, S., and S. Mase, "Multi-Layered Zirconia Oxygen Sensor for Lean Burn Engine Application," SAE Paper 850378, *SAE National Automobile Engineering Meeting,* Detroit, 1985.

PETITIONER'S EXHIBIT 1002
US PATENT NO. 6,581,565

Takami, A., "Development of Titania Heated Exhaust-Gas Oxygen Sensor," *Ceramic Bulletin*, vol. 67, no. 12, 1988, pp. 1956–1960.

Wiedenmann, H. M., "Characteristics of Oxygen Sensors for Lean Exhaust Gas," *VDI Berichte* 578, S.129–151, VDI-Verlag, Düsseldorf, 1985.

ABOUT THE AUTHORS

HANS-MARTIN WIEDENMANN studied physics and meterology in Tübingen and Munich, where he received his Ph.D. in Physics in 1969. He joined Bosch in 1970 and is now senior manager for the development of lambda oxygen sensors.

GERHARD HÖTZEL studied chemistry in Konstanz and received his Ph.D. in 1986 at the University of Stuttgart. At Bosch, he is responsible for physical bases and measurement techniques for lambda oxygen sensors.

HARALD NEUMANN studied solid-state electronics in Aachen where he received a Ph.D. in 1988. Since that time, at Bosch he has been responsible for the technology of planar-type ceramic sensors.

JOHANN RIEGEL studied electrical engineering in Karlsruhe and received a Ph.D. in 1989. At Bosch he is responsible for the investigation of planar-type ceramic sensors.

HELMUT WEYL studied mechanical engineering in Darmstadt and was graduated from there in 1966. He has been with Bosch since 1968 and is now responsible for proving lambda oxygen sensors.

PETITIONER'S EXHIBIT 1002
US PATENT NO. 6,581,565

PETITIONER'S EXHIBIT 1002
US PATENT NO. 6,581,565

CHAPTER 7
SPEED AND ACCELERATION SENSORS

William C. Dunn
Motorola Inc.
Semiconductor Products Sector

7.1 INTRODUCTION

In the automotive arena, speed and acceleration sensors are used in a wide variety of applications, from improving engine performance through safety to helping to provide creature comforts.

Speed sensing can be divided into rotational and linear applications. Rotational speed sensing has two major application areas: engine speed monitoring to enhance engine control, and performance and antilock breaking and traction control systems for improved road handling and safety. Linear sensing can be used for ground-speed monitoring for vehicle control, obstacle detection, and crash avoidance. Acceleration sensors are used in air bag deployment, ride control, antilock brake, traction, and inertial navigation systems.

In most cases, there are a number of different sensor types available for a specific monitoring function. However, the choice of sensor for a specific application can be difficult to make. The selection may be determined by the familiarity of the system's designer with the sensor. On the other hand, the output from one sensor can be used for several applications, and the individual requirements of each application may eventually determine the sensor to be used.

Electronics and electronic sensors are making rapid inroads into the automotive market. In order to analyze the large amounts of sensor data needed for low emissions and efficient engine control, it is necessary to process the information using microcontrollers (MCUs), which can operate at high speeds and in real time. Sensors that can convert information directly into a digital format for MCU compatibility have a distinct advantage over an analog output format. Digital signals are also supply-line voltage-insensitive, virtually unaffected by noise, and have better resolution than can be obtained with analog signals. If the addition of an analog-to-digital converter (on or off the MCU) is required for compatibility, the system cost is increased. The accuracy of the control system is only as good as the integrity of the sensor data supplied to the MCU. Hence, the importance of the performance of the sensor.

This chapter concentrates on speed and acceleration, and therefore does not go into all the other different types of applications for which many of these sensors can be used in the automobile.

PETITIONER'S EXHIBIT 1002
US PATENT NO. 6,581,565

7.2 SPEED-SENSING DEVICES

In automotive applications, the environment must be taken into consideration. The sensing must be accurate, the devices must be rugged and reliable, and they must function in the presence of oil, grease, dirt, and inclement weather conditions. These requirements have severely limited the use of a number of otherwise practical alternatives, such as optical sensors and contact sensing.

In the area of rotational speed monitoring, the most practical devices use magnetic field sensing. These sensors are Hall effect devices, variable reluctance (VR), and magnetoresistive or magnetic resistance element (MRE) devices. Both the Hall effect and VR devices have been widely used and have a proven track record. The MRE device has only recently come into its own with improved technology and provides a viable alternative to the Hall effect device. The MRE device has a higher sensitivity and a wider operating temperature range than the Hall effect device.

For the measurement of ground speed and object detection, optical, radar, laser, infrared, and ultrasonics have been explored. Linear sensing devices typically use the Doppler effect for speed sensing and pulse modulation for distance measuring. These devices are used for object detection in blind spots when reversing or changing lanes, and in such applications as collision avoidance systems.

7.2.1 Variable Reluctance Devices

Variable reluctance devices are in effect small ac generators with an output voltage proportional to speed, but they are limited in applications where zero speed sensing is required. The operating frequency range of the VR device is from about 10 Hz to 50 kHz. It is insensitive to mechanical stress and has a wide temperature operating range from −40 to 190 °C. The supply voltage and offset drift will depend upon the control electronics. The VR device, originally designed around existing automotive electromechanical systems, was adapted for electronic control. The ferrous metal in the VR system is designed for maximum output voltage at low rpm (revolutions per minute), to get as close as possible to zero speed sensing without generating excessive voltages at maximum rpm (up to 150 V). This device gives a linear output voltage with frequency. Most systems use MCUs for data processing, so the VR device needs an analog-to-digital (A/D) converter to generate a digital signal for compatibility with the MCU. Although the VR device itself is inexpensive, the extra costs for data conversion may eventually lead to its demise in many automotive applications.

7.2.2 Hall Effect Devices

The Hall effect exists when a current flowing in a carrier experiencing a magnetic field perpendicular to the direction of current flow results in the current being deflected perpendicular to the field and to the direction of the current. The Hall effect is shown in Fig. 7.1. A current I_c flowing through the device between terminals 1 and 2 will produce a potential VH between terminals 3 and 4, when a magnetic field **B** is applied perpendicular to the device. The potential VH is determined by the strength of the magnetic field and the current flowing. Hall effect devices can be manufactured with indium, gallium arsenide, or silicon. A comparison of their properties is given in Table 7.1.

As can be seen, silicon is the most sensitive material. It is compatible with ICs and has a wide operating temperature range. The Hall effect device is well known both in industry and in the automotive arena for rotational and position-sensing applications. However, recent developments in Hall sensing devices, such as differential sensing and integration, have given improved sensor characteristics, which may result in greater potential in automotive applications.

PETITIONER'S EXHIBIT 1002
US PATENT NO. 6,581,565

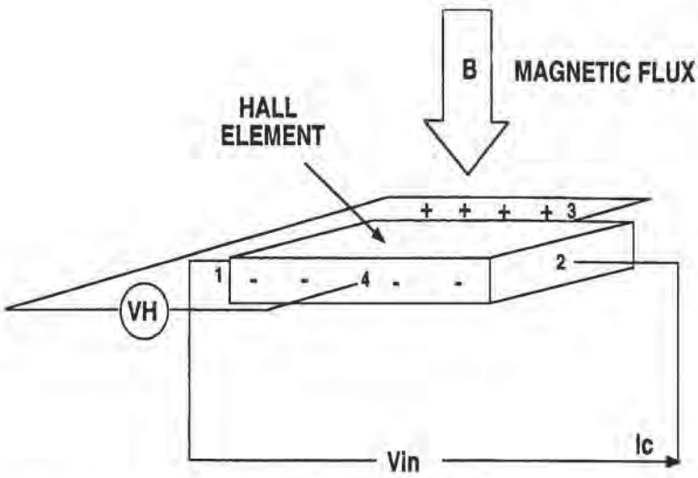


FIGURE 7.1 Hall effect.

The Hall effect device is very versatile, flexible in use, easy to package, and can be used for zero speed sensing (it can give an output when there is no rotation). Hall devices give a frequency output that is proportional to speed, making them compatible with MCUs. The Hall device is normally configured as a bridge to minimize temperature effects and to increase the sensitivity of the sensor.

A typical Hall effect sensor configuration with waveforms is shown in Fig. 7.2. The teeth of the ferrous wheel concentrate the magnetic flux when the teeth come into close proximity to the Hall sensor and magnet. The output from the sensor is a sinusoidal waveform, whose frequency is the rpm of the ferrous wheel multiplied by the number of teeth on the wheel. The resolution of the system depends on the number of teeth in the wheel (typically 20).

7.2.3 Magnetoresistive Devices

The magnetoresistive effect is the property of a current-carrying ferromagnetic material to change its resistivity in the presence of an external magnetic field. For example, a ferromagnetic (permalloy) element (an alloy containing 20 percent iron and 80 percent nickel) will change its resistivity by 2 to 3 percent when it experiences a 90° rotation in a magnetic field.[1] The resistivity value rises to a maximum when the direction of current and magnetic field are coincident, and is a minimum when the fields are perpendicular to each other. This relationship is shown in Fig. 7.3. This attribute is known as the Anisotropic Magneto Resistive Effect. The resistance R of an element is related to the angle q between the current and the magnetic field directions by the expression:

$$R = R_{\parallel} \cos^2 q + R_{l} \sin^2 q \tag{7.1}$$

TABLE 7.1 Comparison of Properties of Hall Effect Materials

Material	Operating temp. °C	Supply voltage	Sensitivity @ 1 kA/m	Frequency range
Indium	–40 to 100	1V	7 mV	0 to 1 MHz
GaAs	–40 to 150	5 V	1.2 mV	0 to 1 MHz
Si (with conditioning)	–40 to 150	12 V	94 mV	0 to 100 kHz

PETITIONER'S EXHIBIT 1002
US PATENT NO. 6,581,565

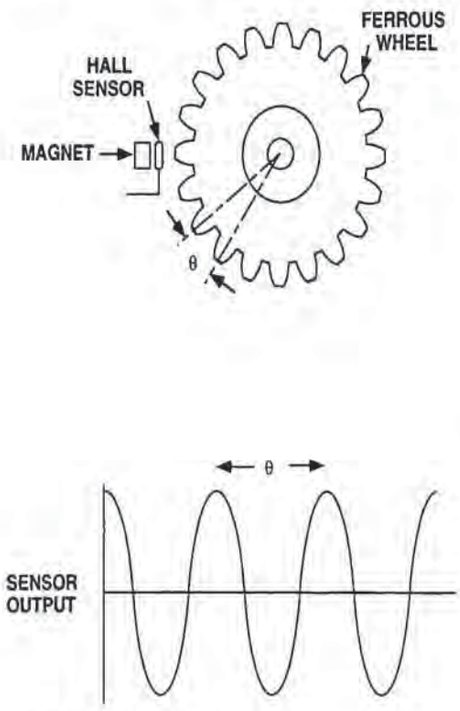


FIGURE 7.2 Hall sensor and output waveforms.

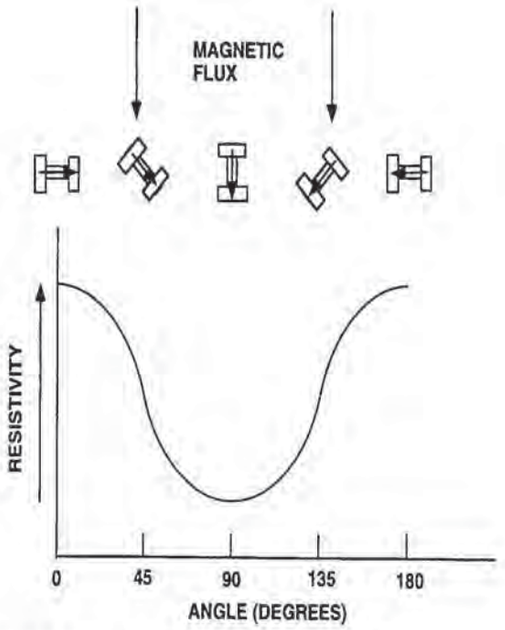


FIGURE 7.3 Relationship between magnetic field and resistivity change in MRE devices.

where $R_{\parallel}$ is the resistance when the current and the magnetic field directions are parallel and $R_{\perp}$ is the resistance when the current and the magnetic field directions are perpendicular.

MRE devices give an output when stationary, which make them suitable for zero speed sensing. MRE devices also give an output frequency that is proportional to speed, making for ease of interfacing with an MCU. For good sensitivity and to minimize temperature effects, a bridge configuration is normally used. In an MRE sensor, aluminum strips can be put across the permalloy element to linearize the device. This configuration is shown in Fig. 7.4 together with a typical MRE characteristic. The low-resistance aluminum stripes cause the current to flow at 45° in the permalloy element, which biases the element into a linear operating region.

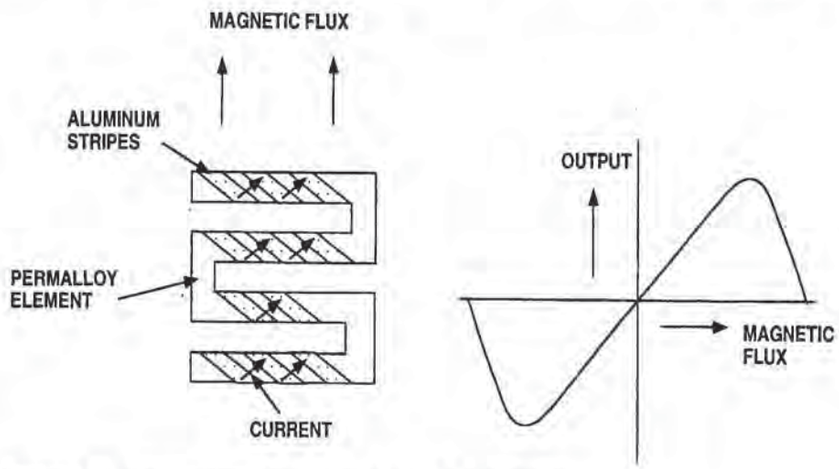


FIGURE 7.4 Use of permalloy strip for linearization in MRE devices.

PETITIONER'S EXHIBIT 1002
US PATENT NO. 6,581,565

Integrated MRE devices can typically operate from –40 to 150 °C, over a supply voltage range of 8 to 16 V, and at frequencies from 0 to 1 MHz. In comparing the MRE sensor to a Hall effect device, the MRE has a higher sensitivity, is less prone to mechanical stress, has a wider operating frequency range, has the potential of being more cost effective, gives better linearity, and is more reproducible. However, it is more sensitive to external magnetic fields. Table 7.2 shows a comparison of rotational sensing devices.

TABLE 7.2 Comparison of Sensing Devices

Sensor type	Operating temperature (°C)	Sensitivity 1 kA/m (mV)	Frequency range	Mechanical stress
Hall effect	–40 to 150	90	0 to 100 kHz	High
MRE	–40 to 150	140	0 to 1 MHz	Low
VR	–40 to 190		1 to 50 kHz	None
Magnetic transistor	–40 to 150	250	0 to 500 kHz	Low

It should be noted that Hall effect and MRE devices have many applications in the automobile outside of rotational speed sensing, such as position sensing, fuel-level sensing, and active suspension. The magnetic transistor is showing potential in rotational speed sensing and position-sensing applications, and may eventually be another viable contender to the Hall effect device in the automotive market.

7.2.4 Ultrasonic Devices

Ultrasonic devices can be used to measure distance, ground speed, and as a proximity detector. To give direction and beam shape, the signals are transmitted and received via specially configured horns and orifices. The transmitter and receiver horns are similar in shape, but are normally separate to accommodate different characteristics. The ultrasonic devices are made from PZT crystal-oriented piezoelectric material ($PbZrO_3$—$PbTiO_3$).

For the measurement of distance or object detection, a pulse of ultrasonic energy is transmitted and the time is measured for the reflected pulse to return to the receiver. The frequency of the transmitted ultrasonic waves are typically about 40 kHz and travel with a velocity of 340 m/s at 15 °C. This velocity changes with temperature and pressure. However, these parameters can be measured and corrections made if high accuracy is required. The repetition frequency and power requirements depend on the distance to be measured. To measure speed, the distance variation with time can be measured and the velocity calculated. A more common method is to use the Doppler effect, which is a change in the transmitted frequency as detected by the receiver due to motion of the target (or, in this case, the motion of the transmitter and receiver).

7.2.5 Optical and Radio Frequency Devices

Optical devices are still being used for rotational speed sensing. They are normally light-emitting diodes (LEDs) with optical sensors. Figure 7.5 shows a typical optical sensor system. An optical sensor detects light from an LED through a series of slits cut into the rotating disc, so that the output from the sensor is a pulse train whose frequency is equal to the rpm of the disc multiplied by the number of slits. The higher the number of slits in the disc, the smaller the angle of rotation that can be measured. The optical sensor can be a single photodiode or a photodiode array as shown. This array gives a more accurate determination of the position of the slit, resulting in higher resolution of the position of the disc.

PETITIONER'S EXHIBIT 1002
US PATENT NO. 6,581,565

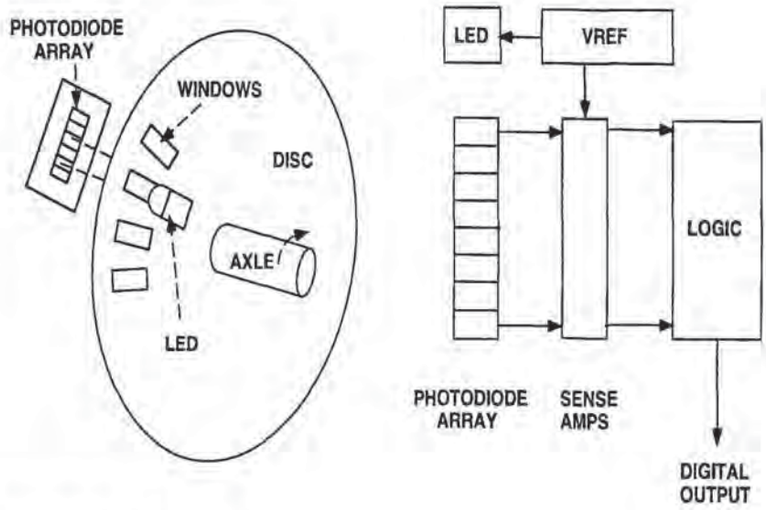


FIGURE 7.5 Optical sensor.

Optical and radio frequency (RF) devices are used for object detection, linear approach speed, and distance measurements in crash avoidance systems where distances greater than about 10 m are involved. These devices use the same principles as the ultrasonic devices. Optical devices normally use lasers or infrared devices for the transmitting source and optical sensors for the receivers. RF devices use gallium arsenide or Gunn devices to obtain the power and high frequency (about 100 GHz) required in the transmitter. The high operating frequency is set to a large extent by the need for a small antenna. These applications are under development and are discussed in Sec. 7.7.2.

7.3 AUTOMOTIVE APPLICATIONS FOR SPEED SENSING

There are several applications for rotational speed sensing. First it is necessary to monitor engine speed. This information is used for transmission control, engine control, cruise control, and possibly for a tachometer. Electronics and electronic sensing in the automobile were brought about by the need for higher-efficiency engines, better fuel economy, increased power and performance, and lower emissions. Second, wheel speed sensing is required for use in transmissions, cruise control, speedometers, antilock brake systems (ABS), traction control (ASR), variable ratio power steering assist, four-wheel steering, and possibly in inertial navigation and air bag deployment applications.

Linear speed sensing can be used to measure the ground speed. This measurement also has the possibly of use in ABS, ASR, and inertial navigation. Similar types of sensors can be used in crash avoidance, proximity, and obstacle detection applications.

7.3.1 Rotational Applications

The high timing accuracy that can be obtained with fuel injection systems and replacement of points by sensors have made cost-effective engine control and low maintenance a reality. Adjustment of the stoichiometric ratio of air to fuel, accurate ignition timing, and oxygen sensors in the exhaust system, have vastly improved engine performance and greatly reduced emissions over widely varying operating conditions. The two important factors in engine con-

PETITIONER'S EXHIBIT 1002
US PATENT NO. 6,581,565

trol are the engine speed in rpm and the crank angle. These signals are used by the engine control MCU for determination of fuel injection and ignition timing. The engine rpm measurement range is from 50 to (say) 8000 rpm. A resolution of about 10 rpm is required for an accuracy of about 0.2 percent. For injection and ignition control in a six-cylinder engine, the interval between combustion at maximum rpm is 2.5 ms, so that this time sets the injection period. In practice, a crank angle accuracy of between 1 and 2 degrees per revolution is required. Newer systems with sequential fuel injection, may also require information on TDC (top dead center) for each cylinder to determine the timing. With the low frequencies involved in this application, either Hall effect or MRE devices can be used for monitoring both the engine rpm and crank angle.

Vehicle speed measurements are in the range 0 to 180 km/h (120 mph) and digital displays must have an accuracy of 1 km/h. Some systems have a mechanical pickoff from the drive shaft, which can then use optical sensors for the measurement of road speed. However, newer systems have a pickoff located directly on the drive shaft, which makes optical devices less practical. It is preferred to eliminate the remote sensing via mechanical coupling to save the cost of the associated mechanical components, seals, maintenance, and so on. One method of pickoff is a ring magnet with between 4 and 20 magnetic poles (depending on the required resolution). Figure 7.6 shows such a system using an MRE sensing device. The magnetic flux changes are sensed by an MRE bridge sensor when the magnet disc is rotating. The bridge is supplied from a voltage reference circuit, and its output is amplified and shaped to give a frequency output that is proportional to shaft rotation speed. A ferrous toothed wheel pickoff with magnet and flux concentrator can also be used (see Fig. 7.2). Vehicle speed sensing can be performed with Hall effect, MRE, or VR devices. The number of pulses P per second from the detector are counted to measure speed S, from the following relationship:

$$P = N \times S \times K \tag{7.2}$$

where N = the number of magnetic poles on ring magnet or wheel teeth
K = a constant determined by axle ratio and wheel size

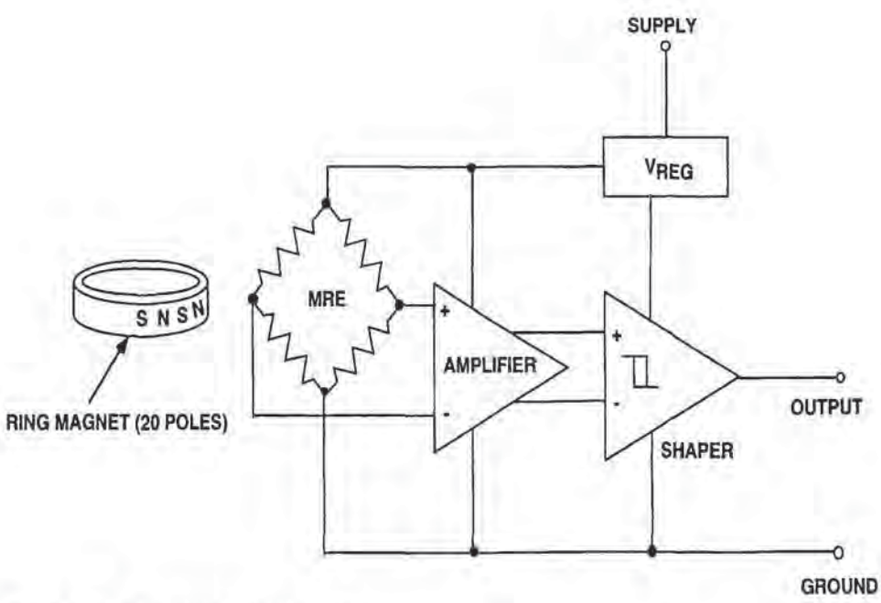


FIGURE 7.6 MRE speed-sensing module.

PETITIONER'S EXHIBIT 1002
US PATENT NO. 6,581,565

The resolution in vehicle speed is then:

$$\frac{P}{S} = N \times K \tag{7.3}$$

The typical system requirements are an operating temperature of –40 to 120 °C, rotational speed detection of 5 to 3000 rpm (1000 p/s), and a duty cycle ratio of 50 ± 10%.

In applications such as ABS, ASR, and four-wheel steering, additional speed sensors are attached to all four wheels so that the slip differential between the wheels can be measured. VR devices have been used and are very cost effective in this application. But the cost of other devices is dropping and as they become cost effective, they are being designed into new systems. In electronic transmission applications, information from the road and engine speed sensors, as well as torque data and throttle position are required for the MCU to select the optimum gear ratio. Electronic control can ensure smooth transition between gear ratios. Transmissions using electronic control are also smaller than conventional automatic transmissions, thus enabling more gear ratios for better performance, higher torque, efficiency, and acceleration.

Cruise control systems require information from the road and engine speed sensors to control the throttle position, and possibly the optimum selection of transmission ratios. Variable ratio assisted power steering also requires information from the wheel speed sensors for adjustment of the steering ratios for ease of turning at low speeds and good road control at high speeds. If automatic tire pressure adjustment becomes a reality, this system may also require information from the wheel speed sensors.

Another application for rotational speed sensing is to control the speed of the radiator cooling fan. The speed of the fan is determined by the coolant temperature. Hall effect devices (MRE can also be used) have been used to monitor the position of the armature and speed of the cooling fan motor. The motor controller uses this information to modulate the power to the motor through a three-phase bridge driving circuit for the control of the fan motor speed.

7.3.2 Linear Applications

Under linear applications are the detection of obstacles close to the vehicle, crash avoidance, distance of the chassis relative to the ground for ride control, measurement of ground speed for ABS, ASR, and inertial navigation. Ultrasonic devices are normally used for short distance measurements (<10 m) and RF devices for long distance measurements (see Sec. 7.6.2). For the measurement of objects from 0.5 to 2 m using ultrasonics, a pulse repetition rate of about 15 Hz is used. The reflected pulses take from 3 to 12 ms to return. The return time T is given by

$$L = C \times \frac{T}{2} \text{ (m)} \tag{7.4}$$

where L = distance to target
C = the transmission speed [given by $C = 331 + 0.6\,t$ (m/sec)]
T = temperature (at 15 °C), the speed of ultrasonic waves is 340 m/s.

In the case of chassis-to-ground measurements for ride control and ground speed measurements, the distance to be measured is from 15 to 50 cm and a higher pulse repetition rate can be used (up to 50 Hz). In this case, the reflected pulse takes from 0.9 to 3 ms to return. For ride control applications, an accelerometer has an advantage over distance measurement, in that it is unaffected by varying distance measurements over rough terrain.

7.4 ACCELERATION SENSING DEVICES

Acceleration sensors vary widely in their construction and operation. In applications such as crash sensors for air bag deployment, mechanical devices (simple mechanical switches) have

PETITIONER'S EXHIBIT 1002
US PATENT NO. 6,581,565

been developed and are in use. Mechanical switches are normally located at the point of impact in the crash zone. With the development of micromachined devices, solid state analog accelerometers have been designed for air bag applications. The analog accelerometers are centrally placed on the automotive frame. These devices can be very cost effective when compared to mechanical switches and are rapidly replacing the electromechanical devices. Silicon micromachined sensors provide a higher degree of functionality, can be programmed, have high reliability, have excellent device-to-device uniformity, and can be integrated with memory circuits to create a more accurate sensor. Additional features such as self-test and diagnostics are also available.

7.4.1 Mechanical Sensing Devices

Mechanical switches are simple make-break devices. Figure 7.7 shows the cross section of a Breed type of switch or sensor. The device contains a spring, a metal ball, and electric contacts in a tube. On impact, the inertia in the ball causes it to move against the retaining force of the spring and closes the electric contacts at the end of travel. An alternative to this device is the one shown in Fig. 7.8. It consists of a cylindrical mass wound in a flat spring. The seismic mass

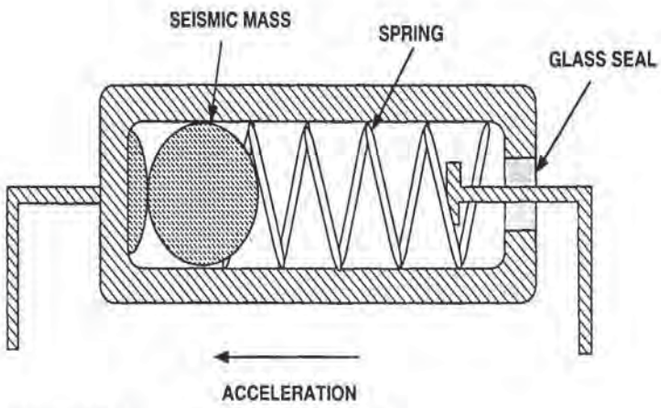


FIGURE 7.7 Cross section of mechanical sensor.

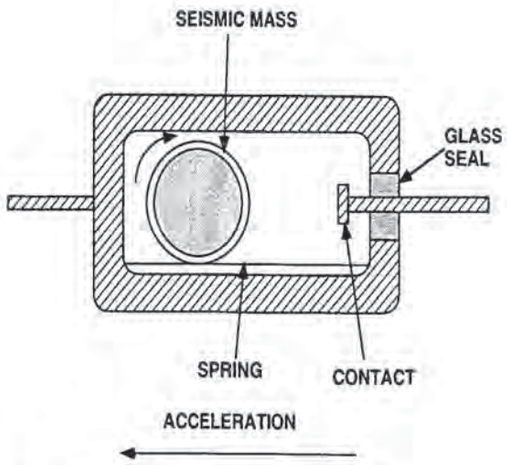


FIGURE 7.8 Cross section of mechanical switch.

PETITIONER'S EXHIBIT 1002
US PATENT NO. 6,581,565

rolls on impact against the spring tension, and again makes electrical contact at the end of travel. The machining tolerances on these devices are high and give wide variations in the acceleration trigger point.

7.4.2 Piezoelectric Sensing Devices

Piezoelectric devices consist of a layer of piezoelectric material (such as quartz) sandwiched between a mounting plate and a seismic mass. Electric connections are made to both sides of the piezoelectric material. The cross section of such a device is shown in Fig. 7.9. Piezoelectric material has the unique property that when a force or pressure is applied to opposite faces of the material, an electrical charge is produced. This charge can be amplified to give an output voltage that is proportional to the applied force. Piezoelectric devices can be effective in some applications, but are not suitable for sensing zero- or low-frequency acceleration, that is <5 Hz due to offset and temperature problems (pyroelectric effect). Piezoelectric sensors have a high Q, low damping, and a very high output impedance. Self-test features are also difficult to implement. The main advantages of piezoelectric devices are their wide operating temperature range (up to 300 °C), and high operating frequency (100 kHz).

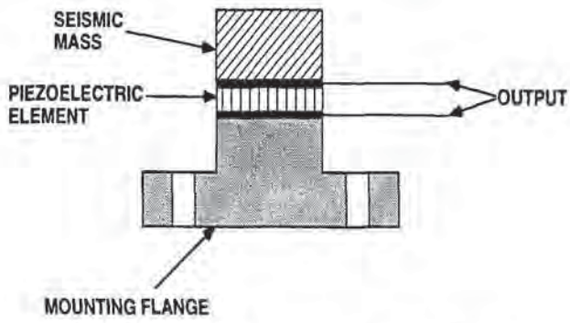


FIGURE 7.9 Cross section of a piezoelectric accelerometer.

Figure 7.10 shows a typical signal-conditioning circuit[2] and the trimming network used with piezoelectric sensors. The output from the sensor is fed to a charge amplifier, which converts the charge generated by the sensor into a voltage proportional to the charge. The circuit

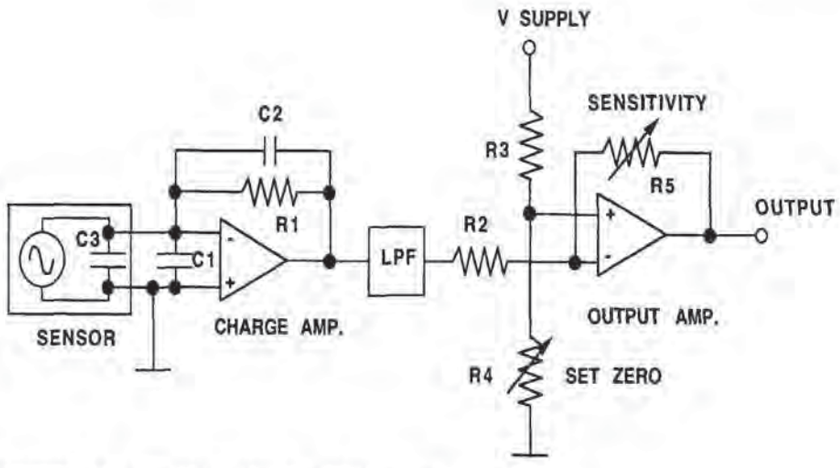


FIGURE 7.10 Piezoelectric signal-conditioning circuit.

PETITIONER'S EXHIBIT 1002
US PATENT NO. 6,581,565

is a modified virtual ground voltage amplifier. Feedback via capacitor C2 and resistor R1 is used to maintain the input at a virtual ground potential. This type of circuit minimizes the effect of stray or ground capacitance C1. The output voltage from the amplifier is fed via a low-pass filter (LPF) to an output amplifier, where it is trimmed for offset by R4 and sensitivity by R5. In system development, the sensitivity is set by the piezoelectric material used. Higher-sensitivity materials however, exhibit higher sensitivity to temperature variations.

7.4.3 Piezoresistive Sensing Devices

The property of some materials to change their resistivity when exposed to stress is called the piezoresistive effect. In silicon, the sensing resistors can be either P or N type doped regions, which can be very sensitive to strain. The resistors are also sensitive to temperature, so that the strain gauge is normally designed as a bridge configuration to minimize temperature effects and to obtain higher sensitivities (see also Chap. 2). In order to maintain good linearity, the operating temperature of piezoresistive devices is limited to about 100 °C. The nonlinearity is caused by excessive junction leakage current at high temperatures. Higher operating temperatures have been obtained using oxide-isolated strain gages (up to 175 °C). An uncompensated strain gauge has a typical error of 3 percent over the operating temperature range –20 to 80 °C. This error can be reduced with a compensating resistor, and still further reduced to about 0.5 percent by the use of thermistors, over an improved operating temperature range of –40 to 110 °C.

Piezoresistive sensing can be used with bulk micromachined accelerometers. Such a device is shown in Fig. 7.11. The strain-sensing elements are diffused into the suspension arms. These elements can then detect strain in the arms caused by acceleration forces on the seismic mass.

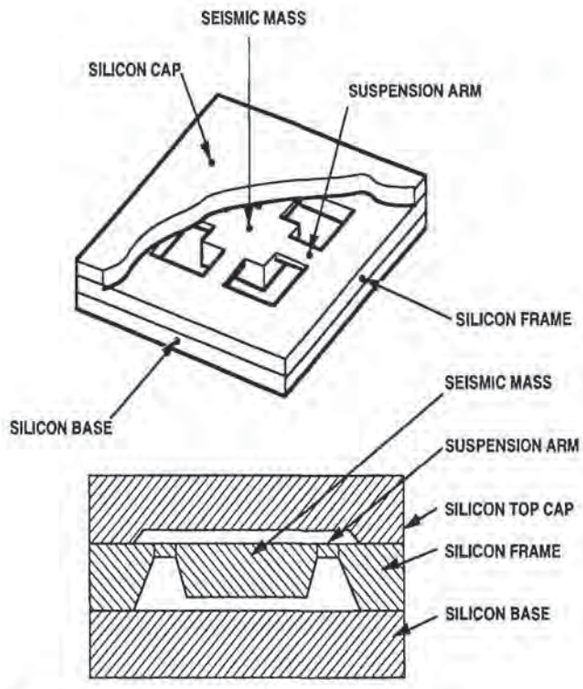


FIGURE 7.11 Bulk micromachined accelerometer.

PETITIONER'S EXHIBIT 1002
US PATENT NO. 6,581,565

7.4.4 Capacitive Sensing Devices

When used with micromachined structures as shown in Figs. 7.11 and 7.12, differential capacitive sensing has a number of attractive features when compared to other methods of sensing: easily implemented self-test, temperature insensitivity, and smaller size. In addition, comparing capacitive sensing to piezoelectric sensing reveals that capacitive sensing has the advantages of dc and low-frequency operation and well-controlled damping. When compared to piezoresistive sensing; differential capacitive sensing has the advantage of a wider operating temperature range and requires less complex trimming. Capacitive sensing has one other major advantage over other sensing methods in that it can be used in closed-loop servo systems. In these systems, voltages can be applied to the capacitive plates to produce electrostatic forces, which will balance the forces on the seismic mass due to acceleration. The main advantage of closed-loop operation is to make the sensor to a large extent independent of process variations. Signal-conditioning circuits can be designed to detect changes in capacitance of <0.1 fF, so that plate capacitances in the range of 200 to 400 fF can be used. The small spacing between capacitor plates in micromachining technology (2 μ) enables practical acceleration sensors as small as 500 μ × 500 μ. When designing capacitive sensors, care must be taken to ensure that the sensing voltages are properly balanced to minimize offsets due to electrostatic forces. These forces can also be produced by internal noise sources. The attributes of capacitive sensing are a linear response, operation over wide temperature ranges (–40 to 150 °C), and a frequency response from dc to about 2 kHz.

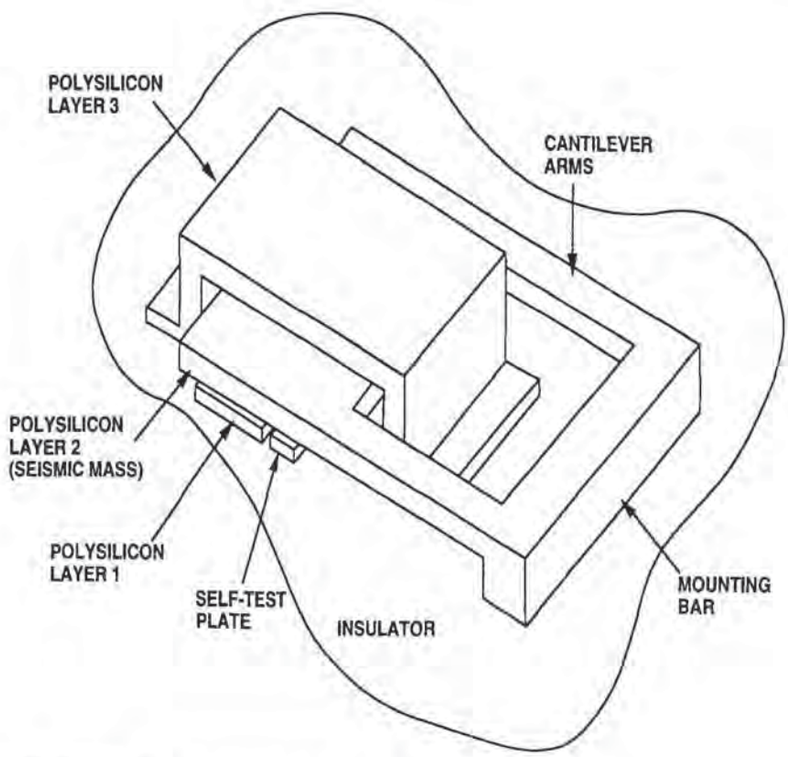


FIGURE 7.12 Surface micromachined accelerometer.

Micromachined Structures. There are a variety of types of micromachined structures that can be used in accelerometers. These structures fall into two technologies: bulk micromachined structures and surface micromachined structures. Bulk micromachined devices are structures

PETITIONER'S EXHIBIT 1002
US PATENT NO. 6,581,565

etched out of silicon wafers. Figure 7.11 shows the cross section of a bulk micromachined device consisting of three layers of silicon bonded together. The center layer is shaped to form a seismic mass suspended by four arms[3] (a cantilever structure has also been designed with two suspension arms[4]). When acted upon by acceleration forces, the seismic mass moves between the top and bottom plates. In this case, the movement can be sensed using piezoresistive elements diffused into the suspension arms, or differential capacitive sensing can be used between the seismic mass and the upper and lower silicon plates. The top and bottom plates can also be made of glass with metalized areas to form the top and bottom capacitors. Such devices have been designed to operate from the high g range (>1000 g), down to sensors with resolution in the μg range. Closed-loop control techniques are normally used in these lower g ranges.

The surface micromachined device shown in Fig. 7.12 is built using layers of polysilicon and sacrificial glass, which are alternately deposited and shaped. In this case, three layers of polysilicon and two layers of sacrificial glass were used. After deposition of the third polysilicon layer, the sacrificial glass is etched away leaving the freestanding structure as shown. A number of etch holes are normally placed in the second and third layer of polysilicon to speed up the etch process. These etch holes are also used to control the squeeze film damping and bandwidth of the device. The seismic mass of the second-layer polysilicon in these devices is of the order of 5×10^{-10} kg. A second plate under the middle polysilicon can be used for self-test. This function is achieved by applying a voltage to the self-test plate, which in turn will produce an electrostatic force on the center polysilicon plate causing it to deflect. This deflection will simulate an external acceleration force. An alternative to the polysilicon and glass structure is nickel with sacrificial copper.[5]

Differential capacitive sensing is used with all of these structures. Both bulk and surface micromachined devices have a very rugged construction. These devices use squeeze film damping to control bandwidth and to ensure critical damping of the resonant frequency (about 2 kHz for bulk and 10 kHz for surface micromachined devices). Film damping also ensures high resistance to shock in the sensing direction. In the directions perpendicular to the sensitive axes, the devices are rugged by construction with low cross-axis sensitivity (<3 percent). An accelerometer designed to sense a few g will typically have a shock tolerance of well over 5000 g. As already noted, surface micromachined devices that have been developed for air bag deployment have analog outputs. These devices normally operate from a 5-V supply, have a bandwidth of about 1 kHz and a sensitivity of 40 mV per g, giving a full-scale output with ±50 g input. Both open- and closed-loop techniques have been used for sensing. In comparing bulk and surface micromachined devices, the bulk structure is larger, using crystal-oriented etching with end stops, which require extra diffusions; whereas, the surface micromachined device uses isotropic etching (masking) with different materials acting as end stops. Surface structures have the potential for easier integration and use a simpler less costly process, but do require annealing.

Open-Loop Sensing. Open-loop signal-conditioning circuits amplify and convert the capacitance changes into a voltage. Such a CMOS circuit using switched capacitor techniques is shown in Fig. 7.13. The circuit contains a virtual ground amplifier to minimize the effect of stray capacitance. The positive input of the amplifier is referenced to a voltage of $V_{REF}/2$, when switch $S2$ is closed the amplifier has unity gain, and the voltage on the middle plate of the sensor is set to $V_{REF}/2$. After $S2$ is opened, $S1$ is switched so that any differences between sensor capacitors C_1 and C_2 produces a charge at the negative input of the amplifier. This charge produces a voltage (V_{out}) at the output of the integrating amplifier. The output voltage of the amplifier is given by

$$V_{out} = V_{REF} \frac{C_1 - C_2}{C_3} \tag{7.5}$$

where C_1 and C_2 are the sensor capacitances
C_3 is the integrator capacitance

PETITIONER'S EXHIBIT 1002
US PATENT NO. 6,581,565

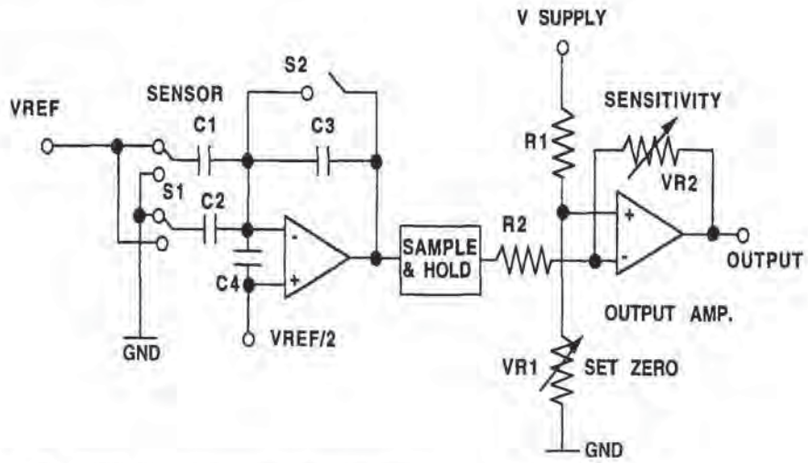


FIGURE 7.13 Capacitive sensing integrator circuit.

If the reference voltage is made proportional to the supply voltage, a ratiometric output is obtained. That is, the system gain is proportional to the supply voltage. This is a requirement in some systems to facilitate the design of the A/D converter.

A block diagram of the system is shown in Fig. 7.14. The system contains an internal oscillator, voltage reference, amplifier, sample and hold, switched capacitor filter, trim network, and output buffer. The output voltage in such a circuit is proportional to the capacitance change. This change is proportional to 1/displacement, or 1/acceleration, giving rise to some nonlinearities. However, the displacement is small compared to the spacing between the plates, so that the output voltage approximates to acceleration, giving less than 3 percent nonlinearity. The filter is used for noise reduction and to set the bandwidth for specific applications. Trimming is used to set the zero operating point and sensitivity of the system.

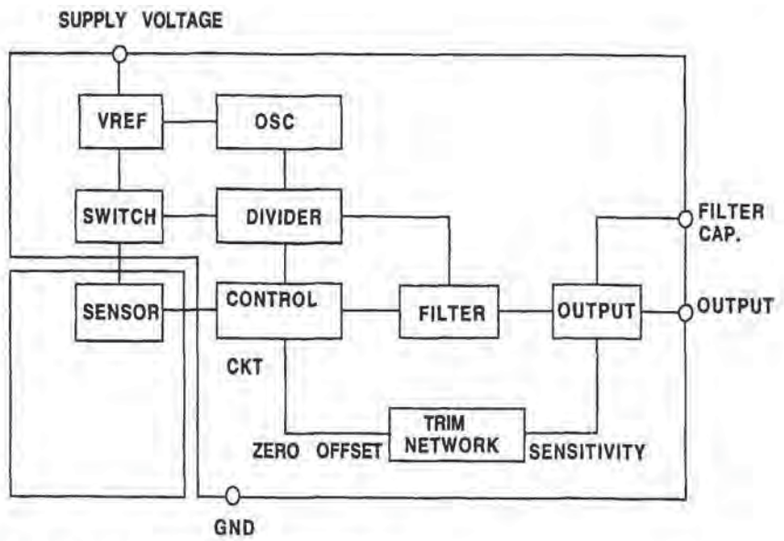


FIGURE 7.14 Signal-conditioning block diagram.

PETITIONER'S EXHIBIT 1002
US PATENT NO. 6,581,565

An alternate circuit with improved linearity is shown in Fig. 7.15. In this case, the output voltage is fed back to the input of the integrator, forming a bridge circuit. The feedback also sets the amplitude of the driving voltage across the sensing capacitors, so that it is proportional to their displacement. This also balances the electrostatic forces on the middle plate.

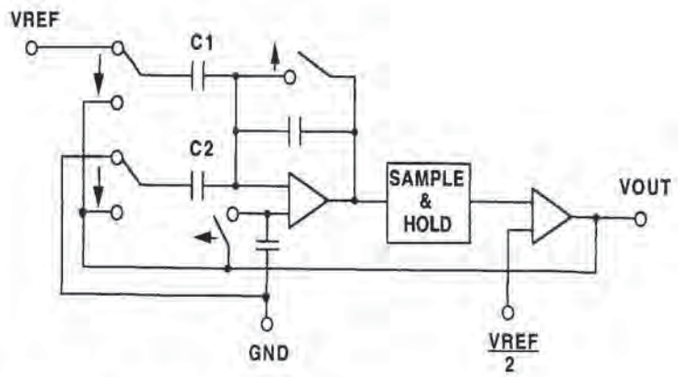


FIGURE 7.15 Linearized circuit schematic.

In this case

$$V_{out} = \frac{(C_1 - C_2)}{(C_1 + C_2)} \frac{V_{REF}}{2} \tag{7.6}$$

where $C_1 \propto 1/d_1$
$C_2 \propto 1/d_2$
$d_1 + d_2 = K$ (constant)

so that

$$V_{out} = V_{in} \frac{(d_1 - d_2)}{K} \tag{7.7}$$

showing that, in this case, V_{out} is proportional to displacement and acceleration giving improved linearity (<1 percent nonlinearity).

Closed-Loop Sensing. An alternative to the open-loop sensing circuit is the closed-loop sensing circuit, which can be configured to give an analog or digital output. Figure 7.16*a* shows the balanced electrostatic forces exerted on a seismic mass by upper and lower capacitor plates, which are at voltages of $+V$ and $-V$. If the seismic mass experiences a force due to acceleration, and a voltage δV is applied to the middle plate to generate enough electrostatic force to counterbalance the acceleration force, then the forces are as shown in Fig. 7.16*b*.

That is

$$m \times a = \frac{C(V + \delta V)^2}{2d} - \frac{C(V - \delta V)^2}{2d} \tag{7.8}$$

from which

$$m \times a = 2\,C \times V \times \frac{\delta V}{d} \tag{7.9}$$

PETITIONER'S EXHIBIT 1002
US PATENT NO. 6,581,565

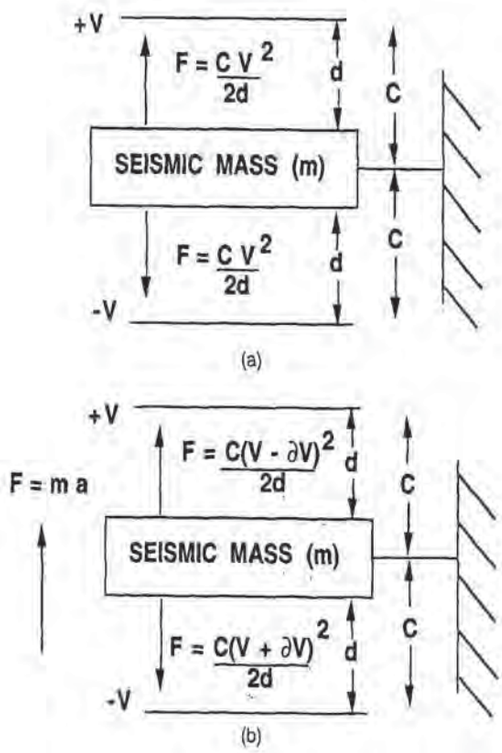


FIGURE 7.16 Electrostatic force diagram.

This shows that an acceleration force can be balanced by a linear voltage applied to the center plate. This voltage can be amplified to give a linear output voltage proportional to acceleration.[6]

In a micromachined structure, the electrostatic force produced by a δV of about 1 V can counterbalance the force produced by an acceleration of 50 g on the seismic mass. Figure 7.17 shows a block diagram of the analog closed-loop system. The top and bottom plates are dc-biased by the resistor divider network consisting of R1, R2, and R3. The ac antiphase signals used for sensing the position of the center plate are fed to the top and bottom sensor plates via the capacitors (C1, C2) from the control logic. The analog output voltage from the filter is feedback to the positive input of the integrator. When the integrator is clocked into the unity gain phase, the feedback voltage is applied to the center plate of the sensor. The electrostatic forces produced on the center plate by the differential voltage between the top and bottom plates, and the feedback voltage on the center plate, will force the center plate back to its normalized position as given in Eq. (7.9). Other methods that have been used for closed-loop operation are pulse width modulation (PWM), and delta sigma modulation (DSM).

The block diagram and waveforms of a PWM system are shown in Fig. 7.18. In this case, the center plate is held at a fixed voltage (0). The output of the integrator is amplified and converted into a PWM signal (VP), this signal and the inverted signal (VPN) are fed to the top and bottom plates of the sensor. The leading edges of the VP and VPN signals are used to sense the position of the middle plate. The electrostatic force generated by the voltage × time differential between the middle plate and the top and bottom plates, will act on the middle plate to counterbalance the forces on the plate due to acceleration. With zero acceleration, the PWM signal has a 50 percent duty cycle, so that the resulting electrostatic forces on the seismic mass are zero. The transfer function of the PWM system is given by

$$\text{Duty cycle} = \frac{\text{Acc} \times g \times d}{C \times V_{\text{REF}}^2} \tag{7.10}$$

PETITIONER'S EXHIBIT 1002
US PATENT NO. 6,581,565

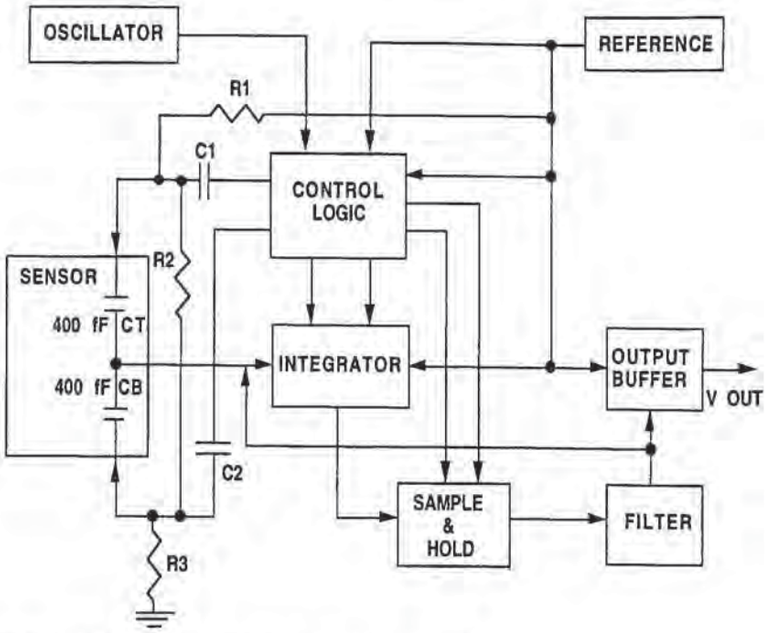


FIGURE 7.17 Block diagram of analog closed-loop system.

where g = gravitational constant
d = plate spacing
C = plate capacitance

The output can either be the PWM digital signal, or an analog output (obtained by feeding the PWM signal through a low pass filter).

Figure 7.19 shows the block diagram and waveforms of a DSM system. In this case, the middle plate is held at VF (volts). As can be seen, transient edges of the plate-drive waveforms are used for sensing the position of the center plate. The output from the integrator is fed to a comparator, whose output is then clocked into a latch where it sets up a "1" or a "0" (high or low) depending on the output from the integrator. The output from the latch is used to apply a voltage V_{REF} to the appropriate top or bottom capacitor plate, so that the electrostatic forces generated by the voltage V_{REF} – VF will maintain the center plate in its no-load position. The one-bit serial data stream from the latch can be fed directly to the MCU, or fed via a decimator circuit (which will convert the data into an 8-bit word) to the MCU. Alternatively, an LPF can be used to convert the data into an analog output. Bipolar or CMOS circuits can be used for signal conditioning. However, CMOS signal conditioning has the following advantages: a very high input impedance, good switching characteristics, low power requirements, small size, compatibility with MCU processes with the prospect of future integration, switched capacitor filters are available for noise reduction and bandwidth control, and EPROM technology is available for trimming (see Fig. 7.14). BiMOS circuits have also been used for signal conditioning.[6] In the BiMOS circuits, thin-film resistors are used to enable laser trimming of the zero offset and voltage reference; external capacitors and resistors are used for filtering and gain control.

Single vs. Multichip Control Circuits. The processing of sensors is not completely compatible with IC fabrication. Consequently, for the integration of sensors and ICs, a number of additional steps are required, which can have a detrimental effect on yields. The question then arises as to which is the most cost effective: a sensor die plus a control die with the additional cost of assembly, or a monolithic approach.

PETITIONER'S EXHIBIT 1002
US PATENT NO. 6,581,565

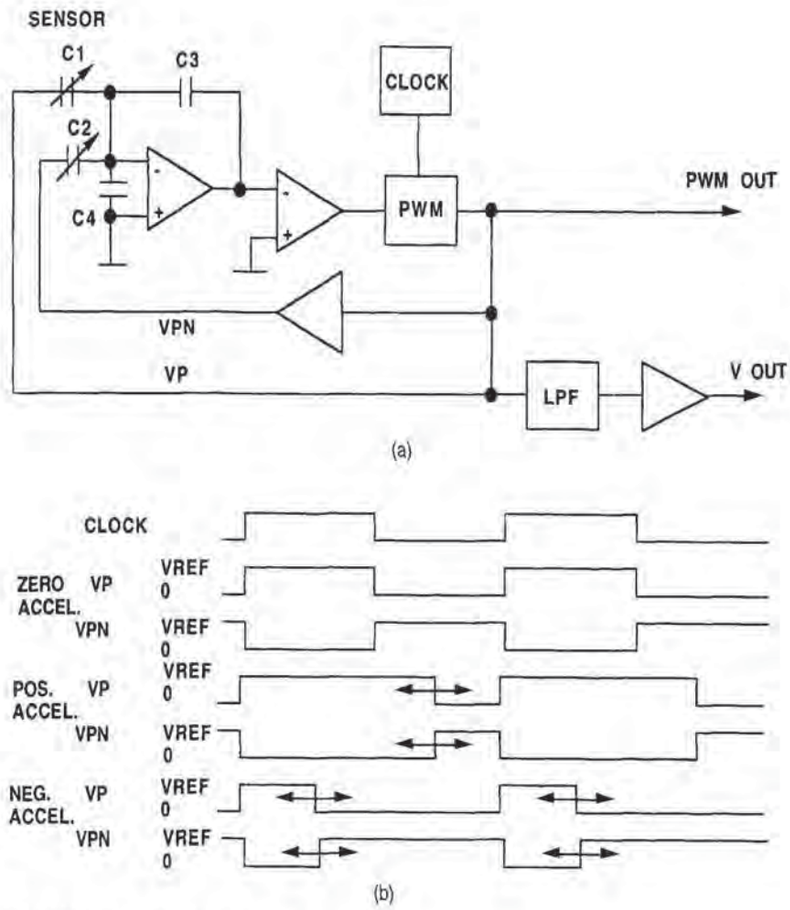


FIGURE 7.18 PWM block diagram.

In the case of micromachined devices, there are a number of advantages to using the dual-chip approach, such as flexibility, in that one type of sensor can be interfaced with a number of different types of control die, or several types of sensors can be interfaced with one type of control die. This provides a variety of input and output options. The control die and sensor can be developed simultaneously, minimizing development time. Problem solving is made easier, and the processing for both die can be optimized for performance. With the two-die approach, the sensor can also be capped and sealed during processing in a clean room atmosphere, thus eliminating contaminants and particles for good longevity. In the monolithic approach, this is not the case. In the monolithic approach, changes required to improve one section can affect the other section, which may then require additional changes in that section. The main disadvantage of the dual-chip approach is the introduction of parasitic capacitances. However, these can be addressed by existing control circuit design techniques.

7.5 AUTOMOTIVE APPLICATIONS FOR ACCELEROMETERS

Accelerometers have a wide variety of uses in the automobile. The initial application is as a crash sensor for air bag deployment. This application is normally associated with head-on collisions, but can also be applied to rear-end impact collisions to prevent rebound impact between the passengers and the windshield. An extension of this application is the use of

PETITIONER'S EXHIBIT 1002
US PATENT NO. 6,581,565

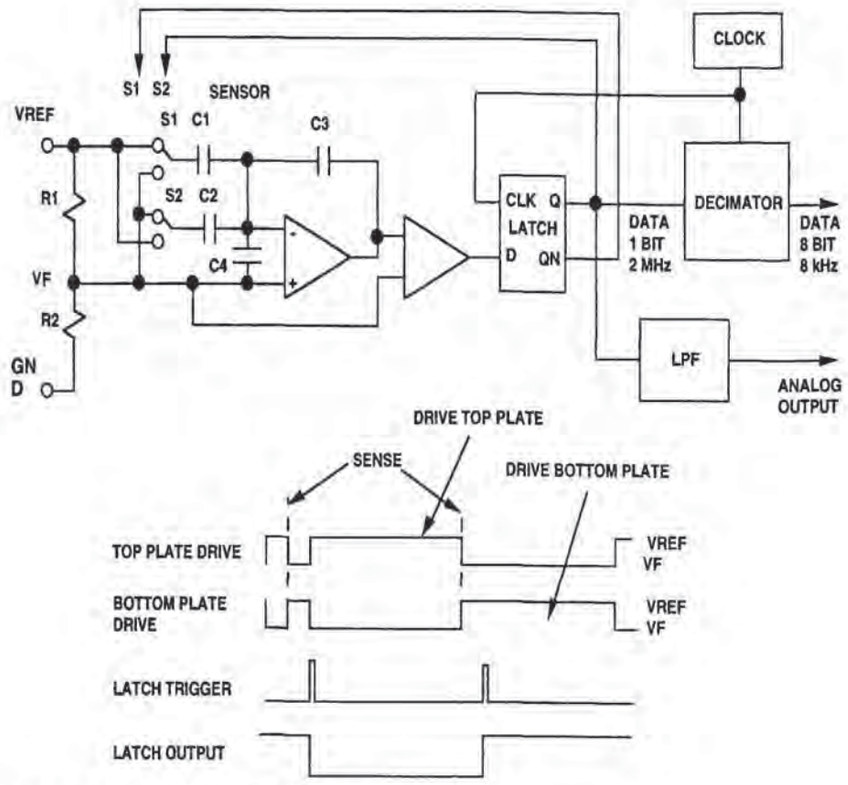


FIGURE 7.19 *Block diagram of Delta Sigma Modulator.*

accelerometers for the detection of side impact. This application will require additional air bags to the side of the occupants. Other low g linear accelerometers are being developed for ride control, ABS, traction, and inertial navigation applications.

Solid state acceleration sensors have special mounting requirements that are different from normal integrated circuits. These are to ensure that acceleration forces are transmitted to the sensor package. An advantage of the solid state device is self-test features for diagnostics. In acceleration applications, the devices are required to operate over the temperature range –40 to 85 °C (125 °C under the hood), and to withstand >2000 *g* shock. Other similar devices that have application in the automotive arena are vibration devices.

7.5.1 Air Bag Deployment Application

Crash sensors that use mechanical switches (sensors) are typically located some 40 cm from the point of impact, which necessitates the use of multiple sensors (normally 3 to 5 sensors are used in multipoint sensing) for crash sensing and air bag deployment. These devices are velocity change detectors, and are calibrated to make contact when the change of velocity in the passenger compartment is at least 20 km/h, this being the velocity change at which the front seat occupants will strike the windshield.

A centrally located analog sensor can be used as a crash sensor (single point). In the case of a centrally located accelerometer, the g level to be sensed is lower than that of a point-of-impact device. However, only one device is required to monitor the crash signature. This signature will vary with different types of chassis and different types of impacts. Consequently, an MCU is used to monitor the output of the accelerometer to determine if a crash has occurred. The typical output of a centrally located accelerometer during a 48 km/h crash is shown in Fig. 7.20. Deceleration of the vehicle and occupant displacement are also shown. At 48 km/h, the sensor has 20 ms to detect the crash and trigger the air bag. This results in infla-

PETITIONER'S EXHIBIT 1002
US PATENT NO. 6,581,565

tion of the air bag 50 ms after impact, at which time the occupant has moved about 18 cm or approximately halfway to the windshield and at the contact point with the inflated air bag. During the initial 20 ms, deceleration can reach 20 *g*, but the average is about 5 *g* when the air bag is triggered. The centrally located accelerometer can take one of several forms: a piezoelectric sensor, a piezoresistive device, or a capacitive sensor.

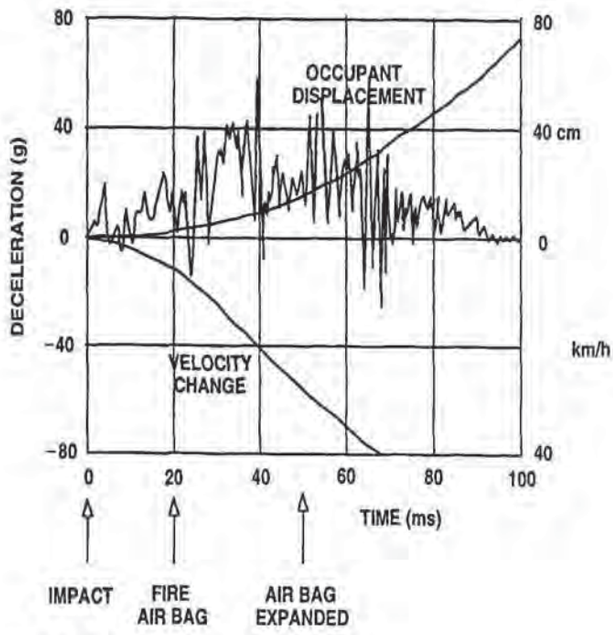


FIGURE 7.20 Typical 48 km/h crash waveform.

The centrally located accelerometer has a number of performance advantages over its mechanical counterpart. These are the reduction in the number of sensors and required bussing, which makes the centrally located system much more cost effective. There is an improvement in sensing and signal-processing accuracy with the single-point sensing accelerometer over the mechanical sensor. This gives a better-defined trigger point and overall improved performance across different chassis types. Capacitive sensors appear to have the edge in this application, because they have the potential of being cost effective, meet the requirements of the application, and have self-test features plus diagnostics available. In this application, a typical accelerometer specification is ±50 *g* full-scale output, accuracy ±5 percent over temperature, bandwidth dc to 750 Hz, and cross-axis sensitivity <3 percent. During impact, the crash sensor can also be used for seat belt locking.

7.5.2 Ride Control Application

In ride control systems, the leaf or coil springs located on the axles are replaced by four *wheel stations,* which form an active suspension. Each wheel station contains an oil-filled cylinder with a piston to set the distance of the frame above the axles and to isolate the frame from axle vibration. This is achieved using a servo feedback system. When a vehicle with conventional suspension encounters a foreign object on the highway, the load on the wheel increases as it moves up to negotiate the obstacle. This load increase makes the vehicle rise up. With a fully active suspension, the increase in load is detected and a servo valve is opened to transfer the necessary amount of oil from the appropriate cylinder to a storage container. Consequently, the load exerted on the chassis by each wheel is maintained at its specific level and

PETITIONER'S EXHIBIT 1002
US PATENT NO. 6,581,565

the chassis remains at its static level. After the object has been traversed, oil is pumped back into the cylinder to reestablish the static load conditions.

An alternative to the active suspension is the adaptive suspension system. In this case, information from the front wheels is gathered and used to predict road conditions for the control of the rear wheels. The advantage over the fully active suspension is one of cost, as the number of acceleration sensors is halved. During cornering, oil is also pumped into the outside wheel cylinders to minimize roll angle.[7]

A combination of sensors is used for active suspension. These are accelerometers, wheel speed sensors, chassis-to-ground sensing, and piston-level sensing in the suspension system. The low g accelerometers used on the axles of the four wheels to detect the load changes on the wheels have the following specifications: ±2 *g* full-scale, accuracy ±5 percent over temperature, bandwidth dc to 10 Hz, and cross-axis sensitivity <3 percent. The acceleration information and data from the wheel speed sensors is used to provide the information necessary for the MCU to operate the servo control valves. Hall effect, MRE, and opto sensors have been used for monitoring the level of the pistons in the wheel stations cylinders.

7.5.3 Vibration Applications

Lean-burn engines are being developed for improved emission levels and for better fuel economy (10 to 15 percent improvement). NO_x emissions are greatly reduced to meet federal standards. Lean-burn engines use high stoichiometric ratios; 20:1 and higher are necessary. At these ratios, combustion becomes unstable and torque fluctuations large. Consequently, antiknock and vibration sensors are required to supply the information necessary to the MCU, so that it can adjust the injected fuel amount and ignition timing for stability over widely varying conditions.

There are two types of solid state sensors that can be used in this application: piezoelectric devices and capacitively coupled vibration sensors. A typical vibration sensor contains a number of fingers of varying length which vibrate at their resonant frequencies when those frequencies are encountered. The resonance is capacitively coupled to the sensing circuit, and the outputs as shown are obtained. Optical sensors have also been used as antiknock sensors. In this case, the ignition spectrum is monitored for the detection of misfiring or knocking. Vibration sensors can also be used for vibration monitoring in maintenance applications.

7.5.4 Antilock Brake System Applications

In antilock brake systems, speed sensors are attached to all wheels to determine wheel rotation speed and slip differential between wheels. VR devices, as well as Hall effect and MRE devices, can be used in this application, as zero speed sensing is not required. VR devices have been used and shown to be cost effective in this application, but Hall effect and MRE devices are now being designed into these systems. Pressure sensors are used to monitor brake fluid pressure, and an accelerometer or ground-speed sensor can be used to provide information on changes in the vehicular speed. Brake pedal position and brake fluid pressure information are also required for control. All of this information is fed to an MCU, which processes the data and adjusts the brake fluid pressure to each wheel for optimum braking. Many of the elements of the ABS system can be used for the detection of lateral slippage on high-speed cornering, and can be used for traction and the direction of power to the wheels. Traction control applies in particular to slippery surfaces and with four-wheel-drive vehicles. Additional information over that used in ABS systems is required by the MCU for ASR applications, such as engine speed and throttle angle. In this application, servo feedback to the throttle may also be necessary.

A more cost-effective, but less accurate, system for ABS and ASR is the adaptive control system in which accelerometers are normally used to measure deceleration when braking, and

PETITIONER'S EXHIBIT 1002
US PATENT NO. 6,581,565

acceleration when the throttle is opened. If skidding occurs during braking, the brake pressure is reduced and adjusted for maximum deceleration, or the throttle adjusted for maximum traction. Typical specifications for the accelerometer required in this application are: ±1 g full-scale output, accuracy ±5 percent over temperature, bandwidth 0.5 to 50 Hz, and cross-axis sensitivity <3 percent.

7.6 NEW SENSING DEVICES

New cost-effective sensors are continually being developed. The technology and cost are often pushed by the application and volume requirements of the automotive industry and federal mandates. Today's silicon sensors and control electronics are limited in operating temperature to 150 °C to ensure long life of the devices. This operational temperature is adequate for most applications, but higher temperature operation may be required for sensors mounted in the engine compartment. The limit on the operating temperature of silicon devices can be extended to between 200 and 250 °C by the use of special isolation techniques such as dielectric isolation (this operating temperature applies to surface micromachined devices). For higher-temperature operation, alternative materials such as GaAs or SiC are being developed, but the cost of these devices limits their use at present.

A list of semiconductor conductor materials and maximum practical operating temperatures is given in Table 7.3. Higher operating temperatures have been reported but with poor longevity.

TABLE 7.3 Device Operating Temperatures

Material	Maximum practical operating temperature, °C
Si	150
Si (dielectric iso.)	250
GaAs	300
AlGaAs	350
GaP	400
SiC	500

7.6.1 New Rotational Speed-Sensing Devices

A number of new devices are being investigated to detect magnetic fields. These are flux gate, Weigand effect, magnetic transistor, and magnetic diode. The magnetic transistor at present is showing the most promise. The device operates on a similar principle to the Hall effect device. That is, the current division between split collectors (bipolar) or split drains (MOS) can be changed by a magnetic field. This current differential can then be detected and amplified to give an output voltage proportional to magnetic field strength. These devices can use either majority or minority carriers, and can be either vertical or lateral bipolar or MOS devices. The magnetic transistor has the potential of higher sensitivity than the Hall effect device.

Figure 7.21 shows the cross section of a lateral PNP magnetic transistor. The current from each collector is equal until a magnetic field is applied perpendicular to the surface of the device. The magnetic field causes an imbalance of current between the two collectors. Sensitivities with this type of structure have been reported as being an order of magnitude greater than in the Hall effect device.[8] Magnetic transistors and diodes can be directly integrated with the signal-conditioning circuits, which could make them very cost effective in future applications. A comparison of the magnetic transistor to other practical devices is given in Table 7.2.

PETITIONER'S EXHIBIT 1002
US PATENT NO. 6,581,565

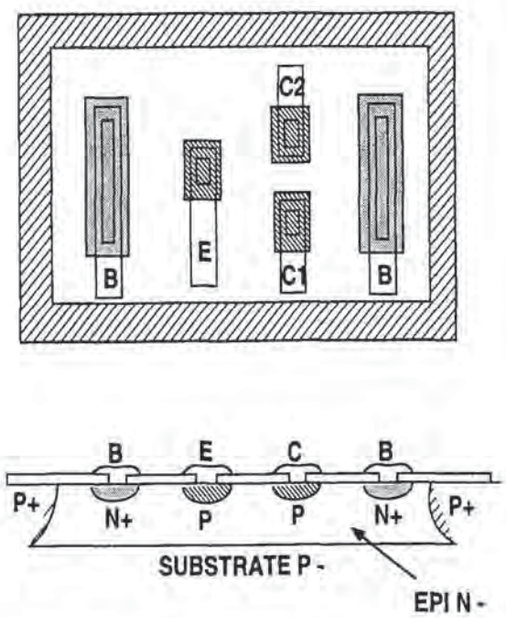


FIGURE 7.21 Cross section of a field-assisted *PNP* magnetic transistor.

7.6.2 New Linear Speed-Sensing Devices

A number of different sensing technologies can be used for distance, object detection, and approach speed measurements. Shown in Fig. 7.22 are the areas covered by blind-spot, rear, and forward-looking sensors. Ultrasonics, infrared, laser, and microwaves (radar) can be used in the detection of objects behind vehicles and in the blind areas. From a practical standpoint, no technology has come to the forefront. However, with new innovations in technology the situation may change very rapidly. Ultrasonics and infrared sensors are cost effective but degrade with inclement weather conditions such as ice, rain, snow, and the accumulation of road grime. Infrared devices are also color-sensitive, in that the sensitivity to shiny black objects is very low compared to other colors. Microwave devices appear to have the edge

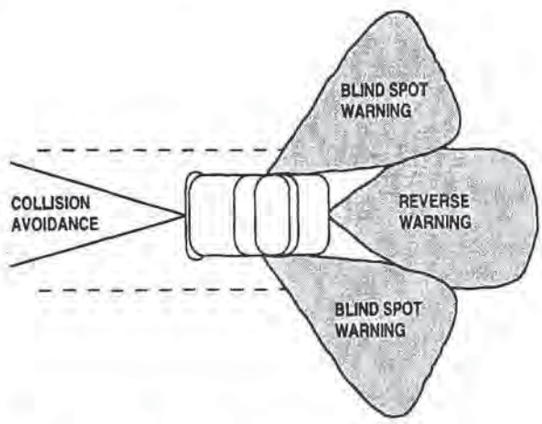


FIGURE 7.22 Collision-avoidance patterns.

PETITIONER'S EXHIBIT 1002
US PATENT NO. 6,581,565

when considering environmental conditions,[9] but are expensive, and radar can be affected by false return signals and clutter.

For the detection of obstacles and vehicles in front of a vehicle, the choice is between laser and microwaves due to the distances involved (up to 90 m). Microwaves have the disadvantage of high cost and large antenna size when considering available devices in the 60 GHz range. Frequencies greater than 100 GHz are preferred for acceptable antenna size. However, collision avoidance radar in the 76/77-GHz band has been developed in Europe. Collision avoidance radar in the 77, 94, and 144 GHz is being considered in the United States. A typical system uses a 38.5-GHz VCO (voltage controlled oscillator) with frequency-doubling to obtain about 40 mW of power at 77 GHz. A frequency-modulated continuous wave or pulse-modulated system can be used. The system uses GaAs devices to meet the frequency and power requirements. Lasers can be cost effective in this application, but also have their drawbacks: degradation of performance by fog, reflections from other light sources (sun, etc.), build-up of road grime on sensor surfaces, and poor reflecting surfaces at laser frequencies, such as grimy and shiny black surfaces.

7.6.3 New Inertial and Acceleration-Sensing Devices

Recent developments in solid state technology have made possible very small cost-effective devices to sense angular rotation. The implementation of one such gyroscopic device is shown in Fig. 7.23. This device is fabricated on a silicon substrate using surface micromachining techniques. In this case, three layers of polysilicon are used, with the first and third layers being fixed and the second layer free to vibrate about its center. The center is held in position by four spring arms attached to four mounting posts as shown. This device can sense rotation about the X and Y axes and sense acceleration in the direction of the Z axis. The center layer of polysilicon, driven by electrostatic forces, vibrates about the Z axis. These forces are produced by voltages applied between the fixed comb fingers and the comb fingers of the second polysilicon. Capacitor plates as shown are formed between the first and third polysilicon on the X and Y axes, and the second layer of polysilicon. Differential capacitive sensing techniques can then be used to sense any displacement of the vibrating disc caused by angular rotation. For example, if angular rotation takes place about the X axis, Coriolis forces produce a deflection of the disc about the Y axis. This deflection can be detected by the capacitor plates on the X axis. The sensing of the three functions is achieved by using a common sensing circuit that alternatively senses the X rotation, Y rotation, and acceleration. The gyroscope is designed to have a resolution of <10 degrees per hour for angular rate measurements, and an acceleration resolution of 0.5 mg.

7.7 FUTURE APPLICATIONS

New applications to increase creature comfort and safety are constantly being developed, but their rate of introduction will depend on the cost effectiveness of the technology, demand, and government mandates. Other concerns of automotive manufacturers are size, weight, power requirements, and adverse effects on styling and appearance. Many of the new sensor technologies are in their infancy, and thus are not yet cost effective on medium- and low-priced automobiles, but are being made available as options on luxury cars.

7.7.1 Future Rotational Speed-Sensing Applications

A future application for speed-sensing devices will be in continuously variable transmissions. In this application, engine and wheel speed, as well as torque, will be measured, and the infor-

PETITIONER'S EXHIBIT 1002
US PATENT NO. 6,581,565

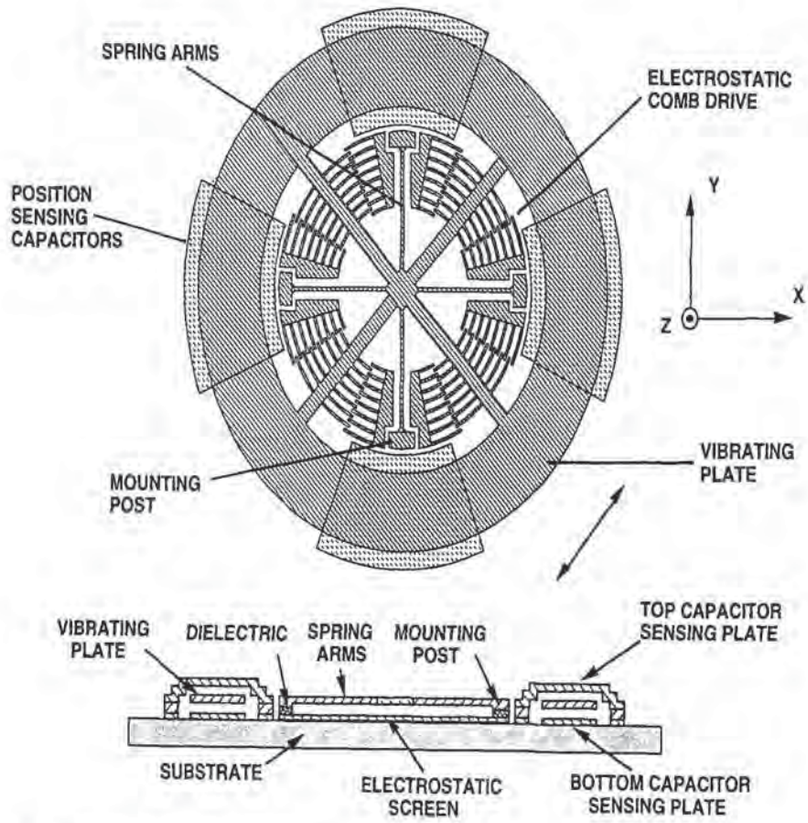


FIGURE 7.23 Solid state gyroscope.

mation processed by an MCU to optimize transmission ratios for engine performance and efficiency. All-wheel steering is also under development, and requires speed-sensing information, in addition to steering, front-, and rear-wheel angle position data for processing and control.

7.7.2 Future Linear Speed-Sensing Applications

Another application that has been developed is the use of speed- and distance-measuring devices for collision avoidance. These devices fall into three categories: near-obstacle detection (rear), blind-spot detection, and semiautomatic frontal object detection and control[9] (see Fig. 7.22).

Near-obstacle detection is used to prevent accidents during reversing. Blind-spot detection is used to prevent accidents due to careless lane changing, and when backing out of a driveway, garage, or alley into traffic. The semiautomatic frontal detection is a long-range system. The distance and closing speed between vehicles, or between a vehicle and a fixed object, can be measured and the speed adjusted as necessary to avoid a collision,[10] or the driver can be warned of impending danger. An addition to this is to monitor road surface conditions for friction—for example, dry roads compared to wet or icy roads—and also to use this information to adjust approach speeds and distance. Without collision avoidance, road condition monitoring can be used to caution vehicle operators. Collision avoidance systems can be used to minimize collisions, or can be used to operate protection systems before an unavoidable collision happens to protect the automobile passengers. In this case, vehicles closing at or approaching an obstacle at 80 km/h will be less than 7 m apart before a collision-is-imminent

PETITIONER'S EXHIBIT 1002
US PATENT NO. 6,581,565

determination can be made. This gives 200 ms decision-making time for the system MCU. This is, however, long compared to today's air bag deployment systems, which have 20 ms decision-making time after the event. In the future, an idealistic system may be a combination of the two systems.

7.7.3 Future Acceleration Applications

One of the future applications being considered is the expansion of the air bag system to include side impact protection. The sensor used for crash sensing is unidirectional, so that it can only detect forward impact. A similar sensor, mounted perpendicular to the air bag sensor, can be added to the system to detect side impact and to deploy protection for the passengers. This device will typically require a 250-*g* accelerometer. Another application for accelerometers is to detect slippage during cornering in advanced steering systems. These systems will employ a low-*g* accelerometer (1–2 *g*).

7.7.4 Inertial Navigation Applications

A number of inertial navigation systems are being developed for short- and long-range travel. Long-range inertial navigation systems normally obtain their location by using a triangulation method. This method references three navigation satellites with known locations in fixed orbits. However, there are certain conditions under which contact with all three satellites is lost. This occurs when the vehicle is in the shadow of tall buildings or high hills, and triangulation is not possible. Under these conditions, the guidance system has to rely on such devices as gyroscopes, which sense angular rotation or change in direction, and/or monitor vehicular motion relative to the road.

Short-range inertial navigation systems or inertial measurement units (IMU) rely to a large extent on high-accuracy accelerometers and gyroscopes. A typical accelerometer specification for this application is: ±2-*g* full-scale output, accuracy 0.5 percent over temperature, bandwidth dc to 20 Hz, and a cross-axis sensitivity <0.5 percent. A centrally located IMU can be expanded to cover other applications such as suspension, ABS, ASR, and working with crash avoidance sensors. This may be the way to handle cost-effective system design in the future. The IMU can also be designed to provide location data for intelligent vehicle highway systems. These systems (Prometheus,[11] Amtics[12]) improve travel efficiency and reduce fuel consumption and pollution by selecting the optimum route to a given destination. The route is chosen to avoid traffic congestion, road construction, and accidents (see Chap. 29).

7.8 SUMMARY

In this chapter, a number of speed-sensing devices, both rotary and linear, have been described, together with potential applications. VR, MRE, Hall effect, and opto devices (possibly magnetic transistor in future applications) can be used in rotational applications for engine control, transmission, and wheel speed sensing. Of these devices, Hall effect, VR, and opto have been widely used. With the tendency for direct pickoff, optical devices may become impractical. MRE devices are being designed in and will become a serious contender to the Hall effect device. In linear applications for crash avoidance, microwave devices have the edge over performance and optical devices in terms of cost. However, as the cost of microwave devices declines, they could become cost effective. For blind-area alert and reversing obstacle detection, ultrasonics and infrared devices are cost effective, but performance degrades during inclement weather.

PETITIONER'S EXHIBIT 1002
US PATENT NO. 6,581,565

The accelerometer has possibly the greatest potential for applications in the automobile. These applications range from crash sensing, ride control, ABS, and ASR to IMU systems. Accelerometers needed will range in sensitivities from 50 *g* in crash sensing to 1 *g* in the IMU. Advances in technology are providing a number of new sensors that are showing potential, such as the magneto transistor and the micromachined gyroscope. To summarize, Figs. 7.24 and 7.25 show the types of sensors used in specific applications, and the technologies used for specific sensors. As can be seen, one type of sensor can be used in a number of applications. In applications where a sensor output is shared, care must be taken to ensure that a failure in one system does not disable the sensor or other systems. Because of the similarities in several of the systems and the use of shared sensors, the greatest potential for cost-effective system design is a single control system. The IMU shows great potential to be the controller for ride control, ABS, ASR, four-wheel-drive, and steering applications. The rate of introduction of new sensors and systems will depend on federal mandates, customer demand, and the need to improve engine fuel efficiency and to reduce emissions.

GLOSSARY

Adaptive suspension A suspension system that monitors motion of the front wheels and adjusts the suspension of the rear axle accordingly.

Arntics Acronym for Advanced Mobile Traffic Information and Communication System.

ASR (traction) A system to prevent wheel spin on slippery surfaces, to give maximum traction and acceleration.

Sensor / Application	Air Bag Deployment	Ride Control	ABS	Engine Control	Transmission	4 Wheel Drive	All Wheel Stearing	Engine Vibrarion	Cruise Control	Seat Belts	Power Steering Assist	Traction (ASR)	Collision Avoidance	Obstacle Detection	Inertial Navigation
Speed Rotation	▨	▨	▨	▨	▨	▨	▨		▨		▨	▨			
Speed Linear			□		□				□		□	□	□	□	□
Acceleration	▨	▨	▨	▨						▨		▨			▨
Vibration								▨							
Angular Rotation															▨

▨ USED □ MAY BE USED

FIGURE 7.24 Sensor applications.

PETITIONER'S EXHIBIT 1002
US PATENT NO. 6,581,565

Measurand / Sensing Technique	Mechanical	Piezoelectric	Piezoresistive	Capacitive	Optical	Infrared	Radar	Laser	Ultrasonic	Hall Effect	Variable Reluctance	Magnetoresistive
Speed Rotation					☒					☒	☒	☒
Speed Linear						☒	☒	☒	☒			
Acceleration	☒	☒	☒	☒								
Vibration		☒		☒								
Angular Rotation				☒								

FIGURE 7.25 Sensor technologies.

Coriolis forces Forces exerted by a spinning body to oppose any motion at right angles to the axle.

Crash signature Shock waveform projected through a chassis during a collision.

Inertial navigation Guidance system giving accurate location.

IMU (inertial measurement unit) System used for guidance between two locations indicates road hazards and delays.

Lean burn Engine with high compression ratios and high air-to-fuel ratios for increased efficiency and low emissions.

Micromachining Manufacturing technology for micromechanical structures using chemical etching techniques.

NO_x Chemical symbol for oxides of nitrogen.

Prometheus Acronym for PROgraM for a European Traffic with Highest Efficiency and Unprecedented Safety.

Switched capacitor filter Technique for switching capacitors to simulate high-value resistors for low-frequency filters to minimize size.

REFERENCES

1. Osamu Ina, Yoshimi Yoshino, and Makio Lida, "Recent Intelligent Sensor Technology in Japan," S.A.E. paper 891709, 1989.
2. D. E. Bergfried, Mattes, B., and Rutz, R., "Electronic Crash Sensors for Restraint Systems," *Proceedings of the International Congress on Transportation Electronics,* Detroit, Oct. 1990, pp. 169–177.

PETITIONER'S EXHIBIT 1002
US PATENT NO. 6,581,565

3. E. Peeters, Vergote, S., Puers, B., and Sansen, W., "A Highly Symmetrical Capacitive Microaccelerometer with Single Degree of Freedom Response," *Tranducers 91,* 1991, pp. 97–103.
4. J. T. Suminto, "A Simple High Performance Piezoresistive Accelerometer," *Transducers 91,* 1991, pp. 104–107.
5. J. C. Cole, "A New Capacitive Technology for Low-Cost Accelerometer Applications," *Sensors Expo. International,* 1989.
6. T. A. Core, Tsang, W. K., and Sherman, S. J., "Fabrication Technology for an Integrated Surface-Micromachined Sensor," *Solid State Technology,* Oct. 1993, pp. 39–47.
7. H. Wallentowitz, "Scope for the Integration of Powertrain and Chassis Control Systems: Traction Control—All Wheel Drive—Active Suspension," *Proceedings of the International Conference on Transportation Electronics,* S.A.E. paper 901168, 1990.
8. H. Kaneko, Muro, H., and French, P. J., "Optimization of Bipolar Magneto-Transistors," *Micro Systems Technologies 90,* 1990, pp. 599–604.
9. L. Raffaelli, Stewart, E., Borelli, J., and Quimby, R., "Monolithic Components for 77 GHz Automotive Collision Avoidance Radars," *Proceedings Sensors Expo,* 1993, pp. 261–268.
10. S. Aono, "Electronic Applications for Enhancing Automotive Safety," *Proceedings of the International Conference on Transportation Electronics,* SAE 901137, 1990, pp. 179–186.
11. J. Hellaker, "Prometheus-Strategy," *Proceedings of the International Congress Transportation Electronics,* SAE 901139, 1990, pp. 195–200.
12. H. Okamoto, and Hase, M., "The Progress of Amtics-Advanced Mobile Traffic Information and Communication System," *Proceedings of the International Congress Transportation Electronics,* SAE 901142, 1990, pp. 217–224.

ABOUT THE AUTHOR

William C. Dunn is a member of the technical staff in the Advanced Custom Technologies group at Motorola's Semiconductor Product Sector in Phoenix, Arizona. He has over 30 years' experience in circuit design and systems engineering. For the past 15 years he has been involved in the development of semiconductor sensors, smart power devices, and control systems for the automotive market. Prior to joining Motorola, he worked for several large corporations in the United Kingdom and United States, has written over 30 papers, and has over 30 patents issued and pending on mechanical sensor structures, semiconductor technology, and circuit design.

PETITIONER'S EXHIBIT 1002
US PATENT NO. 6,581,565

PETITIONER'S EXHIBIT 1002
US PATENT NO. 6,581,565

CHAPTER 8
ENGINE KNOCK SENSORS

William G. Wolber
Executive Engineer
Cummins Electronics Co., Inc.

8.1 INTRODUCTION

Knock is a phenomenon characterized by undesirable structural vibration and noise generation and is peculiar to spark-ignited engines. Knock is undesirable both from a customer acceptance standpoint and also because severe knock can cause engine damage. The terms *ping* (light, barely observable knock) and *predetonation* (knock caused by ignition of the charge slightly before the full ignition of the flame front by the spark plug) are also commonly used in the industry, and not always with precision.

Historically, knock became an important engine phenomenon in the 1930s. In their search for performance improvements, designers of spark-ignited engines increased compression ratios beyond the capabilities of the gasoline formulations available to provide smooth, knock-free combustion. The discovery of gasoline additives such as tetraethyl lead, which improve the stability of the combustion process primarily by decreasing burn rate, permitted the fuel suppliers to provide a range of fuel knock properties at the pump to match with the range of engine requirements. As a result, by 1950, knock was not regarded as a significant engine performance limiting parameter since the car company could specify what fuel should be selected, ranging from "regular" to "super premium" grades. A blending fuel pump was even provided by one fuel company which allowed the operator of the vehicle to select exactly what grade of fuel he or she wished to use from a selection of six grades.

In the late 1960s, the situation began to change drastically. In response to public concern about air quality and health, legislation on automotive emissions became a new constraint on automotive engine design, first in the United States and more recently worldwide. The use of fuel additives to improve gasoline knock characteristics fell into disfavor for two reasons:

- Many of the better additives resulted in combustion products not desirable in the air. For example, most lead compounds are toxic at low levels to human and animal life.
- As engine designers strove to provide lower engine emissions, the use of the three-way catalytic converter cleanup device in the exhaust system became nearly universal. Unfortunately, most good fuel additives that improve knock characteristics poison the catalyst of the converter, rendering it ineffective. Also, many engine controls began to make use of the oxygen sensor feedback control loop. The catalyst on the oxygen sensor also is poisoned by the better additives.

This situation led to gradually more stringent federal regulation of the fuel industry, a trend which, in the end, legislated fuels with knock-improving additives completely off the

PETITIONER'S EXHIBIT 1002
US PATENT NO. 6,581,565

market, so that by the mid 1980s, all spark-ignited automobile engines in the United States were being operated using lead-free gasoline. Of course, as leaded gasoline disappeared, the knock phenomenon returned. The auto industry knew what to do—lower compression ratios—but this step alone has accompanying negative consequences, such as lower fuel economy. Thus, the situation was one driven by the need to optimize between several principal goals: emission regulations, fuel supply characteristics, fuel economy goals, customer acceptability, and vehicle performance.

8.2 THE KNOCK PHENOMENON

8.2.1 Definition

Spark-ignited engine knock has been defined as "an undesirable mode of combustion that originates spontaneously and sporadically in the engine, producing sharp pressure pulses associated with a vibratory movement of the charge and the characteristic sound from which the phenomenon derives its name."[1] This definition at once conveys some of the difficulties of measuring the phenomenon and devising engine controls to minimize it. First, the ultimate standard is the reaction of the human to the vibration felt or the sound heard as a result of the knock. An attempt to measure the cause of the phenomenon leads one to the difficult problem of observing pressure waves in the cylinder. In fact, over the years these difficulties led the industry to devise an experimental comparison measurement technique which measured the octane rating of the *fuel*, not of the engine.

8.2.2 Laboratory Measurements

The CFR Engine. The basic comparison method which evolved for rating fuel knock quality involved the use of a simple, single-cylinder, spark-ignited engine called the CFR engine, and a pure hydrocarbon fuel—100 percent isooctane. Researchers discovered that they could reproduce knock phenomenon, laboratory to laboratory, by running this engine under specified conditions with this fuel.

Gasoline Octane Rating. A system of rating the knock characteristics of fuels, called the octane rating, was developed based on a comparison of the CFR engine performance with the test fuel compared to pure isooctane. On this scale, osooctane has an octane rating of 100; passenger car engine fuels ranged from the high 70s for "regular" to the high 90s for "super premium." (Fuel formulations with an octane rating over 100 were possible but were used mainly for aircraft engines.)

As the industry strove to put knock on a solid engineering basis, methods of measuring the resulting phenomena on the CFR engine, and commercial engines as well, were developed. The parameter on which the industry standardized was "jerk," the third-time derivative of engine block displacement. Scales evolved for comparing the relative knock performance of fuels and of engines based on the output of this kind of sensor. Much work was also done to correlate jerk sensor measurements with cylinder pressure phenomena.

The fundamental resonant frequency of the knock-generated pressure signal is dependent on engine cylinder geometry and the speed of sound in the charge gas. The structural vibration characteristics of the engine block that are excited by the fundamental knock event are determined by the engine block transfer function. Testing conducted on one cylinder of a six-cylinder spark-ignited engine demonstrates that high-frequency structural vibration components are good indicators of knock, despite the relatively low frequency high-pressure excitation event.[2] Structural vibration induced by mechanical events, such as valves opening

PETITIONER'S EXHIBIT 1002
US PATENT NO. 6,581,565

and closing, introduces noise that can be confused with knock-induced vibrations. Careful signal analysis is required to overcome a sometimes poor signal-to-noise ratio.

The reverberation resonance of the cylinder typically lies in the range between 2 and 12 kHz. A useful rough estimate of the knock frequency for a given engine cylinder geometry is given by Draper's equation[3]:

$$\text{fr} = \frac{\text{Pmn} \times C}{\pi B} \tag{8.1}$$

where fr is the knock resonant frequency
Pmn is a vibration mode constant
C is the velocity of sound in the gas in the cylinder
and B is the radius of the cylinder

Using this equation, assuming that the average gas temperature is 2000 K so that C is 900 m/s, the first circumferential mode resonant frequency is estimated at 5.75 kHz for a cylinder of 10-cm bore.

As better cylinder pressure sensors have become available, cylinder pressure wave measurements, along with signal analysis techniques for deriving a knock rating number, have supplemented jerk measurements in the laboratory. The most popular signal analysis approach is to declare the maximum amplitude or peak-to-peak value of the bandpass filtered pressure data as a knock number, usually referred to as *knock intensity.*

Other ways of describing knock level are the root-mean square, mean square, or integral of the absolute value of the bandpass pressure oscillations during the knocking portions of the cycle. The spectral power of the pressure transformed into the frequency domain has been used for measurement. Derivative-based methods have also been established, based on rapid changes of cylinder pressure during the knock phenomenon, using the first, second, and third derivatives of the cylinder pressure history.

8.2.3 On-Board Knock Control

Improved Fuel Economy by Lowering Engine Compression Ratio. As engine control using microcomputers became established in the late 1970s and early 1980s for gasoline passenger car engines, and the octane rating of the fuels available for them dropped below 90, the automotive industry responded by lowering engine compression ratios. However, some of these smaller engines were equipped with turbochargers to recover some of the lost performance at wide open throttle. It was found that these engines could experience destructive high-speed knock at maximum speed and power. Not only were the knock reverberations in the cylinder large, but they were modulating a high base pressure wave. This could occur because the extra boost pressure from the turbocharger permits additional fuel to be metered to the engine without violating emissions restrictions on the control, since the amount of oxygen available to react with the fuel is greater. This could result in knock wave peaks exceeding the cylinder head pressure limit, as well as excessive vibration of the entire engine.

The knock occurring at wide open throttle had to be decreased, but retaining the additional power from the turbocharger at part throttle was very desirable. The electronic control was available to modulate the amount of fuel injected during the dangerous engine state; however, a means of sensing engine knock on-board in real time was needed. The sensors used are described in Sec. 8.3. The control operates by sensing that knock is over the permissible limit, and then reduces it either by retarding ignition timing or by opening a wastegate valve on the boosted manifold pressure.

Improved Fuel Economy by Raising Compression Ratio. Following the successful implementation of knock limit control on turbocharged engines, considerable experimentation was carried out to assess whether or not there is value in applying knock limit control to naturally aspirated spark-ignited engines. It was determined that if the engine knock was always kept

PETITIONER'S EXHIBIT 1002
US PATENT NO. 6,581,565

less than an empirically determined limit for that type of engine and stored in the microcomputer control memory, then the knock level would not be objectionable even to the more critical car operators. Moreover, this could be accomplished while raising the compression ratio one full number—for example, from 8:1 to 9:1. If used to improve fuel economy, this change results in a 3 percent improvement in the corporate average fleet economy (CAFE) rating for that model/engine combination. At today's CAFE values, this is close to a one-mile-per-gallon improvement.

CAFE values are extremely important to a passenger car original equipment manufacturer (OEM). The larger, heavier luxury cars cannot achieve as low a CAFE value as the smaller, lighter cars. However, the larger cars are more profitable to produce. Thus, the mix of cars produced by an OEM can depend on just how close his CAFE results are coming to the mandated value. A way of improving fuel economy without downsizing, adding significant cost, or losing performance is very valuable.

Starting in the early 1980s, more and more passenger cars had a knock limit control and increased compression ratio. Such a change is usually scheduled at a time when the engine design and the tooling to make the engine are changing for other reasons. By 1990, 25 to 30 percent of the naturally aspirated passenger car engines produced in the United States (and all of the turbocharged engines) featured knock limit control.

8.2.4 Measurement and Control System Considerations

In addition to the problem of developing a suitable on-board sensor for knock, once the parameter to use had been selected, a number of other considerations had to be settled in effecting a satisfactory control. It was already pointed out that engine knock can be reduced either by retarding spark timing or by opening a manifold boost wastegate valve. In the United States, the candidate engines already had electronic control of spark timing, so that all that was needed to implement the knock control was an easily added change in the timing command in the control microcomputer. However, many control strategies exist for processing the knock signal. Perhaps the most elaborate of these was implemented on the first turbocharged engine knock limit control:

- The vibration frequency of the knock is specific to the engine model but lies between 2 and 12 kHz for passenger car engines. The sensor used was mechanically bandpass-tuned to match this characteristic with a Q of about 2.
- The major knock reverberations for a given cylinder occur during a time window that starts shortly after the cylinder reaches top dead center and ends 60 to 90 crank-angle degrees later. The control opened a signal gate to allow the knock signal to pass through and be averaged only when the engine was in these time windows.
- To prevent engine damage, whenever the knock signature exceeded the limit value, the control very rapidly retarded ignition by as much as 10 crank-angle degrees so that the engine would not be in severe knock even for the next few cylinder events. Then the control would very slowly advance the timing until the process repeated. This resulted in somewhat less than best engine performance but assured a comfortable margin of safety for the engine.
- The knock threshold limit in the control was modulated to increase with engine speed so as to compensate for greater noise background at high engine speed.

8.3 TECHNOLOGIES FOR SENSING KNOCK

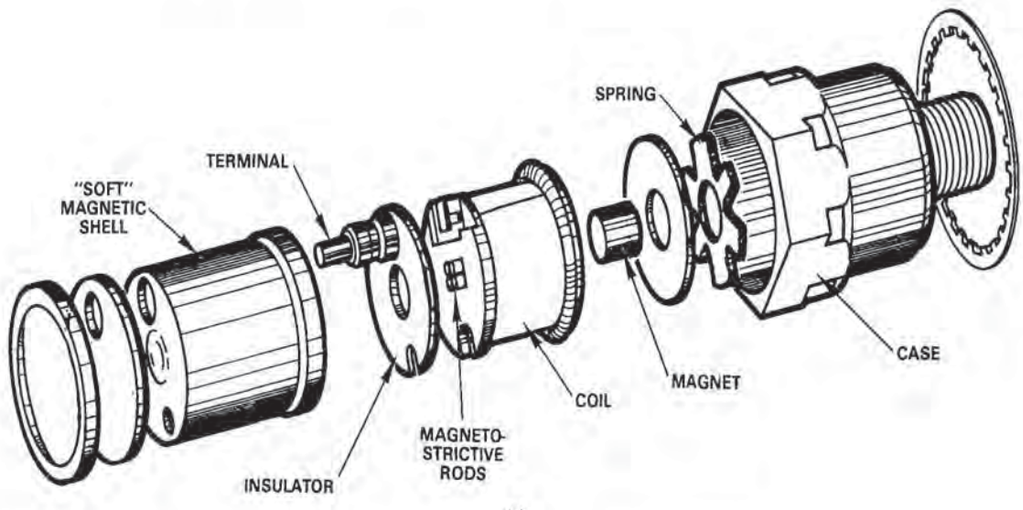
A number of different parameters have been selected for measuring knock in real time on board, and sensors have been developed for this purpose. It must be recognized that these

PETITIONER'S EXHIBIT 1002
US PATENT NO. 6,581,565

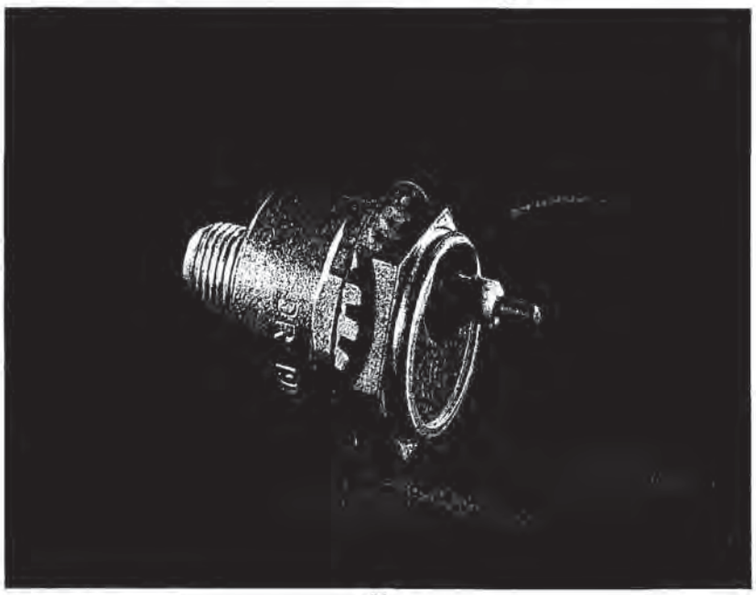
sensors measure the magnitude of a consequential parameter driven by the knock, rather than the knock phenomenon itself. The overall effectiveness of the control is therefore determined not only by the intrinsic performance and stability of the sensor and control, but also by how robust the chain of causality is between the knock phenomenon and the parameter measured.

8.3.1 Jerk Sensors

Naturally enough, the first turbocharged engine knock limit control used a jerk sensor, a productionized version of the kind of sensor used for laboratory CFR engine testing. An exploded view of this sensor is shown in Fig. 8.1.



(a)



(b)

FIGURE 8.1 (*a*) An exploded view of a jerk sensor, and (*b*) a photograph of the sensor.

PETITIONER'S EXHIBIT 1002
US PATENT NO. 6,581,565

Referring to the exploded view, it must be understood that when the sensor is fully assembled, the spider spring is preloaded, and all parts of the sensor except the coil cover are in compression. The nickel alloy magnetostrictive rods are biased mechanically in lengthwise compression and magnetically by the field impressed through the rods from the permanent magnet, returning through the ferromagnetic soft iron coil cover. The nickel alloy rods are the highest reluctance element in this magnetic circuit, and are in magnetic saturation.

The vibrations which are picked up and transmitted from the engine block through the mounting stud appear in the nickel alloy rods. These rods are of such a length that they comprise a broad passband mechanically resonant element. The compressive mechanical bias is sufficiently strong that the compression and rarefraction waves picked up are never large enough to take the rods out of net compression. The waves present in the rods therefore linearly modulate the magnetic reluctance of the magnetic circuit.

The many-turn coil wound around the magnetostrictive rods generates a voltage proportional to the rate of change of the magnetic flux; the flux, in turn, is inversely proportional to the magnetic reluctance of the rods. Since the vibrations picked up are already due to accelerations from the knock reverberations transmitted through the engine block, the voltage from the coil represents the third-time derivative of displacement, or jerk.

The vibration signal from a knocking engine is present virtually everywhere on the engine block, with signals from all cylinders superimposed. For passenger car engines, which rarely have more than eight cylinders, the major part of the knock signatures from the successive cylinder events are not superimposed in time, but rather consecutive without overlap. The time delay due to the distance from the cylinder to the sensor is always much less than 1 ms, whereas the cylinder-to-cylinder time is 2.5 ms even for an eight-cylinder engine at 6000 rpm.

However, the *absolute amplitude* of the knock signal does vary from location to location on the block. There is no best place to mount the sensor; rather, a site with a strong amplitude should be selected for a given engine model, and the sensor should always be mounted at that point on that engine model. The knock threshold is experimentally determined on that engine model with the sensor mounted at that location.

The method used for processing the knock signal and effecting control was described in Sec. 8.2.4. As time has gone on, the knock signal processing has tended to become simpler, although in the 1990s this may be changing. Time windows and mechanically resonant sensors have largely disappeared, and much of the filtering is now done digitally.

8.3.2 Accelerometer Sensors

The magnetostrictive jerk sensor, while satisfactory in performance, has too many parts to be a low-cost solution to measuring knock on board. Moreover, its mechanical assembly is not simple. In an effort to achieve lower-cost solutions, the industry found that the second-time derivative of displacement—acceleration—could be measured and used to implement a satisfactory knock control. The drawback to using an accelerometer compared to a jerk sensor is that it does not yield as good a signal-to-noise ratio; however, by using appropriate filtering, a good control signal can be achieved.

The first accelerometers used were mechanically bandpass-tuned, and some still are. However, in the 1990s, the trend has been to broadband sensors, again used with much electronic filtering. This has the advantage that one sensor model can be used for all engines, with the engine-specific frequency filtering characteristics built into the electronics module, which has to be engine-specific anyway. If the crucial filtering features are provided digitally, they can be installed as part of the engine-specific software.

Piezoelectric Accelerometer. Certain crystals of a specific cut or orientation possess the property that, when stressed, they produce a corresponding voltage. If such a crystal is loaded with a mass and spring, vibrations entering the assembly squeeze and pull the crystal with respect to the mass, and result in a signal which is a measure of the acceleration of the body to

PETITIONER'S EXHIBIT 1002
US PATENT NO. 6,581,565

which the assembly is attached. These signals can be substantial in size but appear electrically to be sourced at a high (capacitive) driving point impedance. Thus, care has to be taken to ensure that capacitively coupled noise does not contaminate the signal.

There are a variety of single crystals which exhibit the piezoelectric effect, but silicon is not one of them. Efforts to devise a silicon micromachined accelerometer were stymied for a long time by this fact, but a solution will be described below. Single crystal quartz is the material which was used in the single-crystal piezoelectric accelerometers.

In some cases, it is possible to use the mass of the piezoelectric element itself as the mass, and to combine the spring with one of the crystal electrodes. In such a design, the only parts are a spring, a contact, the crystal, and the housing.

Piezoceramic Accelerometer. Another type of piezoelectric element is the piezoceramic device. Piezoceramics are not single crystals. They can be fired into just about any shape, just like a ceramic insulator or a vase. By impressing a high voltage across electrodes on the ceramic while the material is at a high temperature—above its Curie temperature—and then gradually lowering the temperature, the piezoceramic becomes *poled*, or piezoelectric across the electrodes.

The best piezoceramics tend to belong to the lead-zirconate-titanate (PZT) family. These materials have a Curie temperature from 250 to 500 °C. If the sensor ever gets above its Curie temperature, its poling becomes degraded, and its calibration is no longer valid. However, these engine block-mounted sensors will not experience temperatures higher than about 125 to 150 °C, even during hot soak, so they can be used for the knock sensor.

Single-crystal piezoelectric accelerometers also have a Curie temperature, but it is typically much higher than for the piezoceramics. Quartz, for example, has a Curie temperature over 600 °C.

Because the piezoceramic materials can be molded into any shape, handled roughly, sawn and machined, coated with thick-film metallic electrodes, and so on, they lend themselves to easy, low-cost mass production. As a result, they have become pretty much the knock sensor of choice for the automobile industry. A drawing of a piezoceramic accelerometer knock sensor is shown in Fig. 8.2. In this particular design, the spring and top electrode have been combined into one part, but the mass is a separate metallic part between the piezoceramic disc and the spring. The whole assembly is stacked on a mandrel which extends up from the base-stud which forms most of the package.

8.3.3 Silicon Accelerometer

As previously noted, silicon itself cannot be made piezoelectric. However, it is possible to make a silicon micromachined accelerometer by anisotropically machining a cantilevered T-shaped structure into each cell of a silicon wafer, using a chemical etch. Strain gauges are diffused or implanted into the cantilever—the vertical bar of the T. The mass of the horizontal crossbar of the T and the spring constant of the cantilever provide the mechanical-to-strain transduction. Such accelerometers are in mass production for use in antiskid braking systems and as triggers for air bag safety devices. Whether or not they will replace piezoceramic knock sensors is primarily a matter of economics. Technically, the silicon accelerometer is satisfactory; its temperature limit is about 150 °C, which is adequate for on-block mounting.

8.3.4 Other Sensors

Instantaneous Cylinder Pressure Sensor. The direct measurement of instantaneous cylinder pressure permits the extraction of the pressure reverberation signal, which is the direct cause of knock. While this would be a very desirable signal to use for knock detection, it has not been implemented in on-board knock control systems for several reasons:

PETITIONER'S EXHIBIT 1002
US PATENT NO. 6,581,565

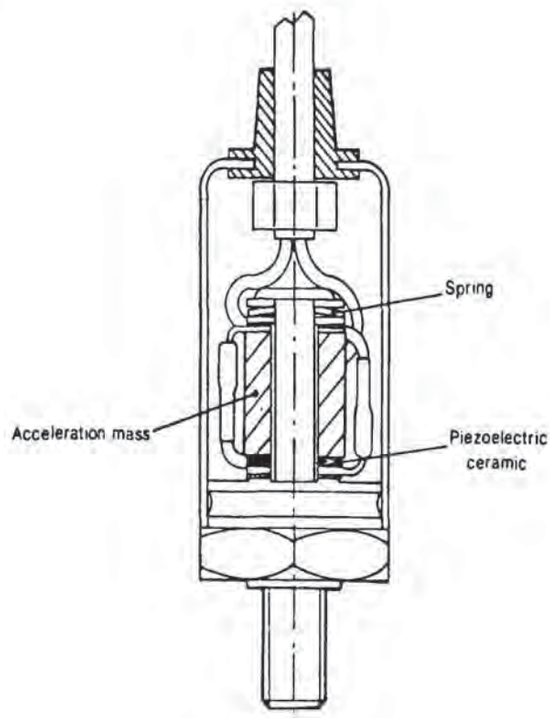


FIGURE 8.2 A piezoceramic accelerometer knock sensor.

- Either the same cylinder must always be the one to experience knock first and most severely, or one must have a sensor on every cylinder.
- The cylinder pressure wave is complex, and knock is only one of many signature elements present. Deriving a unique knock signal requires considerable signal processing in real time.
- While cylinder pressure sensors exist which are suitable for test purposes, a durable, low-cost, mass-producable on-board pressure sensor is not yet available.

In spite of these difficulties, work continues on cylinder pressure sensors for on-board control use, not so much to be used as knock-sensing devices as for use in deriving an instantaneous torque measurement (see Chap. 9). If this approach succeeds, then it is reasonable to suppose that the cylinder pressure sensor will be used to provide the inputs for obtaining both torque and knock measurements.

Since a spark-ignited engine already has a spark plug mounted in each cylinder head, it is possible to convert the spark plug into a kind of "poor man's pressure sensor" by mounting a piezoceramic washer held in compression between the spark plug and the cylinder head when the plug is torqued down. This arrangement has in fact appeared on a commercial passenger car engine. While the signal is not presently being used to extract a knock signal, suitable signal processing would make this possible.

Hydrophone in Coolant. In Sec. 8.3.1, it was mentioned that the knock signal appears virtually everywhere on the block. In fact, it even appears in the coolant fluid faithfully reproduced. This fact led to experiments in which hydrophones were mounted in the coolant and used as knock sensors. This approach has never reached production because it has no advantage over a block-mounted sensor and is in fact more difficult to package and to mount on the engine.

PETITIONER'S EXHIBIT 1002
US PATENT NO. 6,581,565

8.4 SUMMARY

In a remarkably short span of time, the on-board sensing of knock and its control have become a rather standard feature of passenger car engine control electronics. At the same time, the on-board sensors have been developed and are now largely mature. Acceleration has become the parameter of choice for most of these control systems, and the required accelerometers are typically based upon piezoceramic technology; it seems likely that this will remain the case at least through the 1990s. The rapid proliferation of these systems was facilitated by three factors:

- A solid background of experimental knowledge about knock and how to control it was established in the laboratory during the several decades before lead-free gas was mandated.
- The three legislated pressures of emissions limits, CAFE fuel economy goals, and no-lead fuel, combined with a customer base used to engines without knock, made solving the knock problem a high priority.
- The already widespread use of digital microcomputer engine control made the addition of knock limit control a straightforward design change.

GLOSSARY

Curie temperature The temperature above which a piezoelectric crystal or piezoceramic element no longer reliably retains its original piezoelectric characteristics.

Jerk sensor A sensor which measures the third-time derivative of displacement.

Knock Acoustic engine noise and vibration of characteristic frequency caused by uneven combustion in the engine cylinder(s).

Octane rating A measure of the resistance of a gasoline fuel to knock, as compared to pure isooctane hydrocarbon.

Retarding Causing engine combustion to occur at a larger angle past top dead center, by delaying the time at which the signal to start the spark event occurs.

Turbocharger A device which compresses engine intake manifold air by using the engine exhaust to drive a turbine and compressor.

Wastegate valve A valve in the exhaust system of a turbocharged diesel engine which causes part of the exhaust to bypass the turbine. The same name is also applied to a valve on a turbocharged gasoline engine which causes part of the boosted intake manifold air to dump to the atmosphere, dropping the manifold pressure.

REFERENCES

1. Paulius V. Puzinauskas, "Examination of methods used to characterize knock," SAE Paper 920808, Superflor Corp.
2. Karp P. Schmillen (FEV Motorentechnik, Aachen, Germany) and Manfred Rechs (Institute for Applied Thermodynamics, Technical University of Aachen, Germany), "Different methods of knock detection and knock control," SAE Paper 910858.
3. Masayoshi Kaneyasu (Hitachi America, Ltd.), Nobuo Kurihara, Kozo Katogi, and Hiroatsu Tokuda (Hitachi Ltd.), "Engine knock detection using multi-spectrum method," SAE Paper 920702.

ENGR & MATH SCI LIBRARY UMC

PETITIONER'S EXHIBIT 1002
US PATENT NO. 6,581,565

ABOUT THE AUTHOR

William G. Wolber, executive engineer, Cummins Electronics Co., Inc., has 38 years' experience in the development of sensors, actuators, and instruments for application in automobiles and other products. Since 1981, he has been involved principally in the development of sensors and controls for heavy duty diesel engines for Cummins Electronics Co. He holds 15 U.S. patents and is the author of over 50 technical papers. He has lectured and conducted seminars internationally for the Society of Automotive Engineers and other organizations.

PETITIONER'S EXHIBIT 1002
US PATENT NO. 6,581,565

CHAPTER 9
ENGINE TORQUE SENSORS

William G. Wolber
Executive Engineer
Cummins Electronics Co. Inc.

9.1 INTRODUCTION

Torque is one of the primary state parameters of an engine; along with speed it is a fundamental measure related to the output power. Torque can be defined as the moment produced by the engine crankshaft tending to cause the output driveline to turn and thereby deliver power to the load. For rotary motion, the torque multiplied by the rotational speed equals the power delivered by the shaft. In derivative form, Newton's law states that torque T equals the rotational moment of inertia I times the angular acceleration α. Hence, at constant rotational speed, instantaneous power is proportional to instantaneous torque. This is an important relationship because torque and, thus, delivered power can change rapidly compared to rotational speed.

Portraying the engine as a torque-delivering device is a useful concept. When an engine is used in road service as prime mover power, the operator of the vehicle tends to ask the vehicle for positive or negative incremental acceleration, as the operator perceives it to be falling behind or closing upon the vehicle ahead. Hence, the operator asks the engine for more or less torque. If the engine is spark ignited, this happens naturally through the modulation of the engine air intake flow path. In a diesel engine, it happens indirectly. The operator controls fuel rate, which to first approximation is linearly related to power. For slowly varying engine speed and load, an incremental change in power results in a change in torque and therefore a change in acceleration.

9.1.1 Time-Scale Definitions

At this point, it is useful to define two time scales which will be used with regard to the engine. A reciprocating engine is never truly operating steady state. It is a cyclic succession of batch processes, a kind of system which chemical engineers have termed "continuous-by-jerks." Each cylinder absorbs shaft energy during the compression stroke and releases a larger amount of shaft energy through combustion during the power stroke. These actions are so interleaved that the drive shaft is continually accelerating and decelerating in step with cylinder events. Nevertheless, a quasi-steady-state model for the engine can be defined in which these rapid fluctuations are ignored and attention is focused on the more slowly varying state parameters which are nearly stationary during one engine revolution. This is the situation the operator senses and controls and it is also the primary focus of the control algorithms in a microcomputer-based engine control today. (As of 1994, all electronic engine controls operate on the "engine time scale.")

PETITIONER'S EXHIBIT 1002
US PATENT NO. 6,581,565

Quasi-Steady-State Torque. Quasi-steady-state torque is defined as that running average value of torque that varies slowly with respect to the cylinder-to-cylinder period, but rapidly with respect to vehicle changes in motion and load. To quantize this state, it is noted that an unloaded engine coupled to flywheel inertia may accelerate from idle to maximum speed in one to five seconds when subjected to wide open throttle and that this performance is essentially reproduced whether the change in throttle position occurs in 20 ms or 1 ms. Quasi-steady-state torque is what the operator is interested in commanding, and so, if we visualize a torque command-feedback engine control, it is the parameter of interest.

Instantaneous Torque. Today's electronic engine control can usefully respond much more rapidly than this for those state parameters having to do with each cylinder batch process itself. The preparation of the fuel and air charges and the timing of ignition take place on a time scale measured in fractions of a cylinder period, and thus the time scale of interest ranges from 30 μs to 20 ms. This time scale corresponds to the instantaneous engine state. It is the time scale of the torque impulses that are termed instantaneous torque.

In order to use instantaneous torque measurements, it must be recognized that the reciprocating engine is a cyclic machine in which major functions and the parameters that characterize them are tied together in sequence mechanically by the crankshaft and camshaft. Proper adjustment of those other parameters that are free to be changed independently of the train of instantaneous cylinder events allows optimization of the overall torque impulse generation in real time. For example, a theoretical examination of the internal combustion engine cycle has shown that the centroid of the cylinder pressure wave should occur about 15 crank-angle degrees after top dead center ("Powell's Magic Angle") to maximize the instantaneous incremental torque from that cylinder.[1,2] No spark or injection timing algorithm can do any better than to effect such timing of the torque impulse. Note, however, that we are stating where the centroid of the pressure wave should be for the best torque impulse, not where the fuel injection or ignition should be commanded.

State-of-the-art scheduled spark timing controls are based upon test data from one or more prototype engines run extensively in the laboratory on a dynamometer under quasi-steady-state conditions. From the data obtained, families of spark plug or injection timing (crank angle) surfaces versus engine speed, load, etc., are derived that correspond to optimum economy and performance while meeting emission requirements. These data then form the schedule embedded in the control microcomputer memory for all engines of that model produced. This type of scheduled computer control is standard throughout the industry today for all electronically controlled engines, both spark-ignited and compression ignition, with just two exceptions. These are the oxygen sensor feedback control loop, which keeps an engine equipped with a three-way catalyst in the stoichiometric "window" of the catalyst efficiency performance, and the speed governing feedback control algorithm used for power takeoff (PTO) operations, diesel all-speed governors, and generator-set frequency control.

By contrast, the addition of an on-board instantaneous torque measurement would permit the direct feedback control of several key engine control parameters. To take maximum advantage of such feedback control, an advanced instantaneous crankshaft position sensor is also required.

The controls which could be implemented through use of an instantaneous torque feedback control system are:

- Quasi-steady-state torque feedback control in response to torque command.
- Spark-ignition or compression-ignition timing control by feedback of instantaneous torque impulse timing compared to the norm of the "Magic Angle." Torque impulse amplitude can also be optimized against timing. These controls can be implemented on a cylinder-by-cylinder basis, for spark-ignited pulse sequential fuel injected engines, and for unit-injected diesel engines.
- Cylinder-by-cylinder torque-leveling feedback control can be implemented by adjusting the amount of fuel injected into each cylinder to obtain equal torque impulses from each one.

PETITIONER'S EXHIBIT 1002
US PATENT NO. 6,581,565

This results in a quiet, smoothly running engine with a somewhat improved maximum power, because the torque limit can be set for a more nearly constant cylinder event instead of for the worst case cylinder.

- The instantaneous torque signal is also rich in a variety of diagnostic information—for example, to measure engine power or for use as a miss detector.

9.2 AUTOMOTIVE APPLICATIONS OF TORQUE MEASUREMENT

9.2.1 Off-Board Measurement

The principal automotive use of torque measurement today is in the testing and evaluation of engines using the engine dynamometer. The torque sensor is inserted as a drive shaft between the engine and the dynamometer; the shaft of the sensor is a torsional Hooke's law member and its twist is measured. Typically the torque is actually measured using a strain gage bridge on the drive shaft. Full-scale twist is limited to no more than about a degree per foot of shaft for engines in the 50 to 500 hp range.

In a dc torque sensor, the strain gage bridge is powered from an external source through slip rings, and the offset voltage is taken off the bridge the same way (Fig. 9.1). The sensor is necessarily bulky, large, fragile, and costly. A more rugged ac strain gage sensor can be made using rotational transformers, as shown schematically in Fig. 9.2.

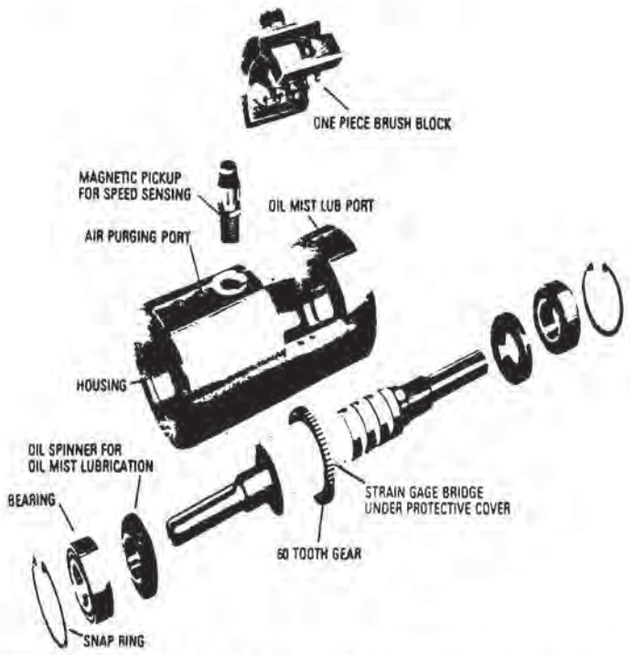


FIGURE 9.1 Exploded view of rotating shaft torque sensor with slip rings. *(Courtesy of the Lebow Div., the Eaton Corp.)*

Developmental Tests. In engine development, a good bit of the work involves fine-tuning the engine to get the maximum power and minimum fuel consumption at various engine conditions. Since power equals torque multiplied by engine speed, if tests are carried out at constant speed, maximum power occurs at maximum torque. Thus, the torque sensor can be used as a direct indicator of whether changes in the engine design or control will improve power.

PETITIONER'S EXHIBIT 1002
US PATENT NO. 6,581,565

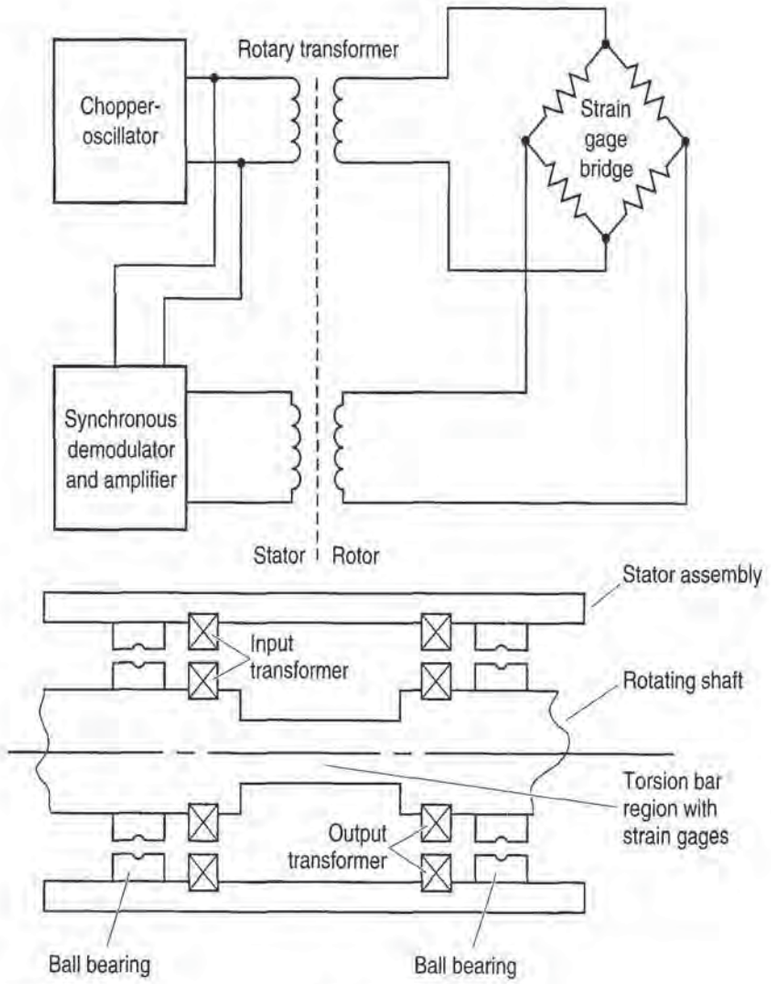


FIGURE 9.2 Rotary transformer rotating shaft torque sensor.

End-of-Line Manufacturing Tests. Particularly in the case of heavy duty diesel engines, the price of the engine is directly related to engine rated horsepower. Such engines are in a real sense sold by the horsepower. The manufacturer certifies that a certain model will deliver no less than a certain horsepower when run at rated conditions. The engine is tested at the end of the assembly line for a number of attributes, chief among which is assurance that it exceeds stated horsepower at rated speed. The assurance is provided by accurate torque and speed measurements.

In-Service Tests. Occasionally, torque sensors may be used with an engine that is being tested under field conditions. This is relatively straightforward when the engine is being used in a stationary application, but not if it is installed in a vehicle.

9.2.2 On-Board Measurements

To be most useful on board, a torque sensor should not only be accurate but also fast in response. Most of the sensors available today do not have this attribute, because they were developed for use in dynamometer tests.

To be a useful on-board engine control sensor, the torque sensor of the future also needs several other attributes:

PETITIONER'S EXHIBIT 1002
US PATENT NO. 6,581,565

- It must be extremely rugged, which for practical purposes means noncontacting with respect to the driveline.
- It must be able to withstand torque impulses of 10 to 20 times its full-scale measuring capability without degrading its accuracy. For strain gage type sensors, this means that the sensor would always have to measure in the lowest 5 to 10 percent of its range, where it is not very accurate.
- Installation of the sensor must not cause any significant change in the compliance of the driveline. This is a requirement imposed by engine application engineers to avoid spoiling the tradeoffs that have been made to avoid severe torsional vibrations.
- Ideally, the shaft of the sensor should be very short in length (in part to achieve the preceding characteristics). Unfortunately, for a torsional Hooke's law device, that means the full-scale shaft twist angle will be very small.

In spite of these formidable barriers to a satisfactory design, a wide variety of desirable applications could be made using an on-board instantaneous torque sensor. As a result, many researchers and developers both in academia and industry are working to achieve such a measurement directly or indirectly.

Power Measurement of Large Engines. Means exist for field service personnel to measure engine power in the field for engines installed in a vehicle and rated at up to 400 to 500 hp. For larger vehicle-mounted engines, this measurement is a difficult problem for a number of reasons:

- A rugged on-board sensor is not available.
- These engines are often installed in very large machines such as mine-haul trucks and front-end loaders located off the road in remote areas.
- Dynamometers large enough to load down the engine to full power are not available except in a very few locations.

One of the most frequent customer complaints about heavy duty engines is perceived loss of power. Often such complaints must be resolved at the field location and on a subjective basis. The engine and vehicle can be fully loaded in actual work operation, and engine speed is known accurately. If an on-board torque sensor were available, such complaints could be quickly resolved, and it would be well worth installing on large engines.

Miss Detection. The California Air Resources Board has mandated that all passenger vehicles shall be equipped with an engine diagnostic capability that includes a miss detector. While the regulation is not yet in force as of the time of this writing, the automotive industry knows that every segment will be affected by the requirement by the end of the decade. Many vehicle OEMs, first-tier automotive suppliers, entrepreneurial sensor firms, and academic researchers are working hard to meet the miss detector requirements, mainly basing their efforts on the same technologies useful for measuring or inferring torque.[3]

Torque Feedback Control. The reciprocating engine could be configured in a feedback control mode if equipped with an on-board quasi-steady-state torque sensor capable of responding at least as fast as the engine/driveline. In a torque command drive-by-wire system, the operator input would be a command for a new torque, greater or less than the present torque. The engine control would do its best to provide the new torque as rapidly as possible. The feedback error signal would be the difference between the torque command and the sensor output. Of course, the new torque and the resulting acceleration or deceleration would have to be limited within bounds set by maxima for cylinder pressure, emissions production, exhaust gas temperature, fuel economy, and so on.

Feedback Control of Timing. As was described in the introduction to this chapter, the measurement of instantaneous torque, on board, along with instantaneous crank angle position,

PETITIONER'S EXHIBIT 1002
US PATENT NO. 6,581,565

would allow the engine control computer to use signature recognition to measure the crank angle at which the centroid of the torque impulse is located, for each cylinder. From this information, probably with some compensation for seriously off-normal engine conditions as stored in computer memory, the engine control can determine if that impulse was centered at Powell's Magic Angle, and, if not, how much earlier or later the chain of combustion events needs to be started. Most likely, the computer also needs to decide between updating that cylinder based upon that information alone and waiting a whole engine revolution to update, or also basing the correction upon abrupt changes in operator input, load, knock level, etc. In any case, under quasi-steady-state conditions, the best efficiency of that engine for converting chemical energy into shaft power by proper engine timing could be achieved this way whether the engine is spark-ignited or compression-ignition.

Cylinder Torque Leveling. Individual trimming of the amount of fuel for each cylinder can be realized on pulse sequential fuel injected spark-ignited engines and on unit injector diesel engines by matching the torque impulse for each cylinder to the average of all cylinders. Then the average impulse can be raised to very nearly the maximum value the engine is designed for. In today's engines, the control must provide a guard band between the maximum torque for the worst case cylinder and the design limit for the engine (commonly called the maximum cylinder pressure limit or the peak torque limit). If the torque impulses delivered by each cylinder were known to be controlled to be equal, the guard band could be reduced and more power obtained from a given engine.

While cylinder-to-cylinder torque leveling is not the same as compression leveling, an engine controlled cylinder by cylinder for timing and torque leveling intuitively would appear to be as smoothly running and low in acoustic noise emission as can be visualized.

Engine Diagnostics. The instantaneous torque signature is very rich in diagnostic information. A figure of merit for engine roughness can easily be obtained in real time, from which a lean-limit control signal can be derived. The miss detector responds to an extreme case of roughness. Ragged ignition and flame front formation, imperfect injection, poor distribution, and many other engine and control problems can be measured or inferred from such a signal, on board and in real time.

9.3 DIRECT TORQUE SENSORS

9.3.1 Reaction Force

The use of a strain-gaged torsional Hooke's law shaft to measure torque at the dynamometer has been described in Sec. 9.2.1. Torque can also be measured in the test cell by instrumenting the engine or dynamometer mounting with strain gage load cells to measure reaction torque. This is a useful way to measure quasi-steady-state torque, but is not a good measuring system for instantaneous torque, as both the engine and its load have considerable inertia and damping which attenuate the torque impulse and may introduce phase delay. It is also not a good on-board measurement because the engine mounts on a vehicle are designed to attenuate and damp out bouncing from road and load irregularities. Also, as a function of time, temperature, ozone concentration, and other variables, they tend to stiffen substantially and change the deflection of the engine at its mounts as a function of torque.

9.3.2 Torsional Strain (Twist) Sensors

Magnetic Vector Sensors. The strain-gaged torsional Hooke's law sensor was described in Sec. 9.2.1. A more practical approach to an on-board torque sensor is a noncontacting design

PETITIONER'S EXHIBIT 1002
US PATENT NO. 6,581,565

called a magnetic vector sensor.[4,5] This sensor operates on the principle that the magnetic domains in a ferromagnetic shaft delivering torque are randomly distributed when no torque is being delivered, but that each domain, on average, is slightly rotated in the tangential direction when torque is delivered by the shaft and twists it. If an ac-driven coil is placed near the shaft and surrounded by four sensing coils arranged mechanically and electrically as a bridge, the amplitude of the bridge offset is proportional to the magnetic vector tangential component, and therefore to twist and torque.

If the magnetic domains were truly statistically distributed over a small range of shaft angle, such a sensor would be able to measure instantaneous torque. Unfortunately, they are not. Over a small shaft angle increment, the average torque vector does not net to zero when torque is zero, and the output is characterized by a fixed pattern noise which repeats every 360°. The magnetic vector sensor is reasonably accurate measuring quasi-steady-state torque, but the signal-to-noise ratio becomes poor when an attempt is made to measure instantaneous torque.

Further work on this sensor simplified and miniaturized it.[6] The bridge was replaced by a single tangential coil, and the sensor was made small enough so that it could be mounted in the rear crankshaft bearing. However, it still was not able to measure instantaneous torque.

Investigation continues on techniques to reduce the fixed pattern noise, and some claims of progress have been made. However, at this writing, a production on-board torque sensor is not available.

Optical Twist Measurement. Research work has been reported on a sensor that changes the duty factor of light pulses sensed after passing through sets of slits at both ends of a shaft.[7] The principle of its operation is shown in Fig. 9.3. Such a sensor is noncontacting and can be made robust, but it requires appreciable shaft length and therefore adds compliance to the driveline. The work has not been engineered to produce an economical on-board device.

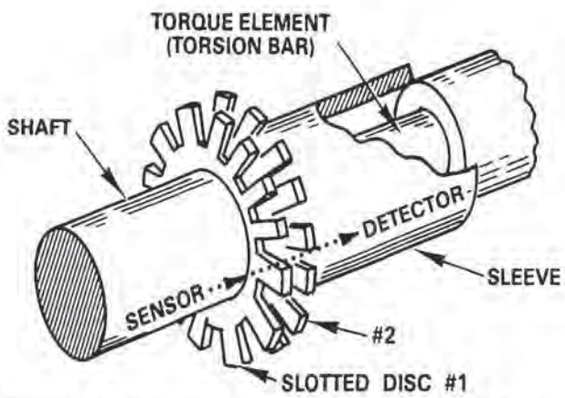


FIGURE 9.3 Optical torque meter. *(Courtesy of The Bendix Corp.)*

Capacitive Twist Sensor. An electrode pattern can be made using interdigitated electrodes spaced one or two degrees apart on two facing flat discs.[8] One of the discs is stationary; the other rotates with the crankshaft. Two such pairs of electrodes can be operated with phase detection measurement to provide a virtually instantaneous signal proportional to the twist of the shaft; the rotating halves of the electrode pairs are attached to the ends of the Hooke's law torsional spring. Obviously, this arrangement has the same drawback as the optical sensor in that it has to have some shaft length to twist and, therefore, some compliance. However, it is robust, has good accuracy, and is a more practical on-board device than the optical twist sen-

PETITIONER'S EXHIBIT 1002
US PATENT NO. 6,581,565

sor. This sensor can also yield an accurate crankshaft position measurement. Nevertheless, an on-board version is not available today.

9.4 INFERRED TORQUE MEASUREMENT

Indirect measurements of torque-related parameters can be made with a view to inferring torque from the measurements. Typically, such measurements require considerable real-time computation in the control microcomputer, along with precision measurement of the instantaneous crank angle position. Much work is in progress in a variety of locations to make these methods into practical instantaneous torque control signals.

9.4.1 Instantaneous Cylinder Pressure Sensors

Engine development engineers have long used piezoelectric crystal cylinder pressure sensors in the laboratory to make engine power and heat release measurements and as an aid to development. The best of these sensors use doped quartz single crystals. They are accurate and reasonably robust, but expensive and unforgiving if overranged or subjected to excessive temperatures. Much work continues on development of a mass-producable on-board cylinder pressure sensor.[9] One of the Japanese car manufacturers is reported to have a top-of-the-line passenger car model, available only in Japan, with engine control using piezoceramic cylinder pressure sensors.

The signals from cylinder pressure sensors need considerable real-time data processing to produce inferred "torque" signals. In one method, the noise always present is filtered, the pressure signal is multiplied by an instantaneous shaft angle term, and integrated over the angle range representative of the power stroke of the cylinder. From this a measure of torque contribution from that cylinder is obtained. The best digital signal processing (DSP) chips available in the early 1990s are barely able to keep up with cylinder events in such a process. Nevertheless, we can be confident that if the proper sensors are available in the late 90s, the microcomputer chip performance required will be available and cost effective too.

9.4.2 Digital Period Analysis (DPA)

When an engine is run at low speed and heavy load, the instantaneous angular velocity of its output shaft on the engine side of the flywheel varies at the fundamental frequency of the cylinders, since the compression stroke of each cylinder abstracts torque and the power stroke adds a larger amount. The signal-to-noise ratio of the measurement of instantaneous angular velocity (or rather of its reciprocal, instantaneous period) degrades with increasing engine speed and lighter load, but is a useful way to infer torque-like measures of engine performance.

Figure 9.4 shows an idealized plot of instantaneous crankshaft period against crank angle under constant speed, lean conditions. The instantaneous period wave is seen to be a variation about the mean period value. This waveform can actually be measured using a precision, multitoothed crankshaft position sensor. For reasons which will be explained later, the instantaneous angular velocity lags the torque inputs producing it. As a result, the period wave appears to lead the torque or cylinder pressure variations.

Timing Control by DPA. The general case of the variation in crankshaft velocity in a four-cylinder engine can be described by:

$$T_N = AL\,P_N(\theta)\sin\theta = AL\,P_{(N+3)}(\theta)\sin\theta + T_F(\theta) + T_L + I\ddot{\theta} \qquad (9.1)$$

PETITIONER'S EXHIBIT 1002
US PATENT NO. 6,581,565

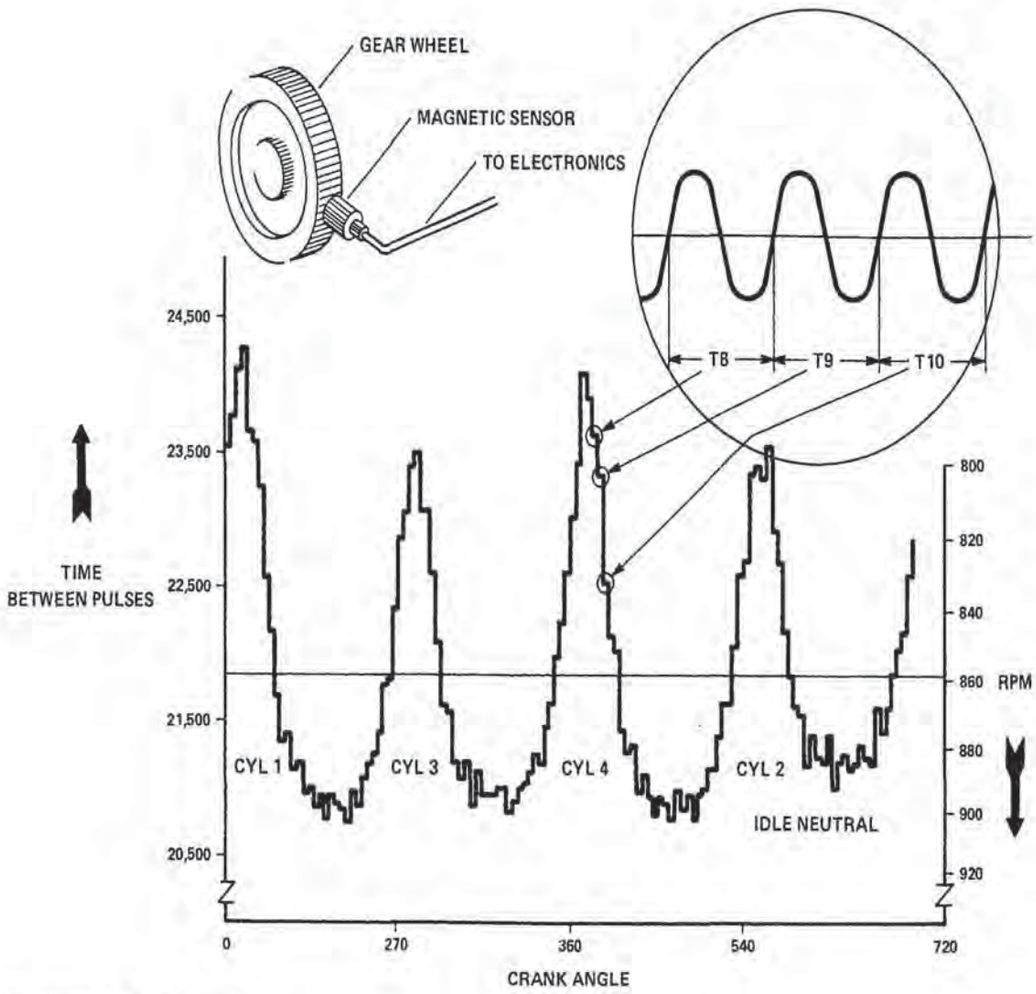


FIGURE 9.4 Digital period input.

where T_N = instantaneous torque due to burning gases in cylinder N at angle θ
A = area of piston
L = maximum effective crank lever arm
$P_N(\theta)$ = pressure in cylinder N (a function of crank angle and many other variables)
$P_{(N+3)}(\theta)$ = pressure in third cylinder to fire after N which is in its compression stroke when cylinder N is in its power stroke
$T_F(\theta)$ = so-called "fixed load" torque due to friction, accessories, etc., and is generally a function of $d\theta/dt$
T_L = torque delivered to the load
I = inertia of the engine, drivetrain, and vehicle reaction through the wheels
$\ddot{\theta}$ = instantaneous angular acceleration of the crankshaft

In order for Eq. (9.1) to remain valid, as T_N varies with angle θ due to the variations of $P_N(\theta)$ and the sin θ term, some term in the right-hand side of the equation must vary correspondingly. In fact, the major effect is upon $\ddot{\theta}$, the angular acceleration, which varies both in magnitude and sign; being positive when P_N is large and θ is near $\pi/2$, and negative when P_N is small and θ is near 0 and π. If Eq. (9.1) is integrated as a function of θ from $\theta = 0$ to $\theta = \pi$ and

PETITIONER'S EXHIBIT 1002
US PATENT NO. 6,581,565

then the summation is extended to angles larger than π by adding in the contributions of cylinders $N + 1$ and $N + 3$, the term in $I\ddot{\theta}$ becomes an average angular velocity over a complete engine cycle.

One important consequence of the preceding analysis is that, upon integration of the equation, the sin θ term becomes cos θ—that is, the angular velocity wave lags the torque impulses causing it by $\pi/2$. Another consequence is that the amplitude of the period wave reflects the net contribution of the cylinders—if the load increases, and $P_N(\theta)$ increases to keep average angular velocity constant, the amplitude of the period wave must increase. The $I\ddot{\theta}$ term has become an $I\omega$, it is the reciprocal of this term which was plotted in Fig. 9.4.

When a spark plug fires or fuel is injected into a diesel cylinder, the pressure in the cylinder takes a finite length of time to build—first, because of a delay to get the fire started and then because of the finite and relatively constant flame propagation time, and second, because the temperature rise which causes pressure to rise, peaks only shortly before combustion is completed. Thereafter, pressure falls as the piston displaces under the pressure of the gases. Mean best torque (MBT) will be achieved from that cylinder when the pressure pulse, convolved with sin θ yields a maximum upon integration. As described previously, researchers at Stanford University have found analytically and confirmed experimentally that this condition prevails for a fairly wide range of engine conditions when the centroid of the pressure pulse occurs at 15 degrees past top dead center (TDC). Because of the delays described previously, ignition must occur early enough to position the pressure peak near this value. It is this "anticipation" in spark plug firing that is termed *ignition advance*. The reason why advance angle has to be larger at higher speeds is now obvious: the flame propagation delay time covers more degrees of crank angle when the engine is running faster.

Further experiments by the Stanford researchers and others confirmed the suspicion that the period wave is a strong function of the crank angle, and that the angle associated with the centroid of the pressure wave is a unique function of the phase of the fundamental component of the period wave measured with respect to a crankshaft angle index point, say top dead center of cylinder no. 1. The period wave is measured with a sensor which is a precision version of a crankshaft position sensor.[10] It produces a fast, sharp pulse for every small and equal angle increment—say one degree—through which the shaft turns. Pulses from a high-frequency quartz crystal clock are counted to measure each period. The crankshaft angle index is available from the crankshaft position sensor. In principle, the period wave could be Fourier analyzed into the Fourier integral coefficients A_n and B_n by computing the Fourier integrals, and the phase of the fundamental (first harmonic) is then arctan B_1/A_1. To perform this computation in real time is a bit much to ask of today's microcomputer (but not tomorrow's!) and various shortcuts are utilized to achieve an approximate result. Remembering that the period wave appears to lead the torque impulses that cause it by $\pi/2$, the spark timing can now be varied so as to place the centroid of the pressure wave, on the average, at or very near the 15-degree-after-TDC point.

It is instructive to consider what performance is required of the DPA and crankshaft position sensors to achieve a given signal-to-noise ratio. The repeatability of the crankshaft angle marked by the sensor is a function of the diameter of the sensing disc. For the various magnetic sensors, a repeatability better than ±0.5 degree can be achieved with a 10-cm-diameter disc. In the DPA sensor, the concern is for the period-to-period jitter. It is obviously worse for smaller angle increments both because the angle jitter is a larger part of the period, and also because the period-counting roundoff error is larger for any given clock frequency. At the same time, the more periods measured per revolution, the more fidelity the period wave will have for its high-frequency components. The period-to-period jitter of the magnetic sensor in this example is about ±0.5 degree. This is satisfactory for 24 periods per revolution but marginal for 60 periods; a typical period wave amplitude is only ±3 percent of the average period. On the other hand, even 60 periods per revolution is marginal for ignition or injection timing control.

The granularity due to counting roundoff also needs to be considered. Today's low-cost LSI circuits can count reliably at 20 MHz, so that is a practical clock frequency. If a four-cylin-

PETITIONER'S EXHIBIT 1002
US PATENT NO. 6,581,565

der engine is running at 1800 rev/min (30 Hz), the associated period wave will have a fundamental of 60 Hz. If the DPA sensor has one degree angle indices, referred to the crankshaft, each period will have about 2000 counts from the clock. Therefore, the period counting round-off noise will be ±1 part per 2000. Referred to a nominal ±3 percent amplitude period wave, this jitter amounts to ±2 percent of the peak value of the period wave (not of the period itself), not counting any smoothing.

For the fundamental of the period wave, the phase of which is used for DPA timing control, a good deal of smoothing can be realized, so that for a "clean" engine, estimation of the correct angle to ± one crankshaft degree is feasible.

Figure 9.5 shows an actual period wave measured using an electromagnetic DPA sensor with one-degree increments and a 10-MHz clock. Both the jitter described previously and a fixed pattern noise can be discerned in the signal. The latter effect is due to slight imperfections in the tooth spacing of the precision gear used as the sensing disc. Such systematic errors can be eliminated in the microcomputer, but they are troublesome and consume integration time. The better solution is to design a precision DPA sensor which minimizes fixed pattern noise.

DPA Used for Diagnostics. During the 1980s, one of the heavy duty diesel engine manufacturers introduced an off-board diagnostic instrument capable of doing DPA on the engine with the clutch disengaged and using snap acceleration and deceleration to load the engine

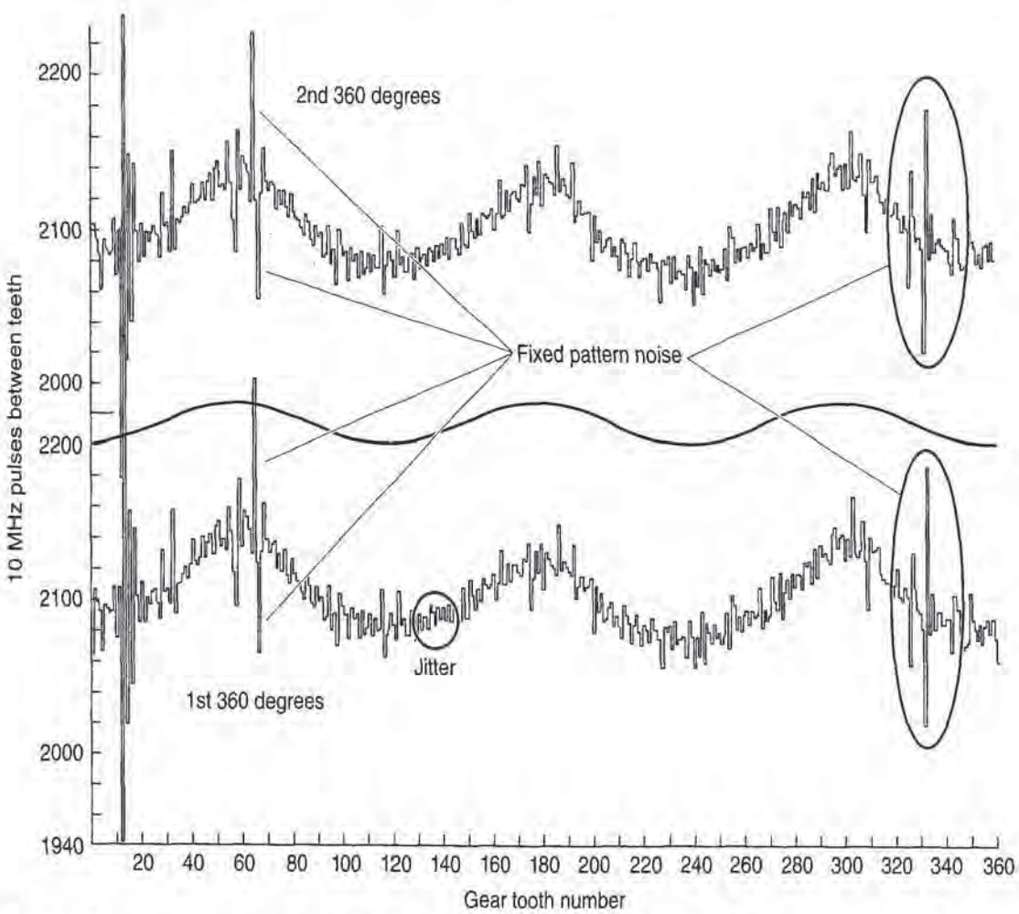


FIGURE 9.5 Actual period wave data from engine crankshaft; unsmoothed data. *(Courtesy of The Bendix Corp., Diesel Operation)*

ENGR & MATH SCI LIBRARY UCLA

PETITIONER'S EXHIBIT 1002
US PATENT NO. 6,581,565

inertially. This instrument used the very imperfect engine ring gear as the DPA target but solved the fixed pattern noise problem in a very elegant way.[11] The position sensor is actually a dual sensor, with the two magnetic circuits disposed tangential to the ring gear and closer together than one tooth pitch. A particular tooth is sensed by the first magnetic circuit and then by the second before the next tooth is sensed by the first circuit. Virtually all of the fixed pattern noise is eliminated.

What would be achieved in an on-board DPA system would be real-time, nearly ideal closed-loop control of spark timing. As with most controls for spark-ignited engines, there are some trims required to make the system work. Flame front propagation is in fact a complex process which has a substantial jitter in the time of propagation, so it is necessary to average the computation of the phase angle over a number of cylinder pulses in order to obtain a good phase estimator. Under transient conditions, the shape of the pressure pulse may change enough so that the angle for mean best torque (MBT) shifts slightly. These factors can also be incorporated in the control. A similar method could be used for compression-ignition engines; in fact, the period wave has a more reproducible signature than for a spark-ignited engine.

It is useful at this point to emphasize again that these principles hold under any conditions, but that the control works well only in the lean regime. As the air/fuel ratio nears stoichiometry, the amplitude of the period wave becomes quite small. Because the method of measuring the instantaneous period—counting clock pulses over a finite angle increment—is a differencing method, the signal-to-noise ratio (S/N) is always a problem, since a differencing process always yields a poorer S/N than that of the original function. Hence, the DPA technique yields poorer results the nearer the engine is to stoichiometry and the higher the engine speed.

Referring to Fig. 9.6, if a figure of merit is formed

$$R = \left| \frac{T_2 - T_1}{t_1 + t_2} \right| \tag{9.2}$$

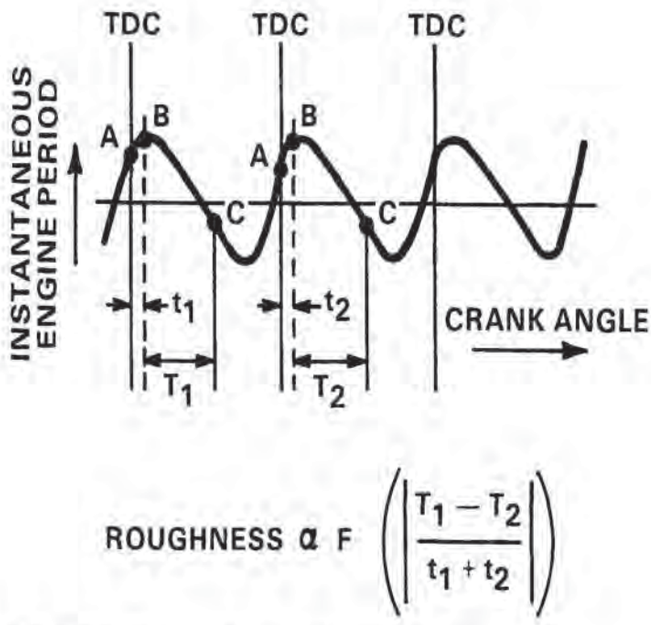


FIGURE 9.6 Digital roughness control.

PETITIONER'S EXHIBIT 1002
US PATENT NO. 6,581,565

we have a measure of the "roughness" of the engine useful for lean limit control or misfire detection. This is one example of many such optimizing algorithms which may be derived from DPA

9.5 SUMMARY

One can conclude from this chapter that torque measurement, whether direct or inferred, is a useful parameter for engine evaluation off-board, but that the proper sensors and computer analysis equipment for on-board control are not yet available. Yet the number of facilities working to advance this art, the resources being added, and the sporadic reports of progress are such that one can predict with some confidence that a breakthrough is imminent. Just what kind of control will first appear, and what kind or kinds will ultimately be successful, is not yet clear.

GLOSSARY

Algorithm A set of software instructions causing a digital computer to go through a prescribed routine. Because embedded computer engine controls have become so common, algorithm has become essentially synonymous with control law for automotive engineers.
Compression leveling A (theoretical) type of engine control which would cause each piston in each cylinder to compress its air charge to the same maximum pressure.
Dynamometer A machine to absorb power in a controlled manner, especially from an engine under test.
Hooke's law A relationship for an ideal elastic member which says that the displacement is proportional to the force.
Interdigitated An arrangement of two multiple-finger structures such that each pair of fingers from one structure has a finger from the other interposed.
Pulse sequential A type of fuel control for gasoline spark-ignited engines in which the fuel for each cylinder is injected into the air manifold near the intake valve for that cylinder just as it opens.
Robust Able to survive and operate properly in a severe environment.
Stoichiometric Pertaining to a combustion process in which the oxidizing agent (oxygen) and the reducing agent (fuel) are in balance such that, were the reaction to go to completion, there would be neither oxygen nor fuel left over, and all the reaction products such as carbon monoxide would be oxidized to their highest state—carbon dioxide.
Torsional Hooke's law A relationship for an ideal elastic shaft which says that the angle through which the shaft twists is proportional to the torque.
Torque The moment tending to make the output shaft of an engine turn. Torque can be expressed as a force acting perpendicular to a lever arm at a distance from the center of rotation. Its units are Newton-meters (pound force-feet).
Unit injector A type of fuel control for diesel engines which has fuel metered into a piston-barrel injector for injection into a specific cylinder at a specific time. Each engine cylinder has its own cam-driven injector, which operates something like a hypodermic syringe.

PETITIONER'S EXHIBIT 1002
US PATENT NO. 6,581,565

REFERENCES

1. J. A. Tennant, Rao, H. S., and Powell, J. David, "Engine characterization and optimal control," *Proceedings of the IEEE Conference on Decisions and Control* (including the 18th Symposium on Adaptive Processes), Ft. Lauderdale, Fla., Dec. 12–14, 1979. IEEE 79CH 7486-OCS, vol. 1, pp. 114–119.
2. Itshak Glaser and Powell, J. David, "Optimal closed-loop spark control of an automotive engine," SAE Paper No. 810058, Society of Automotive Engineers Inc., Warrendale, Pa.
3. Anders Unger and Smith, Kent, "Second-generation on-board diagnostics," *Automotive Engineering* vol. 102, no. 1, Jan. 1994, pp. 107–111.
4. William J. Fleming, "Automotive torque measurement: a summary of seven different methods," *IEEE Transactions on Vehicular Technology,* VT-31, No. 3, Aug. 1982, pp. 117–124.
5. William J. Fleming and Wood, P. W., "Non-contact miniature torque sensor for automotive applications," SAE Paper No. 820206.
6. Yutaka Nonomura; Sugiyama, Jun; Tsukado, Koja; Masahoru, Takeuchi; Itoh, Koji; and Konami, Toshiaki; "Measurements of engine torque with the intra-bearing torque sensor," SAE Paper No. 87042.
7. G. W. Pratt Jr., "An opto-electronic torquemeter for engine control," SAE Paper No. 760007.
8. Charles D. Hoyt, "DC excited capacitive shaft position transducer," U.S. Patent No. 4 862 752 Sept. 5, 1989.
9. Hiroki Kusakabe; Okauchi, Tohru; and Takigawa, Masuo; "A cylinder pressure sensor for internal combustion engine," SAE Paper No. 92071.
10. Stephen J. Citron and Orter, Kevin C., "On-line engine torque measurement utilizing crankshaft speed fluctuations," SAE Paper No. 850496.
11. Clarence E. Kincaid, "Computerized diagnostics for Cummins engines," *Proceedings of Convergence '84,* IEEE '84 CH 1988–5.

ABOUT THE AUTHOR

For biographical information on William G. Wolber, see Chap. 8.

PETITIONER'S EXHIBIT 1002
US PATENT NO. 6,581,565

CHAPTER 10
ACTUATORS

Klaus Müller
Manager, Development of Magnet Valves, Pressure Supply
Automotive Equipment Division 1
Robert Bosch GmbH, Stuttgart

10.1 PREFACE

10.1.1 Introductory Remarks

Numerous open- and closed-loop control systems find application in modern production vehicles, where they provide improved operating characteristics together with enhanced safety, comfort, and environmental compatibility.

The actuators respond to position commands from the electronic control unit to regulate energy, mass, and volume flows.

10.1.2 Actuators: Basic Design and Operating Principles

Conventional final-control elements (standard and spool valves, etc.) have been familiar for some time. A provision for electronic control is required for actuator applications in modern vehicles. The actuator consists of a transformer to convert the input signal from the control unit into (usually) mechanical output quantities, and the conventional final-control element which it governs. (See Fig. 10.1.)

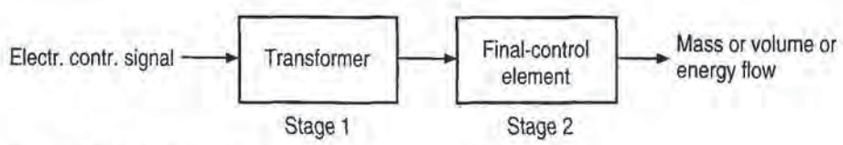


FIGURE 10.1 Basic actuator elements.

Either the control unit or the actuator itself will feature an integral electronic output amplifier. The energy conversion principles (stage 1) determine the classification of the actuators. Electromechanical actuators will also be discussed in the following pages.

ENGR & MATH SCI LIBRARY

PETITIONER'S EXHIBIT 1002
US PATENT NO. 6,581,565

10.2 TYPES OF ELECTROMECHANICAL ACTUATORS

10.2.1 Magnetic Actuators

dc Solenoids

Actuator Principles. In order to operate, actuators depend on the forces found at the interfaces in a coil-generated magnetic field when current passes through it. The solenoid actuation force F_m is calculated as

$$F_m = \frac{A\,B^2}{2\,\mu_o} \tag{10.1}$$

where A = pole face area
B = magnetic induction
μ_o = permeability constant ($\mu_o = 4\,\pi\,10^{-7}$ Vs/Am)

On the flat-armature solenoid illustrated in Fig. 10.2*a*, the total solenoid force is 2 F_m. Equation (10.1) can also be applied to versions equipped with a permanent magnet (Fig. 10.2*b*). A particular solenoid force is specified for each technical application. The pole face area, the magnetic circuit, and the coil are then determined for this force.

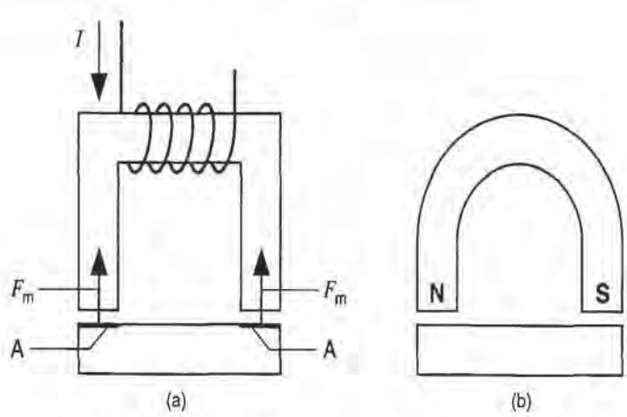


FIGURE 10.2 Flat-armature solenoid featuring field excitation (*a*) via coil; (*b*) via permanent magnet.

Determining Magnetic Circuit and Coil Specifications. The magnetic circuit consists of the working gap (between the armature and the base) and the ferrous regions. Permeability in iron is approximately three orders of magnitude greater than in air. For this reason, the iron regions conduct the field. If the effects of leakage flux are discounted, the absence of magnetic charge, $\oint\!\!\oint B\,\mathrm{d}A = 0$, means that the magnetic flux Φ_m remains constant for all cross sections A in the magnetic circuit:

$$\Phi_m = \iint_{A_1} B\,\mathrm{d}A_1 = \iint_{A_2} B\,\mathrm{d}A_2 = \iint_{A_i} B\,\mathrm{d}A_i = \text{const.} \tag{10.2}$$

If the magnetic induction is assumed to be homogeneous for all cross sections A_i, then Eq. (10.2) can be simplified to:

$$\Phi_m = B_1\,A_1 = B_2\,A_2 = B_i\,A_i = \text{const.} \tag{10.3}$$

PETITIONER'S EXHIBIT 1002
US PATENT NO. 6,581,565

The induction lines run at a 90° angle to the surfaces A_i. Equation (10.3) defines the magnetic induction in each section of the magnetic circuit (Fig. 10.3). If, as an example, Index 1 is assigned to the gap section, then B_1 and A_1 are derived with the assistance of Eq. (10.1), and one can proceed to calculate B_i for the other sections.

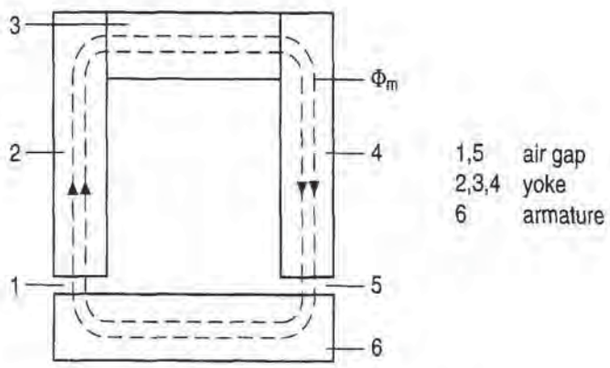


FIGURE 10.3 Magnetic circuit divided into individual sections.

The magnitude of the magnetic field strength $\mathbf{H}_i$ is determined by the material properties (permeability μ_{ri}) of the section in question. Field strength $\mathbf{H}_i$:

$$\mathbf{B}_i = \mu_o \mu_{ri} \mathbf{H}_i \tag{10.4}$$

In air, $\mu_r = 1$. In ferromagnetic materials, μ_r does not remain constant. Rather, it varies as a function of the magnetic field strength **H** (see Fig. 10.4). The relationship between **B** and **H** is defined by the **B-H**-curve.

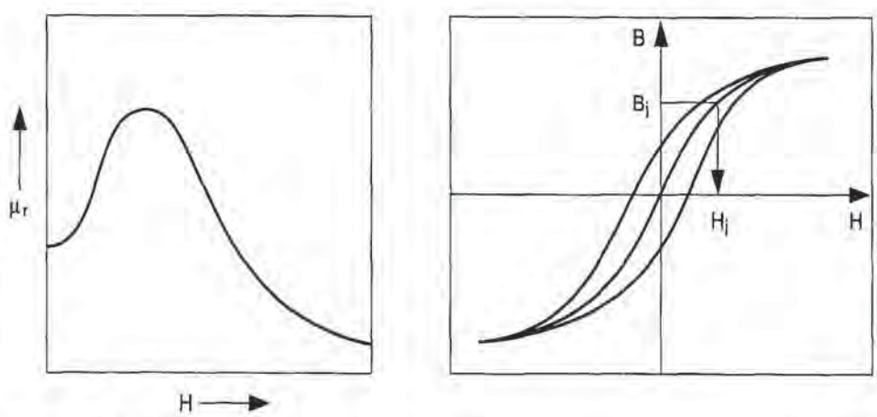


FIGURE 10.4 Progression of permeability and **B-H** curve.

Using the magnetic voltage $V_{mi} = \int \mathbf{H}_i \, d\mathbf{s}$ for the individual section, it is possible to calculate the peripheral magnetic voltage as the sum of the individual magnetic voltages V_{mi}. According to Ampere's law,

$$\Theta = \int \mathbf{H} \, d\mathbf{s} \tag{10.5}$$

this magnetic peripheral voltage is equal to the magnetomotive force Θ. It defines the *total current* of the coil, $\Theta = I\,w$. (I = current, w = number of windings.)

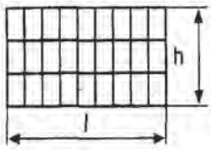
ENGR & MATH SCI LIBRARY UNIV.

PETITIONER'S EXHIBIT 1002
US PATENT NO. 6,581,565

Because the preceding calculation fails to consider leakage flux, the results must frequently be treated as approximations only. It is possible to increase the precision of the calculations by portraying the magnetic circuit as a general network (with gaps and iron regions as reluctance elements) instead of as a series circuit. The results will then reflect the effects of a large proportion of the leakage flux. Maximum precision is achieved with numeric field calculations, which provide numerical solution of Maxwell's equations.

After magnetomotive force Θ has been determined, the field coil must be dimensioned to produce the required magnetic field. The formulas contained in Fig. 10.5 can be employed to determine the field coil's specifications. For a graphic interpretation, see Fig. 10.6.

$A_W = h \cdot l$



Winding cross section area:

$$A_W = \frac{R\,\pi\,\rho\,(d_a+d_i)(1+\alpha\,\Delta\vartheta)^2\,\Theta^2}{2\,k_W\,U^2}$$

Winding number:

$$w = \left(\frac{2\,A_W\,k_W\,R}{\Pi\,\rho\,(d_a+d_i)}\right)^{1/2}$$

Wire diameter:

$$d = \left(\frac{8\,\rho\,(d_a+d_i)\,A_W\,k_W}{\pi\,R}\right)^{1/4}$$

A_W	Winding cross section area	$\Delta\vartheta$	Temperature differential between coil and room temperature
R	Coil resistance	Θ	Magnetomotive force
ρ	Specific resistance of coil wire	k_W	Coil space factor (ratio of total wire area (w/o insulation) to winding cross section area)
d_a	Outer diameter of windings	U	Voltage at coil
d_i	Inside diameter of windings		
α	Thermal resistivity coefficient of coil wire		

FIGURE 10.5 Determining coil data for specified coil resistance and voltage levels.

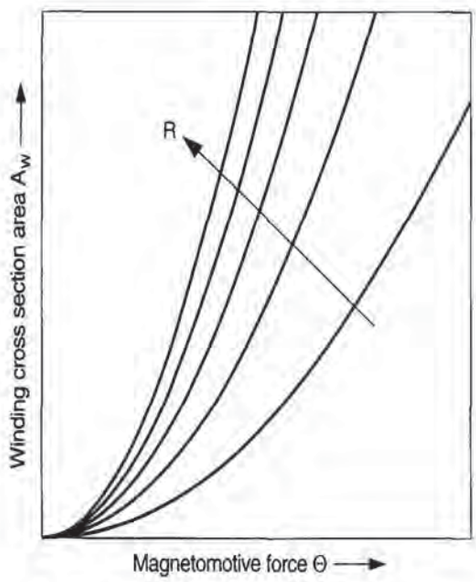


FIGURE 10.6 Area of winding A_w as function of magnetomotive force Θ (parameter coil resistance).

PETITIONER'S EXHIBIT 1002
US PATENT NO. 6,581,565

To minimize the size of the solenoid assembly, the magnetic circuit and the coil must be dimensioned to produce the smallest overall size. The formulas for coil dimensions (Fig. 10.7) can be used to minimize the volume of pot-shaped solenoids.

$$\frac{l}{d} \approx 1.5 \qquad \frac{h}{d} \approx 0.4 \ldots 0.5$$

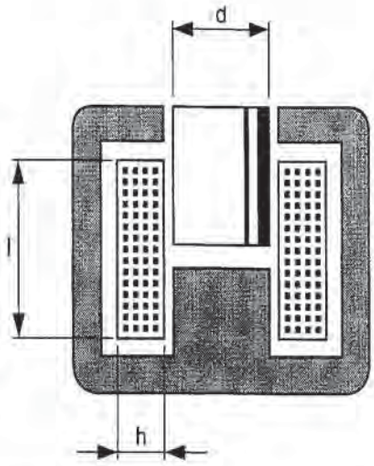


FIGURE 10.7 Selecting coil dimensions for pot-shaped solenoids.

In general, the solenoid is iteratively optimized by changing geometry in those critical areas within the magnetic circuit requiring a high magnetic voltage V_{mi}. The magnetomotive force Θ is then recalculated for the modified magnetic circuit. Figure 10.8 shows the optimization of solenoid diameter D for a particular armature diameter d.

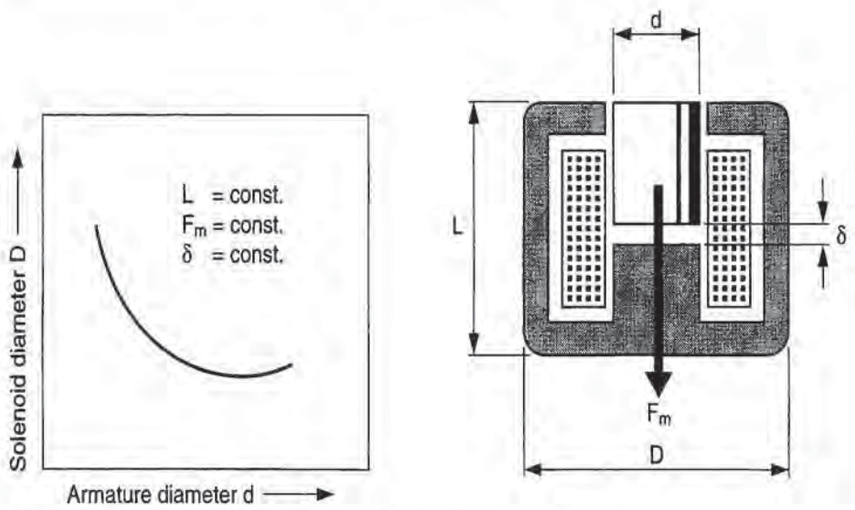


FIGURE 10.8 Relationship between solenoid and armature diameters.

Magnetic Force Curve. When the unit is intended for use in an actuator, the relationship between magnetic force and stroke will be required. With a flat armature and base, and without including the iron regions, Ampere's law [Eq. (10.5)] and Eq. (10.4) provide the following:

$$\Theta = H_\delta \delta = \frac{B_\delta \delta}{\mu_o} \tag{10.6}$$

where δ = working gap

ENGR & MATH SCI LIBRARY

PETITIONER'S EXHIBIT 1002
US PATENT NO. 6,581,565

Together with the force relationship, Eq. (10.1), the following result is obtained:

$$F_m = \frac{\Theta^2 \mu_o A_1}{2\,\delta^2}, \text{ i.e., } F_m \sim \frac{1}{\delta^2} \tag{10.7}$$

The substantial drop in magnetic force will be undesirable in many applications. Modifications to the curve for magnetic force versus stroke represent an alternative to increases in solenoid dimensions. This expedient can be effected through control of the current in the coil or by means of design modifications to the armature and base (see Fig. 10.9).

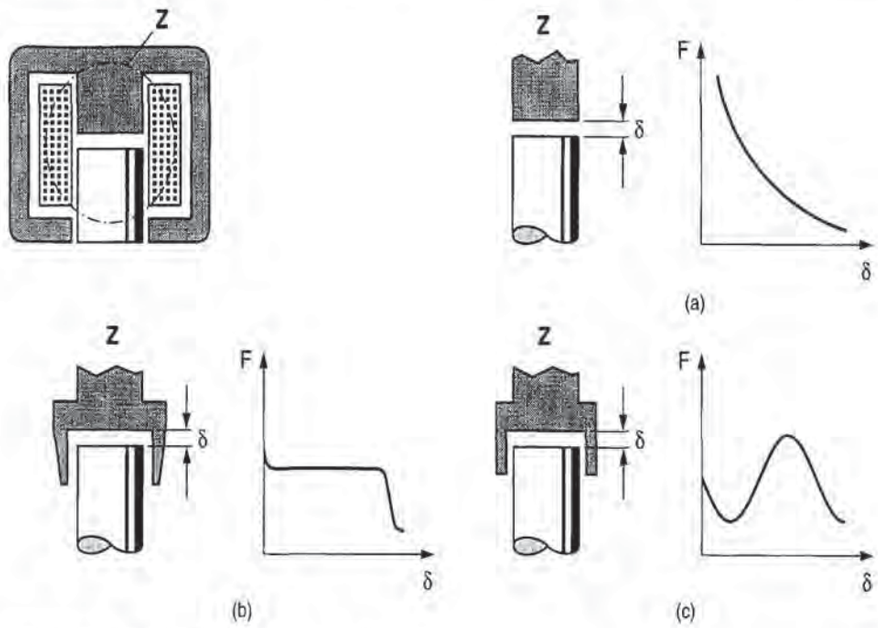


FIGURE 10.9 Design modifications and force curve.

The areas below the force-travel curves, a measure of the work performed, are always the same.

$$\int_0^\infty F_m(\delta)\, d\delta = \text{const.} \tag{10.8}$$

$$\text{with} \quad I = \text{const.}$$

Configuration c can be employed together with a spring to produce a proportional solenoid in which armature travel can be regulated as a function of current. This type of system is sensitive to interference from extraneous factors such as mechanical friction, and hydraulic and pneumatic forces. Thus, final-control systems for high-precision applications must also incorporate a position sensor and a controller (Fig. 10.10).

Dynamic Response. To show the dynamic response pattern more clearly, Fig. 10.11 provides a schematic illustration of the progression over time of three parameters: voltage u at the excitation coil, excitation current i, and armature position s.

The dynamic response pattern can be calculated using computer programs that apply Maxwell's equations (field propagation with eddy currents, self-induction) in conjunction with the motion equation.

Approximation formulas can be employed to derive rapid estimates (eddy currents and magnetic resistance in the iron regions are not taken into account):

PETITIONER'S EXHIBIT 1002
US PATENT NO. 6,581,565

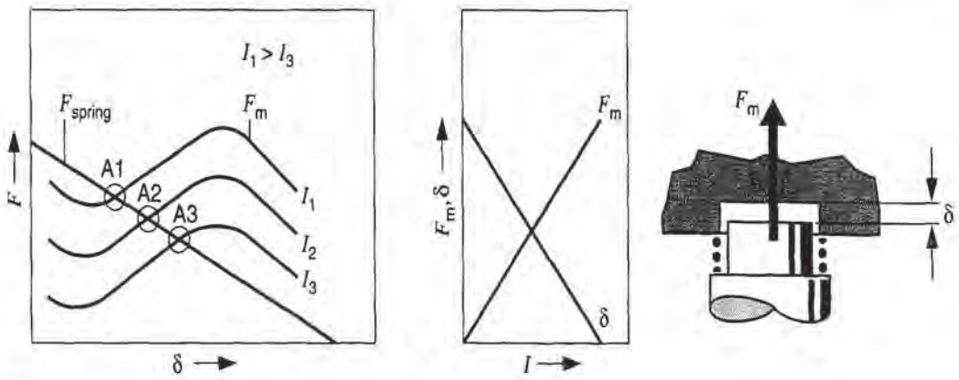


FIGURE 10.10 Operating points of a proportional solenoid.

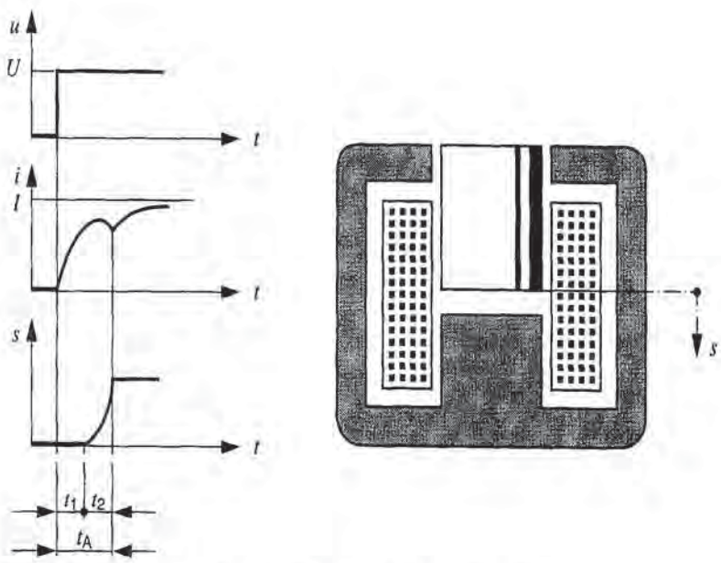


FIGURE 10.11 Progression of voltage, current, and armature travel.

$$t_1 \approx \frac{L_o}{R} \ln \frac{1}{1 - \frac{R}{U}\left(\frac{2 F_{mech}\, \delta_o}{L_o}\right)^{1/2}} \tag{10.9a}$$

$$t_2 \approx \left(\frac{3\, \delta_o m}{U\left(\frac{F_{mech}}{2\, \delta_o L_o}\right)^{1/2} - R\frac{F_{mech}}{L_o}}\right)^{1/3} \tag{10.9b}$$

where L_o = initial inductance
R = coil resistance
U = voltage at solenoid
δ_o = gap with armature lowered
F_{mech} = armature counterforce (treated as constant)
and t_1, t_2, see Fig. 10.11

ENGR & MATH SCI LIBRARY

PETITIONER'S EXHIBIT 1002
US PATENT NO. 6,581,565

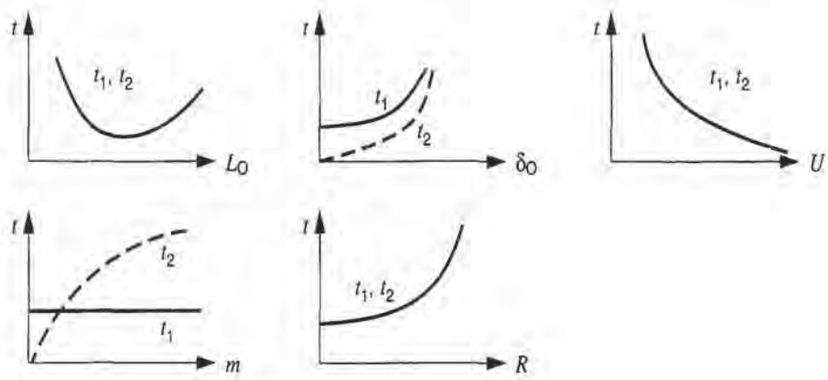


FIGURE 10.12 Relationships of t_1 and t_2.

Figure 10.12 provides an overview of the relationships between t_1 and t_2 and the parameters.

The eddy currents must also be considered in calculations dealing with electromagnets intended for operation at high speeds or switching frequencies. When the excitation current is applied suddenly, the progress over time for the magnetic force is

$$F_m(t) = F_{m0}(1 - e^{-t/\tau})^2 \qquad \text{for field generation}$$

and

$$F_m(t) = F_{m0}\, e^{-2t/\tau} \qquad \text{for field dissipation}$$

with

$$\tau = \frac{\mu_0 l_{Fe} ab}{\pi^2 \rho \delta (a/b + b/a)} \qquad \text{for rectangular cross sections}$$

with

$$\tau = \frac{\mu_0 l_{Fe} d^2}{4(2.405)^2 \rho \delta} \qquad \text{for circular cross sections}$$

where F_{m0} = static solenoid force according to Eq. (10.1)
t = time
l_{Fe} = length of iron core in which eddy currents occur
a/b = height/width of iron core (rectangular cross section)
d = diameter of iron core (circular cross section)
ρ = specific resistance
δ = working gap

Lamination to inhibit eddy currents in dc solenoids is not a standard procedure; its application is restricted to extreme cases.

Figures 10.6 and 10.12 illustrate the fact that at a given voltage, small coil resistances will furnish a small coil and short activation times. However, these benefits are accompanied by a simultaneous increase in the power loss $P_v = U^2/R$. The coil is thus designed to operate at the maximum permissible temperature.

Torque Motors. The torque motor consists of a stator and an armature—both made of soft magnetic material—and a permanent magnet. The pivoting armature can be equipped with either one or two coils.

Figure 10.13*a* shows only the magnetic flux generated by the permanent magnet. The armature is resting at the center position. The magnitude of the magnetic induction is the same at all

PETITIONER'S EXHIBIT 1002
US PATENT NO. 6,581,565

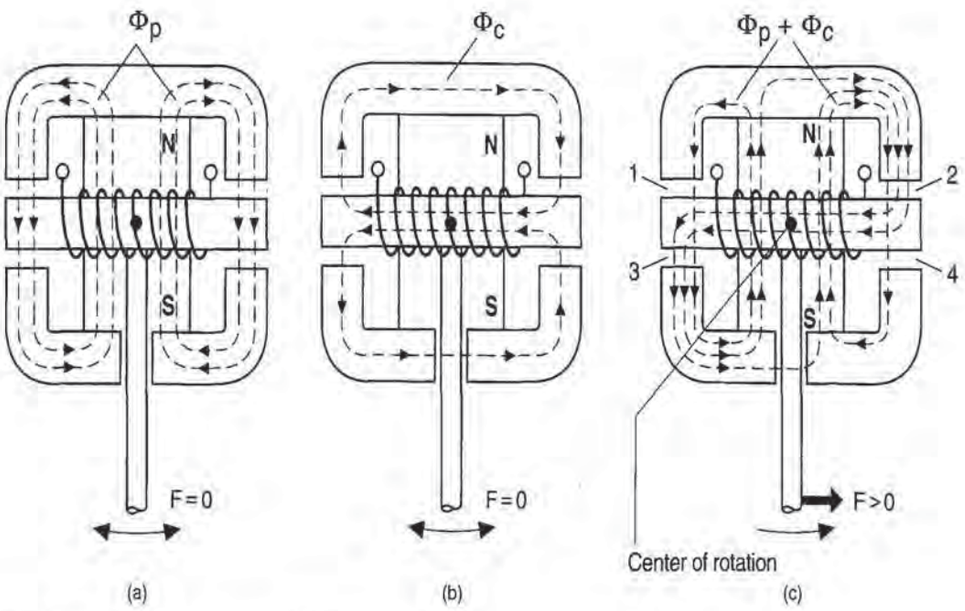


FIGURE 10.13 Design and operation of the torque motor.

gaps. Because equal amounts of force are generated at the armature ends, the forces acting on it exercise a mutual canceling effect.

Figure 10.13*b* illustrates only that magnetic flux which is generated at the coil. Figure 10.13*c* shows the cumulative pattern for the fluxes from *a* and *b*, with increased flow at gaps 2 and 3 ($\Phi_p/2 + \Phi_c/2$) accompanied by reductions at gaps 1 and 4 ($\Phi_p/2 - \Phi_c/2$). Using Eq. (10.1), the torque in the center position is

$$M = F_m r = \frac{r A B_p}{2 s} w I, \text{ i.e., } M \sim I \tag{10.10}$$

where r = armature radius
A = pole face area
B_p = magnetic induction in gap generated by permanent magnet
s = length of gap
w = number of coil windings
I = current.

Torque motors are used for applications in which substantial forces are required over small operating angles. They react more rapidly than electromagnets. In hydraulic and pneumatic applications, torque motors deliver good performance as drive units for flapper and nozzle systems.

Electromagnetic Step Motors. Electromagnetic step motors are drive elements in which a special design operates in conjunction with pulse-shaped control signals to carry out rotary or linear stepped movements. Thus, one complete rotation of the motor shaft will be composed of a precisely defined number of increments, step angles ϕ_0. The magnitude of these angles is determined by the phase number q, the pole pair number p, and by the number of teeth z in the step motor. The step motor is thus capable of transforming digital control signals directly into discontinuous rotary motion. In principle, the step motor is essentially a combination of dc solenoids. The calculations employed for dc solenoids are thus also suitable for application with electromagnetic step motors. Depending upon the configuration of the magnetic circuit, a distinction is made between three types of step motors: the variable-reluctance step motor (neutral magnetic circuit), heteropolar units (polarized magnetic circuit), and hybrid devices.

ENGR & MATH SCI LIBRARY

PETITIONER'S EXHIBIT 1002
US PATENT NO. 6,581,565

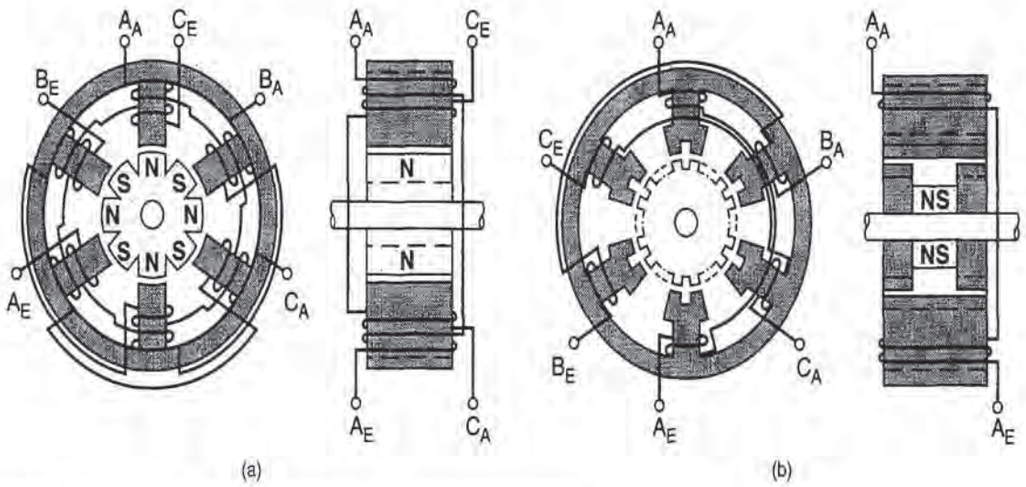


FIGURE 10.14 (*a*) Heteropolar step motor and (*b*) hybrid step motor.

Due to its positive operating characteristics (holding force available in power-off state, improved cushioning, lower control power requirement for a given volume), the polarized step motor has come to be the most widely applied (see Fig. 10.14).

Drive systems featuring electromagnetic step motors combine the following characteristics:

- Field forces induce controllable, incremental movements (minimal wear).
- Precisely graduated movements can be generated using an open-loop control circuit (without position monitors or feedback signals).
- High torque remains available at low angular velocities and in single-step operation.
- Brushless motor design makes it possible to create drive systems which combine reliability with long service life.

The operating characteristics of the rotational step motor can be described with the aid of a stationary torque-angle (M-ϕ) curve. A reasonable approximation can be obtained using sinus-shaped curves with a phase displacement reflecting the switching states of the phase windings (A, B, C) (Fig. 10.15*a*). Assuming that external torque inputs can be excluded, the

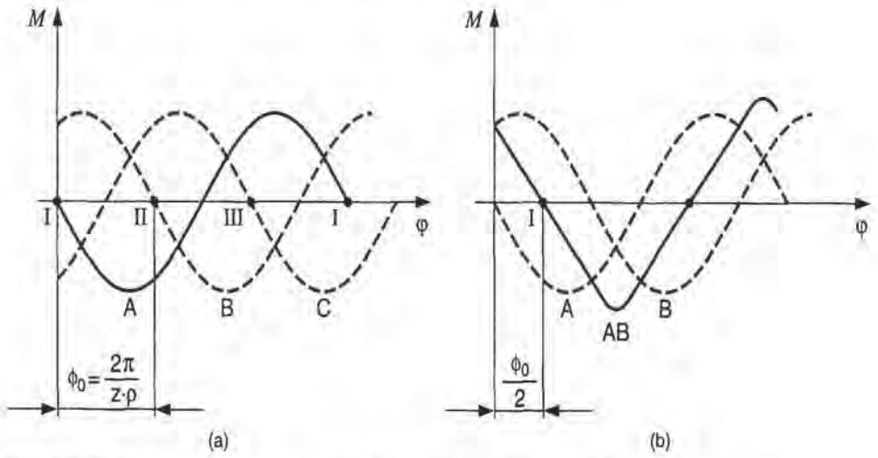


FIGURE 10.15 (*a*) Stationary torque-angle characteristics and (*b*) step-halved.

PETITIONER'S EXHIBIT 1002
US PATENT NO. 6,581,565

armature's stable position will be found where the backslope of the curve intersects the abscissa ($I, \Sigma M = 0, dM/d\phi < 0$). Phase B, C, etc., can then be activated to perpetuate rotation. The periodicity of the stable positions I, II, III is the step angle ϕ_0.

If phase A is followed by simultaneous excitation of A and B with current pulses of the same amplitude, the result is a summing pattern corresponding to Fig. 10.15*b*. The geometric step angle ϕ_0 can then be halved. Alternatively, simultaneous excitation with current pulses of different amplitudes (current control) can be used to subdivide ϕ_0 to almost any degree desired (microstep operation). However, the use of this strategy to enhance the step motor's positioning precision is not possible due to manufacturing tolerances. When step motors are used in drive systems which rely upon open-loop control methods, avoiding stepping errors becomes an important priority (synchronous response).

For critical applications, dynamic simulation of the step drive system's dynamic response pattern is recommended. Here, a good approximation is derived by portraying the step motor using a transfer function of a second-order system. Dynamic response can also be evaluated using the torque-step frequency pattern (*M-f* pattern) for potential step-error-free operation in a start-stop frequency range, Fig. 10.16*a*, and an operating frequency range, Fig. 10.16*b*.

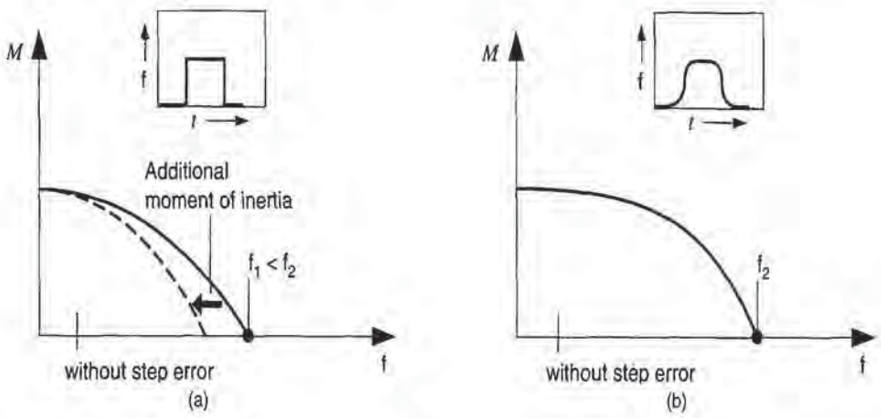


FIGURE 10.16 Torque-step frequency characteristic.

The range in which step error does not occur contracts in response to additional inertial torques or mobile masses. Impressed current induces an upward shift in the potential frequency range which is larger than that derived from impressed voltage. This demonstrates that the step motor's response pattern is strongly influenced by the electronic control strategy. The stepping frequency controls the angular velocity, the pulse distribution (A → B or A → C, see Fig. 10.15) determines the direction of rotation, and the number of pulses governs the pivot angle.

Step motors are only suitable for use as direct-drive elements (the motor's armature operates directly against the actuated unit, no gear drive) in those applications where the influence of load fluctuations and interference factors remains limited, as stepping errors can otherwise occur. For this reason, digital linear actuators featuring integrated rotary step motors and threaded spindles are becoming increasingly popular as linear-motion generators in high-demand applications. When operated within a closed-loop control system, step motors can provide improvements in dynamics, positioning precision, and sturdiness. However, the cost advantages associated with open-loop operation are forfeited.

Moving Coils. The moving coil is an electrodynamic device (force applied to current-saturated conductor in a magnetic field). A spring-mounted coil is located in the ring gap of a magnetic circuit featuring a permanent magnet. When current flows through the coil, a force is exerted against it. The direction of this force is determined by the flow direction of the current itself.

ENGR & MATH SCI LIBRARY

PETITIONER'S EXHIBIT 1002
US PATENT NO. 6,581,565

The positioning force can be calculated using

$$F = B_A L_W I, \text{ i.e., } F \sim I \tag{10.11}$$

where B_A = magnetic induction in the gap
L_W = length of the coil wire
I = excitation current

As the force is not affected by the travel position, a spring can be included to produce a proportional relationship between travel and current.

The advantages of the moving coil include low hysteresis and good linear response. Low mass acts in combination with low coil inductance to provide excellent dynamic-response characteristics. The main liabilities of this design lie in the low force and limited work per stroke for any given unit dimensions.

dc Motors. dc motors are used to discharge a multiplicity of functions in modern cars (today up to 70 motors per vehicle). These motors are generally permanently excited dc devices, as the magnetic field remains continually available without additional energy consumption. For economic reasons, these units are virtually always equipped with ferrite magnets.

Design and Operation. The dc motor depends for its operation on the forces generated in a conductor within a magnetic field when current is applied.

The permanent-magnet-excited motor consists of

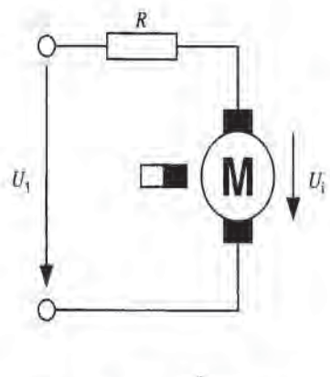
- The magnetic circuit consisting of a permanent magnet for generation and an iron core and a stator frame to conduct the magnetic flux
- Energized coils
- Carbon brushes and commutator, arranged to direct the current to the rotating coil while maintaining the force flow in a single direction

The stationary characteristic can be represented using the following equations (see Fig. 10.17).

$$U_1 = IR + U_i \tag{10.12a}$$

$$U_i = c\, z\, \Phi\, \omega \tag{10.12b}$$

$$M_i = M_v + M = c\, z\, \Phi\, I \tag{10.12c}$$



U_1 – Terminal voltage
U_i – Induction voltage
M – Shaft torque
M_a – Starting torque
M_i – Internal torque
M_v – Torque loss
c – Constant
z – Number of conductors
Φ – Magnetic flux
ω – Armature rotation frequency
I – Current
R – Armature resistance

FIGURE 10.17 dc motor, circuit diagram.

PETITIONER'S EXHIBIT 1002
US PATENT NO. 6,581,565

After inserting Eqs. (10.12*b*) and (10.12*c*) in (10.12*a*), with

$$\omega_{0i} = \frac{U_1}{c\, z\, \Phi} \qquad \text{(ideal idle speed)} \tag{10.13a}$$

$$M_a = c\, z\, \Phi\, \frac{U_1}{R} - M_v \qquad \text{(stall torque)} \tag{10.13b}$$

one obtains

$$\omega = \omega_{0i}\left(1 - \frac{M + M_v}{M_a + M_v}\right) \tag{10.14}$$

or, with idle speed $\omega_0 = \omega(M = 0)$

$$\omega = \omega_0\left(1 - \frac{M}{M_a}\right) \tag{10.15}$$

The motor draws power P_1 from the dc circuit.

$$P_1 = U_1 I \tag{10.16}$$

or

$$P_1 = \frac{U_1}{c\, z\, \Phi}\,(M_v + M) = \omega_0\,\frac{M_v + M_a}{M_a}\,(M_v + M) \tag{10.17}$$

The output at the shaft is the mechanical power P_2

$$P_2 = M\,\omega = M\,\omega_0\left(1 - \frac{M}{M_a}\right) \tag{10.18}$$

Using Eqs. (10.17) and (10.18), the efficiency η can be calculated as a function of the shaft torque.

$$\eta = \frac{P_2}{P_1} = \frac{M(M - M_a)(M_v + M_a)}{M_a(M_v + M)} \tag{10.19}$$

Maximum efficiency as a function of load is obtained by setting the derivative $d\eta/dM = 0$ with

$$M_{\max} = M_v + [M_v(M_v + M_a)]^{1/2} \tag{10.20}$$

In comparison, the output power derived with Eq. (10.18) reaches a maximum at $M = M_a/2$, and thus at a higher value.

Figure 10.18 shows a performance diagram with speed n, current I, and efficiency η as function of the load torque M. It is not possible to determine speed and current separately.

Equations (10.12*a*) through (10.20) illustrate the interactions and the factors that affect the motor's performance curve. The influence of the design parameters is shown in Fig. 10.19.

The magnetic flux Φ is determined by the dimensions and intrinsic material characteristics of the magnet, and by the stack length of the armature and the rest of the magnetic circuit. The speed/torque curve responds to increasing magnetic flux Φ by tilting progressively to the horizontal axis; this response pattern is indicative of a more powerful motor (see Fig. 10.19*a*).

Variations in the number of turns z change the idle speed n_o at the same starting torque (see Fig. 10.19*b*); changes in the armature's resistance (produced by selecting a different wire diameter d) affect the stall current, and thus the stall torque, obtained at any given idle speed n_o (see Fig. 10.19*c*). The maximum achievable copper content is determined by the winding technique.

ENGR & MATH SCI LIBRARY

PETITIONER'S EXHIBIT 1002
US PATENT NO. 6,581,565

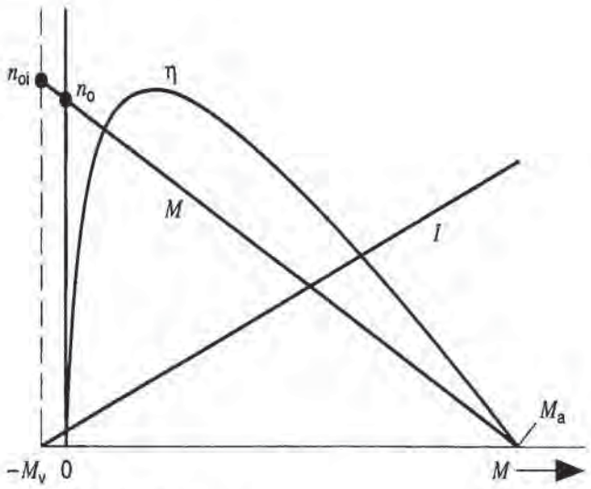


FIGURE 10.18 Motor performance curve.

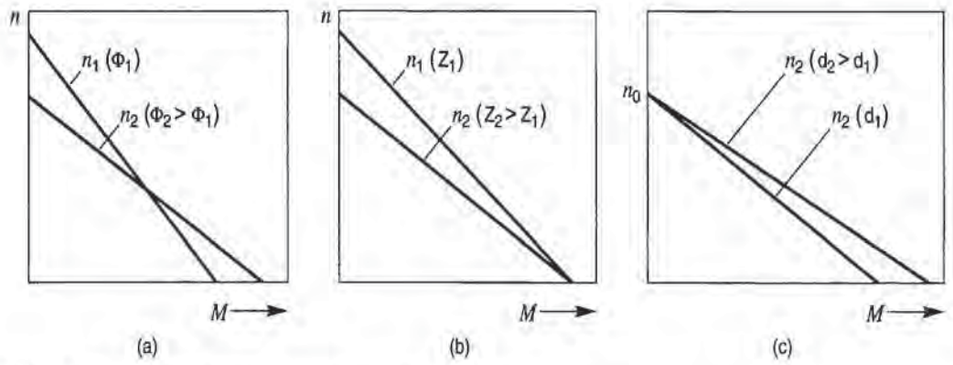


FIGURE 10.19 Effect of design parameters on rotational speed.

Units used in real-world applications display small deviations from the theoretical performance curve as a result of voltage drop at the carbon brushes, the current transfer to the commutator, the armature reaction field produced by the motor's current, and, finally, various rotational and flux losses.

The options for using the electrical parameters to affect the rotating speed are illustrated in Fig. 10.20. Variations in the voltage U (e.g., of the kind produced electronically with a pulse-width modulation) produce a parallel displacement in the speed curve (Fig. 10.20*a*). Other common options include the installation of a ballast resistor R_v and the inclusion of a third carbon brush. Less common (due to cost) is a design in which the winding is divided between two commutators; these can then be activated individually, in parallel, or in series. Servo motors generally operate for brief periods of time, but also over the entire range represented by the unit's characteristic curve.

Each motor must be built specifically for the operating conditions anticipated for the individual vehicle. Ferrite magnets must be selected for the lowest potential temperature, as it is here that the resistance to demagnetization is lowest. When circumstances demand, thermoswitches can also be included to provide protection against overheating.

Automotive actuators must be small and light. Motor volume is directly proportional to torque requirement. At the same time, the power output is proportional to torque multiplied

PETITIONER'S EXHIBIT 1002
US PATENT NO. 6,581,565

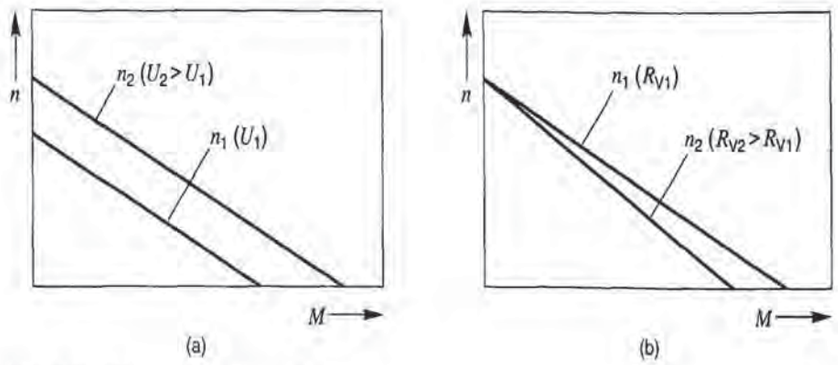


FIGURE 10.20 Speed variations in dc motors.

by rotating speed. Thus, the output can be increased by raising the operating speed; here the accompanying rise in noise levels is the limiting factor. Small motors are equipped with gear-drive units to obtain the required levels of actuating force.

Magnetostrictive Actuators. Ferromagnetic materials respond to increased magnetic field strength by expanding or contracting (magnetostrictive effect). This is due to the Weiss' domains turning in the field direction. The maximum contraction obtained with iron is –8 μm/m. Highly magnetostrictive materials composed of rare-earth/iron alloys display a maximum elongation of 1500 to 2000 μm/m. Maximum potential elongation is obtained at the optimal mechanical pre-tension T_0 (Fig. 10.21).

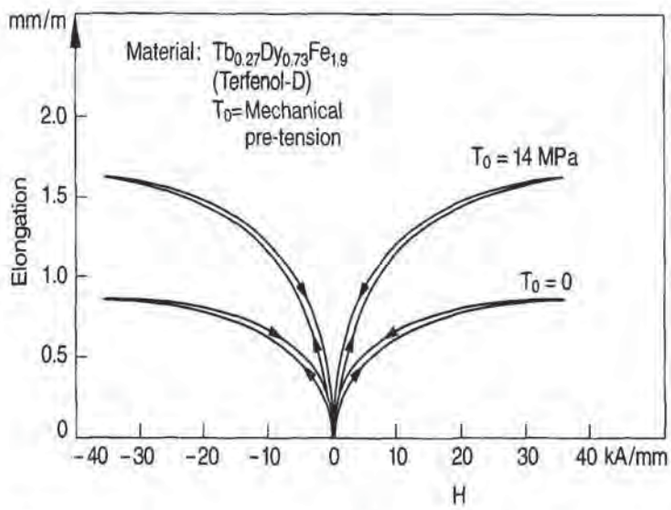


FIGURE 10.21 Magnetostrictive form variations as a function of field strength.

The specific advantages of the magnetostrictive transformer are high actuator forces, rapid response, good rigidity, and a high level of electromechanical efficiency.

The disadvantages include the small variations in length, the high power loss associated with generation of the large maximum field strengths which the unit requires (also in static operation), the length variation with hysteresis, the expense, and the limited availability of the requisite materials. The material is also brittle and difficult to machine.

The commercial availability of the transformers is limited to units designed for research purposes. We are not familiar with any applications in production motor vehicles.

ENGR & MATH SCI LIBRARY

PETITIONER'S EXHIBIT 1002
US PATENT NO. 6,581,565

10.2.2 Electrical Actuators

Piezoelectric Actuators. When mechanical compression and tension are brought to bear on a piezoelectric body, they produce an asymmetrical displacement in the crystal structure and in the charge centers of the affected crystal ions. The result is charge separation. An electric voltage proportional to the mechanical pressure can be measured at the metallic electrodes (direct piezoelectric effect).

If electric voltage is applied to the electrodes on this same body, it will respond with a change in shape; the volume remains constant. This reciprocal piezoelectric effect can be exploited to produce actuators. Sintered ceramics, lead-zirconate-titinate (PZT), are the commonly used materials for these applications. The precise composition can be modified to obtain the desired material characteristics. The magnitude of the shape change depends on the electric field strength E. The relevant equation is $E = U / s$ (U = voltage, s = electrode gap). Single-element actuators require field strengths of up to 2 kV/mm and therefore very high voltage to achieve maximum travel (see Fig. 10.22).

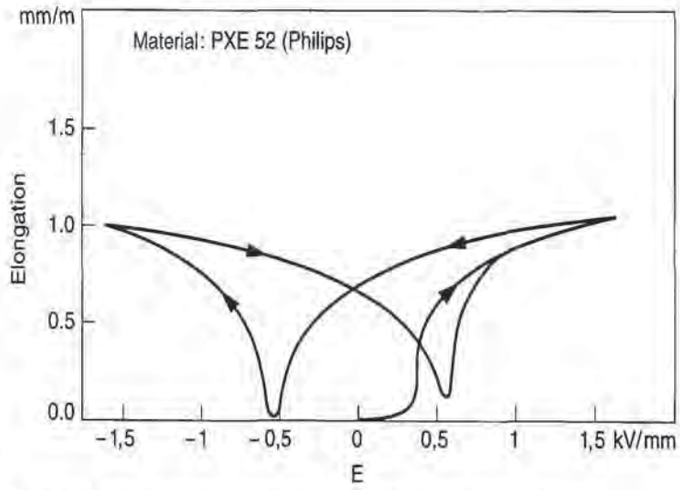


FIGURE 10.22 Form changes as a function of electric field strength.

Stacked-design translational devices consist of piezoelectric layers of between 0.3 and 1 mm in thickness, featuring a metallic electrode between each layer. This design is employed to lower the voltage (down to, for instance, 800 V) while simultaneously increasing the excursion rate. The layers are electrically parallel and form a series circuit (see Fig. 10.23*a*).

Flex elements are formed by joining two layers with varying intrinsic rates of elongation. The elongation occurs along the vertical axis of the direction in which the field strength is projected (transverse effect). Flex elements display larger excursion rates with lower actuating forces (see Fig. 10.23*b*).

New manufacturing techniques make it possible to produce multilayer piezoelectric devices with thinner layers; these can be used to obtain the required field strength at voltages as low as approximately 100 V and below.

However, due to the numerous parallel elements, the advantages associated with the low control voltage are obtained only at the price of increased capacitance and higher operating currents.

The positive attributes of the piezoelectric actuator include a high dynamic response level, substantial actuator force, voltage-proportional elongation, excursion with no power consumption in static operation, and (practically) no wear in the piezoelectric element.

The corresponding liabilities include minimal elongation changes, high operating voltage, hysteresis during elongation, a temperature-sensitive stroke, and a drift in operating response as the unit ages. The material itself is brittle and difficult to machine.

PETITIONER'S EXHIBIT 1002
US PATENT NO. 6,581,565

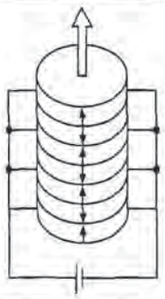
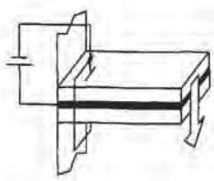
	a	b
Elongation Δl	Parallel to electrical field	Perpendicular to electrical field
Design types		
Typical regulation distance and elongation	$\frac{\Delta l}{l_0} = 0.17\ \%$	$\Delta l \leq 1000\ \mu m$ and more
max. statical load	≤ 35 000 N	≤ 0.01 ... 0.05 N
Typical operation voltage	150 ... 1000 V 50 ... 150 V (multilayer)	10 ... 300 V

FIGURE 10.23 Design and specifications of different transformer versions.

Piezoelectric actuators are applied in precision positioning devices and as active oscillation dampers. Potential automotive applications (with a voltage supply of 12 V) have yet to be thoroughly investigated. However, it is expected that the piezoelectric actuator—and the multilayer stacked-design device in particular—will gain popularity in closed-loop automotive control systems, where they will serve as a replacement for the conventional actuator in applications requiring a higher level of performance.

Electrostatic Actuators. In the past, use of electrical field forces was restricted to some measurement devices and to the acceleration of charged particles. Microactuator technology makes it possible to apply these small forces in mechanical drive devices. These devices combine high switching speeds with much smaller energy loss than that found in electromagnetic actuators. The disadvantages are the force/travel limitations and the high operating voltages. At present, microactuators are rarely encountered outside the research laboratories; thus, the electrostatic actuator's current commercial significance is negligible.

Electrorheological Fluids. The electrorheological effect is based on polarization processes in minute particles suspended in a fluid medium. These particles modify the fluid's viscosity according to the orientation in the electrical field. The effect can be employed to adjust the viscosity between "freely flowing" and "rigid." Reaction times are measured in ms. Among the disadvantages are interference factors, temperature sensitivity, high voltages, control powers of several hundred watts, and the price, which is still high. The electrorheological effect is exploited in controlled transfer and damping elements.

10.2.3 Thermal Actuators

Temperature-Sensitive Bimetallic Elements. The temperature-sensitive bimetallic element is composed of at least two bonded components of varying thermal-expansion coefficients. When heat is applied, the components expand at different rates, causing the bimetallic element to bend. When electrically generated heat is applied, these devices become actuators.

ENGR & MATH SCI LIBRARY UCLA

PETITIONER'S EXHIBIT 1002
US PATENT NO. 6,581,565

The passive component is characterized by a lower thermal-expansion coefficient. Meanwhile, the active component should maintain a constant coefficient of thermal expansion over the largest possible range.

The passive element in the most common type of temperature-sensitive bimetallic device is invar ($FeNi_{36}$), while the active component is an alloy of iron, nickel, and manganese ($FeNi_{20}Mn_6$). Common element configurations include strips, coils, spirals, and wafers. Temperature-sensitive bimetallic devices are readily available and inexpensive. They can be applied at temperatures of up to roughly 650 °C, and display a high degree of consistency in their shape-change response (up to several million cycles). The drawbacks include the modest actuator forces, the low work potential for a given volume (energy density), and the fact that only a single type of shape modification (flexural) is possible.

Memory Alloys. Memory alloys are metallic materials which exhibit a substantial degree of "shape memory." The explanation for this phenomenon can be found in the reversible, thermoelastic martensitic transformation, in which two different crystal structures are adopted. As long as the temperature remains below the transformation threshold, the structure remains martensitic. However, when the alloy is heated beyond the transformation temperature, it responds by becoming austenitic.

The element's shape is changed permanently by the one-way effect. If the element is heated to beyond the transformation temperature, it returns to its former shape. If the component is then reshaped after cooling, the entire process can be repeated. Thermomechanical pretreatment processes can be employed to achieve a two-way effect. The component then assumes one defined shape when heated, and another when cooled.

Yet another phenomenon is superelasticity. Application of loads produces an extension of up to 10 percent; the effect is reversed once the load is removed. However, because this effect is extremely sensitive to temperature, it has yet to be employed in the construction of actuators. The materials are commercially available, the base materials are nickel-titanium (NiTi–) and copper-zinc-aluminum alloys (CuZnAl–). The transformation temperatures of these alloys lie between –100 and +100 °C, with the one-way effect also being obtained outside this range.

The benefits of memory alloys include the high effective output for a given volume and the ability to complete work cycles within a minimal temperature interval of 10 to 30 °C. The memory components can be formed to suit the particular application. The wire's resistance can be employed for direct heating. The material itself can be formed with or without physical machining, and can also be welded. Among the disadvantages must be counted the limited thermal range of application and the high price.

Memory alloys are used as drive, final-control, and triggering elements in various technical applications (automotive, household appliances, heating and climate control, medical technology, etc.). The forms assumed by the actual components include triggering wires, coil springs, and flex and torsion elements.

The memory element can be used as sensor and actuator—for instance, in a liquid medium—in which temperature changes will induce shape changes in the component.

Expansion Elements. The expansion element exploits the volume-versus-temperature response of specific solid and fluid media which exhibit large coefficients of thermal expansion. The volumetric response is converted to a stroke motion. The expansion medium is housed in a rigid container. The motion is converted to a stroke using diaphragms or elastomer inserts. Electrically controlled expansion elements find application as actuators. Expansion elements are inexpensive and robust, and combine large stroke travel with substantial positioning forces.

However, these devices are only suitable for application within a limited temperature range. Their dynamic response is also less than overwhelming. Expansion elements are widely applied in automotive technology (for instance, choke actuators on carbureted engines).

PETITIONER'S EXHIBIT 1002
US PATENT NO. 6,581,565

10.3 AUTOMOTIVE ACTUATORS

10.3.1 Antilock Braking

(See Chap. 15 and **traction control systems**, Chap. 16.)

Both antilock braking systems (ABS) and traction control systems (ASR) limit the rate of slip between tire and road surface. These systems enhance vehicle stability and steering response while maintaining optimal braking and acceleration characteristics. ABS and ASR employ a single set of actuators to modulate braking pressure. In addition, ASR devices supplement braking intervention by adjusting engine output.

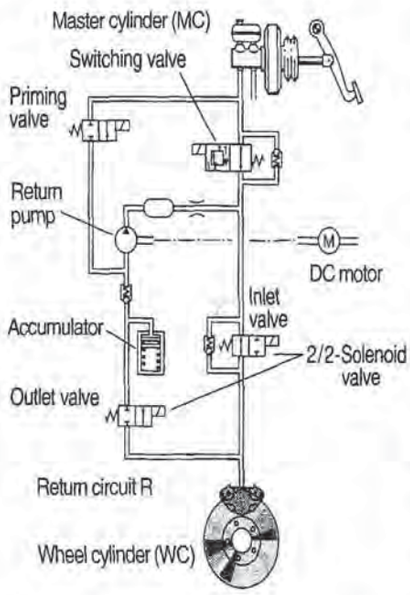


FIGURE 10.24 ABS/ASR hydraulic circuitry.

Actuators for Braking Intervention. Braking pressure is regulated normally via 2/2 solenoid valves (valves with two ports and two switch positions, see Fig. 10.24). When no current is applied, the inlet valve remains open and the outlet valve is closed, allowing unrestricted wheel braking.

ABS/ASR systems modulate pressure by controlling two 2/2 solenoids for each wheel or for two wheels of one axle. With no current, the inlet valve remains open while the outlet valve stays closed. To maintain pressure, current is applied to the inlet valve. Pressure release is obtained by transmitting current to both valves.

Various pulse sequences applied to the inlet valve generate a step-by-step increase of the wheel braking pressure (wheel brake pressure modulation).

Using the same pulse sequence for the outlet valve while the inlet valve remains closed, a step-by-step brake pressure decrease in the wheel cylinders is achieved. Switching and priming valves of a 2/2 type can be incorporated in the circuit to provide the additional functions required for the ASR (Fig. 10.25).

Solenoid Valve Design. One part of the magnetic circuit is located in the hydraulic chamber; here the armature and the pole piece simultaneously serve as valve elements in a design known as the wet solenoid. The solenoid coil and the other part of the magnetic iron circuit are located outside the hydraulic chamber. This design requires the presence of a pressure-resistant sealing element. This element must also be nonmagnetic, in order to ensure that the magnetic flux flows through the working gap and the armature in the desired fashion.

The solenoid circuit is designed to provide reliable switching and pressure maintenance at maximum temperature (maximum coil resistance), minimum voltage, and maximum pressure. At the same time, armature clearance and residual gap must both be adequate to ensure that the valve continues to function at low temperatures (brake-fluid viscosity changes exponentially (by three powers of ten) in the range between –40 and +120 °C). The maximum operating pressures can extend in extreme cases to more than 200 bar. Typical switching times are 4 to 10 ms. Dynamic response is evaluated according to the pressure variation at a specified control pulse. The duty-cycle requirements for ABS are minimal, but ASR switching and priming valves must be capable of 100 percent permanent duty. The maximum cycle numbers correspond to several million actuations.

ENGR & MATH SCI LIBRARY UCLA

PETITIONER'S EXHIBIT 1002
US PATENT NO. 6,581,565

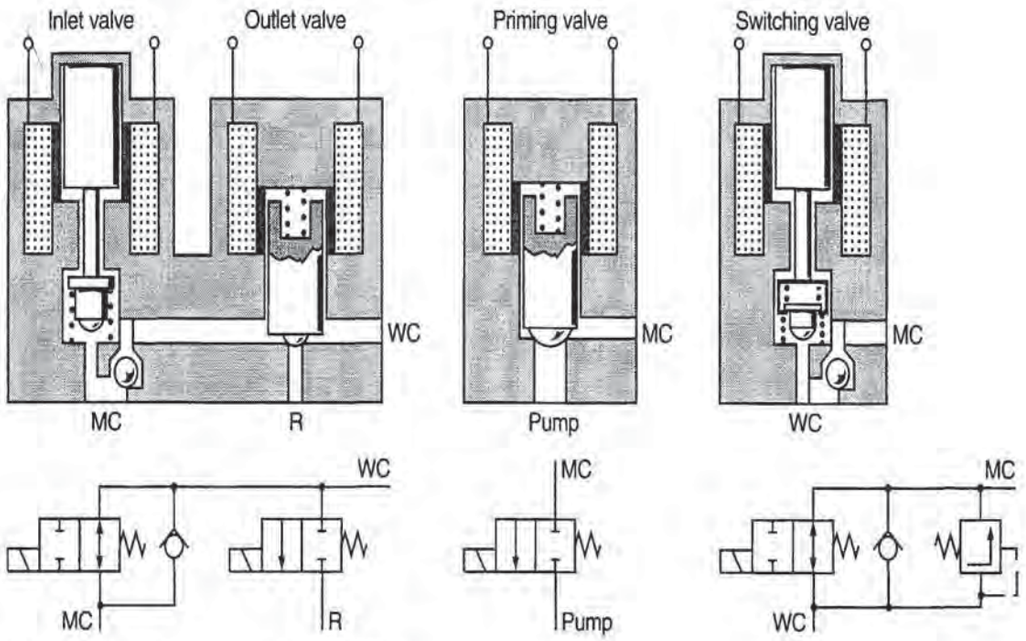


FIGURE 10.25 2/2 solenoid valves for ABS/ASR.

ETC with Throttle-Aperture Adjustment. Either of two standard methods can be employed for throttle regulation. Electronic Throttle Control (ETC) systems feature an actuator (servo motor) mounted directly at the throttle valve. On systems incorporating a traction-control actuator, the actuator (servo motor) is installed in the throttle cable (Bowden cable).

The design configuration of the electronic throttle-control actuator is illustrated in Fig. 10.26. To enhance clarity and facilitate understanding, all rotating components (except the throttle plate) are portrayed as linear-motion devices. The throttle shaft travels between two

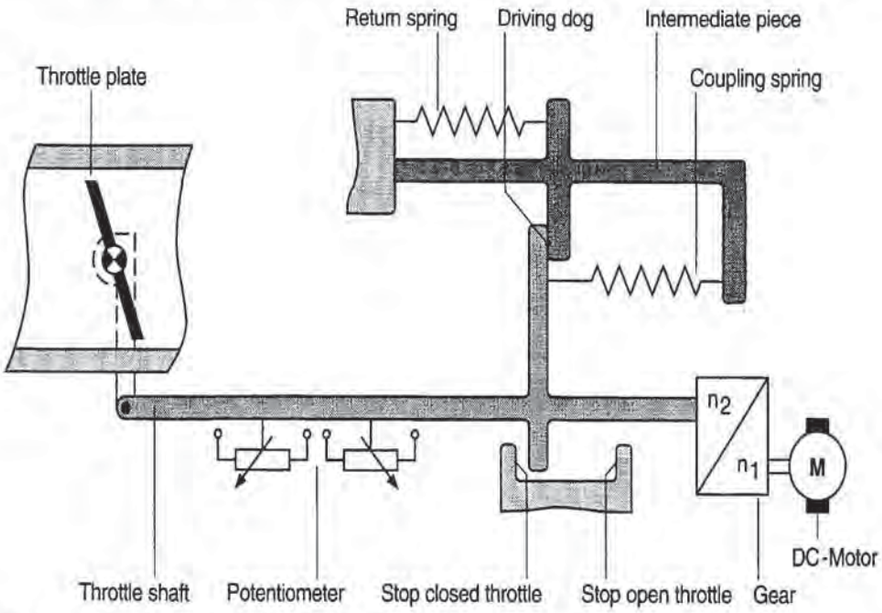


FIGURE 10.26 Operation of electronic throttle control.

PETITIONER'S EXHIBIT 1002
US PATENT NO. 6,581,565

motion limiters; these define the closed throttle and maximum aperture positions. The shaft is powered by a dc motor via a dual-gear drive. When the motor is off, a return spring pulls the intermediate piece back toward the idle-air stop. The driving dog pushes the throttle shaft toward the idle position. The coupling spring holds it in a defined idle position. This position corresponds to an idle speed ensuring adequate engine power to maintain power-steering and brake operation in the event of system failure.

Current can be applied to the dc motor in either direction. One direction opens the throttle plate and tensions the return spring. The other direction closes the throttle plate. When the throttle plate closes all the way, the coupling spring is tensioned. Two potentiometric throttle-position sensors are included in a design calculated to provide redundant system capacity. The electronic control unit uses the signals from these sensors to regulate motor current for the desired throttle position; the signals thus represent part of a closed-loop control system.

Traction-Control Actuator. The actuator can be installed in any of several locations within the engine compartment. No modifications to the throttle body are required.

Figure 10.27 illustrates the operating principles in a simplified linear flow pattern (the actuator components are actually rotary elements). The ends of the Bowden cable sections are connected to rotary cam/linkage spring assemblies.

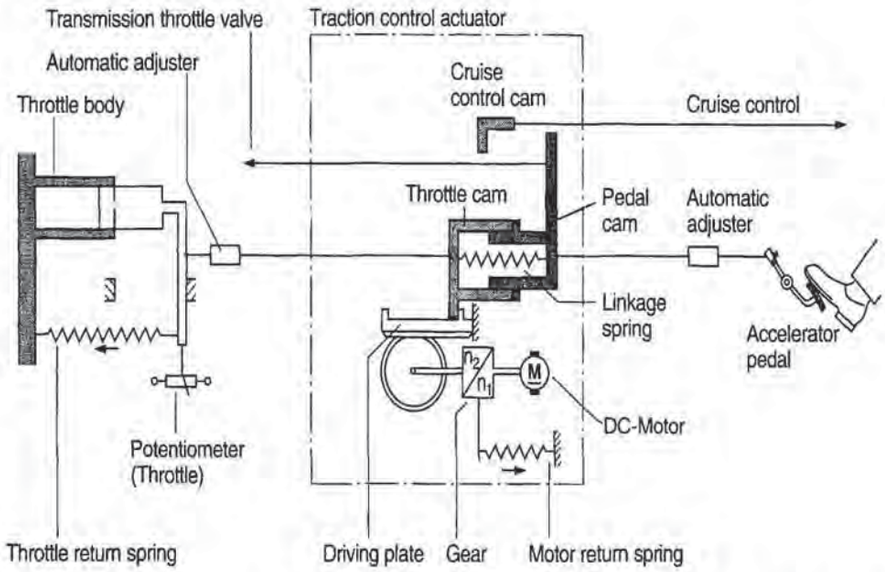


FIGURE 10.27 Operation of a traction-control actuator located between the accelerator pedal and throttle body.

Under normal operating conditions, the pressure applied at the accelerator pedal is relayed through the Bowden cable and linkage spring coupling to open the throttle valve. The servo motor comes to life when the ABS/ASR control unit transmits a command to reduce the throttle-valve aperture. The servo motor pulls the engagement mechanism to the left via gear drive and Bowden cable. Once the initial take-up range has been covered, the linkage is activated to reduce the throttle-valve opening. The servo motor is deactivated as soon as the ASR no longer requires throttle-valve regulation. A return spring then brings the motor back into its original position, allowing the traction control actuator to drive back to its original at rest position.

The traction-control actuator can also be used in conjunction with a cruise-control system. A separate cam connects the Bowden cable for the cruise control to the actuator assembly. This layout is employed to retain the option of traction-control intervention when the cruise-control system is activated.

ENGR & MATH SCI LIBRARY UCLA

PETITIONER'S EXHIBIT 1002
US PATENT NO. 6,581,565

Because the linkage spring must be considerably stronger than the throttle-return spring, it exerts a perceptible effect on the resistance at the accelerator pedal.

Another approach to engine intervention is embodied in a design in which the linkage spring is integrated within the throttle body. Yet a further option is to install a second throttle valve which remains open during normal operation; a separate Bowden cable is installed between this throttle body and the actuator to regulate the valve for active traction-control duties. Because the linkage spring is installed parallel to the throttle-return spring, the preload is substantially lower than that generated by the design described here; there is almost no perceptible feedback at the accelerator pedal. Actuator weight and dimensions are also reduced substantially.

10.3.2 Fuel-Injection for Spark-Ignition Engines

(See Chap. 12.)

Electronically controlled fuel injection systems meter fuel with the assistance of electromagnetic injectors. The injector's opening time determines the discharge of the correct amount of fuel.

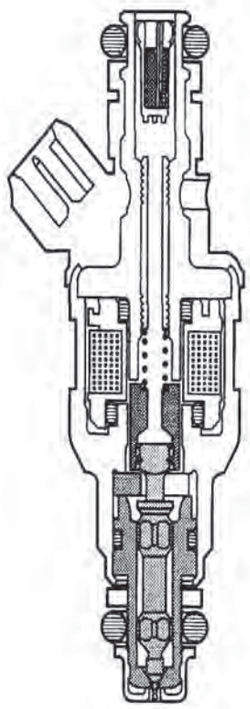


FIGURE 10.28 Injector unit for multipoint fuel injection system.

On single-point injection units, one injector unit is installed at a central location upstream from the throttle valve. Multipoint injection systems feature a separate injector at each cylinder (Fig. 10.28). This type of injector is located in the manifold tract just above the intake port into which it discharges its fuel.

Operating Requirements. The injectors are 2/2 valves with coaxial fuel inlet and lateral plug. They operate with minimal strokes of less than $\frac{1}{10}$ mm.

Besides the precise opening and closing, the reliable sealing and the discharge pattern which an individual injector provides are all largely determined by the design of its metering apparatus, thus exercising a major effect on starting and response, fuel consumption, and emissions.

Electromagnetic injectors have to fulfill the demand for precise fuel metering, consistent linear response at minimal quantities, extended dynamic flow range (DFR), good spray formation and atomization, positive seal at injector seat, resistance to corrosion, operating consistency, and low noise.

Low-resistance injectors with current-controlled output stages achieve shorter switching times. See Table 10.1.

10.3.3 Fuel Injection for Diesel Engines

Distributor-Type Fuel Injection Pumps contain rotary solenoid actuators for injection quantity, and two position valves for engine operation and shutoff.

The fuel quantity injected by an in-line pump is a function of control-rack position and pump speed (Fig. 10.29).

PETITIONER'S EXHIBIT 1002
US PATENT NO. 6,581,565

TABLE 10.1 Typical Injector Specifications

	Units	Multipoint injection	Single-point injection
Line pressure . . . max.	kPa	200–380	100–300
Static flow at 250 kPa,	g/min	100–430	—
at 100 kPa,	g/min	—	200–520
Opening time	ms	1.5	0.75
Closing time	ms	0.8	0.65
Variation ratio (DFR)		1:10	1:16
Durability >mio.cycle		1000	1000
Needle/armature weight	g	4.3	2.7
Length	mm	77	53

The control rack of an EDC in-line pump is shifted by a linear-motion solenoid with a conic armature and base for long stroke application (see pages 10.5 and 10.6). The actuator is attached directly to the pump.

When no current is applied to the linear-motion solenoid, a spring pushes the control rack into the stop position and thus interrupts fuel delivery. As current increases, the control-rack travel and, with it the injection quantity, increase.

Typical operating data of the solenoid actuator are (full load, stationary condition): rack travel 13 mm, spring force 32 N, ECU current output 6 A, 200 Hz. By pulsation of the ECU-current, the actuator friction is minimized. Maximum rack travel is about 20 mm.

The electronically controlled unit injector (Fig. 10.30) has been developed to meet the future emissions regulations by realizing high injection pressures and precise control of start of injection and injection quantity.

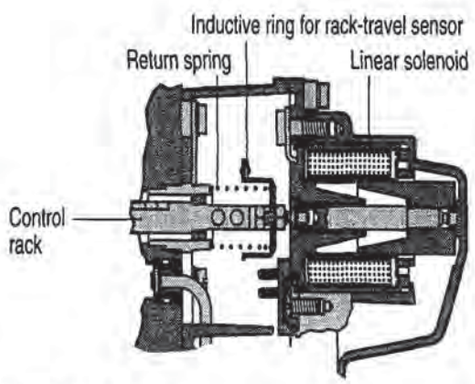


FIGURE 10.29 EDC linear-solenoid actuator.

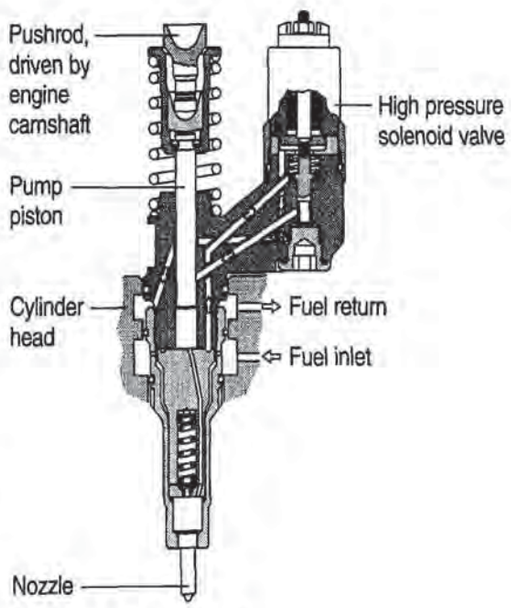


FIGURE 10.30 Unit injector.

ENGR & MATH SCI LIBRARY

PETITIONER'S EXHIBIT 1002
US PATENT NO. 6,581,565

The unit injector combines injection pump and injection nozzle into a single unit, which is installed directly into the engine cylinder head and driven by the engine camshaft. High injection pressures of 1600 bar and more are readily attainable due to low dead volume of compressible fuel.

In order to control start and end of injection, each unit injector contains a time-controlled high-speed solenoid valve. When the valve is open, the unit injector plunger delivers fuel to the low-pressure fuel supply circuit without any injection into the engine cylinder. When the solenoid valve is closed, fuel is delivered to the nozzle for injection into the engine cylinder. Thus, the fuel injection quantity is determined by the time interval between closing and opening of the valve.

Typical switching times for a medium duty/heavy duty truck application are: closing period at rated power, 1000 μs; opening period at rated power, 600 μs. The whole injection process must be completed within a period of about 1 to 2 ms. Consequently, the solenoid-valve motion must occur with an accuracy of less than 10 μs in order to ensure compliance with the usual tolerances for fuel injection quantity and start of injection.

10.3.4 Actuators for Passenger Safety

(See Chap. 24.) Pyrotechnical actuators are used for passenger-restraint systems such as the air bag and the automatic seat belt tensioner. When an accident occurs, the actuators inflate the air bag (or tension the seat belt) at precisely the right instant. Specifications call for the belts to be fully tensioned ~ 10 ms after ignition, while ~ 30 ms are allowed between the ignition point and total inflation for the air bag.

Air bag actuators are available in various sizes, according to vehicle type and application (driver or passenger side), and they are dimensioned to generate gas volumes of between 30 and 200 dm^3. The gases and gas mixtures used for these devices are nontoxic. The section following describes the operating principles for various actuator types.

Pyrotechnical Air Bag Inflator (Gas Generator). Figure 10.31 is an example of a driver-type inflator. When sufficient current is sent through the initiator, or squib, a thin metal filament covered by a sensitive pyrotechnic charge heats up and ignites this charge (Fig. 10.31*a*). The ignition of the squib provides enough energy to light a booster charge, whose combustion

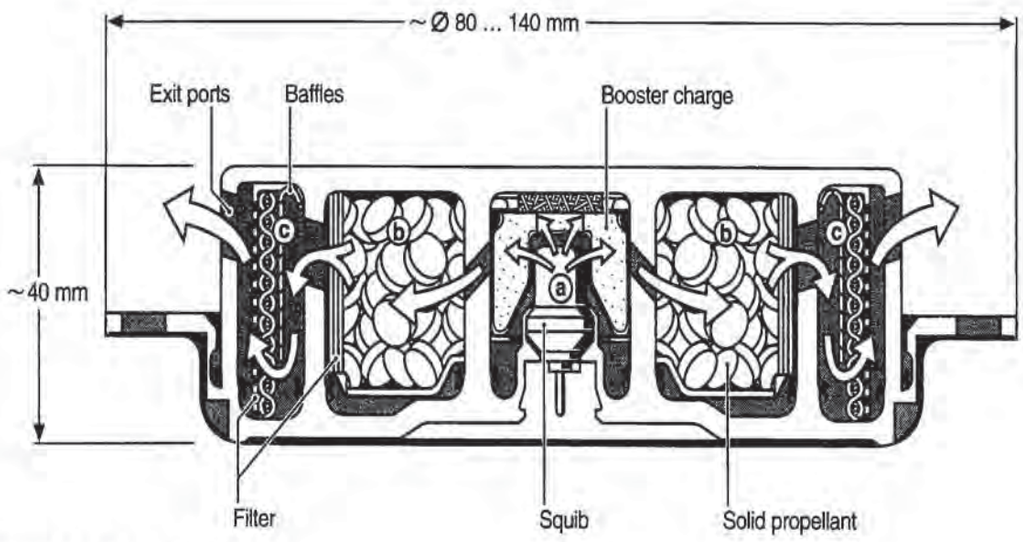


FIGURE 10.31 Gas generator.

PETITIONER'S EXHIBIT 1002
US PATENT NO. 6,581,565

builds up adequate pressure and heat to start the chemical reaction, converting the solid propellant, or gas generant, into gas (Fig. 10.31*b*). The resulting nontoxic hot gas flows over a series of screens, filters, and baffles, cooling down prior to leaving the inflator through exit ports located inside the air bag (Fig. 10.31*c*). The duration of this process is less than one-tenth of a second.

Hybrid (Compressed Gas and Pyrotechnic) Air Bag Inflator. Figure 10.32 is an example of a passenger-type tubular inflator. When sufficient current is sent through the initiator, or squib, a thin metal filament covered by a sensitive pyrotechnic charge heats up and ignites this charge (Fig. 10.32*a*). The ignition of the squib provides enough energy to propel a projectile through a rupture disk, allowing the escape of stored nontoxic compressed gas (Fig. 10.32*b*). The projectile also strikes two primers, lighting a solid pyrotechnic mass, which in turn heats the remaining stored gas (Fig. 10.32*c*). The expanding heated gas flows out of the inflator through exit ports located inside the air bag (Fig. 10.32*d*). The duration of this event is less than one-tenth of a second.

10.3.5 Actuators for Electronic Transmission Control

Continuous operation actuators are used to modulate pressure, while switching actuators function as supply and discharge valves for shift-point control.

In automatic transmissions, response times of 2 ms must be ensured in circuits with flow diameters of up to 2.4 mm, carrying up to 4 dm^3 per minute at a differential pressure of 200 kPa, all within a temperature range extending from –40 to 150 °C; pressure can increase up to 2000 kPa.

On/Off Solenoids. Various versions of the on/off solenoid valve are in use (two-port, three-port, open base state, closed base state). These valves are normally employed for shifting gears, but can also serve in special applications such as control of converter lockup mechanisms or reverse lockouts. Substantial weight savings can be obtained from the use of plastics. On/off valves are controlled through basic switching output stages. Peak-and-hold control strategies can provide weight and size savings.

Variable-Pressure Solenoids (Pressure Regulators). Pressure regulation must remain precise during switching operations and when holding line pressure. Here, analog valves have

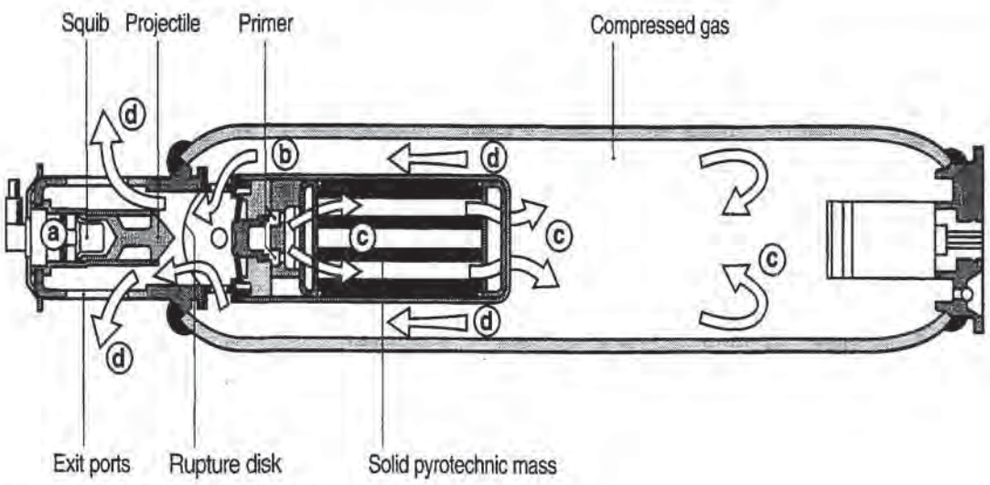


FIGURE 10.32 Hybrid air bag inflator.

ENGR & MATH SCI LIBRARY UCLA

PETITIONER'S EXHIBIT 1002
US PATENT NO. 6,581,565

proven extremely effective. Extremely stable output pressures are achieved by recirculating the controlled pressure to the valve element, making it possible to maintain stable output pressures in the face of interference factors like downstream leakage, supply-pressure fluctuations, and viscosity variations in the hydraulic fluid. Figure 10.33 shows a typical version of the three-way pressure-control valve, the spool valve. This design provides flow rates of 4 dm^3/min at pressure differentials of 2 bar. In order to limit the effects of hysteresis on the pressure/flow response characteristic, mechanical friction must be minimized and materials with low coercive field force must be employed and heat-treating processes are also needed to minimize material-related hysteresis. Choppers in the current-controlled end stage reduce power loss and induce friction-reducing micromovement in the armature. Pressure regulators are also available as seat valves.

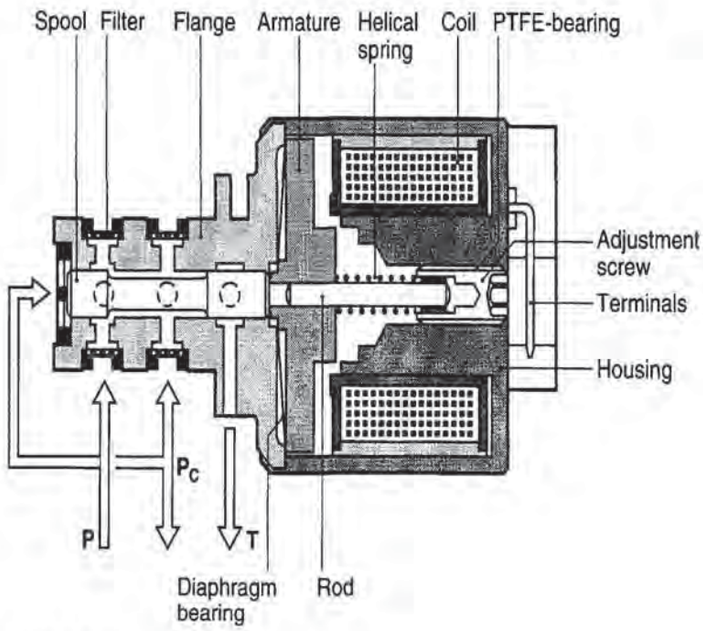


FIGURE 10.33 Variable-pressure solenoid.

PWM Solenoids (Pulse-Width Modulated Solenoid Valves). On/off poppet valves are particularly well suited for direct actuation from microcomputers. The component layout is less complicated than that found in proportional valves, allowing reductions in manufacturing costs. Because microcomputers operate on the basis of discrete time, equidistant setpoint selection, direct valve actuation via constant-frequency pulse represents the optimum design configuration.

When the solenoid-actuated valve is switched on and off at a constant supply pressure, the resulting average outlet pressure is a function of the ratio between open and closed states. However, this design lacks the proportional valve's ability to compensate for interference due to such factors as system leakage, temperature, and fluctuations in supply pressure. This type of actuator thus represents a reasonably priced alternative for applications in which the control pressure is not the controlled variable, but rather is used as a manipulated variable.

These units can be used in automatic transmissions to select gear ratios, or to reduce torque-converter slip losses by modulating the contact pressure of the lockup clutch. Simple switching output stages or peak-and-hold circuits govern the electric control signal to the PWM valve. When used in conjunction with the appropriate valve design, this type of control can be used to obtain cycle frequencies in excess of 100 Hz. In some applications, such as continiously variable transmissions (CVT), a life expectancy of 2×10^9 cycles is demanded.

PETITIONER'S EXHIBIT 1002
US PATENT NO. 6,581,565

10.3.6 Actuators for Headlight Vertical Aim Control

Devices enabling adjustment of headlight range enhance safety by maintaining the correct aim under all vehicle-load conditions. Range adjustment can be manual, with a driver-operated switch, or it can be automatic. The same headlight-adjustment actuators are employed for both designs. The actuator is mounted directly on the headlamp bracket or housing, and adjusts the headlight insert or the reflector.

The actuators are dc or step motors producing a rotary motion which gear-drive units then convert to linear movement. Due to the fixed relationship between the motor's incremental response (steps) and the attendant linear motion, no travel sensor is required with step motors. The total adjustment range extends as far as 8 mm. A single step corresponds to a turning angle of 15 degrees, or an adjustment travel of 0.03 mm. The motor returns to the initial (zero) position (mechanical travel limiter) each time the system is activated in order to prevent step losses.

The step motor combines the following advantages:

- Extremely precise positioning through digital control.
- High adjustment speeds of up to 8 mm/s; different control frequencies can be selected to obtain variations. This system allows graduated adjustment at constant vehicle speeds (consistent lighting) and rapid response during acceleration and braking.

10.4 TECHNOLOGY FOR FUTURE APPLICATION

The motivation to develop new actuators is created by the potential advantages of new manufacturing and driving techniques in combination with new materials. The following examples illustrate representative fields of innovation.

10.4.1 Micromechanical Valves

Micromechanics technology stems from the adaptation of production methods employed in microelectronics. Lithographic miniaturization procedures and etching and assembly techniques make it possible to manufacture minute structures with a high degree of precision. Micromechanical production methods have already become established in the field of sensor manufacture. Electronic circuitry and sensors can be manufactured from the same material (primarily silicon) in simultaneous production processes to furnish integrated components; the benefits associated with this process represent numerous potential advantages.

In automotive applications, microactuators display potential as elements in open-loop control systems where low control power is to be converted, for instance, regulating the flow of fluids in hydraulic or pneumatic systems and metering fuel.

For micromechanical manufacturing, valve designs are required in which planar units with relatively low structure heights are stacked. The energy conversion principles employed to operate the valves correspond to the planar structure (e.g., electrostatic drive, electrothermal or piezoelectric flux converters).

The pressure-balanced seat valve is a basic example of this kind of microvalve (Fig. 10.34). This type of microvalve is produced in a manufacturing process entailing sequential structuring and bonding of four wafers. Depending on the required dimensions for the single valve and the resulting surface requirement, as many as several hundred elements can be produced simultaneously on each wafer stack. Further efforts must be directed to solving packaging problems before these microstructures can be used to control fluid supply and discharge processes.

ENGR & MATH SCI LIBRARY UCLA

PETITIONER'S EXHIBIT 1002
US PATENT NO. 6,581,565

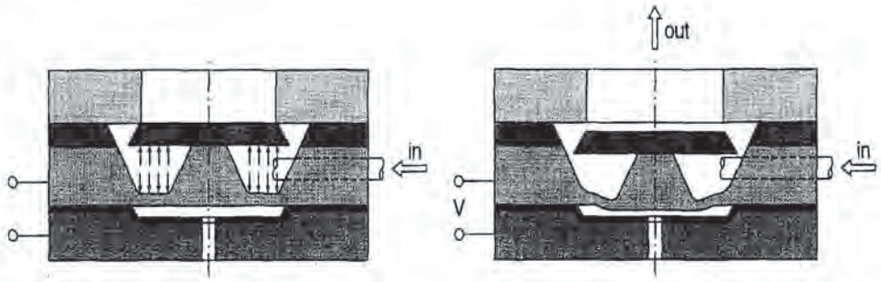


FIGURE 10.34 Pressure-compensated seat valve.

10.4.2 Positive-Engagement Friction Drives

Single piezoelectric actuators provide high dynamic positioning response over short actuating distances. The search for suitable mechanisms employing active piezoceramics to extend the effective travel range has given rise to a multiplicity of drive concepts sharing common attributes:

- Combination of single high-frequency motions (up to the ultrasonic range) to achieve a continuous drive movement
- Output element actuation using friction engagement

Ultrasonic Motor. Of all the designs utilizing piezoelectric actuator technology, the ultrasonic traveling wave device has reached the most advanced stage of development (Fig. 10.35). A stator ring featuring teeth on the upper surface, and made of a material providing low material damping (bronze), is flex-mounted on an end shield via a central diaphragm. A flat piezoceramic ring is bonded to the underside of the stator ring. This piezoring is polarized along the vertical axis of the ring plane. The direction of the polarization changes segmentally (Fig. 10.36).

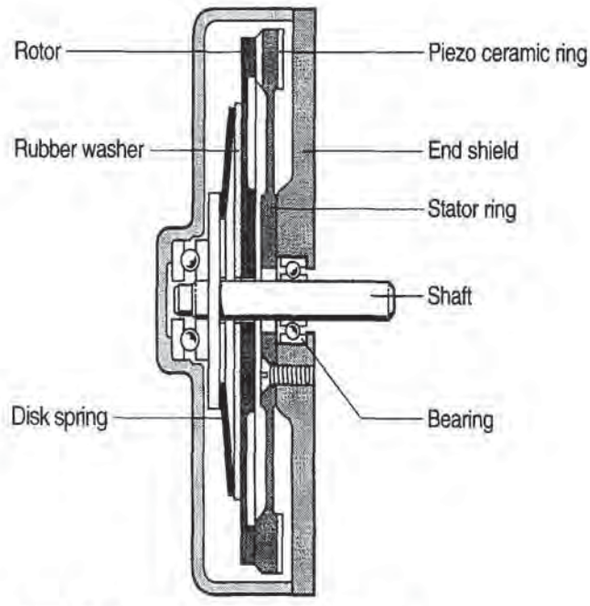


FIGURE 10.35 Traveling-wave motor, Shinsei type.

PETITIONER'S EXHIBIT 1002
US PATENT NO. 6,581,565

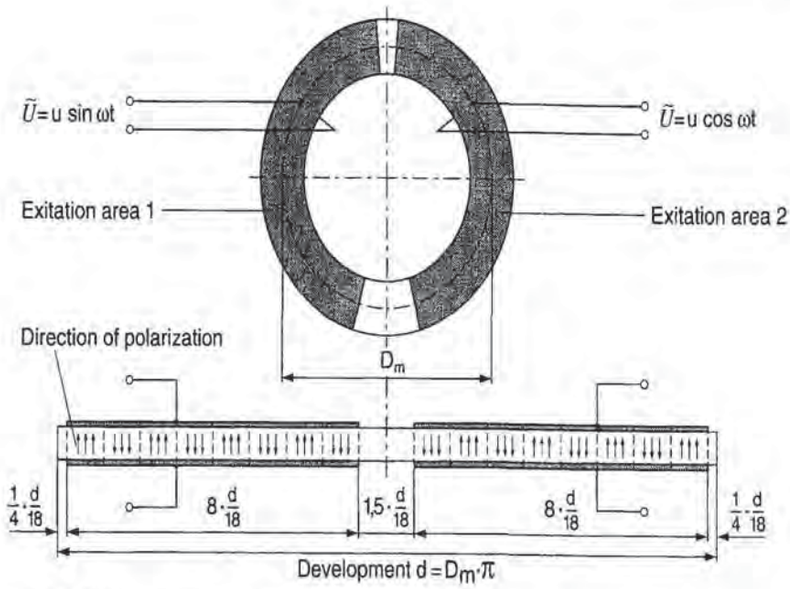


FIGURE 10.36 Segmentation and control of the piezoring.

The electrical contacts are arranged to provide two excitation regions, each featuring eight segments and two small zones. The zone length corresponds to either ½ or 1½ segments. Thus a segment of the excitation zone extends through ⅛ of the stator's circumference. When voltage is applied to an excitation region, the piezos of one polarization direction contract along the circumference direction (lateral piezo effect), while the piezos of the opposite polarization orientation expand. This effect produces a wave-shaped flux in the stator ring in the affected region.

If the region is then excited with ac voltage (for example, 100 V at approximately 40 kHz in existing motors), the result is an oscillation pattern which extends to encompass the entire stator ring. Excitation in the frequency of the ninth flex mode of the stator provokes a standing wave on the entire stator. Resonance step-up is employed to achieve amplitudes of 20 μm.

If an excitation current is now applied at the second excitation region with ac voltage at a 90° lateral displacement, the two waves overlap to form a traveling wave.

In addition to the up and down motion, one point on the upper surface of the stator produces—by means of tilting movement of those teeth which are situated above the neutral axis—a motion along the periphery (±2 μm). When the two motions combine, the surface points move in an elliptical pattern (Fig. 10.37).

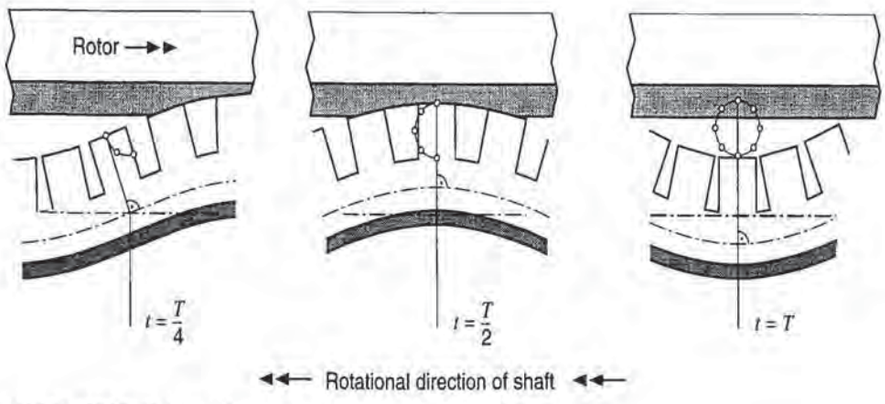


FIGURE 10.37 Drive mechanism.

ENGR & MATH SCI LIBRARY UCLA

PETITIONER'S EXHIBIT 1002
US PATENT NO. 6,581,565

A disc spring and a rubber washer are pressing the disk-shaped rotor in Fig. 10.35 against the stator. The elliptical motion of the stator teeth drives the rotor through friction contact with its contact layer. Speed is adjusted by, for example, varying the excitation frequency, with the stator's oscillation amplitude being monitored.

The salient characteristics of the ultrasonic motor are: high torque (up to 1.3 Nm), low rpm range (30 . . . 130 rpm), bidirectional operation, substantial characteristic retension force, free of clearance, no run-on, potentially precise positioning, noiseless operation, and flat unit configuration.

Ultrasonic motors are suitable for use as direct-drive devices. The disadvantages include the substantial, high-frequency control voltage, and the limitations on service life due to wear on the friction surface.

ACKNOWLEDGMENTS

The author wishes to acknowledge the contributions of D. Baumann, W. Brehm, O. Engfer, G. Genter, H. Gnuschke, U. Hafner, G. Hartz, Prof. E. Kallenbach, Technische Universität Ilmenau; T. Kamitsis, Morton International Inc., Odgen Utah; G. Keuper, H. M. Streib, U. Zillgitt. Unless otherwise stated, the collaborators are employees of Robert Bosch GmbH, Stuttgart.

The author acknowledges with gratitude the support of theoretical revision by Dietmar Baumann and the coordination done by Mr. Ortwin Engfer, as well as the typing of the manuscript by Dorothee Ludmann.

GLOSSARY

Actuator The part of an open-loop or closed-loop control system which connects the electronic control unit with the process. The actuator consists of a transformer and a final-control element. Electric positioning signals are converted to mechanical output.

Closed-loop control A process by which a variable is continuously measured, compared with a reference variable, and changes as a result of this comparison in such a manner that the deviation from the reference variable is reduced. The purpose of closed-loop control is to bring the value of the output variable as close as possible to the value specified by the reference variable in spite of disturbances. In contrast to open-loop control, a closed-loop control system acts to offset the effect of all disturbances.

Commutator The commutator is a current switcher. For dc machines, the commutator switches the armature windings so that the resultant force always acts in the same rotary direction. This requires a reversal of the armature winding connection every 180°. The current supply to the armature is via brushes which contact the commutator.

Eddy current In metals moving in an inhomogeneous magnetic field or located in a changing magnetic field, induced currents circulate throughout the volume. Because of their general circulatory nature, these currents are referred to as eddy currents.

Ferrite magnet In small transformers where eddy current losses must be kept to a minimum, the cores are made of ferrites which are complex oxides of iron and other metals. These materials are ferromagnetic, but have relatively high resistivity.

PETITIONER'S EXHIBIT 1002
US PATENT NO. 6,581,565

Final-control element The second or last stage of an actuator to control mechanical output.

Numeric field calculation A method of numerically calculating fields with the help of computer programs, such as the methods of finite differences or finite elements.

Open-loop control A process within a system in which one or more input variables act on output variables based on the inherent characteristics of the system. An open control loop is a series of elements that act on one another as links in a chain. In an open control loop, only disturbances that are measured by the control unit can be addressed. The open loop has no effect on other disturbances.

Peripheral magnetic voltage The line integral of the magnetic field strength around a closed path.

$$V_m = \oint \mathbf{H} \cdot d\mathbf{s}$$

According to Ampere's law, the peripheral magnetic voltage is equal to the magnetomotive force Θ.

Piezoelectric effect The direct piezoelectric effect is the ability of a piezoelectric crystal to produce an electric voltage when subjected to a force. The inverse piezoelectric effect is the ability of a piezoelectric crystal to deform when subjected to an electric voltage.

Pilot-controlled actuator An actuator that uses one or more additional energy sources to transform the input signal to an output signal. The pilot-controlled actuator consists of a chain of energy positioners and energy transformers that produces an amplification due to their series configuration.

Self-induction Every current is surrounded by a magnetic field with field lines that are interlinked with the current lines. This leads to an induced source voltage in the conductor or coil when the current strength is changed. This phenomenon is called self-induction.

Weiss' domains Ferromagnetic materials have strong interaction among the atoms. Spontaneous local magnetization can occur, even though no external magnetic field is present. These so-called Weiss' domains, sized from 0.01 to 1 mm, are small elementary magnets, which are randomly distributed in the material and are first directed when an external field is applied.

BIBLIOGRAPHY

Actuators Basics

"DIN 19226 Regelungstechnik und Steuerungstechnik: Begriffe und Benennungen."

Janocha, H., *Aktoren: Grundlagen und Anwendungen,* Springer-Verlag, Berlin, Heidelberg, New York, 1992.

Kupfmüller, K., *Einführung in die theoretische Elektrotechnik,* Springer-Verlag, 1973.

Pregla, R., *Grundlagen der Elektrotechnik,* Teil I u. II, Hüthig-Verlag, Heidelberg, 1990.

Raab, U., "Modellgestützte digitale Regelung und Überwachung von Kraftfahrzeugaktuatoren," Reihe 8: Meβ-, Steuerungs- und Regelungstechnik Nr. 313, VDI-Verlag, Düsseldorf 1993.

Robert Bosch GmbH, *Automotive Handbook,* 3d ed., 1993.

Robert Bosch GmbH, "Elektronik und Mikrocomputer," 1987.

VDI/VDE-Technologiezentrum Informationstechnik GmbH, "Neue Aktoren," Fachbeilage Mikroperipherik, 1990.

ENGR & MATH SCI LIBRARY UCLA

PETITIONER'S EXHIBIT 1002
US PATENT NO. 6,581,565

dc Solenoids

Aldefeld, B., "Numerical Calculation of Electromagnetic Acutators," *Archiv für Electrotechnik,* Bd. 61, 1979, pp. 347–352.

Hickmann, W., "Ein Beitrag zur Rechnerunterstützten Auslegung und Optimierung von Gleichstrommagnetsystemen," Dissertation, TH Darmstadt, 1984.

Kallenbach, E., *Der Gleichstrommagnet,* Akademische Verlagsgesellschaft Geest & Portig KG, Leipzig, 1969.

Kallenbach, E., Bögelsack, G., *Gerätetechnische Antriebe,* Carl Hanser-Verlag, München, Wien, 1991.

Müller, W., "Numerical solution of 2- or 3-dimensional nonlinear field problems by means of the computer program PROFI," *Archiv für Elektrotechnik 6,* 1982, p. 299–307.

Roters, H. C., *Electromagnetic Devices,* John Wiley & Sons, New York, 1967.

Rüdenberg, *Elektrische Schaltvorgänge,* Springer, 1974.

Seely, S., *Electromechanical Energy Conversion,* McGraw-Hill New York, 1962. (Moskau: Energija, 1968).

Step Motors

Kuo, B. C., *Incremental Motion Control—Step Motors and Control Systems,* SRL Publishing Company, Champaign Ill., 1979.

Kuo, B. C., *Theory and Applications of Stepmotors,* West Publishing Co., New York, 1974.

Miller, T. J. E., *Brushless Permanent Magnet and Reluctance Motor Drives,* Clarendon Press, Oxford, 1989.

Takashi, Kenjo, *Stepping Motors and Their Microprocessor Controls,* Clarendon Press, Oxford, 1985.

dc Motors

Moeller, W. *Leitfaden der Electrotechnik,* Band II, Teil I, -Gleichstrommaschinen, Teubner, Stuttgart, 1979.

Ruschmeyer, K., *Motoren und Generatoren mit Dauermagneten,* Expert-Verlag, Grafenau, 1983, ISBN 3-88508-914-9.

Schüler, K., and K. Bringmann, *Dauermagnete,* Springer, Berlin, 1970.

Magnetostrictive Actuators

Clark, A. E., "Ferromagnetiv Materials," Chap. 7, Ed. E.P. Wohlfarth, North-Holland, 1980, pp. 531–589.

Dyberg, J., "Magnetostrictive Rods in Mechanical Applications," *Proc. 1st International Conference on Giant Magnetostrictive Alloys and Their Impact on Actuator and Sensor Technology,* Marbella, Spain, 1986.

Edge Technologies Inc., *TERFENOL-D Notes,* Vol. 3, No. 1, 1990.

Fahlander, M., and M. Richardson, "New Material for the Rapid Conversion of Electric Energy to Mechanical Motion," Feredyn AB, Uppsala, Sweden, 1988.

Janocha, H., and J. Schäfer, "Design Rules for Magnetostrictive Actuators," *Proc. Actuators 92,* VDI/VDE-Technologiezentrum Informationstechnik GmbH, Berlin, 1992.

Kvarnsjo, L., "Principles and Tools for Design of Magnetomechanical Devices Based on Giant Magnetostrictive Materials," Royal Institute of Technologie, Dept. of Plant Engineering, S-10044, Stockholm, Sweden, 1990.

Piezo Actuators

Galvagni, J., and B. Rawal, *Multilayer Electroactive Ceramic Actuators,* AVX Corporation, Myrtle Beach, 1991.

Janocha, H., and D. J. Jendritza, "Piezoaktuatoren—Möglichkeiten und Grenzen einer innovativen Stellgliedtechnologie," *VDI Berichte* Nr. 960, 1992.

Janocha, H., and D. J. Jendritza, "Piezoelektrische Aktoren praxisgerecht einsetzens," *Design & Elektronik 22;* Magna MediaVerlag, Haar bei München, 1992.

PETITIONER'S EXHIBIT 1002
US PATENT NO. 6,581,565

VDI/VDE-Technologiezentrum Informationstechnik GmbH, Piezokeramische Aktoren, Fachbeilage Mikroperipherik me Bd. 5, Heft 1, 1991.

Waanders, J. W., *Piezoelectric Ceramics: Properties and Applications,* Philips Components, 1991.

Electrostatic Actuators

Bart, S. E., T. A. Lober, R. T. Howe, J. H. Lang, and M. F. Schlecht, "Design considerations for microfabricated electric actuators," *Sensors and Actuators,* 14, 1988, pp. 269–292.

Price, R. H., J. E. Wood, and S. C. Jacobsen, "The modelling of electrostatic forces in small electrostatic actuators," *IEEE Solid-State Sensor and Actuator Workshop,* Hilton Head Island, S.C., 1988.

Trimmer, W. S., and K. J. Gabriel, "Design Considerations for a Practical Electrostatic Micromotor," *Sensors and Actuators,* 11, 1987, pp. 189–206.

Electrorheological Fluids

Block, H., and J. P. Kelly, "Electro-rheology—A Review Article," *J Phys. D. Appl. Phys,* 21, 1988, pp. 1661–1667.

Bonnecaze, R. T., and J. F. Brady, "Yield stress in electrorheological fluids," *J. Rheol.,* Vol. 36, No. 1, 1992, pp. 73–115.

Simmonds, A. J., "Electro-rheological valves in a hydraulic circuit," *IEE Proc-D,* Vol. 138, No. 4, 1991.

Stangroom, J. E., "Electrorheological Fluids," *J Physics Technology,* 14, 1983, pp. 290–296.

Memory Alloys

Brinson, L. C., "One Dimensional Constitutive Behavior of Shape Memory Alloys: Thermomechanical Derivation with Noncourtant Material Functions and Redefined Martensite Internal Variable," submitted for publication in *Journal of Intelligent Material Systems and Structures,* 1991.

Duerig, T. W., "Applications of shape memory," *Material Science Forum,* 56–58, 1990, pp. 679–692.

Duerig, T. W., K. N. Melton, D. Stoeckel, and C. M. Wayman, *Engineering Aspects of Shape Memory Alloys,* Butterworth-Heinemann, 1990.

Golestaneh, A., "Shape-memory phenomena," *Phys. Today,* Apr. 1984, pp. 62–70.

Tuominen, S. M., and R. J. Biermann, "Shape Memory Wires," *J. Metals,* 1988, p. 32.

Automotive Actuators for ABS/ASR-Systems

Huber, W., B. Lieberoth-Leden, W. Maisch, and A. Reppich, "New Approaches to Electronic Throttle Control," SAE 910085.

Maisch, W., W. D. Jonner, R. Mergenthaler, and A. Sigl, "ABS5 and ASR5: The New ABS/ASR Family to Optimize Directional Stability and Traction," SAE 930505.

Fuel Injection for Spark-Ignition Engines

Fuel Metering (Spark Ignition Engines), SAE 891832, Nov. 89.

Robert Bosch GmbH, *Automotive Electric/Electronic Systems,* SAE ISBN 0-89883-509-7, VDI ISBN 3-18-419110-9.

Fuel Injection for Diesel Engines

Fischer, W., W. Fuchs, H. Laufer, and U. Reuter, "Solenoid-Valve Controlled Diesel Distributor Injection Pump," SAE 930327.

Franke, G., B. G. Barker, and C. T. Timus, "Electronic Unit Injectors," SAE 885013.

ENGR & MATH SCI LIBRARY UCLA

PETITIONER'S EXHIBIT 1002
US PATENT NO. 6,581,565

Lauvin, P., A. Löffler, A. Schmitt, W. Zimmermann, and W. Fuchs, "Electronically Controlled High Pressure Unit Injector System for Diesel Engines," SAE 911819.

Mardell, J. E., and R. K. Cross, "An Integrated, Full Authority, Electrohydraulic Engine Valve and Diesel Fuel Injection System, SAE 880602.

Electronic Transmission Control

Brehm, W., and K. Neuffer, "Fast switching PWM-solenoid for automatic transmissions," *Proc. Seventh International Conference on Automotive Electronics,* London, Oct. 9–12, 1989, C 391/046 I Mech E, 1989.

Henry, James P., and David S. Dennis, "Predicting Solenoid Transient Performance," SAE Paper 870473.

Robinson, G., "A Practical Approach to Automatic Transmission Reliability," SAE Paper 910640.

U.S. Patent 4,535,816, "Pressure controller," 1985.

U.S. Patent 4,577,143, "Method and apparatus to convert an electrical value into a mechanical position by using an electromagnetic element subject to hysteresis," 1986.

Technology for Future Application

Fröschle, A., "Analyse eines Piezo-Wanderwellenmotors," Dissertation, Universität Stuttgart, 1992.

Huff, M. A., M. Mettner, A. A. Lober, and M. A. Schmidt, "A Pressure-Balanced Electrostatically-Actuated Microvalve," *Technical Digest, IEEE Solid-State Sensor and Actuator Workshop,* Hilton Head, S.C., June 4–9, 1990, p. 123.

Mettner, M., M. A. Huff, T. A. Lober, and M. A. Schmidt, "How to Design a Microvalve for High Pressure Application," *MME Micromechanics Europe '90,* Berlin, Nov. 26–27, 1990, p. 108.

ABOUT THE AUTHOR

Klaus Müller, after studying mechanical engineering, was employed at the University of Karlsruhe, Germany, investigating the field dynamic behavior of air conditioning system components. In 1976, he joined Robert Bosch GmbH, Stuttgart, where he began his work in advanced engineering of planar oxygen sensors, combustion sensors, and signal evaluation. This was followed by product development of hydraulic units for antilock braking systems and traction control.

PETITIONER'S EXHIBIT 1002
US PATENT NO. 6,581,565

P · A · R · T · 3

CONTROL SYSTEMS

ENGR & MATH SCI LIBRARY UCLA

PETITIONER'S EXHIBIT 1002
US PATENT NO. 6,581,565

CHAPTER 11
AUTOMOTIVE MICROCONTROLLERS

David S. Boehmer
Senior Applications Engineer
Intel Corporation

ENGR & MATH SCI LIBRARY UCLA

A microcontroller can be found at the heart of almost any automotive electronic control module or ECU in production today. Automotive systems such as antilock braking control (ABS), engine control, navigation, and vehicle dynamics all incorporate at least one microcontroller within their ECU to perform necessary control functions. Understanding the various features and offerings of microcontrollers that are available on the market today is important when making a selection for an application. This chapter is intended to provide a look at various microcontroller features and provide some insight into their characteristics from an automotive application point of view.

11.1 MICROCONTROLLER ARCHITECTURE AND PERFORMANCE CHARACTERISTICS

A microcontroller can essentially be thought of as a single-chip computer system and is often referred to as a single-chip microcomputer. It detects and processes input signals, and responds by asserting output signals to the rest of the ECU. Fabricated upon this highly integrated, single piece of silicon are all of the features necessary to perform embedded control functions. Microcontrollers are fabricated by many manufacturers and are offered in just about any imaginable mix of memory, I/O, and peripheral sets. The user customizes the operation of the microcontroller by programming it with his or her own unique program. The program configures the microcontroller to detect external events, manipulate the collected data, and respond with appropriate output. The user's program is commonly referred to as code and typically resides on-chip in either ROM or EPROM. In some cases where an excessive amount of code space is required, memory may exist off-chip on a separate piece of silicon. After power-up, a microcontroller executes the user's code and performs the desired embedded control function.

Microcontrollers differ from microprocessors in several ways. Microcontrollers can be thought of as a complete microcomputer on a chip that integrates a CPU with memory and various peripherals such as analog-to-digital converters (A/D), serial communication units (SIO, SSIO), high-speed input and output units (HSIO, EPA, PWM), timer/counter units, and

PETITIONER'S EXHIBIT 1002
US PATENT NO. 6,581,565

standard low-speed input/output ports (LSIO). Microcontrollers are designed to be embedded within event-driven control applications and generally have all necessary peripherals integrated onto the same piece of silicon. Microcontrollers are utilized in applications ranging from automotive ABS to household appliances in which the microcontroller's function is predefined and limited user interface is required.

Microprocessors, on the other hand, typically require external peripheral devices to perform their intended function and are not suited to be utilized in single-chip designs. Microprocessors basically consist of a CPU with register arrays and interrupt handlers. Peripherals such as A/D and HSIO are rarely integrated onto microprocessor silicon. Microprocessors are designed to process large quantities of data and have the capability to handle large amounts of external memory. Although microprocessors are typically utilized in applications which are much more human-interface and I/O intensive such as personal computers and office workstations, they are beginning to find their way into embedded applications.

Choosing a microcontroller for an application is a process that takes careful investigation and thought. Items such as memory size, frequency, bus size, I/O requirements, and temperature range are all basic requirements that must be considered when choosing a microcontroller. The microcontroller family must possess the performance capability necessary to successfully accomplish the intended task. The family should also provide a memory, I/O, and frequency growth path that allows easy upgradability to meet market demands. Additionally, the microcontroller must meet the application's thermal requirements in order to guarantee functionality over the intended operating temperature range. Items such as these must all be considered when choosing a microcontroller for an automotive application.

11.1.1 Block Diagram

Usually the first item a designer will see when opening a microcontroller data book or data sheet is a block diagram. A block diagram provides a high-level pictorial representation of a microcontroller and depicts the various peripherals, I/O, and memory functions the microcontroller has to offer. The block diagram gives the designer a quick indication if the particular microcontroller will meet the basic memory, I/O, and peripheral needs of their application. Figure 11.1 shows a block diagram for a state-of-the-art microcontroller. It depicts 32 Kbytes

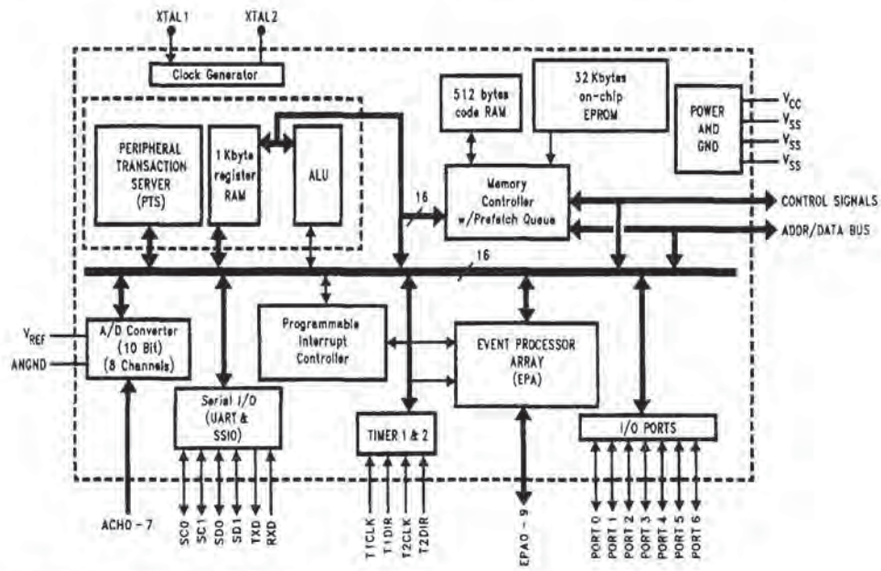


FIGURE 11.1 Microcontroller block diagram.

PETITIONER'S EXHIBIT 1002
US PATENT NO. 6,581,565

of EPROM, 1 Kbyte of register RAM, 6 I/O ports, an A-to-D converter, 2 timers, high-speed input/output (I/O) channels, as well as many other peripherals. These features may be "excessive" to a designer looking for a microcontroller to implement in an automotive trip-computer application but would be excellently suited for automotive ABS/traction control or engine control.

11.1.2 Pin-Out Diagram

A microcontroller's pin-out diagram is used to specify the functions assigned to pins relative to their position on a given package. An example pin-out diagram is shown in Fig. 11.2. Note that most pins have multiple functions assigned to them. Pins that can support more than one function are referred to as multifunction pins. The default function for multifunction pins is normally that of low-speed input and output (discussed later in this chapter). If the user should wish to select the secondary or special function associated with the pin, he or she can do so by writing to the appropriate special function register. There are some exceptions. A good example is pins used for interfacing to external memory. If the device is instructed to power-up executing from external memory as opposed to on-chip memory, the address data bus and associated control pins will revert to their special function as opposed to low-speed I/O.

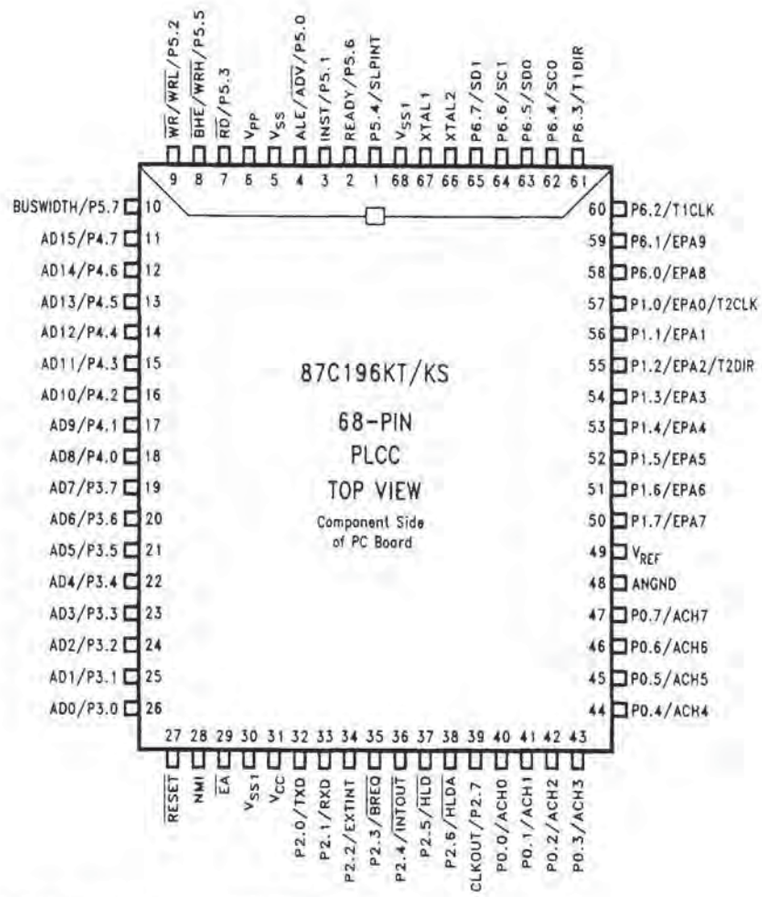


FIGURE 11.2 Microcontroller pin-out diagram.

ENGR & MATH SCI LIBRARY UCLA

PETITIONER'S EXHIBIT 1002
US PATENT NO. 6,581,565

11.1.3 Central Processing Unit

The central processing unit or CPU can be thought of as the brain of a microcontroller. The CPU is the circuitry within a microcontroller where instructions are executed and decisions are made. Mathematical calculations, data processing, and control signal generation all take place within the CPU. Major components of the CPU include the arithmetic logic unit (ALU), register file, instruction register, and a microcode engine. The CPU is connected to the bus controller and other peripherals via a bidirectional data bus.

Microcontrollers are, for the most part, digital devices. As digital devices, microcontrollers utilize a binary numbering system with a base of 2. Binary data digits or *bits* are expressed as either a logic "1" (boolean value of true) or a logic "0" (boolean value of false). In a 5-V system, a logic "1" may be simply defined as a +5-V state and a logic "0" may be defined as a 0-V state. A bit is a single memory or register location that can contain either a logic "1" or a logic "0" state. Bits of data can be arranged as a *nibble* (4 bits of data), a *byte* (8 bits of data), or as a *word* (16 bits of data). It should also be noted that, in some instances, a word may be defined as the data width that a given microcontroller can recognize at a time, be it 8 bits or 16 bits. For purposes of this chapter, we will refer to a word as being 16 bits. Data can also be expressed as a double word which is an unsigned 32-bit variable with a value between 0 and 4,294,967,295. Most architectures support this data only for shifts, dividends of a 32-by-16 divide, or for the product of a 16-by-16 multiply.

The most common way of referring to a microcontroller is by the width of its CPU. This indicates the width of data that the CPU can process at a time. A microcontroller with a CPU that can process 8 bits of data at a time is referred to as an 8-bit microcontroller. A microcontroller with a CPU that can process 16 bits of data at a time is referred to as a 16-bit microcontroller. With this in mind, it is easy to see why 16-bit microcontrollers offer higher performance than their 8-bit counterparts. Figure 11.3 illustrates a typical 16-bit CPU dia-

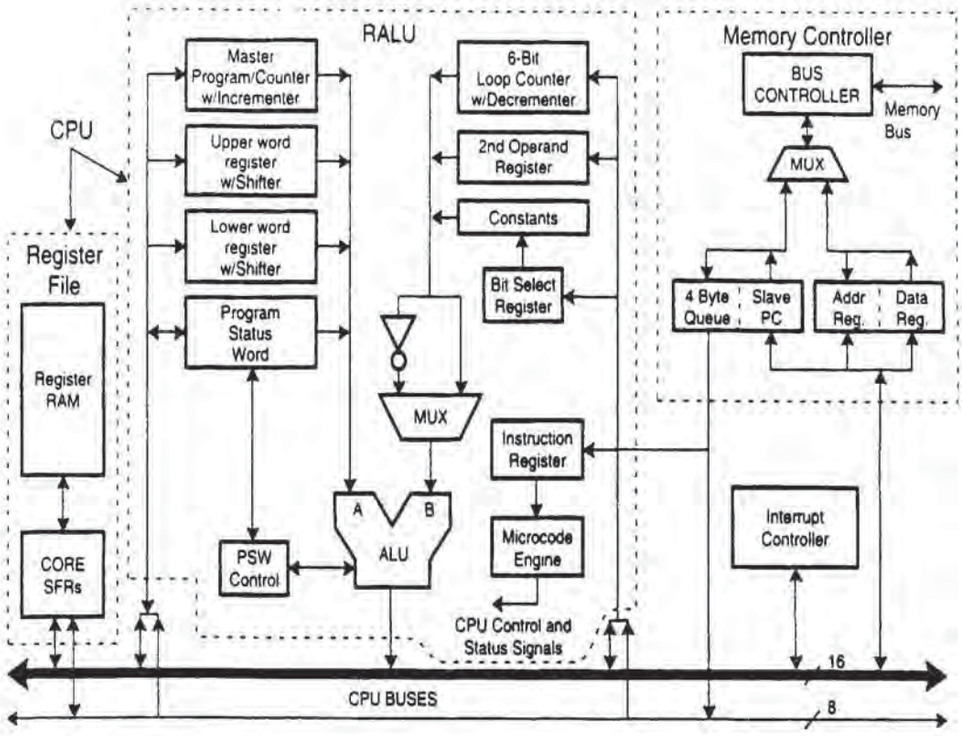


FIGURE 11.3 16-bit CPU.

PETITIONER'S EXHIBIT 1002
US PATENT NO. 6,581,565

gram. The microcode engine controls the CPU. Instructions to the CPU are taken from the instruction queue and temporarily stored in the instruction register. This queue is often referred to as a *prefetch queue* and it decreases execution time by staging instructions to be executed. The microcode engine then decodes the instructions and generates the correct sequence of events to have the ALU perform the desired function(s).

Arithmetic Logic Unit. The ALU is the portion of the CPU that performs most mathematical and logic operations. After an instruction is decoded by the microcode engine, the data specified by the instruction is loaded into the ALU for processing. The ALU then processes the data as specified by the instruction.

Register File. The register file consists of memory locations that are used as temporary storage locations while the user's code is executing. The register file is implemented as RAM and consists of both RAM memory locations and special function registers (SFRs). RAM memory locations are used as temporary data storage during execution of the user's code. After power-up, RAM memory locations default to a logic "0" and data in SFR locations contain default values as specified by the microcontroller manufacturer.

Special Function Registers. SFRs allow the user to configure and monitor various peripherals and functions of the microcontroller. By writing specific data to an SFR, the users can configure the microcontroller to meet the exact needs of their application. Figure 11.4 shows an example of a serial port SFR used for configuration. Note that each bit location within the SFR determines a specific function and can be programmed to either a logic "1" or "0". If more than two configuration choices are possible, two or more bits will be combined to produce the multiple choices. An example of this would be the mode bits (M1 and M2) in the example SFR (Fig. 11.4). Bit locations marked "RSV" are reserved and should be written to with a value as indicated by the manufacturer.

SP_CON (1FBBH)

7	6	5	4	3	2	1	0
0	0	PAR	TB8	REN	PEN	M2	M1

M2, M1	Mode	Function
	00	Mode 0: Synchronous
	01	Mode 1: Standard asynchronous
	10	Mode 2: Asynchronous (receiver interrupt on 9th bit = 1)*
	11	Mode 3: Asynchronous (9th bit = parity or data)**
PEN	Parity Enable. Enables the Parity function for Mode 1 or Mode 3; cannot be enabled for Mode 2.	
REN	Receiver Enable. Enables the receiver to write to SBUF_RX.	
TB8	Transmission Bit 8. Set the ninth data bit for transmission (Modes 2 and 3). Cleared after each transmission; not valid if parity is enabled.	
PAR***	0 = even parity 1 = odd parity	
Bits 6, 7	Reserved; write as zeros for future product compatibility.	

* Mode 2: Asynchronous (receiver: interrupt on 9th bit = 1; transmitter: 9th bit = TB8)
** Mode 3: Asynchronous (receiver: always interrupt on 9th bit; transmitter: 9th bit = parity for PEN = 1
*** Par bit only available on 8XC196KT and KS devices. 9th bit = TB8 for PEN = 0
For 8XC196KR, JR, KQ, JQ devices, this bit should be written as a zero to maintain compatibility with future devices.

FIGURE 11.4 Special function control register example.

ENGR & MATH SCI LIBRARY UCLA

PETITIONER'S EXHIBIT 1002
US PATENT NO. 6,581,565

SP_STAT (1FB9H)

7	6	5	4	3	2	1	0
RB8/RPE	RI	TI	FE	TXE	OE	X	X

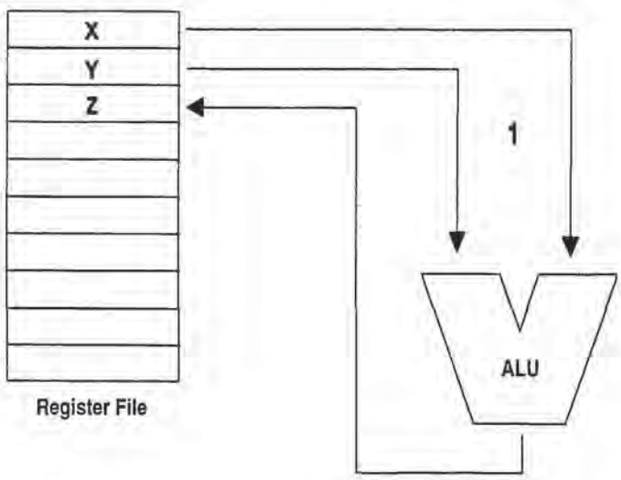
Bits 0, 1	Reserved; ignore data.
OE	Set on buffer overrun error.
TXE	Set on transmitter empty. When set may write 2 bytes to transmit buffer.
FE	Framing error; set it no STOP bit is found at the end of a reception. When set may write 1 byte to transmit buffer.
TI	Transmit interrupt; set at the beginning of the STOP bit transmission.
RI	Receive interrupt; set after the last data bit is received.
RPE	(Parity enabled) Receive parity error (Modes 1 and 3 only); set if parity is enabled and a parity error occurred.
RB8	(Parity disabled) Received Bit 8 (Modes 2 and 3 only); set if the 9th bit is high on reception.

FIGURE 11.5 Special function status register example.

Some SFRs can be read by the user to determine the current status of a given peripheral. Figure 11.5 shows an example of a serial port status register that, when read, indicates the current status of the microcontroller's serial port. Note that each bit location corresponds to a particular state of the serial port. Bit locations marked "RSV" are reserved and should be ignored when read.

Register Direct vs. Accumulator-Based Architectures. Microcontroller architectures can be classified as either the register-direct or accumulator-based type. These terms refer to the means by which the CPU must handle data when performing mathematical, logical, or storage operations.

Register-direct architectures allow the programmer to essentially use most, if not all, of the microcontroller's entire RAM array as individual accumulators. That is, the programmer can perform mathematical or storage operations directly upon any of the RAM locations. This simplifies task switching because program variables may be left in their assigned registers while servicing interrupts. Figure 11.6 illustrates a register-to-register type architecture (such



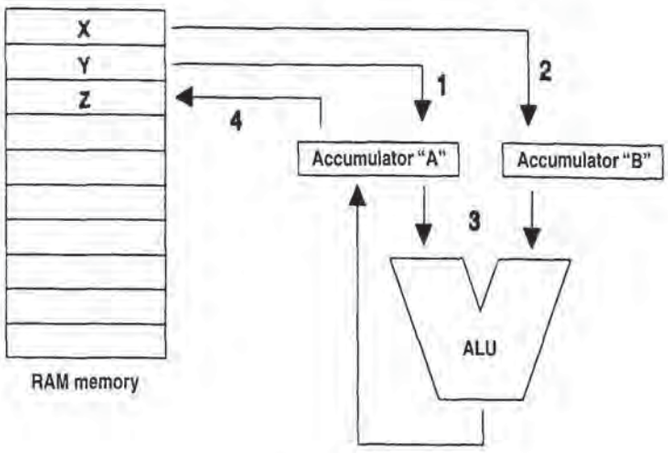

```
Z=X+Y
1. MUL Z,X,Y
```

FIGURE 11.6 Register-to-register architecture example.

PETITIONER'S EXHIBIT 1002
US PATENT NO. 6,581,565

as Intel's MCS®-96). This architecture essentially has 232 "accumulators" (more are available through a windowing mechanism) of which any can be operated on directly by the RALU. The true advantage of this type of architecture is that it reduces accumulator bottleneck and speeds throughput during program execution.

Accumulator-based architectures require the user to first store the data to be manipulated into a temporary storage location, referred to as an "accumulator," prior to performing any type of data operation. After the operation is completed, the user program must then store the result to the desired destination location. Figure 11.7 depicts an example of an accumulator-based architecture.




```
Z = X + Y

1. LD A,Y
2. LD B,X
3. MUL A,B
4. ST A,Z
```

FIGURE 11.7 Accumulator-based architecture.

Program Counter. The Program Counter (PC) controls the sequencing of instructions to be executed. The PC is a 16-bit register located within the CPU which holds the address of the next instruction to be executed. After an instruction is fetched, the PC is automatically incremented to point to the next instruction.

SP starting address (SP+12):	
(SP+10):	80FFh
(SP+8):	A5A5h
(SP+6):	6E20h
(SP+4):	5555h
(SP+2):	0000h
SP ending address (SP):	8000h

FIGURE 11.8 Stack pointer example.

Stack and Stack Pointer. The stack is an area of memory (typically user-assigned) that is used to store data temporarily in a FILO (first-in, last-out) fashion. The stack is primarily used for storing program information (such as the program counter or interrupt mask registers) when an interrupt service routine is invoked. It is also sometimes used to pass variables between subroutines. The stack is typically accessed through PUSH and POP instructions. Execution of the PUSH instruction "pushes" the contents of the specified operand onto the stack whereas the

ENGR & MATH SCI LIBRARY UCLA

PETITIONER'S EXHIBIT 1002
US PATENT NO. 6,581,565

POP instruction "pops" the contents of the specified operand off of the stack. The stack pointer (SP) is a register which points to the next available word location on the stack. Consider the example shown in Fig. 11.8 which shows the contents of the stack after the following code sequence is executed:

PUSH #80FFh	pushes immediate data 80FFh onto stack
PUSH #0A5A5h	pushes immediate data A5A5h onto stack
PUSH 82h	pushes data @ 82h (assume it's 6E20h) onto stack
PUSH #5555h	pushes immediate data 5555h onto stack
PUSH 4Eh	pushes data @ 4Eh (assume it's 0000h) onto stack
PUSH #8000h	pushes immediate data 8000h onto stack

Continuing with the preceding example, if a POP instruction were executed, the data at the current SP address (SP) would be "popped" off the stack and stored to the address specified by the instruction's operand. Executing the POP instruction results in the SP being incremented by 2.

Program Status Word and Flags. The program status word (PSW) is a collection of boolean flags which retain information concerning the state of the user's program. These flags are set or cleared depending upon the result obtained after executing certain instructions as specified by the microcontroller manufacturer. PSW flags are not directly accessible by the user's program; access is typically through instructions which test one or more of the flags to determine proper program flow. Following is a summary of common PSW flags as supported by Intel's MCS-96® architecture:

Z: The *Zero* flag is set when an operation generates a result equal to zero. The Z flag is never set by the add-with-carry (ADDC/ADDCB) or subtract-with-carry (SUBC/SUBCB) instructions, but is cleared if the result is nonzero. These two instructions are normally used in conjunction with ADD/ADDB and SUB/SUBB instructions to perform multiple-precision arithmetic. The operation of the Z flag for these instructions leaves it indicating the proper result for the entire multiple-precision calculation.

N: The *Negative* flag is set when an operation generates a negative result. Note that the N flag will be in the algebraically correct state even if overflow occurs. For shift operations, the N flag is set to the same value as the most significant bit of the result.

V: The *oVerflow* flag is set when an operation generates a result that is outside the range for the destination data type. For shift-left instructions, the V flag is set if the most significant bit of the operand changes at any time during the shift. For an unsigned word divide, the V flag is set if the quotient is greater than 65,535. For a signed word divide, the V flag is set if the quotient is less than –32,768 or greater than 32,767.

VT: The *oVerflow Trap* flag is set when the V flag is set, but it is only cleared by instructions which are specially designated to clear the VT flag (such as CLRVT, JVT, and JNVT). The VT flag allows for testing possible overflow conditions at the end of a sequence of related arithmetic operations. This is normally more efficient than testing the V flag after each instruction.

C: The *Carry* flag is set to indicate either (1) the state of the arithmetic carry from the most significant bit of the ALU for an arithmetic operation or (2) the state of the last bit shifted out of an operand for a shift. Arithmetic borrow after a subtract operation is the complement of the C flag (i.e., if the operation generated a borrow, then C = 0).

ST: The *STicky* bit flag is set to indicate that, during a right shift, a 1 has been shifted first into the C flag and then shifted out. The ST flag can be used along with the C flag to control rounding after a right shift. Imprecise rounding can be a major source of error in a numerical calculation; use of both the C and ST flags can increase accuracy as described in the following paragraphs.

PETITIONER'S EXHIBIT 1002
US PATENT NO. 6,581,565

Consider multiplying two 8-bit quantities and then scaling the result down to 12 bits:

```
MULUB   AX, CL, DL    (CL * DL = AX)
SHR     AX, #4        (AX is shifted right by 4 bits)
```

If the C flag is set after the shift, it indicates that the bits shifted off the end of the operand were greater than or equal to one-half the least significant bit of the 12-bit result. If the C flag is cleared after the shift, it indicates that the bits shifted off the end of the operand were less than half the LSB of the 12-bit result. Without the ST flag, the rounding decision must be made on the basis of the C flag alone. (Normally the result would be rounded up if the C flag is set.) The ST flag allows a finer resolution in the rounding decision as shown here:

C	ST	Bits shifted off
0	0	Value = 0
0	1	0 < Value < ½ LSB
1	0	Value = ½ LSB
1	1	Value > ½ LSB

Jump instructions are the most common instructions to utilize PSW flags for determining the operation to perform. Instructions that test PSW flags are very useful when program flow needs to be altered dependent upon the outcome of an arithmetic operation. The most common example of this would be for program loops that are to be executed a certain number of times. Following are examples of several MCS-96 instructions whose operation is dependent upon the state of one or more program status word flags:

JC (Jump if C flag is set.) If the C (carry) bit is set, the program will jump to the address location specified by the operand. If the C flag is cleared, control will pass to the next sequential instruction.

JGT (Jump if signed greater than.) If both the N (negative) and the Z (zero) flags are clear, the program will jump to the address location specified by the operand. If either of the flags is set, control will pass to the next sequential instruction.

JLE (Jump if signed less than or equal.) If either the N or Z flags is set, the program will jump to the address location specified by the operand. If both the N and Z flags are cleared, control will pass to the next sequential instruction.

11.1.4 Bus Controller

The bus controller serves as the interface between the CPU and the internal program memory and the external memory spaces. The bus controller maintains a queue (commonly called the prefetch queue) of prefetched instruction bytes and responds to CPU requests for data memory references. The prefetch queue decreases execution time by staging instructions to be executed. The capacities of prefetch queues vary but for the MCS-96 architecture, it is 4 bytes deep.

When using a logic analyzer to debug code it is important to consider the effects of the prefetch queue. It is not possible to accurately determine when an instruction will execute by simply watching when it is fetched from external memory. This is because the prefetch queue is filled in advance of instruction execution. It is also important to consider the effects when a jump or branch occurs during program execution. When the program sequence changes because of a jump, interrupt, call, or return, the PC is loaded with the new address, the queue is flushed and processing continues. Consider the situation in which the external address/data bus is being monitored when a program branch occurs. Because of the prefetch queue, it will appear as if instructions past the branch point were executed, when in fact they were only loaded into the prefetch queue.

ENGR & MATH SCI LIBRARY UCLA

PETITIONER'S EXHIBIT 1002
US PATENT NO. 6,581,565

11.1.5 Frequency of Operation

Microcontrollers are being offered in an ever-increasing range of operating frequencies. Most high-end automotive applications currently use microcontrollers operating in the 12- to 20-MHz range, with 24 MHz becoming not so uncommon. Microcontrollers with frequencies as high as 30 and 32 MHz are available as prototypes and will soon be available for production. Operating frequency becomes especially important when a microcontroller must perform high-speed event control such as required in ABS braking and engine control. Applications such as these typically have to detect, calculate, and respond to external events within a given amount of time. In ABS applications, this time is commonly referred to as loop time and defines the amount of time that the microcontroller has to execute the main loop of the software algorithm to achieve optimal performance.

Operating frequency can be directly related to the speed at which a microcontroller will execute the user's code. For instance, let's look at how long it takes for a particular microcontroller to execute the following generic subroutine. For this example, consider the execution times rather than the operations each instruction is performing.

```
(6)  PUSHF
(3)  NOTB   PTS_COUNT_EPA1
(5)  ADDB   NUM_OF_PULSES_1, PTS_COUNT_EPA1, #00h
(5)  SUB    INV_SPEED_1, FTIME_1, ITIME_1
(27) DIV    INV_SPEED_1, NUM_OF_PULSES_1
(5)  LD     Temp1+2, #Speed_high_constant
(5)  LD     Temp1, #Speed_low_constant
(27) DIV    Temp1, INV_SPEED_1
(4)  ST     Temp1, EPA1_FREQ
(11) RET
```

In this example, the numbers in brackets {} denote how many state times it will take the microcontroller to execute the given line of code. A state time is the basic time measurement for all microcontroller operations. For this MCS-96 family microcontroller, a state time is based on the crystal frequency divided by two. A state time for other microcontrollers may be based upon the crystal frequency divided by three. For this particular microcontroller, a state time can be calculated by the following formula (other microcontroller families use similar formulas):

$$1 \text{ state time} = 1[(\text{frequency of operation})/2]$$

Applying this formula, 1 state time = 125 ns when operating at 16 MHz, and 167 ns when operating at 12 MHz. The example code sequence takes the microcontroller 98 state times to execute. This equates to 16.37 μs to execute at an operating frequency of 12 MHz. At 16 MHz, it takes only 12.25 μs for the microcontroller to execute the subroutine. An operating frequency of 16 MHz results in the microcontroller executing approximately 34 percent more instructions in a given time than at a frequency of 12 MHz.

Another consideration when choosing an operating frequency is the clocking resolution of on-chip timer/counters. The maximum clocking rate of on-chip timer/counters is limited by the frequency the microcontroller is being clocked at. As an example, if an on-chip timer/counter is set up to increment/decrement at a rate determined by CLOCK/4, this would result in 333 ns resolution at 12 MHz. However, if the clock speed were increased to 16 MHz, a higher and more desirable resolution of 250 ns is achieved.

11.1.6 Instruction Set

An often overlooked feature that gives a microcontroller the capability to perform desired operations and manipulate data is its instruction set. A microcontroller's instruction set con-

PETITIONER'S EXHIBIT 1002
US PATENT NO. 6,581,565

sists of a set of unique commands which the programmer uses to instruct the microcontroller on what operation to perform.

An *instruction* is a binary command which is recognized by the CPU as a request to perform a certain operation. Examples of typically supported operations are loads, moves, and stores which transfer data from one memory location to another. There are also jumps and branches which are used to alter program flow. Arithmetic instructions include various multiples, divides, subtracts, additions, increments, and decrements. Instructions such as ANDs, ORs, XORs, shifts, and so forth, allow the user to perform logical operations upon data. In addition to these basic instructions, microcontrollers often support specialized instructions unique to their architecture or intended application.

Instructions can be divided into two parts, the *opcode* and *operand.* The opcode (sometimes referred to as the machine instruction) specifies the operation to take place and the operand specifies the data to be operated upon. Instructions typically consist of either 0, 1, 2, or 3 operands to support various operations. As an example, consider the following MCS-96 architecture instructions:

PUSHF (0 operands) is an instruction that pushes the program status word (PSW) onto the stack. Since this instruction operates on a predefined location, no operand is necessary.

Format: PUSHF

PUSH (1 operand) is an instruction that pushes the specified word operand onto the stack.

Format: PUSH (SRC)

ADD (2 operands) adds two words together and places the result in the destination (leftmost) operand location.

Format: ADD (DST),(SRC)

ADD (3 operands) adds two words together as the 2-operand ADD instruction, but in this case, a third operand is specified as the destination.

Format: ADD (DEST),(SRC1),(SRC2)

Instructions support one or more of six basic addressing types to access operands within the address space of the microcontroller. If programmers wish to take full advantage of a microcontroller architecture, it is important that they fully understand the details of the supported addressing types. The six basic types of addressing modes are termed register-direct, indirect, indirect with autoincrement, immediate, short-indexed, and long-indexed. The following descriptions describe these modes as they are handled by hardware in register-to-register architectures.

The *register-direct* addressing mode is used to directly access registers within the lower 256 bytes of the on-chip register file. The register is selected by an 8-bit field within the instruction and the register address must conform to the operand type's alignment rules. Depending upon the instruction, typically up to three registers can take part in the calculation.

Examples:

ADD AX,BX,CX	AX = BX + CX
MUL AX,BX	AX = AX*BX
INCB CL	CL = CL + 1

The *indirect addressing* mode accesses a word in the lower register file containing the 16-bit operand address. The indirect address can refer to an operand anywhere within the address space of the microcontroller. The register containing the indirect address is selected by an 8-bit field within the instruction. An instruction may contain only one indirect reference; the remaining operands (if any) must be register-direct references.

ENGR & MATH SCI LIBRARY UCLA

PETITIONER'S EXHIBIT 1002
US PATENT NO. 6,581,565

Examples:

LD BX,[AX] BX = mem_word(AX)

In this example, assume that before execution:

contents of AX = 2FC2h

contents of 2FC2h = 3F26h

Then after execution,

contents of BX = 3F26h

ADDB AL,BL,[CX] AL = BL + mem_byte(CX)

The *indirect with autoincrement* addressing mode is the same as the indirect mode except that the variable that contains the indirect address is autoincremented after it is used to address the operand. If the instruction operates on bytes or short integers, the indirect address variable is incremented by one; if it operates on words or integers, the indirect address will be incremented by two.

Examples:

LD BX,[AX]+	BX = mem_word(AX)
	AX = AX + 2
ADDB AL,BL,[CX]+	AL = BL + mem_byte(CX)
	CX = CX + 1

For the *immediate addressing* mode, an operand itself is in a field in the instruction. An instruction may contain only one immediate reference; the remaining operand(s) must be register-direct references.

Example:

ADD AX,#340 AX = AX + 340 (decimal)

For the *short-indexed addressing* mode, an 8-bit field in the instruction selects a word variable (which is contained in square brackets) in the lower register file that contains an address. A second 8-bit field in the instruction stream is sign-extended and summed with the word variable to form an operand address.

Since the 8-bit field is sign-extended, the effective address can be up to 128 bytes before the address in the word variable and up to 127 bytes after it. An instruction may contain only one short-indexed reference; the remaining operand(s) must be register-direct references.

Example:

LD AX,4[BX] AX = mem_word(BX + 4)

In this example, assume that before execution:

contents of BX = A152h

The operand address is then A152h + 04h = A156h

The *long-indexed addressing* mode is like the short-indexed mode except that a 16-bit field is taken from the instruction and added to the word variable to form the operand. No sign extension is necessary. An instruction may contain only one long-indexed reference and the remaining operand(s) must be register-direct references.

Examples:

ST AX,TABLE[BX]	mem_word(TABLE + BX) = AX
AND AX,BX,TABLE[CX]	AX = BX and mem_word(TABLE + CX)

PETITIONER'S EXHIBIT 1002
US PATENT NO. 6,581,565

11.1.7 Programming Languages

The two most common types of programming languages in use today for automotive microcontrollers are *assembly languages* and *high-level languages* (HLLs). Program development begins with the user writing code in either an assembly language or an HLL. This code is written as a text file and is referred to as a source file. The source file is then assembled or compiled using the appropriate assembler/compiler program. The assembler translates the source code into object code and creates what is referred to as an object file. The object file contains machine language instructions and data that can be loaded into an evaluation tool for debugging and validation. The object can also be converted into a hex file for EPROM programming or ROM mask generation as discussed later in this chapter. The program development process is illustrated in Fig. 11.9.

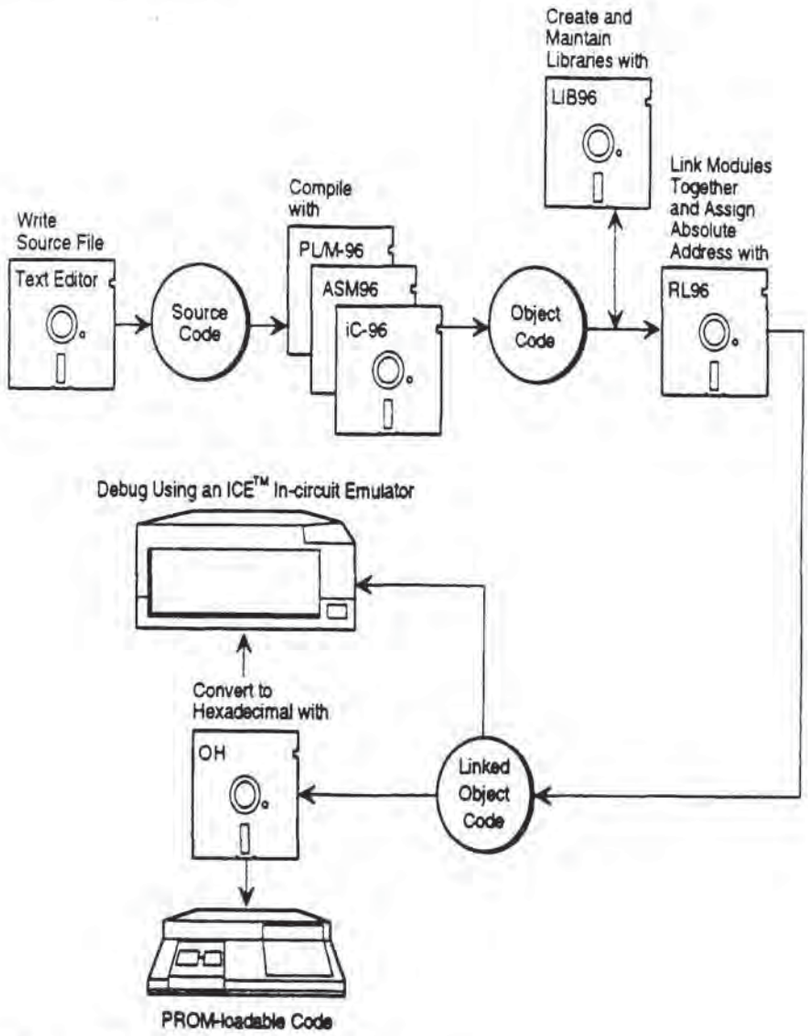


FIGURE 11.9 The program development process.

Assembly Language Programming. An assembly language is a low-level programming language that is specific to a given microcontroller family. Assemblers translate language operation codes (mnemonics) directly into machine instructions that instruct the microcontroller

ENGR & MATH SCI LIBRARY UCLA

PETITIONER'S EXHIBIT 1002
US PATENT NO. 6,581,565

on what operation to perform. Because the programmer is essentially using the microcontroller's machine code to write assembly language programs, more precise control of the device can be achieved through the direct manipulation of individual bits within registers. Because of their efficiency, assembly language programs require less code space than high-level languages. Assembly language programs consist of three parts: machine instructions, assembler directives, and assembler controls.

A *machine instruction* is a machine code that can be executed by the microcontroller's CPU. The collection of machine instructions that a particular microcontroller can execute is referred to as its instruction set. An example of a machine instruction is the opcode for the MULB instruction (Fig. 11.10) from Intel's MCS-96 assembly language. MULB is the mnemonic that represents the machine instruction which performs the specified multiplication operation. When executed by the microcontroller, the MULB opcode results in the multiplication of the two byte operands with the result being placed in a word destination location.

MULB (Three Operands)

Format

```
MULB   wreg,breg,baop
```

Operation

The second and third byte operands are multiplied using signed arithmetic and the 16-bit result is stored into the destination (leftmost) operand. The sticky bit flag is undefined after the instruction is executed.

```
(DEST) ← (SRC1) * (SRC2)
```

Opcode Pattern

11111110	01011aa	baop	breg	wreg

Flags Affected ST

Examples

```
MULB    DELTA, TIMER1, #2
MULB    ALPHA, BETA, GAMMA
MULB    ALPHA, DELTA, 10[GAMMA]
```

FIGURE 11.10 Machine instruction example: MULB.

Assembler directives allow the user to specify auxiliary information (such as storage reservation, location counter control, definition of nonexecutable code, object code relocation, and flow of assembler processing) that determines the manner in which the assembler generates object code from the user's source file input.

Assembler controls set the mode of operation for the assembler and direct the flow of the assembly process. Assembler controls can be classified into primary controls and general controls. Primary controls are set at the beginning of the assembly process and cannot be changed during the assembly. Primary controls allow the user to specify items such as print options, page lengths and widths, error messages, and cross-referencing. General controls can be specified in the invocation line or on control lines anywhere in the source file and can appear any number of times in the program. General controls either cause an immediate action or an immediate change of conditions in which the condition specified remains in effect until another general control causes it to change.

High-level Language Programming. Unlike low-level languages (such as assembly languages), a high-level language is a general purpose language that can support numerous microcontroller architectures. The most common high-level language used for automotive

PETITIONER'S EXHIBIT 1002
US PATENT NO. 6,581,565

applications is C. C programs are written with statements rather than specific instructions from a microcontroller's instruction set. High-level languages utilize a software program known as a *compiler* to translate the user's source code into the specific microcontroller's machine language. Each microcontroller family has its own unique compiler to support selected high-level languages. Although high-level languages tend to be less efficient than assembly languages, their advantage lies in ease of writing code and better debugging capability. The use of statements as opposed to specific instructions better suits high-level languages toward control of procedures (to implement complex software algorithms) as opposed to the microcontroller itself.

11.1.8 Interrupt Structure

The interrupt structure is one of the more important features of an automotive microcontroller. Applications such as automotive ABS and engine control can be referred to as event-driven control systems. Event-driven control systems require that normal code execution be halted to allow a higher-priority task or event to take place. These higher-priority tasks are known as interrupts and can initiate a change in the program flow to execute a specialized routine. When an interrupt occurs, instead of executing the next instruction, the CPU branches to an interrupt service routine (ISR). The branch can occur in response to a request from an on-chip peripheral, an external signal, or an instruction. In the simplest case, the microcontroller receives the request, performs the desired operation and returns to the task that was interrupted.

ISRs are typically serviced via software but it is becoming common for microcontroller manufacturers to implement special on-chip hardware ISR functions for commonly performed operations. These ISRs are typically microcoded or *hardwired* into the microcontroller as described later in this section.

Software, or Normal, Servicing of Interrupts. The software servicing of interrupts is fairly straightforward as shown in Fig. 11.11. When an interrupt source is enabled by the user and a

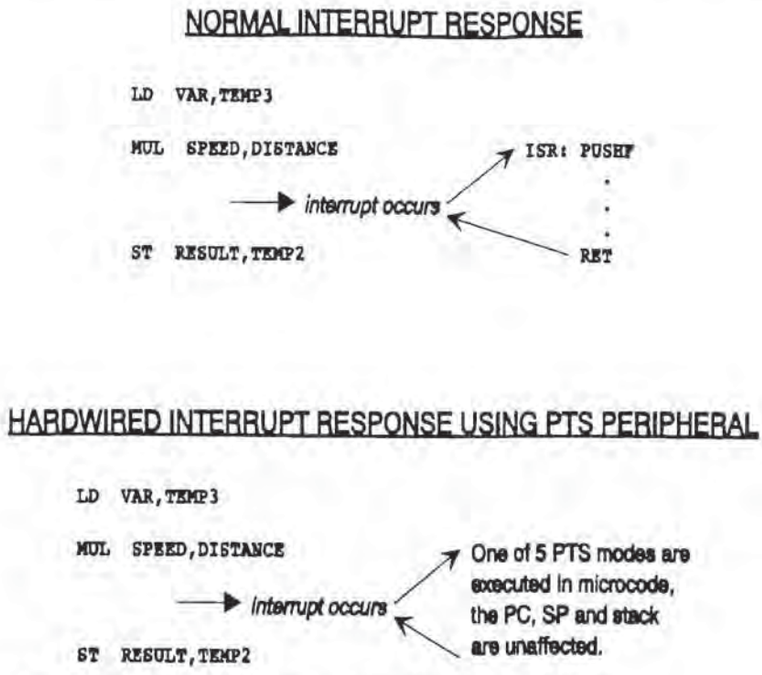


FIGURE 11.11 Comparison of normal interrupts and hardwired interrupts.

ENGR & MATH SCI LIBRARY

PETITIONER'S EXHIBIT 1002
US PATENT NO. 6,581,565

valid interrupt event occurs, the CPU will fetch the starting address of the ISR from the interrupt vector table. The interrupt vector table is a dedicated section of memory that contains the user-programmed start address of the various ISRs. After fetching the ISR address, the CPU automatically pushes the current program counter (PC) onto the stack and loads the PC with the ISR beginning address. This results in the program flow vectoring to the ISR address. The user-programmed ISR is then executed. The last instruction within the ISR is a return instruction that pops the old PC off the stack. This results in program flow continuing from where it was interrupted.

Interrupt mask registers allow the user to prevent or *mask* undesirable interrupts from occurring during various sections of the program. This is a very desirable feature and allows for custom tailoring of the interrupt structure to meet the needs of a particular application. Enabling or disabling of all interrupts (known as globally enabling/disabling) is typically supported with a software instruction such as DI (globally disable all interrupts) or EI (globally enable all interrupts).

Hardware, or Microcoded, Interrupt Structures. Hardware interrupt structures differ from software interrupts in that the user doesn't have to provide the ISR to be executed when the interrupt occurs. With a hardware interrupt structure, the ISR is predefined by being hardwired or *microcoded* into the microcontroller. This is advantageous because it requires less code space and requires less CPU overhead. Stack operations are not necessary since interrupt vectors do not have to be fetched. Most microcontroller manufacturers have their own proprietary solution for hardware ISR's, which are all somewhat similar to one another. For purposes of this section, we will briefly describe the peripheral transaction server as implemented on members of Intel's MCS-96 family of microcontrollers.

The PTS provides a microcoded hardware interrupt handler which can be used in place of a normal ISR. The PTS requires much less overhead than a normal ISR since it operates without modification of the stack. Any interrupt source can be selected by the user to trigger a PTS interrupt in place of a normal ISR. The PTS is similar to a direct memory access (DMA) controller in that when a PTS interrupt, or *cycle*, occurs, data is automatically moved from one location of memory to another as specified by the user. Figure 11.11 compares a regular ISR to a PTS interrupt cycle.

The PTS allows for five modes of operation; single-byte transfer, multiple-byte transfer, PWM, PWM toggle, and A/D scan mode. Each mode is configurable through an 8-byte, user-defined PTS control block (PTSCB) located in RAM. The user may enable virtually any normal interrupt source to be serviced by a PTS interrupt by simply writing to the appropriate bit in an SFR known as the PTS_SELECT register. When a PTS interrupt is enabled and the event occurs, a microcoded interrupt service routine executes in which the contents of the PTSCB are read to determine the specific operation to be performed. More details on the PTSCB can be found in the application example found in this section.

The major advantage of the PTS for automotive applications is its fast response time. The PTS is ideally suited for transferring single or multiple bytes/words of data in response to an interrupt. An example of this is the serial port example which will be described shortly. Another example of the usefulness of the PTS (using A/D scan mode) would be if the user wanted to automatically store A/D conversion results every time a conversion completed within a user-defined scan of A/D channels. The PTS could also be configured to automatically transfer a block of data between memory locations every time an interrupt occurs.

Application Example of PTS Single-Byte Transfer Mode. This example shows how the PTS can be used to automatically transmit and receive 8-byte messages over the serial port. Data to be transmitted and received data are stored in separate tables. The use of the PTS for this purpose greatly reduces CPU overhead and code-space requirements. The layout of the user-defined PTSCB for single-byte transfer mode is shown in Fig. 11.12. PTS_DEST within the PTSCB contains the destination address for the data transfer and PTS_SOURCE contains the source address for the transfer.

PETITIONER'S EXHIBIT 1002
US PATENT NO. 6,581,565

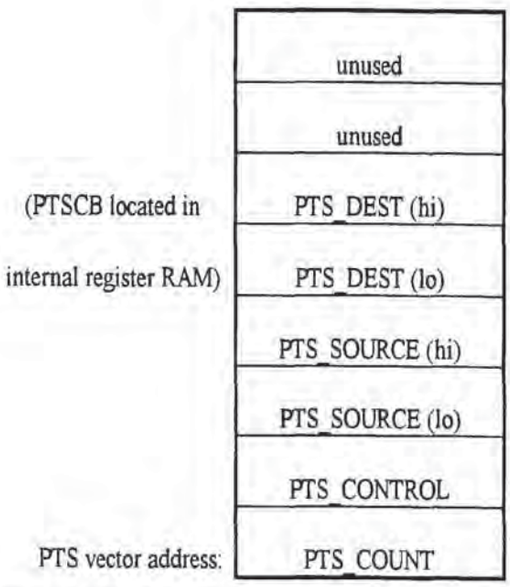


FIGURE 11.12 PTS control block for single-byte transfer mode.

Two PTSCBs are set up for this example, one in response to receive (RX) interrupts and one in response to transmit (TX) interrupts. The RX PTSCB's PTS_DEST is initialized with the start address of the receive data table and the TX PTSCB's PTS_DEST is initialized with the address of the serial port's transmit buffer.

PTS_CONTROL is a byte that specifies the PTS operation to be performed. Its layout is shown in Fig. 11.13.

PTS_COUNT is a down counter that is used to keep track of how many PTS interrupts or cycles have occurred since the last initialization. PTS_COUNT is initialized by the user to any value below 256 and is decremented everytime the corresponding PTS cycle occurs. It is often used to keep track of how many pieces of data have been transferred. In this example, PTS_COUNT is used to determine when a complete 8-byte message has been transmitted or received. After PTS_COUNT expires, an "end-of-PTS" or "normal" ISR occurs, in which the user utilizes the data as required by the application. When an interrupt source is enabled by the user to be a PTS interrupt, the following sequence of events occurs every time the corresponding interrupt occurs:

1. Instead of a normal interrupt, the user has selected it to do a PTS cycle.
2. The microcoded PTS routine fetches the PTS_CONTROL byte from the PTSCB whose start address is specified by the user in the PTS interrupt vector table. The microcoded PTS routine then:

   reads data to be transferred from address specified by PTS_SOURCE

   writes the data to address specified by PTS_DEST

   optionally increments/updates PTS_SOURCE and PTS_DEST addresses

   decrements PTS_COUNT
3. When PTS_COUNT reaches "0", an end of PTS interrupt occurs and the normal ISR is executed in which the user utilizes the received data as necessary (for RX interrupts) or reloads the transmit table with new data (for TX interrupts).

Interrupt Latency. Interrupt latency is defined as the time from when the interrupt event occurs (not when it is acknowledged) to when the microcontroller begins executing the first

ENGR & MATH SCI LIBRARY UCLA

PETITIONER'S EXHIBIT 1002
US PATENT NO. 6,581,565

PTS_CONTROL BYTE (for single and multiple-byte transfers)

7	6	5	4	3	2	1	0
M2	M1	M0	B/W	SU	DU	SI	DI

M2, M1, M0:	Mode	Function
	000	PTS Block Transfer
	100	PTS Single Transfer

B/W:	Byte/Word:	"0" = Word; "1" = Byte
SU:	Source Update:	"1" = update source address
DU:	Destination Update:	"1" = update destination address
SI:	Increment Source:	"1" = Increment Source address
DI:	Increment Destination:	"1" = Increment Destination address

FIGURE 11.13 PTS control byte for single- and multiple-byte transfer modes.

instruction of the interrupt service routine. Interrupt latency must be carefully considered in timing-critical code as is found in many automotive applications.

There is a delay between an interrupt's triggering and its acknowledgment. An interrupt is not acknowledged until the currently executing instruction is finished. Further, if the interrupt signal does not occur at least some specified (assume four for this discussion) state times before the end of the current instruction, the interrupt may not be acknowledged until after the next instruction has been executed. This is because an instruction is fetched and prepared for execution a few state times before it is actually executed. Thus, the maximum delay between interrupt generation and its acknowledgment is approximately four state times plus the execution time of the next instruction.

It should also be noted that most microcontrollers have protected instructions (such as RETURN, PUSH, POP) which inhibit interrupt acknowledgment until after the following instruction is executed. These instructions can increase interrupt-to-acknowledgment delay.

When an interrupt is acknowledged, the interrupt pending bit is cleared and a call is forced to the location indicated by the corresponding interrupt vector. This call occurs after the completion of the current instruction, except as noted previously. For the MCS-96 architecture, the procedure of fetching the interrupt vector and forcing the call requires 16 state times. The stack being located in external memory will add an additional two state times to this number.

Latency is the time from when an interrupt is generated (not acknowledged) until the microcontroller begins executing interrupt code. The maximum latency occurs when an inter-

PETITIONER'S EXHIBIT 1002
US PATENT NO. 6,581,565

rupt occurs too late for acknowledgment following the current instruction. The worst case is calculated assuming that the current instruction is not a protected one. The worst-case latency is the sum of three terms:

1. The time for the current instruction to finish (assume four state times).
2. The state times required for the next instruction. This time is basically the time it takes to execute the longest instruction used in the user's code (assume it's a 16-state DIV instruction).
3. The response time (assume 16 states, 18 for an externally located stack).

Thus, for this scenario, the maximum delay would be 4 + 16 + 16 = 36 state times. This equates to approximately 4.5 μs for a MCS-96 microcontroller operating at 16 MHz. This latency can increase or decrease depending upon the longest execution-time instruction used. Figure 11.14 illustrates an example of this worst-case scenario.

Interrupt latency can be reduced by carefully selecting instructions in areas of code where interrupts are expected. Using a protected instruction followed immediately by a long instruction increases the maximum latency because an interrupt cannot occur after the protected instruction.

11.1.9 Fabrication Processes

The basic fabrication processes that are widely used for automotive microcontrollers today are NMOS (N-channel metal-oxide semiconductor) and CMOS (complementary MOS). The scope of this chapter does not allow for an in-depth discussion of these processes, although a brief description of the structures used to build on-chip circuitry will be discussed. These terms refer to the components used in the construction of MOSFET (MOS field effect transistor) inverters which are the basis of logic on digital devices. NMOS inverters are constructed of N-channel transistors only, whereas CMOS inverters are constructed of both N-channel and P-channel transistors. This section will describe the basic operation of each inverter along with its pros and cons.

Simply stated, a P-channel transistor conducts when a logic "0" is applied to its gate. Conversely, N-channel transistors conduct when a logic "1" is applied to their gate. Figures 11.15 and 11.16 show a simplified cross-sectional view and the electrical symbol for N- and P-channel devices, respectively.

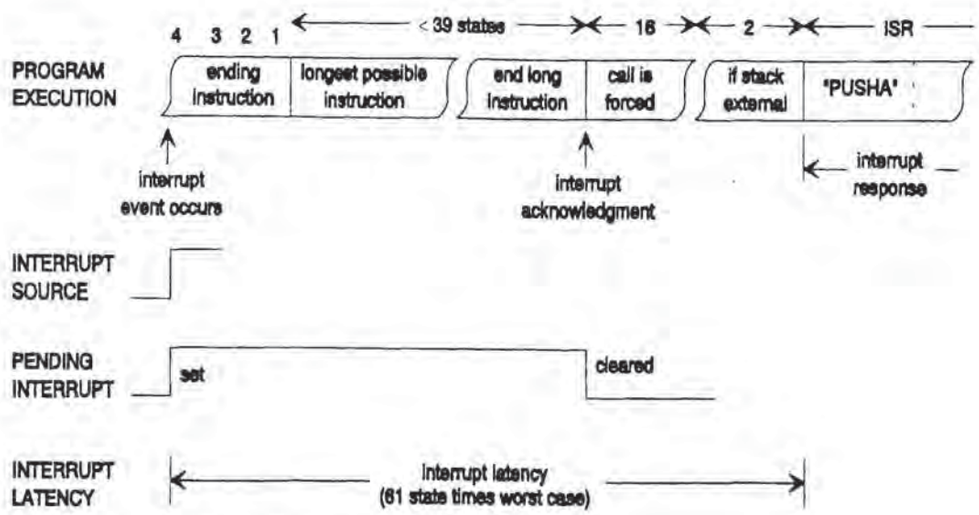


FIGURE 11.14 Worst case interrupt latency example.

ENGR & MATH SCI LIBRARY UCLA

PETITIONER'S EXHIBIT 1002
US PATENT NO. 6,581,565

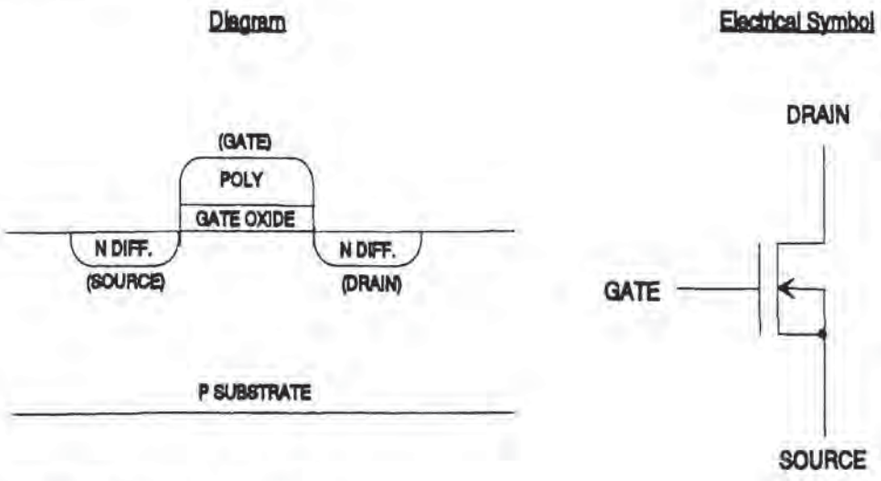


FIGURE 11.15 N-channel transistor.

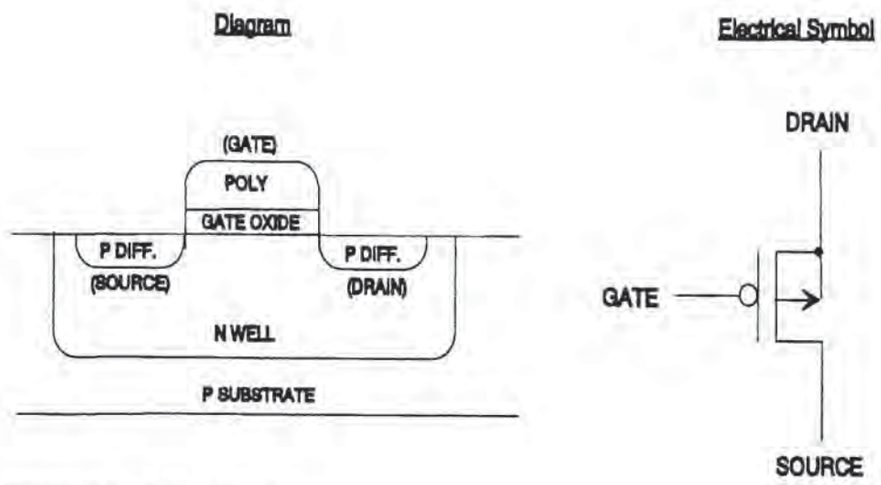


FIGURE 11.16 P-channel transistor.

NMOS Inverters. NMOS inverters are constructed of two NMOS transistors in which one is utilized as a resistance (Q2) and the other is utilized as a switch (Q1). A depletion-mode NMOS transistor is commonly utilized for the resistance device. A basic NMOS inverter is shown in Fig. 11.17. Note that Q2 is always on and acts as a resistor.

When a logic "0" is applied to the inverter's input, Q1 is turned off, which results in Q2 driving a logic 1 at the output. When a logic "1" is applied to the inverter's input, Q1 is turned on and overcomes Q2. This results in a logic "0" at the output.

NMOS microcontrollers are still produced in large quantities today. An advantage of NMOS processes is the simplistic circuit configuration which results in higher chip densities. NMOS devices are also less sensitive to electrostatic discharge (ESD) than CMOS devices. An inherent disadvantage of NMOS design is the slower switching speeds and higher power dissipation due to the dc current path from power to ground through Q1 and Q2 when the inverter is driving a logic "0".

PETITIONER'S EXHIBIT 1002
US PATENT NO. 6,581,565

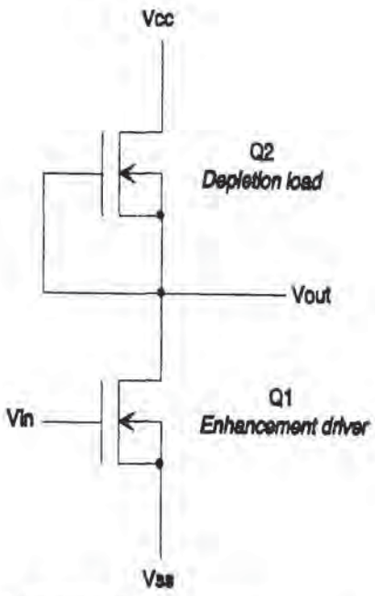


FIGURE 11.17 NMOS inverter.

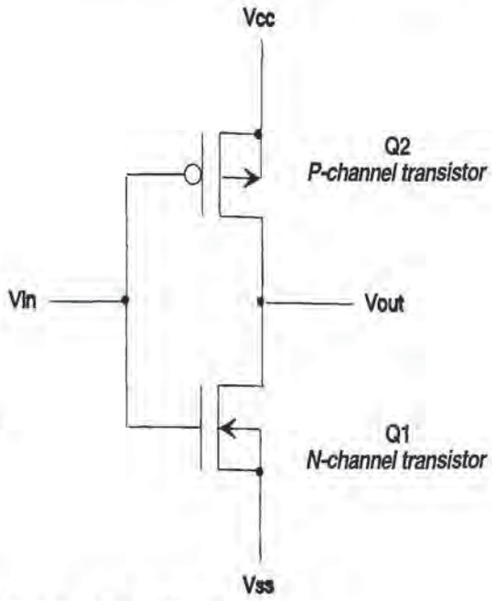


FIGURE 11.18 CMOS inverter.

CMOS Inverters. The CMOS is the most widely used process for automotive microcontrollers today. CMOS inverters are constructed of both P-channel and N-channel transistors that have their inputs tied together as shown in Fig. 11.18. When a logic "0" is applied to the inverter's input, Q1 is turned off and Q2 is turned on, which results in Q2 driving a logic "1" at the output. When a logic "1" is applied to the inverter's input, Q2 is turned off and Q1 is turned on, which results in Q1 driving a logic "0" at the output. Note that only one of these two devices will conduct at a time when the input is "1" or "0". While the input switches, both Q1 and Q2 may conduct for a short time resulting in a small amount of power dissipation.

The main advantages of CMOS logic are greatly improved switching times and lower power consumption, which is due to the complementary design of the inverter. A disadvantage of CMOS logic is that it is more expensive due to its increased complexity and more demanding fabrication process. CMOS logic is more susceptible to ESD damage, although microcontroller manufacturers have countered this by incorporating very effective ESD protection devices onto the silicon.

11.1.10 Temperature Range

Another important factor that must be considered when choosing a microcontroller is the temperature range in which it will be required to operate. The two most common temperature specifications specified by microcontroller manufacturers are *ambient temperature under bias* (TA) and *storage temperature*. These specifications are based upon package thermal characteristics as determined through device and package testing. Storage temperature refers to the temperature range that a microcontroller can be subjected to during periods of nonoperation. Storage temperature specifications are more extreme than ambient temperature under bias temperatures and are usually all the same regardless of the specified ambient temperature range. The common storage temperature range in industry is −60 to +150 °C. While powered-down, a given microcontroller must not be subjected to temperatures that exceed its specified storage temperature range.

ENGR & MATH SCI LIBRARY

PETITIONER'S EXHIBIT 1002
US PATENT NO. 6,581,565

Ambient temperature under bias (TA) refers to the temperature range that the microcontroller is guaranteed to operate at within a given application. While powered-up or operating, a microcontroller must not be subjected to temperatures that exceed its specified ambient temperature range. The most common ambient temperature ranges in industry are:

Commercial	0 to +70 °C
Extended	–40 to +85 °C
Automotive	–40 to +125 °C

11.2 MEMORY

Microcontrollers execute customized programs that are written by the user. These programs are stored in either on-chip or off-chip memory and are often referred to as the *user's code*. On-chip memory is actually integrated onto the same piece of silicon as the microcontroller and is accessed over the internal data bus. Off-chip memory exists on a separately packaged piece of silicon and is typically accessed by the microcontroller over an external address/data bus.

A memory map shows how memory addresses are arranged in a particular microcontroller. Figure 11.19 shows a typical microcontroller memory map.

<table>
<tr><th>Address</th><th colspan="3">Memory Function</th></tr>
<tr><td>0FFFFh
0A000h</td><td colspan="3">External Memory</td></tr>
<tr><td>9FFFh
2080h</td><td colspan="3">Internal ROM/EPROM or External Memory</td></tr>
<tr><td>207Fh
2000h</td><td colspan="3">Internal ROM/EPROM or External Memory
(Interrupt vectors, CCB's, Security Key, Reserved locations, etc.)</td></tr>
<tr><td>1FFFh
1F00h</td><td colspan="3">Internal Special Function Registers (SFR's)</td></tr>
<tr><td>1EFFh
0600h</td><td colspan="3">External Memory</td></tr>
<tr><td>05FFh
0400h</td><td colspan="3">INTERNAL RAM (Address with Indirect or Indexed modes.)
(Also know as Code RAM)</td></tr>
<tr><td>03FFh
0100h</td><td>Register RAM</td><td>Upper Register File (Address with Indirect or Indexed modes or through windows.)</td><td rowspan="3">Register File</td></tr>
<tr><td>00FFh
0018h</td><td>Register RAM</td><td rowspan="2">Lower Register File (Address with direct, Indirect or Indexed modes.)</td></tr>
<tr><td>0017h
0000h</td><td>CPU SFRs</td></tr>
</table>

FIGURE 11.19 Microcontroller memory map.

PETITIONER'S EXHIBIT 1002
US PATENT NO. 6,581,565

Memory is commonly referred to in terms of Kbytes of memory. One Kbyte is defined as 1024 bytes of data. Memory is most commonly arranged in bytes which consist of 8 bits of data. For instance, a common automotive EPROM is referred to as a "256k × 8 EPROM". This EPROM contains 256-Kbytes 8-bit memory locations or 2,097,152 bits of information.

11.2.1 On-Chip Memory

On-chip microcontroller memory consists of some mix of five basic types: random access memory (RAM), read-only memory (ROM), erasable ROM (EPROM), electrically erasable ROM (EPROM), and flash memory. RAM is typically utilized for run-time variable storage and SFRs. The various types of ROM are generally used for code storage and fixed data tables.

The advantages of on-chip memory are numerous, especially for automotive applications, which are very size and cost conscious. Utilizing on-chip memory eliminates the need for external memory and the "glue" logic necessary to implement an address/data bus system. External memory systems are also notorious generators of switching noise and RFI due to their high clock rates and fast switching times. Providing sufficient on-chip memory helps to greatly reduce these concerns.

RAM. RAM may be defined as memory that has both read and write capabilities so that the stored information can be retrieved (read) and changed by applying new information to the cell (write). RAM found on microcontrollers is that of the static type that uses transistor cells connected as flip-flops. A typical six-transistor CMOS RAM cell is shown in Fig. 11.20. It consists of two cross-coupled CMOS inverters to store the data and two transmission gates, which provide the data path into or out of the cell. The most significant characteristic of static memory is that it loses its memory contents once power is removed. After power is removed, and once it is reapplied, static microcontroller RAM locations will revert to their default state of a logic "0". Because of the number of transistors used to construct a single cell, RAM memory is typically larger per bit than EPROM or ROM memory.

Although code typically cannot be executed from register RAM, a special type of RAM often referred to as *code RAM* is useful for downloading small segments of executable code. The difference between code and register RAM is that code RAM can be accessed via the

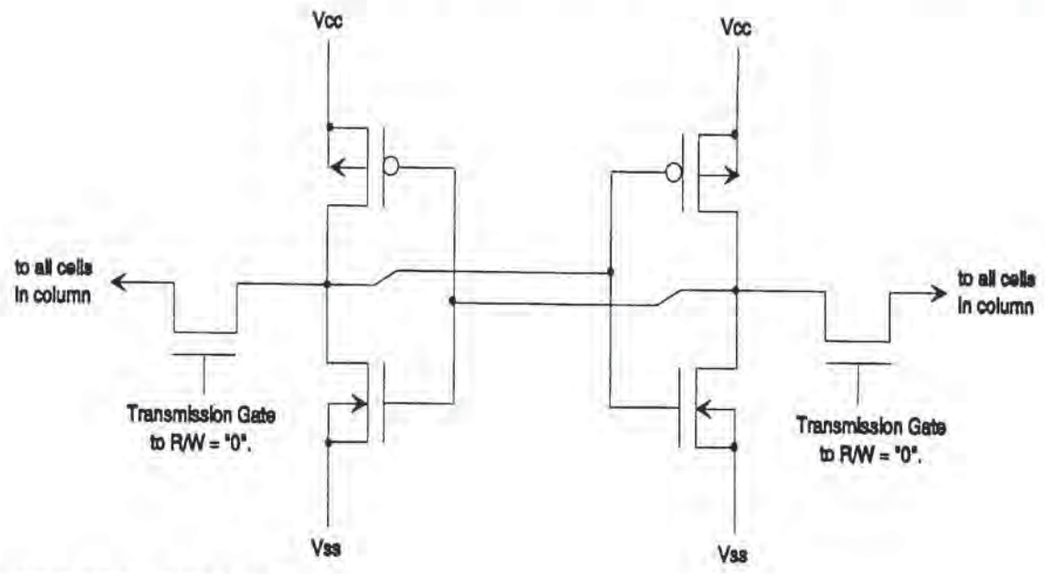


FIGURE 11.20 CMOS RAM memory cell.

ENGR & MATH SCI LIBRARY

PETITIONER'S EXHIBIT 1002
US PATENT NO. 6,581,565

memory controller, thus allowing code to be executed from it. Code RAM is especially useful for end-of-line testing during ECU manufacturing by allowing test code to be downloaded via the serial port peripheral.

ROM. Read-only memory (ROM), as the name implies, is memory that can be read but not written to. ROM is used for storage of user code or data that does not change since it is a non-volatile memory that retains its contents after power is removed. Code or data is either entered during the manufacturing process (masked ROM, or MROM) or by later programming (programmable ROM, or PROM); either way, once entered it is unalterable.

A ROM cell by itself (Fig. 11.21) is nothing more than a transistor. ROM cells must be used in a matrix of word and bit lines (as shown in Fig. 11.22) in order to store information. The word lines are connected to the address decoder and the bit lines are connected to output buffers. The user's code is permanently stored by including or omitting individual cells at word and bit line junctions within the ROM array. For MROMs, this is done during wafer fabrication. For PROMs, this is done by blowing a fuse in the source/drain connection of each cell. To read an address within the array, the address decoder applies the address to the memory matrix. For any given intersection of a word and bit line, the absence of a cell transistor allows no current to flow and causes the transistor to be off. This indicates an unprogrammed ROM cell. The presence of a complete cell conducts and is sensed as a logical "0", indicating a programmed cell. The stored data on the bit lines is then driven to the output buffers.

MROMs are typically used for applications whose code is stable and in volume production. After the development process is complete and the user's program has been verified, the user submits the ROM code to the microcontroller manufacturer. The microcontroller manufacturer then produces a mask that is used during manufacturing to permanently embed the program within the microcontroller. This mask layer either enables or disables individual ROM cells at the junctions of the word and bit lines. An advantage of MROM microcontrollers is that they come with user code embedded, which saves time and money since post-production programming is not necessary. A disadvantage of MROM devices is that, since the mask with the user code has to be supplied early in the manufacturing process, throughput time (TPT) is longer.

Some versions of ROM (such as Intel's Quick-ROM) are actually not ROMs, but rather EPROMs, which are programmed at the factory. These devices are packaged in plastic devices, which prevents them from being erased since ultraviolet light cannot be applied to the actual EPROM array. Throughput time for QROMs is faster since the user code isn't required until after the actual manufacturing of the microcontroller is complete. As with

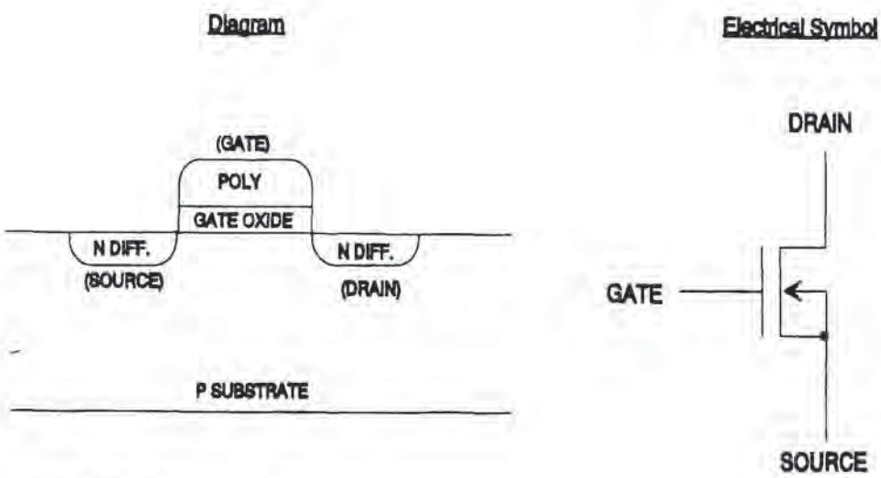


FIGURE 11.21 ROM memory cell.

PETITIONER'S EXHIBIT 1002
US PATENT NO. 6,581,565

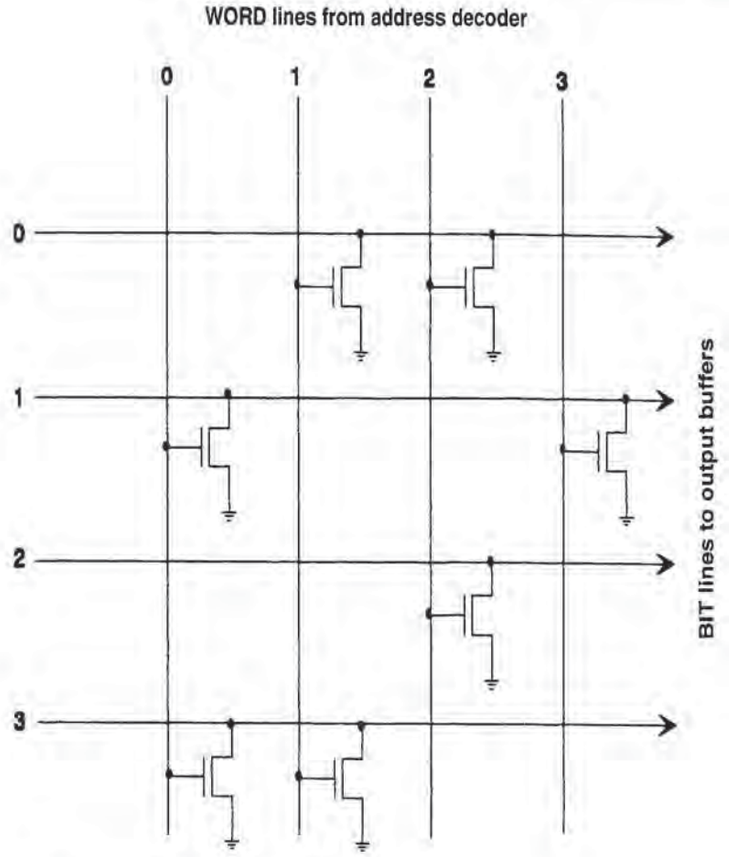


FIGURE 11.22 Simplified ROM memory matrix.

MROMs, the user supplies the ROM code to the microcontroller manufacturer. Instead of creating a mask with the ROM code, the manufacturer programs it into the device just prior to final test.

EPROM. EPROM devices are typically used during application development since this is when user code is changed often. EPROMs are delivered to the user unprogrammed. This allows the user to program the code into memory just prior to installation into an ECU module. Many EPROM microcontrollers actually provide a mechanism for in-module programming. This feature allows the user to program the device via the serial port while it is installed in the module. EPROM devices come assembled in packages either with or without a transparent window. Windowed devices are true EPROM devices that allow the user to erase the memory contents by exposing the EPROM array to ultraviolet light. These devices may be reprogrammed over and over again and thus are ideally suited for system development and debug during which code is changed often. EPROM devices assembled in a package without a window are commonly referred to as *one-time programmable devices* or OTPs. OTPs may only be programmed once, since the absence of a transparent window prevents UV erasure. OTPs are suited for limited production validation (PV) builds in which the code will not be erased.

A typical EPROM cell is shown in Fig. 11.23. It is basically an N-channel transistor that has an added poly1 floating gate to store charge. This floating gate is not connected and is surrounded by insulating oxide that prevents electron flow. The mechanism used to program an EPROM cell is known as *hot electron injection.* Hot electron injection occurs when very high drain (9-V) and select gate (12-V) voltages are applied. This gives the negatively charged electrons enough energy to surmount the oxide barrier and allows them to be stored on the gate.

ENGR & MATH SCI LIBRARY UCLA

PETITIONER'S EXHIBIT 1002
US PATENT NO. 6,581,565

This has the same effect as a negative applied gate voltage and turns the transistor off. When the cell is unprogrammed, it can be turned on like a normal transistor by applying 5 V to the poly2 select gate. When it is programmed, the 5 V will not turn on the cell. The state of the cell is determined by attempting to turn on the cell and detecting if it turns on. Erasure is performed through the application of ultraviolet (UV) light, which gives just the right amount of energy necessary for negatively charged electrons to surmount the oxide barrier and leave the floating gate.

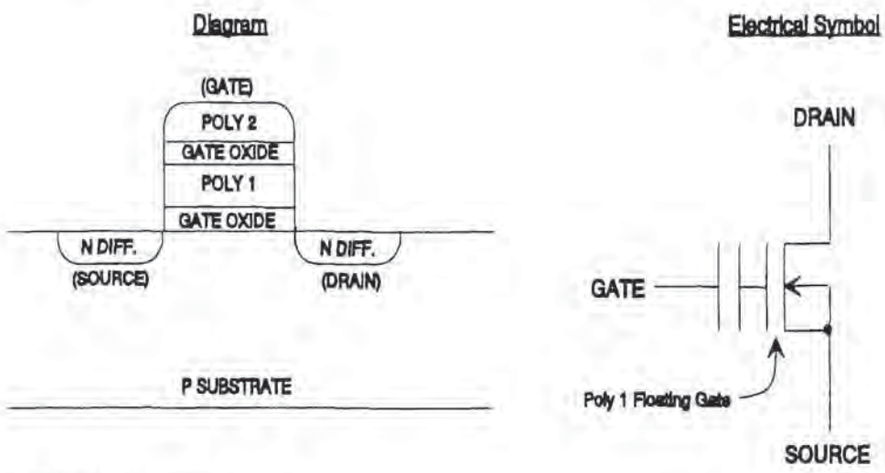


FIGURE 11.23 EPROM memory cell.

Flash. Flash memory is the newest nonvolatile memory technology and is very similar to EPROM. The key difference is that flash memory can be electrically erased. Once programmed, flash memory contents remain intact until an erase cycle is initiated via software. Like EEPROM, flash memory requires a programming and erase voltage of approximately 12.0 V. Since a clean, regulated 12-V reference is not readily available in automotive environments, this need is often provided for through the incorporation of an on-chip charge pump. The charge pump produces the voltage and current necessary for programming and erasure from the standard 5-V supply voltage. The advantage of flash is in its capability to be programmed *and* erased in-module without having to be removed. In-module reprogrammability is desirable since in-vehicle validation testing doesn't always allow for easy access to the microcontroller. Flash also allows for last-minute code changes, data table upgrades, and general code customization during ECU assembly. Since a flash cell is nearly identical in size to that of an EPROM cell, the high reliability and high device density capable with EPROM is retained. The main disadvantage of flash is the need for an on-chip charge pump and special program and erase circuitry, which adds cost.

A flash memory cell is essentially the same as an EPROM cell, with the exception of the floating gate. The difference is a thin oxide layer which allows the cell to be electrically erased. The mechanism used to erase data is known as *Fowler-Nordheim tunneling,* which allows the charge to be transferred from the floating gate when a large enough field is created. Hot electron injection is the mechanism used to program a cell, exactly as is done with EPROM cells. When the floating gate is positively charged, the cell will read a "1", when negatively charged, the cell will read a "0".

EEPROM. EEPROM (electrically erasable and programmable ROM, commonly referred to as E^2ROM) is a ROM that can be electrically erased and programmed. Once programmed, EEPROM contents remain intact until an erase cycle is initiated via software. Like flash, programming and erase voltages of approximately 12 V are required. Since a clean, regulated 12-V reference is not readily available in automotive environments, this requirement is satisfied using an on-chip charge pump as is done for flash memory arrays. Like flash, the advantage of EEPROM is its

PETITIONER'S EXHIBIT 1002
US PATENT NO. 6,581,565

capability to be programmed and erased in-module. This allows the user to erase and program the device in the module without having to remove it. EEPROM's most significant disadvantage is the need for an on-chip charge pump. Special program and erase circuitry also adds cost.

An EEPROM cell is essentially the same as an EPROM cell with the exception of the floating gate being isolated by a thin oxide layer. The main difference from flash is that Fowler-Nordheim electron tunneling is used for *both* programming and erasure. This mechanism allows charge to be transferred to or from the floating gate (depending upon the polarity of the field) when a large enough field is created. When the floating gate is positively charged, the cell will read a "1"; when negatively charged, the cell will read a "0".

11.2.2 Off-Chip Memory

Off-chip memory offers the most flexibility to the system designer, but at a price; it takes up additional PCB real estate as well as additional I/O pins. In cost- and size-conscience applications, such as automotive ABS, system designers almost exclusively use on-chip memory. However, when memory requirements grow to sizes in excess of what is offered on-chip (such as is common in electronic engine control), the system designer must implement an off-chip memory system. Off-chip memory is flexible because the user can implement various memory devices in the configuration of his choice. Most microcontrollers on the market today offer a wide variety of control pins and timing modes to allow the system designer flexibility when interfacing to a wide range of external memory systems.

Accessing External Memory. If circuit designers must use external memory in their applications, the type of external address/data bus incorporated onto the microcontroller should be considered. If external memory is not used, this will have, if any, impact upon the application. There are two basic types of interfaces used in external memory systems. Both of these are parallel interfaces in which bits of data are moved in a parallel fashion and are referred to as *multiplexed* and *demultiplexed* address/data buses.

Multiplexed Address/Data Buses. As the name implies, multiplexed address/data buses allow the address as well as the data to be passed over the same microcontroller pins by multiplexing the two in time. Figure 11.24 illustrates a typical multiplexed 16-bit address/data bus system as is implemented with Intel's 8XC196Kx family of microcontrollers.

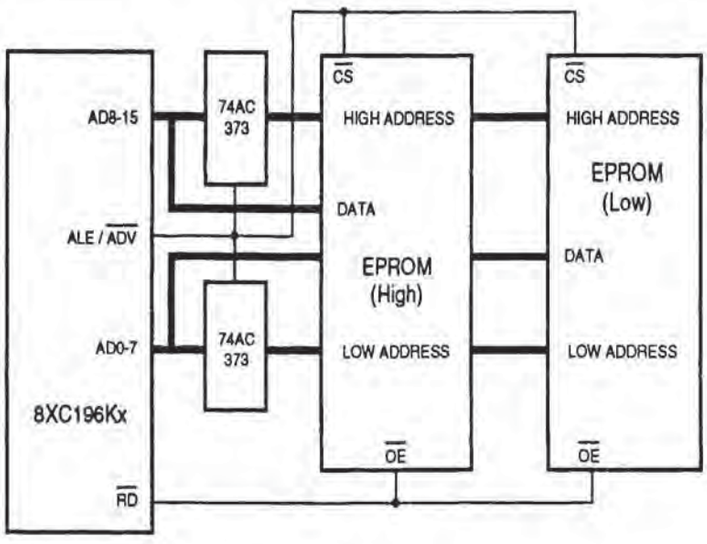


FIGURE 11.24 Multiplexed address/data bus system.

ENGR & MATH SCI LIBRARY

PETITIONER'S EXHIBIT 1002
US PATENT NO. 6,581,565

During a multiplexed bus cycle (refer to Fig. 11.25), the address is placed on the bus during the first half of the bus cycle and then latched by an external address data latch. The signal to latch the address comes from a signal generated by the microcontroller, called address latch enable (ALE). The address must be present on the bus for a specified amount of time prior to ALE being asserted. After the address is latched, the microcontroller asserts either a read (RD#) or a write (WR#) signal to the external memory device.

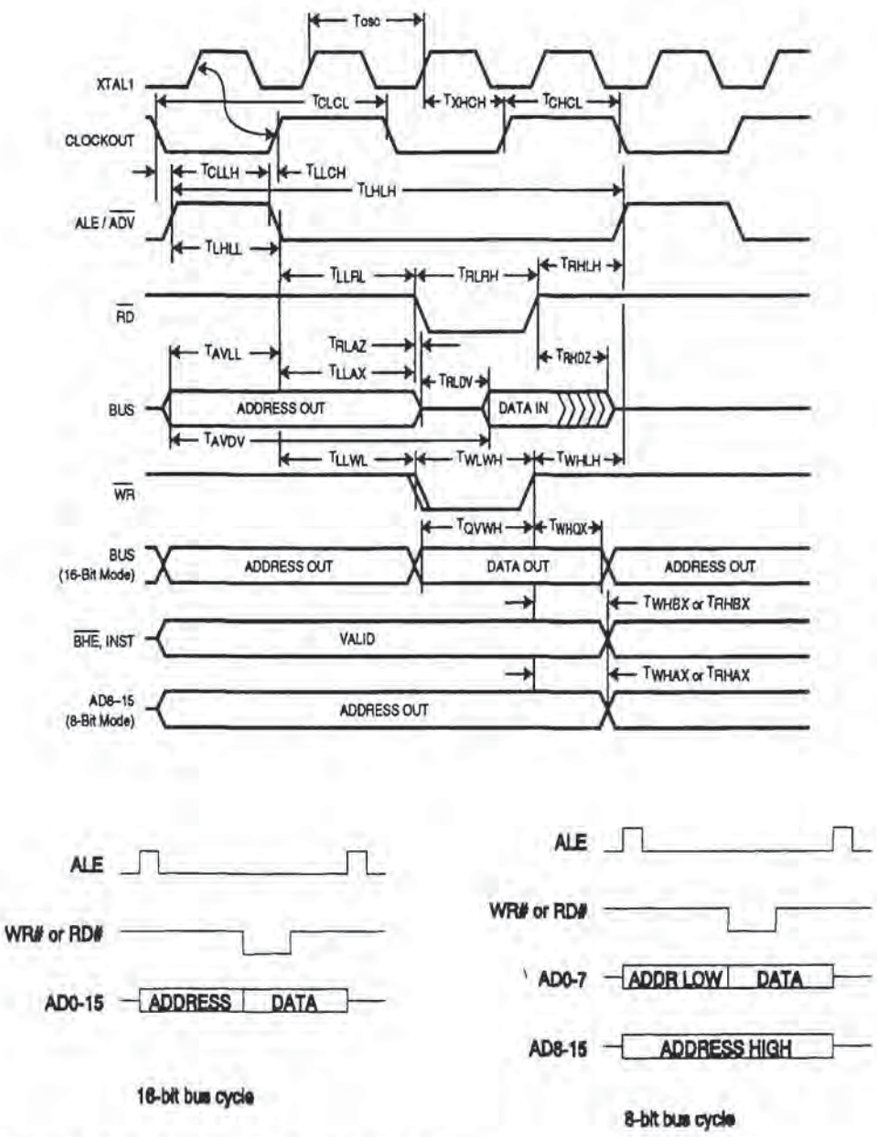


FIGURE 11.25 Multiplexed bus cycle and timing diagram.

For a read cycle, the microcontroller will pull its RD# output pin low and float the bus to allow the memory device to output the data located at the address latched on its address pins. The data returned from external memory must be on the bus and stable for a specified setup time before the rising edge or RD#, which is when the microcontroller latches the data.

For a write cycle, the microcontroller will pull its WR# pin low and then output data on the bus to be written to the external memory. After a specified setup time, the microcontroller will

PETITIONER'S EXHIBIT 1002
US PATENT NO. 6,581,565

release its WR# signal, which signals to the memory device to latch the data on the bus into the address location present on its address pins.

Advantages of multiplexed address/data bus systems are that fewer microcontroller pins are required since address and data share the same pins. For a true 16-bit system, this translates into a multiplexed system requiring 16 fewer pins (for address and data) than would be required by a demultiplexed system. A disadvantage is that an external latch is required to hold the address during the second half of the bus cycle; this adds to the component count.

Demultiplexed Address/Data Buses. Microcontrollers with demultiplexed address/data buses implement separate, dedicated address and data buses as shown in Fig. 11.26.

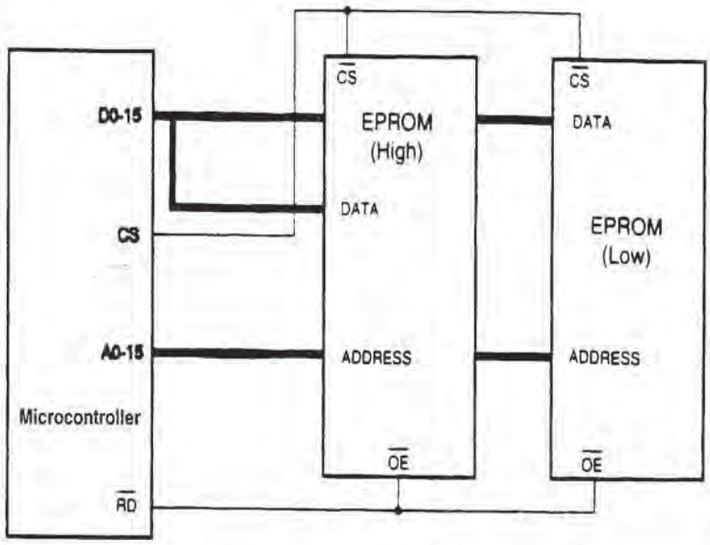


FIGURE 11.26 Typical demultiplexed address/data bus system.

The operation of a demultiplexed address/data bus is basically the same as the multiplexed type with the exception of not having an ALE signal to latch the address for the second half of the bus cycle. The operation of the RD#, WR#, address, and data lines is essentially the same as for that of a multiplexed system.

During a demultiplexed bus cycle, the microcontroller places the address on the address bus and holds it there for the entire bus cycle. For a read of external memory, the microcontroller asserts the RD# signal (or WR# for a write signal) just as would be done for a multiplexed bus cycle. The memory device will respond accordingly by either placing the data to be read on the data bus or by latching the data to be written off of the data bus. Figure 11.27 illustrates a simplified demultiplexed bus cycle.

An advantage of multiplexed address/data bus systems is that external data latches are not necessary, which saves on system component count. A disadvantage, as mentioned earlier, is that more microcontroller pins must be allocated for the interface, which leaves fewer pins for other I/O purposes.

11.3 LOW-SPEED INPUT/OUTPUT PORTS

Low-speed input/output (LSIO) ports allow the microcontroller to read input signals as well as provide output signals to and from other electronic components such as sensors, power drivers,

ENGR & MATH SCI LIBRARY UCLA

PETITIONER'S EXHIBIT 1002
US PATENT NO. 6,581,565

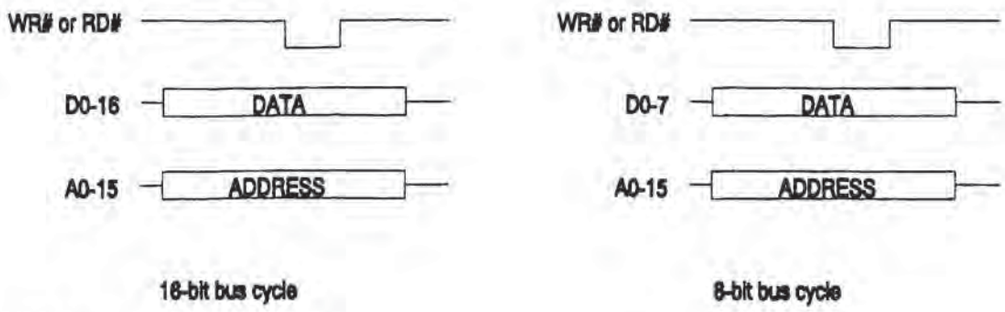


FIGURE 11.27 Demultiplexed bus cycle.

digital devices, actuators, and other microcontrollers. The term "low-speed" is used to describe these ports because unlike high-speed I/O (HSIO) ports which are interrupt driven, LSIO port data must be manually read and written by the user program. Interrupt-driven I/O is typically not possible on port pins configured for LSIO operation. It is common for modern high-performance microcontrollers to utilize multifunctional port pins which can be configured for a special function as well as LSIO. LSIO ports most commonly consist of eight port pins in parallel, which are supported by byte registers. For example, by writing to a single-byte special function register, an entire port can be configured, read, or written. Manipulating individual bits in the port register allows the user flexibility in accessing either single or multiple port pins.

11.3.1 Push-Pull Port Pin Configuration

The term *push-pull*, or *complementary*, output is commonly used to define a port pin that has the capability to output either a logic "1" or "0". Figure 11.28 shows a basic push-pull port pin configuration. Referring to Fig. 11.28, writing a "1" to the data output register enables the P-channel MOSFET and pulls the pin to +5 V, thus driving a logic "1" at the port pin. When a "0" is written

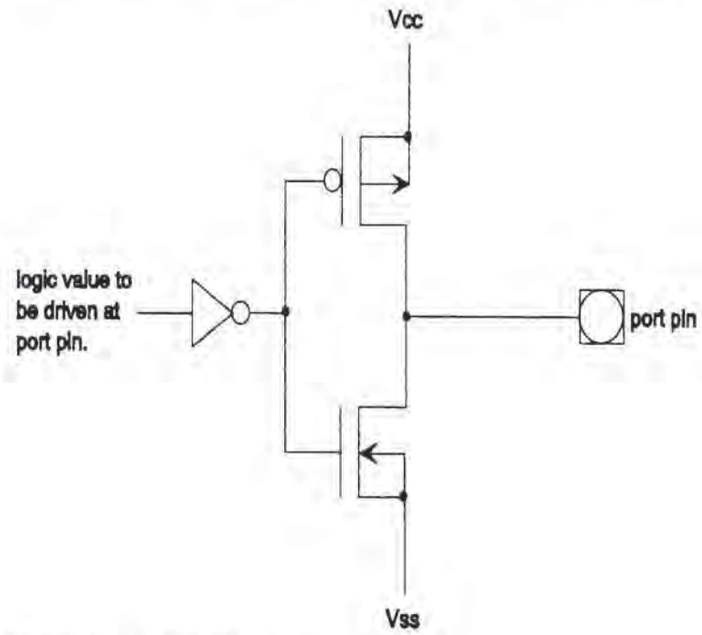


FIGURE 11.28 Push-pull port pin.

PETITIONER'S EXHIBIT 1002
US PATENT NO. 6,581,565

to the data register, the N-channel MOSFET is enabled and thus provides a current path to ground which results in a logic 0 at the port pin. Note that during this time the P-channel pull-up MOSFET is disabled to prevent contention at the port pin. Also note that the port logic design does not allow both the P-channel and the N-channel devices to be driving at the same time.

11.3.2 Open-Drain Port Pin Configuration

Open-drain port pins (Fig. 11.29) are useful for handshaking signals over which multiple devices will have control. The fact that the P-channel transistor is either omitted or disabled dictates the need for an external pull-up resistor. An example of an application for open-drain port pins would be for a bus contention line between two microcontrollers communicating on a common bus. During normal operation, the line is pulled high by the external pull-up resistor to signal to either microcontroller that no contention exists. If one of the microcontrollers should detect contention on the bus, it simply outputs a logic "0", which signals the contention to the other processor. To output the "0", the port only has to overcome the external pull-up which the user should appropriately size to match the port drive specifications.

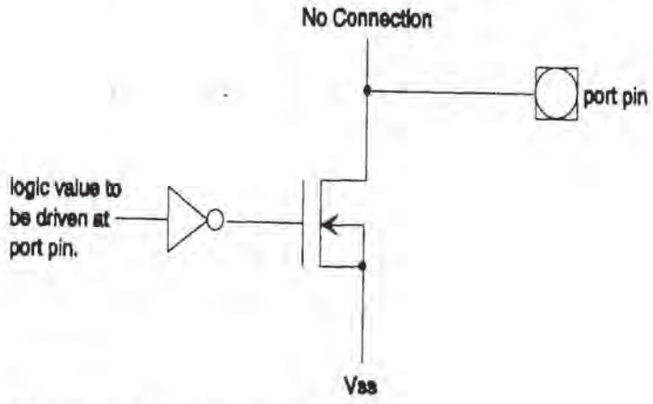


FIGURE 11.29 Open-drain port pin.

11.3.3 High-Impedance Input Port Pin Configuration

High impedance, or "Hi-z," port pins (Fig. 11.30) are used strictly as inputs since no drivers exist on these types of pins. Hi-z refers to the relatively high input impedance of the port pin. This high input impedance prevents the port pin circuitry from actively loading the input signal. Note that the pin is connected to the gates of a CMOS inverter, which drives internal circuitry. Usually a certain amount of hysteresis is built into these pins and is specified in the data sheet.

11.3.4 Quasi Bidirectional Port Pin Configuration

Quasi bidirectional (QBD) port pins are those that can be used as either input or output without the need for direction control logic. QBD port pins can output a strong low value or a weak high value. The weak high value can be externally overridden, providing an input function. Figure 11.31 shows a QBD port pin diagram and its transfer characteristic.

Writing a "1" to the port pin disables the strong low driver (Q2) and enables a very weak high driver (Q3). To get the pin to transition high quickly, a strong high driver (Q1) is enabled for one state time and then disabled (leaving only Q3 active).

It is important to keep in mind that since the port pin can be externally overridden with a logic "0", reading the port pin could falsely indicate that it was written as a logic "0".

ENGR & MATH SCI LIBRARY UCLA

PETITIONER'S EXHIBIT 1002
US PATENT NO. 6,581,565

The ability to overdrive the weak output driver is what gives the quasi bidirectional port pin its input capability. To reduce the amount of current that flows when the pin is externally pulled low, the weak output driver (Q4) is turned off when a valid logic "0" is detected. The input transfer characteristic of a quasi bidirectional port pin is shown in Fig. 11.31.

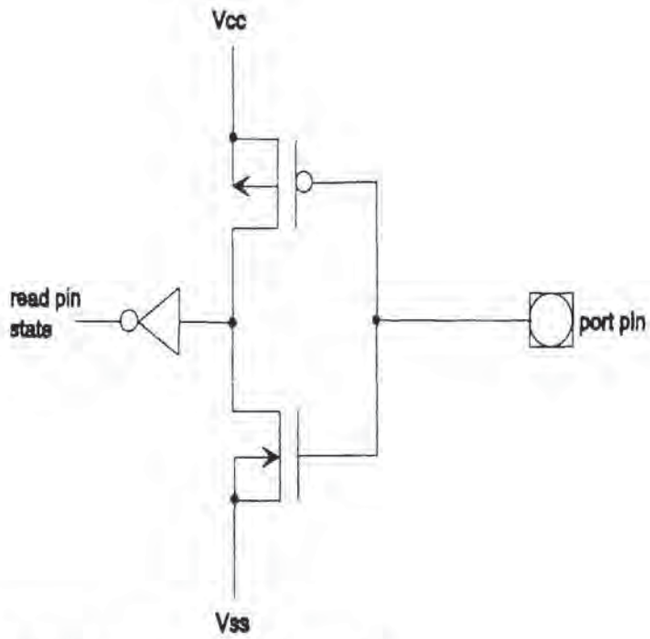


FIGURE 11.30 High-impedance input port pin.

11.3.5 Bidirectional Port Example

The following example describes the operation of a state-of-the-art bidirectional port structure. This particular structure is used upon newer members of Intel's MCS-96 automotive microcontroller family. A single port consists of eight multifunction, parallel port pins (see Fig. 11.32), which are controlled (on a by-pin basis) with four special function registers referred to as Px_PIN, Px_REG, Px_MODE, and Px_DIR. As is common with other high-performance microcontrollers, the pins of this port are shared with alternate special functions controlled by other on-chip peripherals. The Px_MODE register allows the programmer to choose either LSIO or the associated special function for any given port pin. Writing a "1" to the appropriate bit selects the corresponding pin as special function whereas a "0" selects LSIO. The function of the Px_PIN and Px_REG registers is fairly straightforward. In order to read the value on the pin, the user simply reads the Px_PIN register. To write a value to the Px_REG register, the user simply writes the desired output value to the Px_REG register. The Px_DIR register allows the user to configure the port pin as either input or output.

In order to prevent an undefined pin state during reset, port pins revert to a default state during reset. For the Intel Kx bidirectional port structure, this state is defined as a weak logic "1". The transistor that drives this state is labeled as WKPU in Fig. 11.32 and is asserted in reset until the user writes to the Px_MODE register to configure the port pin.

Ports such as this offer the user much flexibility in assigning their function within an application. Following are three examples that depict how these ports may be configured by the user by writing values to the appropriate bit within the port SFR. Also note that the eight pins of a port may be configured individually on a pin-by-pin basis.

To configure a given port pin as a high-impedance input pin, the user must write the following values to the corresponding bit within the port SFR.

PETITIONER'S EXHIBIT 1002
US PATENT NO. 6,581,565

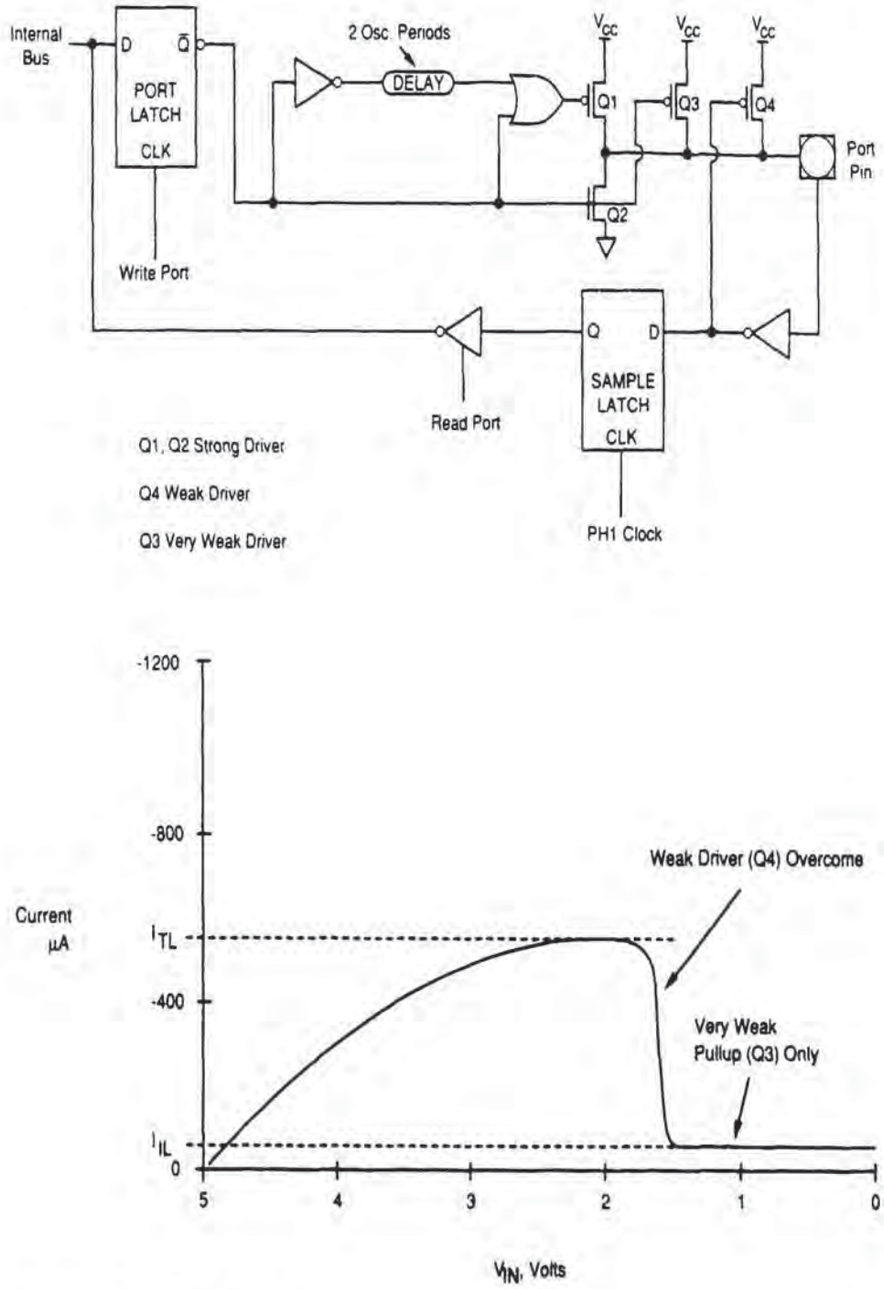


FIGURE 11.31 Quasi bidirectional port pin and transfer characteristic.

Px_MODE: "0" selects the pin as LSIO and disables weak pull-up.
Px_DIR: "1" disables operation of the N-channel transistor.
Px_REG: "1" disables the N-channel transistor.

To configure a given port pin for push-pull operation, the following values must be written to the corresponding bit within the port SFR.

ENGR & MATH SCI LIBRARY TEXAS

PETITIONER'S EXHIBIT 1002
US PATENT NO. 6,581,565

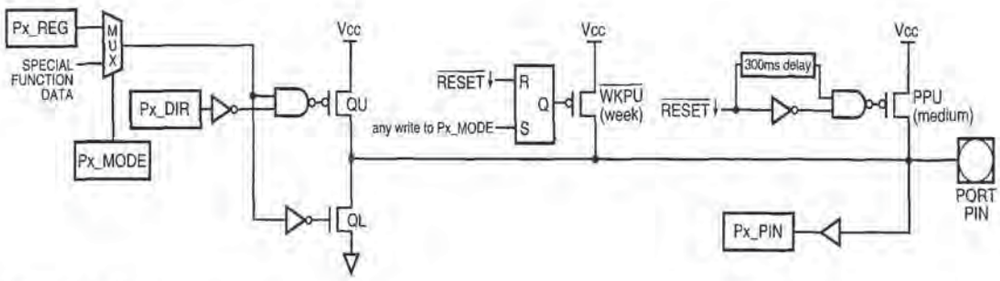


FIGURE 11.32 Bidirectional port structure example.

Px_MODE: "0" selects the pin as LSIO and disables weak pull-up transistor.

Px_DIR: "0" enables operation of both the N- and P-channel transistors.

Px_REG: "0" or "1" drives that value at the port pin.

To configure a port pin for open-drain operation, the user must write the following values to the corresponding bits within the port SFR.

Px_MODE: "0" selects the pin as LSIO and disables weak pull-up transistor.

Px_DIR: "1" disables operation of the N-channel transistor.

Px_REG: "1" disables the P-channel transistor / achieves Hi-Z state.
"0" enables the N-channel transistor / drives "0" at pin.

11.4 HIGH-SPEED I/O PORTS

Perhaps the most demanding of automotive microcontroller applications is electronic engine control and antilock braking/traction control. These applications both require the microcontroller to detect, process, and respond to external signals or "events" within relatively short periods of time. Sometimes referred to as a capture/compare module, a microcontroller's HSIO (high-speed input/output) peripheral allows the microcontroller to capture an event as it occurs. The term *capture* refers to a series of events that begins with the microcontroller detecting a rising or falling edge upon a high-speed input pin. At the precise moment this edge is detected, the value of a software timer is loaded into a time register and an interrupt is triggered. This gives the microcontroller the relative time at which the event occurred. An HSIO peripheral also provides compare functions by detecting an internal event, such as a timer reaching a particular count value. When the particular count value is detected, the HSIO unit will generate a specified event (rising or falling edge) on a port pin. This feature is ideal for generating PWM waveforms or synchronizing external events with internal events.

For example, consider a typical ABS microcontroller which must detect, capture, and calculate wheel speeds; respond with signals to hydraulic solenoids; and perform many other background tasks all within a loop time of about 5 ms. The wheel speed signals are input to the microcontroller as square waves with frequencies up to 7000 Hz (approximately one edge every 71 μs). The microcontroller must have the performance necessary to capture and process these edges on as many as four wheel speed inputs. HSIO peripherals, along with the interrupt structure, play a major role in the microcontroller's ability to perform this function.

Nearly every microcontroller manufacturer has its own proprietary HSIO peripheral. For purposes of this section, the event processor array (EPA) HSIO peripheral, which is used by Intel's 87C196KT automotive microcontroller, will be discussed.

PETITIONER'S EXHIBIT 1002
US PATENT NO. 6,581,565

11.4.1 High-Speed Input and Output Peripheral

High-speed input/output peripherals typically consist of a given number of capture/compare modules, a timer/counter structure, control and status SFRs, and an interrupt structure of some type. Figure 11.33 shows a block diagram of the EPA peripheral. The main components of the EPA are ten capture/compare channels, two compare only channels, and two timer/counters. The capture/compare channels are configured independently of each other. The two timer/counters are shared between the various capture/compare channels. Each capture/compare channel has its own dedicated SFR's: EPAx_TIME and EPAx_CON (x designates the channel number).

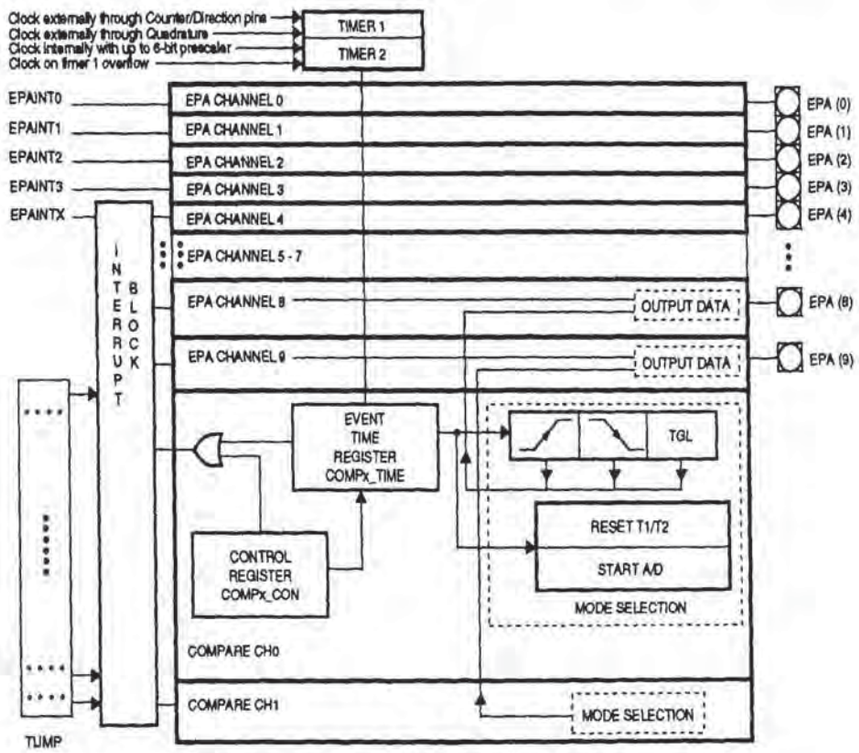


FIGURE 11.33 Example HSIO peripheral: Intel's EPA peripheral.

11.4.2 Timer/Counter Structures

High-performance microcontrollers typically integrate one or more timer/counters onto their silicon. A microcontroller's timer/counter structure provides a time base to which all HSIO events are referenced. Timers are clocked internally, whereas counters are clocked from an external clock source. Timers are often very flexible structures, in which programmers have the capability to configure the timer/counters to meet their application's particular needs. The 87C196KT has two 16-bit timer/counters referred to as TIMER1 and TIMER2. As 16-bit timer/counters, each timer has the capability of counting to 2^{16} or 65,536 before overflowing. The user has the option of triggering an interrupt upon overflow of a timer/counter. Each of these two timers can be independently configured using the TxCONTROL SFR as shown in Fig. 11.34, where x specifies either 1 or 2 for Timer1 or Timer2, respectively.

Bits number 3, 4, and 5 are the mode bits that allow the user to configure the clocking source and direction of each timer/counter. The clock rate can be based either upon the fre-

PETITIONER'S EXHIBIT 1002
US PATENT NO. 6,581,565

TxCONTROL SFR

7	6	5	4	3	2	1	0
CE	UD	M2	M1	M0	P2	P1	P0

CE: Count Enable: "0" = disable timer, "1" = enable timer

UD: Up/Down: "0" = count up, "1" = count down

MODE:	M2, M1, M0	Clock source	Direction determined by:
	0 0 0	XTAL/4	state of UD bit
	0 0 1	TxCLK pin	state of UD bit
	0 1 0	XTAL/4	state of TxDIR pin
	0 1 1	TxCLK pin	state of TxDIR pin
	1 0 0	Timer1 overflow	state of UD bit
	1 1 0	Timer1 overflow	same as Timer1
	1 1 1	Quadrature clocking using TxCLK and TxDIR pins	

Prescale:	P2, P1, P0	Clock prescale values
	0 0 0	÷ by 1 (250 ns @ 16 MHz xtal frequency)
	0 0 1	÷ by 2 (500 ns @ 16 MHz xtal frequency)
	0 1 0	÷ by 4 (1 µs @ 16 MHz xtal frequency)
	0 1 1	÷ by 8 (2 µs @ 16 MHz xtal frequency)
	1 0 0	÷ by 16 (4 µs @ 16 MHz xtal frequency)
	1 0 1	÷ by 32 (8 µs @ 16 MHz xtal frequency)
	1 1 0	÷ by 64 (16 µs @ 16 MHz xtal frequency)
	1 1 1	reserved

FIGURE 11.34 Timer control SFR example.

PETITIONER'S EXHIBIT 1002
US PATENT NO. 6,581,565

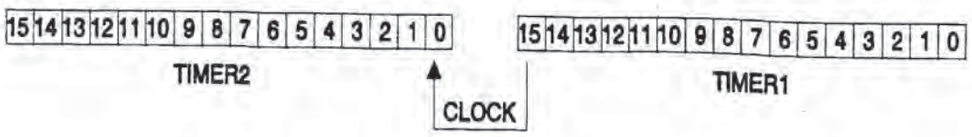


FIGURE 11.35 Cascading of timer/counters.

quency that the microcontroller is being clocked at the XTAL pins or upon the input frequency on another pin referred to as TxCLK. The user also has the option of either having the logic level of another pin (TxDIR) or the UD bits in TxCONTROL determine the direction (up/down) that the timer/counter is clocked.

For those applications that require a 32-bit timer/counter, the user has the option (using the mode bits) to direct the overflow of TIMER1 to clock TIMER2. This is known as cascading and essentially creates a 32-bit timer/counter as shown in Fig. 11.35.

11.4.3 Input Capture

Input capture refers to the process of capturing a current timer value when a specific type of event occurs. An excellent example of high-speed input capture can be illustrated with a basic automotive ABS input capture algorithm that calculates the frequency of a wheel speed input. The signals from the wheel speed sensors are input into the microcontroller's EPA pins as square waves. Consider the generic wheel speed input capture example shown in Fig. 11.36.

Two timers (1 and 2) are used in this example. Timer1 is used in conjunction with an EPA channel to provide a 5-ms software timer (this is a compare function that will be discussed in the next section). The 5 ms is the main loop time used in generic ABS algorithms. Timer2 is used in conjunction with one or more EPA channels to capture the relative times at which edges occur on wheel speed inputs. The EPA is configured to capture falling edges and initiate an interrupt, which stores the event time and increments an edge count. To simplify this example, we will consider only a single input channel.

The process starts by EPA interrupts being enabled after Timer1 starts a new 5-ms timer count. The first falling edge causes an interrupt that stores the event time (T2) into a variable *initial time* and increments an edge count. The next edge causes an interrupt in which the event time (T2+x) is stored into a variable called *final time* and increments the edge count.

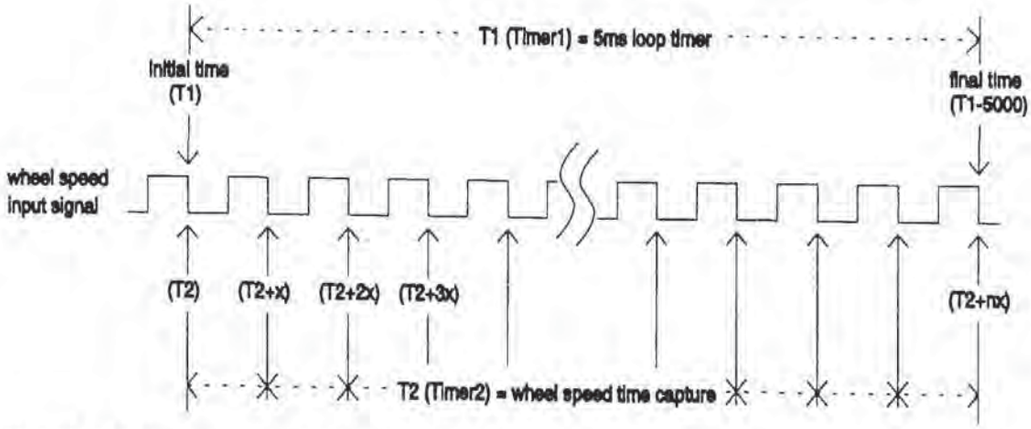


FIGURE 11.36 Input capture example using EPA peripheral.

ENGR & MATH SCI LIBRARY

PETITIONER'S EXHIBIT 1002
US PATENT NO. 6,581,565

Subsequent edges' event times are also stored into *final time* until Timer1's 5-ms count expires. At this point, final time contains the time at which the last edge to occur was captured. The average period of the input waveform can then be calculated with the following equation:

$$\text{input period} = (\textit{final time} - \textit{initial time}) / \text{edge count}$$

11.4.4 Output Compare

Output compare refers to the process of generating an event when a timer value matches a predetermined time value. The event may be to generate an interrupt, toggle an output pin, perform an A/D conversion, and so forth. Following is an example that shows the steps necessary to generate an event every 50 μs:

1. Enable the output compare channel's interrupt.
2. Initialize the timer to count up at 1 μs per timer tick.
3. Initialize the output compare channel to re-enable and reset the timer (to zero) when a timer match occurs.
4. Initialize the output compare channel to produce the desired event when a timer match occurs.
5. Write 32h (50 decimal) to the appropriate output compare channel's time register.
6. Enable the timer to start the process.
7. A compare channel interrupt will be generated every 50 μs.

Since the example re-enables and zeros the timer, the event will occur continuously until the user's program halts the process.

Software Timers. Software timers such as the 5-ms timer used in the ABS wheel speed capture example can be set up easily using a compare channel and a timer. The following software timer procedure is very similar to that used in the previous output compare example:

1. Enable the compare channel's interrupt.
2. Initialize the timer to count up at 1 us per timer tick.
3. Initialize the output compare channel to re-enable and reset the timer (to zero) when a timer match occurs.
4. Initialize the output compare channel to produce an interrupt (5-ms ISR) when a timer match occurs.
5. Write 1388h (5000 decimal) to the appropriate output compare channel's time register.
6. Enable the timer to start the process.
7. An compare channel interrupt will be generated every 5 ms.

11.4.5 Pulse-Width Modulation (PWM)

Pulse-width modulation (PWM) peripherals provide the user with the ability to generate waveforms that have specified frequencies and duty cycles. PWM waveforms are typically used to generate pulsed waveforms used for motor control or they may be filtered to produce a smooth analog signal. HSIO peripherals typically provide for PWM waveform generation, although the methods are not usually as efficient as dedicated PWM peripherals. A basic example of creating a PWM waveform using an HSIO peripheral's output compare function is described in Sec. 11.4.4.

PETITIONER'S EXHIBIT 1002
US PATENT NO. 6,581,565

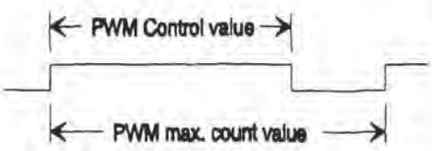


FIGURE 11.37 PWM waveform time values.

PWM Peripheral. The components of a basic automotive microcontroller's PWM peripheral include a counter (typically 8-bit), a comparator, a holding register, and a control register. The counter typically has a prescaler that allows the user to select the clock rate of the counter, which allows for selectable PWM frequencies. Without prescaling capability, an 8-bit counter would only allow for a period of 256 state times. The PWM control register determines how long the PWM output is held high during the pulse, effectively controlling the duty cycle as shown in Fig. 11.37. For an 8-bit PWM counter, the value written to the PWM control register can be from 0 to 255 (equating to 255 state times with no prescaling). Note that PWM peripherals do not typically allow for a 100 percent duty cycle because the output must be reset when the counter reaches zero.

The operation of a PWM peripheral is rather simple. The PWM control register's value (assume 8-bit for this example) is loaded into a holding register when the 8-bit counter overflows. The comparator compares the contents of the holding register to the counter value. When the counter value is equal to zero, the PWM output is driven high. It remains high until the counter value matches the value in the holding register, at which time the output is pulled low. When the counter overflows, the output is again switched high. Figure 11.38 shows typical PWM output waveforms.

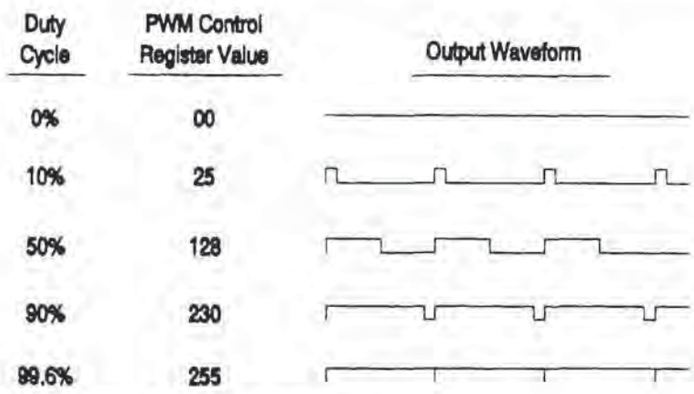


FIGURE 11.38 PWM output waveforms.

11.5 SERIAL COMMUNICATIONS

It is often necessary for automotive microcontrollers to have the capability to communicate with other devices both internal and external to the ECU. Within an ECU a microcontroller may have to communicate with other devices such as backup processors, shift registers, watchdog timers, and so forth. It is not uncommon for automotive microcontrollers to communicate with devices external to the ECU, such as other modules within the vehicle and even diagnostic computers at a service station. All of these communication examples require a large quantity of data to be transmitted/received in a short period of time. Also consider that this communication must utilize as few pins of the microcontroller as possible in order to save valuable PCB board space. These requirements all support the need for serial communications.

Serial communications provides for efficient transfer of data while utilizing a minimum number of pins. Serial communications is performed by transferring a group of data bits, one at a time, sequentially over a single data line. Each transmission of a group of bits (typically a

ENGR & MATH SCI LIBRARY

PETITIONER'S EXHIBIT 1002
US PATENT NO. 6,581,565

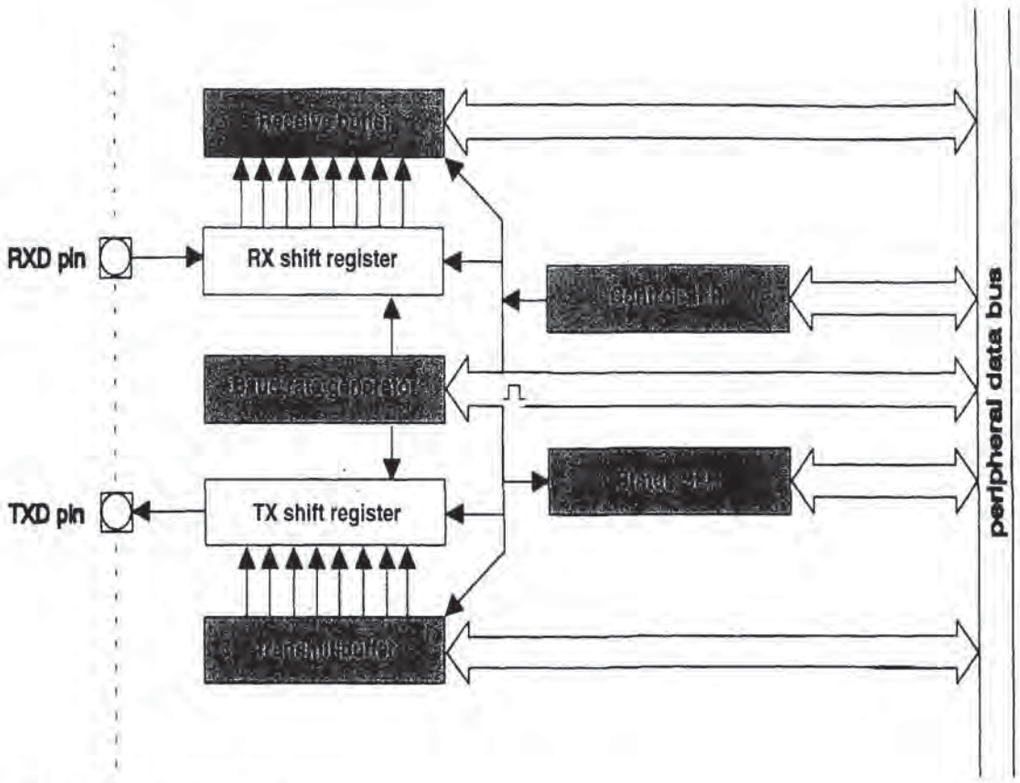


FIGURE 11.39 Serial port block diagram.

byte of data) is known as a data frame. This transfer of data takes place at a given speed, which is referred to as the baud rate and is typically specified in bits/second.

A typical microcontroller serial port consists of data buffers, data registers, and a baud rate generator. Interface to the outside world takes place via the transmit (TXD) and receive (RXD) pins. A block diagram for a typical serial port peripheral is shown in Fig. 11.39. By writing to the serial port control register, users are able to customize the operation of the serial port to their particular application's requirements.

The baud rate generator is used to provide the timing necessary for serial communications and determines the rate at which the bits are transmitted. In synchronous modes, the baud rate generator provides the timing reference used to create clock edges on the clock output pin. In asynchronous modes, the baud rate generator provides the timing reference used to latch data into the RX pin and clock it out of the TX pin.

11.5.1 Synchronous Serial Communications

Sometimes an application does not allow asynchronous serial communications to take place due to variations in clock frequency, which results in unacceptable baud rate error. Some applications simply require some sort of shift register I/O. Synchronous communication involves an additional clock pin, which is used to signal the other device that data being transferred are valid and ready to be read. Often when the user configures the serial port to work in a synchronous mode, the TXD pin automatically reverts to supplying the clock and the RXD pin automatically becomes the data pin. This configuration prevents an additional pin from having to be reserved for use as a serial clock pin. When a synchronous data transfer is initiated, a series of eight clock pulses is emitted from the clock pin at a predetermined baud rate as shown in Fig. 11.40.

PETITIONER'S EXHIBIT 1002
US PATENT NO. 6,581,565

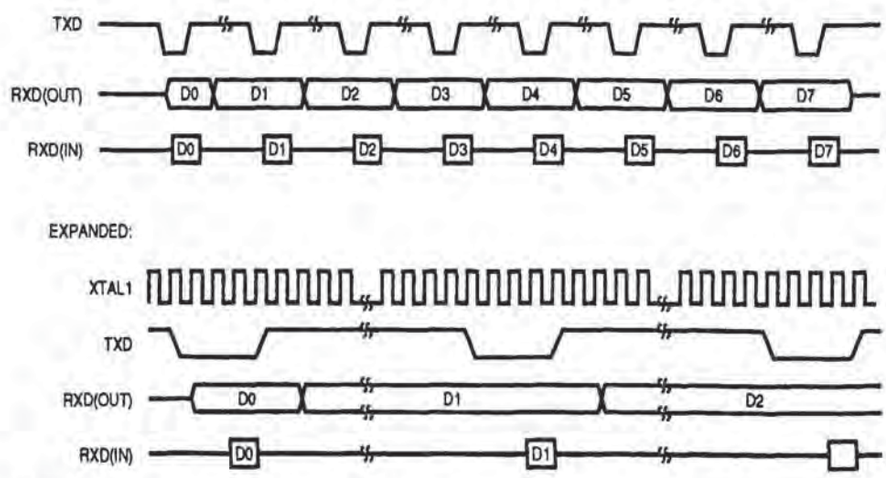


FIGURE 11.40 Synchronous serial mode data frame.

An example of synchronous serial communications is shown in Fig. 11.41. Assume that processor A is to transfer a byte of data to processor B. The program executing in processor A initiates a serial transmission by writing the data byte to be transmitted into the transmit buffer. Assuming microcontroller A's serial port is enabled for transmission, writing to the transmit buffer results in a series of eight clock pulses to be emitted from microcontroller A's clock pin. The first falling edge of the clock will signal to processor B that bit 0 (LSB) is ready to be read into its receive buffer. Microcontroller A will place the next data bit on the TXD pin with each rising clock edge. With B's serial port enabled for reception, each falling edge will result in another data bit being shifted into B's receive buffer. When B's receive buffer is full, the received data byte will be loaded into its receive register and will signal its CPU that the reception has been completed and the data is ready for use.

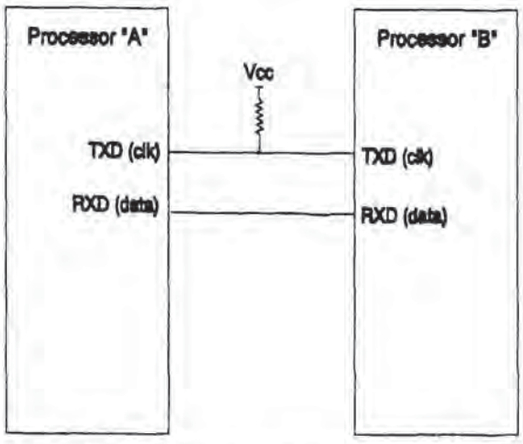


FIGURE 11.41 Synchronous serial communications example.

Shift Register Based I/O Expansion. A common application for synchronous serial transmission is shift register based I/O expansion as shown in Fig. 11.42. In this circuit, a 74HC164 8-bit serial-in/parallel-out shift register is used to provide eight parallel outputs with a single serial input. The 74HC165 8-bit parallel-in/serial out shift register shown provides a single serial input resulting from eight parallel input signals. This allows the system designer to

ENGR & MATH SCI LIBRARY

PETITIONER'S EXHIBIT 1002
US PATENT NO. 6,581,565

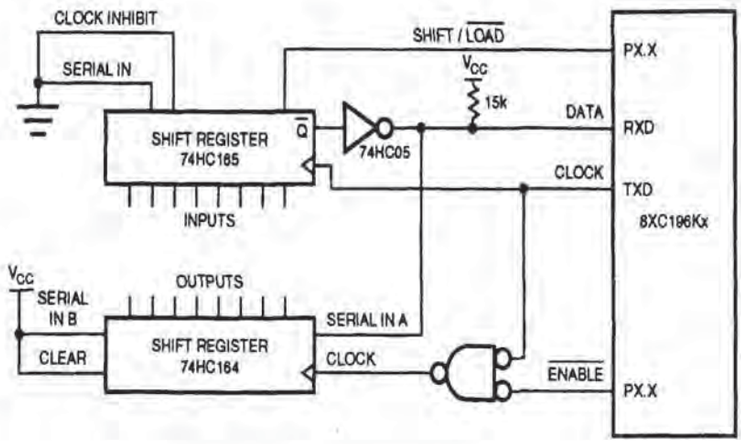


FIGURE 11.42 Shift register based I/O expansion example.

implement an additional 8-bit output port and additional 8-bit input port (16 signals total) using only four pins on the microcontroller. This expansion scheme allows a designer to achieve a greater number of I/O pins without having to upgrade to a microcontroller with a higher pin count.

To output data using this I/O expansion method, the user code simply writes a byte to the serial port transmit register to initiate data transfer. This causes the written byte to be shifted out of the microcontroller's RXD pin and into the 74HC164 one bit at a time. The data is reflected at the output pins of the 74HC164 as each bit is shifted in. For address/data bus emulation, another microcontroller pin may be utilized to indicate valid data to the intended receiving device.

To receive eight bits of data in parallel using this method, the user's code must latch the data on the 74HC165's input pins into its shift register by asserting the *shift/load* signal. After this is accomplished, the user's code simply needs to enable the serial port receive circuitry to receive the data one bit at a time into its receive buffer.

11.5.2 Asynchronous Serial Communications

The most common type of serial communications is asynchronous. As its name implies, asynchronous communication takes place between two devices without use of a clock line. Data is transmitted out the transmit buffer and received into the receive buffer independently at a speed determined by the baud rate generator. Most microcontrollers offer several modes of asynchronous serial communication.

Standard Asynchronous Mode. The standard asynchronous mode consists of 10 bits: a start bit, eight data bits (LSB first), and a stop bit, as shown in Fig. 11.43. After the user initiates a transmission, data is automatically transmitted from the TX pin at the specified baud rate.



FIGURE 11.43 Standard asynchronous mode data frame.

PETITIONER'S EXHIBIT 1002
US PATENT NO. 6,581,565

A parity function is also implemented, which provides for a simple method of error-detection. Data transmitted will consist of either an odd or even number of logical "1"s. If even parity is enabled, the parity bit will either be set to a "1" or a "0" to make the number of "1"s in the data byte even. If odd parity is enabled, the parity bit will be set to the appropriate value to make the number of "1"s in the data byte odd. For instance, consider the data byte 11010010b. If even parity is enabled, the parity bit will be set to a "0" since there is already an even number of "1"s. If odd parity were enabled, the parity bit would be set to a "1" since another "1" would be needed to provide an odd number of "1"s. If the parity function is enabled (usually through a serial port control register), the parity bit is sent instead of the eighth data bit and parity is checked on reception. The occurrence of parity errors is typically flagged in a serial port status register to alert the microcontroller to corrupted data in the receive register.

Multiprocessor Asynchronous Serial Communications Modes. Two other common serial communications modes which are used on automotive microcontrollers are the asynchronous 9th-bit recognition mode and the asynchronous 9th-bit mode. These two modes are commonly used together for multiprocessor communications where selective selection on a data link is required. Both modes are similar to the standard asynchronous mode with the exception of an additional ninth data bit in the data frame as shown in Fig. 11.44.

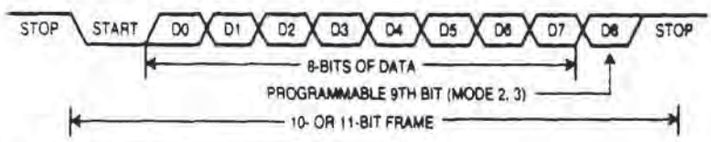


FIGURE 11.44 Asynchronous 9th-bit data frame.

The 9th-bit recognition mode consists of a start bit, nine data bits (LSB first), and a stop bit. For transmission, the ninth bit can be set to "1" by setting a corresponding bit in the serial port control register before writing to the transmit buffer. During reception, the receive interrupt bit is *not* set unless the ninth data bit being received is set to a logic "1".

The 9th-bit mode uses a data frame identical to that of the 9th-bit recognition mode. In this mode, a reception will always cause a receive interrupt, regardless of the state of the ninth data bit.

A multiprocessor data link is fairly simple to implement using these two modes. Microcontrollers within the system are connected as shown in Fig. 11.45. The master microcontroller is set to the 9th-bit recognition mode so that it is always interrupted by serial receptions. The slave microcontrollers are set to operate in the 9th-bit recognition mode so that they are interrupted on receptions only if the ninth data bit is set. Two types of data frames are used: address frames, which have the ninth bit set, and data frames, which have the ninth bit cleared. When the master processor wants to transmit a block of data to one of several slaves, it first sends out an address frame which identifies the target slave. Slaves in the 9th-bit recognition mode are not interrupted by a data frame, but an address frame interrupts all slaves. Each slave can examine the received byte and see if it is being addressed. The addressed slave then switches to the 9th-bit mode to receive data frames, while the slaves that were not addressed stay in the 9th-bit recognition mode and continue without interruption.

11.6 ANALOG-TO-DIGITAL CONVERTER

Analog-to-digital converter (A/D) peripherals allow automotive microcontrollers to sense and assign digital values to analog input voltages with considerable accuracy. An analog input

ENGR & MATH SCI LIBRARY

PETITIONER'S EXHIBIT 1002
US PATENT NO. 6,581,565

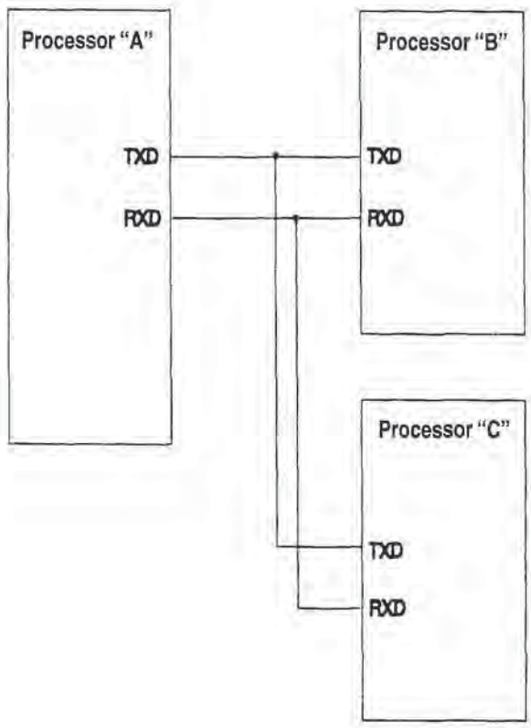


FIGURE 11.45 Asynchronous 9th-bit data frame.

may be defined as a voltage level that varies over a continuous range of values as opposed to the discrete values of digital signals.

11.6.1 Types of A/D Converters

The vast majority of A/D converters available on microcontrollers are of the successive approximation (S/A) type. Other types include flash A/D converters, in which conversions are completed in a parallel fashion and are performed at speeds measuring tens-of-nanoseconds. The drawback is that flash A/D converters require a great deal of die space when integrated on a microcontroller. It is because of their relatively large size that flash A/D converters are seldom offered on microcontrollers. Dual-slope A/D converters offer excellent A/D accuracy but typically take a relatively long period of time to complete a conversion. S/A A/D converters are very popular because they offer a compromise among accuracy, speed, and die-size requirements. The main drawback to successive approximation converters is that implementing the capacitor and resistor ladders takes a considerable amount of die space, although somewhat less than flash A/Ds. These converters are also somewhat susceptible to noise, although there are proven ways to reduce the effects of noise within a given application. The advantage of S/A converters is that they combine the best of other types of converters. They are relatively fast and do not take up excessive die space.

S/A converters typically consist of a resistor ladder, a sample capacitor, an input multiplexer, and a voltage comparator. A typical S/A converter is shown in Fig. 11.46. The resistor ladder is used to produce reference voltages for the input voltage comparison. A sample capacitor is utilized to capture the input voltage during a given period of time known as the sample time. Sample time can be defined as the amount of time that an A/D input voltage is applied to the sample capacitor.

PETITIONER'S EXHIBIT 1002
US PATENT NO. 6,581,565

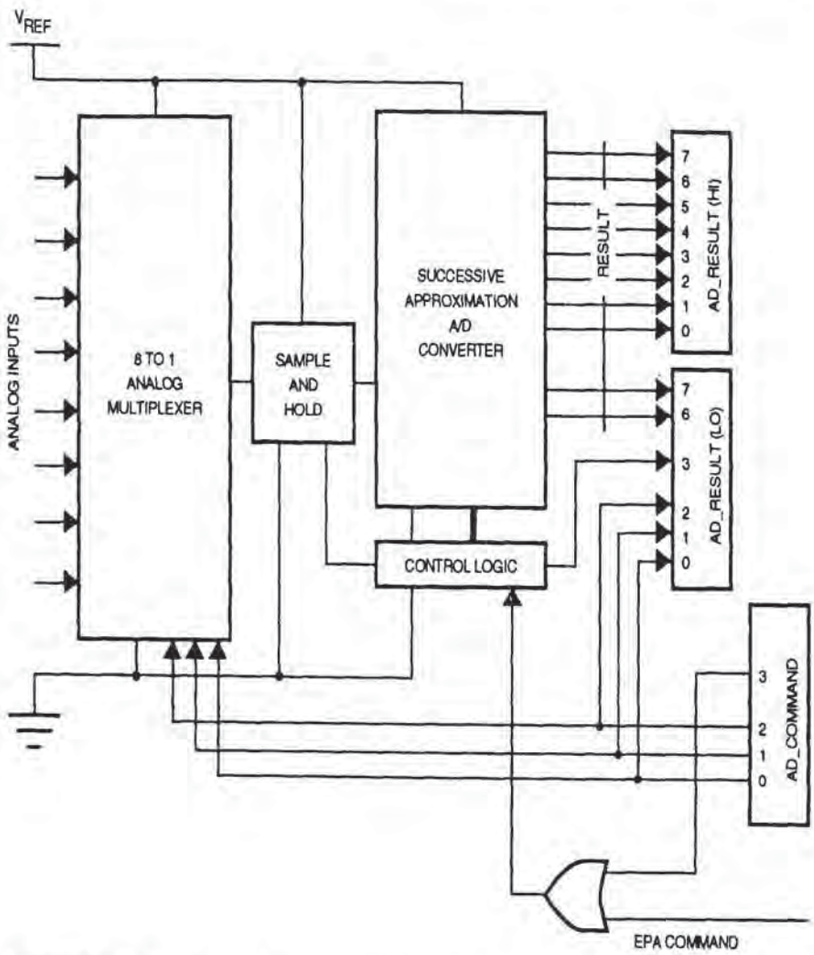


FIGURE 11.46 Typical successive approximation converter.

A successive approximation algorithm is used to perform the A/D conversion. A typical S/A converter consists of a 256-resistor ladder, a comparator, coupling capacitors, and a 10-bit successive approximation register (SAR), along with SFRs and logic to control the process. The resistor ladder provides 20-mV steps (with V_{ref} = 5.12 V), while capacitive coupling creates 5-mV steps within the 20-mV ladder voltages. Therefore, 1024 internal reference voltage levels are available for comparison against the analog input to generate a 10-bit conversion result. Eight-bit conversions use only the resistor ladder, providing 256 levels.

11.6.2 The A/D Conversion Process

The successive approximation conversion compares a reference voltage to the analog input voltage stored in the sampling capacitor. A binary search is performed for the reference voltage that most closely matches the input. The ½ full-scale reference voltage is the first tested. This corresponds to a 10-bit result in which the most significant bit is zero and all other bits are one (0111 1111 11b). If the analog input is less than the test voltage, bit 10 is left at zero and a new test voltage of ¼ full scale (0011 1111 11b) is tested. If this test voltage is less than the analog input voltage, bit 9 of the SAR is set and bit 8 is cleared for the next test (0101 1111

ENGR & MATH SCI LIBRARY UM-A

PETITIONER'S EXHIBIT 1002
US PATENT NO. 6,581,565

11b). This binary search continues until 8 or 10 tests have occurred, at which time the valid 8-bit or 10-bit result resides in the SAR where it can be read by software.

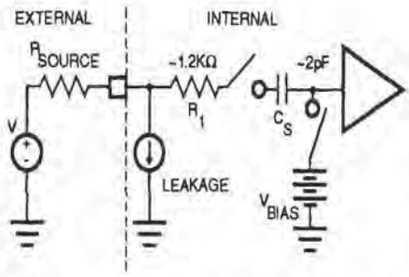


FIGURE 11.47 Idealized interface circuitry.

11.6.3 A/D Interfacing

The external interface circuitry to an analog input is highly dependent upon the application and can impact converter characteristics. Several important factors must be considered in the external interface design: input pin leakage, sample capacitor size, and multiplexer series resistance from the input pin to the sample capacitor. These factors are idealized in Fig. 11.47.

The following example is for a 1-μs sample time and a 10-bit conversion. The external input circuit must be able to charge a sample capacitor (C_S) through a series resistance (R_1) to an accurate voltage, given a dc leakage (I_L). For purposes of this example, assume C_S of 2 pf, R_1 of 1.2 kΩ, and I_L of 1 μA.

External circuits with source impedances of 1 kΩ or less can maintain an input voltage within a tolerance of about 0.2 LSB (1.0 kΩ × 1.0 μA = 1.0 mV) given the dc leakage. Source impedances above 5 kΩ can result in an external error of at least one LSB due to the voltage drop caused by the 1-μA leakage. In addition, source impedances above 25 kΩ may degrade converter accuracy because the internal sample capacitor will not charge completely during the sample time.

Typically, leakage is much lower than the maximum specification specified by the microcontroller manufacturer. Given typical leakage, source impedance may be increased substantially before a one-LSB error is apparent. However, a high source impedance may prevent the internal sample capacitor from fully charging during the sample window. This error can be calculated using the following formula:

$$\text{Error (LSBs)} = \left(e^{\frac{-T_{SAM}}{RC}} \right) \times 1024$$

where T_{SAM} = sample time, μs
$R = R_{SOURCE} + R_1$, Ω
$C = C_S$, μf

The effects of this error can be minimized by connecting an external capacitor C_{EXT} from the input pin to ANGND. The external signal will charge C_{EXT} to the source voltage. When the channel is sampled, a small portion of the charge stored in C_{EXT} will be transferred to the internal sample capacitor. The ratio of C_S to C_{EXT} causes the loss in accuracy. If C_{EXT} is .005 μf or greater, the maximum error will be –0.6 LSB.

Placing an external capacitor on each analog input also reduces the sensitivity to noise because the capacitor combines with series resistance in the external circuit to form a low-pass filter. In practice, one should include a small series resistance prior to the external capacitor on the analog input pin and choose the largest capacitor value practical, given the frequency of the signal being converted. This provides a low-pass filter on the input, while the resistor also limits input current during overvoltage conditions.

11.6.4 Analog References

To achieve maximum noise isolation, on-chip A/D converters typically separate the internal A/D power supply from the rest of the microcontroller's power supply lines. Separate supply

PETITIONER'S EXHIBIT 1002
US PATENT NO. 6,581,565

pins, V_{ref} and An_{gnd}, usually supply both the reference and digital voltages for the A/D converter. Keep in mind that V_{ref} and An_{gnd} are the reference for a large resistor ladder on successive approximation converters. Any variation in these supplies will directly affect the reference voltage taps within the ladder, which in turn directly affect A/D conversion accuracy.

If the on-chip A/D converter is not being used, or if accuracy is not a concern, the Vref and Angnd pins can simply be connected to V_{cc} and V_{ss}, respectively. However, since the reference supply levels strongly influence the absolute accuracy of the A/D converter, a precision, well-regulated reference should be used to supply V_{ref} to achieve the highest performance levels. It is also important to use bypass capacitors between V_{ref} and An_{gnd} to minimize any noise that may be present on these supplies. In noise-sensitive applications running at higher frequencies, the use of separate ground planes within the PCB (circuit board) should be considered, possibly as shown in Fig. 11.48. This will help minimize ground loops and provide for a stable A/D reference.

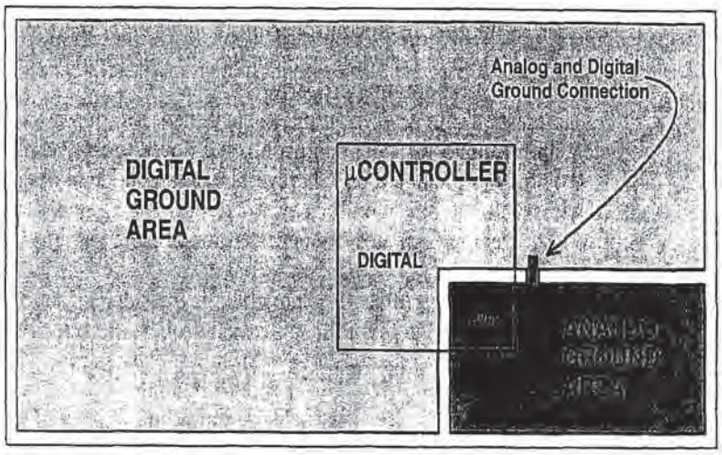


FIGURE 11.48 Example of separate analog and digital ground planes.

11.7 FAILSAFE METHODOLOGIES

The amount and complexity of automotive electronics incorporated into automobiles has increased at an incredible rate over the last decade. This trend has contributed significantly towards the impressive safety record of modern automobiles. Although microcontrollers are extremely reliable electronic devices, it is possible for failures to occur, either elsewhere in the module or within the microcontroller itself. It is critical that these failures be detected and responded to as quickly as possible in safety-related applications such as automotive antilock braking. If proper failsafe methodologies and good programming practices are followed, the chances of a failure going undetected are drastically reduced. The application of *failure mode and effect analysis* (FMEA) is an excellent tool for identifying potential failure modes, detection strategies, and containment methods. Used properly, FMEA will assist the designer in providing a high-quality, reliable automotive module. Although the scope of this chapter does not provide for a discussion on this topic, the author highly encourages the use of FMEA.

11.7.1 Hardware Failsafe Methods

Sometimes a hardware solution is required for detection of and response to certain failure modes. It is difficult for software alone to detect failures external to the device. As an example, consider a case in which electrical overstress (EOS) has damaged a port pin, causing it to

ENGR & MATH SCI LIBRARY UNLV

PETITIONER'S EXHIBIT 1002
US PATENT NO. 6,581,565

read or drive an incorrect value. In this case, it can be difficult for software to detect because it would base its response on an incorrect value read from a pin.

Watchdog Timers (WDTs). An on-chip hardware watchdog is an excellent method of detecting failures which otherwise may go undetected. An example of this would be a microcontroller fetching either erroneous address or data (due to noise, etc.) and becoming "lost." WDTs commonly utilize a dedicated 16-bit counter, which provides for a count of 2^{16}(65,536) clocked at a rate of one tick per state time. If users wish to take advantage of this feature, they simply write to a register to enable the count. Once enabled, the user program must periodically clear the watchdog by writing a specific bit pattern to the Watchdog SFR. Clearing the WDT at least every 4.1 ms (65,535 * 1 state time at 16 MHz) will prevent the device from being reset. The strategy is that if the WDT initiates a reset, the assumption can be made that a failure has occurred and the microcontroller has became lost.

External Failsafe Devices. It is common for systems to incorporate an external failsafe device, such as another microcontroller or an *application-specific integrated circuit* (ASIC). The function of a failsafe device is to monitor the operation of the primary microcontroller and determine if it is operating properly.

The simplest failsafe devices output a signal such as a square wave for the microcontroller to detect and respond to. If the microcontroller doesn't respond correctly, a reset is typically asserted by the failsafe and the ECU reverts to a safe mode of operation. More complex failsafe devices will actually monitor several critical functions for failures such as low Vcc, stopped or decreased oscillator frequency, shorted/opened input signals, and so forth.

Oscillator Failure Detection. It is possible for the clocking source (typically an oscillator) to fail for various reasons. Since most microcontrollers are static devices, a particularly difficult failure mode to detect is the clocking of the device at a reduced frequency. To detect this failure, an *oscillator failure detection* circuit is often integrated upon the microcontroller. This circuitry will detect if the oscillator clock input signal falls below a specified frequency, in which case an interrupt will be generated or the device will reset itself.

Redundancy/Cross-checking. A common failsafe methodology is achieved by designing a redundant, or backup, processor into the module. In this case, the secondary microcontroller usually executes a subset of the main microcontroller's code. The secondary microcontroller typically processes critical input data and performs cross-checks periodically with the main microcontroller to insure proper operation. A failsafe routine is initiated if data exchanged between the two devices did not correlate.

11.7.2 Software Failsafe Techniques

Failsafe methodologies implemented in software are ideal for detecting failure modes that can interfere with proper program flow. Examples of these types of failures include noise glitches, which are notorious for causing external memory systems to fetch invalid addresses. ROM/EPROM memory corruption could cause an ISR start address to be fetched from an invalid interrupt vector location. Interrupts occurring at a rate faster than anticipated can cause problems such as an overflowing stack. Fortunately, failure modes such as these can be dealt with by implementing software failsafe methods. It is simply good programming practice to anticipate these types of failure modes and provide a failsafe strategy to deal with them. Following are several software strategies commonly used to deal with specific types of failure modes:

Checksum. One possible error that must be accounted for is ROM/EPROM memory corruption. An effective method of detecting these types of failures is through the calculation of

PETITIONER'S EXHIBIT 1002
US PATENT NO. 6,581,565

a checksum during the initialization phase of a user's program. A checksum is the final value obtained as the result of performing some arithmetic operation upon every ROM/EPROM memory location. The obtained checksum is then compared against a stored checksum. If the two match, the ROM/EPROM contents are intact. An error routine is called if the two checksums do not match. The most common arithmetic operation used to perform a checksum is addition. The checksum is calculated by adding the contents of all memory locations. When the addition is performed, the carry is ignored which provides for a byte or word checksum. The final result is then used as the checksum.

Unused Interrupt Vectors. It is a rare occasion when all interrupt sources are enabled within an application. If, for some unforeseen reason, the program should vector to an unused interrupt source, some sort of failsafe routine should be implemented to respond to the failure. The failsafe routine could be as simple as vectoring to a reset instruction or it can be as complicated as the programmer wishes.

Unused Memory Locations. A strategy should be in place to detect if, for some unforeseen reason, the program sequence should begin to execute in an unused area of ROM/EPROM. It is uncommon for the user's code to fill the entire ROM/EPROM array of a microcontroller. It is good programming practice to fill any unused locations with the opcode of an instruction such as *Reset.* On the MCS-96 family, executing the opcode FFh (which happens to be the blank state of EPROM) will initiate a reset sequence. Other microcontroller families have similar instructions.

Unimplemented Opcode Interrupt Vectors. Microcontrollers often dedicate one or more interrupt vectors for failsafe purposes. An *unimplemented opcode* interrupt is designed to detect corrupted instruction fetches. The corresponding interrupt service routine is executed whenever an unsupported opcode is fetched for execution. The interrupt service routine contains the user's failsafe routine, which is tailored to address this failure for the specific application.

11.8 FUTURE TRENDS

There are several significant trends developing in automotive electronics as ECU manufacturers strive to meet the challenges of a demanding automotive electronics market. The challenges that are bringing about these trends are: decreasing cost targets, decreasing form-factor goals, increasing performance requirements, and increasing system-to-system communication requirements. As the most significant component of an ECU, microcontrollers are bearing the brunt of these demands. This section will discuss these challenges and provide some insight into some of the ways microcontroller manufacturers are addressing these trends.

11.8.1 Decreasing Cost Targets

Microcontroller manufacturers are aproaching cost reduction in two ways: indirectly and directly. *Indirect* cost reductions are achieved by integrating features onto the microcontroller which allow the system designer to reduce cost elsewhere in the system. The key to this approach being successful is in the microcontroller manufacturer's ability to integrate the feature cheaper than the cost of providing an external solution. Integration is not always the cheaper solution, therefore each feature must be evaluated individually to determine the feasability of integration. An example of an indirect cost reduction would be the integration of watchdog and failsafe functions onto the microcontroller. This would eliminate the need for external watchdog components and thus reduce cost.

ENGR & MATH SCI LIBRARY

PETITIONER'S EXHIBIT 1002
US PATENT NO. 6,581,565

Another example would be through the integration of communications protocols such as CAN (Controller Area Network) or J1850 onto the same piece of silicon as the microcontroller. This will reduce the system chip count (and thus cost) by at least one integrated circuit device (the CAN chip) and several interfacing components. In most cases, a reduced chip count will translate into a PCB size decrease and a cost savings.

By *directly* addressing decreasing cost targets, microcontroller manufacturers actually reduce the manufacturing cost of the microcontroller itself. An example of this would be utilizing smaller geometry processes for manufacturing. Process geometry refers to the transistor channel width that is implanted onto a piece of silicon for a given fabrication process. Smaller processes allow for a higher transistor density on an integrated circuit. Higher densities allow for smaller die sizes which relate to lower costs. Most automotive microcontrollers manufactured today are fabricated with a 1.0-micron, or larger, process. As technology advances, future automotive microcontrollers will be manufactured upon submicron processes, such as 0.6 micron.

11.8.2 Increasing Performance Requirements

Automotive applications, such as ABS and engine control, require the processing of a substantial amount of data within a limited period of time. Higher-performance microcontrollers are required as system complexity increases and new features, such as traction control and vehicle dynamics, are incorporated into the ECU.

Microcontroller performance can be directly related to speed. Therefore, a rather straightforward approach to increased performance is through increasing clock speed. Today, most automotive microcontrollers have the capability to operate at frequencies of 16 MHz with speeds up to 20 MHz becoming common. Future microcontrollers will have the ability to be operated at frequencies of 24 or even 32 MHz. This allows more code to be executed in the same amount of time, and thus improves performance.

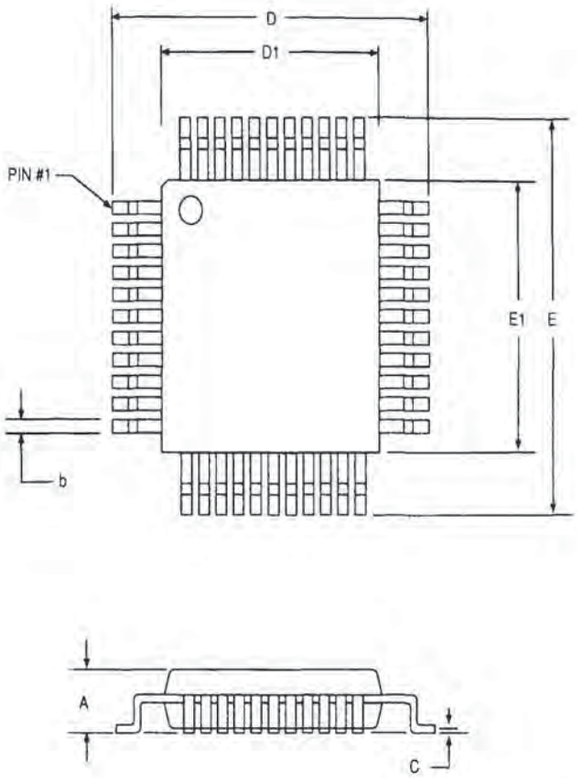
The method of increasing performance is not limited to just increasing the clock frequency. Microcontrollers can also achieve higher performance by enhancing existing peripherals for more efficient operation. This may be in the form of improved data handling or new features which suit the needs of a specific automotive application.

11.8.3 Increasing System-to-System Communication Requirements

The increasing complexity of automotive electronics requires that an increasing amount of information (diagnostics, etc.) be shared between various ECUs within an automobile. To fulfill this need, high-speed data links are utilized to transfer messages between multiple ECUs utilizing protocols such as Bosch's Controller Area Network (CAN) and SAE's J1850. To provide further size and cost savings, it is becoming more and more common to see these protocols supported or integrated onto automotive microcontrollers as opposed to separate integrated circuits.

The theory of centralized body computing is also receiving a closer look due to increased government regulations concerning fuel economy and diagnostics. A centralized body computer would link all ECUs (ABS and traction control, engine, transmission, suspension, instrumentation, etc.) together over a high-speed, in-vehicle serial network. One common scenario would have the central computer (possibly a microprocessor as opposed to a microcontroller) performing the more intense data-crunching tasks, while peripheral microcontrollers located in each individual ECU would perform system I/O functions. These communication protocols provide for efficient two-wire, high-speed serial communications between multiple ECUs utilizing protocols such as CAN and J1850. Supporting these protocols places additional loading upon the microcontroller. Increased microcontroller performance is necessary to manage this loading.

PETITIONER'S EXHIBIT 1002
US PATENT NO. 6,581,565



SHRINK QUAD FLATPACK				
SYMBOL	DESCRIPTION	MIN.	NOM.	MAX.
N	Lead Count		80	
A	Overall Height			1.66
A1	Stand Off	0.00		
b	Lead Width	0.14	0.20	0.26
c	Lead Thickness	0.117	0.127	0.177
D	Terminal Dimension	13.70	14.00	14.30
D1	Package Body		12.0	
E	Terminal Dimension	13.70	14.00	14.30
E1	Package Body		12.0	
e1	Lead Pitch	0.40	0.50	0.60
L1	Foot Length	0.35	0.50	0.70
T	Lead Angle	0.0°		10.0°
Y	Coplanarity			0.10

FIGURE 11.49 Shrink quad flat pack (SQFP) package.

ENGR & MATH SCI LIBRARY UCLA

PETITIONER'S EXHIBIT 1002
US PATENT NO. 6,581,565

11.8.4 Decreasing Form Factor Goals

Automobile manufacturers striving to build compact, more fuel efficient automobiles are putting pressure upon ECU suppliers to build smaller, lighter modules.

ECU size is directly affected by PCB size. The easiest way to achieve a smaller PCB is through integration and utilization of smaller integrated circuit packages. To support this demand, automotive microcontroller manufacturers are beginning to offer smaller, fine-pitch packages. A package commonly used today is the 68-lead plastic leaded chip carrier (PLCC) which has its pins placed on 1.27-mm centers and a body that is 24.3 mm^2. An example of a possible automotive package solution for the future would be the 80-lead shrink quad flat pack (SQFP, Fig. 11.49) which has pins on 0.50-mm centers and a body that is 12.0 mm^2. It is relatively easy to see that the SQFP package offers 12 additional pins in a package that is half the size of the PLCC. This high pin density, fine-pitch packaging allows for a smaller package to be utilized for the same size microcontroller die.

Another technology that is quickly becoming popular for automotive applications is referred to as *multichip modules* (MCMs). An MCM is a collection of unpackaged integrated circuit die (from various manufacturers) which are mounted upon a common substrate and packaged together. The advantage of MCMs is that they require much less PCB space than if the ICs were packaged separately.

GLOSSARY

Accumulator A register within a microcontroller that holds data, particularly data on which arithmetic or logic operations are to be performed.

Arithmetic logic unit (ALU) The part of a microcontroller that performs arithmetic and logic operations.

Analog-to-digital converter An electronic device that produces a digital result that is proportional to the analog input voltage.

Assembly language A low-level symbolic programming language closely resembling machine language.

Central processing unit (CPU) The portion of a computer system or microcontroller that controls the interpretation and execution of instructions and includes arithmetic capability.

EPROM Erasable and programmable read-only memory.

High-speed input/output unit (HSIO) A microcontroller peripheral which has the capability to either capture the time at which a certain input event occurs or create an output event at a predetermined time, both relative to a common clock. HSIO events are configured by the programmer to occur automatically.

Interrupt service routine (ISR) A predefined portion of a computer program which is executed in response to a specific event.

Low-speed input/output The input/output of a digital signal by "manually" reading or writing a register location in software.

Machine language A set of symbols, characters, or signs used to communicate with a computer in a form directly usable by the computer without translation.

Program counter (PC) A microcontroller register which holds the address of the next instruction to be executed.

PETITIONER'S EXHIBIT 1002
US PATENT NO. 6,581,565

Program status word (PSW) A microcontroller register that contains a set of boolean flags which are used to retain information regarding the state of the user's program.

Pulse-width modulation (PWM) The precise and timely creation of negative and positive waveform edges to achieve a waveform with a specific frequency and duty cycle.

Random access memory (RAM) A memory device which has both read and write capabilities so that the stored information (write) can be retrieved (reread) and be changed by applying new information to the inputs.

Read-only memory (ROM) A memory that can only be read and not written to. Data is either entered during the manufacturing process or by later programming; once entered, it is unalterable.

Register/arithmetic logic unit (RALU) A component of register-direct microcontroller architectures that allows the ALU to operate directly upon the entire register file.

Serial input/output (SIO) A method of digital communication in which a group of data bits is transferred one at a time, sequentially over a single data line.

Special function register (SFR) A microcontroller RAM register which has a specific, dedicated function assigned to it.

BIBLIOGRAPHY

ASM96 Assembler User's Manual, Intel Corp., 1992.

Automotive Electrics/Electronics, Robert Bosch GmbH, 1988.

Automotive Handbook, Intel Corporation, 1994.

Automotive Handbook, 2d ed., Robert Bosch GmbH, 1986.

Corell, Roger J., "How are semiconductor suppliers responding to the growing demand for automotive safety features?," *Intel Corp.,* 1993.

Davidson, Lee S., and Robert M. Kowalczyk, "Microcontroller technology enhancements to meet ever-increasing engine control requirements," Intel Corp., 1992.

Fink, Donald G., and Donald Christiansen, *Electronics Engineers' Handbook,* 3d ed. McGraw-Hill, 1989.

iC-96 Compiler User's Manual, Intel Corp., 1992.

Introduction to MOSFETS and EPROM Memories, Intel Corp., 1990.

MCS®-51 Microcontroller Family User's Manual, Intel Corp., 1993.

Millman, Jacob, and Arvin Grabel, *Microelectronics,* McGraw-Hill, 1987.

Packaging Handbook, Intel Corporation, 1994.

Ribbens, William B., *Understanding Automotive Electronics,* Howard Sams Company, Carmel, Ind. 1992.

8XC196Kx User's Manual, Intel Corporation, 1992.

8XC196KC/8XC196KD User's Manual, Intel Corp., 1992.

ABOUT THE AUTHOR

David S. Boehmer is currently a senior technical marketing engineer for the Automotive Operation of Intel's Embedded Microprocessor Division located in Chandler, Ariz. He is a member of SAE.

ENGR & MATH SCI LIBRARY

PETITIONER'S EXHIBIT 1002
US PATENT NO. 6,581,565

PETITIONER'S EXHIBIT 1002
US PATENT NO. 6,581,565

CHAPTER 12
ENGINE CONTROL

Gary C. Hirschlieb, Gottfried Schiller, and Shari Stottler
Robert Bosch GmbH

ENGR & MATH SCI LIBRARY

12.1 OBJECTIVES OF ELECTRONIC ENGINE CONTROL SYSTEMS

The electronic engine control system consists of sensing devices which continuously measure the operating conditions of the engine, an electronic control unit (ECU) which evaluates the sensor inputs using data tables and calculations and determines the output to the actuating devices, and actuating devices which are commanded by the ECU to perform an action in response to the sensor inputs.

The motive for using an electronic engine control system is to provide the needed accuracy and adaptability in order to minimize exhaust emissions and fuel consumption, provide optimal driveability for all operating conditions, minimize evaporative emissions, and provide system diagnosis when malfunctions occur.

In order for the control system to meet these objectives, considerable development time is required for each engine and vehicle application. A substantial amount of development must occur with an engine installed on an engine dynamometer under controlled conditions. Information gathered is used to develop the ECU data tables. A considerable amount of development effort is also required with the engine installed in the vehicle. Final determination of the data tables occurs during vehicle testing.

12.1.1 Exhaust Emissions

Exhaust Components. The engine exhaust consists of products from the combustion of the air and fuel mixture. Fuel is a mixture of chemical compounds, termed hydrocarbons (HC). The various fuel compounds are a combination of hydrogen and carbon. Under perfect combustion conditions, the hydrocarbons would combine in a thermal reaction with the oxygen in the air to form carbon dioxide (CO_2) and water (H_2O). Unfortunately, perfect combustion does not occur and in addition to CO_2 and H_2O, carbon monoxide (CO), oxides of nitrogen (NO_x), and hydrocarbons (HC) occur in the exhaust as a result of the combustion reaction. Additives and impurities in the fuel also contribute minute quantities of pollutants such as lead oxides, lead halogenides, and sulfur oxides. In compression ignition (diesel) engines, there is also an appreciable amount of soot (particulates) created. Federal statues regulate the allowable amount of HC, NO_x, and CO emitted in a vehicle's exhaust. On diesel engines, the amount of particulates emitted is also regulated.

PETITIONER'S EXHIBIT 1002
US PATENT NO. 6,581,565

Spark Ignition Engines

Air/fuel Ratio. The greatest effect on the combustion process, and therefore on the exhaust emissions, is the mass ratio of air to fuel. The air/fuel mixture ratio must lie within a certain range for optimal ignition and combustion. For a spark ignition engine, the mass ratio for complete fuel combustion is 14.7:1; i.e., 14.7 kg of air to 1 kg of fuel. This ratio is known as the stoichiometric ratio. In terms of volume, approximately 10,000 liters of air would be required for 1 liter of fuel. The air/fuel ratio is often described in terms of the excess-air factor known as lambda (λ). Lambda indicates the deviation of the actual air/fuel ratio from the theoretically required ratio:

$$\lambda = \frac{\text{quantity of air supplied}}{\text{theoretical requirement (14.7 for gasoline)}}$$

At stoichiometry: $\lambda = 1$
For a mixture with excess air (lean): $\lambda > 1$
For a mixture with deficient air (rich): $\lambda < 1$

Effect of Air/Fuel Ratio on Emissions

CO emissions. In the rich operating range ($\lambda < 1$), CO emissions increase almost linearly with an increasing amount of fuel. In the lean range ($\lambda > 1$), CO emissions are at their lowest. With an engine operating at ($\lambda = 1$), the CO emissions can be influenced by the cylinder distribution. If some cylinders are operating rich and others lean with the summation achieving $\lambda = 1$, the average CO emissions will be higher than if all cylinders were operating at $\lambda = 1$.

HC emissions. As with CO emissions, HC emissions increase with an increasing amount of fuel. The minimum HC emissions occur at $\lambda = 1.1 \ldots 1.2$. At very lean air/fuel ratios, the HC emissions again increase due to less than optimal combustion conditions resulting in unburned fuel.

NO_x emissions. The effect of the air/fuel ratio on NO_x emissions is the opposite of HC and CO on the rich side of stoichiometry. As the air content increases, the oxygen content increases and the result is more NO_x. On the lean side of stoichiometry, NO_x emissions decrease with increasing air because the decreasing density lowers the combustion chamber temperature. The maximum NO_x emissions occur at $\lambda = 1.05 \ldots 1.1$.

Catalytic Converters. To reduce the exhaust gas emission concentration, a catalytic converter is installed in the exhaust system. Chemical reactions occur in the converter that transform the exhaust emissions to less harmful chemical compounds. The most commonly used converter for a spark ignition engine is the three-way converter (TWC). As the name implies, it simultaneously reduces the concentration of all three regulated exhaust gases: HC, CO, and NO_x. The catalyst promotes reactions that oxidize HC and CO, converting them into CO_2 and H_2O, while reducing NO_x emissions into N_2. The actual chemical reactions that occur are:

$$2CO + O_2 \rightarrow 2CO_2$$

$$2C_2H_6 + 7O_2 \rightarrow 4CO_2 + 6H_20$$

$$2NO + 2CO \rightarrow N_2 + 2CO_2$$

In order for the catalytic converter to operate at the highest efficiency for conversion for all three gases (HC, CO, NO_x), the average air/fuel ratio must be maintained within less than 1 percent of stoichiometry. This small operating range is known as the *lambda window* or *catalytic converter window.* Figure 12.1 is a graph of lambda (λ) versus the exhaust emissions both before and after the catalytic converter. Up to 90 percent of the exhaust gases are converted to less harmful compounds by the catalytic converter.

PETITIONER'S EXHIBIT 1002
US PATENT NO. 6,581,565

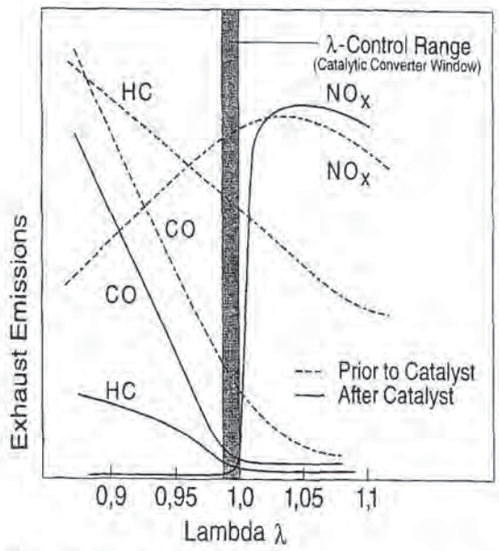


FIGURE 12.1 Lambda effect on exhaust emissions prior to and after catalyst treatment.

To remain within the catalytic converter window, the air/fuel ratio is controlled by the lambda closed-loop fuel control system, which is part of the electronic engine control system. The key component in this system is the lambda sensor. This sensor is installed in the exhaust system upstream of the catalytic converter and responds to the oxygen content in the exhaust gas. The oxygen content is a measure of the excess air (or deficiency of air) in the exhaust gases. A detailed discussion of the lambda closed-loop control system occurs in Sec. 12.2.1.

Ignition Timing. The ignition timing is defined as the crankshaft angle before top dead center (TDC) at which the ignition spark occurs. The ignition timing of the air/fuel mixture has a decisive influence on the exhaust emissions.

Effect of ignition timing on exhaust emissions.

- CO emissions are almost completely independent of the ignition timing and are primarily a function of the air/fuel ratio.
- In general, the more the ignition is advanced, the higher the emissions of HCs. Reactions initiated in the combustion chamber continue to occur after the exhaust valve opens, which depletes the remaining HCs. With advanced timing due to lower exhaust temperatures, these postreactions do not readily occur.
- With increased timing advance, the combustion chamber temperatures increase. The temperature increase causes an increase in NO_x emissions regardless of air/fuel ratio.

To provide the optimal ignition timing for exhaust emissions, precise control of the ignition timing is required. It is imperative that the ignition timing be coordinated with the air/fuel ratio since they have a combined effect on exhaust emissions as well as fuel consumption and driveability. Ignition timing is generally controlled by the ECU. Ignition timing control is discussed in detail in Sec. 12.2.1.

Exhaust Gas Recirculation (EGR). Exhaust gas recirculation (EGR) is a method of reducing emissions of oxides of nitrogen. A portion of the exhaust gas is recirculated back to the combustion chamber. Exhaust gas is an inert gas and, in the combustion chamber, it lowers the peak combustion temperature. Depending on the amount of EGR, NO_x emissions can be reduced by up to 60 percent, although an increase in HC emissions would occur at such high levels of EGR.

Some internal EGR occurs due to the overlap of the exhaust and intake valves. Additional quantities are supplied by a separate system linking the exhaust manifold to the intake mani-

ENGR & MATH SCI LIBRARY

PETITIONER'S EXHIBIT 1002
US PATENT NO. 6,581,565

fold. The quantity of EGR flow to the intake system is metered by a pneumatic or electronic valve. The EGR valve is controlled by the ECU. The maximum flow of EGR is limited by an increase in HC emissions, fuel consumption, and engine roughness. EGR control is discussed in detail in Sec. 12.2.1.

Compression Ignition (Diesel) Engines. There are some key distinctions between an SI engine and a CI engine. The CI engine uses high pressure and temperature instead of a spark to ignite the combustible air/fuel mixture. To achieve this, the CI engine compression ratio is in the range of 21:1, as opposed to roughly 10:1 for an SI engine. In a CI engine, the fuel is injected directly into the cylinder near the top of the compression stroke. Mixing of the fuel and air, therefore, occurs directly in the cylinder.

Air/fuel ratio. Diesel engines always operate with excess air ($\lambda > 1$). Where:

$$\lambda = \frac{\text{quantity of air supplied}}{\text{theoretical requirement}}$$

The excess air ($\lambda = 1.1 \ldots 1.2$) reduces the amount of soot (particulates), HC, and CO emissions.

Catalytic Converters. An oxidizing catalyst is used that converts CO and HC to CO_2 and H_2O. The NO_x reduction that occurs for an SI engine three-way catalyst (TWC) is not possible with a diesel because the diesel operates with excess air. The optimal conversion of NO_x requires a stoichiometric ratio ($\lambda = 1$) or a deficiency of air ($\lambda < 1$).

Injection Timing. In a compression ignition engine, the start of combustion is determined by the start of fuel injection. In general, retarding the injection timing decreases NO_x emissions, while overretarding results in an increase in HC emissions. A 1° (crankshaft angle) deviation in injection timing can increase NO_x emissions by 5 percent and HC emissions by as much as 15 percent. Precise control of injection timing is critical. Injection timing on some systems is controlled by the ECU. Feedback on injection timing can be provided by a sensor installed on the injector nozzle. Further discussion on injection timing occurs in Sec. 12.3.1.

Exhaust Gas Recirculation (EGR). As with an SI engine, exhaust gas can be recirculated to the combustion chamber to significantly reduce NO_x emissions. The quantity of EGR allowed to enter the intake is metered by the EGR valve. If the quantity is too high, HC emissions, CO emissions, and soot (particulates) increase as a result of an insufficient quantity of air. The EGR valve is controlled by the ECU, which determines how much EGR is tolerable under the current engine operating conditions.

12.1.2 Fuel Consumption

Federal statutes are currently in effect that require each automobile manufacturer to achieve a certain average fuel economy for all their models produced in one model year. The requirement is known as *corporate average fuel economy* or CAFE. The fuel economy for each vehicle type is determined during the federal test procedure, the same as for exhaust emissions determination, conducted on a chassis dynamometer. Because of the CAFE requirement, it is critical that fuel consumption be minimized for every vehicle type produced.

The electronic engine control system provides the fuel metering and ignition timing precision required to minimize fuel consumption. Optimum fuel economy occurs near $\lambda = 1.1$. However, as discussed previously, lean engine operation affects exhaust emissions and NO_x is at its maximum at $\lambda = 1.1$.

During coasting and braking, fuel consumption can be further reduced by shutting off the fuel until the engine speed decreases to slightly higher than the set idle speed. The ECU determines when fuel shutoff can occur by evaluating the throttle position, engine RPM, and vehicle speed.

The influence of ignition timing on fuel consumption is the opposite of its influence on exhaust emissions. As the air/fuel mixture becomes leaner, the ignition timing must be advanced to compensate for a slower combustion speed. However, as discussed previously,

PETITIONER'S EXHIBIT 1002
US PATENT NO. 6,581,565

advancing the ignition timing increases the emissions of HC and NO_x. A sophisticated ignition control strategy permitting optimization of the ignition at each operating point is necessary to reach the compromise between fuel consumption and exhaust emissions. The electronic engine control system can provide this sophisticated strategy.

12.1.3 Driveability

Another requirement of the electronic engine control system is to provide acceptable driveability under all operating conditions. No stalls, hesitations, or other objectionable roughness should occur during vehicle operation. Driveability is influenced by almost every operation of the engine control system and, unlike exhaust emissions or fuel economy, is not easily measured. A significant contribution to driveability is determined by the fuel metering and ignition timing. When determining the best fuel and ignition compromises for fuel consumption and exhaust emissions, it is important to evaluate the driveability. Other factors that influence driveability are the idle speed control, EGR control, and evaporative emissions control.

12.1.4 Evaporative Emissions

Hydrocarbon (HC) emissions in the form of fuel vapors escaping from the vehicle are closely regulated by federal statutes. The prime source of these emissions is the fuel tank. Due to ambient heating of the fuel and the return of unused hot fuel from the engine, fuel vapor is generated in the tank. The evaporative emissions control system (EECS) is used to control the evaporative HC emissions. The fuel vapors are routed to the intake manifold via the EECS and they are burned in the combustion process. The quantity of fuel vapors delivered to the intake manifold must be metered such that exhaust emissions and driveability are not adversely affected. The metering is provided by a purge control valve whose function is controlled by the ECU. Further discussion on the operation of the evaporative emissions control system occurs in Sec. 12.2.1.

12.1.5 System Diagnostics

The purpose of system diagnostics is to provide a warning to the driver when the control system determines a malfunction of a component or system and to assist the service technician in identifying and correcting the failure (see Chap. 22). To the driver, the engine may appear to be operating correctly, but excessive amounts of pollutants may be emitted. The ECU determines a malfunction has occurred when a sensor signal received during normal engine operation or during a system test indicates there is a problem. For critical operations such as fuel metering and ignition control, if a required sensor input is faulty, a substitute value may be used by the ECU so that the engine will continue to operate.

When a failure occurs, the malfunction indicator light (MIL), visible to the driver, is illuminated. Information on the failure is stored in the ECU. A service technician can retrieve the information on the failure from the ECU and correct the problem. Detailed examples of system diagnostics are discussed in Sec. 12.2.3.

12.2 SPARK IGNITION ENGINES

12.2.1 Engine Control Functions

Fuel Control. For the purpose of discussing fuel control strategies, a multipoint pulsed fuel injection system is assumed. Additional discussions of fuel control for different types of fuel

ENGR & MATH SCI LIBRARY

PETITIONER'S EXHIBIT 1002
US PATENT NO. 6,581,565

systems such as carbureters, single-point injection, and multipoint continuous injection appear in Sec. 12.2.4 (Fuel Delivery Systems).

In order for the fuel metering system to provide the appropriate amount of fuel for the engine operating conditions, the mass flow rate of incoming air, known as the air charge, must be determined.

$$F_m = \frac{A_m}{\text{requested air-fuel ratio}}$$

where F_m = fuel mass flow rate
A_m = air mass flow rate

The air mass flow rate can be calculated from:

$$A_m = A_v A_d$$

where A_v = volume flow rate of intake air
A_d = air density

There are three methods commonly used for determining the air charge: speed density, air flow measurement, and air mass measurement. In the speed density method, the air charge is calculated by the engine electronic control unit based on the measurement of air inlet temperature, intake manifold pressure, and engine RPM. The temperature and pressure are used to determine the air density and the RPM is used to determine the volume flow rate. The engine acts as an air pump during the intake stroke. The calculated volume flow rate can be determined as follows:

$$A_{\text{RPM}} = \frac{\text{RPM}}{60} \times \frac{D}{2} \times V_{\text{E}}$$

where RPM = engine speed
D = engine displacement
V_{E} = volumetric efficiency

In an engine using exhaust gas recirculation (EGR), the volume flow rate of EGR must be subtracted from the calculated volume flow rate.

$$A_v = A_{\text{RPM}} - A_{\text{EGR}}$$

The volume flow rate of EGR can be determined empirically based on the EGR valve flow rate and the EGR control strategy being used.

In the air flow measurement method, the air flow is measured using a vane type meter and air density changes are compensated for by an air inlet temperature sensor. The vane meter uses the force of the incoming air to move a flap through a defined angle. This angular movement is converted by a potentiometer to a voltage ratio. Because only the fresh air charge is measured, no compensation is required for EGR.

In the air mass measurement method, the air charge is measured directly using a hot-wire or hot-film air mass flow sensor. The inlet air passes a heated element, either wire or film. The element is part of a bridge circuit that keeps the element at a constant temperature above the inlet air temperature. By measuring the heating current required by the bridge circuit and converting this to a voltage via a resistor, the air mass flow passing the element can be determined. Again, because only the fresh air charge is measured, no compensation for EGR is required. However, sensing errors may occur due to strong intake manifold reversion pulses, which occur under certain operating conditions. In such cases, a correction factor must be determined and applied.

PETITIONER'S EXHIBIT 1002
US PATENT NO. 6,581,565

Calculation of Injector Pulse Width. The base pulse width is determined from the required fuel mass flow rate (F_m) and an empirical injector constant. The injector constant is determined by the design of the injector and is a function of the energized time versus the flow volume. This constant is normally determined with a constant differential pressure across the injector (from fuel rail to intake manifold). When the pressure across the injector does not remain constant (i.e., there is no pressure regulator intake manifold vacuum reference), an entire map of injector constants for different manifold pressures may be required.

The effective injector pulse width is a modification of the base pulse width. The base pulse width is adjusted by a number of correction factors depending on operating conditions. For example, a battery voltage correction is required to compensate for the electromechanical characteristics of the fuel injectors. Injector opening and closing rates differ depending on the voltage applied to the injector, which affects the amount of fuel injected for a given pulse width. Other common correction factors may include hot restart, cold operation, and transient operation corrections. Figure 12.2 is a flowchart of a typical injector effective pulse-width calculation method.

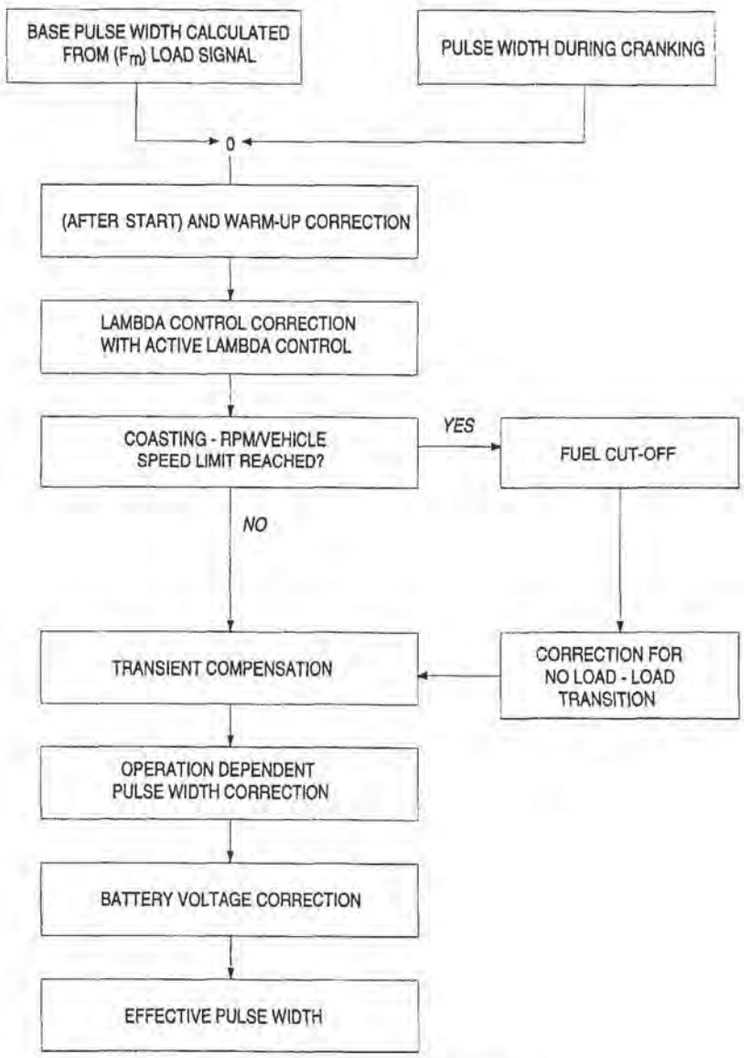


FIGURE 12.2 Determination of effective injector pulse width.

ENGR & MATH SCI LIBRARY UNLV

PETITIONER'S EXHIBIT 1002
US PATENT NO. 6,581,565

Injection Strategies. There are three commonly used fuel injection strategies for multipoint fuel metering systems: simultaneous injection, group injection, and sequential injection. Figure 12.3 is a diagram of the different strategies. Some engines use simultaneous injection during crank and switch over to sequential after the engine is running. This allows for shorter starting times since no synchronization with the camshaft is necessary before fuel injection begins. A description of each strategy follows.

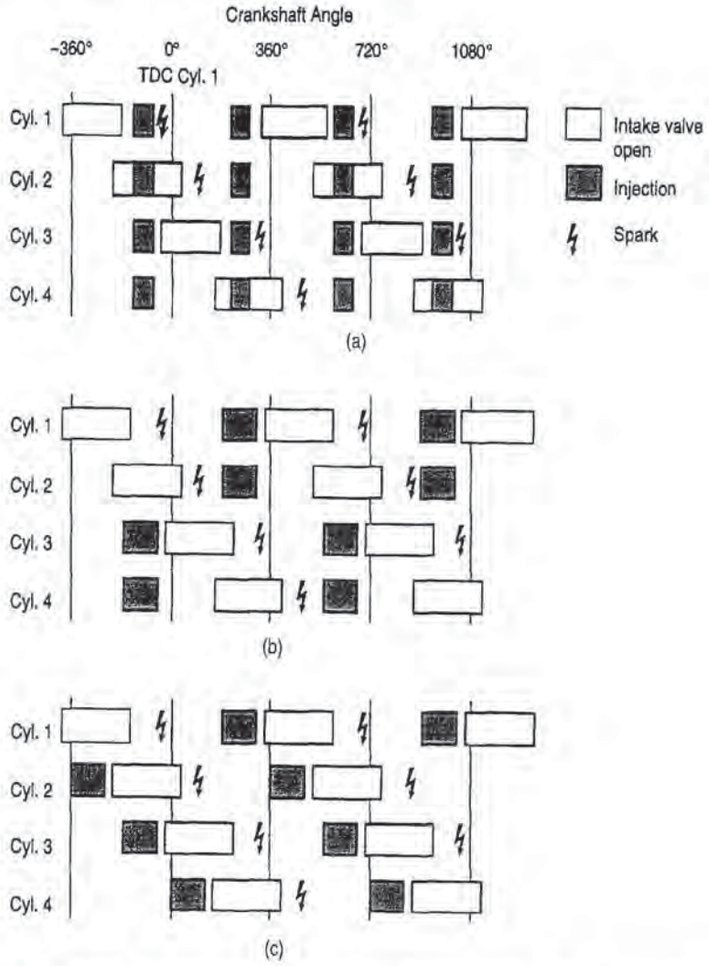


FIGURE 12.3 Fuel injection strategies: (*a*) simultaneous injection, (*b*) group injection, and (*c*) sequential injection.

Simultaneous injection. Injection of fuel occurs at the same time for all cylinders every revolution of the crankshaft. Therefore, fuel is injected twice within each four-stroke cycle. The injection timing is fixed with respect to crank/camshaft position.

Group injection. The injectors are divided into two groups that are controlled separately. Each group injects once per four-stroke cycle. The offset between the groups is one crankshaft revolution. This arrangement allows for injection timing selection that eliminates spraying fuel into an open intake valve.

Sequential injection. Each injector is controlled separately. Injection timing, both with reference to crank/camshaft position and pulse width, can be optimized for each individual cylinder.

PETITIONER'S EXHIBIT 1002
US PATENT NO. 6,581,565

Lambda Control. A subsystem of the fuel control system is lambda closed-loop control. Lambda (λ) is defined as the excess-air factor that indicates the deviation of the actual air/fuel ratio from the theoretically required ratio:

$$\lambda = \frac{\text{quantity of air supplied}}{\text{theoretical requirement (14.7 for gasoline)}}$$

The lambda sensor, or exhaust gas oxygen sensor, is installed in the engine exhaust stream upstream of the catalytic converter. The sensor responds to the oxygen content of the exhaust gas. The signal from the lambda sensor serves as feedback to the fuel control system. This provides the fine-tuning needed to remain within the limited catalytic converter window for optimal catalyst performance. (See Sec. 12.1.1 for more discussion on the catalytic converter window.) For a lean mixture ($\lambda > 1$), sensor voltage is approximately 100 mV. For a rich mixture ($\lambda < 1$), the sensor voltage is approximately 800 mV. At roughly $\lambda = 1$ (a stoichiometric mixture), the sensor switches rapidly between the two voltages. The input from the lambda sensor is used to modify the base pulse width to achieve $\lambda = 1$.

Lambda closed-loop control requires an operationally ready lambda sensor, typically one which has reached an operating temperature threshold. Sensor output is monitored by the ECU to determine when the sensor is supplying usable information. An active sensor signal, along with other requirements, such as engine temperature, must be achieved before lambda closed-loop control will be activated.

Under steady state conditions, the lambda control system oscillates between rich and lean around the lambda window. As the lambda sensor switches, the injector pulse width is adjusted by the amount determined by a control factor until the lambda sensor switches again to the opposite condition. The control factor can be defined as the allowable increase or decrease in the commanded fuel injector pulse width. The frequency of oscillation is determined by the gas transport time and the magnitude of the control factor. The gas transport time is defined as the time from air/fuel mixture formation to lambda sensor measurement.

Under transient conditions, the gas transport time results in a delay before the lambda sensor can indicate that the operating conditions have changed. Using only the lambda sensor for closed-loop fuel control would result in poor driveability and exhaust emissions because of this delay. Therefore, the engine control unit uses an anticipatory control strategy that uses engine load and RPM to determine the approximate fuel requirement. The engine load information is provided by the manifold pressure sensor for speed density systems and by the air meter for air flow and air mass measurement systems and by the throttle valve position sensor. The engine control unit contains data tables for combinations of load and RPM. This allows for rapid response to changes in operating conditions. The lambda sensor still provides the feedback correction for each load/RPM point. The data used for these data tables are largely developed from system modeling and engine development testing.

Due to production variations in engines, variations in fuel and changes due to wear and aging, the control system must be able to adapt to function properly for every engine over the engine's life. Therefore, the electronic control unit has a feature for adapting changes in the fuel required for the load/RPM points. At each load/RPM point, the lambda sensor continuously provides information that allows the system to adjust the fuel to the commanded A/F ratio. The corrected information is stored in RAM (random access memory) so that the next time the engine reaches that operating point (load/RPM), the anticipatory value will require less correction. These values remain stored in the electronic control unit even after the engine is shut off. Only if power to the electronic control unit is disrupted (i.e., due to a dead battery), will the correction be lost. In that case, the electronic control unit will revert back to the original production values that are written in ROM (read-only memory).

Lambda sensors do not switch symmetrically from lean to rich and rich to lean. Because of this, the control strategy is modified to account for the asymmetry. This can be accomplished either by delaying the modification by the control factor after the sensor switches or by using control factors of different magnitudes for rich-to-lean and lean-to-rich switching.

ENGR & MATH SCI LIBRARY

PETITIONER'S EXHIBIT 1002
US PATENT NO. 6,581,565

Ignition Timing Control. The goal of the engine control system for ignition timing is to provide spark advance which optimizes engine torque, exhaust emissions, fuel economy, and driveability, and which minimizes engine knock. Data tables with the base ignition timing, depending on engine load and RPM, are stored in ROM in the electronic control unit. The values in these tables are optimized for fuel economy, exhaust emissions, and engine torque. They are developed through engine experimentation, usually with an engine dynamometer. Corrections to the base timing values are needed for temperature effects, EGR, hot restart, barometric pressure, and engine knock. In addition, some systems use ignition timing to vary the engine torque for improvement in automatic transmission shift quality or for idle speed control. Figure 12.4 is a flowchart of a typical ignition timing calculation method.

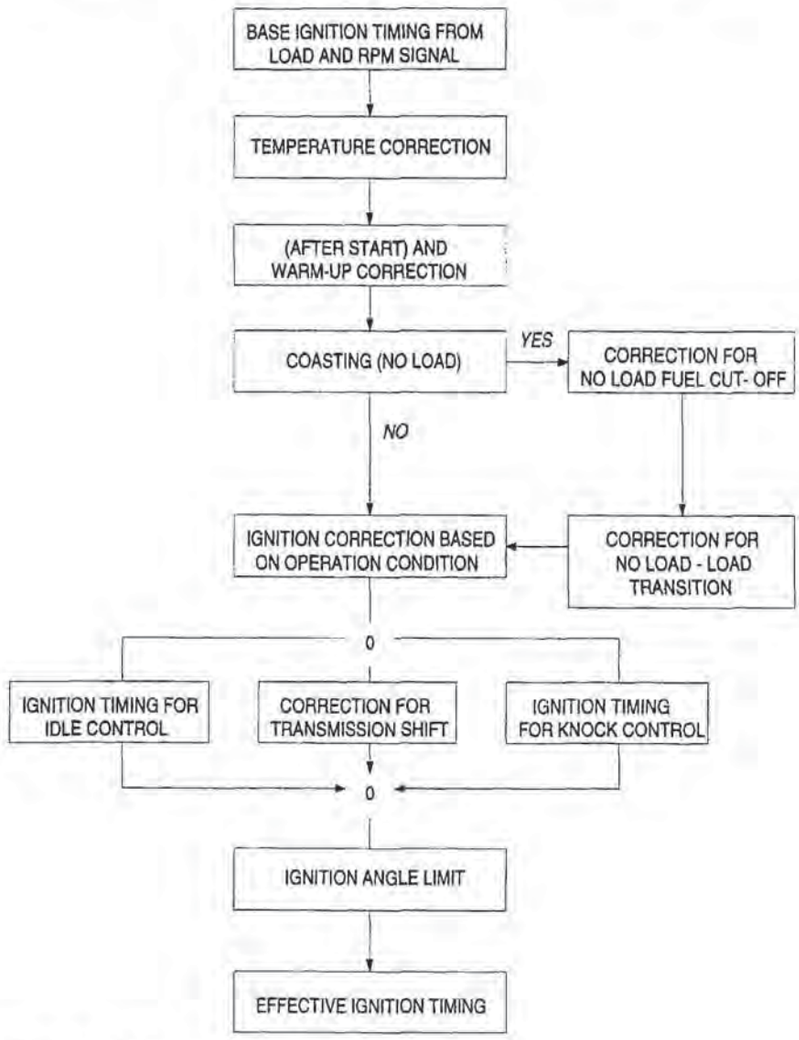


FIGURE 12.4 Determination of effective ignition timing.

Dwell Angle Control. The dwell angle performance map stored in the electronic control unit controls the charging time of the ignition coil, depending on RPM and battery voltage. The dwell angle is controlled so that the desired primary current is reached at the end of the charging time just prior to the ignition point. This assures the necessary primary current, even with quick transients in RPM. A limit on the charge time in the upper RPM ranges allows for the necessary spark duration.

PETITIONER'S EXHIBIT 1002
US PATENT NO. 6,581,565

Knock Control. The ignition timing for optimization of torque, fuel economy, and exhaust emissions is in close proximity to the ignition timing that results in engine knock. Engine knock occurs when the ignition timing is advanced too far for the engine operating conditions and causes uncontrolled combustion that can lead to engine damage, depending on the severity and frequency. If a factor of safety was used when developing the base timing map for all conditions that contribute to knock, such as fuel quality and variations in compression ratio, the ignition timing would be significantly retarded from the optimum level, resulting in a significant loss in torque and fuel economy. To avoid this, a knock sensor (one or more) is installed on the engine to detect knocking (see Chap. 8). Knock sensors are usually acceleration sensors that provide an electric signal to the electronic control unit. From this signal, the engine control unit algorithm determines which cylinder or cylinders are knocking. Ignition timing is modified (retarded) for those cylinders until the knock is no longer detected. The ignition timing is then advanced again until knock is detected. (See Fig. 12.5.) Information on the amount of spark retard required to eliminate the knock for each cylinder under each load/RPM condition is saved in the electronic control unit RAM. This allows for quick access to the appropriate "learned" ignition timing for each condition. With this control system, the base timing can be more advanced for improved fuel economy and torque.

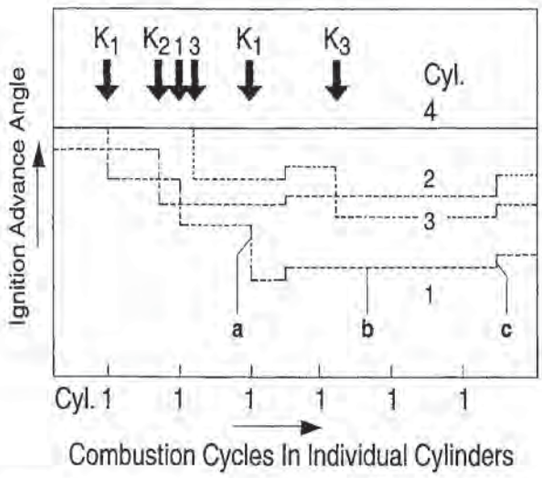


FIGURE 12.5 Knock control. Control algorithm for ignition adjustments for a four-cylinder engine. $K_{1\ldots3}$ (knock in cylinders 1 . . . 3), cylinder number four (no knock), (*a*) (ignition retard), (*b*) (delay before return to original point, (*c*) (spark advance).

Evaporative Emissions Control. Hydrocarbon (HC) emissions in the form of fuel vapors escaping from the vehicle, primarily from the fuel tank, are closely regulated by federal statutes. There are two principal causes of fuel vapor in the fuel tank: increasing ambient temperature and return of unused hot fuel from the engine. In order to control the release of these emissions to the atmosphere, the evaporative emissions control system was developed.

Evaporative Emissions Control System. A vapor ventilation line exits the fuel tank and enters the fuel vapor canister. The canister consists of an active charcoal element which absorbs the vapor and allows only air to escape to the atmosphere. Only a certain volume of fuel vapor can be contained by the canister. The vapors in the canister must therefore be purged from and burned by the engine so that the canister can continue to store vapors as they are generated. To accomplish this, another line leads from the charcoal canister to the intake manifold. Included in this line is the canister purge solenoid valve. Figure 12.6 shows a layout of a typical evaporative emissions control system.

During engine operation, vacuum in the intake manifold causes flow through the charcoal canister because the canister vent opening, at the charcoal filter end, is at atmospheric pres-

ENGR & MATH SCI LIBRARY

PETITIONER'S EXHIBIT 1002
US PATENT NO. 6,581,565

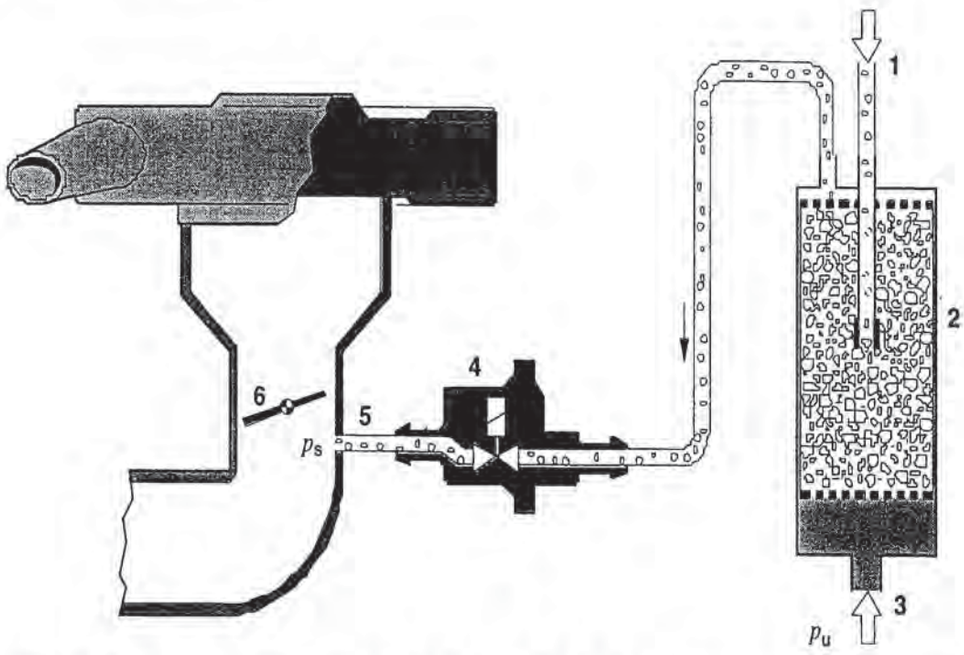


FIGURE 12.6 Evaporative emission control system: fuel vapor from fuel tank (1), charcoal canister (2), ambient air (3), canister purge control valve (4), purge line to intake manifold (5), throttle valve (6), p_s is intake manifold vacuum, and p_u is atmospheric pressure.

sure. The canister purge valve meters the amount of flow from the canister. The amount of fuel vapor in the canister and, therefore, contained in the flow stream, is not known. Therefore, it is critical that the lambda control system is operating and adjusting the fuel requirement as the vapors are being purged. Purge vapors could otherwise result in up to a 30 percent increase in air/fuel mixture richness in the engine.

Purge Valve Control. Control of the purge valve must allow for two criteria:

- There must be enough vapor flow so that the charcoal canister does not become saturated and leak fuel vapors to the atmosphere
- Purge flow must generally occur under lambda closed-loop control so that the effect of the purge vapors on A/F ratio can be detected and the fuel metering corrected

When the electronic control unit commands the purge valve to meter vapor from the canister, it requests a duty cycle (ratio of ON time to total ON and OFF time). This allows the amount of vapor flow to be regulated depending on the engine operating conditions. When lambda control is not operating, only low duty cycles and, therefore, small amounts of purge vapors, are allowed. Under deceleration fuel cutoff, the purge valve is closed entirely to minimize the possibility of unburned HCs in the exhaust.

Turbocharger Boost Pressure Control. The exhaust turbocharger consists of a compressor and an exhaust turbine arranged on a common shaft. Energy from the exhaust gas is converted to rotational energy by the exhaust turbine, which then drives the compressor. The compressed air leaves the compressor and passes through the air cooler (optional), throttle valve, intake manifold, and into the cylinders. In order to achieve near-constant air charge pressure over a wide RPM range, the turbocharger uses a circuit that allows for the bypass of the exhaust gases away from the exhaust turbine. The valve that regulates the bypass opens at a specified air charge pressure and is known as the wastegate.

PETITIONER'S EXHIBIT 1002
US PATENT NO. 6,581,565

Engines that have turbochargers benefit significantly from electronic boost pressure control. If only a pneumatic-mechanical wastegate is used, only one boost pressure point for the entire operating range is used to divert the exhaust gas. This creates a compromise for part-load conditions, which results in increased exhaust backpressure, more turbocharger work, more residual exhaust gas in the cylinders, and higher-charge air temperatures.

By controlling the wastegate with a pulse-width modulated solenoid valve, different wastegate opening pressures can be specified, depending on the engine operating conditions (Fig. 12.7). Therefore, only the level of air charge pressure required is developed. The electronic control unit uses information on engine load from either manifold pressure or the air meter and RPM and throttle position. From this information, a data table is referenced and the proper boost pressure (actually a duty cycle of the control valve) is determined. On systems using manifold pressure sensors, a closed-loop control system can be developed to compare the specified value with the measured value.

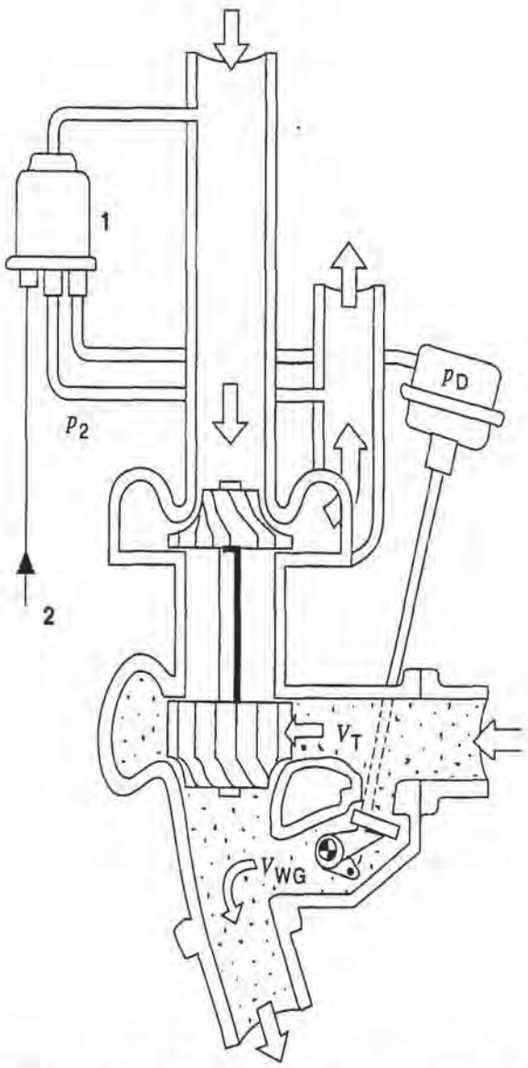


FIGURE 12.7 Electronic turbocharger boost control: solenoid valve (1), control signal from ECU (2), boost pressure (p_D), volume flow through turbine (V_T), volume flow through wastegate (V_{WG}).

ENGR & MATH SCI LIBRARY

PETITIONER'S EXHIBIT 1002
US PATENT NO. 6,581,565

The boost pressure control system is usually used in combination with knock control for turbocharged engines. When the ignition timing is retarded due to knock, an increase in already high exhaust temperatures for turbocharged engines occurs. To counteract the temperature increase, the boost pressure is reduced when the ignition timing is retarded past a predetermined threshold.

Engine/Vehicle Speed Control. Using the inputs of engine RPM and vehicle speed to the electronic control unit, thresholds can be established for limiting these variables with fuel cutoff. When the maximum speed is achieved, the fuel injectors are shut off. When the speed decreases below the threshold, fuel injection resumes.

EGR Control. By mixing a portion of the exhaust gas with the fresh intake air/fuel mixture, oxides of nitrogen (NO_x) can be reduced by lowering the peak combustion temperatures. However, the addition of exhaust gas can degrade driveability by causing combustion instability, especially at idle and low speeds and with a cold engine. The ECU references an engine RPM/load table of optimal EGR valve openings. The data table is developed on the engine dynamometer by analyzing the exhaust emissions. With increasing EGR, a point is reached where hydrocarbon (HC) emissions begin to increase. The optimal percent of EGR is just prior to that point.

The electronic control unit regulates a pneumatic- or solenoid-type valve to meter a certain quantity of exhaust gas back to the intake manifold. Typically, an engine coolant temperature threshold is also required before EGR is activated to avoid poor driveability. Under acceleration and at idle, EGR is deactivated.

Camshaft Control. There are two types of camshaft controls: phasing (i.e., overlap or intake/exhaust valve opening point) and valve lift and opening duration.

Camshaft Phasing Control. Valve overlap is a function of the rotation of the intake camshaft with respect to the exhaust camshaft. Overlap can be controlled by an electrohydraulic actuator. At idle and at high RPM, it is desirable to have the intake valves open and close later, which reduces the overlap. For idle, this reduces the residual exhaust gases that return with the fresh charge air and improves idle stability. At high RPM, late closing of the intake valve provides the best condition for maximum cylinder filling and, therefore, maximum output. For partial loads, a large valve overlap, where the intake opens early, is desirable. This allows for an increase in residual exhaust gas for improved exhaust emissions (Fig. 12.8).

Valve Lift and Opening Duration Control. Control of the valve lift and opening duration is accomplished by switching between two camshaft profiles. An initial cam specifies the optimal lift and duration for the low to middle RPM range. A second cam profile controls a higher valve lift and duration for high-RPM operation. By monitoring engine load and RPM, the ECU actuates the electrohydraulic device that switches from one cam profile to the other (Fig. 12.9).

Variable Intake Manifold Control. The goal of the engine design is to achieve the highest possible torque at low engine RPM as well as high output at high engine RPM. The torque curve of an engine is proportional to the air charge at any given engine speed. Therefore, a primary influence on the torque is the intake manifold geometric design. The simplest type of air charging uses the dynamics of the drawn-in air. The standard intake manifolds for multipoint engines consist of several intake runners and collectors converging at the throttle valve.

In general, short intake runners result in a high output at high RPM with a simultaneous loss of torque at low RPM. Long intake runners have the opposite effect. Due to intake valve and piston dynamics, pressure waves occur that oscillate within the intake manifold. Proper selection of runner lengths and collector sizes can result in the pressure waves arriving at the intake valves just before they are closing. This has a supercharging effect. The limitation of this method is that, for a given intake manifold configuration, the tuning peak can only occur at one operating point.

PETITIONER'S EXHIBIT 1002
US PATENT NO. 6,581,565

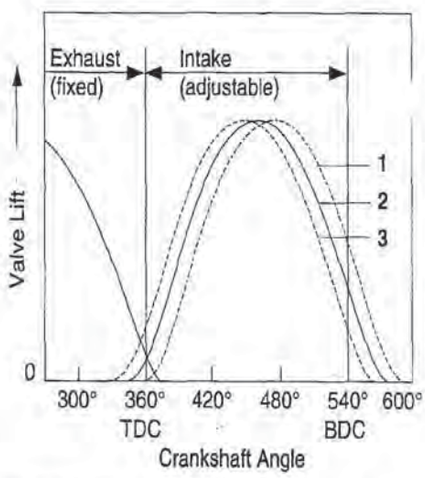


FIGURE 12.8 Adjustment angle for intake camshaft: retard (1), standard (2), advance (3).

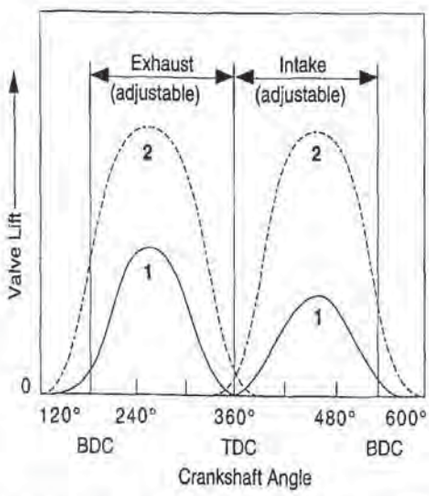


FIGURE 12.9 Selective camshaft lobe actuation: base cam lobe (1), auxiliary cam lobe (2).

Variable Intake Systems. To optimize the benefits of intake manifold charging, several systems have been developed that allow for changes in runner length and collector volume, depending on engine operating conditions. This allows for tuning peaks at more than one operating point. One method developed uses electronically controlled valves to close off areas of the intake manifold (Fig. 12.10). Inputs of engine load, RPM, and throttle angle determine the position of the valves.

12.2.2 Engine Control Modes

Engine Crank and Start. During engine cranking, the goal is to get the engine started with the minimal amount of delay. To accomplish this, fuel must be delivered that meets the requirements for starting for any combination of engine coolant and ambient temperatures. For a cold engine, an increase in the commanded air/fuel ratio is required due to poor fuel vaporization and "wall wetting," which decreases the amount of usable fuel. Wall wetting is the condensation of some of the vaporized fuel on the cold metal surfaces in the intake port and combustion chamber. It is critical that the fuel does not wet the spark plugs, which can reduce the effectiveness of the spark plug and prevent the plug from firing. Should plug wetting occur, it may be impossible to start the engine.

Fuel Requirement. Within the ECU ROM there are specific data tables to establish cold-start fuel based on engine coolant temperature. For two reasons, the lambda sensor output cannot be used during crank: the lambda sensor is below its minimum operating temperature and the air/fuel ratio required is outside the lambda sensor control window.

Many starting sequences use a front-loading strategy for fueling whereby the quantity of fuel is reduced after a speed threshold (RPM) is achieved, after a certain number of revolutions or at a defined time after the initial crank. Some systems also switch over from simultaneous injection to sequential injection after a speed threshold is achieved. For cold temperature starting, the fuel mixture may remain richer than $\lambda = 1$ after starting, due the continuing poor mixture formation in the cold induction system.

Ignition Timing Requirement. Ignition timing is controlled by the ECU during crank and is determined by engine coolant temperature and cranking speed. For a cold engine with low cranking speeds, ideal timing is near TDC. For higher cranking speeds, a slightly more advanced timing is optimal. Timing advance must be limited during cranking to avoid igniting

PETITIONER'S EXHIBIT 1002
US PATENT NO. 6,581,565

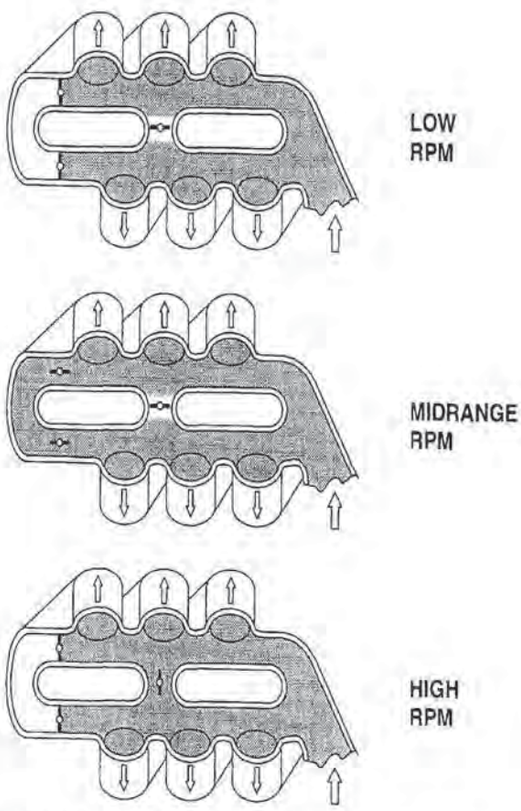


FIGURE 12.10 Variable configuration intake manifold.

the air/fuel mixture before the crankshaft reaches top dead center (TDC). A damaging torque reversal could occur that would damage the starter. After the engine starts, ignition timing is advanced to improve cold engine running as well as to reduce the need for fuel enrichment.

Engine Warm-Up. During the warm-up phase, there are three conflicting objectives: keep the engine operating smoothly (i.e., no stalls or driveability problems), increase exhaust temperature to quickly achieve operational temperature for catalyst (light-off) and lambda sensor so that closed-loop fuel control can begin operating, and keep exhaust emissions and fuel consumption to a minimum. The best method for achieving these objectives is very dependent on the specific engine application.

If the engine is still cold, fuel enrichment will be required to keep the engine running smoothly due, again, to poor fuel vaporization and wall wetting effects. The amount of enrichment is dependent on engine temperature and is a correction factor to the injector pulse width. This enrichment, combined with secondary air injection, also helps achieve the desired increase in catalyst temperature. To provide secondary air injection, an external air pump delivers fresh air downstream of the exhaust valves for a short time after start. The excess air causes oxidation (burning) of the excess HC and CO from the rich mixture in the exhaust manifold, which rapidly increases the temperature of the catalytic converter. The oxidation also removes harmful pollutants from the exhaust stream.

It is possible to increase the exhaust temperature by increasing the idle speed during warm-up. The increased idle speed may also be combined with a slightly retarded ignition timing, which increases temperatures in the exhaust, thereby promoting rapid warm-up of the catalyst.

PETITIONER'S EXHIBIT 1002
US PATENT NO. 6,581,565

Transient Compensation. During transitions such as acceleration or deceleration, the objective of the engine control system is to provide a smooth transition from one engine operating condition to another (i.e., no hesitations, stalls, bumps, or other objectionable driveability concerns), and keep exhaust emissions and fuel consumption to a minimum.

Acceleration Enrichment. When an increase in engine load and throttle angle occurs, a corresponding increase in fuel mixture richness is required to compensate for the increased wall wetting. The sudden increase in air results in a lean mixture that must be corrected swiftly to obtain good transitional response. The rate of change of engine load and throttle angle are used to determine the quantity of fuel during acceleration enrichment. The amount of fuel must be enough to provide the desired performance, but not so much as to degrade exhaust emissions and fuel economy.

During acceleration enrichment, the ignition timing is set for maximum torque without knocking. Additionally, when a large change in engine load occurs, some systems delay the ignition timing advance briefly to prevent engine knock, which may arise from a momentary lean mixture or from transient ignition timing errors.

Deceleration Enleanment. During deceleration modes, such as coasting or braking, there is no torque requirement. Therefore, the fuel may be shut off until either an increase in throttle angle is detected or the engine speed falls to a speed slightly above the idle RPM. Fuel shutoff or cutoff can decrease exhaust emissions by eliminating unburned HC and CO and may also improve fuel consumption. Fuel cutoff is also used to protect the catalytic converter from extreme high temperatures during extended overrun conditions. During transition to fuel cutoff, the ignition timing is retarded from its current setting to reduce engine torque and to assist in engine braking. The fuel is then shut off. During the transition, the throttle bypass valve or the main throttle valve may remain open for a short period to allow fresh air to oxidize the remaining unburned HC and CO to further reduce exhaust emissions. During development of the fuel cutoff strategy, the advantage of reduced emission effects and catalyst temperature control must be balanced against driveability requirements. The use of fuel cutoff may change the perceived amount of engine braking felt by the driver. In addition, care must be taken to avoid a "bump" feel when entering the fuel cutoff mode, due to the change in torque.

Full Load. Under steady state full-load conditions, such as for climbing a grade, it is desirable to control the air/fuel mixture and ignition timing to obtain maximum power and to also limit engine and exhaust temperatures. The best engine torque is typically delivered at about $\lambda = 0.9$ to 0.95. When the ECU determines the engine is operating at full load via the throttle valve sensor (at WOT), the commanded air/fuel mixture, if required, can be enriched. The lambda sensor signal cannot be used to provide correction to the air/fuel mixture because the rich operating point lies outside the lambda control window.

The ignition timing at full load is set to achieve the maximum torque without knocking. This initial value is determined through engine dynamometer testing. With a knock control system (see Sec. 12.2.1), the ignition timing is modified (retarded) when engine knock occurs. The modification required to eliminate the knock may be saved in the ECU so that the next time that engine RPM/load point occurs, less knocking will occur and less correction will be required.

Idle Speed Control. The objectives of the engine control system during idle are:

- Provide a balance between the engine torque produced and the changing engine loads, thus achieving a consistent idle speed even with various load changes due to accessories (i.e., air conditioning, power steering, and electrical loads) being turned on and off and during engagement of the automatic transmission. In addition, the idle speed control must be able to compensate for long-term changes in engine load, such as the reduction in engine friction that occurs with engine break-in.
- Provide the lowest idle speed that allows smooth running to achieve the lowest exhaust emissions and fuel consumption (up to 30 percent of a vehicle's fuel consumption in city driving occurs during idling).

PETITIONER'S EXHIBIT 1002
US PATENT NO. 6,581,565

To control the idle speed, the ECU uses inputs from the throttle position sensor, air conditioning, automatic transmission, power steering, charging system, engine RPM, and vehicle speed. There are currently two strategies used to control idle speed: air control and ignition control.

Air Control. The amount of air entering the intake manifold is controlled either by a bypass valve or by an actuator acting directly on the throttle valve. The bypass valve uses, for example, an electronically controlled motor controlled by the ECU that opens or closes a fixed amount. For large throttle valves, it may be desirable to use a bypass valve because a small change in throttle angle may result in a large change in air flow and, therefore, idle speed may be difficult to control. Using engine RPM feedback input, the ECU adjusts the air flow to increase or decrease the idle speed. A disadvantage to air control is that the response to load changes is relatively slow. To overcome this, air control is often combined with ignition timing control to provide acceptable idle speed control. The fuel quantity required at idle is determined by engine load and RPM. During closed-loop operation, this value is optimized by the lambda sensor closed-loop control.

Ignition Timing Control. Engine torque may be increased or decreased by advancing or retarding the ignition timing within an established window. This principle can be employed to help control idle speed. Ignition timing control is particularly desirable for responding to idle load changes because engine torque output changes more rapidly in response to a change in ignition timing than to a change in air valve position. Using the same inputs as for air control, the ECU adjusts the spark advance to either raise or lower the idle speed.

Anticipating Accessory Loads. Specific electric inputs to the ECU, such as a pressure switch located in the power steering system, are used to anticipate accessory loads so that the idle control system can compensate more quickly. This "feed forward" strategy allows better idle control than a strictly feedback system which does not respond until the idle speed begins to fall. When an accessory can be controlled by the ECU, further improvement in idle speed control is obtained. By delaying the load briefly after it is requested, the compensation sequence can begin before the load is actually applied. Such a load delay strategy is effective for controlling air conditioning compressor loads, for example. In this case, when the air conditioner is requested, the ECU begins to increase the idle speed first and then activates the A/C compressor.

12.2.3 Engine Control Diagnostics

The purpose of system diagnostics is to provide a warning to the driver when the control system determines that a malfunction of a component or system has occurred and to assist the service technician in identifying and correcting the failure (see Chap. 22). In many cases, to the driver, the engine may appear to be operating correctly, but excessive amounts of pollutants may be emitted. The ECU determines that a malfunction has occurred when a sensor signal received during normal engine operation or during a system test indicates there is a problem. For critical operations such as fuel metering and ignition control, if a required sensor input is faulty, a substitute value may be used by the ECU so that the engine will continue to operate, but likely not at optimal performance. It is also possible to apply an emergency measure if the failure of a component may result in engine or emission system damage. For example, if repeated misfires are detected in one cylinder, perhaps due to an ignition failure, the fuel injector feeding that cylinder can be shut off to avoid damage to the catalytic converter. When a failure occurs, the malfunction indicator light (MIL), visible to the driver, is illuminated. Information on the failure is stored in the ECU. A service technician can retrieve the information on the failure from the ECU and correct the problem.

Air Mass Sensor. For air mass measurement systems, the pulse width of the fuel injectors is calculated in the ECU from the air mass sensor input. As a comparison, the pulse width is also calculated from the throttle valve sensor and the engine RPM. If the pulse width values devi-

VW EX1015 (Part 2 of 3)
U.S. Patent No. 6,581,565

PETITIONER'S EXHIBIT 1002
US PATENT NO. 6,581,565

ate by a predetermined amount, the discrepancy is stored in the ECU. Then, while the vehicle is being driven, plausibility tests determine which input is incorrect. When this has been determined, the appropriate failure code is saved in the ECU.

Misfire Detection. Misfiring is the lack of combustion in the cylinder. Misfiring can be caused by several factors including fouled or worn spark plugs, poor fuel metering, or faulty electrical connections. Even a small number of misfires may result in excessive exhaust emissions due to the unburned mixture. Increased misfire rates can damage the catalytic converter.

To determine if the engine is experiencing a misfire, the crankshaft speed fluctuation is monitored. If a misfire occurs, no torque is created during the power stroke of the cylinder(s) that is misfiring. A small decrease in the rotational speed of the crankshaft occurs. Because the change in speed is very small, highly accurate sensing of the crankshaft speed is required. In addition, a fairly complicated calculation process is required in order to distinguish misfiring from other influences on crankshaft speed. As was mentioned previously, if a cylinder repeatedly misfires, it is possible to shut off the fuel to that cylinder to prevent damage to the catalytic converter.

Catalytic Converter Monitoring. During the useful life of a catalytic converter, its efficiency decreases. If subjected to engine misfire, the decrease in efficiency occurs more rapidly. A loss in efficiency results in an increase in exhaust pollutants. For this reason, the catalytic converter is monitored. A properly operating catalytic converter transforms O_2, HC, CO, and NO_x into H_2O, CO_2, and N_2. The incoming air/fuel ratio oscillates from rich to lean due to the lambda closed-loop control strategy discussed in Sec. 12.2.1. Only a properly functioning catalytic converter is able to dampen these oscillations by storing and converting the incoming components. As the catalyst ages, this storage effect is diminished. To monitor the catalytic converter, an additional lambda sensor is installed downstream of the catalyst. The ECU compares the signal of the lambda sensor upstream with the lambda sensor downstream and determines if the catalytic converter is operating properly. If not, the ECU illuminates the malfunction indicator light (MIL) and stores a failure code.

Lambda Sensor Monitoring. To minimize exhaust emissions, the engine must operate within the catalytic converter window for air/fuel ratio (see Sec. 12.1.1 for a detailed description of the catalytic converter window). Output from the lambda sensor serves as feedback to the ECU to control the fuel within that window. When a lambda sensor is exposed to high heat for a long period of time, it may respond more slowly to changes in the air/fuel mixture. This can cause a deviation in the air/fuel mixture from the window, which would affect the exhaust emissions.

If the upstream lambda sensor operation is determined to be too slow, which can be detected by the system operation frequency, the ECU illuminates the malfunction indicator light (MIL) and a failure code is stored. Additionally, the ECU compares the output signal of the additional lambda sensor downstream of the catalytic converter with the lambda sensor signal upstream. With this, the ECU is able to detect deviations of the average value in air/fuel ratio.

For heated lambda sensors, the electric current and voltage of the heater circuit is monitored. To accomplish this, the heater is directly controlled by the ECU, not through a relay.

Fuel System Monitoring. To provide the correct air/fuel ratio, the ECU uses a preset data map with the optimal fuel required for each load and RPM point. The lambda closed-loop control system (see Sec. 12.2.1) provides feedback to the ECU on the necessary correction to the preset data points. The corrected information is stored in the ECU's RAM so that the next time that operating point is reached, less correction of the air/fuel ratio will be required. If the ECU correction passes a predetermined threshold, it is an indication that some component in the fuel supply system is outside of its operating range. Some examples are defective pressure regulator, defective manifold pressure sensor, intake system leakage, or exhaust system leakage. When the ECU determines a problem exists, the MIL is illuminated and a code is stored in the ECU.

PETITIONER'S EXHIBIT 1002
US PATENT NO. 6,581,565

Exhaust Gas Recirculation (EGR) Monitoring. There are currently two methods used to monitor EGR operation. One method confirms that hot exhaust gases are returning to the intake manifold during EGR operation by use of a temperature sensor in the intake manifold. The second method requires the EGR valve to be fully opened during coast operation, where high intake manifold vacuum occurs. The exhaust gas flowing into the manifold causes a measurable increase in pressure. Thus, if a measured increase in pressure does not occur, the EGR system is not operating.

Evaporative Emissions Control System (EECS) Monitoring. In general, a valve will be installed at the atmospheric side of the purge canister. During idle, this valve would close and the purge valve would open. Intake manifold vacuum would occur in the entire EECS. A pressure sensor in the fuel tank would provide a pressure profile during this test to the ECU, which would then determine if a leak existed in the system.

12.2.4 Fuel Delivery Systems

Overview. Fuel management in the spark ignition engine consists of metering the fuel, formation of the air/fuel mixture, transportation of the air/fuel mixture, and distribution of the air/fuel mixture. The driver operates the throttle valve, which determines the quantity of air inducted by the engine. The fuel delivery system must provide the proper quantity of fuel to create a combustible mixture in the engine cylinder. In general, two fuel delivery system configurations exist: *single-point* and *multipoint* (Fig. 12.11).

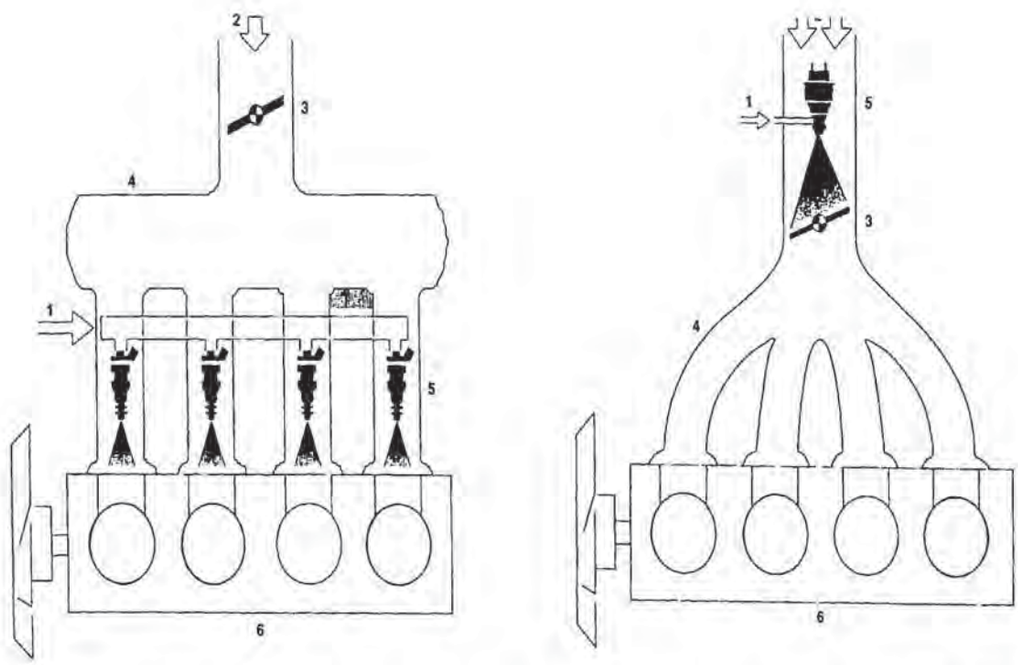


FIGURE 12.11 Air-fuel mixture preparation: right, single-point fuel injection; left, multipoint fuel injection with fuel (1), air (2), throttle valve (3), intake manifold (4), injector(s) (5), and engine (6).

PETITIONER'S EXHIBIT 1002
US PATENT NO. 6,581,565

For single-point systems such as carburetors or single-point fuel injection, the fuel is metered in the vicinity of the throttle valve. Mixture formation occurs in the intake manifold. Some of the fuel droplets evaporate to form fuel vapor (desirable) while others condense to form a film on the intake manifold walls (undesirable). Mixture transport and distribution is a function of intake manifold design. Uniform distribution under all operating conditions is difficult to achieve in a single-point system.

For multipoint systems, the fuel is injected near the intake valve. Mixture formation is supplemented by the evaporation of the fuel on the back of the hot intake valve. Mixture transport and distribution occurs only in the vicinity of the intake valve. The influence of the intake manifold design on uniform mixture distribution is minimized. Since mixture transport and distribution is not an issue, the intake manifold design can be optimized for air flow.

Single-Point Injection Systems A single-point injection system uses one or, in some cases, two electronic fuel injectors to inject fuel into the intake air stream. The main component is the fuel injection unit which is located upstream of the intake manifold.

Component Description. An electric fuel pump provides fuel at a medium pressure (typically 0.7 to 1.0 bar) to the electronic fuel injection unit (Fig. 12.12). The fuel injection unit houses the solenoid-operated fuel injector, which is located in the intake air flow above the throttle valve. This allows for homogeneous mixture formation and distribution. The injector spray pattern is designed to allow fuel to pass between the throttle valve and the throttle bore. To prevent vapor lock of the injector, fuel flows through the injector at all times. Fuel not used by the engine is returned to the fuel tank. The injector is activated in relation to the speed of the engine, typically once per ignition event. The length of the pulse width determines the quantity of fuel provided.

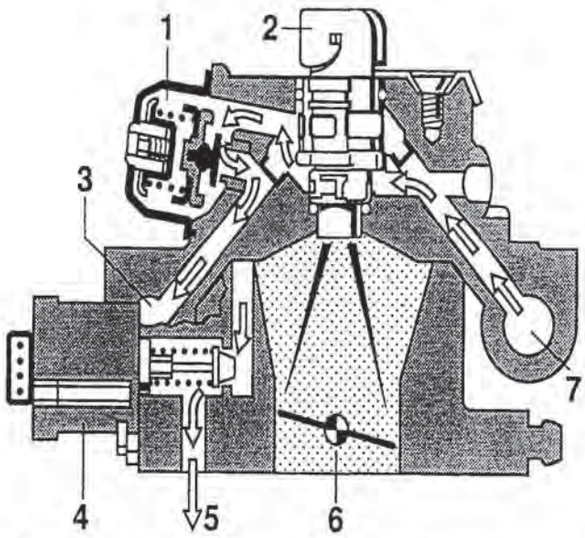


FIGURE 12.12 Single-point injection unit: pressure regulator (1), injector (2), fuel return (3), stepper motor for idle speed control (4), to intake manifold (5), throttle valve (6), and fuel inlet (7).

The electronic injection unit also houses the throttle position sensor and, in some cases, an inlet air temperature sensor which provides operating condition information to the ECU. The throttle valve actuator and fuel pressure regulator are also mounted on the injection unit. In addition, some units contain an air bypass valve for idle speed control. Engine temperature, battery voltage, and engine speed via the ignition system are all inputs to the ECU. The single-

PETITIONER'S EXHIBIT 1002
US PATENT NO. 6,581,565

point injection system also uses lambda closed-loop fuel control to optimize fuel metering within the lambda control window (see Sec. 12.2.1).

Adaptation to Operating Conditions. For cold-start and engine warm-up, the ECU uses engine temperature information to determine the correct amount of fuel and commands the fuel injector via a pulse width. Due to wall wetting and poor fuel vaporization when the engine is cold, an increase in mixture richness is required. As the engine warms up to operating temperature, the commanded pulse width is reduced.

During an acceleration transition, the ECU adds a correction factor (an increase) to the commanded injector pulse width. The sudden increase in air results in a lean mixture which must be corrected swiftly to obtain good transitional response. During a deceleration transition, the fuel can be shut off by simply not providing a pulse width signal to the injector to minimize exhaust emissions and fuel consumption.

During full-load operation, the air/fuel mixture can be enriched ($\lambda < 1$) to deliver maximum torque. The ECU determines full-load operation by the throttle position sensor (at or near wide-open throttle) and adds a correction to the injector pulse width to achieve the desired air/fuel mixture richness.

The single-point system can control the idle speed by ECU control of either a throttle valve actuator or a bypass valve. Idle speed is a function of engine operating temperature, whether the transmission is in drive, and what accessories are in use. Fuel metering at idle is determined by engine RPM and load as well as lambda closed-loop control.

Multipoint Fuel Injection Systems. A multipoint fuel injection system supplies fuel to each cylinder individually via a mechanical or solenoid-operated fuel injector located just upstream of the intake valve. Advantages of this system type compared to SPI systems are numerous:

- *Increased fuel economy.* On an SPI engine, due to the intake manifold configuration, mixture formation will differ at each cylinder. To provide adequate fuel for the leanest cylinder, too much fuel must be metered overall. In addition, during engine load changes, a film of fuel is deposited on the intake manifold walls. This leads to further variations in mixture from cylinder to cylinder. Multipoint injection provides the same quantity of fuel to each cylinder.
- *Higher power output.* With the fuel being injected near the intake valve, the rest of the intake manifold can be optimized for maximum air flow. The result is increased torque.
- *Improved throttle response.* Because the fuel is injected onto the intake valves, responses to increases in throttle position are swift. With an SPI system, the increased fuel required must travel the length of the intake manifold before entering the cylinder.
- *Lower exhaust emissions.* As was discussed for fuel economy, mixture variation in an SPI system creates increased exhaust emissions. Metering of the fuel at the intake valve decreases this variation. In addition, the system transport time is reduced, increasing the frequency at which the lambda closed-loop control system can switch air/fuel ratio. Catalytic converter efficiency is increased.

Although there are numerous advantages of the MPI systems over the SPI systems, there is still one important advantage the SPI systems have over the MPI systems. In general, SPI systems have better fuel preparation, similar to a carburetor.

Mechanically Controlled Continuous Injection System. This type of system meters the fuel as a function of the intake air quantity and injects it continuously onto the intake valves. This is accomplished by measuring the air flow as it passes through the air flow meter by means of deflection of a meter plate. The fuel is supplied through a fuel accumulator to the fuel distributor by an electric fuel pump. A primary-pressure regulator in the fuel distributor maintains constant fuel pressure. The fuel distributor, through its interface with the air flow meter and warm-up regulator, meters fuel to the continuously flowing fuel injectors.

Component Description

Mixture control unit. The mixture control unit houses the air flow meter and the fuel distributor. In the air flow meter, the measurement of the intake air serves as the basis for

PETITIONER'S EXHIBIT 1002
US PATENT NO. 6,581,565

determining the amount of fuel to be metered to the injectors. The air flow meter is located upstream of the throttle valve so that it measures all the air entering the engine. It consists of an air funnel, in which a sensor plate is free to pivot. Intake air flowing through the funnel causes a deflection of the sensor plate. The sensor plate is mechanically linked to a control plunger and movement of the plate results in movement of the control plunger. The control plunger movement determines the amount of fuel to be injected.

In the fuel distributor, the control plunger moves up and down in a cylindrically shaped device (barrel) with rectangular openings (metering slit), one for each engine cylinder. Increased air flow causes the control plunger to move upward, uncovering a larger area of the metering slit and increasing the fuel metered. Downstream of each metering slit is a differential-pressure valve that maintains a constant pressure drop across the metering slits at different flow rates. Due to the constant pressure, the fuel flow through the slits is directly proportional to the position of the control plunger (Fig. 12.13).

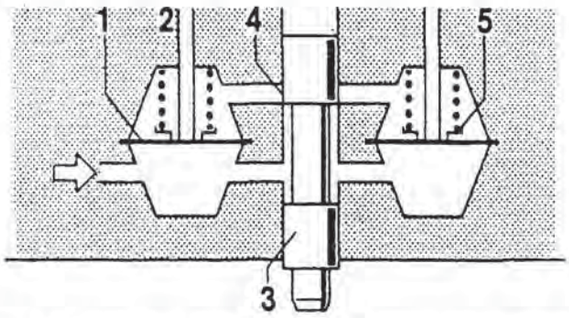


FIGURE 12.13 Fuel distributor for mixture control unit: diaphragm (1), to injector (2), control plunger (3), metering slot (4), differential pressure regulator (5).

Warm-up regulator. The warm-up regulator is used to richen the fuel mixture under cold engine conditions. It consists of a diaphragm valve and an electrically heated bimetallic spring. Under cold conditions, the warm-up regulator lowers the control pressure on the control plunger. The control pressure acts on the opposite end of the plunger from the air flow meter plate. A lower control pressure results in a lower force required to move the meter plate. Therefore, the same air flow causes the meter plate and control plunger to move a greater distance and additional fuel is metered to the injectors.

Fuel injectors. The injectors open at a pressure of approximately 3.6 bar. Atomization of the fuel occurs through oscillation (audible chatter) of the valve needle caused by the fuel flowing through it. The injectors remain open as long as fuel is provided above the opening pressure. Fuel is injected continuously into the intake port. When the intake valve opens, the mixture is drawn into the cylinder.

Auxiliary air valve. The auxiliary air valve provides additional air to the engine by bypassing the throttle valve during cold engine operation. This creates an increase in the idle speed needed during cold operation.

Thermo-time switch. The thermo-time switch controls the cold start valve as a function of time and engine temperature. Fuel enters the intake manifold from the cold start valve and further enriches the mixture to improve cold-starting at low ambient temperatures. When the engine is warm, the contacts in the thermo-time switch open and the cold-start valve is not used in starting the engine.

Lambda sensor. With the addition of a lambda sensor in the exhaust stream, a frequency valve, a modified fuel distributor, and an electronic control unit, the mechanically controlled fuel system can operate under lambda closed-loop control. The lambda sensor sig-

PETITIONER'S EXHIBIT 1002
US PATENT NO. 6,581,565

nal is read by the ECU. The ECU outputs electric pulses to an electromagnetic (frequency) valve. The frequency valve modulates the pressure to the lower chambers of the differential-pressure valves in the fuel distributor. This results in a modification of the pressure drop across the metering slits, effectively increasing or decreasing the amount of fuel injected. Figure 12.14 is a schematic of a typical mechanically controlled continuous injection system.

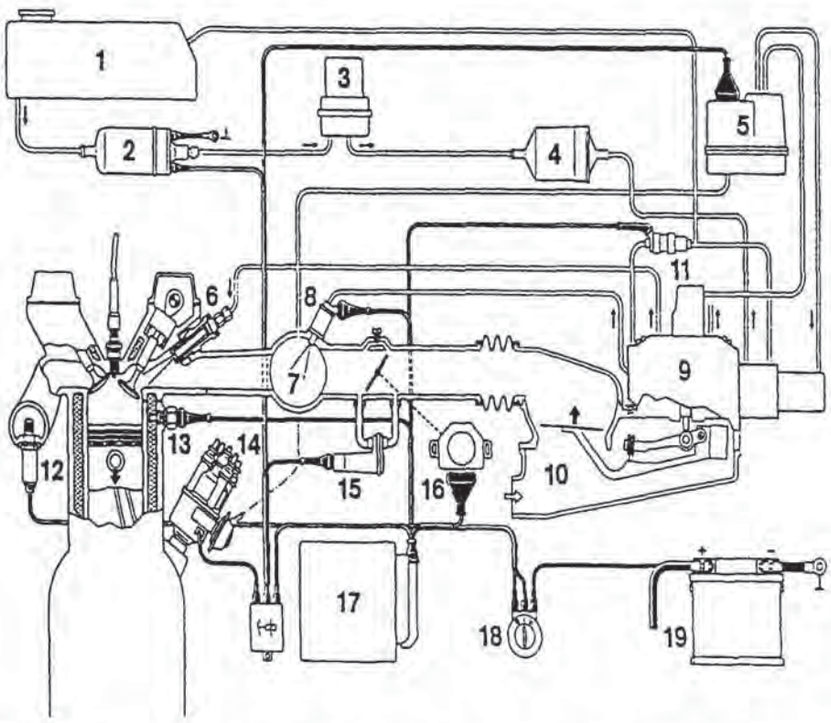


FIGURE 12.14 Schematic of mechanically controlled continuous injection system: fuel tank (1), electric fuel pump (2), fuel accumulator (3), fuel filter (4), warm-up regulator (5), injector (6), intake plenum (7), cold-start valve (8), fuel distributor (9), air flow sensor (10), electrohydraulic pressure actuator (11), lambda sensor (12), thermo-time switch (13), ignition distributor (14), auxiliary air valve (15), throttle switch (16), ECU (17), ignition switch (18), and battery (19).

Depending on the engine temperature, the cold-start valve injects extra fuel into the intake manifold for a limited period during cold start. The injection period is determined by a combination of time and temperature and is controlled by the thermo-time switch. As the engine temperature increases, this additional enrichment is no longer required and the thermo-time switch turns off the cold-start valve. For repeated start attempts or long cranking, the thermo-time switch turns off the cold-start injector after a given time. This minimizes engine flooding when engine start has not occurred.

As the engine continues to warm up, wall wetting and poor fuel vaporization still occur and mixture enrichment is still required until the engine reaches operating temperature. This enrichment is controlled as a function of temperature by the warm-up regulator. As the temperature increases, the warm-up regulator commands less and less additional fuel by increasing the control pressure.

For acceleration response, the air flow sensor "overswings" during quick throttle increases. This causes an additional quantity of fuel to be injected for acceleration enrichment. For full-load enrichment to achieve maximum power, a special warm-up regulator

PETITIONER'S EXHIBIT 1002
US PATENT NO. 6,581,565

that uses intake manifold pressure is required. At increased manifold pressures, i.e., during wide-open throttle, the warm-up regulator lowers the control pressure, which results in an increase in fuel delivery. Deceleration fuel shutoff is accomplished by diverting all intake air through an air bypass around the air flow sensor plate. With no air flow past the air flow sensor plate, the fuel pressure to the injectors is decreased below the opening pressure.

Idle speed for the cold-running engine is increased by the auxiliary air valve. The amount of additional air varies with engine temperature until the auxiliary air valve is closed and the idle speed is then controlled only be the air passing the throttle valve.

Electronically Controlled Continuous Injection. The basis of the electronically controlled continuous injection is still the mechanical hydraulic injection system discussed previously. This is supplemented by an electronic control unit (ECU) that allows for an increase in flexibility and the use of additional functions. This system incorporates additional sensors for detecting the engine temperature, the throttle valve position (load signal), and the air flow sensor plate deflection. This information is processed by the ECU, which then commands an electrohydraulic pressure actuator to adapt the injected fuel quantity for the present operating conditions.

In contrast to the mechanical system mentioned previously, the control pressure or counterpressure on the control plunger is not varied by a warm-up regulator. The control pressure remains constant and is the same as the primary pressure. The function of the warm-up regulator is now handled by the ECU and the electrohydraulic pressure actuator. Figure 12.15 is a schematic of a typical electronically controlled continuous injection system.

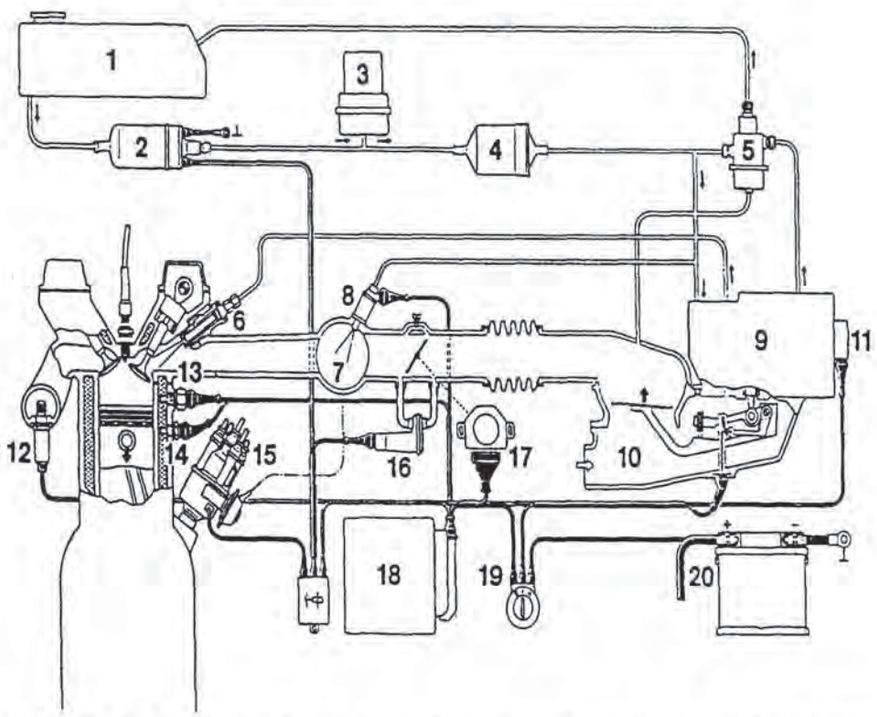


FIGURE 12.15 Schematic of an electronically controlled continuous fuel injection system: fuel tank (1), electric fuel pump (2), fuel accumulator (3), fuel filter (4), fuel pressure regulator (5), injector (6), intake plenum (7), cold-start valve (8), fuel distributor (9), air flow sensor (10), electrohydraulic pressure actuator (11), lambda sensor (12), thermo-time switch (13), coolant temperature sensor (14), ignition distributor (15), auxiliary air valve (16), throttle valve switch (17), ECU (18), ignition switch (19), and battery (20).

PETITIONER'S EXHIBIT 1002
US PATENT NO. 6,581,565

Component description—electrohydraulic pressure actuator. The main difference in the componentry between the purely mechanical system and the electronically controlled system is the addition of the electrohydraulic actuator and the elimination of the warm-up regulator. With the addition of the ECU control of fuel metering, the purely mechanical warm-up regulator is no longer required. Depending on the signal received from the ECU, the electrohydraulic pressure actuator varies the pressure in the lower chambers of the differential pressure valves. This changes the amount of fuel delivered to the injectors.

Lambda closed-loop control. As with the mechanical system, the lambda sensor signal is processed by the ECU to determine mixture composition. The difference is that the ECU now commands the electrohydraulic actuator to modify the fuel metered, as opposed to the separate frequency valve, which is no longer necessary.

Adaptation to operating conditions. Depending on the engine temperature, the cold-start valve injects extra fuel into the intake manifold for a limited period during cold-start. The quantity to be injected is controlled by the ECU and is a function of engine temperature (from the engine temperature sensor). The thermo-time switch controls how long the cold-start valve remains active, depending on engine temperature and time.

Acceleration enrichment is controlled by the ECU. Input from the air flow sensor plate position sensor provides the ECU with information on how quickly the engine load has increased. The ECU commands additional enrichment via the electrohydraulic pressure actuator. For full-load enrichment for maximum power, the ECU receives input from the throttle position sensor that the throttle is wide open. The ECU then commands additional enrichment via the electrohydraulic pressure actuator. Deceleration fuel shutoff is also controlled by the ECU when the throttle valve switch indicates the throttle is closed and the engine speed is above idle RPM. The ECU signals the electrohydraulic pressure actuator to interrupt fuel delivery to the injectors.

Idle speed control can be a closed-loop function with the addition of the idle actuator valve. This valve is ECU-controlled and the RPM signal from the ignition, combined with the engine temperature signal, is used to determine its position for the correct idle speed.

Pulsed Fuel Injection Systems. Pulsed fuel injection systems are a further enhancement of the continuous injection systems. Today, most continuous injection systems have been replaced with pulsed fuel injection systems. Instead of injecting fuel continuously and controlling the quantity of fuel by modifying the delivery volume flow rate, the fuel quantity is controlled by the open time of the solenoid-operated injectors. The injectors are controlled directly by the ECU. For most systems, the fuel pressure drop across the injector, from the fuel rail to the intake manifold, is kept constant by using intake manifold air pressure to compensate the fuel pressure regulator. This type of system allows for still greater precision of fuel control and is usually coupled with an equally precise ignition timing control system.

Component description. Several multipoint pulsed injection systems exist in various configurations. The components discussed here serve as a general outline of this system type. Figure 12.16 is a schematic of a typical pulsed fuel injection system.

- *Inlet air sensing.* The inlet air charge can be measured directly using either an air flow meter or a mass air flow meter. The air flow meter is a vane-type meter, which uses the force of the incoming air to move a flap through a defined angle. The angular movement is converted by a potentiometer to a voltage ratio. The air flow meter requires an air inlet temperature sensor to correct for air density changes. The air mass flow meter measures the air mass directly by hot-wire or hot-film element. As the inlet air flow passes the heated element, a bridge circuit keeps the element at a constant temperature above the inlet temperature. The heating current required by the bridge circuit to maintain the element at a constant temperature is measured and converted to an air density value.

  The air charge can also be measured indirectly by measuring the inlet air temperature, intake manifold pressure, and engine RPM and then calculating the air charge (see Sec. 12.2.1 for further discussion on the calculation method which is called speed density air measurement).

PETITIONER'S EXHIBIT 1002
US PATENT NO. 6,581,565

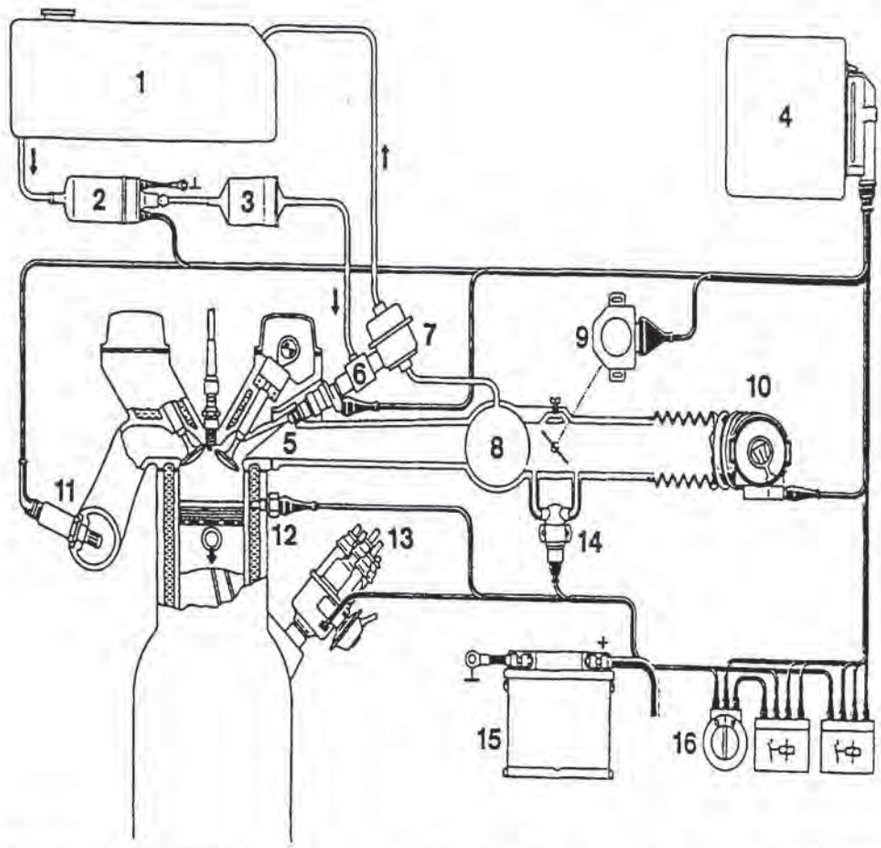


FIGURE 12.16 Schematic of a pulsed fuel injection system: fuel tank (1), electric fuel pump (2), fuel filter (3), ECU (4), injector (5), fuel distributor (6), fuel pressure regulator (7), intake plenum (8), throttle valve switch (9), hot-wire mass air flow sensor (10), lambda sensor (11), coolant temperature sensor (12), ignition distributor (13), idle speed actuator (14), battery (15), and ignition switch (16).

- *Fuel metering.* The fuel supply system includes an electric fuel pump, fuel filter, fuel rail, pressure regulator, and solenoid-operated injectors. The fuel pump provides more fuel than the maximum required by the engine. Fuel not used by the engine is returned to the fuel tank. The fuel rail supplies all injectors with an equal quantity of fuel and ensures the same fuel pressure at all injectors.

  The pressure regulator keeps the pressure differential across the injectors constant. It contains a diaphragm that has intake manifold pressure on one side and fuel rail pressure on the other. Normally, it is mounted at the outlet end of the fuel rail. The diaphragm operates a valve which opens at a differential pressure between 2.0 and 3.5 bar and allows excess fuel to return to the fuel tank.

  The fuel injectors are solenoid-operated valves that are opened and closed by means of electric pulses from the ECU. The injectors are mounted in the intake manifold and spray onto the back of the intake valves. In general, one injector is used for each cylinder.

  In addition, some systems also use a separate cold-start injector mounted in the intake manifold just downstream of the throttle valve. This injector ensures good fuel vaporization during cold-start and supplies the additional enrichment needed to start the cold engine. Control of the cold-start valve is either by the ECU directly or in conjunction with a thermo-time switch.

PETITIONER'S EXHIBIT 1002
US PATENT NO. 6,581,565

- *Lambda closed-loop control.* The lambda sensor signal is processed by the ECU. The ECU determines the required injector pulse width to maintain the air/fuel ratio within the lambda control window (see Sec. 12.2.1 for further discussion on lambda closed-loop control).

Adaptation to operating conditions. For cranking, the fuel required is determined by a data table in the ECU with reference to engine temperature. The ECU then commands a pulse width for the fuel injectors. The air/fuel mixture is greatly enriched due to poor fuel vaporization and wall wetting, which reduces the amount of usable fuel. After start, the fuel mixture remains rich due to continuing poor air/fuel mixture formation. The amount of enrichment should be minimized to obtain good emission results. The target is to stay close to lambda (λ) = 1.

For acceleration enrichment, the throttle valve position sensor indicates that the throttle has moved rapidly. The ECU adds a correction factor to increase the pulse width so that a smooth transition occurs. For deceleration, the ECU uses input from the throttle position sensor and engine RPM to indicate that the throttle has closed and the engine speed is above the idle speed. Since no torque is required under this condition, the ECU provides no pulse width to the injectors and they are therefore closed. For full-load enrichment, when necessary, the ECU can provide an injector pulse width that would result in the engine achieving its maximum torque (roughly $\lambda = 0.9$). Fuel metering during idle is primarily controlled by lambda closed-loop control when the engine has reached operating temperature.

12.2.5 Ignition Systems

Overview. The purpose of the ignition system in the spark ignition engine is to initiate combustion of the air/fuel mixture by delivering a spark at precisely the right moment. The spark consists of an electrical arc generated across the electrodes of the spark plug. Two important factors for proper ignition are the energy of the spark and the point in the four-stroke cycle when the spark occurs (ignition timing).

Electrical Energy. The energy required for a spark to ignite an air/fuel mixture at stoichiometry depends on specific engine conditions. If there is insufficient energy available to ignite the air/fuel mixture, misfiring will occur. Misfiring will result in poor engine operation, high exhaust emissions, and possible catalytic converter damage. Therefore, the amount of ignition energy available must always exceed the amount necessary to ensure ignition even under adverse conditions.

Some of the conditions that affect ignitability of the air/fuel mixture are fuel atomization, access of the mixture to the spark, spark duration, and spark physical length. Fuel atomization is controlled by the fuel system and the engine design. Access to the spark depends on combustion chamber and spark plug design. Spark duration is a function of the ignition system. Spark physical length is determined by the spark plug dimensions (gap).

Ignition Timing. The ignition timing must be selected to meet the following objectives: maximize engine performance, limit fuel consumption, minimize engine knock, and minimize exhaust emissions. Unfortunately, all of these objectives cannot be achieved simultaneously under all operating conditions and compromises must be made.

It is desirable in the SI engine to have ignition of the combustible mixture occur prior to the piston reaching TDC on the compression stroke to achieve the best engine performance. The ignition spark must occur early enough to ensure that the peak cylinder combustion pressure occurs at the correct point after top dead center (ADC) under all operating conditions. Figure 12.17 is a graph of ignition angle vs. combustion pressure. The length of the combustion process from initial ignition to final combustion is approximately 2 ms. This combustion time remains relatively constant with respect to engine speed. Therefore, as the engine speed increases, the ignition spark must occur earlier in terms of crankshaft angle to ensure complete combustion.

PETITIONER'S EXHIBIT 1002
US PATENT NO. 6,581,565

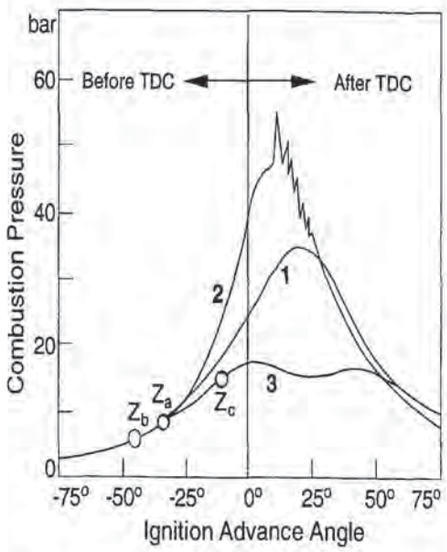


FIGURE 12.17 Combustion pressure curve for various ignition timing points: correct ignition advance Z_a (1), excessive ignition advance Z_b (2), and excessive ignition retard Z_c (3).

At low engine loads, the lower air charge and the residual gas content, due to valve overlap, serve to lengthen the time required for complete combustion. To compensate for this effect, the ignition timing is advanced at low loads to ensure that complete combustion occurs.

Ignition timing influences exhaust emissions and fuel consumption. With more advanced timing, the emission of unburned hydrocarbons (HC) and of oxides of nitrogen (NO_x) increases. Carbon monoxide (CO) emissions are not influenced greatly by ignition timing. To achieve improvements in fuel consumption, the air/fuel mixture must be lean. To ensure complete combustion for a lean mixture, the ignition timing must be advanced. However, as previously stated, advanced timing increases emissions of HC and NO_x.

Spark Ignition Systems. The general configuration of an ignition system consists of the following components: energy storage device, ignition timing mechanism, ignition triggering mechanism, spark distribution system, and spark plugs and high tension wires.

Inductive ignition systems use an ignition coil as the energy storage device. The coil also functions as a transformer, boosting the secondary ignition voltage. A typical turns-ratio of the primary to secondary winding is 1:100. Electrical energy is supplied to the coil's primary winding from the vehicle electrical system. Before the ignition point, the coil is charged during the dwell period to its interruption current. Open- or closed-loop dwell angle control ensures a sufficient interruption current even at high speeds. Sufficient ignition energy at the interruption current is ensured by an adequate coil design. At the ignition point, the primary current will be interrupted. The rapid change of the magnetic field induces the secondary voltage in the secondary winding. A distribution system assigns the high voltage to the corresponding spark plug. After exceeding the arcing over voltage at the spark plug, the coil will be discharged during the spark duration.

The ignition timing mechanism, ignition triggering mechanism, and the spark distribution system differ between ignition systems. Further discussion of these will occur within the discussion of each ignition system type.

The spark plugs provide the ignition energy via the high-tension wires to the air/fuel mixture in the cylinder to initiate combustion. The voltage required at the spark plug can be more

PETITIONER'S EXHIBIT 1002
US PATENT NO. 6,581,565

than 30 kV. Because the spark plug extends into the combustion chamber, it is exposed to extreme temperature and pressure conditions. Spark plug design and materials are chosen to ensure long-term operation under tough operating conditions.

A typical spark plug consists of a pair of electrodes, called a center and ground electrode, separated by a gap. The size of the gap is important and is specified for each plug type and engine. The center electrode is electrically connected to the top terminal of the plug which is attached to the high-tension wire. The electrical energy travels through the high-tension wire to the top terminal and down to the center electrode. The ground electrode is part of the threaded portion of the spark plug that is installed in the cylinder head. The ground electrode is at electrical ground potential because the negative terminal of the battery is also connected to the engine. The spark is produced when the high-voltage pulse travels to the center electrode and jumps the gap to the ground electrode.

Ignition System Types. Table 12.1 summarizes the various ignition systems used on SI engines.

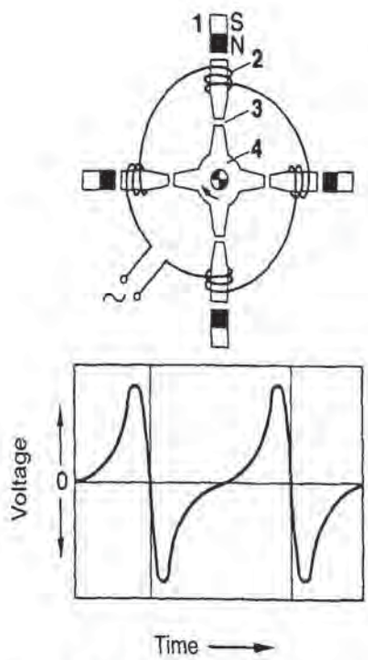


FIGURE 12.18 Induction-type pulse generator: permanent magnet (1), induction winding with core (2), variable air gap (3), trigger wheel (4).

Coil ignition. Breaker-triggered coil ignition systems have been replaced by breakerless transistorized ignition systems and are no longer installed as original equipment.

On breakerless transistorized ignition systems, the contact breaker's function is replaced by a magnetic pulse generator. The pulse generator is installed in the distributor and turns with the distributor shaft. There are commonly two types of pulse generators: induction-type and Hall-type. Induction-type pulse generators consist of a stator and a trigger wheel (Fig. 12.18). The stator consists of a permanent magnet, inductive winding, and core, and remains fixed. The trigger wheel teeth correspond to the number of cylinders, and the trigger wheel turns with the distributor shaft. The operating principle is that as the air gap changes between the stator and the rotor, the magnetic flux changes. The change in magnetic flux induces an ac voltage in the inductive winding. The frequency and magnitude of the alternating current increases with increasing engine speed. The electronic control unit or trigger box uses this information to trigger the ignition timing.

TABLE 12.1 Overview of Various Ignition Systems

	Ignition designation				
Ignition function	Coil system	Transistorized coil system	Capacitor discharge system	Electronic system with distributor	Electronic distributorless system
Ignition triggering	Mechanical	Electronic	Electronic	Electronic	Electronic
Ignition timing	Mechanical	Mechanical	Electronic	Electronic	Electronic
High-voltage generation	Inductive	Inductive	Capacitive	Inductive	Inductive
Spark distribution to appropriate cylinder	Mechanical	Mechanical	Mechanical	Mechanical	Electronic

PETITIONER'S EXHIBIT 1002
US PATENT NO. 6,581,565

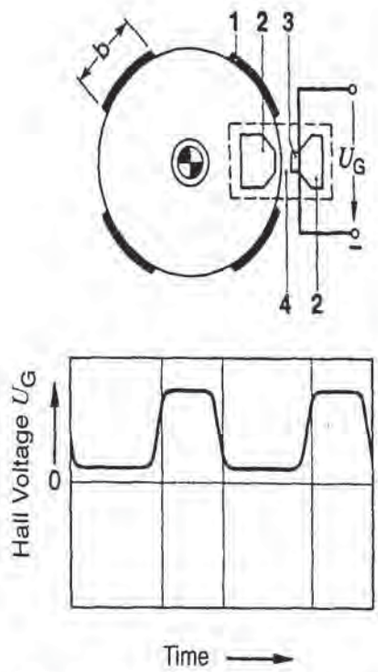


FIGURE 12.19 Hall-type pulse generator: vane (1), soft magnetic conductive elements (2), Hall IC (3), and air gap, UG-Hall sensor voltage (4).

Hall-type pulse generators utilize the Hall effect (Fig. 12.19). As the distributor shaft turns, the vanes of the rotor move through the air gap of the magnetic barrier. When the vane is not in front of the Hall IC, the sensor is subjected to a magnetic field. The magnetic flux density is high and thus the voltage U_G is at a maximum. As soon as the rotor vane enters the air gap, the magnetic flux runs through the vane area and is largely prevented from reaching the Hall layer. The voltage U_G is at a minimum. The resulting pulses switch the primary current off and on.

The distributor disburses the ignition pulses to the spark plugs via the high-tension wires in a specific sequence. It also adjusts the ignition timing by means of spark advance mechanisms. The distributor rotor is turned by the engine at one-half the crankshaft speed. The electrical energy is fed to the center of the rotor. While the rotor turns, the rotor electrode aligns with the outer electrodes that are connected to the high-tension wires. One outer electrode and high-tension wire connection exists for each cylinder. When alignment occurs between the center and outer electrode, the spark is distributed to that particular cylinder.

The spark advance mechanisms advance the ignition timing by rotating the distributor plate relative to the distributor shaft. The centrifugal advance increases the spark advance with increasing engine speed. The vacuum advance, using intake manifold vacuum, increases the spark advance at low engine speeds.

Capacitor discharge ignition system. The capacitive discharge system differs from the coil-type ignition systems previously discussed. Ignition energy is stored in the electrical field of a capacitor. Capacitance and charge voltage of the capacitor determine the amount of energy that is stored. The ignition transformer converts the primary voltage discharged from the capacitor to the required high voltage.

Electronic ignition—with distributor. Electronic ignition calculates the ignition timing electronically (Fig. 12.20). This replaces the function of the centrifugal advance and vacuum advance in the distributor discussed on the previous coil ignition systems. Because the ignition timing is not limited by mechanical devices, the optimal timing can be chosen for each engine operating point. Figure 12.21 is a comparison of an ignition map from a mechanical advance system and a map of an electronically optimized system. Also, additional influences such as engine knock detection can be used to modify the ignition timing. The engine speed input and crankshaft position input can be obtained from a sensor mounted near the crankshaft. Precision is improved over using the distributor-mounted trigger. This input is provided to the electronic control unit (ECU) along with the engine temperature and engine load. The ECU references data tables to determine the optimal spark advance for each engine operating condition. Additional corrections to the spark timing, such as for EGR usage or knock sensor detection, are made in the ECU.

Electronic ignition—distributorless. On distributorless ignition systems, the high voltage distribution is accomplished by using either single or double spark ignition coils. Ignition timing is determined by the ECU, as discussed for electronic ignition with distributor. For the double spark ignition coils, one coil exists for two corresponding cylinders. Two high-tension

PETITIONER'S EXHIBIT 1002
US PATENT NO. 6,581,565

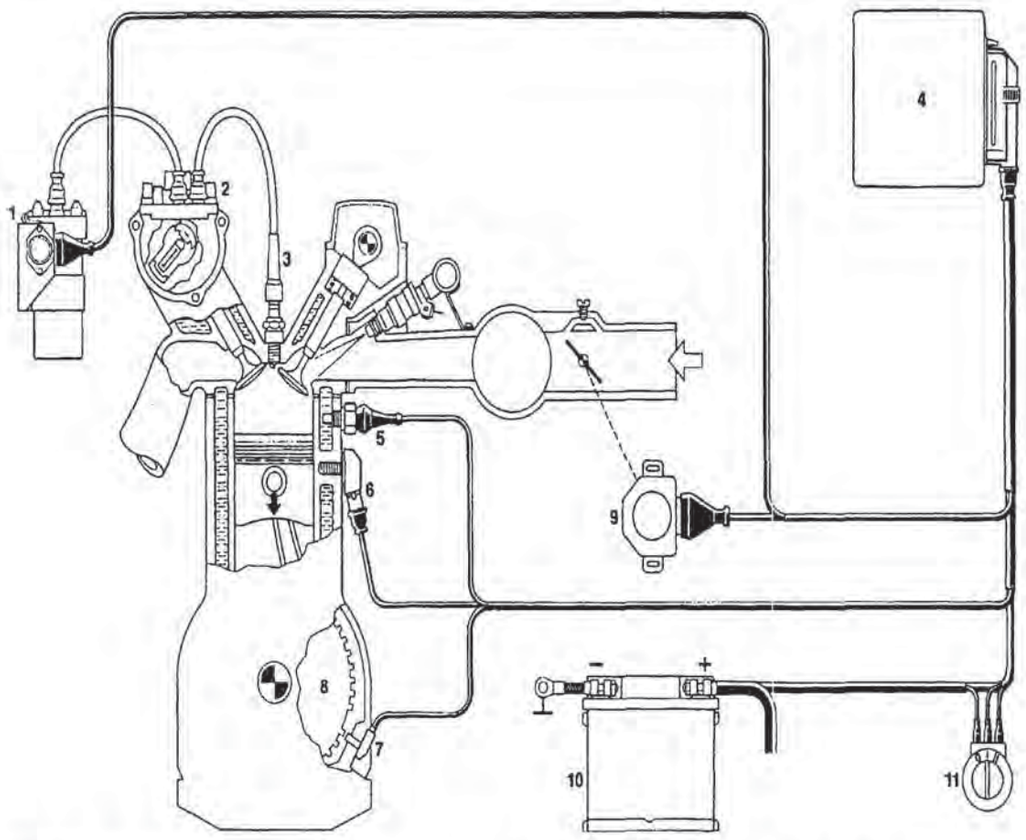


FIGURE 12.20 Schematic of an electronic ignition system with distributor: ignition coil (1), high-voltage distributor (2), spark plug (3), ECU (4), coolant temperature sensor (5), knock sensor (6), engine speed and crankshaft reference sensor (7), sensor wheel (8), throttle valve (9), battery (10), and ignition switch (11).

wires are routed from each coil to two cylinders, which are 360° out of phase. When the coil output stage is triggered via the ECU, a spark is delivered to both cylinders. One cylinder will be on the compression stroke, the other on the exhaust stroke. Because both cylinders are fired together, for a given crankshaft rotation, one will always be on the compression stroke and the other on the exhaust stroke. Therefore, there is no need to know which cylinder is compressing the ignitable mixture.

On single spark ignition coils, one coil exists for each cylinder. Each coil triggers only once during the four-stroke cycle. Because of this, it must be known which cylinder is on the compression stroke. Synchronization with the camshaft must occur. The information needed on camshaft position is supplied by a phase sensor mounted on the camshaft.

12.3 COMPRESSION IGNITION ENGINES

12.3.1 Engine Control Functions

Electronic engine controls are now being used on compression ignition (diesel) engines. These controls offer greater precision and control of fuel injection quantity and timing, engine speed, EGR, turbocharger boost pressure, and auxiliary starting devices. The following inputs

PETITIONER'S EXHIBIT 1002
US PATENT NO. 6,581,565

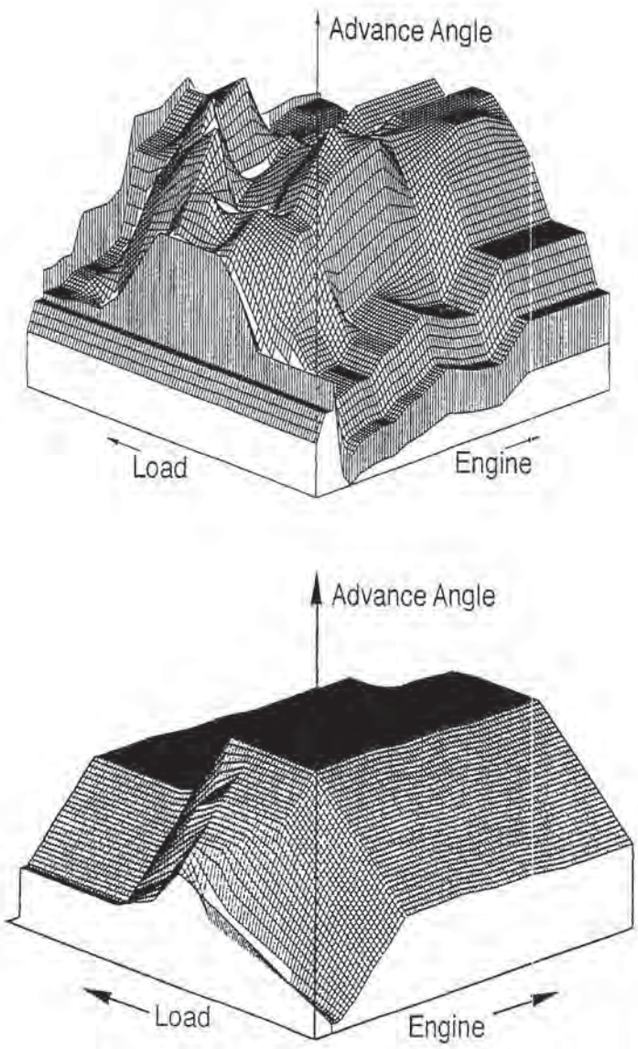


FIGURE 12.21 Ignition timing maps: electronically optimized (*above*) and mechanical advance system (*below*).

are used to provide the ECU with information on current engine operating conditions: engine speed; accelerator position; engine coolant, fuel, and inlet air temperatures; turbocharger boost pressure, vehicle speed, control rack, or control collar position (for control of fuel quantity); and amospheric pressure. Figure 12.22 is a schematic of an electronic engine control system on an in-line diesel fuel injection pump application.

Fuel Quantity and Timing. The fuel quantity alone controls a compression ignition engine's speed and load. The intake air is not throttled as in a spark ignition engine. The quantity of fuel to be delivered is changed by increasing or decreasing the length of fuel delivery time per injection. On the injection pump, the delivery time is controlled by the position of the control rack on in-line pumps and the position of the control collar on distributor-type pumps. An ECU-controlled actuator is used to move the control rack or the collar to increase or decrease the fuel delivery time. The ECU determines the correct length of delivery time (expressed as a function of control rack or collar position) using performance maps based on engine speed and calculated fuel quantity. Corrections and/or limitations as functions of

PETITIONER'S EXHIBIT 1002
US PATENT NO. 6,581,565

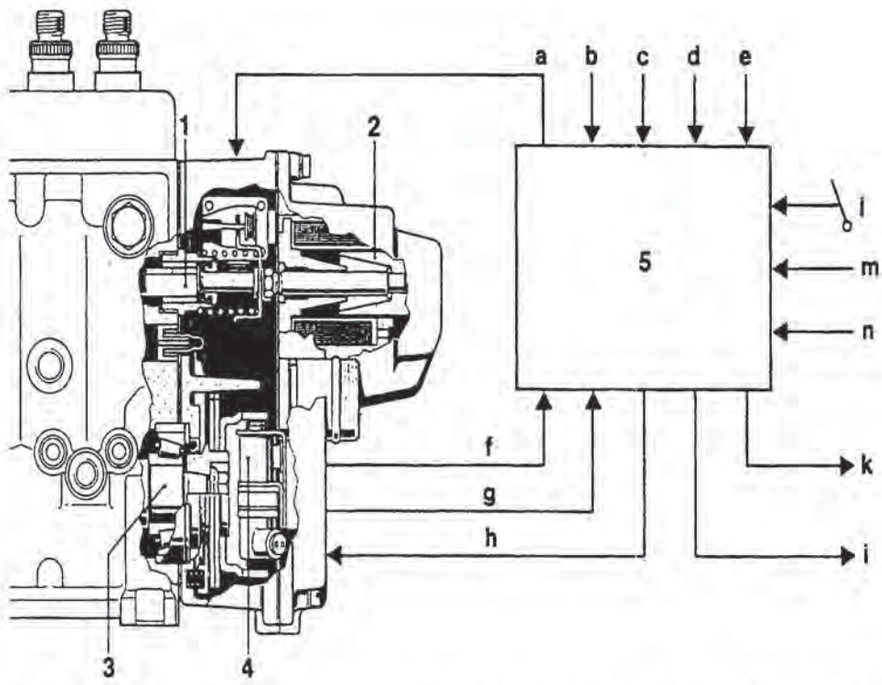


FIGURE 12.22 Electronic engine control system for an in-line injection pump: control rack (1), actuator (2), camshaft (3), engine speed sensor (4), ECU (5). Input/output: redundant fuel shutoff (a), boost pressure (b), vehicle speed (c), temperature—water, air, fuel (d), intervention in injection fuel quantity (e), speed (f), control rack position (g), solenoid position (h), fuel consumption and engine speed display (i), system diagnosis information (k), accelerator position (l), preset speed (m), and clutch, brakes, engine brake (n).

engine speed, temperature, and turbocharger boost pressure are used to modify the delivery time. In addition, the control rack or collar actuator contains a position sensor that provides feedback to the ECU on controller position. If the requested position differs from the commanded position, the ECU continues to move the controller via the actuator until the commanded and actual position are the same.

The start of injection time of the fuel at the cylinder is a function of the wave propagation speed (i.e., the speed of sound) of the fuel from the fuel injection pump to the injector. Because this time remains a constant, at increasing engine speed the delivery of fuel at the cylinder would be delayed with reference to crankshaft angle. Therefore, the timing at the injection pump must be advanced with increasing engine speed so that the start of injection occurs at the same crankshaft angle at higher engine speeds. Selection of injection timing has a large impact on exhaust emissions and engine noise. Delaying the start of injection reduces NO_x emissions, but excessive delay increases HCs in the exhaust. A 1° deviation in injection timing can increase NO_x emissions by 5 percent and HC emissions by as much as 15 percent. Therefore, precise control of the start of injection is essential.

Although many systems use mechanical devices to control injection timing, electronic control of injection timing is being used on some pump types. The advantage of electronic control is that a sophisticated timing data map can be used that provides the best injection timing for exhaust emissions under various operating conditions. On electronic control systems, the start of injection is monitored at the injector nozzle by a needle-motion sensor. The ECU uses this information to determine and control the injection timing. The timing is then modified by control of a pulse-width modulated solenoid valve. The valve varies the pressure exerted on the spring-loaded timing device plunger. The plunger rotates the pump's collar ring (for distributor type pumps) in the opposite direction of the pump's rotation which advances the timing.

PETITIONER'S EXHIBIT 1002
US PATENT NO. 6,581,565

Speed Control. As was mentioned previously, for a CI engine, fuel quantity alone controls the engine's speed and load. Therefore, presuming adequate injected fuel quantity, an unloaded CI engine can speed up out of control and destroy itself. Because of this, a governor is required to limit the engine's maximum speed. In addition, governors are also used for low idle and cruise control to maintain a constant engine or vehicle speed and meter the correct fuel for cold-starting. Fuel is also controlled as a function of speed and boost pressure to limit smoke levels, engine torque, and exhaust gas temperatures. On an electronically controlled CI engine, the governor's functions are controlled by the fuel delivery system described previously. Engine speed is provided by an RPM sensor that monitors the periods of angular segments between the reference marks on the engine's flywheel or in the in-line injection pump.

EGR Control. Rerouting of exhaust gases into the intake air stream is known as exhaust gas recirculation (EGR). EGR reduces the amount of oxygen in the fresh intake charge while increasing its specific heat. This lowers combustion temperatures and results in lower NO_x emissions. However, excessive amounts of EGR result in higher emissions of soot (particulates), CO, and HCs all due to insufficient air. Also, the introduction of EGR can have an adverse affect on driveability during cold-engine operation, full-load operation, and at idle. It is best, therefore, to control the EGR valve with the ECU. Both pneumatically controlled and solenoid-controlled EGR valves are in use. The ECU determines when and how much EGR will occur based on engine temperature and accelerator position.

Turbocharger Boost Pressure Control. Engines that have turbochargers benefit significantly from electronic boost pressure control. If only a pneumatic-mechanical wastegate is used, only one boost pressure point for the entire operating range is used to divert the exhaust gas away from the turbine side of the turbocharger. This creates a compromise for part-load conditions because all the exhaust gases must pass the turbine. The result is increased exhaust backpressure, more turbocharger work, more residual exhaust gas in the cylinders, and higher charge air temperatures.

By controlling the wastegate with a pulse-width-modulated solenoid valve, the wastegate can be opened at different pressures depending on the engine operating conditions. Therefore, only the level of air charge pressure required is developed. The electronic control unit uses information on engine speed and accelerator position to reference a data table and the proper boost pressure (actually, duty cycle of the control valve) is determined. On systems using intake manifold pressure sensors, a closed-loop control system can be developed to compare the specified value with the measured value.

Glow Plug Control. Electronic control of the glow plug duration can be handled by the ECU or a separate control unit. Input for determining glow time is from an engine coolant temperature sensor. At the end of the specified glow period, the controller turns out the start indicator light to signal the driver that the engine can be started. The glow plugs remain energized while the starter is engaged. An engine load monitor is used to switch off the glow process after start. To limit the loads on the battery and the glow plugs, a safety override is also used.

12.3.2 Fuel Delivery Systems

The diesel fuel delivery system comprises a low- and high-pressure side. On the low-pressure side is the fuel tank, fuel filter, fuel supply pump, overflow valve, and fuel supply lines. The high-pressure side is initiated in the plunger and barrel assembly and continues through the delivery valve, high-pressure injection lines, and injection nozzle.

The fuel injection pump must deliver fuel at a pressure between 350 and 1200 bar, depending on the engine's combustion configuration. The quantity and timing of injection must be precisely controlled to achieve good mixture quality and to minimize exhaust emissions.

PETITIONER'S EXHIBIT 1002
US PATENT NO. 6,581,565

Fuel Injection Process. An engine-driven camshaft (in-line pump) or cam plate (distributor pump) drives the injection pump's plunger in the supply direction, creating pressure in the high-pressure gallery. The delivery valve responds to the increase in pressure by opening. This sends a pressure wave to the injection nozzle at the speed of sound. The needle valve in the nozzle overcomes the spring force of the injection nozzle spring and lifts from its seat when the opening pressure is reached. Fuel is then injected from the spray orifices into the engine's combustion chamber. The injection process ends with the opening of the spill port in the plunger and barrel assembly. This causes the pressure in the pump chamber to collapse, which then causes the delivery valve to close. Due to the action of the delivery valve relief collar, the pressure in the injection line is reduced to the "stand-by pressure." The stand-by pressure is determined to ensure that the injector nozzle closes quickly to eliminate fuel dribble, and the residual pressure waves in the lines prevent the nozzles from reopening.

ABOUT THE AUTHORS

GARY C. HIRSCHLIEB is chief engineer, engine management systems, for the Robert Bosch Corp. He previously held various engineering and sales responsibilities with Bosch. In his earlier career, he worked as a senior engineer in powertrain development for Ford tractor operations, and as a sales engineer with GTE, and as an engineer in plant engineering for GM Truck and Coach.

GOTTFRIED SCHILLER is engineering manager, engine management systems, for Robert Bosch Corp. His previous positions with Bosch included applications engineering, engine management systems; application engineer, diesel systems; and development engineer, diesel products.

SHARI STOTTLER is now a self-employed technical writer, but, until 1993, she was a senior application engineer with Robert Bosch Corp. Prior to that she had been an engineering project coordinator for Honda of North America, Manufacturing, and a product engineer with General Motors Corp.

PETITIONER'S EXHIBIT 1002
US PATENT NO. 6,581,565

CHAPTER 13
TRANSMISSION CONTROL

Kurt Neuffer, Wolfgang Bullmer, and Werner Brehm
Robert Bosch GmbH

13.1 INTRODUCTION

In North America and Japan, 80 to 90 percent of all passenger cars sold have automatic transmissions (ATs), but in Europe only 10 to 15 percent of passenger cars sold have ATs. There are two main reasons for the difference. In Europe, drivers tend to view ATs, compared to manual transmissions, as detrimental to driveability and responsible for a somewhat higher fuel consumption. But implementation of electronic control concepts has invalidated both of those arguments.

Since the introduction of electronic transmission controls units (TCUs) in the early 1980s by Renault and BMW (together with a four-speed transmission from Zahnradfabrik Friedrichshafen, or ZF), the acceptance of the AT rose steeply, even in Europe. For this reason, all new ATs are designed with electronic control. The market for ATs is divided into stepped and continuously variable transmissions (CVTs). For both types the driver gets many advantages. In stepped transmissions, the smooth shifts can be optimized by the reduction of engine torque during gear shift, combined with the correctly matched oil pressure for the friction elements (clutches, brake bands). The reduction of shift shocks to a very low or even to an unnoticeable level has allowed the design of five-speed ATs where a slightly higher number of gear shifts occur. In today's standard systems, the driver can choose between sport and economic drive programs by operating a selector switch. In highly sophisticated newer systems, the selection can be replaced by the self-adaptation of shift strategies. This leads not only to better driveability but also to a significant reduction in fuel consumption. Additionally, a well-matched electronic control of the torque converter lockup helps to improve the yield of the overall system. Both automotive and transmission manufacturers benefit from the reduced expense resulting from the application of different car/engine combinations. Different shift characteristics are easy to implement in software, and much adaptation can be achieved by data change, leaving the transmission hardware and TCU unchanged. The reduction of power losses in friction elements increases the life expectancy and enables the optimization of transmission hardware design.

With the CVT, one of the biggest obstacles to the potential reduction in fuel consumption by operating the engine at its optimal working point is the power loss from the transmission's oil pump. Only with electronic control is it possible to achieve the required yield by matching the oil mass-stream and oil pressure for the pulleys to the actual working conditions.

To guarantee the overall economic solution for an electronically controlled transmission, either stepped or CVT, the availability of precision electrohydraulic actuators is imperative.

PETITIONER'S EXHIBIT 1002
US PATENT NO. 6,581,565

13.2 SYSTEM COMPONENTS

The components of an electronic transmission control system are a transmission which is adapted to the electronic control requirements and an electronic control unit with corresponding inputs and outputs and attached sensor elements.

13.2.1 Transmission

The greatest share of electronically controlled transmissions currently on the market consists of four- or five-speed units with a torque converter lockup clutch, commanded by the control unit. Market share for five-speed transmissions is continuously increasing. With electronically controlled transmissions there are numerous possibilities to substitute mechanical and hydraulic components with electromechanical or electrohydraulic components. One basic method is to substitute only the shift point control. In a conventional pure hydraulic AT, the gear shifts are carried out by mechanical and hydraulic components. These are controlled by a centrifugal governor that detects the vehicle speed, and a wire cable connected to the throttle plate lever. With an electronic shift point control, on the other hand, an electronic control unit detects and controls the relevant components. In the transmission's hydraulic control unit, mechanical and hydraulic components are replaced by electrohydraulic controlling elements, usually in the form of electrohydraulic on/off solenoids. This way the number of solenoids, as well as the control logic, can be varied over a wide range. For example, for each gear, one specific solenoid can operate the relevant clutch for this gear shift. Alternatively, there can be one solenoid for each gear change, which is switched corresponding to the shift command. In this way, only three solenoids are required in a four-speed transmission. In some current designs, the gears are controlled by a logical combination of solenoid states. This design needs only two gear-controlling solenoids for a four-speed transmission. For five-speed applications, accordingly, three solenoids are required (Table 13.1)

TABLE 13.1 Example of a Gear-Solenoid Combination for a Five-Speed Transmission Application

	Solenoid 1	Solenoid 2	Solenoid 3
1st gear	on	on	on
2nd gear	on	on	off
3rd gear	on	off	off
4th gear	off	off	off
5th gear	off	on	off

The hydraulic pressure is controlled in this basic application by a hydraulic proportional valve which is, in turn, controlled by a wire cable connected to the throttle plate lever. With this design, the shift points can be determined by the electronic TCU, resulting in a wide range of freely selectable driving behaviors regarding the shift points. It is also possible to use different shift maps according to switch or sensor signals. The influence on driving comfort during gear shifting in this electronic transmission control application has important restrictions. The only possible way to control shift smoothness is with an interface to the electronic engine management. This way, the engine output torque is influenced during gear shifting. A systematic wide-range control of the hydraulic pressure during and after the gear shift necessitates the replacement of the hydraulic pressure governor with an electronically controlled hydraulic solenoid. This design allows the use of either a pulse-width-modulated (PWM) solenoid or a pressure regulator. The choice of which type of pressure control solenoid to use results from the requirements concerning shift comfort under all driving conditions. For

PETITIONER'S EXHIBIT 1002
US PATENT NO. 6,581,565

present-day designs with high requirements for shift comfort during the entire life of the transmission, at all temperatures, and with varying oil quality, the analog pressure control solenoid is superior to the usual PWM solenoid, providing there is no pressure sensor in operation as a guideline for pressure regulation. This application usually uses one central controlling element in the transmission for the pressure regulation to control the shift quality.

In other transmission developments, the shift quality is further increased using electronically controllable brake elements (brake bands) for some specific gear changes. In this case, the flywheel effect of the revolving elements is limited by an electronic control of a brake band according to an algorithm or special timing conditions.

The most sophisticated transmission application to date is so designed that overrunning clutches are eliminated and gear changes are exclusively controlled by the electronic control unit with pressure regulator solenoids.[1] This application is characterized by extremely high demands on the electronic TCU concerning real-time behavior and data handling. The relationship between weight, transmission outline, and transferrable torque has reached a high level. Compared to transmissions with overrun clutches, the necessary fitting dimensions are reduced.

Present electronically controlled ATs usually have an electronically commanded torque converter clutch, which can lock up the torque converter between the engine output and the transmission input. The torque converter clutch is activated under certain driving conditions by a solenoid controlled by the electronic TCU. The solenoid design, depending on the requirements of TCC functions and shift comfort, can either be an on/off solenoid, a PWM solenoid, or a pressure regulator. Locking up the torque converter eliminates the slip of the converter, and the efficiency of the transmission system is increased. This results in an even lower fuel consumption for cars equipped with AT.

13.2.2 Electronic Control Unit

Another important component in electronic transmission control is the electronic control unit, which is designed according to the requirements of the transmission and the car environments. The electronic control unit can be divided into two main parts: the hardware and the corresponding software.

Hardware. The hardware of the electronic control unit consists of the housing, the plug, the carrier for the electronic devices, and the devices themselves. The housing, according to the requirements, is available as an unsealed design for applications inside the passenger compartment or within the luggage compartment. It is also possible to have sealed variants for mounting conditions inside the engine compartment or at the bulkhead. The materials for the housing can be either various plastics or metals. There are many different nonstandardized housings on the market. The various outlines and plug configurations differ, depending upon the manufacturer of the electronic unit. The plug configuration, i.e., the number of pins and the shape, depends on the functions and the requirements of the automotive manufacturer. The number of pins is usually less than 100. Some control unit manufacturers try to standardize their plugs and housings throughout all their electronic control units, such as engine management, ABS, traction control, and others. This is important to simplify and to standardize the unit production and the tests during manufacturing.

The carrier for the electronic devices is usually a conventional printed circuit board (PCB). The number of layers on the PCB depends on the application. For units with a complex device structure and high demands for electromagnetic compatibility, multilayer applications are in use. In special cases, it is possible to use ceramics as a carrier. There are usually some parts of the electronic circuit, resistors for example, designed as a thick-film circuit on the hybrid. In this case the electronic unit is manufactured as a solder hybrid or as a bond hybrid with direct-bonded integrated circuit devices. Some single applications exist with a flex-foil as a carrier for the electronic devices. These applications are limited to very special requirements.

PETITIONER'S EXHIBIT 1002
US PATENT NO. 6,581,565

The transmission control area requires some specially designed electronic devices, in particular, the output stages for the actuators of pressure regulation and torque converter clutch control. These actuators for pressure control have extremely high demands regarding accuracy of the actuator current over the whole temperature range and under all conditions independent of battery voltage and over the entire lifetime. There are some known applications of customer-specific integrated circuits or devices. Here, special attention paid to quality and reliability over the entire lifetime is necessary to meet the continuously increasing quality requirements of the automotive market. Currently, there is an increasing spread of surface-mounted devices in transmission control applications. This is why the unit size is continuously decreasing despite an increasing number of functions.

On the functional side, the hardware configuration can be divided into power supply, input signal transfer circuits, output stages, and microcontroller, including peripheral components and monitoring and safety circuits (Fig. 13.1). The power supply converts the vehicle battery voltage into a constant voltage required by the electronic devices inside the control unit. Accordingly, special attention must be paid to the protection of the internal devices against destruction by transients from the vehicle electrical system such as load dump, reverse battery polarity, and voltage peaks. Particular attention is also necessary in the design of the elec-

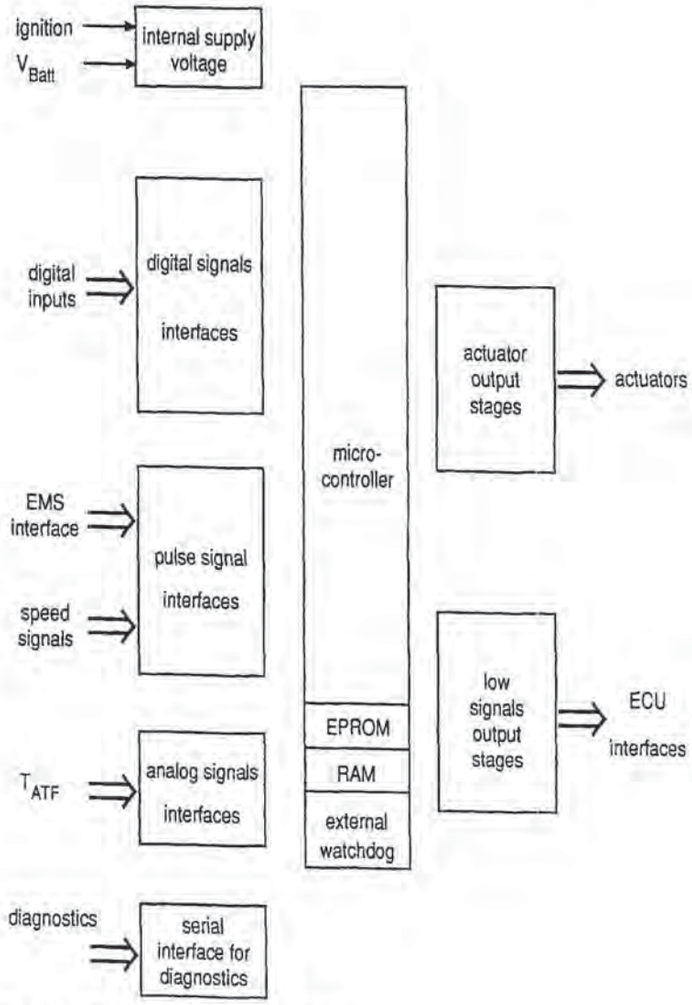


FIGURE 13.1 Overview of hardware parts.

PETITIONER'S EXHIBIT 1002
US PATENT NO. 6,581,565

tronic ground concept for the control unit, especially where the electromagnetic compatibility and RF interference is concerned. This is very important to prevent undesired gear shifting that may be troublesome for drivers. One part of the input circuit is the preparation of the digital signals, such as position switch, program selector, and kickdown switch. A second part is the transfer of the analog signals like ATF temperature and voltages according to potentiometer states. The third part is the interface to other electronic control units, especially to the engine management system. Here the single signal lines between the control units will be increasingly substituted by bus systems like CAN. The fourth part is the preparation of the transmission-specific signals from the speed sensors inside the transmission.

The calculators inside the control units are usually microcontrollers. The real-time requirements and the directly addressable program storage size of the selected microcontrollers are determined by the functions of the transmission control and the car environment. In present applications, either 8-bit or 16-bit microcontrollers are in use. There are systems with 32-bit microcontrollers in development for new, highly sophisticated control systems with increasing functional and extreme real-time requirements originating from the transmission concept. The memory devices for program and data are usually EPROMS. Their storage capacity is, in present applications, up to 64 Kbytes. Future applications will necessitate storage sizes up to 128 Kbytes. The failure storages for diagnostics and the storage for adaptive data are in conventional applications, battery voltage-supplied RAMs. These are increasingly being replaced by EEPROMs.

There are usually watchdog circuits in various configurations in use regarding safety and monitoring. These can be either a second, low-performance microcontroller, a customer-specific circuit, or a circuit with common available devices. The output stages can be divided into high-power stages for the transmission actuator control and low-power stages like lamp drivers or interfaces to other electronic control units. The low-power output stages are mostly conventional output drivers either in single or in multiple applications, which are mainly protected against short circuits and voltage overloads.

For the transmission solenoid control, special output stages are necessary, and they are specialized for operation with inductive actuators. The pressure regulation during shifting in some applications requires high accuracy and current-regulated output stages are needed. These are mainly designed as customer-specific devices. The type and number of solenoid output stages depend on the control philosophy of the transmission: they are generally of a special design for specific transmission applications. During the preparation of the speed sensor signals, attention must be paid to the electromagnetic compatibility and radio frequency interference conditions.

Software. The software within the electronic transmission control system is gaining increasing importance due to the increasing number of functions which, in turn, requires increasing software volume. The software for the control unit can be divided into two parts: the program and the data. The program structure is defined by the functions. The data are specific for the relevant program parts and have to be fixed during the calibration stage. The most difficult software requirements result from the real-time conditions coming from the transmission design. This is also the main criterion for the selection of the microcontroller (Fig. 13.2).

The program is generally made up in several parts:

- Software according to the special microcontroller hardware; e.g., I/O preparation and filter, driver functions, initialization of the microcontroller and the control unit, internal services for the controller peripheral devices, and internal software services like operating systems.
- Software coming from the defined functions, originating from specific transmission and car functions.
- Parts concerning safety functions like output switch-off, substitute values for the input signals, and safety states of the microcontroller environment in case of failures. Depending on the requirements, there can be a software watchdog or a hardware-configured watchdog circuit in use. The watchdog instruction is also part of the security software.

PETITIONER'S EXHIBIT 1002
US PATENT NO. 6,581,565

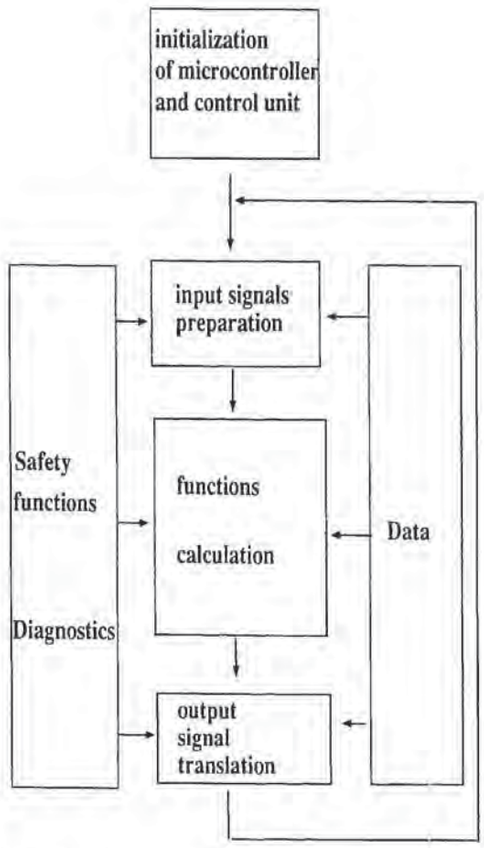


FIGURE 13.2 Software structure overview.

- Diagnostic and communication software for the self-test of the control unit and also the test of the control unit environment.

These functions are related to the defined functions of the electronic control system. Parts of the software component are usually the output stages monitoring, the input monitoring, and the diagnosis of the microcontroller environment. Failure handling and storage is gaining importance as system complexity increases. These diagnostic functions are also very useful for the service station to determine the reason for eventual problems. Part of these functions is reserved for the communication software needed for the test equipment to read the failures stored during car service. Current protocols are standardized communication protocols like ISO 9141. There is an increasing share of bus systems for communication with other electronic control units, using standardized protocols like CAN, VAN, or J1850. These bus systems allow an increasing unit function by changing software when other control units are added to the bus.

Most software models are written directly in an assembler to meet the real-time requirements and because there is a limited memory size in common mass production units. The number of powerful, cost-effective microcontrollers is continuously increasing. The availability of memory components with larger storage sizes suitable for automotive use is also rising, making it possible to use a higher programming language in future developments. This allows an ingenious structure of software models and an application of operating systems. This can be followed by an effective distribution of functions during and outside gear shifting with related time requirements and event management. This type of program structure improves the function of the electronic TCU because of the accelerated handling of time-critical functions during gear shifting.

PETITIONER'S EXHIBIT 1002
US PATENT NO. 6,581,565

The second software part, data, can be divided into fixed data, which is related to fixed attributes of the system; e.g., the number of actuators, and calibration data for system tuning. The calibration data can be adapted to changing parameters of the system such as the engine, vehicle, and transmission characteristics. The fixing of calibration data takes place during the tuning stage of the vehicle and has to be redetermined for each type of vehicle and transmission. With some applications, the calibration data are added to a basic program during the vehicle production according to different types of cars by the so-called end-of-line programming. This means that the units can be programmed with the calibration data with closed housings by a special interface. The share of software development in relation to the total development time is increasing continuously. The requirements for real-time behavior and memory size are rising in accordance with the considerably increasing demands for shift comfort and self-learning functions. This requires an ingenious structure of the software and an event-related distribution of software models, especially during gear shifting. The rising software complexity with simultaneously increasing quality requirements causes higher demands for software quality control.

13.2.3 Actuators

Electrohydraulic actuators are important components of the electronic transmission control systems.[2] Continuously operating actuators are used to modulate pressure, while switching actuators function as supply and discharge valves for shift-point control. Figure 13.3 provides a basic overview of these types of solenoids.

Important qualities for the use of actuators in ATs are low hydraulic resistance to achieve high flow rates, operation temperature range from –40 to +150 °C, small power loss, minimized heat dissipation in the ECU's output stages, small size and low weight, highest reliability in heavily contaminated oils, maximum accuracy and repeatability over lifetime, short reaction times, pressure range up to 2000 kPa, maximum vibration acceleration of 300 m/s^2, and high number of switch operations.

A very important aspect is that the hardware and software of the ECU be developed, taking into account the electrical specifications of the solenoid to obtain an optimized complete system concerning performance and cost.[6,7] For further details in design and application, refer to Sec. 10.3.5.

It should be noted that these characteristics can be varied over a wide range and that many other types of solenoids exist or are in development for the special requirements of new applications.

13.3 SYSTEM FUNCTIONS

Functions can be designated at systems functions if the individual components of the total electronic transmission control system cooperate efficiently to provide a desired behavior of the transmission and the vehicle. There are different stages of functionality which have different effects on driving behavior and shift characteristics (Fig. 13.4). In general, there is an increasing complexity of the system relating to all components to improve the translation of driver behavior into transmission action. That means that the expense of actuators, sensors, and links to other control units is increasing, as is the expense of the TCU software and hardware in the case of high-level requirements regarding driveability and shift comfort. Figure 13.4 shows three main areas. These will be discussed in detail in the following material.

13.3.1 Basic Functions

The basic functions of the transmission control are the shift point control, the lockup control, engine torque control during shifting, related safety functions, and diagnostic functions for

PETITIONER'S EXHIBIT 1002
US PATENT NO. 6,581,565

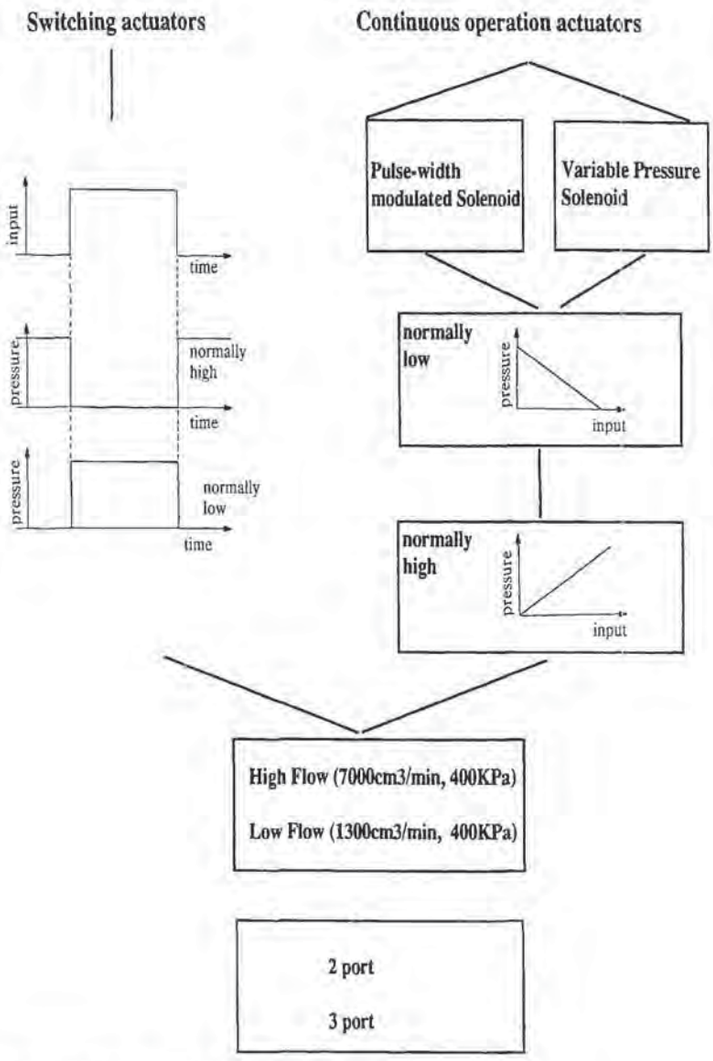


FIGURE 13.3 Electrohydraulic actuators for automatic transmissions.

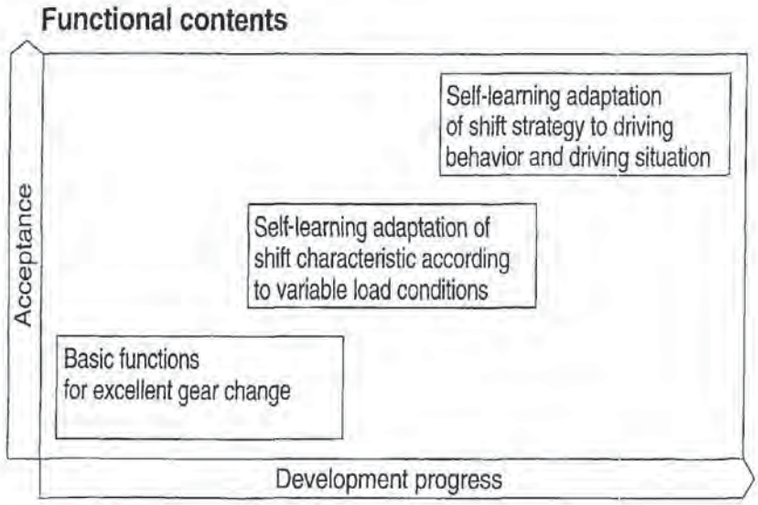


FIGURE 13.4 Relationship between driving characteristic and function complexity.

PETITIONER'S EXHIBIT 1002
US PATENT NO. 6,581,565

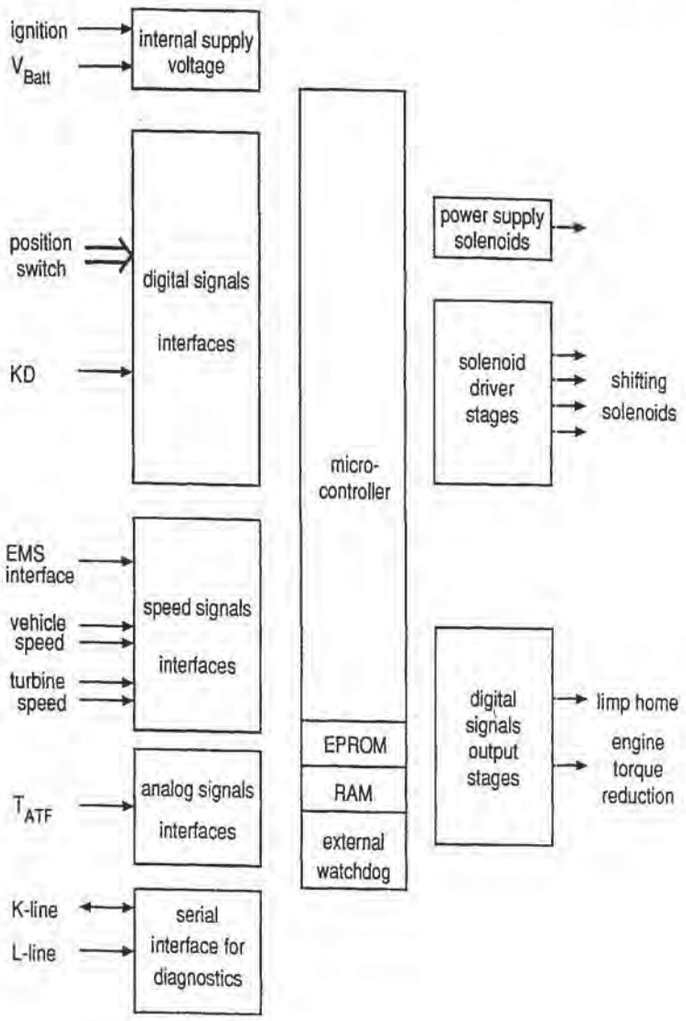


FIGURE 13.5 Structure of a basic transmission electronic control unit.

vehicle service. The pressure control in transmission systems with electrical operating possibilities for the pressure during and outside shifting can also be considered as a basic function. Figure 13.5 shows the necessary inputs and outputs as well as the block diagram of an electronic TCU suitable for the basic functions.

Shift Point Control. The basic shift point control uses shift maps, which are defined in data in the unit memory. These shift maps are selectable over a wide range. The shift point limitations are made, on the one hand, by the highest admissible engine speed for each application and, on the other hand, by the lowest engine speed that is practical for driving comfort and noise emission. The inputs of the shift point determination are the throttle position, the accelerator pedal position, and the vehicle speed (determined by the transmission output speed). Figure 13.6 shows a typical shift map application of a four-speed transmission.

To prevent overly frequent shifting between two gears, a hysteresis between the upshift and the downshift characteristic is incorporated. The hysteresis is determined by the desired shifting habit of the transmission and, alternatively, the car behavior. In the event that the particular shift characteristic is crossed by one of either of the two input valves, the electronic ECU releases the shift by activating the related actuators. This can be a direct shift into the

PETITIONER'S EXHIBIT 1002
US PATENT NO. 6,581,565

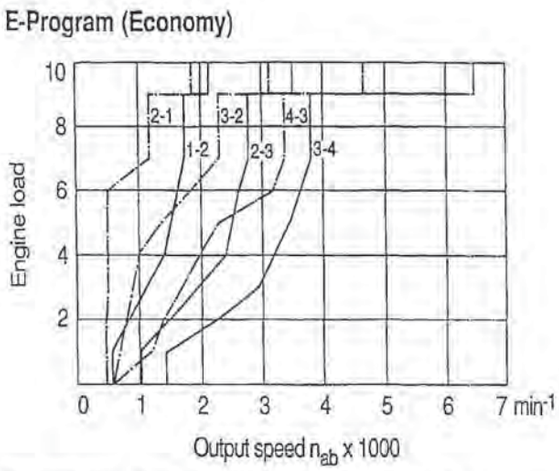


FIGURE 13.6 Shift characteristics of a four-speed application.

target gear or by a serial activation of specific actuators in a fixed sequence to the target gear, depending on the transmission hardware design.

Lockup Control/Torque Converter Clutch.[8] The torque converter clutch connects both functional components of the hydraulic converter, the pump and the turbine. The lockup of the clutch reduces the power losses coming from the torque converter slip. This is a permanent slip because it is necessary in principle to have a slip between the pumpwheel and the turbine to translate torque from the engine output to the transmission input. To increase the efficiency of the lockup, it is necessary to close the clutch as often as possible. On the other hand, the torque converter is an important component to prevent vibrations of the powertrain. The activation of the lockup is, therefore, a compromise between low fuel consumption and high driving comfort. The shift points of the lockup are determined in the same way as the determination of the shift point in the gear shift point control. Usually there is one separate characteristic curve for the lockup for each gear. To prevent powertrain vibrations, it is advisable to open the lockup during coasting to use the damping effect of the torque converter. In the case of a high positive gradient of the accelerator pedal with low engine speed, the converter clutch has to open to use the torque gain of the converter for better acceleration of the car. In some applications, the lockup is opened during shifting for improved shift comfort. After shifting, the lockup can be closed again. When driving in first gear, the lockup is usually open, because the time spent in first gear is usually very low and, therefore, the frequency of lockup shifting versus gear shifting becomes very high. This may result in decreased driving comfort. A second reason is the improved acceleration of the car in first gear when using the converter gain for wheel torque.

Engine Torque Control During Shifting.[8] The engine torque control requires an interface to an electronic engine management system. The target of the engine torque control, torque reduction during shifting, is to support the synchronization of the transmission and to prevent shift shocks.

In conventional applications, the engine torque reduction originates from an ignition angle control. The timing and absolute value of the ignition control depends on the operating conditions concerning actual engine torque and shifting type.

Upshift. The upshift occurs without an interruption of the tractive power. The engine torque reduction may be activated if the clutch of the target gear stays with the translation of torque. The beginning of the engine torque reduction is determined by the course of engine or transmission input speed. There it is important to detect a decreasing speed. The start of the

PETITIONER'S EXHIBIT 1002
US PATENT NO. 6,581,565

torque reduction is characterized by a specific speed difference. The end of the torque reduction is activated at an applicable speed lead before reaching the synchronous speed of the new gear.

The power losses, which have to be picked up by the clutches, are dependent on the engine torque and the slipping time

$$Q = f \times (M_{eng} \times t_s + Q_{kin}) \tag{13.1}$$

where Q = power losses
M_{eng} = engine torque
t_s = slipping time
Q_{kin} = kinetic energy of revolving elements

It is possible to reduce the temperature stress to the clutches by reducing the engine torque and, consequently, by increasing the slipping time at a fixed possible maximum power loss Q [Eq. (13.1)]. Figure 13.7 shows a typical upshift characteristic.

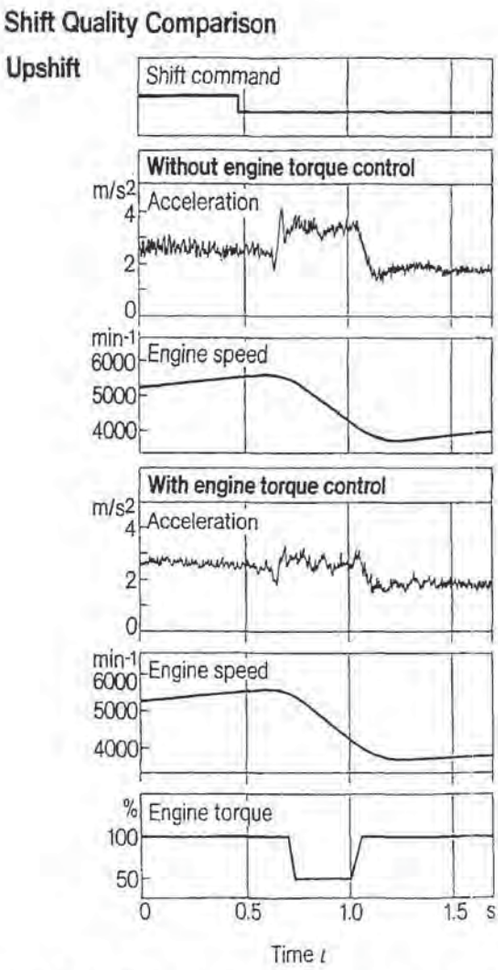


FIGURE 13.7 Timing of engine torque reduction during upshift.

Downshift. Downshift under driving conditions results in a short interruption of the tractive power. At the synchronous point, the tractive power is in operation. The higher revolving energy, on the other hand, results in undesired vibrations of the powertrain. To prevent such

PETITIONER'S EXHIBIT 1002
US PATENT NO. 6,581,565

vibrations, it is necessary to reduce the engine output torque before reaching the synchronous point of the new gear. When the transmission input speed reaches the synchronous speed of the new gear, the engine torque has to increase to the nominal value. The increase is usually applied as a torque ramp. Figure 13.8 shows a typical characteristic of a downshift. The values and timing of the engine torque reduction are generally part of the special calibration data for each combination of vehicle, engine, and transmission.

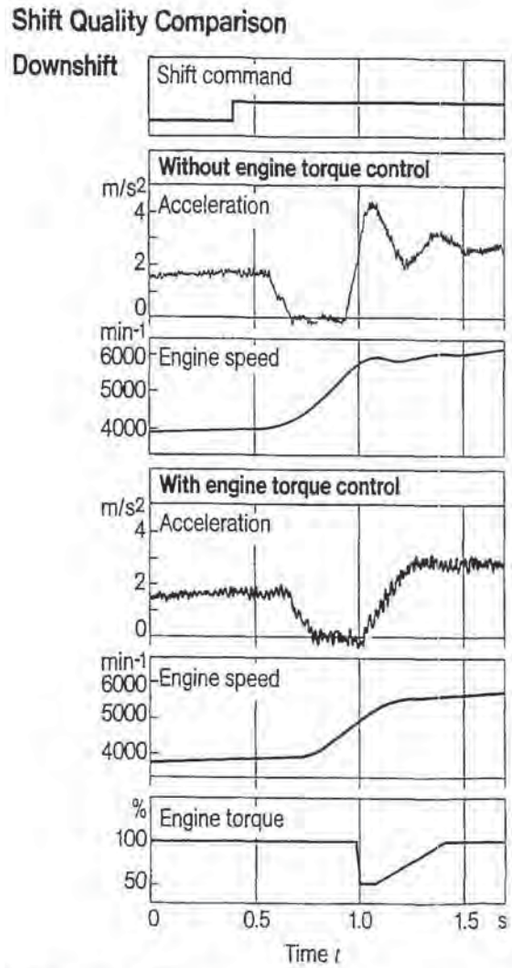


FIGURE 13.8 Timing of engine torque reduction during downshift.

Pressure Control.[8] The timing and absolute values of the pressure, which is responsible for the torque translation of the friction elements, is, aside from the engine torque reduction, the most important influence to shift comfort. The electronic TCU offers additional possibilities for better function than a conventional hydraulic system.

The pressure values during and outside shifting can be calculated by different algorithms or can be determined by characteristic maps. The inputs for a pressure calculation are engine torque, transmission input speed, turbine torque, throttle position, and so on. The inputs depend on the special signal availability in different systems as well as the requirement concerning shift comfort. The variable pressure components are usually added to a constant pressure value according to the different transmission designs. Equation (13.2) gives a typical algorithm for a pressure calculation.

PETITIONER'S EXHIBIT 1002
US PATENT NO. 6,581,565

$$P_{mod} = P_{const} + k_n \times P_n + k_{tor} \times P_{tor} + k_s \times P_s \quad (13.2)$$

where P_{mod} = pressure
P_{const} = constant pressure value
k_n = adaptation factor for input speed
P_n = pressure component dependent on the revolution signal
k_{tor} = adaptation factor for engine torque
P_{tor} = pressure component dependent on torque
k_s = adaptation factor for vehicle speed
P_s = pressure component dependent on vehicle speed

During applications, the factors must be defined in the calibration phase. In general, the determination of these factors requires many vehicle tests, because the dynamic characteristic of the total system has an important influence on shift comfort. Another possibility for the pressure determination is to use characteristic maps which have to be defined during the calibration phase. This kind of pressure determination allows an improved selection of the optimum pressure at various extreme points independent of an algorithm.

Safety and Diagnostic Functions. The functions, which are usually known as diagnostic functions of the electronic TCU, can be divided into real safety functions to prevent critical driving conditions and diagnostic functions which affect an increasing availability of the car and a better failure detection for servicing. The boundary between safety and diagnostic functions depends on the philosophy of the automotive manufacturer. In the category of real safety functions belong all security functions that prevent uncontrollable shifting, especially unintended downshifting. One section is the monitoring of the microcontroller and its related peripheral devices. The monitoring of the transmission, like gear ratio detection, is also a part of this functional block, as are the actuator and speed sensor monitoring. The microcontroller monitor is usually a watchdog circuit. One possibility is to use the controller internal watchdog. In common applications, it is necessary to use an external watchdog circuit for safety reasons. This can be done with a second, low-performance microcontroller or by a separate hardware watchdog designed as an ASIC or as a conventional circuit device. Usually there is a safety logic circuit connected to the watchdog, which, in the case of a microcontroller breakdown, activates the failure signal and switches the outputs for the transmission actuators to a safety condition.

For the detection of the watchdog, it is necessary to test the watchdog function after each power-on during the electronic initialization. The monitoring of the controller peripheral components, in general EPROM, RAM, and chip-select circuits, works continuously with specific algorithms; e.g., by writing fixed data values to the storage cells and following comparison with the read value or by checksum comparison with fixed sum values. The actuator monitoring includes detection of short circuit to supply voltage and ground, as well as open-load conditions.

In case of actuator malfunction, the limp home mode is selected. This means that the transmission runs in a fixed, safe gear, depending on the driving conditions. The safe state of the actuators is the noncurrent condition, which is secured by the electronic control unit. The control unit can put the output stages into the noncurrent stage separate for each output or by a common supply switch, usually a relay or a transistor. There are some applications that use a combination of both the watchdog and safety circuits.

The monitoring of the transmission-specific sensors, such as input speed, output speed, and oil temperature, works as a plausability check. For example the transmission input speed can be calculated as a combination of the transmission output speed and the gear ratio. In case of a detected speed sensor malfunction, the limp home mode is generally required. With a temperature sensor failure, the TCU usually works with a substitute value

The diagnostic functions, which facilitate the finding of failures in the service station, contain the failure storage and the communication to the service tester, which allow the stored

PETITIONER'S EXHIBIT 1002
US PATENT NO. 6,581,565

failures of the electronic TCU to be read. The communication between the control unit and the service tester is mainly car manufacturer-specific and must be defined by the car manufacturer before going into series production. The communication runs on a bidirectional, separate communication link.

The failure storage takes place in a nonvolatile memory device; e.g., in a permanent supplied RAM or in an EEPROM. It is also possible to store sporadic failures to detect such problems during the next service. The failure codes, number of stored failures, the handling of the failure storage, as well as the reaction of the TCU in case of a particular failure, is manufacturer-specific and is part of the unit specification. The real safety functions are part of the basic functions of an electronic TCU. The diagnostic functions concerning service tester and communication protocols are, over a wide range, manufacturer-specific. These range from a simple blink code up to a real self-test of the electronic unit, including all peripheral components.

13.3.2 Improvement of Shift Control

In a second development stage, the basic functions can be revised by a modification of the software functions and by adding new parts to the basic functions. This action results in a significant enhancement of the driving and shifting comfort. By a revision of the basic safety and diagnostic functions with so-called substitute functions, it is possible to increase the availability of the vehicle with AT as well as the driveability in case of a malfunction.

Shift Point Control. The basic function can be improved significantly by adding a software function, the so-called adaptive shift point control.[8] This function requires only signals which are available in an electronic TCU with basic functions. The adaptive shift point control is able to prevent an often-criticized attribute, the tendency for shift hunting especially when hill climbing and under heavy load conditions.

The adaptive function calculates the vehicle acceleration from the transmission output speed over time. The value of the actual acceleration in relation to a set value of the acceleration is the input for the shift point correction. The set value is given by the traction resistance characteristic. For a certain difference between set and actual value, the adaptation of the shift point occurs. The dimension of the shift point correction can be determined by calibration data and depends in general also on the actual vehicle speed and the engine load.

The shift point correction leads to higher hysteresis between upshift and downshift characteristics. With a high difference between set and actual values, it is also possible to forbid certain gears. The return to the basic shift point control is organized by software and can be fixed by calibration data. Usually, in the case of power-on, the adaptive shift point control is reset (Figs. 13.9 and 13.10).

In addition to these functions, different shift maps can be implemented into the data field of the TCU. For example, it is possible to have one shift map for low fuel consumption, which has shift points in the range of the best efficiency of the engine, and additionally to have another map for power operation, where the shift points are placed at points of highest engine output power. The character and number of different shift maps can be selected over a wide range. The choice of the different shift maps can be done by a selector push button or switch commanded by the driver. In further applications, the changing of the different shift programs is possible by self-learning strategies. It is also possible to implement a manual program in which fixed gears are specific to predetermined positions of the selector lever.

Lockup Control. There are some additional functions which can improve considerably the shift comfort of the lockup. In a first step, it is possible to replace the on/off control of the lockup actuator by a pulse control during opening and closing. This can be achieved using conventional hardware only by a software modification. In a further step, the on/off solenoid is replaced by a pressure regulator or a PWM solenoid.

By coordinating intelligent control strategies and corresponding output stages within the electronic TCU, a considerable improvement of the shift behavior of the lockup results. Here

PETITIONER'S EXHIBIT 1002
US PATENT NO. 6,581,565

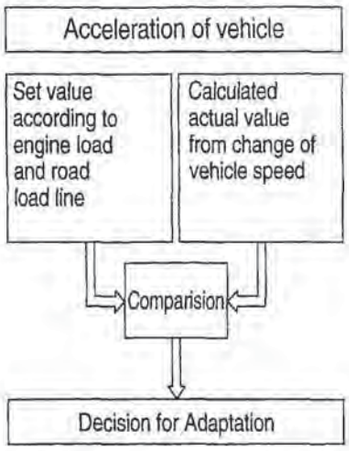


FIGURE 13.9 Basic principle of adaptive shift point control.

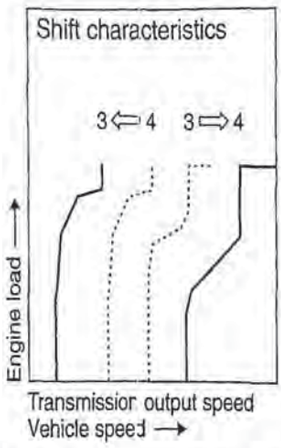


FIGURE 13.10 Shift characteristics before (- - -) and after (—) adaptation.

it is possible to close the lockup at low engine speed and low engine load with good shift comfort, resulting in decreased fuel consumption.

Engine Torque Reduction During Gear Shifting. By an improved interface design to the engine management system, it is possible to extend the engine torque reduction function. It is necessary to use a PWM signal with related fixed values or a bus interface. The engine torque reduction is controlled directly by the TCU. The advantage of such an interface is an independent calibration of the TCU data over a wide range without changing the engine management data. A further advantage is the improved possibility for the coordination of the engine torque reduction and the pressure control within the TCU. The improvement of this interface can be extended up to a real torque interface, especially when using a bus communication link.

Pressure Control.[8] The pressure control can be improved in a similar way as the shift point control with an adaptive software strategy. The required inputs for the adaptive pressure control are calculated from available signals in the transmission control. The main reasons for the implementation of the adaptive pressure control are the variations of the attributes of the transmission components like clutch surfaces and oil quality as well as the changing engine output torque over the lifetime of the car.

The principle of adaptive pressure control is a comparison of a set value for the shift time with an actual value, measured by the transmission input speed course. At a specific difference of the set value to the actual value, the pressure value is corrected by a certain increment in the positive or negative direction. The original adaptation time and the pressure value increment were fixed during the calibration phase. For safety reasons, the total deviation of the pressure value from a given value is limited, depending on the particular application. Usually the correction values are stored in the nonvolatile memory to have the correct values available after power-on of the electronic TCU.

Safety and Diagnostic Functions. The safety functions extend over better monitoring of the selector lever and functions concerning misuse by the driver. With a corresponding transmission hardware design, the implementation of a reverse gear inhibit function is possible; i.e, above a certain vehicle speed, the position R is blocked hydraulically by a single solenoid or by a particular solenoid combination commanded by the electronic TCU. This function pre-

PETITIONER'S EXHIBIT 1002
US PATENT NO. 6,581,565

vents the destruction of the transmission in the event of an unintentional shift to the reverse gear. Downshift prevention is part of the safety function, especially during manual shifting by the driver. Here the synchronous speed of the new gear is calculated and compared with the admissable maximum engine speed. In the case of a calculated synchronous speed above the maximum engine speed, the downshift is prohibited by the TCU. This function can be supported by an overrun safeguard which releases the limp home mode in case of exceeding the admissable maximum engine speed.

All of those functions can be extended and have to be defined during the development stage by the automobile transmission and electronic TCU manufacturers. To increase availability of the AT system, even with the failure of certain signals, it is possible to provide a substitute operation with better drivability than in the limp home mode. This can be done by substitute functions. The electronic TCU falls back on substitute values or signals in the case of a breakdown of certain interfaces. There is, for example, the possibility to run with a programmable fixed throttle value with a breakdown of the throttle position signal. This results in a reduction of the shift characteristics to shift points. Shifting into all gears is possible, however, with reduced shift comfort. A further method is to use secondary signals in case the original signals break down. For example, the calculation of vehicle speed can be from wheel speed during breakdown of the transmission output speed signal. This technique usually requires a connection between ABS and transmission control. The third variant is the canceling of certain functions if the necessary input signals are missed. For example, in the case of a kickdown switch failure, the kickdown function is canceled. This results in no downshift after operation of the kickdown. Downshifts are nevertheless still possible via the full-throttle opening point according to the full-load shift characteristic.

The availability and driveability of automobiles equipped with electronic TCU in case of system failures can be improved significantly with the implementation of substitute functions. This results in a considerable increase in acceptance by the drivers of automobiles with electronic transmission control.

13.3.3 Adaptation to Driver's Behavior and Traffic Situations

In certain driving conditions, some disadvantages of the conventional AT can be prevented by using self-learning strategies.[9] This is especially valid when improving the compromise in the shift characteristics regarding gear selection under particular driving conditions and under difficult environmental conditions. The intention of the self-learning functions is to provide the appropriate shift characteristic suitable to the driver under all driving conditions. Additionally, the behavior of the car under special conditions can be improved by suitable functions. Available input signals of the car, provided by the related electronic TCUs from interfaces and communication links, are processed by the TCU with specific algorithms. The self-learning functions can be divided into a long respectively medium term adaptation for driver's style detection and into a short-term adaptation which reacts to the present driving situation, such as hills or curves.

The core of the adaptive strategies is the driver's style detection. The driver's style can be detected by monitoring of the accelerator pedal movements. The inputs are operation speed, operation frequency, and the rating position of the accelerator pedal. These inputs are processed depending on priorities with special algorithms related to the desired driving behavior of the car. The calculated driver style is related to certain shift maps. There is a large choice of shift maps available. With the currently known applications, there are mostly four different shift maps ranging from fuel economic to extremely sporty vehicle behavior. The calculated driver's style can also depend on the actual vehicle speed and the share of constant driving conditions during a certain driving cycle. These self-learning functions can be calibrated by the car manufacturer, depending on his philosophy and target market. In this way, the number of shift maps and the speed of the adaptation have the main influence. A further possibility to match the driver's style is by rating the accelerator pedal operation during vehicle start, for example, after a red light stop. In this way the operation speed and frequency of the accelera-

PETITIONER'S EXHIBIT 1002
US PATENT NO. 6,581,565

tor pedal below a certain vehicle speed can be interpreted and calculated as part of the driver's style rating. In the event of kickdown, the shift maps of the driver's style rating are shut down by a priority command. The driver has the usual behavior of the car during kickdown, generally a downshift, providing no other safety function is in operation.

To prevent shift hunting, the self-learning functions are carried out over a long respectively medium term adaptation with the adaptation timer ranging from several seconds up to one minute. The second part of the self-learning functions is the driving condition detection. There is a correlation between the input signals of the transmission control and the driving condition.

One of the main disadvantages of a conventional electronic transmission control is the upshifting at constant vehicle speed by crossing the upshift characteristic with a reduction of the accelerator pedal angle. This results in an unintended gear shift, especially when cornering and when approaching a crossing or an obstacle. To prevent these gear shifts it is possible to use so-called upshift prevention. Cornering can be detected by the acceleration of the car along the driving direction related to the vehicle speed. The vehicle speed is calculated from the transmission output speed. The acceleration can be detected by an acceleration sensor or by the difference between the nondriven wheel speeds. In this way it is possible to prevent the upshift when cornering, resulting in a considerable improvement in vehicle stability.

The detection of a crossing or obstacle approach is possible by the detection of a fast off condition of the accelerator pedal. At a certain gradient of the pedal position, the upshift is prevented. This is a considerable advantage especially when overtaking low-speed vehicles. With this strategy the correct gear is available without a shift delay.

Another part of the driving situation detection is the recognition of uphill driving and full-load conditions. This is possible by adding special functions to the adaptive gear shift control. When driving downhill, it makes sense to support the engine braking effect for a better deceleration of the car. Downhill driving can be detected by a comparison of throttle position and vehicle speed gradient. An upshift is prevented and, in some special cases, a downshift is activated by the electronic TCU.

A further section of the self-learning functions is the environmental monitoring with related shift strategies. A special application can be a self-learning winter program. The wheel slip of the driven wheels is compared with a set value of a combination of given wheel torque and vehicle speed. When exceeding a set limit of wheel slip, a special shift strategy is chosen. For example, the vehicle starts off in second gear or an upshift takes place at lower engine speeds.

The development of adaptive shift strategies started a few years ago and is currently one of the main areas in electronic transmission development. The efficiency of the self-learning functions has led to a wide acceptance of AT-equipped vehicles. The future development concerning new adaptive functions and an improvement of the already known functions is an important area in control development. This can be supported by an increasing share of electronic units and interfaces for the communication between units. With multiple use of sensors providing the necessary input signals, the total system gains increased functionality, especially with bus systems.

At present, an increasing share of manual programs with an AT can be registrated. The driver instructs the AT to shift via a switch or a push button. In this manner, the driver can operate the AT like a manual gearbox independently of other shift maps, with only the safety functions in operation. This has led to a broad acceptance, especially in the sports car market. These functions can all be calibrated and applied by the car manufacturer with data relating to his philosophy and to the target market. The result is the prevention of the known disadvantages of the conventional AT control without canceling the advantages in driving comfort and safety.

13.4 COMMUNICATIONS WITH OTHER ELECTRONIC CONTROL UNITS

With the existence of electronic control units for various applications in vehicles, many opportunities exist to link these ECUs and to establish communications between them. The main partner of the TCU is the engine management system. Due to the coupling of engine and

PETITIONER'S EXHIBIT 1002
US PATENT NO. 6,581,565

transmission within the vehicle powertrain, it is necessary to have an interface between these ECUs for a functional coupling and an interchange of signals. It is essential for the pressure control inside the transmission control to sensor the engine load, the engine speed, and the throttle position. The engine torque reduction during shifting is also important to establish a good shift comfort and a satisfactory lifetime for the clutches. By handing over certain signals like position lever state, lockup condition, or shift commands to the engine management, the driving comfort of the vehicle can be improved significantly. An interface to ABS and traction control is useful for some self-learning functions in the transmission control when using the wheel speeds.

It is possible to implement certain shift strategies in the transmission control as an active support for ABS and traction control. A link to the electronic throttle control or cruise control makes it possible to optimize certain functions for the total vehicle. By interfaces between the ECUs, a reduction of the sensor expense results by a multiple use via communications. Suitable links include, especially, PWM or bus configurations for trouble-free communication. Bus systems in particular have the advantage of the link-up of additional ECUs without changing their existing hardware. Additional coupling requires only a software change. The interchange of required supplementary signals for new functions is possible without any problems. An example of powertrain management by coupling the powertrain ECUs to achieve lower fuel consumption, simultaneously improving the driveability, is described as follows.

13.5 OPTIMIZATION OF THE DRIVETRAIN

The newest generation of transmission controllers has overcome the former disadvantage regarding fuel efficiency. Adaptive functions in cooperation with carefully designed torque converter clutch control,[8] which allows the clutch to be closed even at low gears, have improved fuel consumption significantly. Based on the driver's behavior, together with an adaptive shift strategy as previously described, part of the TCU's adaptive program software may select an economy or even super-economy shift strategy whenever possible. There is, however, still more potential for fuel economy by optimization of the drivetrain.

The concept called Mastershift[10] is shown in Fig. 13.11. The basic idea is to interpret the accelerator pedal position as an acceleration request. That acceleration request, or a request for wheel torque, has to be converted by operating the engine at high torque, i.e., open throttle and low rpm values. In order to realize this, it is necessary to use an electronic throttle control system. The communication between the electronic throttle, the engine, and transmission is shown in Fig. 13.12.

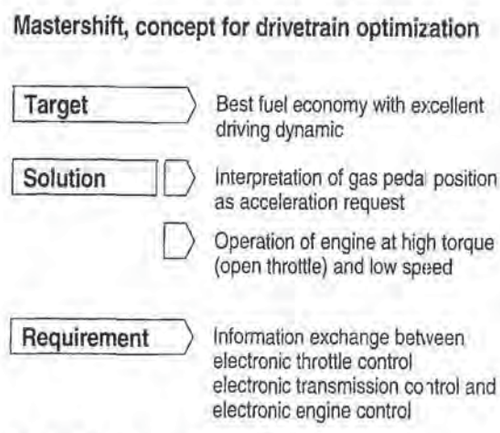


FIGURE 13.11 Drivetrain operation.

PETITIONER'S EXHIBIT 1002
US PATENT NO. 6,581,565

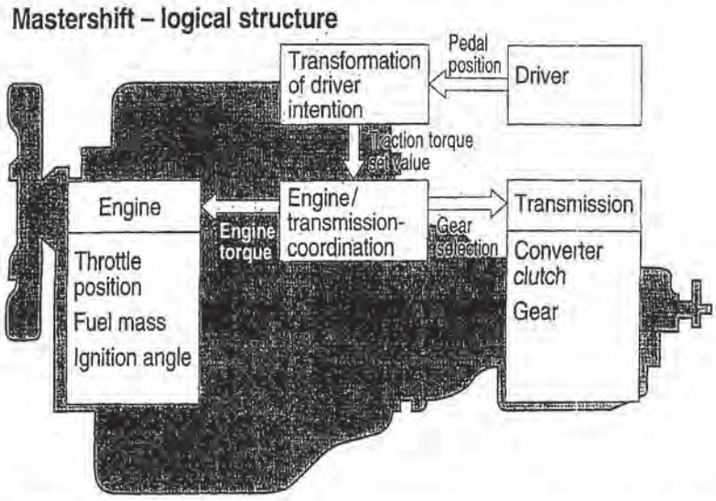


FIGURE 13.12 Mastershift: logical structure and communication between different control systems.

In such a system, a well-defined coordination between the engine torque, mainly given by throttle position (air mass), fuel mass, and ignition angle on one side and selection of the appropriate gear including torque converter clutch on the other side, is imperative. Depending on the type of engine, fuel consumption can be reduced further by 5 to 10 percent with this optimized Mastershift concept. Because the average engine operation is at higher torque levels compared to standard systems, a greater number of gear shifts may occur. This is important to guarantee optimal shift comfort. Figure 13.13 shows how that can be accomplished by using the additional degree of freedom given by the electronic throttle control. It is possible to operate the throttle angle during the gear shift in such a way as to achieve constant wheel torque before and after downshifts.

13.6 FUTURE DEVELOPMENTS

In future years, development work will be concentrated on redesign of hardware components for cost reduction, improvement of yield to reduce fuel consumption, and improvement of driveability. A good approach to meet cost targets on the electronic hardware side would be to integrate two or more individual control modules into a common housing. Regarding the electronic components, one could continue using two separate microcontrollers. This would have the advantage that the software development and application could be done individually for two different systems, for example engine and transmission controllers. Another approach could be to mount the TCU on the transmission housing itself. This could lead to a significant reduction in the expense for the wiring harness. Here, however, the problem of hostile ambient temperatures on electronic components has to be solved. Today's stand-alone actuators could be integrated into a common housing similar to the solution shown by Chrysler Corp. in its A 604 transmission.

The improvement of the yield is a main topic for designers of ATs. Oil pumps and torque converters are a major source of energy losses. A significant improvement of yield will be possible as soon as torque converter clutches are available with the capability for continuous slip operation. The torque converter clutch can then be operated in low gears and at low engine speeds without facing problems from drivetrain oscillations and/or noise emission.

The driveability is the most important feature for the drivers' acceptance of ATs. In addition to the self-adaptive functions described, the implementation of shift strategies benefiting from control algorithms using fuzzy theory may further improve driveability.

PETITIONER'S EXHIBIT 1002
US PATENT NO. 6,581,565

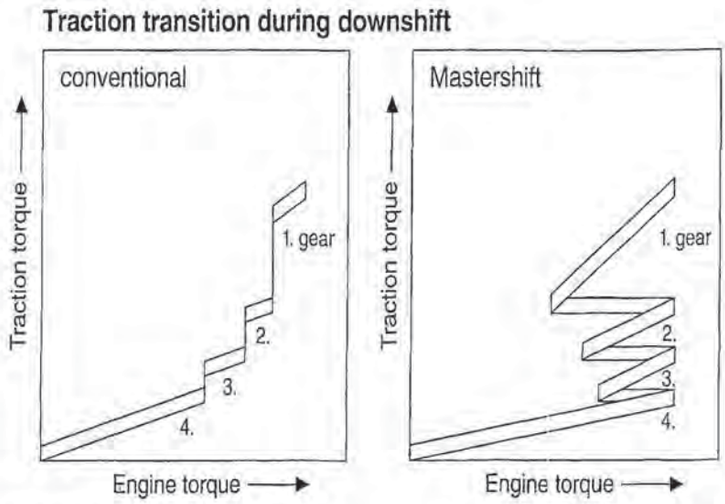


FIGURE 13.13 Constant traction torque by operation of throttle opening during gear shift.

GLOSSARY

ASIC Application-specific integrated circuit.

AT Automatic transmission.

ATF Automatic transmission fluid.

CAN Controller area network.

CVT Continuously variable transmission.

EEPROM Electrically erasable and programmable read-only memory.

EMC Electromagnetic compatibility.

EPROM Erasable programmable read-only memory.

PWM Pulse-width modulation.

RAM Random access memory.

RFI Radio frequency interference.

TCC Torque converter clutch.

TCU Transmission control unit.

REFERENCES

1. F. Kucukay and Lorenz, K., "Das neue Fünfgang-Automatikgetriebe für V8-Motoren in der 7er Baureihe von BMW," *ATZ Automobiltechnische Zeitschrift 94,* Heft 7/8, 1992.
2. K. Neuffer, "Recent development of AT-control: adaptive functions and actuators," Symposium No. 9313, *Advanced Technologies in Automotive Propulsion Systems,* Society of Automotive Engineers of Japan Inc., 1993, pp. 42–49.

PETITIONER'S EXHIBIT 1002
US PATENT NO. 6,581,565

3. J. G. Eleftherakis and Khalil, A., "Development of a laboratory test contaminant for transmissions," SAE Paper 90 0561, Society of Automotive Engineers, Warrendale, Pa.
4. B. Aldefeld, "Numerical calculation of electromagnetic actuators," *Archiv für Elektrotechnik,* Bd. 61, 1979, pp. 347–352
5. K. Hasuuaka, Takagi, K., and Sinji, W., "A study on electro-hydraulic control for automatic transmissions," SAE Paper 89 2000, Society of Automotive Engineers, Warrendale. Pa.
6. P. C. Sen, "Principles of electric machines and power electronics," J. Wiley, New York, 1989.
7. "Method and Apparatus to Convert an Electrical Value into a Mechanical Position by Using an Electromagnetic Element Subject to Hysteresis," U. S. Patent 4,577,143 March 18, 1986.
8. K. Neuffer, "Electronische Getriebesteuerung von Bosch," *ATZ Automobiltechnische Zeitschrift 94,* Heft 9, 1992, pp. 442–449.
9. A. Welter, et al., "Die Adaptive Getriegesteuerung für Automatikgetriebe der BMW-Fahrzeuge mit Zwolfzylindermotor," *ATZ Automobiltechnische Zeitschrift 94,* 1992, pp. 428–436.
10. H. M. Streib and R. Leonhard, "Hierarchical control strategy for powertrain function," *XXIV Fisita Congress,* London, 1992.

ABOUT THE AUTHORS

KURT NEUFFER is responsible at Robert Bosch GmbH for the development of electronic control units for automatic transmissions and also for the development of actuators. He was educated in electronics engineering at the University of Stuttgart and holds a DI. Ing. in the field of basic semiconductor research. He has been in the field of automotive component development for 10 years.

WOLFGANG BULLMER is responsible at Bosch for systems and software development of electronic control units for automatic transmissions. He was educated in electronics engineering at the University of Stuttgart. He has been working in the area of transmission control unit development for eight years.

WERNER BREHM is a Bosch section manager for the design of electrohydraulic actuators used in electronically controlled automatic transmissions. He was educated in mechanical engineering at the University of Stuttgart and has worked on components engineering for antilock braking systems in passenger cars.

PETITIONER'S EXHIBIT 1002
US PATENT NO. 6,581,565

PETITIONER'S EXHIBIT 1002
US PATENT NO. 6,581,565

CHAPTER 14
CRUISE CONTROL

Richard Valentine
Motorola Inc.

14.1 CRUISE CONTROL SYSTEM

A vehicle speed control system can range from a simple throttle latching device to a sophisticated digital controller that constantly maintains a set speed under varying driving conditions. The next generation of electronic speed control systems will probably still use a separate module (black box), the same as present-day systems, but will share data from the engine, ABS, and transmission control systems. Futuristic cruise control systems that include radar sensors to measure the rate of closure to other vehicles and adjust the speed to maintain a constant distance are possible but need significant cost reductions for widespread private vehicle usage.

The objective of an automatic vehicle cruise control is to sustain a steady speed under varying road conditions, thus allowing the vehicle operator to relax from constant foot throttle manipulation. In some cases, the cruise control system may actually improve the vehicle's fuel efficiency value by limiting throttle excursions to small steps. By using the power and speed of a microcontroller device and fuzzy logic software design, an excellent cruise control system can be designed.

14.1.1 Functional Elements

The cruise control system is a closed-loop speed control as shown in Fig. 14.1. The key input signals are the driver's speed setpoint and the vehicle's actual speed. Other important inputs are the faster-accel/slower-coast driver adjustments, resume, on/off, brake switch, and engine control messages. The key output signals are the throttle control servo actuator values. Additional output signals include cruise ON and service indicators, plus messages to the engine and/or transmission control system and possibly data for diagnostics.

14.1.2 Performance Expectations

The ideal cruise system features would include the following specifications:

- *Speed performance:* ±0.5 m/h control at less than 5 percent grade, and ±1 m/h control or vehicle limit over 5 percent grade.
- *Reliability:* Circuit designed to withstand overvoltage transients, reverse voltages, and power dissipation of components kept to minimum.

PETITIONER'S EXHIBIT 1002
US PATENT NO. 6,581,565

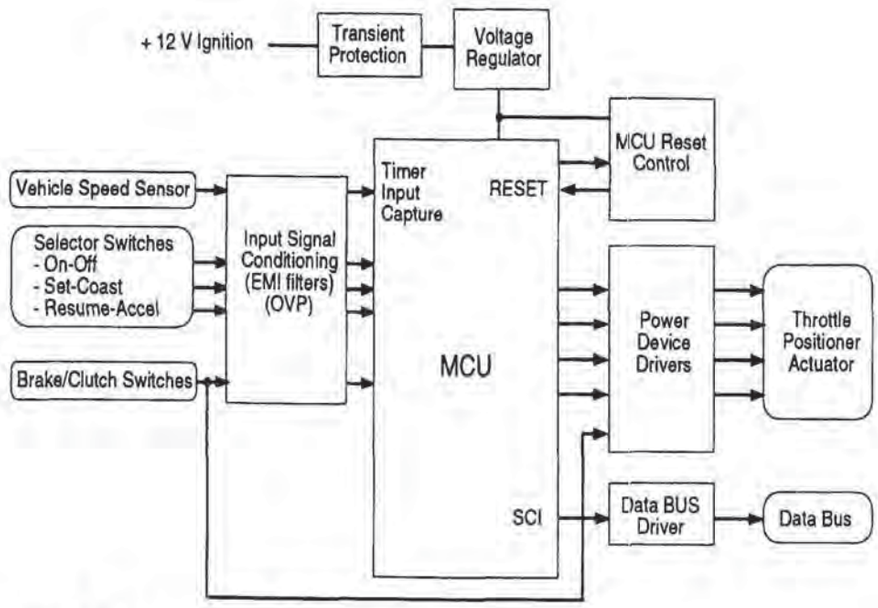


FIGURE 14.1 Cruise control system.

- *Application options:* By changing EEPROM via a simple serial data interface or over the MUX network, the cruise software can be upgraded and optimized for specific vehicle types. These provisions allow for various sensors, servos, and speed ranges.
- *Driver adaptability:* The response time of the cruise control can be adjusted to match the driver's preferences within the constraints of the vehicle's performance.
- *Favorable price-to-performance ratio:* The use of integrated actuator drivers and a high-functionality MCU reduce component counts, increase reliability, and decrease the cruise control module's footprint.

14.1.3 Safety Considerations (Failsafe)

Several safety factors need to be considered for a vehicle speed control design. The most basic is a method designed into the throttle control circuit to insure a failsafe mode of operation in the event that the microcontroller or actuator drivers should fail. This electronic failsafe circuit shuts off the control servos so that the throttle linkage will be released when the brake switch or cruise off switch is activated, no matter the condition of the MCU or servo actuator control transistors. (This assumes the actuators are mechanically in good shape and will release.)

Other safety-related items include program code to detect abnormal operating conditions and preserving into memory the data points associated with the abnormal condition for later diagnostics. Abnormal conditions, for example, could be an intermittent vehicle speed sensor, or erratic driver switch signals. A test could also be made during the initial ignition "key on time" plus any time the cruise is activated to verify the integrity of the cruise system, with any faults resulting in a warning indicator to the driver. Obviously, the most serious fault to avoid is runaway acceleration. Continuous monitoring of the MCU and key control elements will help minimize the potential for this type of fault.

PETITIONER'S EXHIBIT 1002
US PATENT NO. 6,581,565

14.2 MICROCONTROLLER REQUIREMENTS FOR CRUISE CONTROL

The MCU for cruise control applications requires high functionality. The MCU would include the following:

- a precise internal timebase for the speed measurement calculations
- A/D inputs
- PWM outputs
- timer input capture
- timer output compares
- serial data port (MUX port)
- internal watchdog
- EEPROM
- low-power CMOS technology

14.2.1 Input Signals

The speed sensor is one of the most critical parts in the system, because the microcontroller calculates the vehicle speed from the speed sensor's signal to within ½ m/h. Any speedometer cable whip or oscillation can cause errors to be introduced into the speed calculation. An averaging routine in the speed calculations can minimize this effect. The speedometer sensor drives the microcontroller's timer input capture line or the external interrupt line. The MCU then calculates the vehicle's speed from the frequency of the sensor signals and the MCU internal timebase. The vehicle's speed value is continually updated and stored into RAM for use by the basic speed control program. Speed sensors traditionally have been a simple ac generator located in the transmission or speedometer cable. The ac generator produces an ac voltage waveform with its frequency proportional to the sensor's rpm and vehicle speed. Optical sensors in the speedometer head can also be incorporated. Usually the speed sensor produces a number of pulses or cycles per km or mile. With the increasing ABS system usage, a backup speed sensor value could be obtained from the ABS wheel speed sensors. The ABS speed data could be obtained by way of a MUX network.

The user command switch signals could either be single MCU input lines to each switch contact or a more complex analog resistor divider type to an A/D input line. Other input signals of interest to the cruise system program would be throttle position, transmission or clutch status, A/C status, actuator diagnostics, engine status, etc., which could be obtained over the MUX data network.

14.2.2 Program Flow

The microcontroller is programmed to measure the rate of vehicle speed and note how much, and in which direction, the vehicle speed is drifting. The standard PI (proportional-integral) method produces one output signal p that is proportional to the difference between the set-speed and actual vehicle speed (the error value) by a proportional gain block Kp. Another signal i is generated that ramps up or down at a rate set by the error signal magnitude. The gains of both Ki and Kp are chosen to provide a quick response, but with little instability. In effect, the PI system adds up the error rate over time, and, therefore, if an underspeed condition occurs as in a long uphill grade, the error signal will begin to greatly increase to try to compensate. Under level driving conditions, the integral control block Ki will tend toward zero

PETITIONER'S EXHIBIT 1002
US PATENT NO. 6,581,565

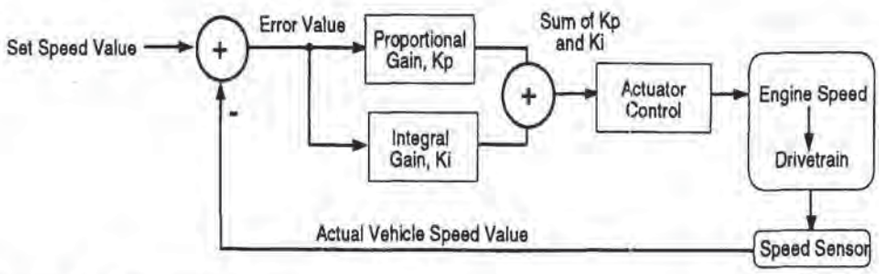


FIGURE 14.2 PI speed error control.

because there is less error over time. The vehicle's weight, engine performance, and rolling resistance all factor in to determine the PI gain constants. In summary, the PI method allows fast response to abrupt grades or mountains and stable operation under light grades or hills. Figure 14.2 shows the traditional PI cruise control diagram.

14.2.3 Output Controls

When the error signal has been computed, an output signal to the servo actuators is generated to increase, hold, or decrease the throttle position. The servo is updated at a rate that is within the servo's mechanical operating specifications, which could be several milliseconds. The error signal can be computed at a much faster rate and, therefore, gives extra time for some averaging of the vehicle speed sensor signal.

Throttle positioning is traditionally either a vacuum type servo or motor. The vacuum supply to the vacuum servo/actuator is discharged as a failsafe measure whenever the brake system is engaged in addition to the normal turn-off of the actuator driver coils. Electric servo type motors require more complex drive electronics and some type of mechanical failsafe linked backed to the brake system.

14.3 CRUISE CONTROL SOFTWARE

The cruise error calculation algorithm can be designed around traditional math models such as PI or fuzzy logic.

14.3.1 Fuzzy Logic Examples

Fuzzy logic allows somewhat easier implementation of the speed error calculation because its design syntax uses simple linguistics. For example: IF speed difference negative and small, THEN increase throttle slightly.

The output is then adjusted to slightly increase the throttle. The throttle position update rate is determined by another fuzzy program which looks for the driver's cruise performance request (slow, medium, or fast reaction), the application type (small, medium, or large engine size), and other cruise system factory preset parameters. Figure 14.3 shows one part of a fuzzy logic design for computing normal throttle position. Other parts would compute the effects of other inputs, such as resume, driver habits, engine type, and the like.

Other program design requirements include verification that the input signals fall within expected boundaries. For example, a broken or intermittent speed sensor could be detected.

PETITIONER'S EXHIBIT 1002
US PATENT NO. 6,581,565

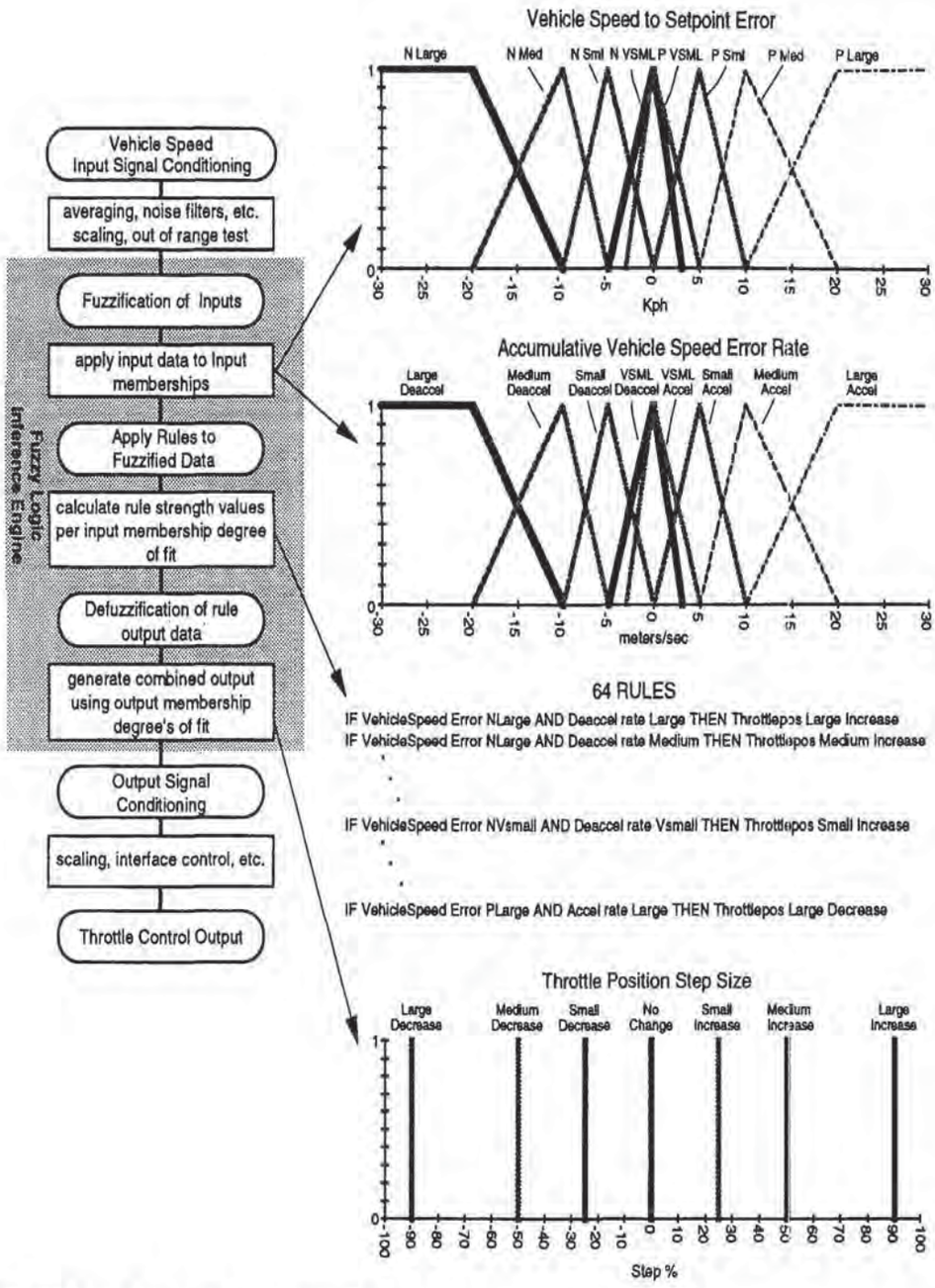


FIGURE 14.3 Fuzzy speed error program flow.

A heavily loaded vehicle with a small engine may not be able to maintain a high setpoint speed up a steep grade, and the cruise control needs to be disengaged to protect the engine from sustained full-throttle operation under a heavy load. This could be preset to occur 20 percent below the setpoint speed. Another program can test the vehicle speed to resume setpoint speed and prevent unsafe acceleration under certain conditions. For example, if a high-performance vehicle (>200-kW or 268-hp engine) has a setpoint speed of 125 km/h (78 mi/h), and drives from the freeway into heavy city traffic doing 48 km/h (30 mi/h) and the vehicle's

PETITIONER'S EXHIBIT 1002
US PATENT NO. 6,581,565

driver fortuitously hits the cruise resume switch at this low speed, the cruise control invokes a near full-throttle action, and an accident is likely. A fuzzy design can limit the acceleration upon resume using simple rules such as IF resume and big speed error, THEN increase throttle slightly.

14.3.2 Adaptive Programming

The response time and gain of the cruise system can be adjusted to match individual drivers. For example, some drivers may prefer to allow the vehicle to slow down somewhat when climbing a grade and then respond quickly to maintain a setspeed; other drivers may prefer a constant speed at all times, while still other drivers may prefer a very slow responding cruise system to maximize fuel efficiency. The cruise system can be adapted either by a user selection switch (slow, medium, fast) or by analyzing the driver's acceleration/deacceleration habits during noncruise operation. Once these habits are analyzed, they can be grouped into the three previously mentioned categories. One drawback of a totally automatic adaptive cruise system is when various drivers with vastly different driving preferences operate the vehicle on the same trip. The cruise system would have to be "retrained" for each driver.

14.4 CRUISE CONTROL DESIGN

Many of the required elements of a cruise control can be integrated into one single-chip MCU device. For example, the actuator drivers can be designed in the MCU if their power requirements are on the low side.

14.4.1 Automatic Cruise System

Figure 14.4 shows an experimental system design for a cruise control based upon a semicustom 8 or 16-bit single-chip MCU that incorporates special high-power output driver elements and a built-in voltage regulator.

14.4.2 Safety Backup Examples

The design of a cruise control system should include many safeguards:

- A test to determine vehicle speed conditions or command inputs that do not fall within the normal conditions for operation of the cruise control function.
- A test to determine if the vehicle speed has decreased below what the cruise routine can compensate for.
- Speed setpoint minimums and maximums (30 km/h min to 125 km/h max, for example) are checked and, if exceeded, will cause the cruise function to turn off.
- Speedometer cable failure is detected by checking for speed sensor electrical output pulses over a 100-ms time period and, if these pulses are absent, the system is disengaged.
- Software program traps should also be scattered throughout the program and, if memory permits, at the end of each program loop. These will catch an out-of-control program and initiate a vector restart.

PETITIONER'S EXHIBIT 1002
US PATENT NO. 6,581,565

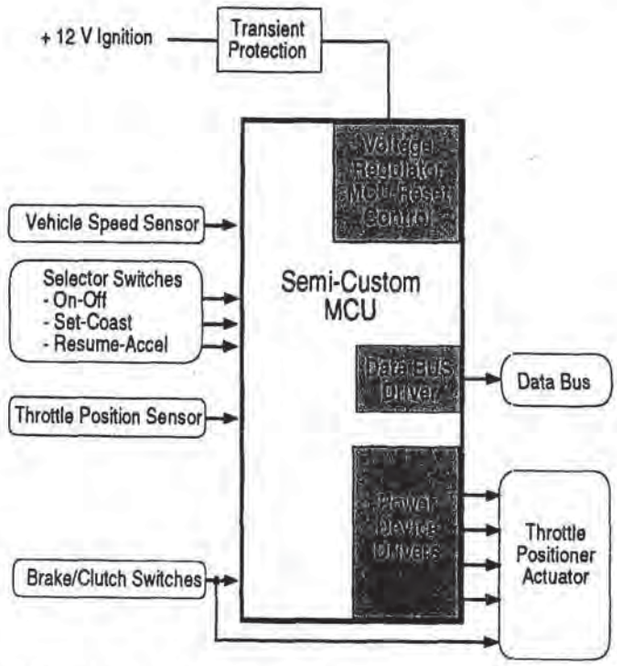


FIGURE 14.4 Automatic cruise control.

14.4.3 EMI and RFI Noise Problems

As with any electronic design, consideration must be given to suppressing RFI (radio frequency interference) from the circuit, besides minimizing effects of external EMI (electromagnetic interference) and RFI to the circuit's normal operation. It is not uncommon that the circuit must operate in RF fields up to 200 V/m intensity. This requires careful layout of the module's PCB (printed circuit board) and RF filters on all lines going in or out of the module. The module case may even have to contain some type of RF shielding. Minimizing generated RFI from the cruise circuit can be accomplished by operating the MCU's crystal oscillator at a minimal power level (this is controlled mostly by the MCU internal design), careful PCB trace layout of the MCU oscillator area, metal shielding over the MCU, ground planes on the PCB under the MCU, and setting the actuator switching edge transition times to over 10 ms. (See Chaps. 27 and 28.)

14.5 FUTURE CRUISE CONCEPTS

Several research projects are underway to develop a crash avoidance system that could be interconnected with a cruise system. The development of a low-cost distance sensor that can measure up to a few hundred meters away with a tight focal point in all weather conditions is proving to be a challenge. When a practical vehicular distance sensor is available, the cruise control can be programmed to maintain either constant speed or constant distance to another vehicle. Other methods of cruise control could include receiving a roadside signal that gives an optimum speed value for the vehicle when travelling within certain traffic control areas.

PETITIONER'S EXHIBIT 1002
US PATENT NO. 6,581,565

14.5.1 Road Conditions Integration with IVHS

The IVHS (Intelligent Vehicle-Highway System) network may be a more practical approach to setting optimum cruise speed values for groups of vehicles. The IVHS can monitor road conditions, local weather, etc., and broadcast optimal speed data values for vehicles in its zone. (See Chap. 29.)

GLOSSARY

Analog input Sensors usually generate electrical signals that are directly proportional to the mechanism being sensed. The signal is, therefore, analog or can vary from a minimum limit to a maximum limit. Normally, an 8-bit MCU A/D input using a 5-V reference, the analog input resolution is 1 bit, which is 1/256 of 5 V or 0.0193 V.

Defuzzification The process of translating output grades to analog output values.

Fuzzification The process of translating analog input values to input memberships or labels.

Fuzzy logic Software design based upon a reasoning model rather than fixed mathematical algorithms. A fuzzy logic design allows the system engineer to participate in the software design because the fuzzy language is linguistic and built upon easy-to-comprehend fundamentals.

Inference engine The internal software program that produces output values through fuzzy rules for given input values. The inference process involves three steps: fuzzification, rule evaluation, and defuzzification.

Input memberships The input signal or sensor range is divided into degrees of membership, i.e., low, medium, high or cold, cool, comfortable, warm, hot. Each of these membership labels is assigned numerical values or grades.

Output memberships The output signal is divided into grades such as off, slow, medium, fast, and full-on. Numerical values are assigned to each grade. Grades can be either singleton (one value) or Mandani (a range of values per grade).

Rule evaluation Output values are computed per the input memberships and their relationship to the output memberships. The number of rules is usually set by the total number of input memberships and the total number of output memberships. The rules consist of IF inputvarA is *x*, AND inputvarB is *y*, THEN outvar is *z*.

Semicustom MCU An MCU (microcontroller unit) that incorporates normal MCU elements plus user-specified peripheral devices such as higher-power port outputs, special timer units, etc. Mixed semiconductor technologies, such as high-density CMOS (HCMOS) and bipolar analog, are available in a semicustom MCU. Generally, HCMOS is limited to 10 V, whereas bipolar-analog is usable to 60 V.

BIBLIOGRAPHY

Bannatyne, R., "Fuzzy logic—A new approach to embedded control solutions," Motorola Semiconductor Design Concept, DC410, 1992.

Catherwood, M., "Designing for electromagnetic compatibility (EMC) with HCMOS microcontrollers," Motorola Semiconductor Application Note, AN1050, 1989.

PETITIONER'S EXHIBIT 1002
US PATENT NO. 6,581,565

Chaudhuri, et al., "Speed control integrated into the powertrain computer," *New Trends in Electronic Management and Driveline Controls,* SAE SP-653, 1986, pp. 65–72.

Hosaka, T., et al., "Vehicle control system and method therefore," U.S. Patent 4809175, May 29, 1990.

Hosaka, T., et al., "Vehicle control system," U.S. Patent 4930084, Feb. 28, 1989.

Mamdani, E. H., "Application of fuzzy logic to approximate reasoning using linguistic synthesis," *IEEE Transactions on Computers,* C-26-12, 1977, pp. 1182–1191.

Ribbens, W., "Vehicle Motion Control," *Understanding Automotive Electronics,* 4th ed., 1992, pp. 247–257.

Takahashi, Hioshi, "Automatic speed control device using self-tuning fuzzy logic," *IEEE Workshop on Automotive Applications of Electronics,* 88THO321, 1988, pp. 65–71.

Self, Kevin, "Designing with fuzzy logic," *IEEE Spectrum,* Nov. 1990, pp. 42–44, 105.

Sibigtroth, J., "Implementing fuzzy expert rules in hardware," *AI Expert,* April 1992.

Stefanides, E. J., "Cruise control components packaged as one unit," *Design News,* Oct. 1, 1990, pp. 162–163.

Zadeh, L. A., "Fuzzy sets, information and control," vol. 8, 1965, pp. 338–353.

ABOUT THE AUTHOR

Richard J. Valentine is a principal staff engineer at Motorola SPS in Phoenix, Ariz. His present assignments include engineering evaluation of advanced semiconductor products for emerging automotive systems. He holds two patents and has published 29 technical articles during his 24 years at Motorola.

PETITIONER'S EXHIBIT 1002
US PATENT NO. 6,581,565

PETITIONER'S EXHIBIT 1002
US PATENT NO. 6,581,565

CHAPTER 15
BRAKING CONTROL

Jerry L. Cage
AlliedSignal Inc.

15.1 INTRODUCTION

This chapter describes braking by first examining vehicle braking fundamentals, including the tire-to-road interface, vehicle dynamics, and conventional brake system components, and progressing to antilock systems objectives, components, safety considerations, control logic, and testing. The chapter concludes with a discussion of future vehicle braking systems.

For simplicity and because of applicability to the majority of automotive vehicles on the road, hydraulic brake systems as used on two-axle, nonarticulated vehicles will be discussed exclusively; this type of brake system is used on passenger cars, light trucks, and, in North America, on medium trucks.

15.2 VEHICLE BRAKING FUNDAMENTALS

Essential to the understanding of the technology associated with modern automotive vehicle braking is knowledge of the tire-to-road interface, vehicle dynamics during braking, and the components of a brake system. This section discusses these subjects to a system level of understanding.

15.2.1 Tire-to-Road Interface

The braking force generated at each wheel of a vehicle during a braking maneuver is a function of the normal force on the wheel and the coefficient of friction between the tire and the road. The simplified relationship between the weight on a wheel and the resulting frictional (braking) force is shown in Eq. (15.1).

$$F_x = \mu W_{wh} \tag{15.1}$$

where F_x = friction force × direction
μ = coefficient of friction, tire-to-road
W_{wh} = static and dynamic weight on the wheel

PETITIONER'S EXHIBIT 1002
US PATENT NO. 6,581,565

The tire-to-road coefficient of friction is not a constant but is a function of factors, most prominent being type of road surface and the relative longitudinal slip between the tire and the road. General curves relating coefficient of friction to wheel slip on various surfaces are shown in Fig. 15.1. From this figure and Eq. (15.1), the following observations are evident:

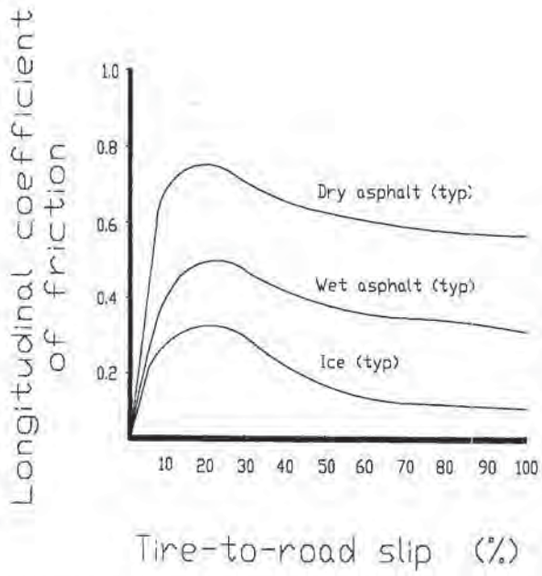


FIGURE 15.1 Longitudinal coefficient of friction as a function of wheel slip.

- The generation of frictional forces depends on wheel slip. If the tire is rolling at the same tangential velocity as the road surface, there is no longitudinal (braking) force. This relationship is fundamental in understanding braking and is not easily observed: wheel slip other than near 100 percent (no rotational wheel speed) is difficult to discern without instrumentation.
- The peak frictional (braking) force occurs under conditions of relatively little slip. This indicates that a hard apply of the brakes which causes a 100 percent slip typically does not produce the most braking force and an evenly modulated, controlled brake pressure applied by a skilled driver or through antilock control tends to produce shorter stops on most surfaces.
- The frictional (braking) force generated varies widely with road surface. The result of this relationship is obvious to both drivers and passengers in terms of stopping distance and deceleration if dry asphalt braking is compared with braking on ice.
- Typically, beyond the peak coefficient of friction attainable on a given road surface, the slope of the curve becomes negative. This phenomenon (essentially indicating that, beyond the slip resulting in peak frictional force, more pedal force results in less braking) explains why a skilled driver can attain significantly shorter stopping distances than can a less experienced driver and why electronic vehicle braking control is as complicated as it is. Also, the amount of "peak" in the coefficient of friction curves varies widely with road surface. More braking force benefit can be gained through slip control on surfaces such as ice than on dry asphalt, for example.

Another characteristic of automotive tires important in braking is lateral force versus slip. Lateral force is the force keeping a tire from sliding in a direction normal to the direction of the vehicle. The equation for lateral force is as follows:

$$F_y = \mu_{\text{lateral}} W_{wh}$$

PETITIONER'S EXHIBIT 1002
US PATENT NO. 6,581,565

where F_y = friction force, by direction
$\mu_{lateral}$ = lateral coefficient of friction, tire-to-road

The lateral coefficient of friction drops off quickly once a wheel begins to slip longitudinally, as can happen during braking. Excessive wheel slip at the rear wheels of a vehicle and the resulting loss of lateral frictional force will contribute to instability as the rear of the vehicle tends to slide sideways with relatively small lateral forces on the vehicle. Excessive wheel slip and the resulting loss of lateral friction force on the front wheels of a vehicle will contribute to loss of steerability; this loss of steering phenomenon is common during panic stops on low coefficient surfaces such as ice, as a hard apply of the brakes puts the tires in a 100 percent slip situation.

15.2.2 Vehicle Dynamics During Braking

An equation for braking performance can be obtained from Newton's second law: the sum of the external forces acting on a body in a given direction is equal to the product of its mass and the acceleration in that direction. Relating this law to straight-line vehicle braking, the significant factors are shown in Eq. (15.2) and the sum of the forces acting on the vehicle is shown in Fig. 15.2.[1]

$$\Sigma F = Ma_x = \frac{+W}{g} D_x = +F_{xf} + F_{xr} + D_A + W \sin\Theta + f_r W \cos\Theta \tag{15.2}$$

where M = mass of the vehicle
a_x = linear acceleration in the x direction
W = weight of the vehicle
g = acceleration due to gravity
$D_x = -a_x$ = linear deceleration
F_{xf} = front axle braking force
F_{xr} = rear axle braking force
D_A = aerodynamic drag (considered to be acting at a point)
Θ = angle of roadway
f_r = rolling resistance coefficient = $(R_{xf} + R_{xr}) / W\cos\Theta$

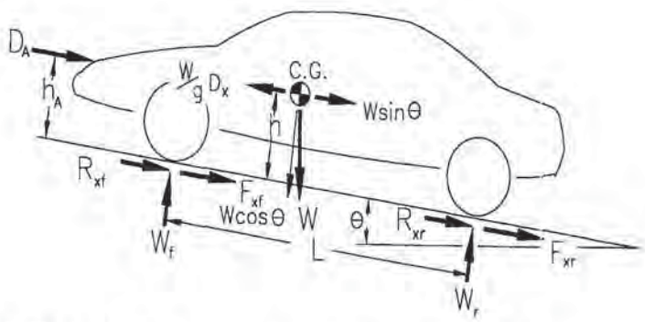


FIGURE 15.2 Significant forces' action on a vehicle during braking.

If braking forces are held constant and the vehicle velocity effects on aerodynamic drag and rolling resistance are neglected, the time for a vehicle velocity change, Eq. (15.3), and the distance traveled during a velocity change, Eq. (15.4), can also be derived from Newton's second law.[2]

$$t = \frac{M}{F_{xt}}(V_o - V_f) \tag{15.3}$$

PETITIONER'S EXHIBIT 1002
US PATENT NO. 6,581,565

where F_{xt} = total of all longitudinal deceleration forces on the vehicle
t = time
V_o = initial velocity
and V_f = final velocity

$$x = \frac{M}{F_{xt}}\left(\frac{V_o^2}{2} - \frac{V_f^2}{2}\right) \tag{15.4}$$

where x = distance in forward direction

These approximations indicate that the time to stop is proportional to vehicle velocity and the stopping distance is proportional to the square of the vehicle velocity.

During braking, the dynamic load transfer that occurs is a function of the height of the center of gravity, the weight of the vehicle, the wheelbase, and the deceleration rate. Equation 15.5 describes this dynamic load shift.

$$W_d = \left(\frac{h}{L}\right)\left(\frac{W}{g}\right)D_x - \frac{h_A}{L}D_A \tag{15.5}$$

where W_d = dynamic weight
h = center of gravity height
L = wheelbase
W = static vehicle weight
g = acceleration due to gravity
D_x = deceleration in the forward direction
h_A = height of the aerodynamic drag

Considering two-axle vehicles, this load transfer is additive to the front wheels and subtractive to the rear wheels during braking, as shown in Eq. (15.6) and (15.7), respectively.

$$F_{xmf} = \mu_p\left(W_{fs} + \frac{hWD_x}{Lg} - \frac{h_A}{L}D_A\right) \tag{15.6}$$

where F_{xmf} = maximum friction force in the longitudinal direction on the front wheels
μ_p = peak coefficient of friction
W_{fs} = static weight on the front wheels

$$F_{xmr} = \mu\left(W_{rs} - \frac{hWD_x}{Lg} + \frac{h_A}{L}D_A\right) \tag{15.7}$$

where F_{xmr} = maximum friction force in the longitudinal direction on the rear wheels
W_{rs} = static weight on the rear wheels

Simplifying Eq. (15.2) for the case of $\Theta = 0°$ and negligible aerodynamic drag and rolling resistance yields the following:

$$\sum F = \frac{W}{g}D_x = +F_{xf} + F_{xr}$$

Solving for D_x and substituting in simplified Eqs. (15.6) and (15.7) yields Eq. (15.8) and (15.9), respectively:

PETITIONER'S EXHIBIT 1002
US PATENT NO. 6,581,565

$$F_{xmf} = \mu \frac{\left(W_{fs} + \frac{hF_{xmr}}{L}\right)}{1 - \mu_p \frac{h}{L}} \tag{15.8}$$

$$F_{xmr} = \mu \frac{\left(W_{rs} + \frac{hF_{xmf}}{L}\right)}{1 - \mu_p \frac{h}{L}} \tag{15.9}$$

These relationships indicate that the maximum braking force on the front wheels is dependent on the braking force on the rear wheels through the deceleration and the associated forward load transfer and, in a similar fashion, the braking force on the rear wheels is dependent on the braking force on the front wheels.

Through application of the preceding equations, brake systems designers can determine the total braking force required to achieve the desired deceleration, and the brake system components can be sized appropriately. Safety and legal requirements dictate that system designers consider deceleration under vehicle loaded and unloaded conditions as well as under partially failed brake system conditions (either half-system failures or loss of brake boost to the entire system). Because of these considerations and numerous others, such as desired customer pedal stroke and pedal force/deceleration expectations, vehicle brake system sizing is a complicated engineering effort usually accomplished with the aid of a vehicle simulator computer program.

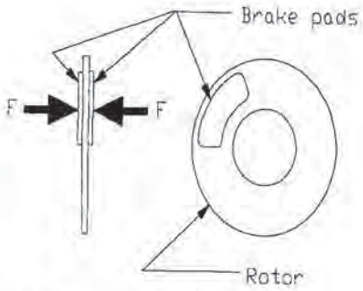


FIGURE 15.3 Disk brake schematic.

15.2.3 Brake System Components

Disk Brakes. Figure 15.3 shows a schematic diagram of a disc brake. In this type of brake, force is applied equally to both sides of a rotor and braking action is achieved through the frictional action of inboard and outboard brake pads against the rotor. The pads are contained within a caliper (not shown), as is the wheel cylinder. Although not a high-gain type of brake, disk brakes have the advantage of providing relatively linear braking with lower susceptibility to fading than drum brakes.

Force applied to the rotor by the pads is a function of hydraulic pressure in the brake system and the area of the wheel cylinder (or cylinders, as the design dictates). Static brake torque can be calculated using the following equation:

$$T = PAER \tag{15.10}$$

where T = brake torque
P = application pressure
A = wheel cylinder area
E = effectiveness factor: ratio of the disk rubbing surface to the input force on the shoes
R = brake radius

PETITIONER'S EXHIBIT 1002
US PATENT NO. 6,581,565

The static brake force can be calculated with the following relationship:

$$F_b = \frac{T}{r}$$

where F_b = brake force
r = tire rolling radius

Drum Brakes. Figure 15.4 depicts a schematic diagram of a drum brake. In drum brakes, force is applied to a pair of brake shoes in a variety of configurations, including leading/trailing shoe (simplex), duo-duplex, and duo-servo. Drum brakes feature high gains relative to disk brakes, but some configurations tend to be more nonlinear and sensitive to fading and other brake lining coefficient-of-friction changes.

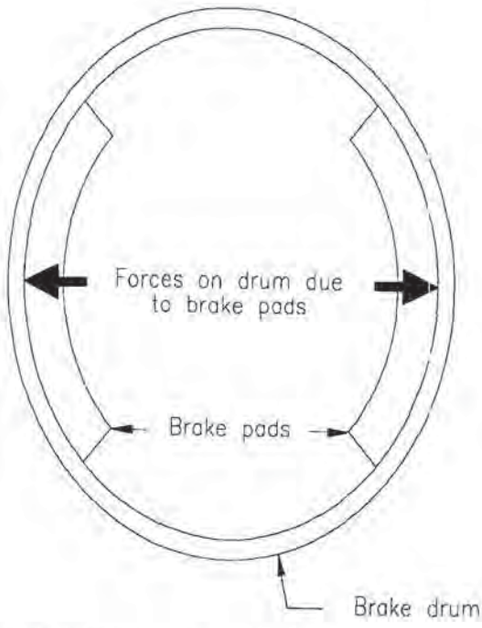


FIGURE 15.4 Drum brake schematic.

The static brake torque equation previously presented for disk brakes, Eq. (15.10), is equally applicable to drum brakes with design-specific changes for drum brake radius and effectiveness factor. By design, the brake radius for a drum brake is one-half the drum diameter. The effectiveness factor represents the major functional difference between drum and disk brakes; the geometry of drum brakes may allow a moment to be produced by the friction force on the shoe in such a manner as to rotate it against the drum and increase the friction force developed. This action can yield a mechanical advantage that significantly increases the gain of the brake and the effectiveness factor as compared with disk brakes. The dynamic brake force calculation for drum and disk brakes is more complex since the brake lining coefficient of friction is a function of temperature; as the lining heats during a braking maneuver, the effective coefficient of friction increases and less pressure is needed to maintain a constant brake torque.

Booster and Master Cylinder. Figure 15.5 is a schematic of a brake pedal, a vacuum booster, and a master cylinder. In actual practice, in passenger cars and light trucks the mechanical force gain due to the brake pedal geometry is usually 3 to 4 and the gain through a vacuum

PETITIONER'S EXHIBIT 1002
US PATENT NO. 6,581,565

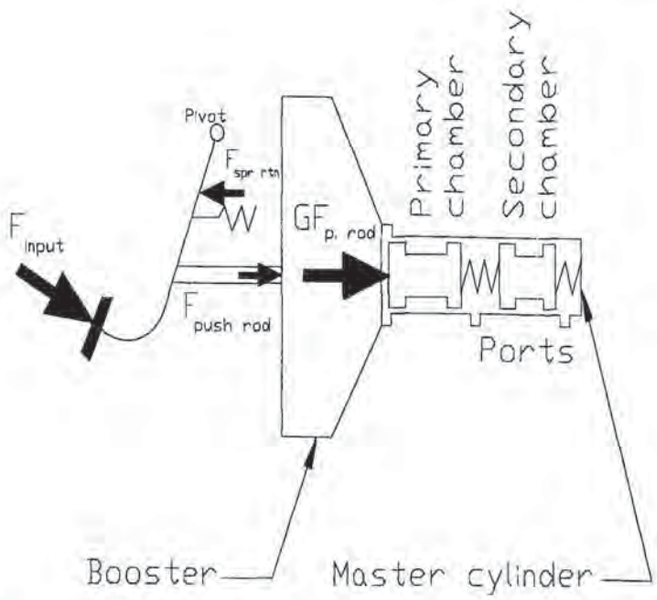


FIGURE 15.5 Brake pedal, vacuum booster, and master cylinder schematics.

booster is typically 5 to 9 after the booster reaches its crack point and before runout occurs. Therefore, force applied by the operator typically will be multiplied by a factor of 12 to 36 at the master cylinder in order to achieve the pressure necessary for braking. The resulting pressure in the master cylinder is as follows:

$$P_{MC} = \eta \frac{(F_{op} G_{mech} G_{boost} - F_s)}{A_{piston}}$$

where η = mechanical efficiency
P_{MC} = master cylinder pressure
F_{op} = operator force on the brake pedal
G_{mech} = mechanical gain primarily related to the brake pedal assembly geometry and the instantaneous return spring force
G_{boost} = brake booster gain, a function with the nonlinearities of a minimum crack force being necessary to initiate boost and a runout phenomenon resulting in a decreased force gain after a given input force is applied
F_s = return spring force
A_{piston} = area in the master cylinder on which the force is acting (chamber piston area)

Master cylinders are separated into primary and secondary chambers to improve safety by avoiding total brake system loss in case of a failure in one portion of the system. The most common configuration is shown in Fig. 15.5 with two chambers in a single bore.

Proportioning Valve. Due to the dynamic weight shift, as shown in Eq. (15.5), brake pressures that are appropriate for high-deceleration braking on front wheels usually are too high for the rear wheels; the result is that the rear wheels will tend to lock during braking. This problem can be decreased significantly through the use of proportioning valves. Standard proportioning valves allow equal front and rear brake pressures during low input pressures (corresponding to low deceleration rates and little dynamic load shift) but decrease the gain through the valve to less than one when a fixed input pressure (crack pressure) is reached. More sophisticated load-sensing valves are used in some applications when necessary, such as

PETITIONER'S EXHIBIT 1002
US PATENT NO. 6,581,565

when dynamic load shifts and vehicle loading changes are wide enough to make a fixed proportioning valve insufficient for proper braking in all conditions. Load-sensing valves feature a means to measure the weight on the rear wheels and adjust the gain through the valve accordingly.

Figure 15.6 shows the two most common passenger car and light truck system schematics including proportioning valves. The vertically split brake system typically is used on rear-wheel-drive vehicles and the diagonally split system is typically used on front-wheel-drive vehicles.

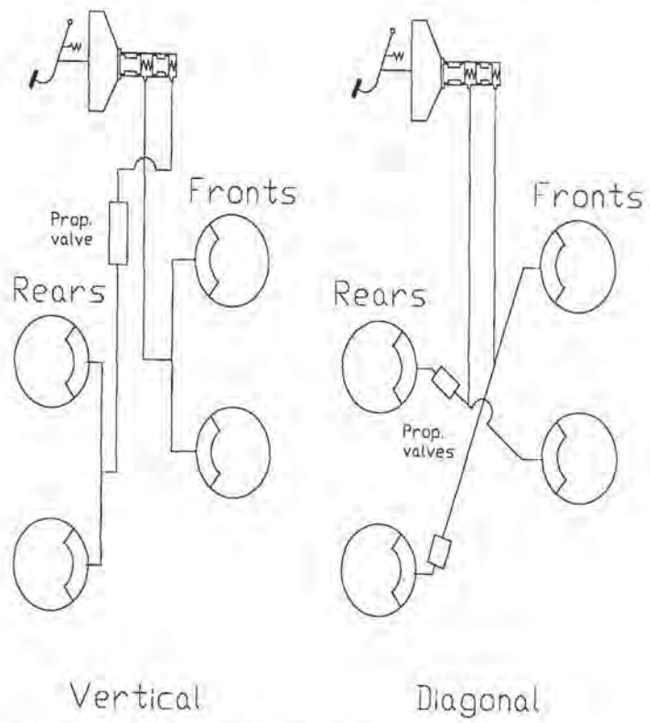


FIGURE 15.6 Vertical and diagonal split brake systems schematics.

Widespread use of diagonally split systems has been a direct result of the popularity of front-wheel-drive vehicles. Current law requires a half-system (hydraulic) failure stopping rate that is difficult to meet if the half system is the rear brakes (on a vertically split system) and the vehicle weight is significantly shifted towards the front as it is in front-wheel-drive vehicles. Diagonally split systems afford the use of one front brake regardless of the half-system failure, and front-wheel-drive vehicles can be made to pass the legal requirements despite the typically large difference between the weight on the front and on the rear wheels. However, diagonally split systems require two proportioning valves and tend to require more complex hydraulic plumbing than do vertically split systems.

15.3 ANTILOCK SYSTEMS

Although antilock concepts have been known for decades, widespread use of antilock (also called antiskid and ABS) began in the 1980s with systems developed with digital microprocessors/microcontrollers replacing the earlier analog units. An antilock system consists of a

PETITIONER'S EXHIBIT 1002
US PATENT NO. 6,581,565

hydraulic modulator and hydraulic power source that may or may not be integrated with the system master cylinder and booster, wheel speed sensors, and an electronic control unit. The fundamental function of an antilock system is to prohibit wheel lock by sensing impending wheel lock and taking action through the hydraulic modulator to reduce the brake pressure in the wheel sufficiently to bring the wheel speed back to the slip level range necessary for near-optimum braking performance.

15.3.1 Objectives

The objectives of antilock systems are threefold: to reduce stopping distances, to improve stability, and to improve steerability during braking.

Stopping Distance. As shown in Eq. (15.4), the distance to stop ($V_f = 0$) is a function of the initial velocity, the mass of the vehicle, and the braking force. From this equation it can be seen that by maximizing the braking force the stopping distance will be minimized, all other factors remaining constant. From Fig. 15.1 it is evident that on all types of surfaces, to a greater or lesser extent, there exists a peak frictional force. It follows that by keeping all of the wheels of a vehicle near the peak, an antilock system can attain maximum frictional force and, therefore, minimum stopping distance. This is an objective of antilock systems; however, it is tempered by the need for vehicle stability and steerability.

Stability. Although decelerating and stopping vehicles constitutes a fundamental purpose of braking systems, maximum friction force may not be desirable in all cases. For example, if a vehicle is on a split-coefficient surface, (asphalt and ice, for example), such that significantly more braking force is obtainable on one side of the vehicle than on the other side, applying maximum braking force on both sides will result in a yaw moment that will tend to pull the vehicle to the high-coefficient side and contribute to vehicle instability. Typically, on short-wheelbase vehicles a control strategy is employed to control the pressure in the rear wheels together to improve stability; similarly, it is common for a front-wheel strategy to be employed to limit the initial side-to-side pressure difference so as to not induce excessive moment changes in the steering wheel and force the operator to make excessive steering corrections to counteract the yaw moment.

If an antilock system can keep the vehicle wheels near the peak frictional force range, then lateral force is reasonably high, though not maximized. This contributes to stability and is an objective of antilock systems.

Steerability. Steerability depends on high lateral force. Good peak frictional force control is necessary in order to achieve satisfactory lateral force and, therefore, satisfactory steerability. Steerability while braking is important not only for minor course corrections but also for the possibility of steering around an obstacle. Antilock systems provide this feature through control to the peak frictional force range.

15.3.2 Antilock Components

The components of an antilock system are the wheel speed sensors, the hydraulic modulator, the hydraulic power source (usually an electric motor/pump), and the electronic control unit.

Wheel Speed Sensors. Due to simplicity and proven reliability, variable reluctance wheel speed sensors typically are used in antilock systems. Used in conjunction with exciter rings, this type of sensor produces a sinusoidal output that is directly proportional in frequency and amplitude to the angular velocity of the sensed wheel.

Depending on the design of the sensor and exciter ring and the gap between them, the sensor output amplitude may be as low as 100 mV at very low vehicle speeds and over 100 V at high vehicle speeds.

PETITIONER'S EXHIBIT 1002
US PATENT NO. 6,581,565

Both single-pole and dual-pole variable reluctance sensors are used, depending on the application: single-pole sensors tend to have higher outputs and dual-pole sensors tend to have better immunity to some types of noise. A limitation of this technology is that the very low speed output tends to be too low to be sensed reliably by the electronic control unit, given the electrically noisy environment typical of vehicles. This can result in errors below 1 to 3 m/h and cumulative inaccuracies if this sensor is used in conjunction with an odometer function; normally, antilock function is inhibited at very low speeds. Both single-ended and balanced inputs are used in electronic control units to receive wheel speed signals. A variety of active sensor technologies, including Hall effect and magnetoresistive, can be used in applications requiring very low speed sensing and in applications in which an appropriate signal level cannot be achieved with conventional variable reluctance sensors.

Hydraulic Modulators. Hydraulic modulators typically take two forms in production antilock systems: solenoid valves and electric motors. A simplified solenoid valve system schematic is shown in Fig. 15.7. In this system, if the solenoid valves are de-energized, hydraulic fluid is free to flow between the master cylinder and the brakes. If too much pressure is presented to the brakes and wheel lock is imminent, the antilock system will actuate a solenoid valve and energize the hydraulic pump. Actuation of the solenoid valve allows pressure to decrease from the brake through the valve to a low-pressure accumulator/sump. The fluid is temporarily stored in the sump prior to being pumped back into the system by the hydraulic pump. Through repetitive energization/de-energization cycles, average pressure to a given wheel can be regulated to the level necessary to achieve the desired braking force. Typical brake pressure and resulting wheel speed cycling is shown in Fig. 15.8.

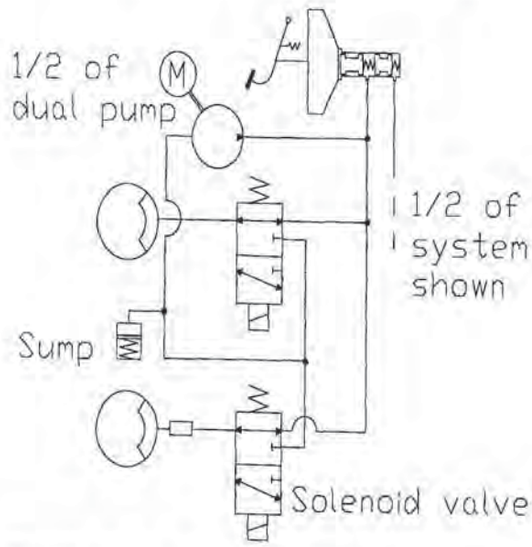


FIGURE 15.7 Simplified solenoid valve antilock system schematic.

Electric Motor/Pump. Although some antilock systems use multiple electric motors driving pistons to provide multiple-channel pressure reduction and rebuild, usually an electric motor-driven pump is used in conjunction with solenoid valves to achieve individual brake or brake channel pressure reduction and rebuild. A dual pump is often used to maintain a complete hydraulic separation of the two channels of the brake system. This is done to ensure that failure in one channel of the brake system will not affect operation of the other channel.

Electronic Control Unit. Control of the hydraulic modulator and electric motor/pump is performed by the electronic control unit. Modern customer expectations coupled with

PETITIONER'S EXHIBIT 1002
US PATENT NO. 6,581,565

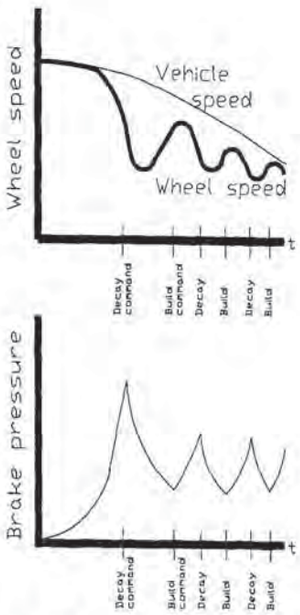


FIGURE 15.8 Typical antilock brake cycling.

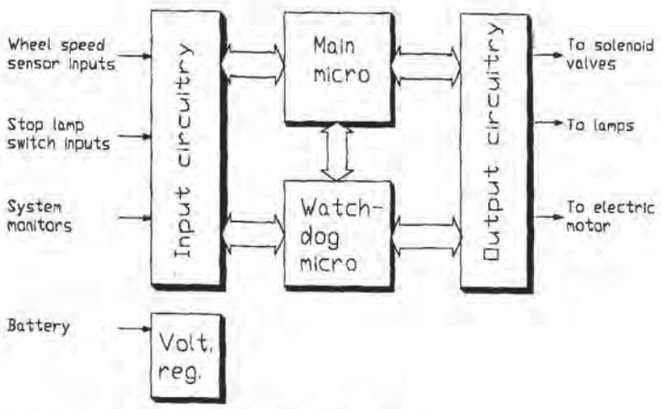


FIGURE 15.9 Electronic control unit block diagram.

decreasing microcontroller costs have made microcontroller-based electronic control units the norm rather than the exception. Although the control units can be either engine compartment-mounted or passenger compartment-mounted, reduced wiring costs favors the former. Also, for enhanced reliability, electronic control units may be either attached to or integrated with the hydraulic modulator.

15.3.3 Safety Considerations

Standard automotive brake systems have been developed and refined over the years to be highly reliable and safe. Because of its ability to decrease pressure in brakes, an antilock system must be designed using a disciplined methodology and must be rigorously tested prior to release for production.

PETITIONER'S EXHIBIT 1002
US PATENT NO. 6,581,565

Failure Mode and Effects Analyses/Fault Tree Analyses. Failure mode and effects analyses (or fault tree analyses) are essential to the proper design of antilock systems. Both system-level and subsystem-level analyses need to be performed and fault effects and detection assumptions must be tested. No single failure can result in an unsafe condition and, if a fault is undetectable in the field, that fault in conjunction with any other fault must not result in an unsafe condition. Because of the complexity of the electronic control units, simulation techniques are used to test those fault effects in which bench or field testing is impractical.

Common Design Techniques to Improve Safety. One of the most common techniques used to improve safety in antilock systems is to include extensive built-in-test within the electronic control unit. Typically, all inputs to the electronic control unit and outputs to the other components of the antilock system are tested for proper signals and loads, respectively, and all functions internal to the electronic control unit are extensively tested.

In addition, redundant processing is commonly used to insure the proper internal working of a microcontroller. This may take the form either of identical microcontrollers or of a main and a watchdog microcontroller that can inhibit operation.

In order to ensure inhibition of faulty antilock operation, antilock systems employ a relay function to remove actuation power from the output actuators; this function may take the form of a discrete relay or it may be a transistorized circuit. This relay function is a key element of the design since it affords a secondary method in which to inhibit energization of valves or the motor/pump and, therefore, a second level of safety relative to improper antilock operation.

Figure 15.9 is a typical electronic control unit block diagram.[3] Inputs are filtered and buffered prior to being presented to the microcontrollers for processing. Likewise, the microcontroller outputs are buffered/amplified and filtered prior to exiting the electronic control unit. In the diagram shown, the main microcontroller is responsible for the majority of processing and control of the outputs; the watchdog microcontroller, as its name implies, is responsible for monitoring for proper operation and inhibiting antilock if faults are indicated. A characteristic of modern antilock electronic control units is bidirectional communication between functional blocks; this is a result of the high level of built-in-test designed into the control units. For example, the output circuitry may be commanded to test the solenoid valves for proper current draw and convey the test results to the microcontrollers; similarly, the input circuitry may be commanded to perform tests on the sensors and other antilock components external to the electronic control unit, and convey the test results to the microcontrollers.

15.3.4 Antilock Control Logic Fundamentals

Due to the complexity of antilock braking and the requirements of stability and steerability as well as good stopping distance, the brake control algorithm is more easily represented as a state-space diagram than as a classical proportional-integrative-derivative control scheme.

A simplified state diagram for a single-channel antilock system is shown in Fig. 15.10. In this diagram, a vehicle not braking or decelerating would be in the NORMAL BRAKING state. If antilock action is warranted, it is because the brake pressure on a given channel has caused the wheel to begin to lock; the first action would be to decrease the brake pressure (DECAY state) in an effort to permit the locking wheel to reaccelerate. Fine control of the brake pressure is indicated by the states labeled HOLD OR BUILD/DECAY and SLOW BUILD and course control is indicated by the FAST BUILD state. (The course control is typically used during rapidly changing road surface conditions such as ice-to-asphalt transitions.) During the antilock cycle the state will change, as needed, to attain the type of brake pressure and resulting wheel speed activity as shown in Fig. 15.8. Once the need for antilock action has ended, the END ANTILOCK state is entered, the pump motor is de-energized, the valves are de-energized, and the system can return to the original NORMAL BRAKING state.[4]

How this state-space approach is integrated into a typical microcontroller flowchart is shown in Fig. 15.11. After RESET and INITIALIZATION, a microcontroller enters into a

PETITIONER'S EXHIBIT 1002
US PATENT NO. 6,581,565

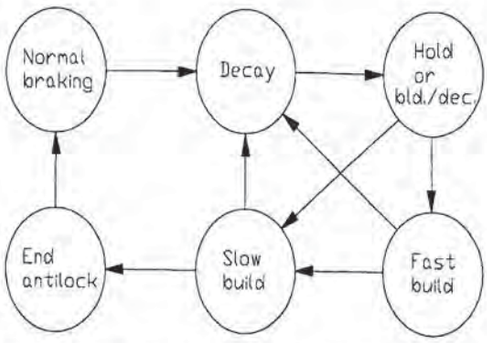


FIGURE 15.10 Simplified single-channel state diagram.

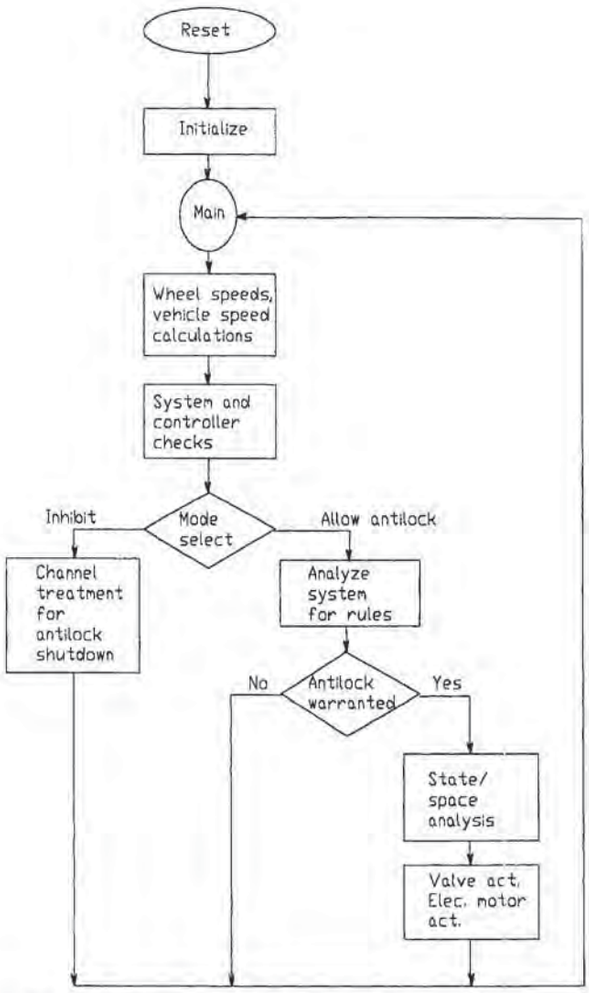


FIGURE 15.11 Simplified antilock flowchart.

PETITIONER'S EXHIBIT 1002
US PATENT NO. 6,581,565

MAIN loop that includes extensive system and electronic control unit checks as well as calculations of wheel speeds, prediction of vehicle speed, analysis of conditions warranting antilock action/state-space control law, and valve and motor/pump actuations.

Calculation of wheel speeds consists of scaling the wheel speed sensor inputs to a more usable form and possibly filtering noise due to axle deflection, brake squeal, other electrical systems, etc. A consideration is that the bandwidth of wheel acceleration and deceleration is large—50 g's may be attainable.

The vehicle velocity prediction is critical to many control schemes because wheel velocity relative to vehicle velocity, as well as wheel slip, may be used as a factor in determining appropriate valve action. Vehicle velocity prediction becomes difficult once the wheels begin to lock because the sensors will no longer be reliable indicators of vehicle speed. The methods used to predict vehicle velocity once the wheels have begun to lock consist of a set of rules that have been developed by antilock manufacturers through years of experience to ensure a prediction that has a high degree of accuracy to true vehicle speed.

The antilock system checks typically consist of sensor and valve/motor continuity tests and system voltage range tests. In addition, the checks normally include tests internal to the electronic control unit, such as inter-microcontroller communication.

Once it is determined that conditions are such that antilock action can be safely invoked if warranted, the wheel speed conditions are analyzed to establish the appropriate state for that channel. Primary indicators for most antilock control schemes are wheel slip and wheel deceleration. Another factor considered is the effect on vehicle stability if a particular state is commanded.

Actuation of the valves or electric motor actuators is a direct result of the decisions made in the analysis/state-space logic. Other than actuators requiring pulse-width modulation drives, the actuators normally will remain in the commanded state until the microcontroller loops back through the code (usually a few milliseconds).

15.3.5 Antilock System Testing

Antilock vehicle testing has evolved over the years to include the following most common tests:

- Straight-line stopping
- Braking in a turn
- Split coefficient stopping with associated stability criteria
- Transitional road surface testing including checkerboard and low/high and high/low coefficient surfaces
- Lane change maneuver

All of these tests may be performed on a variety of surfaces, at a variety of speeds, and with lightly loaded and heavily loaded vehicles.

15.4 FUTURE VEHICLE BRAKING SYSTEMS

A trend that will impact braking systems is the industry's desire to reduce vehicle wiring through the use of multiplexing techniques. As increasing numbers of vehicles are outfitted with antilock, this trend is expected to result in an increased number of antilock systems communicating with other vehicle systems through a multiplex link. In addition to the wheel speed/vehicle velocity information available from the antilock system, the antilock electronic control unit could benefit from this technology by being able to receive engine, transmission, steering angle, and other subsystem information.

PETITIONER'S EXHIBIT 1002
US PATENT NO. 6,581,565

Another trend in advanced electronically controlled braking systems is vehicle dynamics control during nonbraking maneuvers, as well as during braking. This is accomplished through use of the traction control actuators normally integrated in antilock hydraulic modulators, the addition of sensors to more accurately determine the dynamic state of the vehicle, and communication links with the drivetrain electronic controllers. Vehicle dynamic control holds the promise of safer vehicle operation through improved stability in all maneuvers.

The vehicle brake systems engineering community also is investigating the addition of radar to individual vehicles. This addition could lead to semiautomatic or automatic braking in emergency situations as the brake system anticipates the potential problem and aids the operator in safely applying the vehicle brakes in time to avoid a collision. This concept also lends itself to automatic braking in nonemergency situations to maintain safe distances between vehicles at high speeds.

Continuing interest in electric vehicles and the need for regenerative braking in these vehicles likely will significantly impact future braking systems. It is expected that the regenerative braking function will not be sufficient to provide adequate braking deceleration under all conditions and to provide operators the comfort and safety obtainable with conventional friction brake systems augmented by antilock systems. It is expected that a more complex electronic control system will be used in conjunction with electric vehicles to afford optimum power regeneration without sacrificing braking stopping distance, stability, or steerability.

These trends point to a continued use of friction brake systems through the end of the century and a significant expansion of the role of electronics in these systems.

GLOSSARY

Antilock (or ABS or Antiskid) A system designed to prevent wheel lock during overbraking.

Antilock hydraulic modulator A hydraulic brake pressure modulation actuator used in antilock systems.

Booster A brake pedal force amplifier, typically vacuum or hydraulically powered.

Booster crack point The brake pedal/push rod travel point initiating booster force amplification.

Booster runout A condition in which the brake booster can no longer provide the gain required due to high input forces and the input force/output force slope becomes less positive.

Brake caliper A part of a disc brake that contains the brake pads and the brake cylinder.

Braking force A force tending to stop a moving vehicle. Usually applied to the force resulting from brake torque being applied to a wheel of a moving vehicle.

Braking maneuver Any vehicle braking action intended to decelerate a moving vehicle, including partial as well as full stops.

Diagonal split brake system A brake system configuration in which a front brake and its opposing rear brake are included in the same brake channel. This technique is used to allow braking on one front wheel in the case of catastrophic failure of the other brake channel.

Disk brake A type of brake characterized by force being applied to both sides of a rotor, thereby creating braking torque.

Drum brake A type of brake characterized by brake force being applied to the inner surface of a drum, thereby creating braking torque.

Dynamic load transfer The characteristic of weight shift during deceleration that places more weight on the front wheels and reduces weight on the rear wheels.

PETITIONER'S EXHIBIT 1002
US PATENT NO. 6,581,565

Electric motor/pump The typical hydraulic power source used in antilock systems; an electric motor driving a hydraulic pump.

Lateral force Force perpendicular to the direction of travel.

Longitudinal slip Relative slip between the wheels and the road surface in the direction of travel.

Master cylinder A two-chambered hydraulic cylinder operated by the driver through actuation of the brake pedal.

Proportioning valve A hydraulic valve designed to reduce pressure to the rear brakes relative to the front brakes once a crack point is reached. The valve may be fixed or load-sensing.

Regenerative braking A type of braking used in electric vehicles in which the drive motor is used as a generator during braking, and it serves as the load to brake the vehicle. This technique is used to reclaim a portion of the energy expended during vehicle motion.

Vertical split brake system A brake system configuration in which both front brakes are on one channel and both rear brakes are on the other channel.

Wheel slip The difference between tangential wheel speed and road speed. A rolling tire with no braking torque on it exhibits 0 percent slip; a nonrotating tire on a moving vehicle exhibits 100 percent slip.

REFERENCES

1. J. Y. Wong, *Theory of Ground Vehicles,* John Wiley & Sons, New York, 1978.
2. T. D. Gillespie, *Fundamentals of Vehicle Dynamics,* Society of Automotive Engineers, Inc., Warrendale, Pa., 1992.
3. J. L. Cage, "The Bendix ABS underhood electronic control unit," *Automotive Technology International '90,* Sterling Publications International Limited, London, 1990.
4. J. L. Cage, and J. T. Hargenrader, "Safe electronic modules for antilock applications," *Automotive Technology International '91,* Sterling Publications International Limited, London, 1991.

ABOUT THE AUTHOR

Jerry L. Cage is the manager of electrical/electronics engineering, AlliedSignal Braking Systems. He has over 20 years experience in the design and development of automotive and aerospace control systems and harsh environment electronics. He has been awarded five U.S. patents in electronics and electrohydraulics.

PETITIONER'S EXHIBIT 1002
US PATENT NO. 6,581,565

CHAPTER 16
TRACTION CONTROL

Armin Czinczel
Development Engineer
Robert Bosch GmbH

16.1 INTRODUCTION

Traction control systems designed to prevent the drive wheels from spinning in response to application of excess throttle have been on the market since 1987. Vehicles with powerful engines are particularly susceptible to drive-wheel slip under acceleration from standstill and/or on low-traction road surfaces. The results include attenuated steering response on front-wheel-drive (FWD) vehicles, diminished vehicle stability on rear-wheel-drive (RWD) cars, and loss of effective accelerative force.

Large mutual discrepancies in left- and right-side traction levels engender early drive-wheel slip on slick surfaces. Under these conditions, the effective accelerative forces at both drive wheels are limited to a level corresponding to the adhesion available at the low-traction side. The traction control system inhibits wheelspin, allowing the wheel on the high-traction surface to apply maximum accelerative force to the road.

16.1.1 Optimizing Stability (Steering Control)

The essential requirement for systems designed to optimize vehicle stability (with RWD) and steering control (with FWD) is to maintain adequate lateral traction. The most basic arrangements achieve this end by controlling engine torque alone. Both drive wheels transmit the same level of motive force, dosed in accordance with the adhesion available at the low-traction wheel and thereby providing particularly large lateral-traction reserves at the wheel with the greater adhesion. When the traction levels are roughly equal at both drive wheels, the system enhances vehicle stability (steering control) while providing a certain increase in available effective accelerative force beyond that available on an uncontrolled vehicle with slipping wheels.

16.1.2 Optimizing Traction

The optimization of traction becomes a top priority when the motive force must be transmitted to surfaces on which the adhesion varies substantially between sides.

PETITIONER'S EXHIBIT 1002
US PATENT NO. 6,581,565

The typical passenger car features a differential unit at the drive axle; this unit allows virtually loss-free differences in wheel speed (for instance, in corners) in combination with uniform torque distribution to the drive wheels. This layout generally provides favorable dynamic vehicle response, as the equal distribution of drive torque inhibits vehicle yaw. However, a difference in the force-transmission potentials at the drive wheels can combine with demands for maximum traction to expose basic liabilities in the design principle.

Figure 16.1 illustrates the system dynamics of drive shaft, differential, and drive wheels on road surfaces affording differing levels of traction with adhesion coefficients μ_H, μ_L (high wheel, low wheel). The torque emanating from the driveshaft is distributed equally between the drive wheels. The low wheel responds to inadequate adhesion potential by spinning during brief wheel acceleration. The accelerative force transmitted through the high wheel then corresponds to the sum of the accelerative force at the low wheel plus its inertia Θ_R [$\dot{\Omega}$]/R. Once the low wheel reaches its terminal speed, the accelerative force available at both wheels is limited to the maximum at the low wheel.

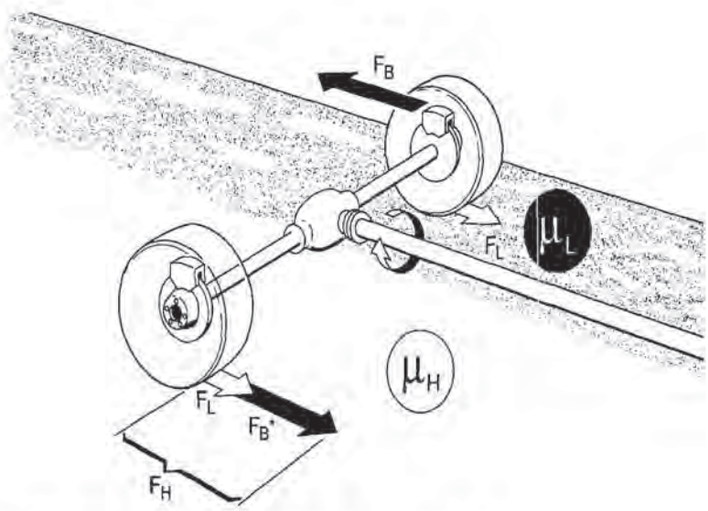


FIGURE 16.1 Braking intervention to limit differential slip.

The only way to increase the accelerative force at the high wheel is to prevent the low wheel from spinning. The first option, application of the wheel brake, is illustrated in Fig. 16.1. The application of braking force F_B at the low wheel prevents it from spinning. This makes the additional accelerative force F_B^* (the product of F_B multiplied by the ratio of effective braking radius to wheel radius) available at the high wheel.

A second option for maximum exploitation of traction potential is represented by the application of fixed, variable, or controlled differential-slip limitation mechanisms. These provide fixed coupling to ensure equal slippage rates at the drive wheels, thereby allowing them to develop maximum accelerative force.

During cornering at high rates of lateral acceleration, lateral variations in drive-wheel load occur, again producing a difference in acceleration potential. Brakes and limited-slip differential arrangements can also be applied to assist in ensuring maximum traction under these conditions.

16.1.3 Optimizing Stability and Traction

Traction-control systems incorporating engine-torque control and supplementary braking intervention (or controlled differentials) can be applied simultaneously to ensure consistent

PETITIONER'S EXHIBIT 1002
US PATENT NO. 6,581,565

vehicle stability (steering control) and optimal acceleration within the limits imposed by physical constraints. Engine-torque control is the preferred method on road surfaces affording uniform adhesion, while application of braking force (or differential control) provides optimal acceleration at both drive wheels for dealing with surfaces displaying lateral variations in traction.

16.2 FORCES AFFECTING WHEEL TRACTION: FUNDAMENTAL CONCEPTS

The dynamic forces that define the tires' braking response on straights and during cornering are already familiar from the technical literature. The transmission of accelerative force in straight-line operation and in curves is subject to the same qualitative principles that apply during braking. The slip ratio which applies for braking.

$$\lambda_B = \frac{V_F - \Theta_R R}{V_F}$$

is replaced by the ratio

$$\lambda_A = \frac{\Theta_R r - V_F}{V_F} \quad \text{with} \quad \Theta_R r \geq V_F$$

Acceleration slip rates can range all the way from 0 to the very high numbers used to describe the conditions that can occur when the drive wheels spin freely during attempts to accelerate from rest.

Figures 16.2 to 16.4 show acceleration and side-force coefficients as a function of the acceleration slip. Figure 16.2 applies for acceleration during straight-line operation. The demand for reserves in lateral adhesion is fairly diminutive under these conditions (including, for instance, compensation for side winds); thus, traction remains the salient factor.

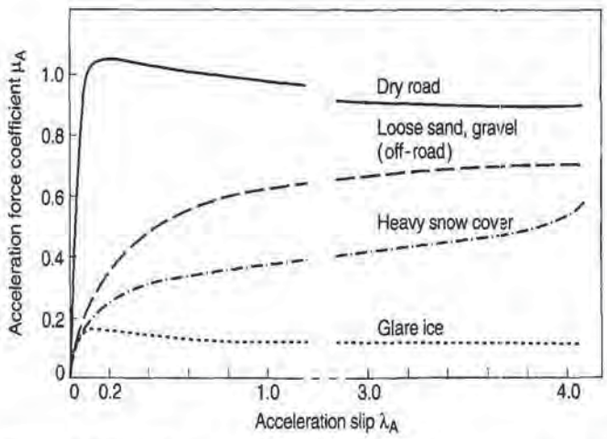


FIGURE 16.2 Adhesion coefficient for acceleration μ_A as a function of acceleration slip λ_A.

PETITIONER'S EXHIBIT 1002
US PATENT NO. 6,581,565

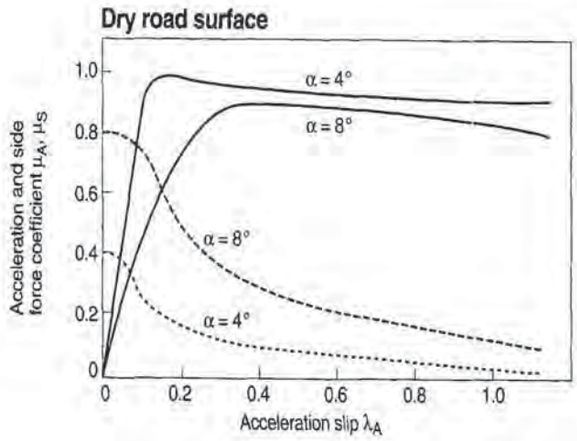


FIGURE 16.3 Acceleration and lateral traction coefficients at different slip angles α.

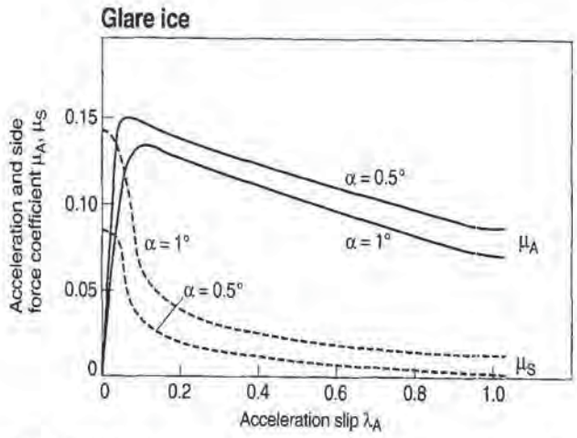


FIGURE 16.4 Acceleration and side-force coefficients at different slip angles α.

On dry road surfaces, maximum accelerative force is available at slip rates of 10 to 30 percent, with traction enhancements of 5 to 10 percent possible relative to spinning drive wheels.

On glare ice, maximum traction is achieved at extremely diminutive acceleration slip levels (2 to 5 percent). On loose sand and gravel and in deep snow (especially in combination with snow chains), the coefficient of acceleration force increases continually along with the slip rate, with the respective maxima only being reached somewhere beyond 60 percent. Thus, the slip rates of 2 to 20 percent found within the ASR's operating range will not provide adequate traction under all operating conditions.

For this reason, all known ASR systems incorporate slip-threshold switches or ASR deactivation switches, which allow the vehicle operator to either reset the ASR slip-control threshold to substantially higher levels, or to switch the system off entirely should the need arise.

Figures 16.3 and 16.4 apply to acceleration during cornering; under these conditions the drive wheels are subject to various degrees of lateral force as a function of the vehicle's rate of lateral acceleration. Increasing acceleration slip (and increasing accelerative forces) cause a drop in the lateral forces, which then respond to still higher slip rates by collapsing to small residual levels.

PETITIONER'S EXHIBIT 1002
US PATENT NO. 6,581,565

Figure 16.3 represents the response pattern on a dry road surface. The curve starts at a rate of acceleration slip of zero. Initially, the side-force coefficient displays a moderate downward trend. However, continuing increases in the coefficient of acceleration force induce a substantial fall in the side-force coefficient. The figure shows that the accelerative force must be limited to a fraction of its ultimate potential if sufficient lateral forces are to be maintained.

On glare ice (Fig. 16.4), the extremely limited friction potential means that vehicle stability under acceleration remains available only at relatively small slip angles (ca. ≤2°). Relatively diminutive slip angles (≤0.05°) will be sufficient to induce a radical drop in the side-force coefficient. This makes it clear that an extremely precise and sensitive slip control is required on glare ice (and other low-friction road surfaces). The traction-control system must thus exhibit a high degree of monitoring accuracy, while signal processing and actuation of the final-control elements must be rapid and precise.

16.3 CONTROLLED VARIABLES

The four wheel speeds used for the ABS supply the following closed-loop control parameters for the ASR traction control system: the acceleration slip from the lateral variation in the rotation speeds of the driven and nondriven wheels, and the angular acceleration of the driven wheels.

The following secondary control parameters are also calculated: vehicle velocity and acceleration based on the speeds of the nondriven wheels, and curve recognition, derived from comparisons of the speeds of the nondriven wheels.

The target value for acceleration slip is defined as the mean rotational velocity of the nondriven wheels plus a specified speed difference known as the slip threshold setpoint. The main goal of regulating acceleration slip can thus be divided into two subsidiary objectives: closed-loop control of acceleration slip to maintain slip rates at the specified levels with maximum precision, and calculation of optimal slip setpoints for different operating conditions and their implementation as control objectives.

Depending on the final-control strategy being used, various control concepts can be employed to meet the first objective. With throttle-valve control, a setpoint calculated from a number of signals is adopted for regulation as soon as the closed-loop control enters operation. The subsequent control process basically corresponds to that of a PI controller. When the brakes are used, arrangements are necessary to compensate for the nonlinear pressure-volume curve which governs the response in the brake calipers. The first stage of the closed-loop control program thus employs a sensing pulse corresponding to a relatively large volume; this compensates for compliance in the brake caliper. In the next stage, the system responds to positive deviations from the setpoint with graduated pressure increases; the rate of increase corresponds to the degree of divergence. A subsequent drop below the control setpoint initiates a pressure-relief stage (sequence of defined pressure-relief and holding phases). This impulse series, in which the length of the pressure-relief phases increases continually, is followed by termination of braking intervention.

Ignition and fuel-injection intervention essentially conform to the D controller closed-loop control concept. The difficulty associated with determining satisfactory setpoint values results from the fact that optimal acceleration and lateral forces cannot be achieved simultaneously. The ASR control algorithm must therefore meet varying operator demands for linear traction and lateral adhesion by using priority-control strategies and adaptive response patterns.

High vehicle speeds are accompanied by lower operator requirements for traction, especially with low coefficients of adhesion. At the same time, reductions in vehicle stability and steering response are not acceptable. The control strategy is thus designed to provide progressively lower slip threshold setpoints as the vehicle speed increases, with priority being shifted from linear traction to lateral adhesion.

PETITIONER'S EXHIBIT 1002
US PATENT NO. 6,581,565

The vehicle's acceleration rate and the regulated level of engine output provide the basis for reliable conclusions regarding the coefficient of friction. Thus, another important strategy takes into account the coefficient of friction at the road surface. The slip threshold setpoint is raised in response to higher friction coefficients. This ensures that an ASR system designed for optimum performance on low-friction surfaces will not intervene prematurely on high-traction surfaces.

Yet another important control strategy is based on the cornering detection mentioned previously. This system employs the difference in the wheel speeds of the nondriven wheels as a basis for reductions in the slip setpoint to enhance stability in curves. This speed differential can be used to calculate the vehicle's rate of lateral acceleration. A large discrepancy indicates a high rate of lateral acceleration, meaning that a high coefficient of friction may also be assumed. In this case, the slip setpoint should not be reduced, but rather increased.

16.4 CONTROL MODES

16.4.1 Modulation of Engine Torque

Various control intervention procedures can be employed, either singularly or in combination, to regulate engine torque:

- Throttle-valve control with the assistance of the electronic performance control or an automatic throttle-valve actuator (ADS)
- Adjustment of the ignition-advance angle
- Selective ignition cutout, combined with suppression of fuel injection
- Fuel injection suppression alone

Slippage at the drive wheels generally occurs in response to an excess of torque relative to the coefficient of friction available at the road surface. Controlled reduction of engine torque is thus a logical step. It is always the most suitable method in cases where virtually identical adhesion is present at both drive wheels. At the same time, the response times for the individual engine controls must be considered if adequate vehicle stability is to be ensured (see Fig. 16.5).

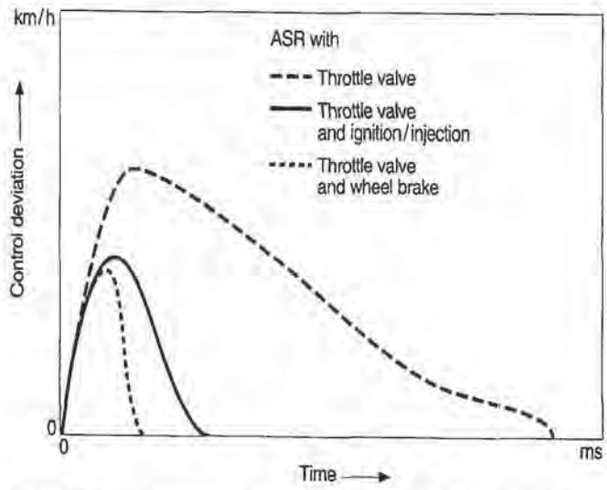


FIGURE 16.5 Deviation of the controlled variable during first control cycle with different actuators.

PETITIONER'S EXHIBIT 1002
US PATENT NO. 6,581,565

If control is restricted to the throttle-valve position alone, the throttle valve's response time, response delays within the intake tract, inertial forces in the engine, and drivetrain compliance will all result in palpable wheel slippage continuing for a relatively long period of time. Throttle regulation alone cannot ensure adequate vehicle stability on rear-wheel-drive vehicles. This qualification is particularly applicable to vehicles with a high power-to-weight ratio. On FWD and 4WD vehicles, throttle-valve control alone can be sufficiently effective if response delays are minimized.

Arrangements combining throttle-valve regulation with interruptions in the fuel injection produce substantial reductions in the amplitude and duration of wheel slip. Thus, this concept can be used to guarantee good vehicle stability regardless of which axles are driven.

In principle, it is also possible to design an ASR system based solely on regulation of the ignition and injection systems. This concept employs a system with sequential fuel injection. It alternately cuts out individual cylinders, while the ignition is also adjusted for the duration of the control process. Although this concept can be employed to ensure adequate vehicle stability regardless of drive configuration, certain sacrifices in comfort are unavoidable, especially during operation on ice and during the warm-up phase.

16.4.2 Brake Torque Control

The brakes at the drive wheels are capable of converting large amounts of kinetic energy into heat, at least for limited periods of time. In addition, the response times can be held extremely short, making it possible to limit slippage increases to very low levels.

ASR systems relying exclusively on braking intervention appear suitable for regulating spin at the drive wheels.

Traction enhancements during starts and under acceleration on road surfaces affording varying levels of adhesion at the left and right sides are especially significant with this system.

The ASR hydraulic unit used to generate the braking forces employs components which are already present for the ABS. Cost considerations make it important that ASR hydraulic systems require an absolute minimum in additional components beyond those already available for the ABS.

The hydraulic concepts can be classified in two categories, according to whether stored hydraulic energy is employed or not. A dual-strategy system including rapid braking intervention with stored hydraulic energy is always to be recommended where the engine torque control is based entirely on throttle valve adjustments with their relatively long response times.

Figures 16.6 and 16.7 illustrate two examples of ASR braking intervention using stored energy.

Brake Torque Control with Stored Energy. In this ASR system, designed for RWD vehicles in the upper price range, engine torque is regulated exclusively by the engine performance control (EPS) unit. Rapid braking intervention is required for enhanced regulation of vehicle stability; this also ensures optimal traction at both drive wheels, especially with lateral variations in adhesion potential. This system offers optimal vehicle stability and traction combined with a high level of comfort. Figure 16.6 illustrates the design of the integrated ABS/ASR hydraulic unit.

The primer pump draws brake fluid from the master-cylinder reservoir and supplies it to the ABS return pump under small positive pressure. To meet the requirements of the ABS system, the dual-circuit ABS return pump is expanded to include a third plunger, which assumes responsibility for the ASR storage charge. For "rapid" braking intervention, the pressure in the wheel cylinder must escalate from 0 to 50 bar in less than 200 ms. A hydropump, with its limited supply capacity, is not capable of providing this order of pressure build-up in the required time, necessitating the use of a high-pressure accumulator to supply the required brake fluid with adequate alacrity.

When the traction control system is activated, the switchover valve moves to the third position and brake fluid from the reservoir is supplied to the two ABS/ASR control valves. While

PETITIONER'S EXHIBIT 1002
US PATENT NO. 6,581,565

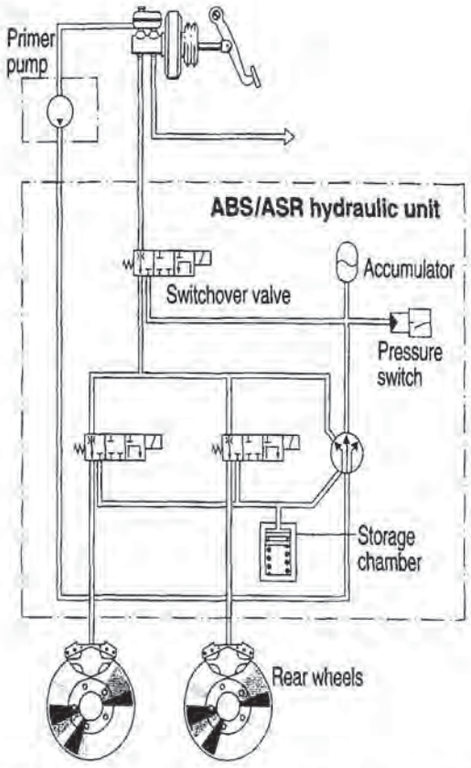


FIGURE 16.6 Diagram showing the ABS/ASR hydarulic circuit using braking force with stored energy (integrated system).

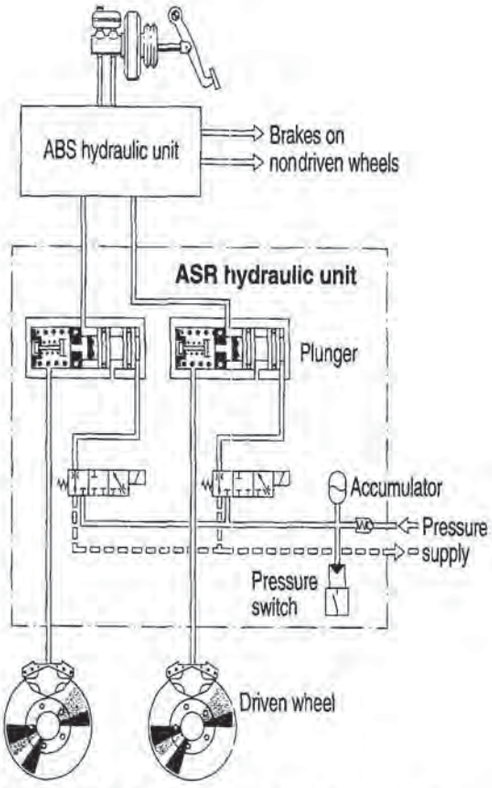


FIGURE 16.7 Diagram showing hydraulic unit for ASR system with braking intervention using stored energy via plunger.

an ABS solenoid valve can satisfy the requirements of the ABS hydraulic circuit, two solenoid valves are needed for the ABS/ASR hydraulic unit in order to allow individual braking control at the drive wheels.

These two solenoid valves regulate brake pressures at the driven wheels in accordance with the ASR control commands. Accumulator charging is controlled by the pressure switch and continues during normal vehicle operation. A special low-noise pump design is employed to meet stringent customer specifications.

ABS/ASR System with Brake Intervention Using Stored Energy (separate design). One version employs a high-pressure accumulator to provide hydraulic energy for ASR braking. An engine-driven pump (level control) supplies hydraulic fluid to the accumulator. The system includes a plunger for each driven-wheel brake. An additional 3/3 ABS valve is also installed to govern the supply of hydraulic fluid from the reservoir to the primary side of the plunger and to separate this medium from the brake fluid present on the secondary side. The solenoid valves respond to the position commands from the ABS/ASR control unit to control pressure accumulation, maintenance, and release operations to maintain the required pressure level on the plungers' primary sides. The plungers move to the left. Initially, a central valve closes to block the connection with the master cylinder. The plunger's displacement pressurizes the brake fluid on the secondary side to produce the desired pressure level in the wheel cylinder.

ASR designs relying on stored energy to activate plungers are always worthy of consideration in those cases where the vehicle is already equipped with a hydraulic energy supply for other purposes (e.g., power steering, level control).

PETITIONER'S EXHIBIT 1002
US PATENT NO. 6,581,565

Brake Torque Control without Stored Energy. Each of the ASR hydraulic units described requires a high-pressure accumulator to ensure that the braking energy can be provided quickly enough. This means additional design complication with attendant expenditure.

Another system differs from those already described by using the supply circuit of the ABS return pump exclusively to regulate the braking force at the drive wheels. The return pump forms part of a self-priming circuit, thus employing the (already installed) ABS return pump as an inexpensive source of energy for braking. The ASR braking function can thus be achieved with a minimum of additional design complication.

Figure 16.8 shows the hydraulic circuit for a passenger car with a K-pattern brake circuit and front-wheel-drive. When the intake valve opens, the self-priming pump extracts brake fluid from the reservoir and draws it into its circuit before supplying it directly to the ABS/ASR control valve at the drive wheel. The control valve regulates braking force by building up, maintaining, and releasing pressure in accordance with the respective position commands from the control unit. The fluid bled by the control valve in the pressure-release mode is returned to the pump's intake side. A switchover valve connects the high-pressure side of the self-priming return pump with the second brake circuit (governing the other front-wheel brake) and the pressure-relief valve responsible for regulating the ASR system pressure. With the exception of the suction line, the second brake circuit features a symmetrical layout. The passage to the master cylinder is also closed.

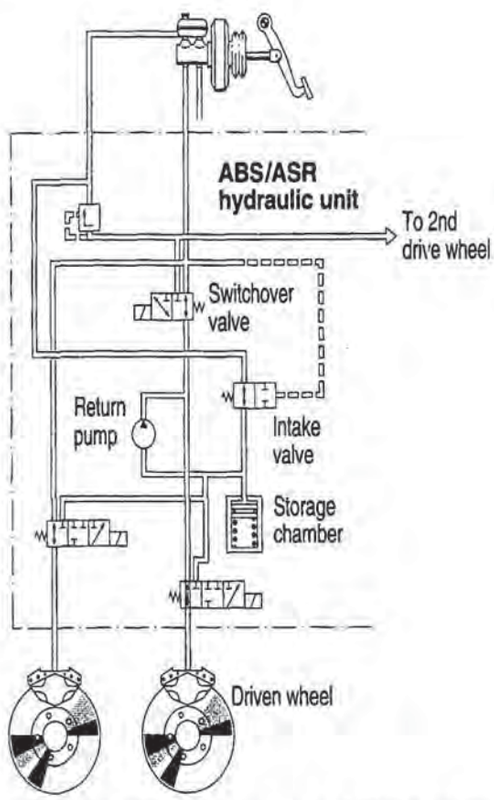


FIGURE 16.8 Diagram showing the ABS/ASR hydraulic unit employed for braking intervention without stored energy.

This ASR system can be installed in rear-wheel-drive vehicles with TT brake circuit configurations with even less expenditure: because both drive-wheel brakes are then in the same circuit, only a single switchover valve is required.

PETITIONER'S EXHIBIT 1002
US PATENT NO. 6,581,565

New Design for Brake Torque Control without Stored Energy. The principle of braking intervention without stored energy has been developed further for a new generation of ASR systems entering production in 1993. (See Fig. 16.9.)

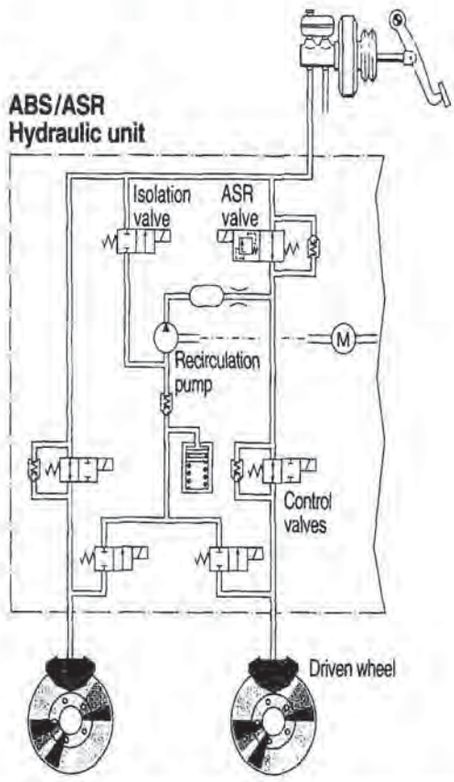


FIGURE 16.9 New design for brake torque control without stored energy.

The self-priming recirculation pump draws fluid from the master cylinder through an electrically controlled isolation valve, obviating the requirement for an additional intake line. Meanwhile, the pressure-relief valve can be integrated within the ASR valve. This configuration allows creation of a self-contained system combining simplified installation with enhanced safety. In addition, the reduction in the number of components improves reliability.

The 3/3 valves employed on earlier versions have been replaced by extremely small 2/2 solenoid valves.

16.4.3 Differential Slip Modulation

ABS/ASR System Regulating Differential Slip on Rear-Wheel-Drive Vehicles. This system controls the differential's lateral slip to improve traction for starting off and for simultaneous acceleration and cornering on road surfaces affording different levels of traction from left to right. The slip-limitation mode remains active until a specific vehicle speed is attained, and is deactivated completely at higher speeds.

When the vehicle starts off, the rotation speeds of the wheels on the outside of the curve are subjected to a mutual comparison. The lock is activated once a specific difference in the two speeds is exceeded. There then follows a comparison of the rotation speeds of the driven

PETITIONER'S EXHIBIT 1002
US PATENT NO. 6,581,565

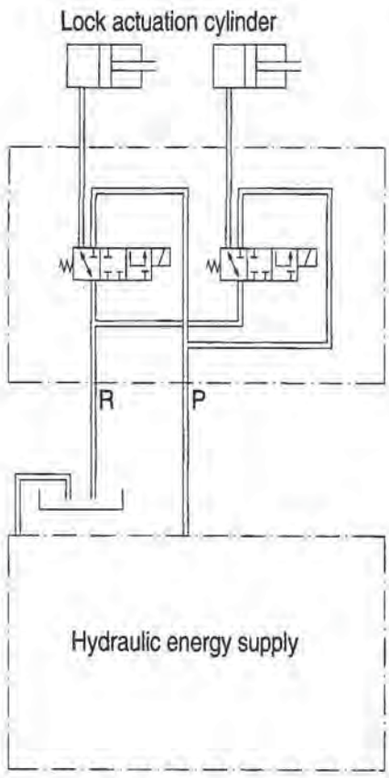


FIGURE 16.10 Hydraulic unit for control of rear-axle and interaxle differential locks.

wheels. The lock is deactivated as soon as the difference in rotation speeds drops below a specified level.

ABS/ASR System for Controlling Rear-Axle and Interaxle Differential Slip Rates on 4WD Passenger Cars. This version incorporates an additional interaxle control feature.

Four-wheel drive passenger cars employ a specific fixed front-to-rear distribution of engine output to provide optimum vehicle characteristics within the stable range (that is, with limited amounts of acceleration slip). One or both wheels at either axle can respond to throttle application on low-traction surfaces with immoderate wheelspin. This is where the interaxle slip limiter is activated to adapt the distribution of engine torque to the traction available at the respective axles, thereby improving traction while also enhancing vehicle stability and steering response.

Figure 16.10 illustrates the design of the hydraulic unit used to control the lateral and interaxle slip-limitation mechanisms. An electric pump supplies a high-pressure accumulator. The accumulator, in turn, provides pressure to a 3/3 solenoid valve for control of the lateral and interaxle locking mechanisms. The return volume from the pressure-relief phase is conducted to a separate reservoir.

16.5 TRACTION CONTROL COMPONENTS

The following is a selection of the components used in Bosch traction control systems.

16.5.1 Wheel-Speed Sensors

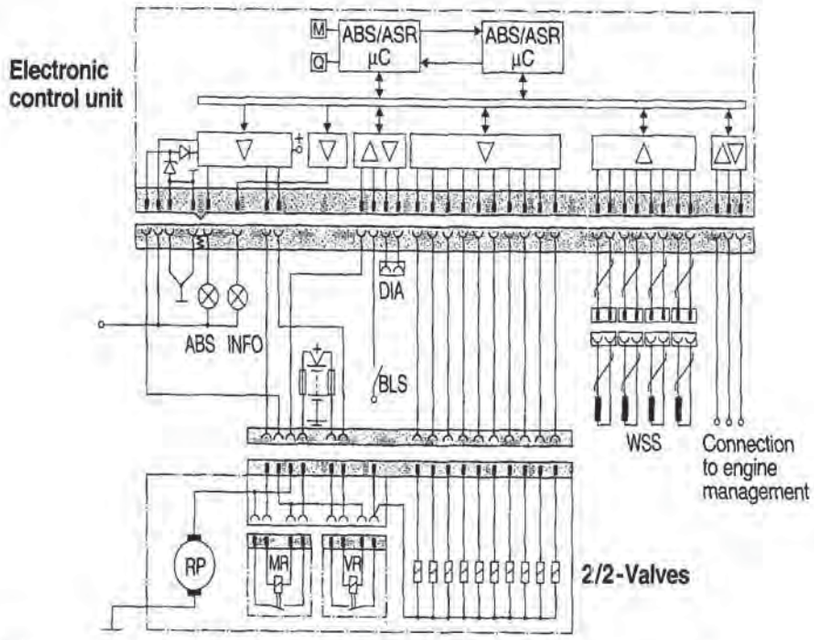
The system employs the same wheel-speed sensors that provide the information for the antilock braking system.

16.5.2 Electronic Control Unit

Figure 16.11 shows an ASR circuit diagram. An input amplifier IC receives the signals from the wheel-speed sensor; the signal frequency indicates the wheel speed. Two microcontrollers then process the signals to determine the wheel speed and acceleration rate. These data, in turn, provide the basis for calculations to determine the actual and desired values for slip control. Overall signal processing, the control algorithm, and the monitoring software are present in each of these microcontrollers to provide the system with backup capabilities.

Three output amplifiers control the solenoid valves, the ABS and ASR indicator lamps, the driver-information lamp, and the motor and valve relay. An additional IC is required to monitor the braking requirement and pump-motor voltage and for diagnosis.

PETITIONER'S EXHIBIT 1002
US PATENT NO. 6,581,565



M :	memory	BLS :	brake light switch
Q :	quartz	WSS :	wheel speed sensors
ABS/ASRµC :	ABS/ASR microcomputer	RP :	recirculation pump motor
ABS :	ABS warning lamp	MR :	motor relay
INFO :	information lamp	VR :	valve relay
DIA :	diagnosis connector		

FIGURE 16.11 Operation diagram for the complete system.

16.5.3 Hydraulic Unit

Four examples of ASR hydraulic units were given in Sec. 16.4.2.

16.5.4 Electronic Throttle Control Actuator

See Sec. 10.3.1.

16.5.5 Simplified Throttle Control Actuator

See Sec. 10.3.1.

16.5.6 Fuel Injection and Ignition Control

This system reduces engine output by suppressing the fuel injection process.

Complete fuel injection suppression would lead to a total loss of engine output—a smooth, graduated response would be impossible with this kind of arrangement. In contrast, selective suppression of the injection process at individual cylinders can be employed to achieve a good compromise between quick response and a graduated reduction of engine power. This is the design principle behind the new concept.

PETITIONER'S EXHIBIT 1002
US PATENT NO. 6,581,565

With suppression according to individual cylinders, the number of control increments is the same as the number of cylinders. Because this limited number of control stages is still inadequate for a (as an example) four-cylinder engine, a supplementary strategy is employed: this is referred to as alternating injection suppression. It consists of varying the number of active cylinders by one after every two crankshaft rotations to produce a mean torque lying between the torques produced at the two cylinder stages. This method doubles the number of control stages to achieve an acceptable level of driving comfort, while complementary reductions in ignition advance can be employed to provide additional incremental adjustments.

In cases where the excess torque is substantial, injection suppression can be supplemented by short-term ignition cutout to provide extremely rapid output reductions. Figure 16.12 shows the design of the system. In addition to the modest expense, this system also offers vehicle manufacturers an additional advantage in the form of space savings (no additional space required) and simplicity (limited amount of extra wiring).

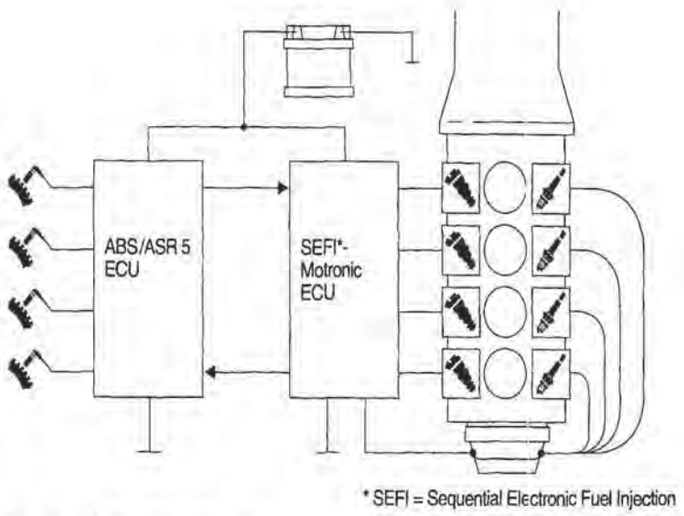


FIGURE 16.12 ASR EZ system.

16.6 APPLICATIONS ON HEAVY COMMERCIAL VEHICLES

Heavy commercial vehicles are used in a highly variegated range of applications. In principle, the ASR installed on these vehicles employs the same control strategies used for passenger cars: engine-output control and braking intervention.

Differences in vehicle application can make it necessary to employ ASR systems in various levels of complexity (for instance, relying on braking control or engine output control exclusively). The control unit recognizes the design stage and carries out its control functions accordingly. This makes it possible to employ the most economical ASR system for each vehicle type and particular application.

Figure 16.13 features a schematic diagram showing a typical 4×2 vehicle equipped with a top-of-the-line ABS/ASR system. During acceleration on μ-split surfaces, the brake-force regulator limits slip between the drive wheels. The ASR valve (4) is activated on the side with the spinning wheel, while the ABS pressure-control valve (3) allows graduated increases in pressure at the wheel cylinder.

If both drive wheels start to spin on a road surface affording equal traction on both sides, the engine-output controller responds by reducing the drive slip to optimum values. In this example, the electric performance control (EPC) (10) assumes the role of final-control ele-

PETITIONER'S EXHIBIT 1002
US PATENT NO. 6,581,565

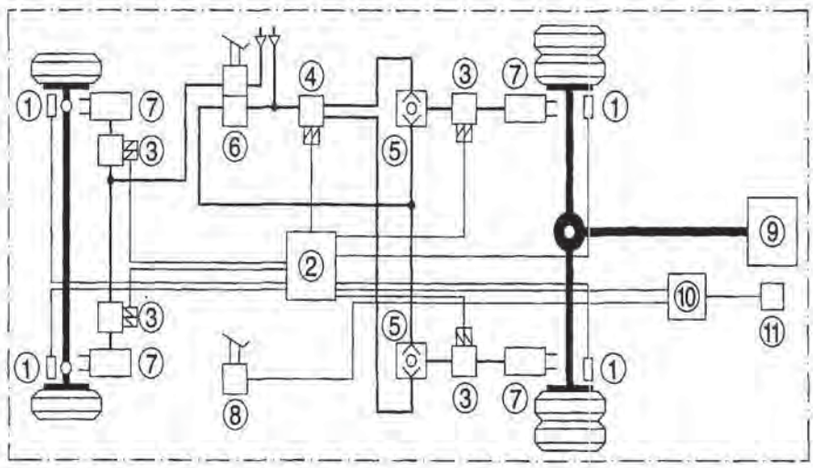


FIGURE 16.13 Four-circuit ABS/ASR, 4 × 2 vehicle.

ment. The ABS/ASR control unit (2) transmits the desired increment of reduction to the EPC control unit via interface, and also controls the electric motor at the injection pump.

16.7 FUTURE TRENDS

Ensuring driving stability is the most important task of ASR with rear-wheel-drive cars. This task can be achieved by a fast engine torque control or a combination of throttle control and a fast brake control.

ASR systems with a fast engine torque control (ignition and injection intervention) and brake control without stored energy will be widely used.

Although the application of controllable differential locks also offers efficient ASR control, the higher costs of this system will prevent wide usage.

The predominant demand on ASR systems for front-wheel-drive cars is that of traction optimization. Therefore, an ASR system with brake torque control is needed. The combination of brake torque control and engine torque control results in a complex, efficient system.

In the future, only ASR systems with brake torque control will be widely used with front-wheel-drive cars. Especially the combination of brake torque control and engine torque control with ignition and injection intervention will be widely used.

GLOSSARY

ABS return pump A piston pump that draws back brake fluid to the master cylinder.

Alternating injection suppression A variation of the number of active cylinders by one after every two crankshaft rotations in order to modulate the engine torque.

PETITIONER'S EXHIBIT 1002
US PATENT NO. 6,581,565

ASR deactivation switch A device to switch off ASR on sand and loose gravel in order to achieve maximum traction on these surfaces.

Automatic throttle valve actuator A simple actuator for automatic throttle angle reduction in case of excessive acceleration slip.

Braking intervention Automatic brake application at drive wheels in case of excessive acceleration slip.

D controller A controller with differentiating characteristics.

Electronic performance control Electronic accelerator control.

Engine torque control An actuator to modulate engine torque in case of excessive acceleration slip.

PI controller Controller with proportional and integral characteristics.

Slip threshold switch Switch to increase desired slip threshold on sand and loose gravel.

Switchover valve A valve to switch hydraulic performance from normal braking to ASR performance.

Throttle valve control ASR actuator to modulate the throttle angle.

3/3 ABS valve A valve with three connections and three positions for ABS wheel pressure modulation.

BIBLIOGRAPHY

Maisch, Wolfgang, Jonner Wolf-Dieter, and Alfred Sigl, "Traction control—a logical addition to ABS," *SAE International Congress and Exposition,* Detroit, Feb. 23–27, 1987.

Kolberg, Gerhard, "Elektronische Motorsteuerung für Kraftfahrzeuge," *Motortechnische Zeitschrift,* Germany, 1985.

Demel, H., and A. Czinczel, "ABS-task, design, and function," *I Mech E Conference,* London, 1988-6, pp. 89–94.

Buschmann, G., N. Ocvirk, and P. Volz, "Integrated traction control function—the consequent extension of highly sophisticated anti-lock systems," *I Mech E Conference,* 1988-6, pp. 103–112.

Klein, Hans-Christof, "PkW-ABV-Bremssysteme mit weiteren integrierten Funktionen," *Automobilindustrie,* May 1989, pp. 659–673.

Kupper, R., and N. Hover, "Anti-slip-control system with high safety and comfort," *I Mech E,* C382/113, 1989, pp. 523–531.

Sigl, A., and H. Demel, "ASR-traction control, state of the art and some prospects," SAE 900.24.

Sigl, A., and A. Czinczel, "ABS/ASR5—the new ABS/ASR system for passenger cars," *I Mech E Conference,* London, 1993, pp. 81–87.

ABOUT THE AUTHOR

Dipl. Ing. Armin Czinczel received a degree in mechanical engineering at the Technical University in Hanover, Germany. He started his professional career with development work on navigation systems. He joined Bosch in 1968, working on ABS development until his retirement in 1994.

PETITIONER'S EXHIBIT 1002
US PATENT NO. 6,581,565

PETITIONER'S EXHIBIT 1002
US PATENT NO. 6,581,565

CHAPTER 17
SUSPENSION CONTROL

Akatsu Yohsuke
Manager, Vehicle Research Laboratory
Nissan Motor Co., Ltd.

The function of a suspension system in an automobile is to improve ride comfort and stability. An important consideration in suspension design is how to obtain both improved ride comfort and stability, since they are normally in conflict. Advances in electronic control technology, applied to the automobile, can resolve this conflict.

17.1 SHOCK ABSORBER CONTROL SYSTEM

During the past 20 years, many different damping control systems have been studied. The main purpose of all these systems is to select the optimum damping force for various driving conditions. The first function of a shock absorber is to control vehicle movement against inertial forces, such as roll when the vehicle turns and pitch when the vehicle is braked. The second function is to prevent vehicle vibration caused by road surface inputs. To satisfy both functions it is necessary to control damping forces.

There are three basic parts of a damping control system: a damping control device (actuator), sensors, and software (control strategy). Optimum damping forces should be set for various running conditions in order to improve ride comfort and handling stability.

17.1.1 System Configuration

One of the damping control system configurations is shown in Fig. 17.1. This system uses five sensors, including a supersonic road sensor, to detect running conditions. Control signals are sent to adjust the damping force of the variable shock absorbers to optimum values. A main advantage to this type of system is that, through the use of a road sensor, it can provide optimum control in accordance with the actual road conditions. This system incorporates three discrete damper characteristics. Sensors used are: a vehicle speed sensor, a steering angle sensor, an acceleration and deceleration sensor, a brake sensor, and a supersonic sensor to detect road conditions.

One system uses four piezo sensors and four piezo actuators on each wheel in order to change the damping forces as quickly as possible. This system incorporates two discrete damper characteristics. Sensors used are: four piezo sensors on each wheel, a stop lamp switch, a steering sensor, and a vehicle speed sensor.

PETITIONER'S EXHIBIT 1002
US PATENT NO. 6,581,565

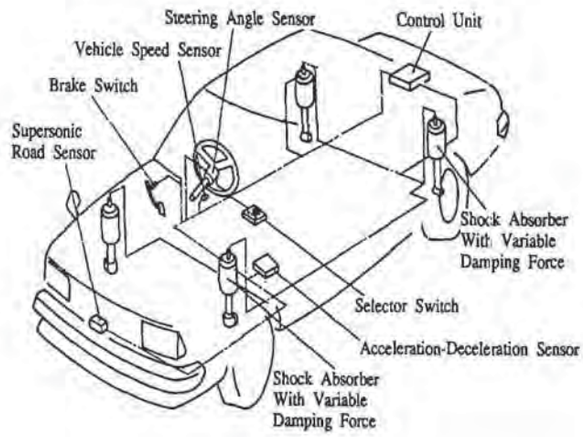


FIGURE 17.1 Principal components of a damping control system.

17.1.2 Actuator and Sensor

Actuator. Discrete damping control actuators often use a built-in motor to change the damping force. This motor turns a rotary valve to select the orifice diameter for three different damping levels: soft, medium, and hard. The stopping position of the rotary valve is controlled by encoder signals.

Another actuator is a piezo actuator consisting of 88 piezo elements, and it is installed in the piston rod of a shock absorber. When a high voltage (500 V) is applied to the piezo actuator, it expands about 50 μm with reverse piezoelectric effect. Elongation in the piezo actuator causes the plunger pin to be pushed out through the displacement hydraulic coupling unit. As a result, the plunger pin moves down to open the bypass of the damping force switching valve. The result is a soft damping force. Figure 17.2 shows this valve.

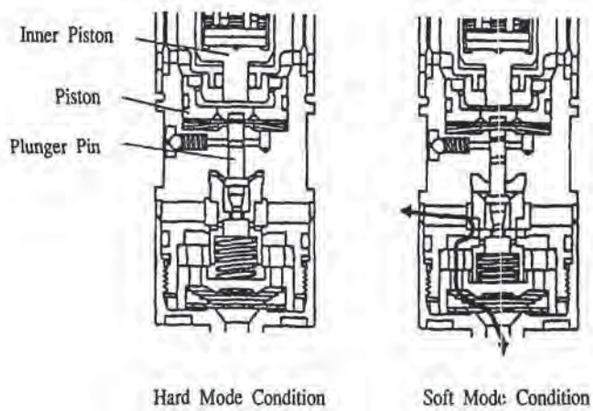


FIGURE 17.2 Damping force switching valve.

Sensor. A sensor using a supersonic wave to detect the road surface is shown in Fig. 17.3. The vehicle height from road to body is calculated on the basis of reflection time T. Judgment of the road condition is made by analyzing the pattern of change in vehicle height.

A sensor using the piezoelectric effect is shown in Fig. 17.4. Installed in the piston rod of a shock absorber, the sensor generates an electric charge in accordance with axial force from the road surface.

PETITIONER'S EXHIBIT 1002
US PATENT NO. 6,581,565

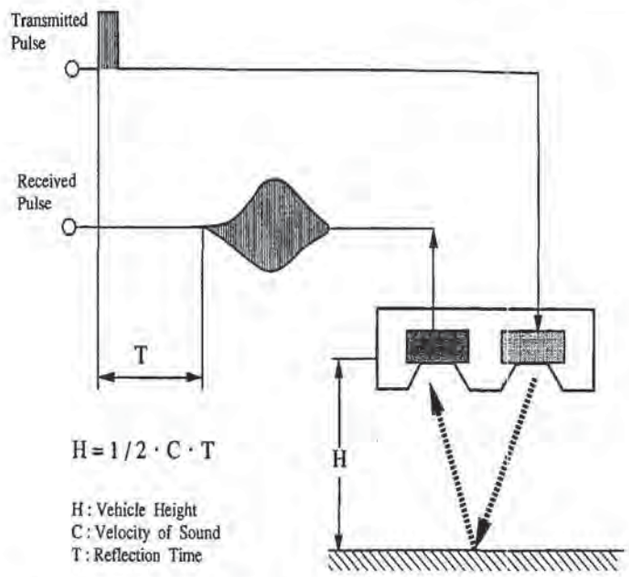


FIGURE 17.3 Supersonic sensor.

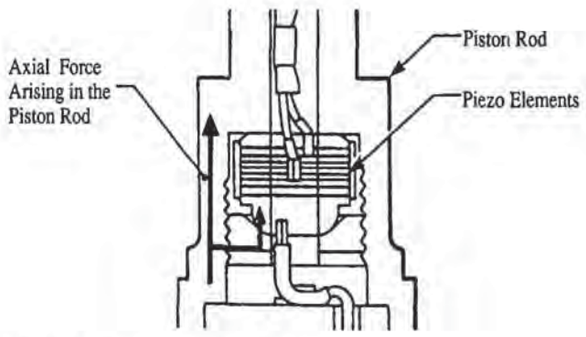


FIGURE 17.4 Piezoelectric sensor.

17.1.3 Control System

The control system of Fig. 17.1 is shown in Table 17.1. The occurrence of roll and pitch can be predicted from various sensors. Single bumps or dips are detected from changes in vehicle height. The outline of the road surface judgment logic is shown in Table 17.2.

The block diagram of the system using four piezo sensors and four piezo actuators is shown in Fig. 17.5. The damping force arising in an absorber increases instantaneously as the tire or wheel goes up or down in accordance with unevenness of the road surface. Each piezo sensor outputs to the electronic control unit continuous signals indicating damping force differential. If the value of damping force differential exceeds a predetermined level, the system switches from firm mode to soft mode. The system is designed so that the firm mode reengages immediately after the vibrations due to poor road surface cease.

Many of the limitations and disadvantages of the conventional shock absorber can be eliminated by the damping control systems. They include semiactive suspension systems which are capable of providing both ride comfort and good handling.

PETITIONER'S EXHIBIT 1002
US PATENT NO. 6,581,565

TABLE 17.1 Damping Force Control System

Control objectives		Sensors used					Damping force Front / Rear
		Vehicle speed	Steering angle	Accel/ decel	Brake	Road condition	
Roll	Roll reduction for quick steering operation	○	○				Hard / Hard
Pitch	Reduction of nose diving by braking				○	○	Hard / Hard
	Reduction of pitching when accelerating and decelerating	○		○			Medium / Medium
Bouncing	Reduction of light, bouncy vibrations in bottoming	○				○	Medium / Medium
	Reduction of light, bouncy vibrations in bouncing on a heaving road	○				○	Medium / Medium
Road holding performance	Road holding performance improvement when running on rough roads	○				○	Medium / Medium
Others	Stability improvement at high speed	○					Medium / Soft
	Prevention of shaking when stopping and rocking when passengers exit or enter	○					Hard / Hard

TABLE 17.2 Road Condition Judgment Logic

High-frequency components	Low-frequency components	
	Small	Large
Small	Smooth road	Heaving road
Large	damping force control unnecessary	Rough road

17.2 HYDROPNEUMATIC SUSPENSION CONTROL SYSTEM

A hermetically sealed quantity of gas is used in the hydropneumatic suspension control system. The gas and hydraulic oil are separated by a rubber diaphragm, as shown in Fig. 17.6*a*. The mechanical springs are replaced by gas. The shock absorber damping mechanism is achieved by the orifice fitted with valves.

17.2.1 System Configuration

As shown in Fig. 17.6*b*, by adding an additional sphere to the hydropneumatic system, a controllable hydropneumatic system can be realized. If the regulator is closed, the system is in a firm mode. If the regulator is open, the spring constant of the suspension system becomes lower by increasing the total volume of the sphere, and the total damping force is reduced.

PETITIONER'S EXHIBIT 1002
US PATENT NO. 6,581,565

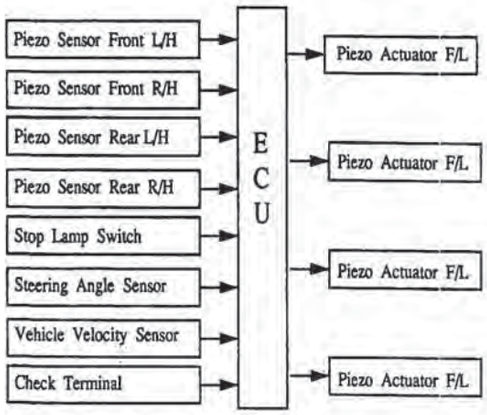


FIGURE 17.5 Block diagram of damping control system.

Depending on the sensors used, which detect vehicle driving and road surface conditions, this system can change the regulator characteristics in order to achieve both good ride comfort and handling stability.

17.3 ELECTRONIC LEVELING CONTROL SYSTEM

In a pneumatic and hydropneumatic suspension, the vehicle body can be maintained at a constant height from the road surface, keeping a low spring constant. The advantages of an electronic control system are:

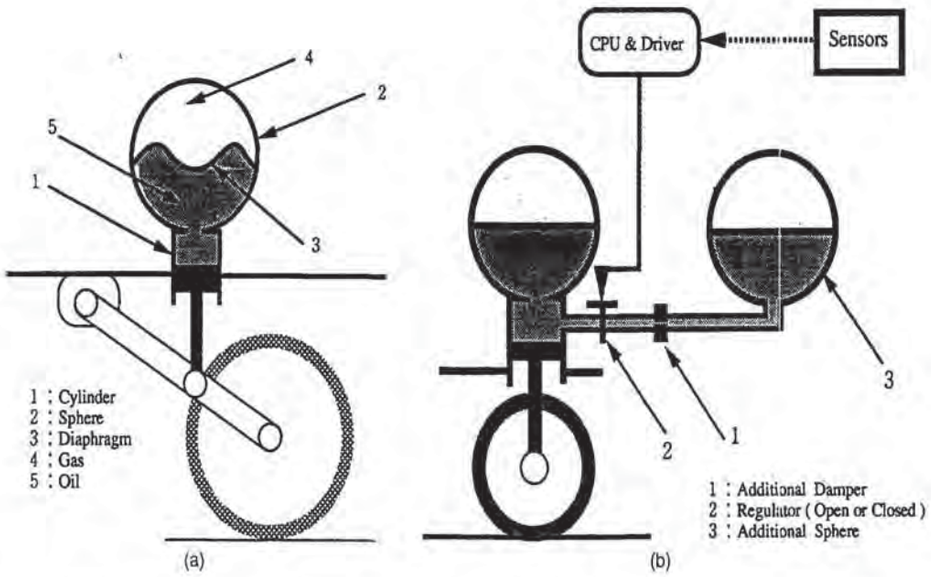


FIGURE 17.6 (*a*) Hydropneumatic suspension system; (*b*) Controllable hydropneumatic suspension system.

PETITIONER'S EXHIBIT 1002
US PATENT NO. 6,581,565

- Keeping a low spring rate to achieve good ride comfort independent of load conditions
- Increase in vehicle body height on rough road surfaces
- Changing spring rate and damping force in accordance with driving conditions and road surfaces

17.3.1 System Configuration

The system is shown in Fig. 17.7. It consists of eight sensors, a mode select switch, air spring/shock absorber units on four wheels, actuators to operate the changing valves in the unit, a compressor unit and five height control valves for air springs, and an electronic control unit (ECU). The system configuration is shown in Fig. 17.8.

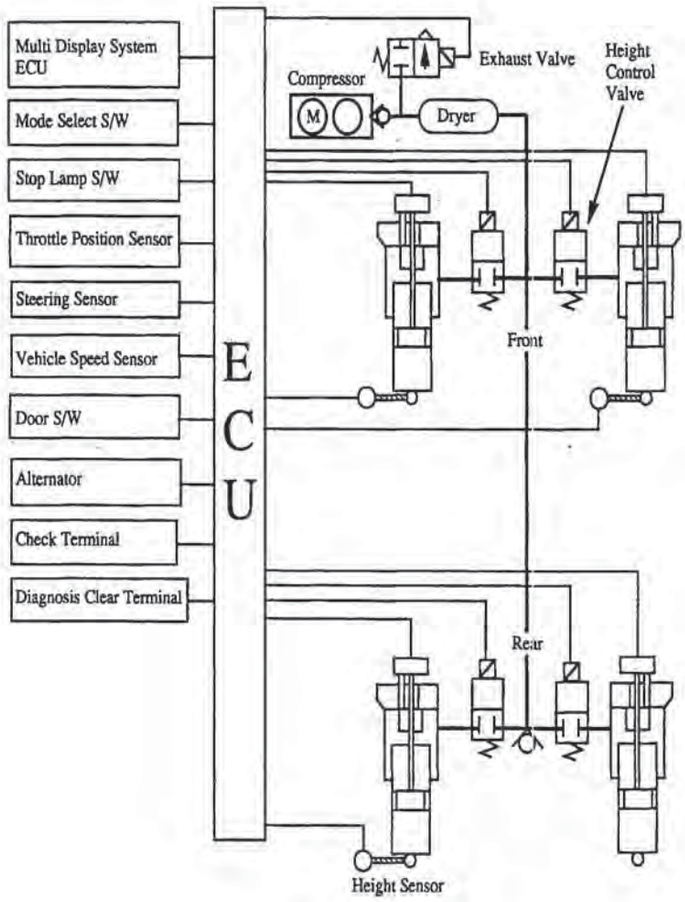


FIGURE 17.7 Principal components of an air suspension system.

17.3.2 Components

The structure of the air suspension unit consists of a shock absorber, a pneumatic piston surrounding the shock absorber, main and sub-air chambers, a rolling diaphragm, and valves which change the suspension stroke.

The actuator uses a dc motor, which has two shafts to operate the valves for the air spring and the shock absorber. The rotation of the motor is reduced by the sector gear and operates

PETITIONER'S EXHIBIT 1002
US PATENT NO. 6,581,565

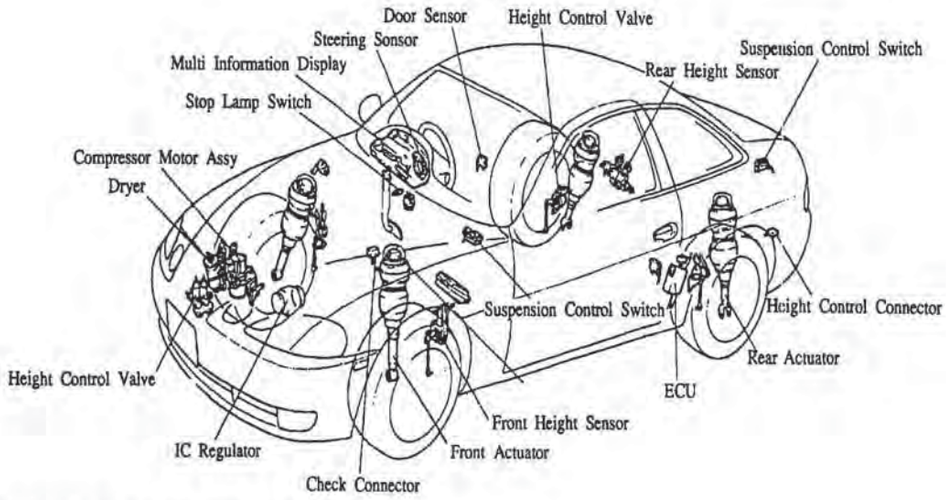


FIGURE 17.8 Configuration of an air suspension system.

the rotary valve to change the damping force. At the same time, another gear engaged with the sector gear operates the air valve to change the spring rate.

17.3.3 Control System

This system can change the spring rate and the damping force into three levels and vehicle height levels of low, normal, or high can be selected. One of the control logics is shown in Table 17.3. This is a control which changes the suspension characteristics in response to vehicle speed and road conditions. The spring rate/damping force and the vehicle height are controlled independently according to each control logic.

Electronic leveling control systems do not need much energy to control vehicle height. They control both spring rate and damping force. As a result of keeping the low spring rate, electronic leveling control systems can provide both good ride comfort and handling stability.

TABLE 17.3 Basic Control Logic of Air Suspension System

		Spring rate, damping force					
		Soft mode			Medium mode		
Function	Operating condition	Soft	Medium	Firm	Soft	Medium	Firm
Antiroll	Rapid steering	○		→ ○		○	→ ○
			○	↗			
Antidive	Braking at V* > 60 km/h	○		→ ○		○	→ ○
			○	↗			
Antisquat	Rapid starting at V < 20 km/h	○		→ ○		○	→ ○

* V: Vehicle speed.

PETITIONER'S EXHIBIT 1002
US PATENT NO. 6,581,565

17.4 ACTIVE SUSPENSION

Suspension control systems for passenger cars have evolved through several stages over the years. Work in the field began with the air suspension for controlling vehicle height and then progressed to the hydropneumatic suspension and suspensions with variable damping force and spring rate control. Now efforts are underway to develop an active suspension. It is defined as one that has the following features:

- Energy is constantly supplied to the suspension and the force generated by that energy is continuously controlled
- The suspension incorporates various types of sensors and a unit for processing their signals that generates forces that are a function of the signal outputs

17.4.1 System Configurations

Basic Configuration. Hydraulic active suspension can be divided into two large systems: the hydraulic system and the control system, as shown in Fig. 17.9. The hydraulic pressure of each of the actuators located on each wheel is controlled in accordance with the output values from the G sensors to suppress changes in vehicle body position (bounce, pitch, roll) and reduce vibration from the road surface.

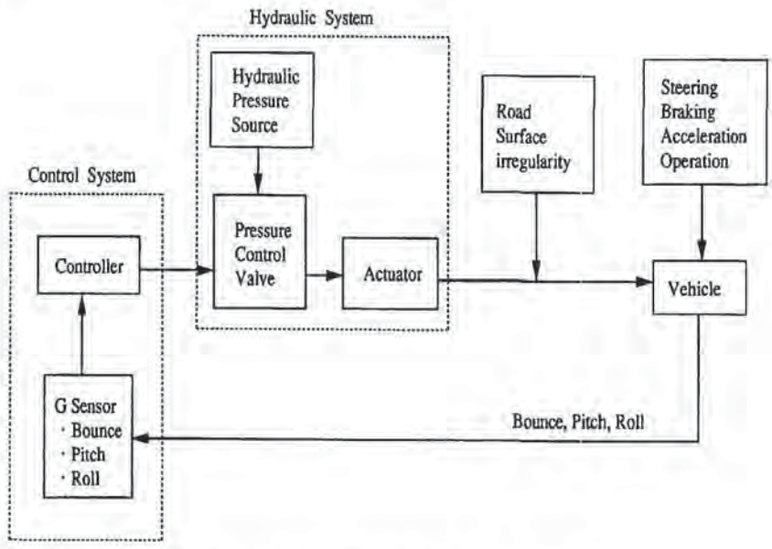


FIGURE 17.9 Hydraulic and control systems for an active suspension.

Hydraulic and Control System Configuration. A basic overview of the system is shown in Fig. 17.10. The functions of the main units of the hydraulic system are shown in Table 17.4.

As shown in Fig. 17.11, the control system contains the controller and all of the sensors including the vertical G sensors, lateral G sensors, fore and aft G sensors, and vehicle height sensors.

17.4.2 Components

Oil Pump. The oil pump has seven cylinders arranged around the circumference and can output a maximum oil flow of 12 liters per minute. The pump is connected in tandem with the power steering vane pump.

PETITIONER'S EXHIBIT 1002
US PATENT NO. 6,581,565

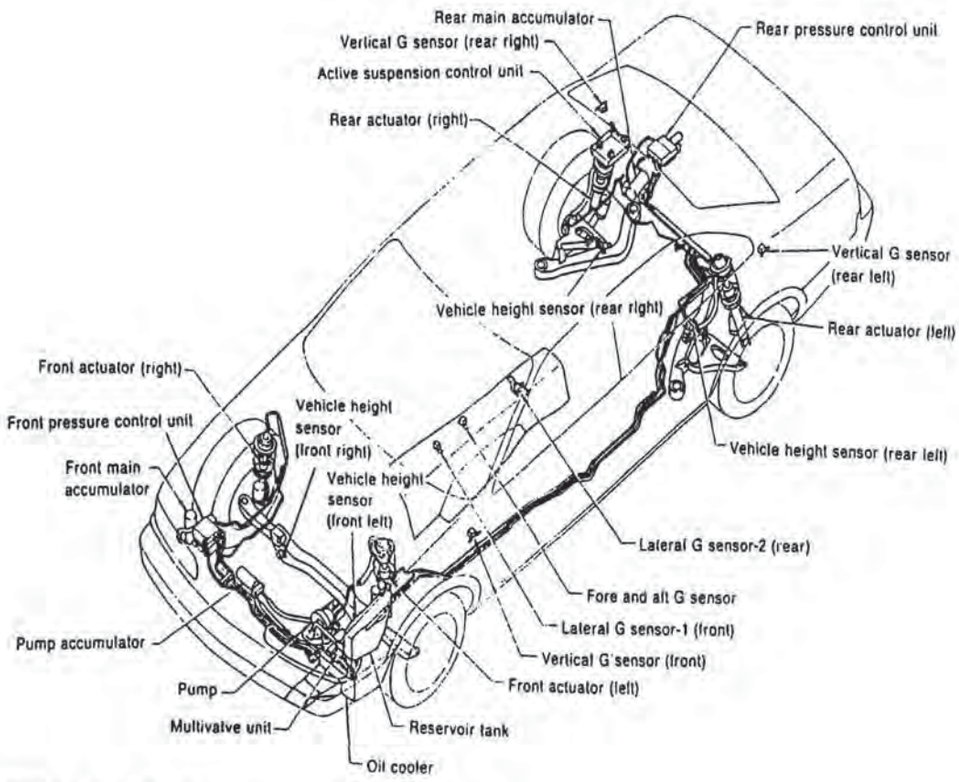


FIGURE 17.10 Principal components of an active suspension system.

Pump Accumulator. To dampen pulsating hydraulic pressure generated by the oil pump, pump accumulators are installed in the hydraulic supply unit, including one on the side of the oil pump. To dampen the high-frequency pulsations, a metal-bellows-type accumulator is used.

Multivalve Unit. As shown in Fig. 17.12, the multivalve unit contains valves for many different functions. The main purpose of the multivalve unit is the basic control of hydraulic pressure for the whole system. The function of the multivalve unit is shown in Table 17.5.

Main Accumulator. The main accumulator is positioned at both the front and rear axles. The main accumulator has two principal functions: it stores oil from the multivalve unit and provides extra flow to the actuators when necessary, and it preserves vehicle height when the engine is turned off.

TABLE 17.4 The Functions of Main Units of the Hydraulic Systems

	Main basic function
Oil pump	Supplies the necessary oil for system operation (power supply)
Pump accumulator	Removes the pulsating action from pressurized oil supplied by the oil pump
Multivalve unit	Controls the supply of pressurized oil, failsafe function, etc.
Main accumulator	Maintains oil pressure, compensates when large amount of flow is required and preserves vehicle body height
Pressure control unit	Controls the hydraulics for the actuators on each wheel according to signals received from the control unit
Actuator	Controls vehicle attitude and absorbs external forces from the road surface

PETITIONER'S EXHIBIT 1002
US PATENT NO. 6,581,565

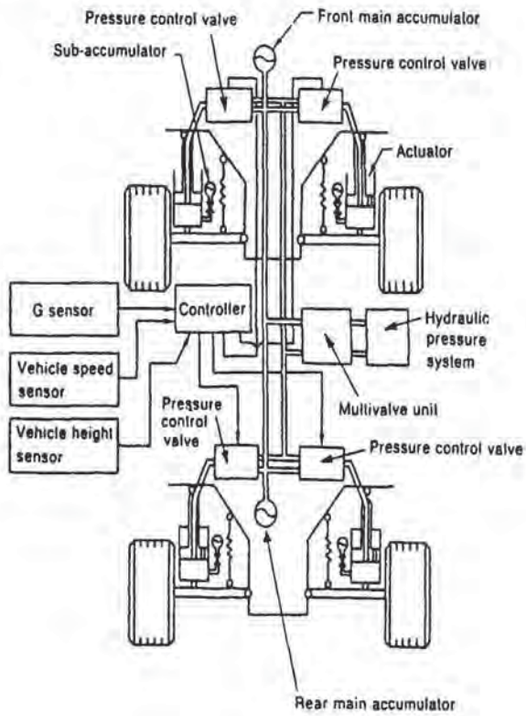


FIGURE 17.11 Controls for an active suspension system.

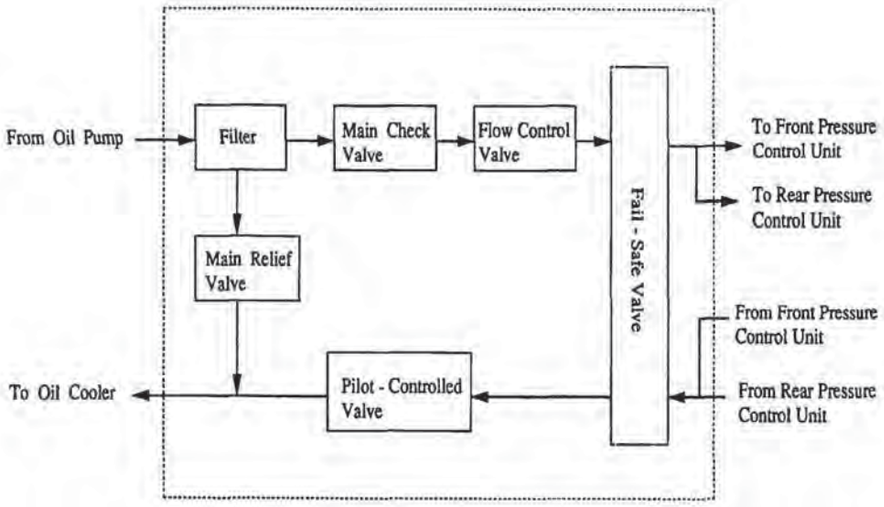


FIGURE 17.12 Multivalve unit configuration.

Pressure Control Unit. As shown in Fig. 17.13, the pressure control unit controls the hydraulic movement of the actuator of each wheel in accordance with instructions received from the control unit. Table 17.6 shows the valve's construction and operating principle.

The electrohydraulic pressure control system consists of a pressure actuator and a pressure control valve. The actuator is of the single acting type and is provided with a damping valve and an accumulator below the cylinder. The pressure control valve is built with three ports

PETITIONER'S EXHIBIT 1002
US PATENT NO. 6,581,565

TABLE 17.5 Multivalve Unit Functions

Function	Valve	Outline
Pressure supply management function	Main relief valve	When the oil pressure exceeds a constant value, the main relief valve will return some of the oil flow. This keeps the oil supply pressure at a constant pressure.
Vehicle height maintenance function	Main check valve Pilot-controlled check valve	The main check valve is a nonreturn valve that controls the flow from the line filter and directs it to the flow control valve. The pilot controlled check valve is a supply-pressure-reaction-type open/closed valve. When the hydraulic pressure exceeds a constant value, the valve opens and when the hydraulic pressure falls below that level, it closes. In addition, it maintains the hydraulic pressure at a constant level when the engine is turned off.
Vehicle height control function	Flow control valve	When the engine is turned off, the flow control valve closes the main passage and directs the flow through the bypass passage orifice, slowly increasing the hydraulic pressure, after which the main passage is opened. This prevents any sudden changes in vehicle height when starting the engine.
Failsafe function	Failsafe valve	When any irregularities occur in the electronic system, it changes the hydraulic passage, preventing any sudden changes in vehicle height.

and employs a pilot type proportional electromagnetic control valve. This pressure control valve has two main functions:

- It controls the pressure of the actuator according to the control input. This is accomplished by driving the solenoid so that it adjusts the pilot valve, causing the spool to move.
- Feedback control is applied to move the spool in response to fluctuations in actuator pressure caused by road surface inputs; the action of the spool works to keep the actuator pressure at a certain fixed level.

Actuator. As shown in Fig. 17.14, the actuator consists of the hydraulic power cylinder, subaccumulator, damping valve, etc. Auxiliary coil springs are also employed to reduce the pressure necessary for the overall system and to reduce the amount of horsepower expended. The subaccumulator and damping valve at the bottom of the hydraulic power cylinder absorb and damp the high-frequency vibration from the road surface.

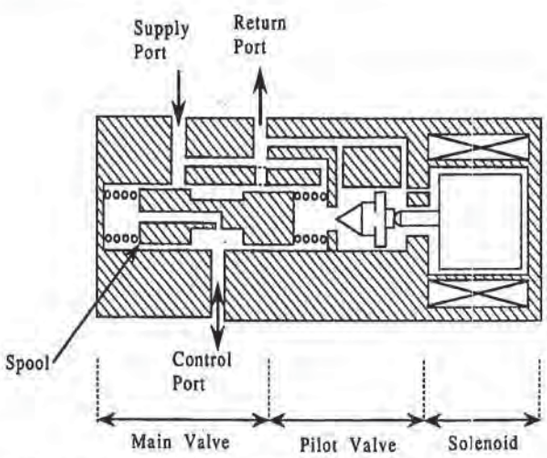


FIGURE 17.13 Pressure control valve construction.

PETITIONER'S EXHIBIT 1002
US PATENT NO. 6,581,565

TABLE 17.6 Pressure Control Valve Functions

Active control function	The pressure in the control port (actuator) is controlled in response to the electric current applied to the solenoid, thus controlling the vehicle attitude.
Passive damping function	When various pressure levels are caused in the interior of the actuator by road surface forces, this pressure passes through the control port, causing feedback on the spool and the generation of appropriate damping forces.

Controller. As shown in Fig. 17.15, the controller is constructed using two 16-bit microcomputers, MCU1 and MCU2.

MCU1 processes signals from the G sensors and then sends attitude control signals to the pressure control valve solenoid drive circuit. MCU2 processes signals from the vehicle height sensors and then sends attitude control signals to the solenoid drive circuit.

MCU1 and MCU2 normally perform mutual transmission, but should an irregularity occur, the signal will be sent to the failsafe circuit, causing the failsafe valve to operate and thus guarantee a high degree of safety.

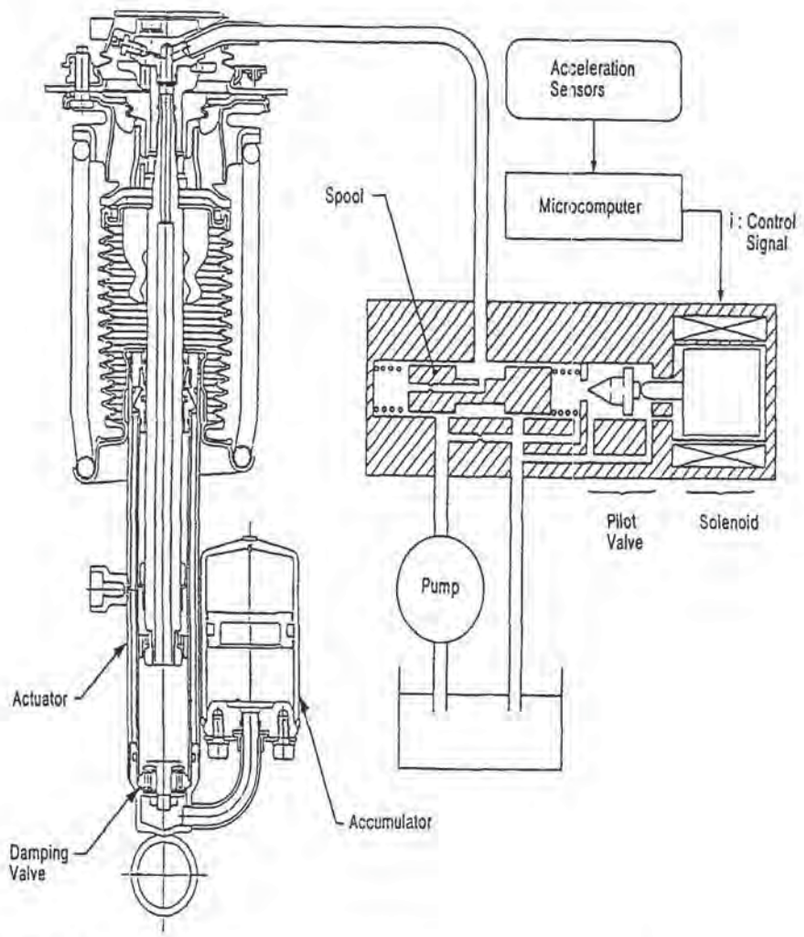


FIGURE 17.14 Schematic diagram of electrohydraulic pressure control system.

PETITIONER'S EXHIBIT 1002
US PATENT NO. 6,581,565

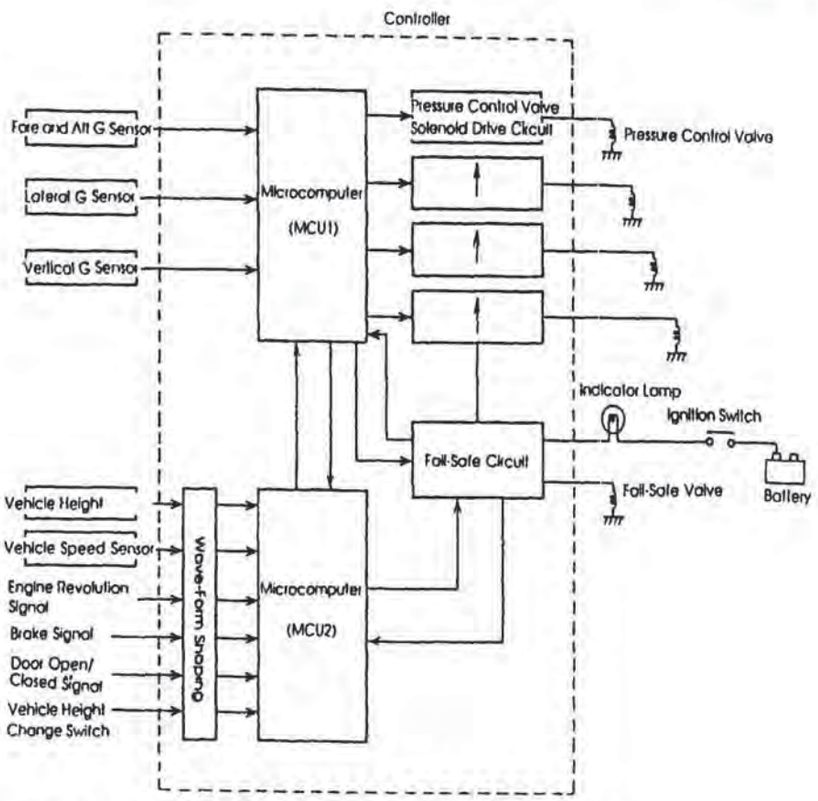


FIGURE 17.15 Interior construction of the electrohydraulic pressure controller.

G Sensors. The G sensors are ball position detection type sensors. They detect changes in the magnetic field caused by the position change of a steel ball as the result of acceleration.

17.4.3 Control System

Roll Control. The inertia force, which causes the car to roll, is detected by the lateral G sensor. Roll control is initiated by increasing the control pressure on the wheels on the outside of the turn and by decreasing the control pressure for the wheels on the inside of the turn. Figure 17.16 shows this operating principle.

The relation between the lateral G and the force generated by the actuator is:

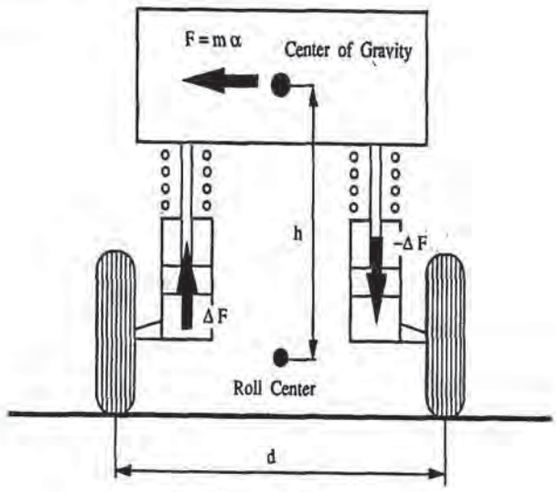
$$F = m\alpha \tag{17.1}$$

$$Fh = \Delta Fd$$

$$\Delta F = \frac{Fh}{d} = \frac{m\alpha h}{d}$$

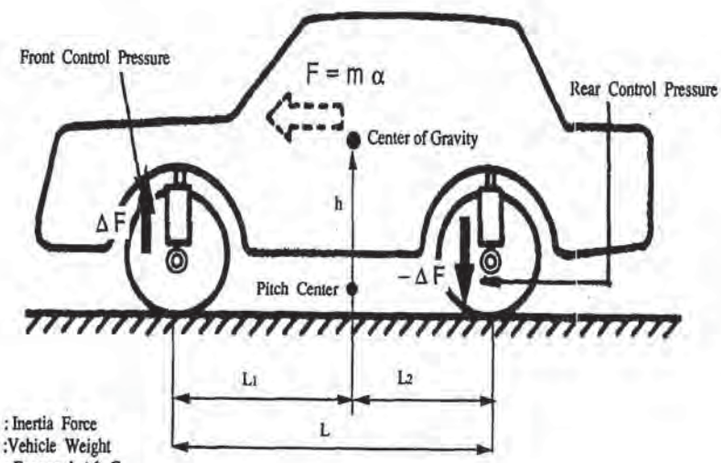
Pitch Control. During braking, inertia is generated at the vehicle's center of gravity and causes pitching. The longitudinal G sensor detects this inertia and cancels it to suppress nose dive by increasing the control pressure to the front and decreasing control pressure to the rear, as shown in Fig. 17.17. The relationship between longitudinal G and the actuator generated force is:

PETITIONER'S EXHIBIT 1002
US PATENT NO. 6,581,565



α : Lateral G
F : Inertia
ΔF : Actuator Generated Force
d : Tread

FIGURE 17.16 Operating principle for roll control.



F : Inertia Force
m : Vehicle Weight
α : Fore and Aft G
ΔF : Actuator - Generated Force
L : Wheel Base

FIGURE 17.17 Pitch control parameters.

$$Fh = \Delta F\,(L_1 + L_2)$$

$$\Delta F = \frac{Fh}{(L_1 + L_2)} = \frac{m\alpha h}{L} \tag{17.2}$$

Bounce Control. The vertical G sensor attached to the vehicle body detects the value for vehicle body acceleration. By integration of the acceleration, the absolute velocity of the body is calculated. A force proportional to the absolute velocity is generated by the pressure control valve.

PETITIONER'S EXHIBIT 1002
US PATENT NO. 6,581,565

This control method, called skyhook damper control, is adapted. It dampens the motion of the car body regardless of any input from the road surface.

In the case of a passive damper, the vertical motion of the body relative to the road surface inputs can be given as:

$$\frac{X_2}{X_1} = \frac{2j\omega_2\xi_2\omega + \omega_2^2}{-\omega^2 + 2j\omega_2\xi_2\omega + \omega_2^2} \tag{17.3}$$

The vibration transmission rate at the resonant point is:

$$\left|\frac{X_2}{X_1}\right|_{\omega=\omega_2} = \sqrt{1 + \frac{1}{4\xi_2^2}} \tag{17.4}$$

and always has a value greater than one.

By contrast, the vibration characteristics of the skyhook damper are given as:

$$\frac{X_2}{X_1} = \frac{2j\omega_2\xi_2\omega + \omega_2^2}{-\omega^2 + 2j\omega_2(\xi_2 + \xi_s)\omega + \omega_2^2} \tag{17.5}$$

The vibration transmission ratio at the resonant point is:

$$\left|\frac{X_2}{X_1}\right|_{\omega=\omega_2} = \frac{\sqrt{4\xi_2^2 + 1}}{2(\xi_2 + \xi_s)} \tag{17.6}$$

hence,

$$\xi_s \geq \sqrt{\xi_2^2 + \frac{1}{4}} - \xi_2 \tag{17.7}$$

and it is possible to reduce the ratio to less than one.

The effects of the hydraulic active suspension are organized in Table 17.7 according to those related to the vehicle.

17.4.4 Effectiveness

Figure 17.18 shows the lateral G and angle of roll during cornering. Figure 17.19 shows the fore and aft G force, angle of nose dive, and squat angle during starts and stops. In either case, the car with the hydraulic active suspension outperformed the other cars with conventional suspensions.

TABLE 17.7 Effect of Active Suspension Control

Control	Vehicle-related effects
Roll control	During transient control of wheel loading, as when changing lanes, the steering characteristics of the vehicle can be optimally controlled. The tires are used to their utmost performance ability because there is minimal roll, minimal change in the camber of the tires to the ground, and because the tires are continually kept in square contact with the road.
Pitch control	Nose dive and tail lift are minimized during braking. Squats are minimized during starts and rapid acceleration.
Bounce control	Vertical vibration of the vehicle is reduced and continuity is improved. Vertical load fluctuation is minimal, and the contact of the tires with the road is greatly improved.

PETITIONER'S EXHIBIT 1002
US PATENT NO. 6,581,565

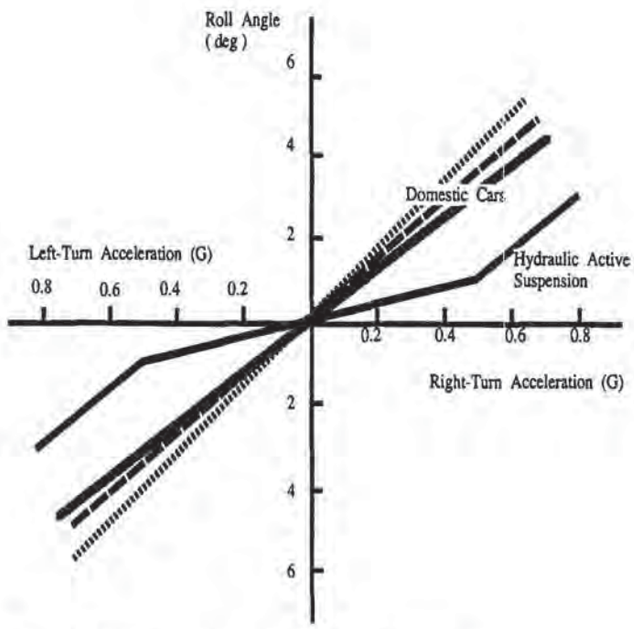


FIGURE 17.18 Comparison of roll angles during cornering.

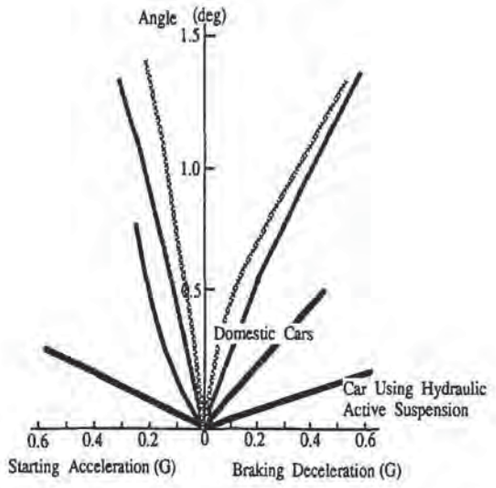


FIGURE 17.19 Comparison of nose dive and squat angles.

Figure 17.20 shows the effects of bounce control for the skyhook damper. Compared with cars using conventional suspension systems, the car with the hydraulic active suspension system exhibited superior performance and low vibration levels.

Figure 17.21 shows the ride characteristics and roll rate for various cars with some suspension systems. As the results clearly demonstrated, the hydraulic active suspension system, through advanced roll control and bounce control, provides a ride and a level of control far superior to that of other suspension systems.

PETITIONER'S EXHIBIT 1002
US PATENT NO. 6,581,565

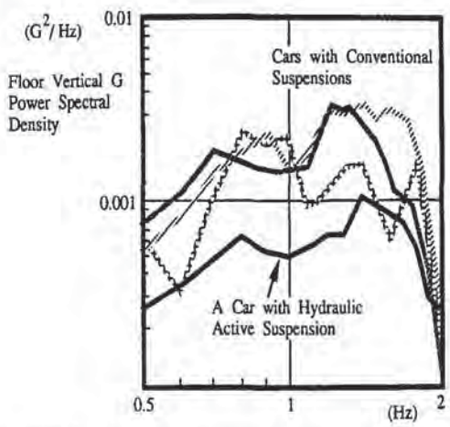


FIGURE 17.20 Comparison of vertical vibrations.

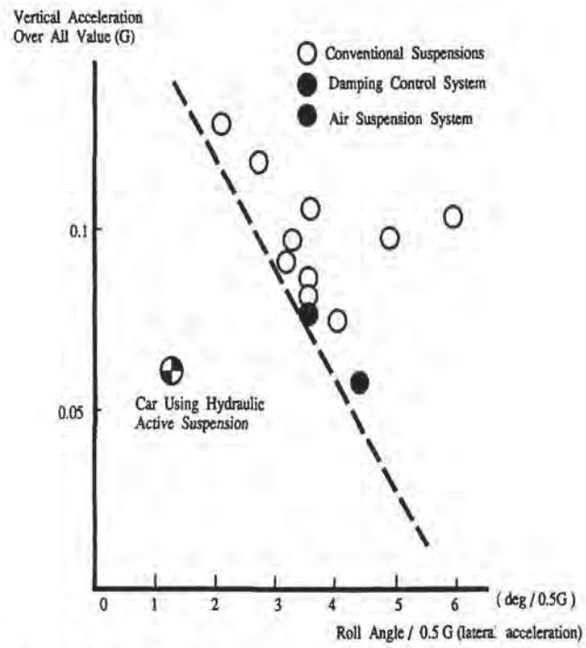


FIGURE 17.21 Ride characteristics and roll rate for various cars with different suspension systems.

17.5 CONCLUSION

The active suspension system provides outstanding levels of performance which are unobtainable with other suspension control systems and conventional passive suspensions. Evaluations made with actual vehicles confirmed the effectiveness of the active suspension system in improving ride comfort and handling properties.

PETITIONER'S EXHIBIT 1002
US PATENT NO. 6,581,565

GLOSSARY

Hydropneumatic suspension A suspension system using oil or air to support the car body.

Skyhook damper control The control law applied to control the vehicle as if it were fixed within absolute space suspended from the sky.

Supersonic sensor A sensor used to measure the distance between a car body and the road surface using supersonic waves.

NOMENCLATURE

C_2: passive damping coefficient
C_s: active damping coefficient
K_1: tire stiffness
K_2: spring stiffness
M_1: unsprung mass
M_2: sprung mass
$\omega_1 = (K_1/M_1)^{1/2}$ natural frequency of unsprung mass
$\omega_2 = (K_2/M_2)^{1/2}$ natural frequency of sprung mass
$\xi_2 = (C_2/2)\,(M_2K_2)^{1/2}$ active damping ratio
$\xi_S = (C_S/2)\,(M_2/K_2)^{1/2}$ passive damping ratio

BIBLIOGRAPHY

Decker, H., and W. Scramm, "An optimized approach to suspension control," SAE Paper 900661, 1990.

Decker, H., W. Scramm, and R. Kallenbach, "A modular concept for suspension control," *XXIII Fisita Congress,* Torino, Italy, 1990, 905124.

Decker, H., W. Scramm, and R. Kallenbach, "A practical approach toward advanced suspension systems," *Proc. IMechE International Conference on Advanced Suspensions,* London, 1988, S. 93–99.

Doi, S., E. Yasuda, and Y. Hayashi, "An experimental study of optimal vibration adjustment using adaptive control methods," *Proceedings of the Institution of Mechanical Engineers,* London, Oct. 24–25, 1988.

Guy, Y., M. B. Lizell, and M. W. Kerastas, "A solenoid-actuated pilot valve in a semi-active damping system," SAE Paper 881139, Aug. 1988.

Haget, K. H., et al., "Continuous adjustable shock absorbers for rapid-acting ride control systems (RCS)," *XXIII Fisita Congress,* Torino, Italy, 1990, 905125.

Hennecke, D., P. Baier, B. Jordan, and E. Walek, "EDCIII—the new variable damper system for BMW's top models—a further development of our adaptive, frequency-dependent damper control," SAE Paper 900662.

Hennecke, D., P. Baier, B. Jordan, and E. Walek, "Further market-oriented development of adaptive damper force control," *XXIII Fisita Congress,* Torino, Italy, 1990, 905143.

Hennecke, D., B. Jordan, and U. Ochner, "Electronic damper control—a fully automatic adaptive system for damping force adjustment on the BMW 635 CSi," *ATZ 89,* 9, 1987, pp. 471–479.

Hrovat, D., D. L. Margolis, and M. Hubbard, "An approach toward the optimal semi-active suspension," *Transactions of the ASME,* 288, vol. 110, Sept. 1988.

PETITIONER'S EXHIBIT 1002
US PATENT NO. 6,581,565

Karnop, D., and D. L. Margolis, "Adaptive suspension concepts for road vehicles," *Vehicle System Dynamics,* 13, 1984, pp. 145–160.

Karnop, D., M. J. Crosby, and R. A. Harwood, "Vibration control using semi-active force generators," *ASME Journal of Engineering for Industry Transactions of the ASME,* No. 96, 1974, S. 613–626.

Margolis, D. L., "Semi-active control of wheel hop in ground vehicles," *Vehicle System Dynamics,* 12, 1983, pp. 317–330.

Sharp, R. S., and S. A. Hassan, "Performance and design considerations for dissipative semi-active suspension systems for automobiles," *Proceedings Institution of Mechanical Engineers,* vol. 201, no. D2, pp. 149–153.

Sugasawa, F., et al., "Electronically controlled shock absorber system used as a road sensor which utilizes super sonic waves," SAE Paper 851652, 1985.

Tsutsumi, Y., H. Sato, H. Kawaguchi, and M. Hirose, "Development of Piezo TEMS (Toyota Electronic Modulated Suspension)," SAE Paper 901745, 1990.

Yokota, Y., K. Asami, and T. Hajima, "Toyota electronic modulated suspension system for the 1983 Soarer," SAE Paper 840341, 1984.

Hydropneumatic Suspension

Akatsu, Y., N. Fukushima, K. Takahashi, M. Satoh, and Y. Kawarazaki, "An active suspension employing an electrohydraulic pressure control system," *XXIII Fisita Congress,* Torino, Italy, 1990, 905123.

Carbonaro, O., "Hydractive suspension electronic control system," *XXIII Fisita Congress,* Torino, Italy, 1990, 905101.

Dominy, J., and D. N. Bulman, "An active suspension for a Formula One Grand Prix racing car," *Transactions ASME, Journal Dynamic Systems Measurement Control,* vol. 107, 1, 1985, pp. 73–78.

Hedrick, J. K., "Railway vehicle active suspensions," *Vehicle System Dynamics* **10**, 1981, pp. 267–283.

Henning, H., "Citroen SM V6," *ATZ 92,* 1990, pp. 23–27.

Hrovat, D., "Optimal active suspension structures for quarter-car vehicle models," *Automatica,* vol. 26, 5, 1990, pp. 845–860.

Karnop, D., "Active damping in road vehicle suspension systems," *Vehicle System Dynamics* **12**, 1983, pp. 291–316.

Sharp, R. S., and S. A. Hassan, "An evaluation of passive automotive suspension systems with variable stiffness and damping parameters," *Vehicle System Dynamics,* **15**(6):1986, pp. 335–350.

Tanahashi, H., K. Shindo, T. Nogami, and T. Oonuma, "Toyota electronic modulated air suspension for the 1986 Soarer," SAE Paper 870541, 1987.

Thompson, A. G., "An active suspension with optimal linear state feedback," *Vehicle System Dynamics* **5**, 1976, pp. 187–203.

Tobata, H., N. Fukushima, K. Fukuyama, and T. Kimura, "Advanced control method of active suspension," *Avec92,* Yokohama, Japan, 1992, 923023.

Wright, P., "The application of active suspension to high performance road vehicle," *I MechE,* C239/84, 1984.

ABOUT THE AUTHOR

Akatsu Yohsuke has been Vehicle Research Manager for Nissan Motor Co., Ltd., since 1980. He was awarded the B.E. degree from the Tokyo Institute of Technology in 1978 and the M.E. degree from there in 1980.

PETITIONER'S EXHIBIT 1002
US PATENT NO. 6,581,565

PETITIONER'S EXHIBIT 1002
US PATENT NO. 6,581,565

CHAPTER 18
STEERING CONTROL

Makoto Sato
Honda R&D Co., Ltd.

The application of electronic control technology to vehicle steering systems is still in the development stage. The structure and functioning of such systems are not yet clearly defined. Accordingly, the material that follows is intended primarily to introduce systems which have already been published, and it is devoted entirely to the electronic aspects of those systems and does not include descriptions of the basic operation of hydraulic power steering systems.

18.1 VARIABLE-ASSIST STEERING

18.1.1 Fundamentals of Electronically Controlled Power Steering

Electronically controlled power steering improves steering feel and power-saving effectiveness, and increases steering performance. It does so with control mechanisms that reduce the steering effort. An electronic control system, for example, may be added to the hydraulic booster or the whole system may be composed of electronic and electric components.

The intent of electronic controls, initially, was to reduce the steering effort when driving at low speeds and to supply feedback for the appropriate steering reaction force when driving at high speeds. In order to achieve those goals, devices such as vehicle speed sensors were used to detect vehicle speed in order to make smooth and continuous changes in the steering assist rate under conditions ranging from steering maneuvers at zero speed to those at high speeds. However, as vehicles became equipped with electrohydraulic systems and fully electronic and electric systems, the emphasis for these systems started to include reduction in power requirements and higher performance.

The main functions required for electronically controlled power steering are listed in Table 18.1.

18.1.2 Types of Electronically Controlled Power Steering

Electronically controlled power steering systems presently available commercially can be classified according to their basic structure and basic principles into three types: hydraulic, hybrid, and full electric systems, as shown in Table 18.2. Detailed explanations of these systems are given as follows.

PETITIONER'S EXHIBIT 1002
US PATENT NO. 6,581,565

TABLE 18.1 Functions Required for Electronically Controlled Power Steering

Reduction of driver's burden when turning the steering wheel and improvement in the steering feel	• Reduction in steering effort • Smoothness of steering operation • Feedback of appropriate steering reaction forces • Reduction of kickback[1] • Improvement in convergence[2] • Creation of other new functions
Power saving	
Failsafe	• Maintaining of manual steering function in the event of any malfunctions

TABLE 18.2 Classification of Electronically Controlled Power Steering System

Basic structure	Control method	Control objects	Sensors				Actuator	Major effects	
			Vehicle speed	Steering torque	Angular velocity	Current		Steering force responsive to vehicle speed	Power saving
Electronically controlled hydraulic system	Flow	Flow supply to power cylinder	O			O	Solenoid	O	O
	Cylinder bypass	Effective actuation pressure given to cylinder	O			O	Solenoid	O	
	Valve characteristics	Pressure generated at control value	O			O	Solenoid	O	
	Hydraulic reaction force control	Pressure acting on the hydraulic reaction force mechanism	O			O	Solenoid	O	
Hybrid system	Flow	Flow supply to power cylinder	O		O	O	Motor	O	O
Full electric system	Current	Motor torque	O	O		O	Motor	O	O
	Voltage	Motor power	O	O	O	O	Motor	O	O

18.1.3 Explanations of Each System

Electronically Controlled Hydraulic System. This system consists of a linear solenoid valve, a vehicle speed sensor, and other electronic devices located in part of the hydraulic circuit of the hydraulic system. The opening of the solenoid valve is controlled based on signals from the vehicle speed sensor. The flow and pressure of the hydraulic fluid is controlled by means of the opening of the solenoid valve.

The assist rate is smoothly and continuously varied in response to the vehicle speed, so that when the vehicle is stationary, the opening of the solenoid valve is small to ensure that the steering effort is appropriately light. When the vehicle is moving at high speed, the opening of the solenoid valve is large to ensure that the steering effort is appropriately heavy.

Flow Control Method. In this method, a solenoid valve is located at the pump discharge port as shown in Fig. 18.1. The electronic control device regulates the solenoid valve opening at high vehicle speeds to reduce the pump discharge volume, thus increasing the required steering effort. By reducing the resistance of the circuit between the pump and the power cylinder, power requirements are reduced. Figure 18.2 shows the position of the solenoid

PETITIONER'S EXHIBIT 1002
US PATENT NO. 6,581,565